Lecture Notes in Mechanical Engineering

Vitalii Ivanov · Justyna Trojanowska · Ivan Pavlenko · Erwin Rauch · Ján Piteľ *Editors*

Advances in Design, Simulation and Manufacturing VII

Proceedings of the 7th International Conference on Design, Simulation, Manufacturing: The Innovation Exchange, DSMIE-2024, June 4–7, 2024, Pilsen, Czech Republic - Volume 1: Manufacturing Engineering

Springer

Lecture Notes in Mechanical Engineering

Series Editors

Fakher Chaari, *National School of Engineers, University of Sfax, Sfax, Tunisia*
Francesco Gherardini, *Dipartimento di Ingegneria "Enzo Ferrari", Università di Modena e Reggio Emilia, Modena, Italy*
Vitalii Ivanov, *Department of Manufacturing Engineering, Machines and Tools, Sumy State University, Sumy, Poland*
Mohamed Haddar, *National School of Engineers of Sfax (ENIS), Sfax, Tunisia*

Editorial Board Members

Francisco Cavas-Martínez, *Departamento de Estructuras, Construcción y Expresión Gráfica Universidad Politécnica de Cartagena, Cartagena, Spain*
Francesca di Mare, *Institute of Energy Technology, Ruhr-Universität Bochum, Bochum, Germany*
Young W. Kwon, *Department of Manufacturing Engineering and Aerospace Engineering, Graduate School of Engineering and Applied Science, Monterey, USA*
Tullio A. M. Tolio, *Department of Mechanical Engineering, Politecnico di Milano, Milano, Italy*
Justyna Trojanowska, *Poznan University of Technology, Poznan, Poland*
Robert Schmitt, *RWTH Aachen University, Aachen, Germany*
Jinyang Xu, *School of Mechanical Engineering, Shanghai Jiao Tong University, Shanghai, China*

Lecture Notes in Mechanical Engineering (LNME) publishes the latest developments in Mechanical Engineering—quickly, informally and with high quality. Original research or contributions reported in proceedings and post-proceedings represents the core of LNME. Volumes published in LNME embrace all aspects, subfields and new challenges of mechanical engineering.

To submit a proposal or request further information, please contact the Springer Editor of your location:

Europe, USA, Africa: Leontina Di Cecco at Leontina.dicecco@springer.com
China: Ella Zhang at ella.zhang@cn.springernature.com
India: Priya Vyas at priya.vyas@springer.com
Rest of Asia, Australia, New Zealand: Swati Meherishi at swati.meherishi@springer.com

Topics in the series include:

- Engineering Design
- Machinery and Machine Elements
- Mechanical Structures and Stress Analysis
- Automotive Engineering
- Engine Technology
- Aerospace Technology and Astronautics
- Nanotechnology and Microengineering
- Control, Robotics, Mechatronics
- MEMS
- Theoretical and Applied Mechanics
- Dynamical Systems, Control
- Fluid Mechanics
- Engineering Thermodynamics, Heat and Mass Transfer
- Manufacturing Engineering and Smart Manufacturing
- Precision Engineering, Instrumentation, Measurement
- Materials Engineering
- Tribology and Surface Technology

Indexed by SCOPUS, EI Compendex, and INSPEC.

All books published in the series are evaluated by Web of Science for the Conference Proceedings Citation Index (CPCI).

To submit a proposal for a monograph, please check our Springer Tracts in Mechanical Engineering at https://link.springer.com/bookseries/11693.

Vitalii Ivanov · Justyna Trojanowska ·
Ivan Pavlenko · Erwin Rauch · Ján Pitel'
Editors

Advances in Design, Simulation and Manufacturing VII

Proceedings of the 7th International Conference on Design, Simulation, Manufacturing: The Innovation Exchange, DSMIE-2024, June 4–7, 2024, Pilsen, Czech Republic - Volume 1: Manufacturing Engineering

Springer

Editors
Vitalii Ivanov
Department of Manufacturing Engineering, Machines and Tools
Sumy State University
Sumy, Ukraine

Ivan Pavlenko
Department of Computational Mechanics Named After V. Martsynkovskyy
Sumy State University
Sumy, Ukraine

Ján Pitel'
Faculty of Manufacturing Technologies with a Seat in Prešov
Technical University of Košice
Prešov, Slovakia

Justyna Trojanowska
Faculty of Mechanical Engineering
Poznań University of Technology
Poznań, Poland

Erwin Rauch
Faculty of Engineering
Free University of Bozen-Bolzano
Bolzano, Italy

ISSN 2195-4356 ISSN 2195-4364 (electronic)
Lecture Notes in Mechanical Engineering
ISBN 978-3-031-61796-6 ISBN 978-3-031-61797-3 (eBook)
https://doi.org/10.1007/978-3-031-61797-3

© The Editor(s) (if applicable) and The Author(s), under exclusive license to Springer Nature Switzerland AG 2024

This work is subject to copyright. All rights are solely and exclusively licensed by the Publisher, whether the whole or part of the material is concerned, specifically the rights of translation, reprinting, reuse of illustrations, recitation, broadcasting, reproduction on microfilms or in any other physical way, and transmission or information storage and retrieval, electronic adaptation, computer software, or by similar or dissimilar methodology now known or hereafter developed.
The use of general descriptive names, registered names, trademarks, service marks, etc. in this publication does not imply, even in the absence of a specific statement, that such names are exempt from the relevant protective laws and regulations and therefore free for general use.
The publisher, the authors and the editors are safe to assume that the advice and information in this book are believed to be true and accurate at the date of publication. Neither the publisher nor the authors or the editors give a warranty, expressed or implied, with respect to the material contained herein or for any errors or omissions that may have been made. The publisher remains neutral with regard to jurisdictional claims in published maps and institutional affiliations.

This Springer imprint is published by the registered company Springer Nature Switzerland AG
The registered company address is: Gewerbestrasse 11, 6330 Cham, Switzerland

If disposing of this product, please recycle the paper.

Preface

This volume of Lecture Notes in Mechanical Engineering contains selected papers presented at the 7th International Conference on Design, Simulation, Manufacturing: The Innovation Exchange (DSMIE-2024), held in Pilsen, Czech Republic, on June 4–7, 2024. The conference was organized by the Sumy State University, University of West Bohemia, and International Association for Technological Development and Innovations in partnership with Poznan University of Technology (Poland), Technical University of Kosice (Slovak Republic), Kielce University of Technology (Poland), Association for Promoting Innovative Technologies – Innovative FET (Croatia), and Society for Robotics of Bosnia and Herzegovina (Bosnia and Herzegovina).

DSMIE Conference Series is the international forum for fundamental and applied research and industrial applications in engineering. The conference focuses on research challenges in the fields of Manufacturing Engineering, Materials Engineering, and Mechanical Engineering, addressing current and future trends in design approaches, simulation techniques, and manufacturing technologies, highlighting the growing role of smart manufacturing systems, artificial intelligence, standards-based integration, and innovations implementation to the transition to sustainable, human-centric, and resilient engineering solutions. DSMIE brings together researchers from academic institutions, leading industrial companies, and government laboratories worldwide to promote and popularize the scientific fundamentals of engineering.

DSMIE-2024 received 148 contributions from 33 countries around the world. After a two-stage single-blind review, the Program Committee accepted 83 papers written by 324 authors from 28 countries. Thank you very much to the authors for their contribution. These papers are published in the present book, achieving an acceptance rate of about 56%. Extended versions of selected best papers will be published in scientific journals: Management and Production Engineering Review (Poland), Journal of Engineering Sciences (Ukraine), Advances in Thermal Processes and Energy Transformation (Slovak Republic), Assembly Techniques and Technology (Poland), special issue of Machines (Switzerland) "Innovations in the Design, Simulation, and Manufacturing of Production Systems", and a special issue of Materials (Switzerland) "Novel Approaches in the Design, Simulation, and Manufacturing for Processes and Systems".

We would like to thank members of the Program Committee and invited external reviewers for their efforts and expertise in contributing to reviewing, without which it would be impossible to maintain the high standards of peer-reviewed papers. About 97 Program Committee members and 13 invited external reviewers devoted their time and energy to peer-reviewing manuscripts. Our reviewers come from around the world, representing 21 countries, and are affiliated with 39 institutions.

Thank you very much to the keynote speakers: Prof. Arkadiusz Gola (Lublin University of Technology, Poland), Dr. Foivos Psarommatis (University of Oslo, Norway & ZerOfect Company, Switzerland), Prof. Jinyang Xu (Shanghai Jiao Tong University,

China), Prof. Francisco J.G. Silva (Polytechnic of Porto, Portugal), and Prof. Andre Batako (Liverpool John Moores University, UK).

We sincerely appreciate the invited speakers of the DSMIE Workshops: Dr. Bohdan Haidabrus (Riga Technical University, Latvia) and Prof. Katarzyna Antosz (Rzeszow University of Technology, Poland).

The book "Advances in Design, Simulation and Manufacturing VII" was organized in two LNME volumes according to the main conference topics: Volume 1—Manufacturing Engineering and Volume 2—Mechanical and Materials Engineering. Each volume is devoted to research in design, simulation, and manufacturing within the main conference areas.

The first volume consists of six parts. The first part includes recent developments in smart and sustainable manufacturing. It presents research works in designing cyber-physical production systems, implementing the technological capabilities of modern laboratories, and studies on streamlining processes for Industry 4.0. Additionally, this part includes studies on laser technologies, sustainable design, and advanced circular economy. Moreover, recent developments in simulation-driven evaluation of reward systems for activity-based manufacturing environments are presented in this part. Problems of an industrial data collection application are also discussed.

The second part includes studies in information management systems, particularly the development of IT systems in warehouse management. Application of AI in delivery management and agile digital projects are also presented. Finally, this part proposes improvements in information resources management at industrial companies.

The third part of manufacturing technologies is devoted to increasing the vibration resistance of finishing and boring machines, ensuring tool run-in during milling, and improving metal cutting tools using data-based failure rate assessment methodology. It presents studies on applying ANFIS systems to predict spindle vibrations for CNC machining centers and enhancing service life and machine parts' durability. This part also includes recent developments in designing technological schemes for rolled metal production, increasing the efficiency of rolling rolls and grinding processes, and preventing cracks formation. Moreover, issues regarding the sustainable machining of automotive parts, evaluating the stiffness of underpinning supports for fixtures, and developing flexible fixtures for fork-type parts are presented. Studies on surface hardness improvement of tool steel, wear behavior of coated tools during milling, adaptive fluid jet support technique for end milling, surface morphology and microstructural features of superalloys, and heat treatment are also discussed in this part. Moreover, the third part proposes ways to improve the profile accuracy of large-pitch tapered threads and the power parameters of forming the screw spirals. Finally, it includes research on the statistical comparison of manual and automatic enterprise sampling.

The fourth part considers studies on quality assurance, including problems in assembly technology and machined surface integrity. Statistical analysis and machine learning techniques are also presented in this part. Moreover, it discusses issues of metrological support in defectoscopy and reliability control for mechanical products depending on the tool's accuracy.

The fifth part aims to discuss modern challenges in supply chain and transportation. It includes risk assessment using fuzzy logic and external supply risk assessment.

The problems of designing green logistics systems and real-time driver detection using transfer learning are also added to this part. Finally, it consists of research on process optimization and supply chain.

The sixth part regarding engineering education is based on studies in designing the educational content for the Industry 4.0 competency model and implementing eco-oriented pedagogical technologies. The model for professional competence development of educators at engineering colleges is also proposed in this part. Finally, it discusses motivation principles of self-management in the professional training of engineers to form creative competencies.

We appreciate the partnership with Springer Nature, iThenticate, EasyChair, International Innovation Foundation, and our sponsors for their essential support during the preparation of DSMIE-2024.

Thank you very much to the DSMIE Team. Their outstanding involvement and hard work were crucial to the success of the conference.

DSMIE's motto is *"Together we can do more for science, technology, engineering, and education"*.

June 2024

Vitalii Ivanov
Justyna Trojanowska
Ivan Pavlenko
Erwin Rauch
Ján Pitel'

Organization

Steering Committee

General Chair

Vitalii Ivanov	Sumy State University, Ukraine

Co-chair

Milan Edl	University of West Bohemia, Czech Republic

Co-chairs, Program Committee Chairs

Oleksandr Liaposhchenko	Sumy State University, Ukraine
Vladimir Duchek	University of West Bohemia, Czech Republic

Co-chairs, Publication Chairs

Ivan Pavlenko	Sumy State University, Ukraine
Justyna Trojanowska	Poznan University of Technology, Poland

Co-chairs, Organizational Chairs

Oleksandr Gusak	Sumy State University, Ukraine
Khrystyna Berladir	Sumy State University, Ukraine
Jan Zdebor	University of West Bohemia, Czech Republic

Program Committee

Katarzyna Antosz	Rzeszov University of Technology, Poland
Liliana-Laura Badita-Voicu	National Institute of Research and Development in Mechatronics and Measurement Technique, Romania
Yevheniia Basova	National Technical University “Kharkiv Polytechnic Institute”, Ukraine
Andre Batako	Liverpool John Moores University, UK

Khrystyna Berladir	Sumy State University, Ukraine
Ricardo Branco	University of Coimbra, Portugal
Anna Burduk	Wroclaw University of Technology, Poland
Suthep Butdee	King Mongkut's University of Technology, Thailand
Emilia Campean	Technical University of Cluj-Napoca, Romania
Vasile G. Cioata	Polytechnic University of Timisoara, Romania
Olaf Ciszak	Poznan University of Technology, Poland
Radu Cotetiu	Technical University of Cluj-Napoca, Romania
Ivan Cvitic	University of Zagreb, Croatia
Predrag Dasic	High Technical Mechanical School of Professional Studies Trstenik, Serbia
Ivan Dehtiarov	Sumy State University, Ukraine
Yuliia Denysenko	Sumy State University, Ukraine
Oleksandr Derevianchenko	Odessa Polytechnic National University, Ukraine
Sergey Dobrotvorskiy	National Technical University "Kharkiv Polytechnic Institute", Ukraine
Tygran Dzuguryan	Maritime University of Szczecin, Poland
Milan Edl	University of West Bohemia, Czech Republic
Mathieu Gautier	University Lyon, France
Renata Gnatowska	Czestochowa University of Technology, Poland
Arkadiusz Gola	Lublin University of Technology, Poland
Marek Gucwa	Czestochowa University of Technology, Poland
Volodymyr Gurey	Lviv Polytechnic National University, Ukraine
Bohdan Haidabrus	Riga Technical University, Latvia
Oksana Haponova	Sumy State University, Ukraine
Alexander Hosovsky	Technical University of Kosice, Slovak Republic
Ihor Hurey	Lviv Polytechnic National University, Ukraine
Angelina Iakovets	Technical University of Kosice, Slovak Republic
Vitalii Ivanov	Sumy State University, Ukraine
Maryna Ivanova	National Technical University "Kharkiv Polytechnic Institute", Ukraine
Jerzy Jedrzejewski	Wroclaw University of Technology, Poland
Lydmila Kalafatova	Donetsk National Technical University, Ukraine
Isak Karabegovic	University of Bihac, Bosnia and Herzegovina
Nadiia Kharchenko	Sumy State University, Ukraine
Gennadii Khavin	National Technical University "Kharkiv Polytechnic Institute", Ukraine
Serhii Khovanskyi	Sumy State University, Ukraine
Imre Kiss	Polytechnic University of Timisoara, Romania
Tibor Krenicky	Technical University of Kosice, Slovak Republic
Agnieszka Kujawinska	Poznan University of Technology, Poland

Monika Kulisz	Lublin University of Technology, Poland
Yaroslav Kusyi	Lviv Polytechnic National University, Ukraine
Maria Lazar	University of Petrosani, Romania
Dmytro Levchenko	Lodz University of Technology, Poland
Oleksandr Liaposhchenko	Sumy State University, Ukraine
Jose Mendes Machado	University of Minho, Portugal
Ole Madsen	Aalborg University, Denmark
Angelos Markopoulos	National Technical University of Athens, Greece
Ievgen Medvediev	Gdansk University of Technology, Poland
Mykola Melnychuk	Lutsk National Technical University, Ukraine
Anthony Xavior Michael	Vellore Institute of Technology, India
Jakub Montewka	Gdansk University of Technology, Poland
Roland Iosif Moraru	University of Petrosani, Romania
Dmitriy Muzylyov	State Biotechnological University, Ukraine
Arun Nagarajah	University of Duisburg-Essen, Germany
Marek Ochowiak	Poznan University of Technology, Poland
Oleh Onysko	Ivano-Frankivsk National Technical University of Oil and Gas, Ukraine
Ruslan Ostroha	Sumy State University, Ukraine
Anatolii Panchenko	Dmytro Motornyi Tavria State Agrotechnological University, Ukraine
Ivan Pavlenko	Sumy State University, Ukraine
Florin Popister	Technical University of Cluj-Napoca, Romania
Oleksandr Povstyanoy	Lutsk National Technical University, Ukraine
Erwin Rauch	Free University of Bolzano, Italy
Paulina Rewers	Poznan University of Technology, Poland
Andrii Rogovyi	National Technical University “Kharkiv Polytechnic Institute”, Ukraine
Joanna Rosak-Szyrocka	Czestochowa University of Technology, Poland
Serhii Sharapov	Sumy State University, Ukraine
Lesya Shkitsa	Ivano-Frankivsk National Technical University of Oil and Gas, Ukraine
Natalya Shramenko	Lviv Polytechnic National University, Ukraine
Robert Sika	Poznan University of Technology, Poland
Francisco J.G. Silva	Polytechnic of Porto, Portugal
Dusan Simsik	Technical University of Kosice, Slovak Republic
Maksym Skydanenko	Sumy State University, Ukraine
Vadym Stupnytskyy	Lviv Polytechnic National University, Ukraine
Anastasiia Symonova	Kremenchuk Mykhailo Ostrohradskyi National University, Ukraine
Antoni Swic	Lublin University of Technology, Poland
Marek Szostak	Poznan University of Technology, Poland

Yuliia Tarasevych	AGH University of Science and Technology, Poland
Amila Thibbotuwawa	University of Moratuwa, Sri Lanka
Anatolii Tkachuk	Lutsk National Technical University, Ukraine
Valentyna Tkachuk	Lutsk National Technical University, Ukraine
Volodymyr Tonkonogyi	Odessa Polytechnic National University, Ukraine
Justyna Trojanowska	Poznan University of Technology, Poland
Piotr Trojanowski	West Pomeranian University of Technology, Poland
Nicolae Ungureanu	Technical University of Cluj-Napoca, Romania
Alper Uysal	Yildiz Technical University, Turkey
George-Christopher Vosniakos	National Technical University of Athens, Greece
Jerzy Winczek	Czestochowa University of Technology, Poland
Jinyang Xu	Shanghai Jiao Tong University, China
Oleg Zabolotnyi	Lutsk National Technical University, Ukraine
Sahin Yildirim	Erciyes University, Turkey
Volodymyr Zavialov	National University of Food Technologies, Ukraine
Przemyslaw Zawadzki	Poznan University of Technology, Poland
Dmytro Zhyhilii	Sumy State University, Ukraine
Justyna Zywiolek	Czestochowa University of Technology, Poland
Predrag Zivkovic	University of Nis, Serbia

Invited External Reviewers

Adrian Dornbach	University of Duisburg-Essen, Germany
Andriy Dzyubuk	Lviv Polytechnic National University, Ukraine
Lyudmyla Dzyubuk	Lviv Polytechnic National University, Ukraine
Madushan Fernando	University of Moratuwa, Sri Lanka
Madushan Jayalath	University of Moratuwa, Sri Lanka
Nikolaos Karkalos	National Technical University of Athens, Greece
Vladyslav Kondus	Sumy State University, Ukraine
Olha Kostiuk	Lviv Polytechnic National University, Ukraine
Sergii Kotliar	National Technical University of Ukraine “KPI named after I. Sikorskyi”, Ukraine
Emmanouil Lazaros Papazoglou	National Technical University of Athens, Greece
Sebastian Sonntag	University of Duisburg-Essen, Germany
Volodymyr Topilnytskyy	Lviv Polytechnic National University, Ukraine
Ihor Yakovenko	National Technical University “Kharkiv Polytechnic Institute”, Ukraine

DSMIE Team

Vladyslav Andrusyshyn	Sumy State University, Ukraine
Khrystyna Berladir	Sumy State University, Ukraine
Yuliia Denysenko	Sumy State University, Ukraine
Vladimir Duchek	University of West Bohemia, Czech Republic
Milan Edl	University of West Bohemia, Czech Republic
Oleksandr Gusak	Sumy State University, Ukraine
Vitalii Ivanov	Sumy State University, Ukraine
Eva Kozakova-Krauzova	University of West Bohemia, Czech Republic
Oleksandr Liaposhchenko	Sumy State University, Ukraine
Martin Melichar	University of West Bohemia, Czech Republic
Ivan Pavlenko	Sumy State University, Ukraine
Marketa Pribylova	University of West Bohemia, Czech Republic
Oleksandr Sokolov	Sumy State University, Ukraine
Justyna Trojanowska	Poznan University of Technology, Poland
Jan Zdebor	University of West Bohemia, Czech Republic

Contents

Smart and Sustainable Manufacturing

Cyber-Physical Production System Design Decomposition for Internal Disruption Avoidance 3
Tanel Aruväli, Matteo De Marchi, Erwin Rauch, and Dominik T. Matt

Implementation of the Technological Capabilities of the Testbed 4.0 Laboratory in Cooperation with Simulation 15
Marek Kliment, Peter Trebuňa, Matúš Matiscák, and Ján Kopec

Studies on Streamlining Processes Using Industry 4.0 Elements 28
Jan Kopec, Miriam Pekarcikova, Marek Kliment, and Marek Mizerak

Material Removal Rate Determination Based on a Laser Displacement Sensor 39
Natalia Lishchenko, Garret O'Donnell, Vasily Larshin, and Igor Dudarev

Advancing Circular Economy: The Product Circularity Index as a Tool for Sustainable Design 51
Foivos Psarommatis, Fotios K. Konstantinidis, Victor Azamfirei, and Gökan May

Simulation-Driven Evaluation of Reward Systems for Activity-Based Manufacturing Environments 63
Unais Sait, Marco Frego, Antonella De Angeli, and Angelika Peer

Creation of a Localization Project in RTLS Studio for the Need of an Industrial Data Collection Application 75
Peter Trebuňa, Marek Mizerák, Miriam Pekarčíková, and Jozef Trojan

Information Management Systems

Directions of IT Systems Development in Warehouses Management: Polish Practitioners Viewpoint 89
Ludmiła Filina-Dawidowicz, Piotr Trojanowski, Piotr Mrowiński, and Anastasiya Troynina

Generative AI in Agile, Project, and Delivery Management 100
Bohdan Haidabrus

Management of Information Resources at Industrial Companies 111
Dmytro Gorovyi, Yevheniia Basova, Olena Lynnyk, Ivan Pavlenko, and Justyna Trojanowska

Deployment and Release Management Process in Agile Digital Projects 124
Janis Grabis, Bohdan Haidabrus, Evgeniy Druzhinin, and Kateryna Kolesnikova

Manufacturing Technologies

An Increase in the Vibration Resistance of Finishing and Boring Machines when Cutting Ends Using the Plunge-In Method 139
Olexandr Badovskyi, Anna Balaniuk, Gennadii Oborskyi, Alexandr Orgiyan, and Milan Edl

Use of the Processing Arrays Theory of Experimental Data for the Analysis of the Technological Scheme in the Rolled Metal Production – Controlled Rolling 152
Oleksandr Beketov, Dmytro Laukhin, Nataliia Rott, Eugene Babenko, and Valentyn Kozechko

Research of Static Stiffness of Flexible Fixtures for Y-Type Fork Parts 164
Ivan Dehtiarov, Vitalii Ivanov, Artem Evtuhov, Ruslan Ostroha, and Olaf Ciszak

Surface Hardness Improvement of AISI D2 Tool Steel by Laser Transformation Hardening Process Using High-Power Disk Laser 178
Vitaliy Dzhemelinskyi, Matej Hruska, Bohdan Mordyuk, Daniel Grochala, and Dmytro Lesyk

Ensuring Tool Run-In When Milling AISI321 Steel in Various Technological Environments 188
Eshreb Dzhemilov, Alper Uysal, Orhan Çakir, Ruslan Dzhemalyadinov, and Eldar Vaniev

Empirical Data-Based Failure Rate Assessment Methodology for Metal-Cutting Tools 200
Mykhaylo Frolov, Volodymyr Tsyganov, and Vasyl Solokha

Spindle Vibration Prediction for the CNC Machining Center Using ANFIS System 212
Pichai Janmanee and Suthep Butdee

Adaptive Fluid Jet Support Technique for Variable Stiffness Thin-Walled Parts End Milling 223
Serhii Kononenko, Sergey Dobrotvorskiy, Yevheniia Basova, Oleksandr Kharchenko, and Dmytro Trubin

The Influence of Cutting Forces on Cracks Formation During the Grinding of Products from Materials Prone to Defect Formation 240
Maksym Kunitsyn, Anatoly Usov, and Yuriy Zaychyk

Stiffness of Underpinning Supports for Fixtures 251
Pavlo Kushnirov, Yuliia Denysenko, Grigore Pop, Bohdan Basov, and Oksana Dynnyk

Design of the Technological Route for Sustainable Machining of Functional Surfaces for Automotive Engineering Parts 263
Yaroslav Kusyi, Nazarii Kusen, Andrii Slipchuk, Iryna Schuliar, and Lolita Pituley

Surface Morphology and Microstructural Features of LPBF-Printed Superalloy Turbine Blade Subjected to HIP, Heat Treatment, and Shot Peening 276
Dmytro Lesyk, Silvia Martinez, Bohdan Mordyuk, Vitaliy Dzhemelinskyi, and Aitzol Lamikiz

Study of Power Parameters of the Screw Spirals Forming 287
Oleg Lyashuk, Roman Rogatynskyi, Ivan Hevko, Tetiana Navrotska, and Andrii Diachun

The Influence of the Geometry of High-Performance Cutters on the Profile Accuracy of Large-Pitch Tapered Threads: Theoretical Study 299
Iuliia Medvid, Oleh Onysko, Lolita Pituley, Zinovii Odosii, and Olena Kornuta

Theoretical Justification for Increasing Efficiency of Grinding Technological Processes Based on the Reduction of Cutting Temperature 309
Fedir Novikov, Andrii Hutorov, Oleksii Yermolenko, Oksana Yermolenko, and Andrii Ivashura

Wear Behaviour and Machining Performance in Milling of INCONEL® 718 of TiAlVN and TiAlN/TiAlVN Coated Tools: A Comparative Study 319
Naiara Sebbe, Filipe Fernandes, Rúben Costa, Rita Sales-Contini, and André Pedroso

Evaluation of Cutting Fluid Penetration into the Cutting Zone During Grinding of Rolling Rolls 331
Mykhaylo Stepanov, Leonid Polonsky, Volodymyr Korniienko, Tetyana Tretyak, and Maryna Ivanova

Enhancing Service Life and Durability of Machine Parts Through Surface Plastic Deformation 341
Anastasiia Symonova, Volodymyr Drahobetskyi, and Viktoriia Kulynych

Statistical Comparison of Manual and Automatic Sampling at Enterprises 352
Jozef Trojan and Milan Fil'o

Quality Assurance

Improvement of the Assembly Technology Quality by Determining the Closing Link Size Under Thermal Stress 365
Hanna Hrinchenko, Roman Trishch, Viktoriia Kniazieva, and Nataliia Antonenko

Integration of Statistical Analysis and Machine Learning Techniques for Enhanced Quality Control in Candle Oil Cartridge Manufacturing 376
Monika Kulisz, Katarzyna Antosz, and Edward Kozłowski

An Analysis of Machined Surface Quality Using TiAlTaN-Coated Tools in AMPCO® Milling Operations 388
Francisca Nogueira, André Pedroso, Francisco Silva, Raul Campilho, and Rita Sales-Contini

Metrological Support of the Thermal Vision Method of Defectoscopy 399
Volodymyr Tonkonogyi, Maryna Holofieieva, Alexandr Orgiyan, Yurii Holofieiev, and Oleksii Buriachenko

Virtual Device for Assessing the Geometric Parameters' Reliability Control for Mechanical Products Depending on the Tool Accuracy 409
Oleksandr Voichyshen, Serhii Patsera, Vitalii Derbaba, and Oleksandr Bohdanov

Supply Chain and Transportation

Real-Time Driver Drowsiness Detection Using Transfer Learning 425
P. M. Fernando, Ranil Sugathadasa, M. Mavin De Silva, Amila Thibbotuwawa, and T. Sivakumar

Risk Assessment at Unsignalized Intersections Based on Human-Road-Environment-Vehicle System Applying Fuzzy Logic 437
Ievgen Medvediev, Dmitriy Muzylyov, Vitalii Ivanov, Jakub Montewka, and Justyna Trojanowska

Green Logistics System: Cargo Bikes as an Alternative to Light Trucks 449
Natalya Shramenko, Christoph Hupfer, Vladyslav Shramenko, and Piotr Trojanowski

Assessing External Supply Risk: Perspectives from a Low Middle-Income Country 462
Praveena Somaweera, Dilina Kosgoda, and H. Niles Perera

Optimizing the Process of Obtaining and Maintaining Rainforest Alliance Certification in the Sri Lankan Supply Chain 475
Kavitha Wickramaarachchi, W. Madushan Fernando, Amila Thibbotuwawa, H. Niles Perera, and Peter Nielsen

Engineering Education

Designing the Educational Content for the Industry 4.0 Competency Model 489
Peter Arras and Galyna Tabunshchyk

Implementation of the Methodical System for the Development and Application of Eco-Oriented Pedagogical Technologies 498
Andrii Kalenskyi, Tetiana Gerliand, Oksana Lapa, Tetyana Pyatnichuk, and Olha Haiduk

The Model for Professional Competence Development of Engineering Teachers at Colleges 509
Petro Luzan, Olena Titova, Iryna Mosia, Tetiana Pashchenko, and Gulshan Navruzova

Motivation Principles of Self-management in the Professional Training of Engineers Under the Conditions of Forming the Creative Competence 521
Viktor Nagayev, Yuliia Sahachko, Galyna Nagayeva, Sergii Chervonyi, and Yevhenii Beznos

Author Index 531

Smart and Sustainable Manufacturing

Cyber-Physical Production System Design Decomposition for Internal Disruption Avoidance

Tanel Aruväli[1], Matteo De Marchi[1], Erwin Rauch[1](✉), and Dominik T. Matt[1,2]

[1] Industrial Engineering and Automation (IEA), Free University of Bozen-Bolzano, 1, Piazza Università, 39100 Bolzano, Italy
erwin.rauch@unibz.it

[2] Innovation Engineering Center, Fraunhofer Research Italia, 13 A, Via A. Volta, 39100 Bolzano, Italy

Abstract. A growing number of manufacturing companies are undergoing digital transformation and moving towards Cyber-Physical Production Systems (CPPS). To ensure the long-term resilience of CPPS by avoiding internal disruptions, the starting point is the proper design of a functional digital shadow. Therefore, the goal was to provide decomposed design guidelines for the digital shadow implementation. The Axiomatic Design (AD) method was applied to discard systems-based categorization and decompose design parameters from functional requirements, which guided a novel approach covering digital shadow design guidelines. Through the zigzagging process, we elaborated collectively exhaustive and mutually exclusive conceptual design parameters. The received results were applied to a cyber-physical demonstrator. The practical value of the received design parameters guided towards alternative digital solutions, and based on AD axioms, the selection of digital solutions was implemented on the demonstrator. Such an approach enabled us to cover the full concerned functionality while avoiding decoupling and overlapping in implemented solutions.

Keywords: Digital Shadow · Axiomatic Design · Resilience · Industrial Growth

1 Introduction

The last four years of multiple external disruptions have led a growing number of manufacturing companies to adopt digital technologies to their processes [1] and deploy principles of Cyber-Physical Production Systems (CPPS). Many of these companies have seen the possibility of maintaining competitiveness and increasing resilience against disruptions in this step. Disruption management starts from the internal processes to ensure the quality of manufacturing processes. Digital Twin (DT), as an enabler for real-time optimization of the processes [2], only adds value when its input data is reliable. This requires real-time knowledge about physical phenomena taking place on the shop floor. Thus, the design of digital shadow influences the efficiency of higher-level manufacturing control. It stands for mirroring the physical changes in a digital space and the reliable representation of the acquired data.

© The Author(s), under exclusive license to Springer Nature Switzerland AG 2024
V. Ivanov et al. (Eds.): DSMIE 2024, LNME, pp. 3–14, 2024.
https://doi.org/10.1007/978-3-031-61797-3_1

The paper aims to provide decomposed design guidelines for the digital mirroring of physical manufacturing through the realization of digital shadow to decrease the occurrence of internal disruptions in cyber-physical shop floors. The research aims to decompose design guidelines for CPPS. More specifically, the Axiomatic Design (AD) method is deployed to the design of a DT for daily manufacturing, focused on achieving reliable digital shadow. The study is limited to the functions of digital shadow to minimize the number of internal disruptions. It does not involve post-disruption management actions of a DT to adapt to disruptions and recover performance.

2 Literature Review

Napoleone et al. [3] divided CPS characteristics into five groups relating to the data: integration, intelligence/smartness, cooperation/collaboration, reconfigurability/adaptability, and predictability. The initial parameter in designing a successful CPS system is accurate and reliable data from the shop floor [4]. This is achieved through a 3-layer architecture: perception, transmission, and application [5]. Having static data about manufacturing parameters enables the creation of a digital model. A digital shadow is created when this data is dynamic, meaning constant near real-time updates from a physical shop floor. The digital shadow does not require the representation of real-time digitally animated movements. The basics of the digital shadow are having the data at a sufficient level of actuality to make knowledge-based decisions. The next level is the DT [6], which enables bidirectional secured communication [7] between cyber and physical space [8, 9]. None of the outputs can have a higher accuracy than the input. Therefore, managing data structures and their communication is essential for applying a structured method of digitalizing manufacturing systems [10]- DT.

Before the introduction of CPPS, Manufacturing System Design Decomposition (MSDD) for various competitive environments using AD and lean approach was applied to manufacturing systems by Cochran et al. [11]. The branch managing disruptions is called “Deliver products on time, “one of the quality production characteristics. The branch lower-level functional requirements (FRs) manage DPs for disruption minimization, identification, and rapid resolution. Later, Cochran et al. [12] expanded the problem with a sustainability dimension and applied a Collective System Design to ensure takt times and efficiency of the manufacturing systems. Lately, Cochran et al. [13] introduced an elaborated version of MSDD called MSDD 10.0, where the study is focused on Industry 4.0 manufacturing processes. Vickery et al. [14] applied the AD method to decompose smart data analytics for small and medium enterprises. They devised an FR, “use available real-time data for prediction needs,” and its following level FR, “gather real-time data from production”. They also highlighted the need for connectivity and data visualization. Aruväli et al. [15] started the decomposition of resilient CPPS by dividing the required functions into two main branches according to a resilience metric Penalty of Change (POC) previously selected as the most practically usable resilience metric for manufacturing companies.

The reviewed AD studies approached the disruption minimization from different digitalization levels. They focused on the internal processes and solutions to improve the quality of the production process and related data. Nevertheless, a solution-neutral

approach for detecting design parameters specifically for digital shadow has yet to be carried out. This is a research gap that needs a further structured approach.

3 Research Methodology

AD, as the primary method, was used for deriving the most inevitable DPs of CPPS to reduce occurrences of internal disruptions. AD is a system engineering methodology that uses matrix methods to analyze the translation of customer systematically needs into FRs and DPs. This methodology is suitable for the design of products, processes, projects, and systems. Suh's axioms [16]: (i) maintain the independence of the FRs and (ii) minimize the information content – were followed in the decoupling and decomposing process. The main characteristics and functions of CPPS were considered to increase the level of resilience in the assurance of quality manufacturing processes. The approach was not subsystems-based but rather functions-based to increase solution neutrality. For instance, a monitoring system was not considered as a DP. Instead, sub-functions and sub-components of the monitoring system were distributed all over the decomposition where needed. The resilience metric POC defined the first-level requirements and thus derivated the two main branches. Through zigzagging, the FRs, with their functional requirement metrics, were decoupled, and related DPs were found. Coupled design was avoided and checked through the design matrices.

3.1 Resilient Manufacturing System Main Branches

The decomposition of resilient CPPS in [15] was considered the starting point for quality manufacturing process decomposition. According to this approach, the resilient manufacturing system has two DPs: avoidance of disruptions occurrence and preparedness for changes caused by disruptions. These parameters were achieved from the resilience metric POC [17] by translating the metric components into FRs. In the second level, the FRs of both branches were divided between external and internal disruptions. In the lower levels, we focused on branch 1.2 with FR "Minimize the occurrence of internal disruptions", functional requirement metric "No of internal disruptions", and DP "Quality manufacturing process".

3.2 Minimize the Occurrence of Internal Disruptions

The decomposition of quality manufacturing was modified compared to [15]. The current approach (Fig. 1) considers CPPS's main characteristics: physical and cyber (digital) manufacturing. This ensures the focus on CPPS needs and strengthens the design. Thus, the quality manufacturing of CPPS is a combination of physical manufacturing processes, digital information, and communication between physical and digital domains to merge them into a seamlessly functioning flexible system.

Quality Manufacturing Process. A design parameter in standardized physical manufacturing processes (DP1.2.1) stands for the efficiency of manufacturing processes

while ensuring safety in workplaces. Efficiency functions are related to Overall Equipment Effectiveness (OEE), which has three main components: availability, performance, and quality. These components, together with safety, are translated into FRs.

While supporting manufacturing with digital information, analytics, and control, the accuracy of the information must be guaranteed. Therefore, the DT of daily manufacturing is proposed as the DP1.2.2. It is crucial to differentiate between daily manufacturing, which must ensure the avoidance of disruptions, and adaptation measures after the occurrence of any disruption. While the DT of daily manufacturing is represented in the branch, which stands for the avoidance of disruptions occurrence (the currently analyzed branch), the DT resolving of disruption consequences is related to the other main branch that minimizes the cost of changes caused by disruptions.

A digital communication infrastructure is needed to provide communication between physical manufacturing, digital space, and humans (DP1.2.3). As in the current branch, the physical manufacturing is mirrored in a digital space, and communication is built according to the needs of the physical and digital spaces, and decoupled design is achieved at the third level (Eq. 1).

$$\begin{Bmatrix} FR1.2.1 \\ FR1.2.2 \\ FR1.2.3 \end{Bmatrix} = \begin{vmatrix} X & 0 & 0 \\ X & X & 0 \\ X & X & X \end{vmatrix} \begin{Bmatrix} DP1.2.1 \\ DP1.2.2 \\ DP1.2.3 \end{Bmatrix} \tag{1}$$

DT of Daily Manufacturing. The DT of daily manufacturing is foreseen to coordinate the daily manufacturing and ensure a seamless production flow in a disruption-free environment. Therefore, it consists of a manufacturing controlling unit (DP1.2.2.1). Digital shadow (DP1.2.2.2) stands for mirroring physical phenomena taking place on the physical shop floor. Strategies comparison and evaluation system (DP1.2.2.3) takes into consideration the mirrored data from the physical shop floor and information systems to simulate and analyze for optimization purposes. Optimization vectors may consider performance, delivery times, throughput, energy usage, customer satisfaction, etc. Such a system can comprise machine learning and artificial intelligence as input for decision-making. The production planning system (DP1.2.2.4) stands for implementing the chosen strategy. As the manufacturing controlling unit coordinates the manufacturing and the DT, it is a prerequisite for other same-level DPs. Information on the digital shadow is needed to select the proper manufacturing strategy and for subsequent planning and scheduling. Therefore, the DPs are decoupled (Eq. 2).

$$\begin{Bmatrix} FR1.2.2.1 \\ FR1.2.2.2 \\ FR1.2.2.3 \\ FR1.2.2.4 \end{Bmatrix} = \begin{vmatrix} X & 0 & 0 & 0 \\ X & X & 0 & 0 \\ X & X & X & 0 \\ X & X & X & X \end{vmatrix} \begin{Bmatrix} DP1.2.2.1 \\ DP1.2.2.2 \\ DP1.2.2.3 \\ DP1.2.2.4 \end{Bmatrix} \tag{2}$$

Digital Communication Infrastructure. Communication occurs between various entities on a shop floor and supporting digital systems. Various digital management systems have gained popularity recently (Enterprise Resource Planning (ERP), Product Lifecycle Management, Warehouse Management System, Customer Relationships Management, etc.). This has led to the data being partially duplicated between different

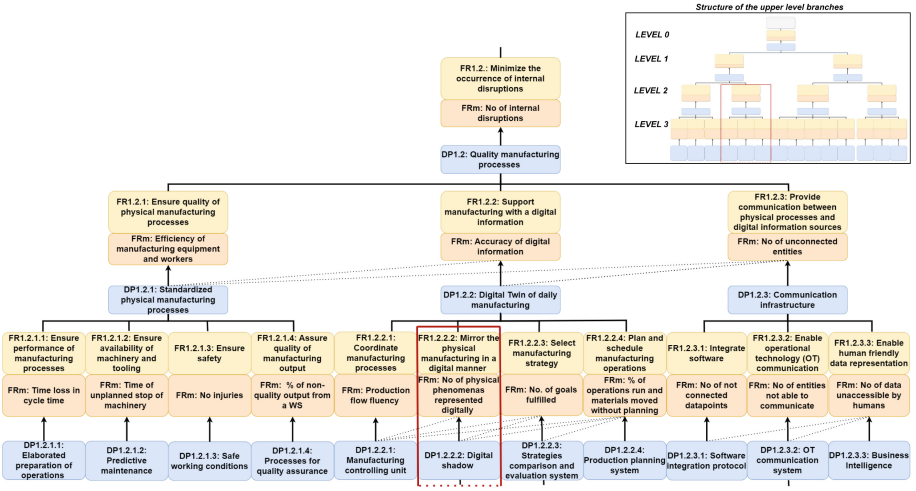

Fig. 1. Main branches of the design decomposition of quality manufacturing processes.

software. Although implementing central management systems has lowered the number of separate locally stored documents (mainly spreadsheets), data still needs to be corrected. If earlier duplication often existed between workers in the same department, then management systems have eliminated that duplication level. Hence, without integrating different digital systems, duplication exists mainly between different (sub)departments, continuously creating data misalignments. To overcome this challenge, a single source of truth must exist at the data level. This requires connecting the existing data points.

3.3 Digital Shadow Decomposition

Digital shadow mirrors the physical world in the best possible manner. For this reason, it must track the status of manufacturing and, at the same time, ensure the quality of data (Fig. 2). The DPs are uncoupled (Eq. 3).

$$\begin{Bmatrix} FR1.2.2.2.1 \\ FR1.2.2.2.2 \end{Bmatrix} = \begin{vmatrix} X & 0 \\ 0 & X \end{vmatrix} \begin{Bmatrix} DP1.2.2.2.1 \\ DP1.2.2.2.2 \end{Bmatrix} \tag{3}$$

For data reliability, each data type must have one single source (DP1.2.2.2.1). The data can be divided into operational data that tracks traditional manufacturing-related parameters such as the movement of parts, machines and operators' status, production orders, and big data for predictive decisions. ERP (DP1.2.2.2.1.1) is a type of software that stores and makes connections between different departments in a single system. It comprises modules for sales, manufacturing, warehouse, quality management, logistics, and bookkeeping. Relational database (1.2.2.2.1.2), on the other hand, is a good option for larger datasets. High-frequency sensor measurements cannot be recorded in ERP; therefore, an additional structured database is needed. After data management in the

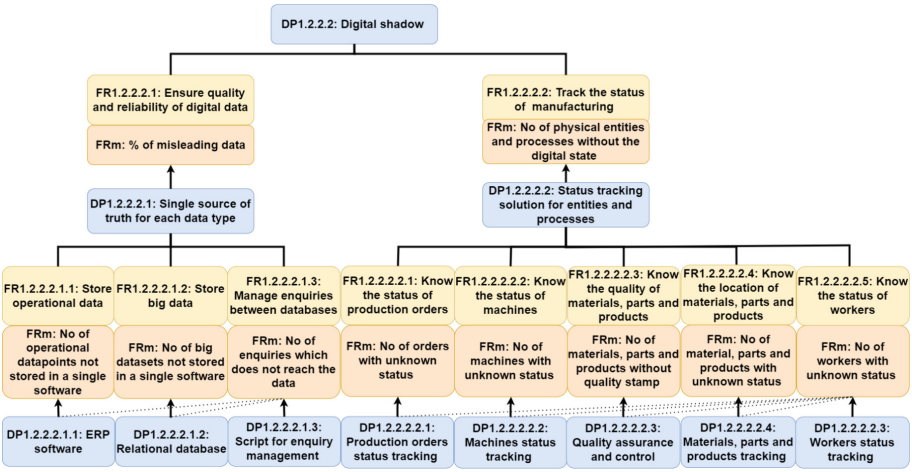

Fig. 2. Decomposition of the digital shadow.

storage systems, a script for inquiry management leads inquiries to a specific single data source (Eq. 4).

$$\begin{Bmatrix} FR1.2.2.2.1.1 \\ FR1.2.2.2.1.2 \\ FR1.2.2.2.1.3 \end{Bmatrix} = \begin{vmatrix} X & 0 & 0 \\ 0 & X & 0 \\ X & X & X \end{vmatrix} \begin{Bmatrix} DP1.2.2.2.1.1 \\ DP1.2.2.2.1.2 \\ DP1.2.2.2.1.3 \end{Bmatrix} \tag{4}$$

However, the central function of digital shadow is tracking manufacturing status, which comprises entities and processes. Therefore, the status tracking solution for entities and processes (DP1.2.2.2.2) plays the central role in data acquisition. The most crucial daily manufacturing operative information is achieved through manufacturing orders output tracking (DP1.2.2.2.2.1), machines status tracking (DP1.2.2.2.2.2), quality assurance and control (DP1.2.2.2.2.3), materials, parts and components tracking (DP1.2.2.2.2.4), and indirect operators status tracking (DP1.2.2.2.2.5). The tracking systems are partly uncoupled as operators' status tracking should be deployed indirectly using the data of other tracking systems to lower the stress level of operators (Eq. 5).

$$\begin{Bmatrix} FR1.2.2.2.2.1 \\ FR1.2.2.2.2.2 \\ FR1.2.2.2.2.3 \\ FR1.2.2.2.2.4 \\ FR1.2.2.2.2.5 \end{Bmatrix} = \begin{vmatrix} X & 0 & 0\,0\,0 \\ 0 & X & 0\,0\,0 \\ 0 & 0 & X\,0\,0 \\ 0 & 0 & 0\,X\,0 \\ X & X & X\,X\,X \end{vmatrix} \begin{Bmatrix} DP1.2.2.2.2.1 \\ DP1.2.2.2.2.2 \\ DP1.2.2.2.2.3 \\ DP1.2.2.2.2.4 \\ DP1.2.2.2.2.5 \end{Bmatrix} \tag{5}$$

4 Results and Discussion

AD-based decomposition of FRs for resilient CPPS led to the specification of conceptual DPs to avoid internal disruptions. The results were implemented in a cyber-physical flexible manufacturing cell demonstrator.

4.1 Results

DPs for internal disruption avoidance in CPPS were identified. More deeply, the analysis was applied to receive the DPs of digital shadow, which is a prerequisite for the DT of daily manufacturing. Additionally, related digital communication means were studied sufficiently to deploy the communication measures. The following DPs for digital shadow were detected: ERP software, relational database, a script for inquiry management, production orders output tracking, machine status tracking, quality assurance and control, materials, parts, and products tracking, and workers status tracking. The following DPs were identified for communication infrastructure: software integration protocol, operational technology communication system, and business intelligence.

4.2 Results Implementation and Discussion in a Use Case: CPPS Demonstrator Design for Minimizing Internal Disruptions

Based on the results, minimizing internal disruptions in a resilient CPPS was applied to a didactic demonstrator. The digital solutions were found based on the conceptual DPs (Table 1). This cyber-physical demonstrator was built in the learning factory 'Smart Mini Factory' at the Free University of Bozen-Bolzano.

Table 1. Digital solutions for minimizing the occurrence of internal disruptions.

Branch of DPs	Conceptual DPs	Digital solutions
Digital shadow (data structures)	ERP	Microsoft Business Central
	Relational DB	PostgreSQL
	Script for inquiry management	Python
Digital shadow (status tracking)	Production orders status tracking	Automatic reporting through IoT weighing scales system
	Machines status tracking	Event logs
	Quality assurance and control	Quality control station
	Materials, parts, and products tracking	ERP extensions (optional)
	Workers' status tracking	Mix of the tracking information
Communication infrastructure	Software integration protocol	Rest API
	OT communication system	MQTT (+ middleware)
	Business intelligence	Grafana

The flexible manufacturing cell demonstrator consists of the following machinery (Fig. 3): a Montrac transfer line with three shuttles for cell-wide transportation; a Universal Robot UR10 collaborative robotic arm for loading components and products between the warehouse and the shuttles; a Universal Robot UR5 collaborative robotic arm for loading components and products between the shuttles and a manual workstation; a 3D-printer/laser work center; a manual workstation with a cognitive assistance

system; quality control station; and a warehouse rack. The manufacturing cell is used to manufacture mechanical components for USB flash drives and assemble the product. The components are moved on blisters (specific bins for storing up to six different components). Each shuttle can carry three blisters at a time.

It needs to be noted that CPPS does not mean full automation and the exclusion of operators. Resilient CPPS must find the best ratio between automation's efficiency and human flexibility [18]. Therefore, the system accommodates the workplace for a human operator. The worker is possibly instructed by a cognitive assistance system integrated into the workstation and can provide step-by-step work tasks.

Digital Shadow Data Structures. Digital shadow data structures must provide a single source of truth. Otherwise, the system's liability suffers. Two different data storage software are used because the data collected from a shop floor may have different data structures.

An implemented ERP system, Microsoft Business Central (BC), covers operational manufacturing data that contains information regarding production scheduling, work centers, products, raw materials, components, production calendars, bill of materials, etc. It covers and links data of other departments. An alternative ERP system Monitor was considered for implementation. Although the Monitor is suitable for smaller enterprises and partly covers the functions of the Manufacturing Execution System (MES), the BC was selected. This ERP is mainly used in mid-size companies. Still, considering the cost and close-by dedicated technical support needed for specific extensions, the selection favored BC. In addition, BC can be integrated easily with Advanced Planning and Scheduling (APS) software Etagis, which is used for production scheduling and is comparable with MES functionality.

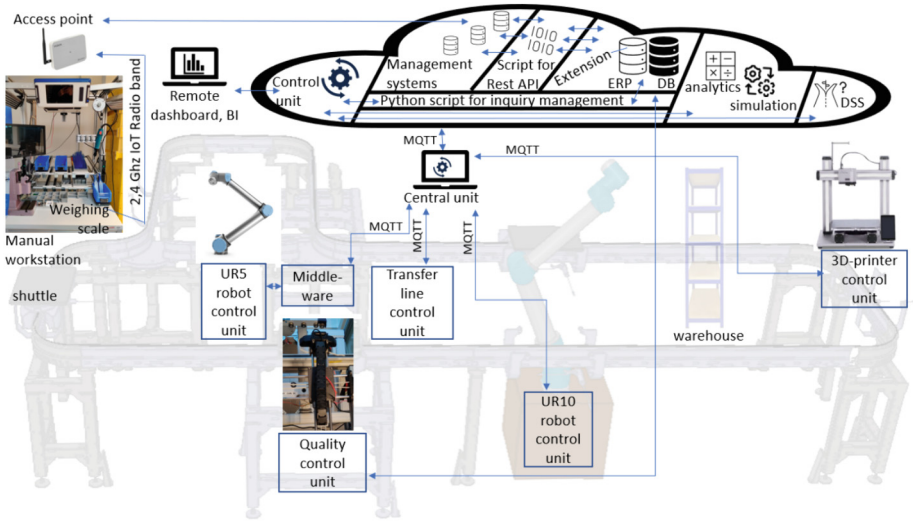

Fig. 3. Digital design solutions in the cyber-physical demonstrator. DB – database, ERP – enterprise resource planning, DSS – decision support system, UR – Universal Robot, API – application programming interface, IoT – Internet of Things.

The relational database covers data structures that are unsuitable or unreasonable for the ERP. The relational database PostgreSQL is deployed to store quality assurance-related data. The quality control unit can directly access the database to compare inspection camera data with previously trained data structures. Python script is adapted to manage the principle of a single source of truth and directs the inquiries to the related data source: BC ERP or PostgreSQL DB. My SQL DB was considered as an alternative. PostgreSQL was chosen because it performs complex queries faster and does not have that tight space constraints compared to My SQL.

Having one single data source, such as a relational database, would eliminate the need for the extra inquiry management layer, but the consequence was losing the links in standardized manufacturing information and scheduling, as well as the links to other departments' data. ERP functions could be theoretically replicated to a single DB in a perfect scenario. Nevertheless, this choice is unfavorable considering small but frequent changes in regulations and related IT management.

Digital Shadow Status Tracking. Tracking for a digital shadow can be divided into five main parts: production orders output tracking, machine status tracking, quality assurance and control, materials, parts, and products tracking, and workers status tracking. Automatic reporting of produced goods eliminates postproduction manual counting by an operator. Manual reporting, even if the results are entered digitally, is often time-consuming and prone to errors. Implemented weighing scales allow the detection of manufactured quantities of goods by measuring the weight of a bin. The measuring is activated by vibration when placing the goods, and results are delivered wirelessly using 2,4 GHz IoT protocol to the access point. Further, the data is delivered to a cloud-scale provider provider management system.

Although ERP systems provide a wide scale of functionality, there is still sometimes a need for customer-specific extensions. In the demonstrator, the system difficulty lies in the description of internal logistics applied untraditionally. The system consists of two-level warehousing: the static warehouse and movable blisters. In the BC, AL language was used to add extra features in the system description to enable tracking of movements. The blisters were defined as micro bins, and the warehouse and workstations were defined as macro bins. This specification allows tracking the location of a specific component and the related blister with other components on it. In addition, the extension allows reservation of workstations and a place on the shuttle when the movement of components starts to avoid scheduling conflicts.

Event logs for machinery status tracking are recorded when the components are moved between workstations and the warehouse. When needed components are delivered to a specific workstation, the production order operation is stated as in progress. Consequently, the event of machine occupation is recorded in the system. After machining, the central unit is informed to organize the pick-up of the parts and change the status. The alternative option would be to use sensors for real-time measuring the machinery vibrations, acoustics, or current to define its status. This demonstrator enables tracking of shuttles and components and communication between operational technology. Therefore, a more data-capacious alternative with sensors was discarded.

A quality control station was built that uses a camera sensor to detect incorrectly assembled products. Additionally, in-process quality assurance is applied to the cognitive assistance system, which launches quality control steps during assembly processes to ensure quality during manufacturing. The operator's status is tracked indirectly, using a combination of assistance system output, materials tracking, and finished product output tracking.

Communication Infrastructure. A Rest Application Programming Interface (API) was applied to communicate between ERP as a central operational information system and other supporting management systems such as Etagis APS and weighing scale system. The data format used in the communication between different software was json. Python script was launched to manage the requests and connect the endpoints in the Rest API format to deliver the payloads. Rest API protocol and payloads in the JSON format were the only options that complied with all the used software. Therefore, other alternatives, such as Soap API, were not considered.

The IoT communication protocol MQTT was launched for operational technology and Central Unit communication. This protocol enables the sending and receiving messages according to each entity's subscription to topics. Alternative OT protocols are, for instance, Zigbee, Lora, and LwM2M. The benefit of MQTT is the ability to communicate to the cloud. Many gateway protocols, such as Lora and Zigbee, are still converted into MQTT protocol in the case of device-cloud communication. MQTT protocol was designed for IoT devices; therefore, it is designed to be lightweight and reliable in a shop floor environment. Protocol conversion is needed for disparate devices to integrate into the network (in our case, UR5). Grafana, as a business intelligence application, was launched to provide easy-to-catch charts for humans. Alternatively, the ThingsBoard application was considered, but the selection was made due to Grafana's compatibility with containerization technology.

5 Conclusions

The AD approach was deployed to CPPS to decouple its FRs and decompose its DPs to launch a digital shadow to support the avoidance of internal disruptions. The delivered DPs were converted into digital solutions implemented in the cyber-physical demonstrator. An interesting result is a guideline for separate data storage for operational and enormous datasets, ERP, and relational DB controlled by the custom script for inquiry management. Although the digital twin solutions mainly use one or another data storage infrastructure [20, 21]. Such diversification enables the integration of management systems and big data into the existing operational data infrastructure, thus creating dedicated spaces for various types of data manipulation and integration. Additionally, the proposed design process helps specify if customized ERP developments are needed, such as for items tracking in the demonstrator. The demonstrator still needs additional effort to launch the proposed solutions for each single entity in the system. The next step will be decomposing DT functionality to lower the cost of changes related to the adaptation to disruptions.

Acknowledgment. This project has received funding from the Autonomous Province of Bozen/Bolzano, Department Innovation, research, universities and museums (ASSIST4RESILIENCE: Increasing Resilience in Manufacturing - Development of a Digital Twin Based Worker Assistance).

References

1. Arica, E., Powell, D.: Digitalization in manufacturing: trends, drivers, challenges, and research areas in Norway. In: Dolgui, A., Bernard, A., Lemoine, D., von Cieminski, G., Romero, Da. (eds.) Advances in Production Management Systems. Artificial Intelligence for Sustainable and Resilient Production Systems: IFIP WG 5.7 International Conference, APMS 2021, Nantes, France, September 5–9, 2021, Proceedings, Part III, pp. 118–125. Springer International Publishing, Cham (2021). https://doi.org/10.1007/978-3-030-85906-0_14
2. Papacharalampopoulos, A., Michail, C.K., Stavropoulos, P.: Manufacturing resilience and agility through processes digital twin: design and testing applied in the LPBF case. Proc. CIRP **103**, 164–169 (2021). https://doi.org/10.1016/j.procir.2021.10.026
3. Napoleone, A., Macchi, M., Pozzetti, A.: A review on the characteristics of cyber-physical systems for the future smart factories. J. Manuf. Syst. **54**, 305–335 (2020). https://doi.org/10.1016/j.jmsy.2020.01.007
4. Sony, M.: Design of cyber physical system architecture for industry 4.0 through lean six sigma: conceptual foundations and research issues. Product. Manufac. Res. **8**(1), 158−181 (2020). https://doi.org/10.1080/21693277.2020.1774814
5. Yaacoub, J.A., Salman, O., Noura, H.N., Kaaniche, N., Chehab, A., Malli, M.: Cyber-physical systems security: limitations, issues and future trends. Microprocess. Microsyst. **77**, 103201 (2020). https://doi.org/10.1016/j.micpro.2020.103201
6. Magalhães, L.C., Magalhães, L.C., Ramos, J.B., et al.: Conceiving a digital twin for a flexible manufacturing system. Appl. Sci. **12**(19), 9864 (2022). https://doi.org/10.3390/app12199864
7. Lydia, M., Edwin Prem Kumar, G., Immanuel Selvakumar, A.: Securing the cyber-physical system: a review. Cyber-Phys. Syst. **9**(3), 193−223 (2023). https://doi.org/10.1080/23335777.2022.2104378
8. Segovia, M., Garcia-Alfaro, J.: Design, modeling and implementation of digital twins. Sensors **22**(14), 5396 (2022). https://doi.org/10.3390/s22145396
9. Attaran, M., Celik, B.G.: Digital twin: benefits, use cases, challenges, and opportunities. Dec. Anal. J. **6**, 100165 (2023). https://doi.org/10.1016/j.dajour.2023.100165
10. Pizoń, J., Gola, A., Świć, A.: The role and meaning of the digital twin technology in the process of implementing intelligent collaborative robots. In: Gapiński, B., Ciszak, O., Ivanov, V. (eds.) Advances in Manufacturing III: Volume 1 - Mechanical Engineering: Research and Technology Innovations, Industry 4.0, pp. 39–49. Springer International Publishing, Cham (2022). https://doi.org/10.1007/978-3-031-00805-4_4
11. Cochran, D.S., Arinez, J.F., Duda, J.W., Linck, J.: A decomposition approach for manufacturing system design. J. Manuf. Syst. **20**, 371–389 (2001). https://doi.org/10.1016/S0278-6125(01)80058-3
12. Cochran, D.S., Hendricks, S., Barnes, J., Bi, Z.: Extension of manufacturing system design decomposition to implement manufacturing systems that are sustainable. J. Manufac. Sci. Eng. **138**(10) (2016). https://doi.org/10.1115/1.4034303
13. Cochran, D.S., Smith J., Fitch, J.: MSDD 10.0: a design pattern for sustainable manufacturing systems. Product. Manufac. Res. **10**(1), 964−989 (2022). https://doi.org/10.1080/21693277.2022.2153184

14. Vickery, A.R., Rauch, E., Rojas, R.A., Brown, C.A.: Smart data analytics in SME manufacturing – an axiomatic design based conceptual framework. MATEC Web Conf. **301**, 1–11 (2019)
15. Aruväli, T., De Marchi, M., Rauch, E., Matt, D.: Design decomposition for cyber resiliency in cyber-physical production systems. In: Puik, E., Cochran, D.S., Foley, J.T., Foith-Förster, P. (eds.) Proceedings of the 15th International Conference on Axiomatic Design 2023, pp. 3–14. Springer Nature Switzerland, Cham (2024). https://doi.org/10.1007/978-3-031-49920-3_1
16. Suh, N.P.: The principles of design. Oxford University Press, New York (1990)
17. Alexopoulos, K., Anagiannis, I., Nikolakis, N., Chryssolouris, G.: A quantitative approach to resilience in manufacturing systems. Int. J. Prod. Res. **60**(24), 7178–7193 (2022). https://doi.org/10.1080/00207543.2021.2018519
18. Cimini, C., Pirola, F., Pinto, R., Cavalieri, S.: A human-in-the-loop manufacturing control architecture for the next generation of production systems. J. Manuf. Syst. **54**, 258–271 (2020). https://doi.org/10.1016/j.jmsy.2020.01.002
19. Lachenmaier, J., Weber, P., Lasi, H.: Enterprise information systems vs. digital twins– a case study on the properties, purpose, and future relationship in the logistics sector. In: Proceedings of the 56th hawaii international conference on system sciences, pp. 4505−4514 (2023)
20. Singh, S., Shehab, E., Higgins, N., et al.: Data management for developing digital twin ontology model. Proc. Inst. Mech. Eng. Part B: J. Eng. Manufac. **235**(14), 2323–2337 (2021). https://doi.org/10.1177/0954405420978117

Implementation of the Technological Capabilities of the Testbed 4.0 Laboratory in Cooperation with Simulation

Marek Kliment(✉), Peter Trebuňa, Matúš Matiscák, and Ján Kopec

Technical University of Kosice, 9, Park Komenského, 040 01 Košice, Slovak Republic
marek.kliment@tuke.sk

Abstract. Technologies such as simulations, detailed modeling, and data collection with the help of sensors and feelers are familiar in industrial practice and industrial engineering. It is more important to apply and integrate all these technologies correctly. If we connect all available options and use all available data sources, we can create authentic digital models of actual operations, the so-called digital twin. Such a relatively perfect simulation can, with the correct configuration and connection of external devices such as PLCs, not only receive but also physically influence the environment. The paper deals with integrating simulation and technological means within the TestBed 4.0 laboratory, such as PLC converters, different types of servers, and devices that can be connected to them. The TestBed 4.0 laboratory dramatically facilitates the verification of the modification of production processes and the creation of various types of digital twins, making it possible to verify various variants of the modification of processes in a digital environment. After tuning the twin and verifying all the advantages and disadvantages of the modification, this already verified one is implemented in actual operation, eliminating production losses. In a way, the post is a guide to connecting the simulation software Tecnomatix Plant Simulation using the available means with a PLC converter, with the help of which it is possible to control the elements of the simulation and, conversely, to control the elements of the physical world with the help of the simulation.

Keywords: Simulation · Testbed 4.0 · PLC · Server · Connection · Industrial Growth

1 Introduction

Models and simulations have always been and will be an integral part of human existence and are a tool through which a person comes to terms with reality. Mental models help people better understand reality, create plans, and consider different options. Digitization and automation, which are part of Industry 4.0, are the bearers of changes entering the current industry at all levels of management of business processes and services [1–5]

An integral part of Industry 4.0 is modern modeling, simulation, and management of production processes. The digital revolution aims to digitize the production process

© The Author(s), under exclusive license to Springer Nature Switzerland AG 2024
V. Ivanov et al. (Eds.): DSMIE 2024, LNME, pp. 15–27, 2024.
https://doi.org/10.1007/978-3-031-61797-3_2

with minimal human intervention. An important factor in companies' success nowadays is optimizing their business processes. Modeling and simulation will become integral to planning and managing their future processes [5–9].

In the future, the dynamic production environment will require modeling and simulation tools that will be able to simulate complex processes and phenomena in production. Artificial intelligence or virtual reality has also become a supporting simulation technique. With the increasing complexity of systems, the importance of simulation is constantly growing. It is essential that a wrong decision could mean ineffective investments, long-term economic losses, or weakening competitiveness [10, 11].

The contribution aims to describe and highlight the importance of connecting simulation software to natural processes to collect data from the external environment. After subsequent editing, these data will make it possible to create authentic and accurate digital models in the form of simulations, in which it will be possible to test possible changes and optimization variants first in digital form. These changes can be projected directly from the simulation into the natural process. Resources such as KepServer and PLC converters help us with these steps. This post contains instructions on how to make such a connection. The research goal of the workplace where it was created is to use these resources further and to create its 3D digital enterprise with the resources already available at the workplace, but those that the workplace plans to import in the future. To achieve this goal, it is planned to use the means of 3D modeling to create equipment and product models. These models will then be implemented in a simulation to make them more authentic and accurate. At the same time, they can be used as templates for 3D printing, providing us with a tangible model of the device, which we can then assemble into a 3D digital enterprise. With such and other means, it will be possible to work towards further possibilities of modeling and optimizing productions and their presentation for practice.

The structure of the post is as follows:

- Description of technology for creating digital twins,
- Description of the possibility of connecting the simulation using KepServer and PLC converter to the natural environment,
- Other possibilities of application and development of digital twin technology in the digital environment, in the field of 3D modeling, and their application in practice.

2 Literature Review

In creating the basis of the contribution, some parts of contributions 1 to 5, which deal with using CAD models in various areas, whether within virtual mixed and augmented reality or simulation, served us. By applying simulation and its combination, for example, with localization elements and systems for process optimization, as well as the expected consequences of the onset of technology in the context of Industry 4.0, such as the integration of simulation or the sustainability and cooperation of these elements in production processes. Papers 6 to 9 deal with logistics and linking simulation to this field and the methodologies that can be used. When processing the simulation models, we also took into account the methodologies within the logistics chain. Literary sources 10 and 11 cooperate and follow up on the context of using simulation in practice and

optimizing individual processes. The authors of the cited contributions 12 to 15, like the entire content of the contribution, deal with the area of simulation, optimization, material flow, etc., in connection with current possibilities within Industry 4.0

3 Research Methodology

The goal of the contribution and its content is to integrate simulation tools with the physical environment and vice versa. Creating a digital twin can validate planned changes in natural processes in a virtual environment without physical intervention in existing production. With the help of technological means in the TestBed 4.0 laboratory, these changes can be tested on physical models and technologies in a digital environment and on physical objects that can demonstrate real devices, production lines, and their parts. A digital twin is a virtual representation of a physical product, process, or system that enables real-time monitoring, analysis, and optimization. Furthermore, it is a two-way transfer or sharing of data between a physical object and a digital object. Using this data, Digital Twin can perform tasks such as [11–13]:

- in-depth analysis of the physical twin,
- design and validation of a new or existing product/process, • simulation of the health status of a physical twin,
- increasing the safety and reliability of the physical twin, • optimization of a part, product, process, or production,
- monitoring the condition of the physical twin during its lifetime, • prediction of physical twin performance,
- physical twin control in real-time.

A digital twin is a created combination of data, analytics, and simulation that mirrors the physical properties and behavior of a system (Fig. 1). It is used in a variety of industries, from manufacturing and engineering to healthcare and transportation, to increase efficiency, reduce costs and improve performance. It provides a way to monitor and analyze system behavior, predict potential problems, and simulate new scenarios before changing the physical system. One of the main advantages of digital twins is their ability to reduce downtime, improve maintenance processes, or identify and solve potential problems before they occur [13].

The simplest way to imagine the working principle of a digital twin is as a bridge between the digital and physical worlds (Fig. 2). First, the most important thing is to get the information from the object (physical). Sensors use intelligent components to collect information about working conditions, positions, and states in real-time, obtained from a physical item and then connected to a cloud system, in which all processed data is received and subsequently detected by the sensors [14, 17].

- Sensors
  - deployment of sensors in the production process,
  - thanks to the sensors, the digital twin can capture environmental data about physical processes and position and state data.

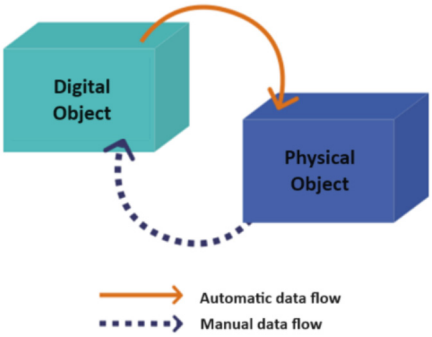

Fig. 1. Digital Twin and our data flow.

- Data
  - sensors provide data drawn from company systems (bill of materials).
- Integration
  - shared data that communicates between the digital and physical worlds.
- Analytical technologies
  - Analyzing data obtained with the help of algorithms and individual simulations.
- Active elements
  - controlled independently or by a human.

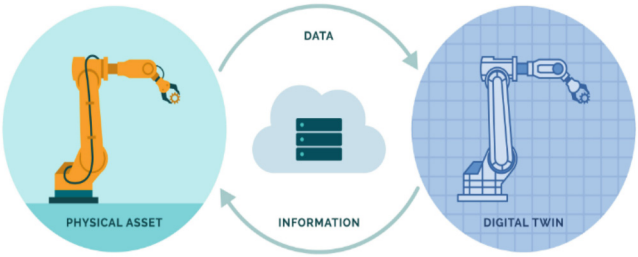

Fig. 2. Digital twin principle.

4 Results and Discussion

4.1 Evaluation of the Possibilities of Cooperation of Simulation with Technologies in the Testbed 4.0 Laboratory

This part will evaluate the possibility of simulation cooperation with technologies in the TestBed 4.0 laboratory. In the TestBed 4.0 laboratory, the simulation of the designed production line and the subsequent connection of the Tecnomatix PlantSimulation program and the PLC will be performed. The following figure (Fig. 3) shows the connection between the individual programs that communicate with each other and exchange information, based on which we can set up the simulation according to our requirements.

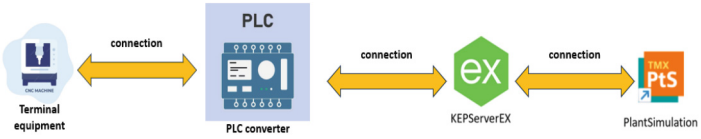

Fig. 3. Connecting simulation software and terminal equipment.

First, after opening the KEPServerEX program, we click "Project" in the menu on the left and create a "New Channel". After creating a "New Channel", the option "Select the type of channel to be created" will appear, and we will select the option "Simulator". The next step will be naming "Specify the identity of this object", where we enter the name of the "object". Subsequently, we set the selection of the method of sending invalid floating-point numbers to the client (Figs. 4 and 5).

We continue to create a simulation link and set up in KepServerEX to access the PLC port and ensure communication between the simulation and the physical device.

We enter a name for "Device", select a specific device type and format, and enter values. In the last step, we have a table summarizing the settings made in this step (Fig. 6).

After creating the "New Channel" and "Device" items, which we also named, we clicked on the "Working" item, in which we set the "Data Type" to "Boolean," and we also adapted the address to the "Data Type", which is why we chose from menu R0001, as these variables are for type "Boolean" (Fig. 7).

The next step was to open the production line in the Tecnomatix PlantSimulation program, where we assigned "OPC UA" to one process in production from the "Toolbox" menu in the "Information Flow" section. OPC UA will serve us so that we can connect the PlantSimualtion program and KEPserverEX and that these programs can communicate with each other. After adding "OPC UA" to the production program, right-click on the KEpserverEX program and select the "OPC UA Configuration" option (Fig. 8).

After opening "OPC UA Configuration", "Server Endpoints" opens, in which we double-click the first option in the URL option, and the "TCP Connection" option opens. In the "TCP Connection" option, we assign a "Port Number", which will generate an "IP Address". In the Tecnomatix PlantSimulation program, we open "OPC UA1" and insert the generated IP address, which was generated for us in "Server Endpoints". The entered IP address will ensure that the PlantSimulation programs and the KEPserverEX program

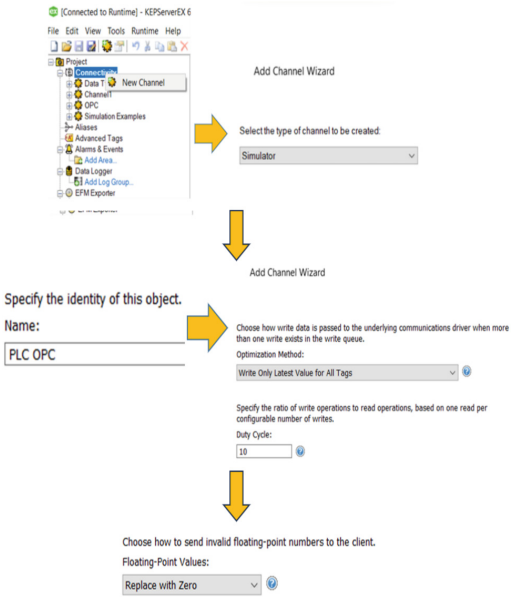

Fig. 4. Project and client creation in KEPServerEX.

will communicate with each other. After opening "OPC UA1", we click on "Items." After opening it, we assign a "Group Name" to it, into which we insert the already created "New Channel", which we named OPC_UA_Bc, we also add "Namespace", "Read Interval' and 'Write Interval'. After clicking "Group Name", another "window" will open, where we have to assign "Identifier", "Alias" (Fig. 9).

The next step was to open a production process called " frezovanieparalelne", where we assigned a product input method and a product output method in the "Controls" column. A process input method named "frezovanieparalelne" describes that the machine will turn on and work if the variable is full. A method for the output of the "milling in parallel" process describes that if the variable is empty, the machine will shut down. If all 4 parts from the input arrive in the "frezovanieparalelne" process, only then will this process be turned on, and the "CNC device" assigned to us will also be turned on immediately (Fig. 10).

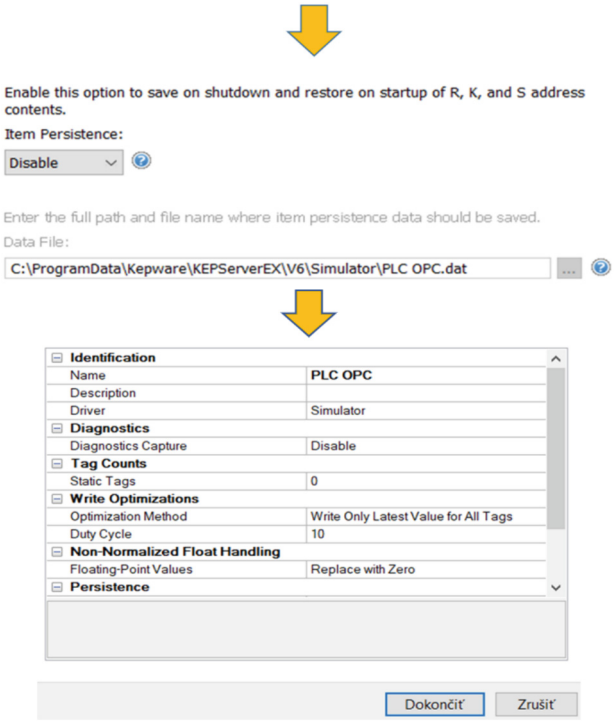

Fig. 5. Summary of set values and names.

4.2 Other Prerequisites for the Use and Development of Technology Linking Simulation with the Real Environment

As mentioned in the introduction, the author's workplace has a lot of technology and possibilities for developing various industrial and digital engineering areas. At the workplace, we have support software for 3D modeling and software such as Solid Works and Solid Edge for creating models of devices or products. Simulation software from the Siemens Tecnomatix range, such as Plant Simulation, Process Simulate, Jack, etc. Software for creating a virtual and mixed reality environment. The models can be created as naturally reduced objects with the help of 3D printing. The printed models can be set in motion with the help of programmable Arduino modules and servo drives. The workplace also has several programmable robots, vehicles, and logistics elements from the company Wlkata, which allow students and workers to validate various production scenarios on miniature models of fundamental production components. For mapping movements in production, we use RTLS technology, which allows the collected data to be edited and implemented in simulation models.

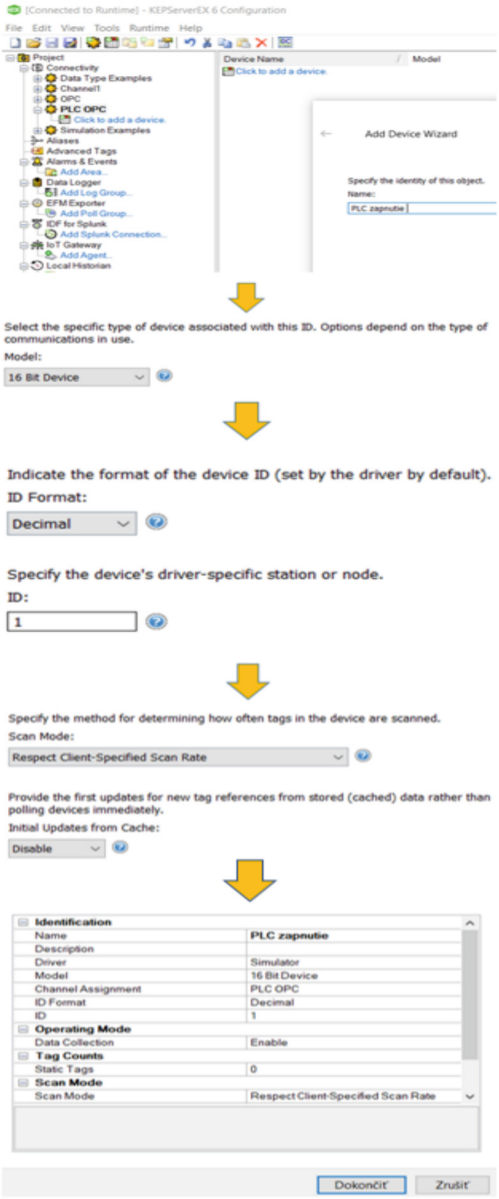

Fig. 6. Creation of a specific device for connection.

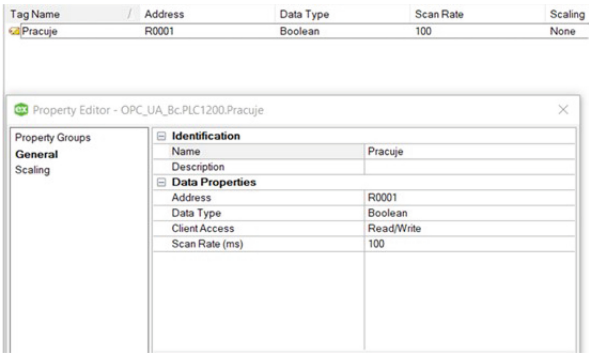

Fig. 7. Defining variables.

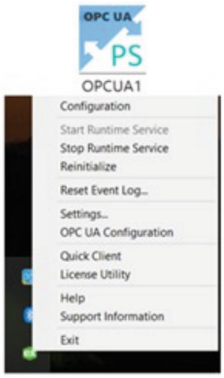

Fig. 8. OPC UA Configuration.

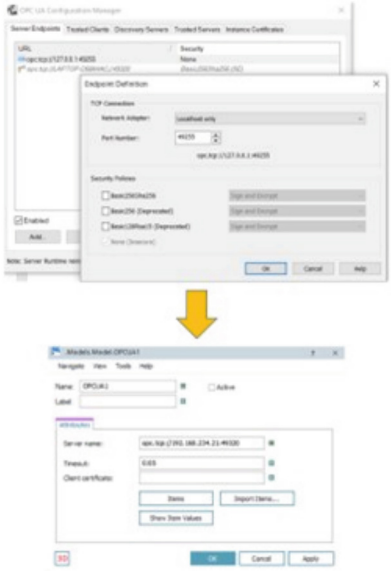

Fig. 9. Endpoints server setting and OPC UA IP address assignment.

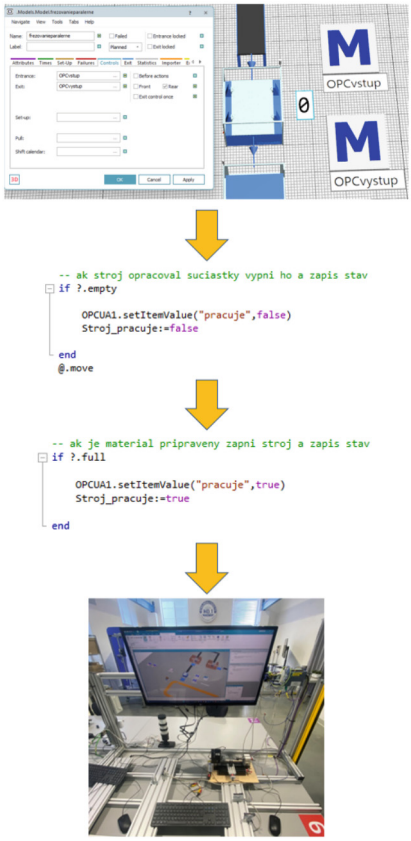

Fig. 10. Assignment of methods for connecting the simulation with OPC UA and the end device.

Last but not least, we can use the technologies of PLC converters and the options they offer in cooperation with HMI panels. Lastly, the workplace houses the first and only TestBed 4.0 laboratory in Slovakia, which only highlights and supports all these possibilities. In the future, the real goal is to integrate all these technologies and use them to create your own scaled-down 3D digital enterprise, which will enable the development of digital twin technology and provide for practice the opportunity to demonstrate verified scenarios, not only in digital form with the help of simulation models but also in a scaled-down form on real moving devices created and manufactured in the workplace of the authors of the post (Fig. 11).

4.3 Discussion

In his paper: Digital Twin Certified: Employing Virtual Testing of Digital Twins in Manufacturing to Ensure Quality Products, Grieves, M talks about eliminating risk and reducing costs while increasing product quality using digital twin technology [16]. In their article on intelligent production, Sameer Mittal and the team describe everything

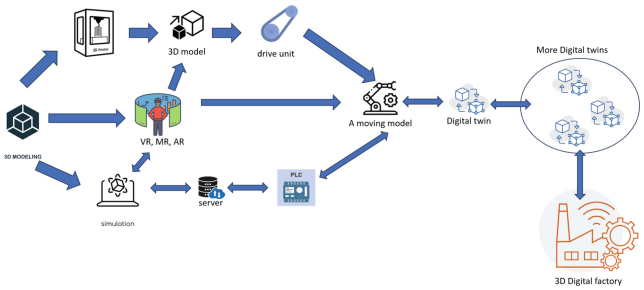

Fig. 11. Integration of multiple technologies to create 3D digital factories.

necessary so that tiny and medium-sized enterprises can start using this concept and make full use of it in their production processes, thereby improving their competitive position in the market [17]. Mozolova, L. and the collective of authors deal with the application of simulation in improving the efficiency of the production process [18]. All these, as well as other contributions by many other authors, make it possible to develop the theory of creating digital twins with the help of the integration of PLC technology and creating your digital enterprise by implementing 3D printing in the production of your own devices from 3D models and setting them in motion with the help of available resources.

5 Conclusions

The goal of the post was to bring the possibility closer to the method of creating a digital twin and to point out the possibilities of connecting the simulation directly to physical instruments in a natural environment in the TestBed 4.0 laboratory. In the described way, it is possible to create a mutual interaction between the external environment and the simulation, for example, with the help of various sensors and light gates. Conversely, it is also possible to control the tools and devices of the physical environment using simulation, such as the Unimat CNC kit. However, the connection can also be demonstrated by more straightforward means, such as lights, beacons, horns, etc. With the help of PLC converters, it is also possible to connect robot models with the simulation, which can perform activities in the simulation. Still, it should be noted that the simulation does not control the robot's movements. It is necessary to program the robot in advance for the given tasks, and the simulation, with the help of PLC, can control its commissioning and its stopping. With the help of these means, the technology moves more and more towards more perfect forms of digital twins, and the sense of simulation grows immeasurably.

Integrating other means and technology within industrial and digital engineering also offers these and other possibilities. Such technologies can be, for example, the further application of models that appear in the simulation and display devices, machines, and semi-finished products moving in the production process. These models can be transformed into formats suitable for 3D printing, and after their materialization, drive and control units can be added to them, which can then be connected to the simulation using PLC converters and used for the needs of the digital twin. By creating several

mutually influencing digital twins in this form, we can create a 3D digital enterprise, which will provide the opportunity to demonstrate the results of optimization not only in a digital but also in an actual reduced form. Models and simulation models can, of course, also be presented with the help of virtual reality; under certain circumstances, these models can also be used in mixed and augmented reality. It follows from the contribution that when integrating several technologies and means of industrial and digital engineering, it is possible to create and optimize business processes both in digital and in reduced actual form. These resources are applicable in practice and the educational process of future graduates of these fields of study.

Acknowledgment. This article was processed within the framework of the grant project: APVV-17-0258 Application of elements of digital engineering in the innovation and optimization of production flows. APVV-19-0418 Intelligent solutions for increasing the innovative capacity of enterprises in the process of their transformation into intelligent enterprises. VEGA 1/0438/20 Interaction of digital technologies for the purpose of supporting software and hardware communication of an advanced production system platform. VEGA 1/0508/22 Innovative and digital technologies in production and logistics processes and systems. KEGA 020TUKE-4/2023 Systematic development of the competence profile of industrial and digital engineering students in the process of higher education.

References

1. Kaščak, J., Husár, J., Knapčíková, L., Trojanowska, J., Ivanov, V.: Conceptual use of augmented reality in the maintenance of manufacturing facilities. In: Trojanowska, J., Kujawińska, A., Machado, J., Pavlenko, I. (eds.) MANUFACTURING 2022. LNME, pp. 241–252. Springer, Cham (2022). https://doi.org/10.1007/978-3-030-99310-8_19
2. Grznar, P., et al.: The use of a genetic algorithm for sorting warehouse optimisation. Processes **9**, 1197 (2021). https://doi.org/10.3390/pr9071197
3. Balog, M., Knapcikova, L.: Advances of intelligent techniques used in Industry 4.0: proposals and testing. Wireless Networks **27**(3), 1665−1670 (2021). https://doi.org/10.1007/s11276-019-02064-w
4. Saniuk, S., Grabowska, S., Straka, M.: Identification of social and economic expectations: contextual reasons for the transformation process of Industry 4.0 into the Industry 5.0 Concept. Sustainability **14**, 1391 (2022). https://doi.org/10.3390/su14031391
5. Patalas-Maliszewska, J, Klos, S., Dostatni, E.: Integrating the assessment of sustainability and an ERP system in small and medium manufacturing enterprise—a case study. In: Trojanowska, J., Kujawińska, A., Machado, J., Pavlenko, I. (eds.) Advances in manufacturing III. MANUFACTURING 2022. LNME, pp. 50–60. Springer, Cham (2022). https://doi.org/10.1007/978-3-030-99310-8_5
6. Paska, M., Malkus, T., Rosova, A., Trebuna, P., Kacmary, P., Behun, M.: International commercial terms and their necessity for the logistics. In: 8th carpathian logistics congress (CLC 2018), pp. 688−696 (2018)
7. Kábele, P., Edl, M.: Increasing the efficiency of the production process due to using methods of industrial engineering. In: Ivanov, V., et al. (eds.) DSMIE 2019. LNME, pp. 126–137. Springer, Cham (2020). https://doi.org/10.1007/978-3-030-22365-6_13
8. Fedorko, G., Vasil, M., Bartosova, M.: Use of simulation model for measurement of MilkRun system performance. Open Eng. **9**(1), 600–605 (2019). https://doi.org/10.1515/eng-2019-0067

9. Burganova, N., Grznar, P., Gregor, M., Mozol, Š: Optimalisation of internal logistics transport time through warehouse management: case study. Transport. Res. Procedia **55**, 553–560 (2021). https://doi.org/10.1016/j.trpro.2021.07.021
10. Sujova, E., Čierna, H., Bambura, R.: Simulation model of production as tool for industry 4.0 implementation into practice. In: Engineering for rural development 2019, pp. 1192−1197 (2019). https://doi.org/10.22616/ERDev2019.18.N279
11. Ding, M.Z., He, K.T., Shi, L., Chen, D.: Production process optimization of the bar screen machine. In: Proceedings of the 10th IEEE conference on industrial electronics and applications, pp. 97–101. Auckland, New Zealand (2015). https://doi.org/10.1109/ICIEA.2015.7334091
12. Gola, A., Plinta, D., Grznar, P.: Modelling and simulation of reconfigurable manufacturing system for machining of casing-class parts. In: Proceedings of the 20th international scientific conference engineering for rural development, pp. 1563–1568 (2021). https://doi.org/10.22616/erdev.2021.20.tf333
13. Weichert, D., Link, P., Stoll, A., Rüping, S., Ihlenfeldt, S., Wrobel, S.: A review of machine learning for the optimization of production processes. Int. J. Adv. Manuf. Technol. **104**, 1889–1902 (2019). https://doi.org/10.1007/s00170-019-03988-5
14. Kasakow, G., Aurich, J.C.: Realising digital connectivity by using interdependencies within a production process. Procedia CIRP **52**, 80–83 (2016). https://doi.org/10.1016/j.procir.2016.07.076
15. Yang, B., He, Y., Yin, H.: Data analysis and production process control. In: Dolgui, A., Bernard, A., Lemoine, D., von Cieminski, G., Romero, D. (eds.) Advances in Production Management Systems. Artificial Intelligence for Sustainable and Resilient Production Systems: IFIP WG 5.7 International Conference, APMS 2021, Nantes, France, September 5–9, 2021, Proceedings, Part I, pp. 555–562. Springer International Publishing, Cham (2021). https://doi.org/10.1007/978-3-030-85874-2_59
16. Grieves, M.: Digital twin certified: employing virtual testing of digital twins in manufacturing to ensure quality products. Machines **11**, 808 (2023). https://doi.org/10.3390/machines11080808
17. Mittal, S., Muztoba, A.K., et. al.: A smart manufacturing adoption framework for SMEs. Int. J. Product. Res. **58**(5), 1555−1573 (2020). https://doi.org/10.1080/00207543.2019.1661540
18. Mozolova, L., Grznar, P., Mozol, S., Krajcovic, M.: Streamlining utilization of the assembly line using computer simulation. Acta Logistica **10**(2), 165–173 (2023). https://doi.org/10.22306/al.v10i2.365

Studies on Streamlining Processes Using Industry 4.0 Elements

Jan Kopec(✉), Miriam Pekarcikova, Marek Kliment, and Marek Mizerak

Technical University of Kosice, 9, Park Komenskeho, 042 00 Kosice, Slovak Republic
jan.kopec@tuke.sk

Abstract. Industry 4.0 is redefining manufacturing paradigms through the integration of advanced digital technologies. This study takes a theoretical and practical look at the implementation of Industry 4.0 elements to increase the efficiency of manufacturing processes through simulation and visualization in the manufacturing sphere of the enterprise. Industry 4.0 concepts are analyzed, highlighting their impact on the transformation of business models. It also describes a specific workplace that has successfully integrated these technologies, detailing their implementation and benefits. The article discusses digitalization in the Tecnomatix Plant Simulation software, which enables real-time modeling. It details its use for optimizing production processes, reducing lead times, and streamlining supply chain efficiency. It concludes with an analysis of the improvements achieved and their impact on the production cycle, presenting concrete results regarding increased efficiency, minimization of errors, and optimization of resources. Overall, it provides a comprehensive view of successful Industry 4.0 implementation through simulation and visualization.

Keywords: Process Innovation · Simulation · Visualization · Tecnomatix Plant Simulation

1 Introduction

In an Industry 4.0 environment, computers and intelligent machines are connected, communicating with each other, interacting with the environment, and ultimately making their own decisions with minimal human intervention in the decision-making process. Digitalization of production processes and business processes and the introduction of smarter machines and equipment can offer a few benefits, such as production productivity, production efficiency, efficiency of use resource efficiency, and waste reduction. In contrast, increased production speed brings some disadvantages. Increased production speed due to industrial automation will also increase consumption of resources and energy and hence an increase in pollution. In terms of social development, digital transformation and restructuring of industry will severely disrupt the labor market. Experts believe that digitalization and the emergence of labor-saving technologies will eliminate most lower-skilled jobs while creating fewer job opportunities in various fields [1].

Industry 4.0 now encompasses the digital transformation of the entire industrial market, from smart manufacturing to the digitization of the entire production process.

© The Author(s), under exclusive license to Springer Nature Switzerland AG 2024
V. Ivanov et al. (Eds.): DSMIE 2024, LNME, pp. 28–38, 2024.
https://doi.org/10.1007/978-3-031-61797-3_3

Industry 4.0 design principles are explicit solutions to problems that provide a systematization of knowledge and a description of the components of the problem. These design principles allow manufacturers to anticipate the process of Industry 4.0 adaptation and provide them with insights in developing the appropriate practices and solutions needed for the transition to Industry 4.0. The basic design principles in Industry 4.0 rely on implementing and integrating various simple to advanced information, digital, and operational technologies such as industrial sensors, controllers, or robots. Manufacturing mainly involves software applications, used by one or more networks, supporting business models. It also includes intelligent monitoring and control of sensors, smart metering devices, and intelligent mobile devices. Finally, it includes intelligent production management that integrates IoT data into its logic [2].

Tecnomatix Plant Simulation is a manufacturing process and logistics simulation software that allows you to model and optimize manufacturing systems before implementing them in a real environment. This software is widely used in industrial engineering to design, plan, and analyze manufacturing operations.

Tecnomatix Plant Simulation's strength is its ability to visualize and analyze the entire manufacturing process. Here are a few aspects that the software can address and optimize:

- Plant Design and Layout: the software allows you to model the physical layout of production equipment and workstations throughout the factory. This feature allows you to explore different layout options to achieve optimal efficiency.
- Material Flow Simulation: Simulation allows you to model the movement of materials throughout the factory. You can analyze the flow of materials, track their movement between different workstations, and identify potential areas of improvement.
- Timing Analysis: the program allows you to simulate the timing aspects of the production process. You can analyze which parts of the process are the most time-consuming and identify opportunities to improve production speed.
- Capacity Optimization: Tecnomatix Plant Simulation allows you to optimize the capacity of production equipment and workstations. This can include adding or removing equipment to achieve optimal production.
- Workflow Improvement: simulation allows you to analyze workflow and identify possible areas of improvement. For example, it can reveal a bottleneck in a process or allow testing of different scenarios to improve workflow.
- Virtual Test Scenarios: Through simulation, you can virtually test different scenarios and strategies, minimizing the risk of errors in real deployments.

This paper aims to prepare the necessary knowledge level for the new application linking the elements of the department and the TestBed 4.0 workplace. New technologies that contribute to the digitalization and the streamlining of production processes and new software elements bring new horizons for research and collaboration with practice (Tecnomatix plant simulation software package and TIA portal linked KEPServerEX, creation of digital manuals in Unity, etc.

2 Literature Review

The TestBed 4.0 (Fig. 1) laboratory facilities are located at the Technical University of Košice, specifically on the premises of the Department of Industrial and Digital Engineering. TestBed 4.0 was created to meet the demand for companies brought about by the fourth industrial revolution, also known as Industry 4.0, and as a support system that serves as a tool for companies to increase their competitive capabilities. In general terms, TestBed 4.0 has a huge benefit for companies that want to design, test, and find the best way to optimize their production processes solution [6]. This means that companies are going digital and starting to work more efficiently. TestBed 4.0 works with large amounts of data, from product design through its logistics operations, all the way to the actual production of the product. This dedicated workplace offers both quality facilities and the collection of this information from production and, finally, expert advice, which evaluates this data and communicates with companies about these blind spots in production and suggests optimizations on how to make them more efficient. The great advantage of TestBed 4.0 is that it can create a tailor-made solution for each company according to its requirements. Possible solutions include the procedures, concept, and methodology for Industry 4.0 applications, which means complex data collection, data gathering, data exchange, and transformation of this data into the necessary information [7, 8]. An essential part of the design, verification, and optimization is the correct application of the digital twin. Its presence helps to control the ecosystem of an industrial enterprise, which includes:

- CAM systems,
- PLM,
- CAD systems,
- RTLS,
- manufacturing machines,
- monitoring energy costs during production [3].

3 Research Methodology

As already mentioned, within the capabilities of TestBed 4.0, it is possible to track the desired product from its birth and thus plan and control the production process in detail, not only on its parts but globally throughout the entire value stream of the product. Within the lifecycle, it is possible to detail models of individual production departments and then insert them into a simulation in which inputs to these departments can be tracked; logistics flows, storage and many other components required in the production area can be addressed. All this knowledge is then used to build a new plant or to optimize an existing plant. TestBed 4.0 offers to test all these insights, such as the effectiveness of the investments made in new plants or plant modules, in a virtual environment [9, 10]. The result of this simulation will show the manager whether this investment is profitable and will bring more profit to the company. At the same time, the creation of these virtual models allows the verification of any inclusion that will affect the process and helps to increase the efficiency of the process. We select a device from the library's offerings to include in a process and observe its impact on that process [4, 5] (Fig. 2).

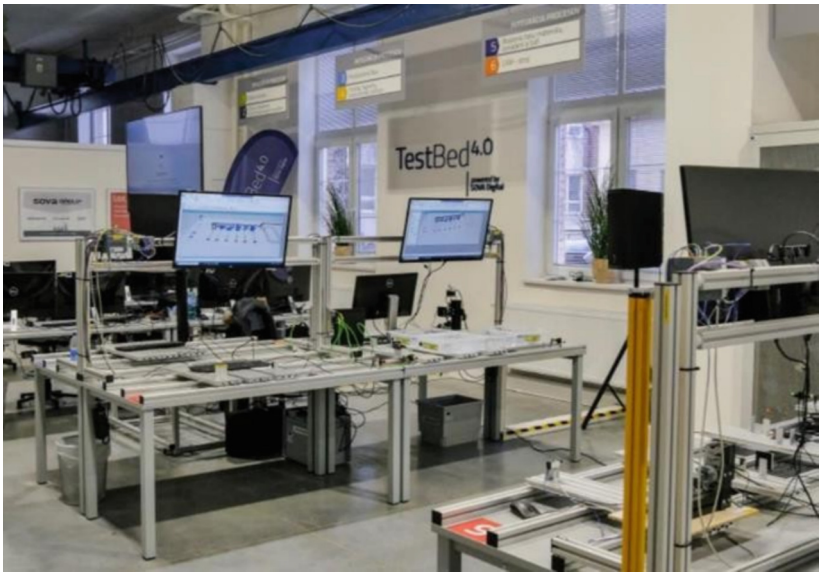

Fig. 1. TestBed 4.0 - a workplace focused on addressing the practical needs of Industry 4.0.

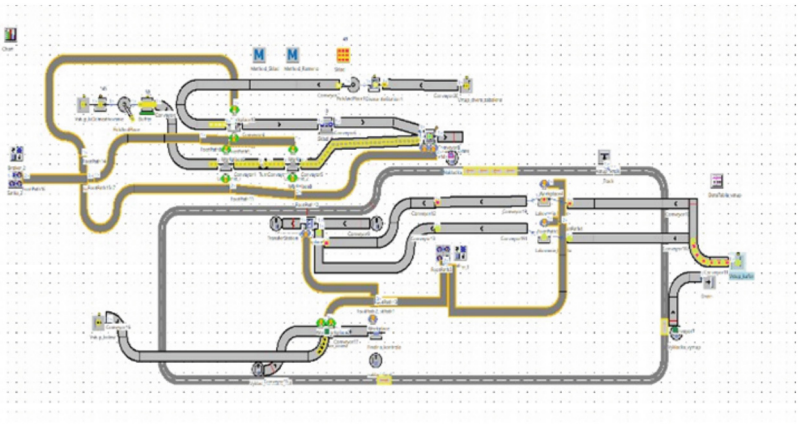

Fig. 2. Simplified car assembly line.

The car assembly simulation was set to an 8-h production time, and a favorable advantage of Tecnomatix Plant Simulation is the output data from the output (Drain). The data accessed is shown in Fig. 3. The control object is the output of the finished cars. Furthermore, the figure contains data such as main production time, transport time, storage, and utilization.

Simulation time:8:00:00.0000

Object	Name	Mean Life Time	Throughput	TPH	Production	Transport	Storage	Value added	Portion
Drain	Auto_final	14:20.8340	44	6	42.07%	57.93%	0.00%	41.82%	

Cumulated Statistics of the Parts which the Drain Deleted

Fig. 3. Statistical output from the simulation.

4 Results and Discussion

4.1 Production Line Simulation in Tecnomatix Plant Simulation

In this chapter, the design and improvement of the efficiency of the production process will be discussed. The manufacturing process was designed and streamlined in laboratory conditions. This process is focused on the production of individual components and the subsequent assembly of the bearing puller. The components are manufactured at separate workstations and moved to the assembly site using various transport options. The overall production consists of two separate buildings. The first building is the production hall for manufacturing the puller body (Fig. 4).

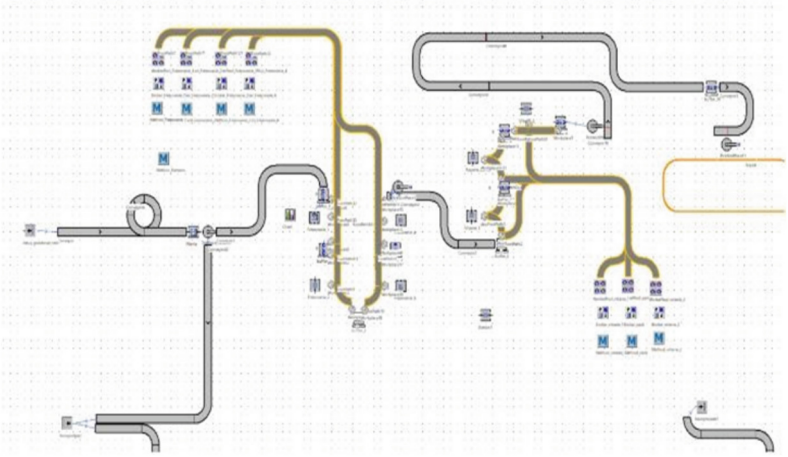

Fig. 4. Production hall of the body puller.

On this production line, the goods for body production enter the production line in a row behind each other, thus burdening and congesting the overall conveyor belt. The suggestions for improving this problem are as follows. The blank entry into the production line is set at an interval (1:50) that simulates the time required to perform the following operation, thus reducing the wear on the conveyor belt due to the high load on its total length. This interval is cyclically triggered after each unloading of material on the conveyor belt [11].

The semi-finished product travels along the conveyor belt to the following production process, which is material cutting. This workstation (Fig. 5a) performs the material

cutting using a band saw. This process is limited due to the manual removal of metal filings and, thus, longer downtimes for cleaning.

The optimization of this workstation is the automatic material transfer and the possibility of automatic sawdust removal provided by a robotic arm (Fig. 5b), thus reducing downtime associated with this issue. The sawdust is then conveyed via a conveyor belt to the warehouse to the ferrous waste. The robotic arm also ensures the transshipment of the separated material to the next conveyor belt.

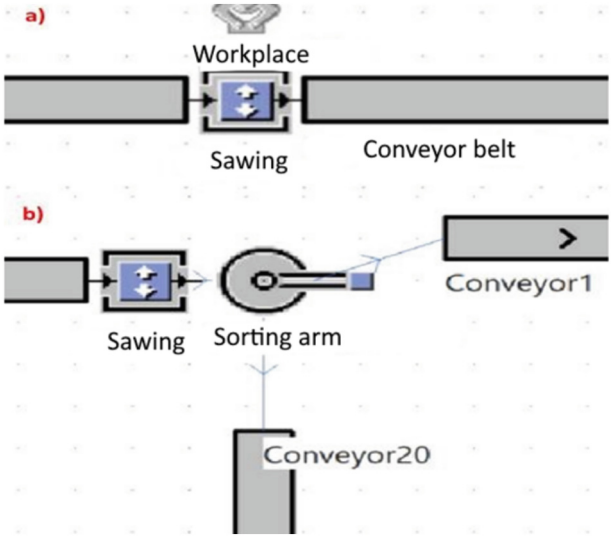

Fig. 5. (a) material separation workstation before optimization, (b) improved part of the production process.

The semi-finished product of the required length is transported to the milling workplace. The milling workplace consists of several milling machines, namely two milling machines. This workplace produces the largest downtime in the entire production line of the body puller. This is due to the production capacity of these machines and the associated machine reset after each milling operation. Increasing the number of production facilities is one possible solution to reduce downtime for capacity reasons. To spread the production requirements, we have chosen to increase the number of production facilities to four (Fig. 6). By increasing the number of production devices. We also eliminated the downtime due to machine readjustment after each operation. The required machine readjustment was created by milling a continuously different part surface, for which different parameters were set repeatedly. After each operation, the machined part is moved to the next production machine. Each machine is set up for a precise operation, so downtime due to machine reset is eliminated. For this workstation, we also considered the wear of the cutting tools themselves [7].

The simulation program was set up with the realistic tool wear numbers (300 cuts; consequently, the cut is inaccurate and can damage the semi-finished product or the cutting tool shatters and injure the operator) given by the company and the time the

operator must replace it. In this case, it is 3 min. After increasing the number of working machines, the company's milling overrun was reduced to 2 min.

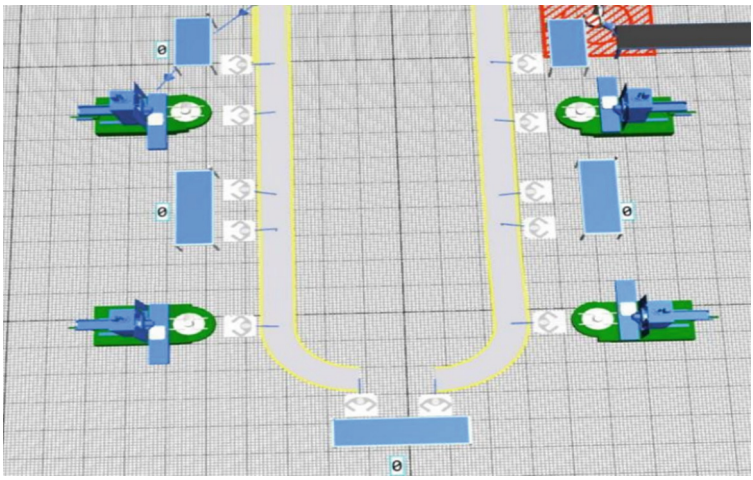

Fig. 6. Milling workplace.

The next technological operation is drilling a hole for the internal thread in the center of the component and then drilling holes for the attachment of the arms using a hexagon head bolt. At this site, we have streamlined production and reduced downtime by adding one piece of production equipment, namely a pillar drill for cutting the internal thread.

Before this piece of production equipment was added, downtime at this site was again caused by insufficient capacity of the production equipment. Most of the downtime comprised the time required to change the tool from the drilling process to the threading process and vice versa. The newly designed workstation consists of a production facility for drilling the hole for thread cutting, a production facility for thread cutting, and a production facility for drilling the three holes for the shoulder attachment [10].

At this workplace, the operators provide transport between the individual production facilities due to the small weight of the workpiece and the small distance between the individual facilities.

The part is stopped for degreasing and inspection before it leaves the production facility and then travels to the intermediate warehouse. The part is removed from the drilling and tapping workstation using a robotic arm on a conveyor belt. The part is stopped on this conveyor belt for the degreasing process. This process takes one minute and thirty seconds. After the process, the part proceeds to the inspection process. After the quality inspection, the part goes to the intermediate warehouse. The quality control process and the degreasing process are indicated in Fig. 8 (Fig. 7).

The finished part is conveyed to the robotic arm, which loads the parts onto the transport autonomous trolley. A transport trolley with a capacity of six pieces takes the finished product to the assembly workstation located in the adjacent production hall (Fig. 9).

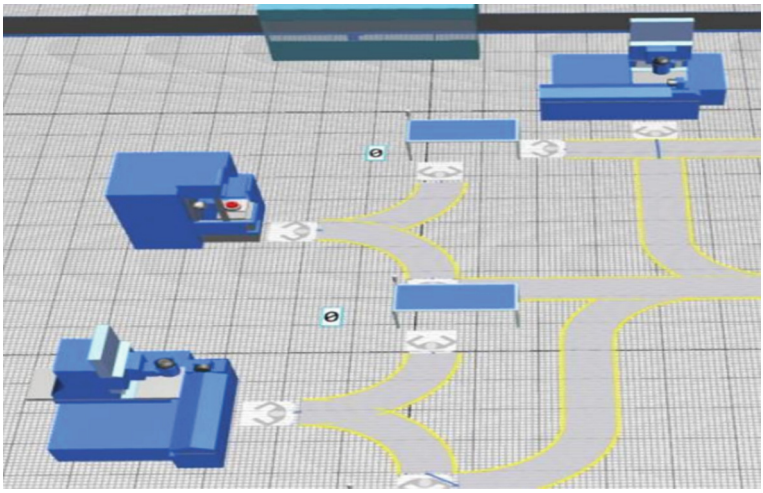

Fig. 7. Drilling and tapping workplace.

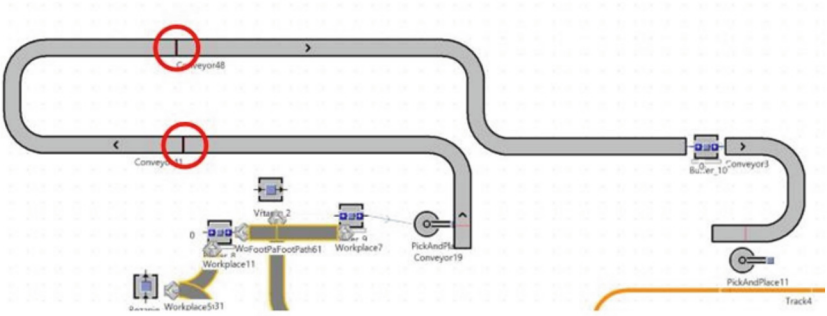

Fig. 8. Degreasing and Inspection.

4.2 Evaluation of the Designs and Elements of Digitization Within the Simulated Processes

The proposed changes or innovations used in the simulation helped increase the number of produced pieces at individual workplaces, whether it was an increase in production facilities or automation of specific processes. To evaluate and analyze the process, we can see statistical data on the number of pieces produced during an eight-hour shift at the workplace milling in the first production hall.

As can already be seen in Fig. 10, before the increase in the number of production facilities, the number of ninety-two pieces were produced during one working shift. These two milling machines needed frequent maintenance because of the heavy workload and constant operation.

Figure 11 shows the difference, reflected not only in the number of pieces but also in the average production time of the component, and the average production time dropped by almost half while the number of parts produced units increased by one hundred and

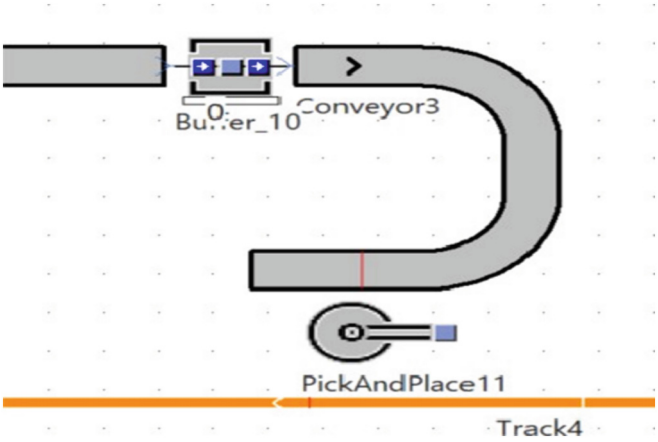

Fig. 9. Loading arm.

Simulation time:8:00:00.0000

Object	Name	Mean Life Time	Throughput	TPH	Production	Transport	Storage	Value added	Portion
Drain	telo	41:12.8696	92	12	34.17%	60.98%	4.85%	21.84%	

Cumulated Statistics of the Parts which the Drain Deleted

Fig. 10. Statistical data before the increase in the number of production facilities.

thirty-five units. It should also be noted that the designs introduced improvements are theoretical as everything that appeared to be a bottleneck in the simulation was improved, and that is why the design result is less than one hundred and fifty percent better than the original state. We could approach a similarly significant improvement if all the proposed changes were implemented. The proposed changes would be phased in over to ensure they are economically more manageable.

Simulation time:8:00:00.0000

Object	Name	Mean Life Time	Throughput	TPH	Production	Transport	Storage	Value added	Portion
Drain	telo	22:26.3634	227	28	43.04%	48.04%	8.91%	33.42%	

Cumulated Statistics of the Parts which the Drain Deleted

Fig. 11. Statistical data after the increase in production facilities.

4.3 Discussion

We have implemented IoT sensors and analytics tools in our industry, allowing us to monitor and optimize our manufacturing process in real-time. This has reduced the time spent on production and minimized unnecessary raw material wastage.

Thanks to Industry 4.0, we can plan the maintenance of our equipment more efficiently. Predictive maintenance allows us to identify potential failures earlier, saving costs and minimizing downtime.

The implementation of Industry 4.0 brings with it new technologies and automation. While this may mean that some routine tasks will be automated, employees can focus on more creative and challenging tasks. However, preparing employees for new technologies is also essential.

Financial investment can also be a challenge. Implementing Industry 4.0 may require significant capital expenditure. It is crucial that companies accurately assess the return on investment and choose the technologies that best suit their needs.

5 Conclusions

The simulation of the study results from the visualization investigation will streamline the production process. The capabilities of simulation software and the combination of different simulation inputs and outputs are beneficial in designing and better understanding the proposed changes to the manufacturing process. By inserting custom 3D objects into the manufacturing process simulation, the simulation mirrors the real production line, ensuring maximum benefit as Tecnomatix Plant Simulation software has a limited library of machines and their parts [9]. Replacing the models with custom models creates a sketch for the digital twin. The content of this section also includes creating custom objects and the project documentation of the objects, then editing them into the required file type needed for interfacing with the simulation. Several innovations to the manufacturing process have also been proposed in this paper.

An evaluation of the designs used in the simulation and an overall analysis of the innovations used form the conclusion of this paper.

Introducing effective individual measures into production brings statistical data that assists managers in making decisions about further innovations. This is one of the reasons why material flow tracking and subsequent statistical analysis in manufacturing processes are so essential and are increasingly emphasized. The fact that the improvements introduced were not investigated from an economic and profitability point of view is also a given, as the outcome of this study was to demonstrate the capabilities of simulation and simulation software in visualization, along with interfacing with VR, 3D printing and designing for a digital twin.

The cost-effectiveness and payback of these designs are a topic for further studies that may build on this work.

Acknowledgment. This article was created by the implementation of the grant projects APVV-17-0258 Digital engineering elements application in innovation and optimization of production flows, APVV-19-0418 Intelligent solutions to enhance business innovation capability in the process of transforming them into smart businesses. VEGA 1/0438/20 Interaction of digital technologies to support software and hardware communication of the advanced production system platform. KEGA 020TUKE-4/2023 Systematic development of the competence profile of students of industrial and digital engineering in the process of higher education. VEGA 1/0508/22 „Innovative and digital technologies in manufacturing and logistics processes and system".

References

1. Lasi, H., Fettke, P., Kemper, H.G., et al.: Industry 4.0. Bus. Inf. Syst. Eng. **6**, 239–242 (2014). https://doi.org/10.1007/s12599-014-0334-4
2. Tava Lennon, O., Brian, T.: Industry 4.0: opportunities and challenges for operations management. Manufac. Serv. Oper. Manage. **22**(1), 113−122 (2020). https://doi.org/10.1287/msom.2019.0796
3. For industry. TestBed 4.0. https://www.testbed.sk/pre-priemysel/. Accessed 15 Dec 2023
4. Trebuňa, P., et al.: Methods and systems of production control in industrial engineering. Technical University of Košice, Košice (2020)
5. Kliment, M., Pekarcikova, M., Trebuna, P., Trebuna, M.: Application of TestBed 4.0 technology within the implementation of Industry 4.0 in teaching methods of industrial engineering as well as industrial practice. Sustainability **13**, 8963 (2021). https://doi.org/10.3390/su13168963
6. Trebuňa, P., et.al.: Modelling in industrial engineering. 1st edn. Košice (2015.)
7. Trebuňa, P., et al.: Production processes and systems digitalization, 1st edn. RAM-Verlag, Lüdenscheid (2022)
8. Bangsow, S.: Tecnomatix plant simulation: modeling and programming by means of examples. Springer, Berlin Heidelberg, Switzerland (2016)
9. Trebuňa, P., et al.: An overview study of the Testbed 4.0 laboratory 2022. In: Proceedings of the 25th international scientific conference «Trends and innovative approaches in business processes 2022», pp. 142−147. Technical University of Košice, Košice (2022)
10. Priemysel 4.0. https://casopis.fit.cvut.cz/tema/priemysel-4-0/. Accessed 15 Dec 2023
11. Mozolová, L., Mozol, Š., Grznár, P., Gregor, M.: Comparison of the use of 2D and 3D views in the Tecnomatix plant simulation platform. In: Proceedings of the XXIV international scientific conference «Trends and innovative approaches in business processes 2021», vol. 24, pp. 25−29. Technical University of Košice, Košice (2021)

Material Removal Rate Determination Based on a Laser Displacement Sensor

Natalia Lishchenko[1], Garret O'Donnell[1], Vasily Larshin[2(✉)], and Igor Dudarev[3]

[1] Trinity College Dublin, 2, College Green, Dublin 02 PN40, Ireland
[2] Odesa Polytechnic National University, 1, Shevchenko Avenue, Odesa 65044, Ukraine
vasilylarshin@gmail.com
[3] Odesa State Agrarian University, 13, Panteleymonovskaya Street, Odesa 65012, Ukraine

Abstract. The non-contact measurement method was used to determine the parameters of the cut layer of material during grinding and other mechanical machining methods. One of these parameters is the specific grinding energy, which equals the ratio of grinding power to the material removal rate. The latter is determined by the cross-sectional area of the material layer being cut. The paper proposes a non-contact method for measuring instantaneous height parameters of the cross-section of the cut layer using a laser displacement sensor with subsequent determination of the cross-sectional area. This is relevant for defectless grinding implants and workpieces with free-form surfaces made of hard-to-machine materials. Studies have been carried out on the accuracy of non-contact measurement of instantaneous height parameters of the cross-section of the cut layer of material by comparing the obtained data with the results of contact measurement of standard block gauges. The developed non-contact distance measurement system has been shown to have a resolution of 0.01 mm with the same standard deviation regardless of the absolute value of the height parameters. The relative error of non-contact indirect measuring of the difference in the height parameters has been established.

Keywords: Industrial Growth · Laser Displacement Sensor · Complex-Shaped Surface · Block Gauges · Non-Contact Method · Cross-Section Area · Measurement Bases

1 Introduction

The implants consist of small multiple curved or free-formed surfaces. The geometrical material engagement parameters vary considerably in the case of concave or convex manufacturing. In freeform surface grinding, the engagement between a workpiece and a tool constantly changes; therefore, the material removal rate (MRR) will vary significantly across the implant surface. The contact conditions influence the material removal mechanisms and the mechanical and thermal load of the material in grinding the complex-shaped surface.

© The Author(s), under exclusive license to Springer Nature Switzerland AG 2024
V. Ivanov et al. (Eds.): DSMIE 2024, LNME, pp. 39–50, 2024.
https://doi.org/10.1007/978-3-031-61797-3_4

To understand the process, it is necessary to quantify the MRR during the process. As the tool-workpiece engagement greatly influences process forces, power, specific energy, and machining efficiency, it is beneficial to analyze the engagement situation during machining, including on-machine measurement. The specific energy of the cutting process is an important quantity for various reasons. It is the work required to convert a cubic metal volume into chips and is approximately independent of other variables. Specific energy can also be used as a general metric to describe the efficiency of the machining process. Knowledge of specific grinding energy is required to control the heat intensity of the grinding process.

It isn't easy to perform such an analysis through purely geometric considerations. To ascertain the amount of MRR and the change in depth of cut over the surface of a freeform part, it is more convenient to measure this quantity directly. This can be achieved through non-contact laser profile measurement of the workpiece before and after machining.

The most cost-effective and flexible solution for this application is laser profilometry. Measurements of MRR during the process using this profile measurement technique, combined with the surface acoustic wave (SAW) monitoring, form a process monitoring platform that can serve as a basis for future process optimization through adaptive control.

This study presents the development of a custom laser profile monitoring system that is capable of measuring the difference in the material heights before and after machining. Physical models of the part - an implant - are proposed for the following purposes: one will be used to study and monitor the process in further research; the other will be to test the algorithm for determining the cross-sectional area of the cut and MRR.

Therefore, the paper aims to study the possibility of non-contact laser measurement of the height parameters of the layer of cut material and the difference in the heights with subsequent calculation of the cross-sectional area of the cut layer and MRR using the appropriate MATLAB script.

2 Literature Review

Today, the parts with freeform shapes are widely used in industries such as automotive (car bodies), aerospace (blades, impellers), household appliances (mobile phones), and medicine (femoral implant for orthopedics). In this case, measuring technological systems for freeform shape parts can be the following: coordinate measuring machine, photogrammetry, fringe projection, laser tracker, laser radar, laser scanner, etc. [1, 2]. Non-contact measurement of freeform surfaces is possible using non-contact laser sensors, including multiple-point sensors such as line sensors and single-point sensors such as laser displacement sensors. The latter have become widespread due to their low cost and high accuracy. They can be used for two research directions: to inspect a specific surface of the machined part and to optimize the machining process based on the sensors measurement results [3, 4].

By the first direction (inspection of a specific surface), the laser displacement sensors are used, e.g., to determine the distance between the walls of a wind tunnel, displacement of the valve spool of a solenoid on-off valve acting directly [5], obtaining 3D surface maps of turbine blades for final control of the part [1, 6]; detecting minute cracks in

parts of concrete structures and establishing a correlation of these values with the crack width [7]; measurement of such parameters as the step height, hole diameter, roundness, flatness of cylindrical part [8]; measurement of the thread profile of ball screws and nuts [9]; obtaining a roundness profile and assessing its parameters for wood species with various colors and densities [10].

Following the second direction (optimizing the machining process), the measuring systems based on the laser displacement sensors are used to perform modeled error compensation, planning path optimization, and accuracy analysis after processing [11], as well as for measuring MRR during the abrasive machining for subsequent construction map specific energy and optimizing the process [12].

Modern laser technology has made it possible to obtain positive results in non-contact measurement of height parameters of objects [13, 14]. However, the error of indirect measurements when determining the difference in the measured height parameters has yet to be studied. This task is also relevant when studying the non-contact imaging of subsurface defects, which are detected by ultrasonic waves excited by a laser [15]. The above second direction needs to be sufficiently represented in the literature.

Therefore, despite the widespread use of non-contact laser sensors and the clear (obvious) advantages of their use, researchers are still studying their capabilities, finding ways to improve both their accuracy [6] and expand their capabilities [3]. In the first case (accuracy), an error-compensation model is proposed, which reduces the impact (influence) of the incident angle error of the laser displacement sensors [6]. In the second case (capabilities), a measurement system determines the distance from the sensor to the surface of the specimen (sample). This distance is used as a feedback signal to control the position of the sensor along the Z axis [3]. This will allow the use of a high-resolution sensor to measure parts with a significant variation in height. Such studies are related to geometric and optical measurement conditions (surface quality, surface color, measurement range, and surface orientation) influencing accuracy [6, 10].

To test the accuracy of the laser displacement sensors, researchers compare results obtained by contact and non-contact methods. For example, one of the sections of the turbine blade was tested by the probe of the coordinate measuring machine and laser displacement sensors Keyence LK-G400. The average error is from 12 μm, along with a fourfold increase in productivity [11].

The laser displacement sensor Keyence LK-G80 has more excellent uncertainty components when measuring repeatability and reproducibility than the mechanical probe, as it is more sensitive to the measurement environment, test-piece surface, and vibration. The uncertainties of on-machine measurement using a mechanical probe and a laser displacement sensor were evaluated, with ranges of 2.4–3.7 μm and 4.8–5.8 μm, respectively [8].

The maximum error band of the measurement for the screw and nut is about 4 μm and 4.5 μm, respectively, in comparison with the coordinate measuring machine [9]. The accuracy of the Keyence LC-2450 laser sensor was tested when measuring the roughness of wood species and compared with the results of measurements by the stylus sensor [10]. The roughness parameters are close, but the stylus method gives overestimated results. However, it was found that the assessment of dark wood surfaces and high-density surfaces was imperfect.

That is why the study, which is related to using measurement results to obtain new technological parameters, such as MRR, specific grinding energy, etc., is now relevant. Also, when testing the laser sensor, it is necessary to perform measurements using contact and non-contact methods to determine the error between them.

3 Research Methodology

3.1 General Principles

This study uses the first of three interconnected and sequentially located in time methodological directions: grinding modeling, optimization, and control, i.e., the grinding modeling. Modeling allows using models to replace complex phenomena with corresponding models and study certain phenomena (geometric, thermophysical, dynamic, etc.). Physical models, such as processes-analogues and computer graphic models, make it possible to purposefully study individual properties of complex processes while eliminating the influence of disturbing factors on them. For example, flat grinding with a toroidal grinding wheel may be used as a physical model of the process of grinding implants. It allows for the study of the relationship between the output signal of the sensor and the volume of material removed per time unit, as well as the change in specific grinding energy depending on the conditions of engagement of a grinding wheel and a workpiece. Replacing the actual implant grinding with its physical model of flat grinding allows testing, for example, an algorithm for determining the actual MRR using laser non-contact measurement.

Since the femoral component of knee replacement is a complex-shaped part, its physical models have been developed for experimental studies. The first is a blank of CoCrMoF-75 alloy, which combines convex, flat, and concave surfaces – representatives of the implant part. This model will be further used to relate the output of the SAW sensor integrated into the CBN grinding wheel and determine the actual MRR measured by the laser displacement sensor. The second model (Fig. 1a) tests the algorithm for determining the MRR (Fig. 1b). The specimen is made of medium-carbon steel, the geometric elements of which are cut using wire electrical discharge machining (WEDM).

Laser measurements allow the comparison of two *X-Y-Z* data point clouds (before and after machining). To accurately compare and determine MRR, it is necessary to find the difference between the two data point clouds: before and after machining. To do this, the curves from two data sets (before and after machining) must lie in the same plane and be measured in the same place on the specimen. When performing a measuring operation, the workpiece must be oriented on the table of the measuring device by the basing theory for a prismatic specimen. Additionally, it is necessary to create artificial measurement bases along the X and Y axis – bases 1 (a stair) and 2 (an artificial crack) in Fig. 1b.

The experimental installation (rig) is a benchtop machine designed for use in a laboratory environment to perform surface displacement and roughness measurements. Its operating principle is gathering 2D line scans of a part by moving it to be measured underneath a chromatic confocal sensor and laser displacement sensor. This is achieved by placing the part in an automated *XY* stage (table of the rig). The sensors are mounted to

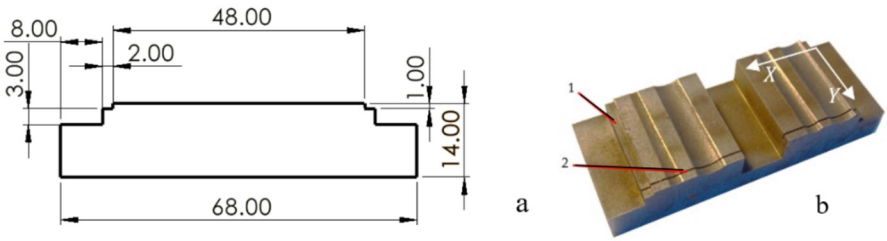

Fig. 1. Specimen for study without (a) and with (b) grooves to be measured.

an automated *Z* axis, which is positioned before measurements so that the part's surface is within the sensor's range.

3.2 Materials and Methods

The experimental rig (Fig. 2), called "SR-Test Precision", is designed as a laboratory benchtop machine for measuring displacement and surface roughness. The main components of the measuring system have been purchased, but the rig is designed and manufactured for the first time. The main part of the rig is the laser displacement sensor IL-S025 based on the triangulation principle (on the left in Fig. 2a) and the laser chromatic confocal sensor CL-PT010 (on the right in Fig. 2a). The "SR-Test Precision" was developed at Trinity College Dublin and is designed for industrial and laboratory applications. It is used for (1) characterizing the surface roughness of sample parts, (2) measuring the geometry and dimensions of the surface and their features, and (3) in-process quality control and dimensional testing.

This study uses a laser displacement sensor Keyence IL-S025 (KEYENCE, Osaka, Japan). The Keyence laser displacement sensor system comprises two main hardware components: the Keyence IL-S025 sensor head unit and the IL-1000 sensor amplifier unit (Fig. 2b). The Keyence IL-S025 sensor head (KEYENCE, Osaka, Japan) specification includes the following characteristics: reference distance is 25 mm $\pm$ 0.25 mm; measurement range 25 mm $\pm$ 5 mm; spot diameter is approximately 25 $\times$ 1200 μm; repeatability 1 μm; sampling rate 0.33/1/2/5 ms; light source type is the red semiconductor laser; wavelength 655 nm (visible light); laser class 2 with output 560 μW.

Triangulation sensors and confocal sensors are the most common laser sensors, but they differ in their operation principle. The laser sensor with the triangulation method (Fig. 3a) measures the distance to an object (Fig. 3b). When the target position is altered, the beam spot on the complementary metal-oxide-semiconductor (CMOS) moves. These devices measure the displacement of targets by detecting the position of the beam spot. This algorithm identifies differences in CMOS received light waveforms generated by changes in surface conditions of the target workpiece and automatically processes the waveforms in the best manner possible. For example, it is possible to perform stable detection without tuning, even on metal hairlines, plastic, rubber, and other workpiece that have always been difficult to detect. The known applications are positioning, thickness measurement, detecting welding seams, counting sheets, detecting molten metal level, controlling marking height, etc.

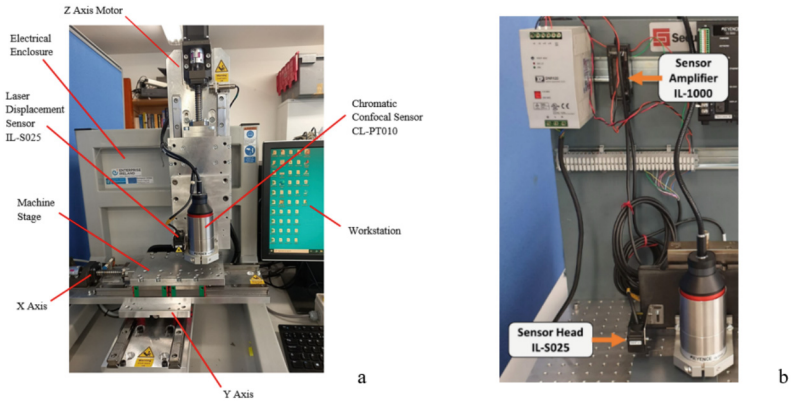

Fig. 2. SR-Test Precision machine general view (a) and its hidden components (b).

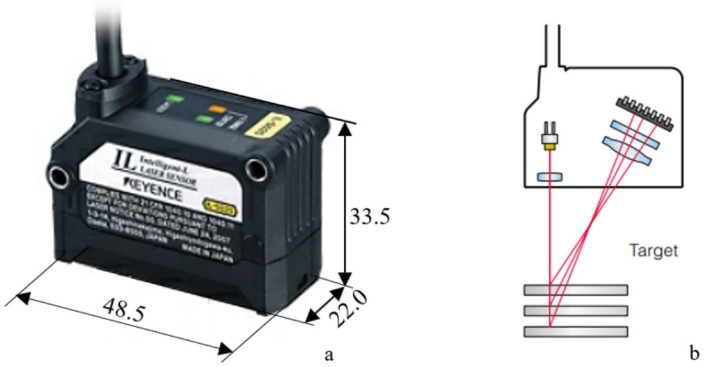

Fig. 3. Keyence laser displacement sensor (a) and its triangulation work principal (b).

The Keyence laser displacement sensor system is set up as shown in Fig. 4. The Keyence IL-S025 laser sensor head is connected directly to the Keyence IL-1000 sensor amplifier unit by aligning, inserting, and tightening the connection cables. A National Instruments compact (cRIO-9066) with an analog input module (NI-9239) was used to interface with the sensor amplifier unit. Once the hardware and software are set up, measurement data from the Keyence laser displacement sensor can be directly read from the cRIO-9066 through LabVIEW.

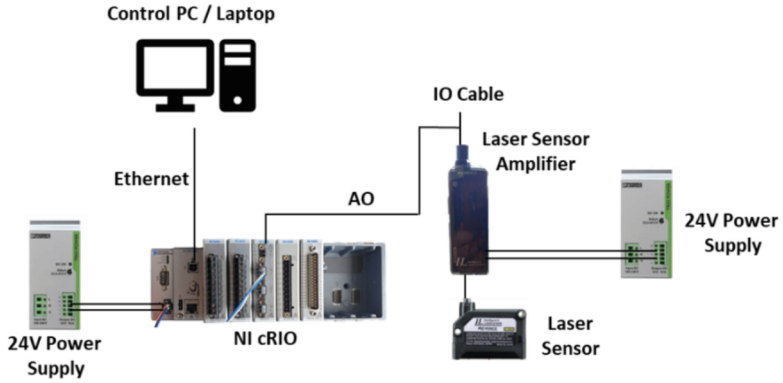

Fig. 4. Chromatic confocal sensor wiring diagram.

4 Results and Discussion

4.1 Measurement Accuracy Study

All block gauges were measured by Keyence IL-S025 laser sensor (Fig. 5) when the length for evaluation is 38 mm, the head speed is 4 mm/s, the ramp distance (or run-on and run-off distance) is 1 mm; the number of tracks is 3, track offset is 5 mm, and acceleration is 5 mm/s^2. The steps, i.e., the difference in the heights measured, were evaluated by measuring three tracks that had a distance of 5 mm between them. Each track was repeated triply by contact electronic digital indicator EDI-125 with resolution 0.001 mm and accuracy $\pm$0.005 mm on the one hand and laser displacement sensor on the other hand. The latter moved with a velocity of 4 mm/s. The results of measuring the steps, sample standard deviation, and error margin of the laser displacement sensor for IL-S025 were calculated. When measuring the same tracks three times on different gauge blocks during measuring steps from 0.01 mm to 1.6 mm, the sample standard deviation values are in the range of 0.00011 mm to 0.010 mm; the margin of error is from 0.000272 mm to 0.025260 mm. As mentioned above, all block gauges were measured using a dial gauge (electronic digital indicator EDI-125) and a laser displacement sensor (Keyence IL-S025 laser displacement sensor). The steps found from the average measurement values for the contact and non-contact methods and the error are presented in Table 1.

The proposed system's ability to measure displacement from 0.01 mm to more is demonstrated in experimental data. The maximum relative error in this range is 8.4% (Table. 1).

4.2 The Cut Layer Cross-Sectional Area Determination

The "SR-Test Precision" was used to determine the cut layer's cross-sectional area and the cut layer's volume. The corresponding scripts were written in MATLAB. Block diagram fragments of the sequence of actions are presented in Fig. 6.

Distance measurements along the profile of the specimen (later, it will be an implant) are accomplished through the following measurement strategy: the laser is fired, displacement is recorded, the motor moves the part by a set step along the *X*-direction,

a

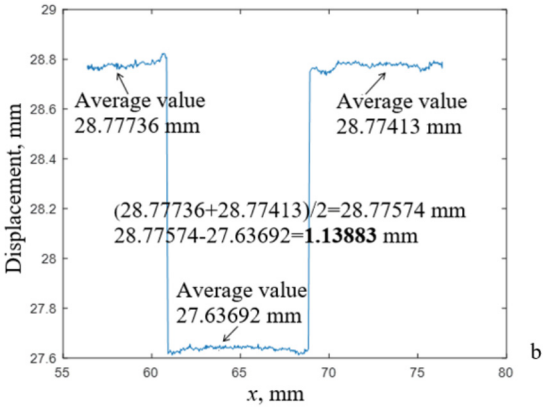

b

Fig. 5. Experimental setup (a) while measuring the block gauges' heights and difference between them (b) using IL-S025 laser displacement sensor for the heights of 1.07 mm,1.08 mm, 1.10 mm, 1.13 mm, 1.18 mm, 1.30 mm, 1.50 mm, 1.80 mm, 3.4 mm, 3 mm, and 4 mm.

Table 1. The steps were measured using a laser displacement sensor and digital indicator.

Nominal heights of gauge blocks, mm	Difference in the adjacent heights (step), mm	The average step, mm		Relative error, %
		Dial gauge (EDI-125) contact method	Laser displacement sensor (Keyence IL-S025) non-contact method	
1	2	3	4	5
1.07	–	–	–	–
1.08	0.01	0.012	0.012789	6.58
1.10	0.02	0.021	0.019224	8.46
1.13	0.03	0.032	0.031444	1.74
1.18	0.05	0.049	0.045553	7.03
1.30	0.12	0.117	0.125314	7.10
1.50	0.2	0.197	0.198435	0.73
1.80	0.3	0.306	0.296655	3.05
3.4	1.6	1.598	1.583146	0.02
3.0	0.4	0.398	0.402041	1.02
4.0	1.0	1.001	0.997166	0.38
Note: columns 3 and 4 show the average values obtained for three tests and three tracks				

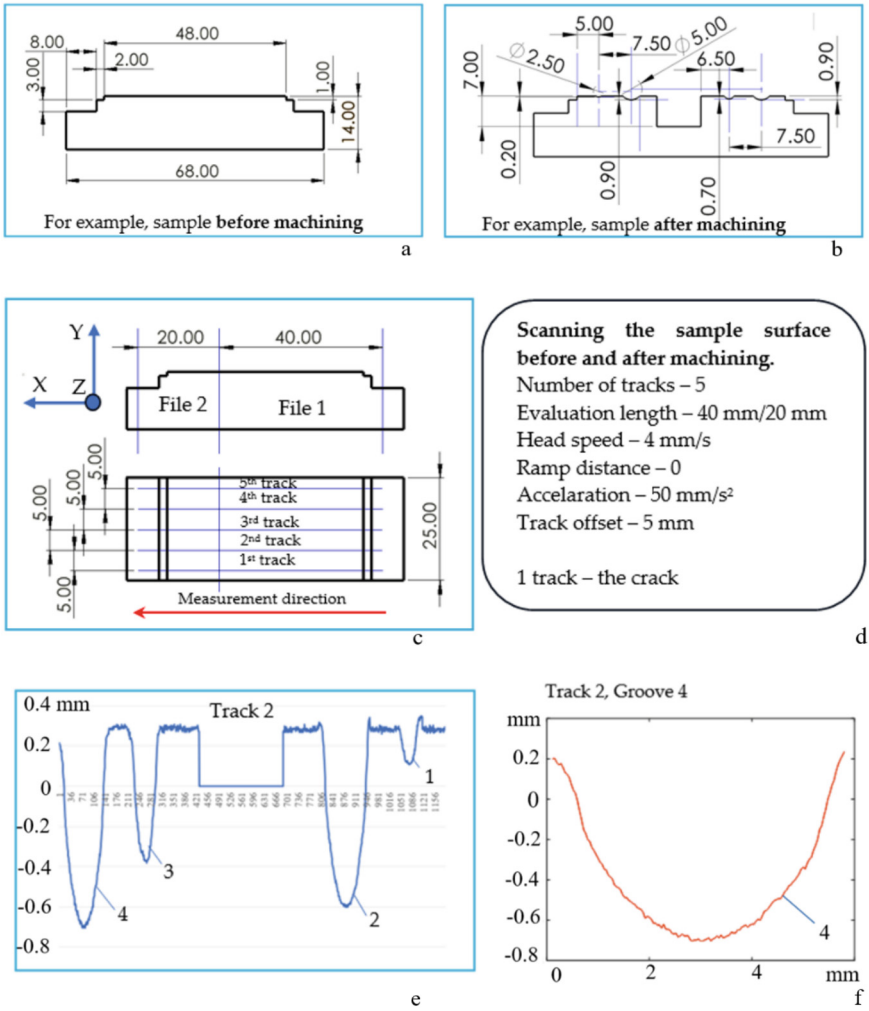

Fig. 6. MATLAB scripts: samples before (a) and after (b) machining, scanning plan (c) and its parameters (d), graphic images of four (1, 2, 3, 4) grooves (e) and an enlarged image of the fourth groove (f).

then the part is moved along the *Y*-direction by a set step, and the scanning procedure along *X*-direction repeats until a complete profile scan is acquired (or specified number of scanned lines). Some blocks in Fig. 6 are omitted, namely: "Formation of files (arrays) for working zone", "Building of surface topography from 4 tracks with a distance 5 mm", and "Determination of cross-sectional areas". Calculating results of the cross-sectional areas according to 4 tracks are 3.4916 mm^2 (track 2), 3.5586 mm^2 (track 3), 3.5005 mm^2 (track 4), and 3.5221 mm^2 (track 5). Average cross-section area value 3.5182 mm^2. The theoretical cross-section area, calculated using the formula for the area of a circle segment, is 3.5012 mm^2. That is a relative error of 0.4855%.

4.3 Discussion

The surface's reflective properties and roughness affect the non-contact measurement method. The smaller the height difference, the greater the relative measurement error (see Table 1). For example, for height difference intervals of 0.01–0.12 mm (average value 0.065 mm) and 1.0–1.6 mm (average value 1.3 mm), we have error intervals of 1.74–8,46% (average value 4.965%) and 0.38–0.02% (average value 0.2%), respectively. It can be seen that an increase in the measured parameter (the average height difference of the measured object) from 0.065 mm to 1.3 mm (20 times) leads to a decrease in the relative measurement error from 4.965% to 0.2% (24.825 times). In addition, it is necessary to consider that the measured parameter (increase in object height or step) is the result of an indirect measurement. The value of this parameter is equal to the difference between the results of two direct measurements, each of which has its measurement error. It is known that the error in the difference between the results of two direct measurements is equal to the sum of the errors of these measurements, i.e., the error of indirect (or oblique) measurement is about twice as significant as each of the indicated errors of direct measurement.

The results obtained on the relative error of non-contact laser measurement of height parameters are consistent with what was known earlier [13, 14] and are even much better. For example, when measuring roughness height parameters, the relative error of non-contact measurement compared to the corresponding contact measurement was within 10% [13] and 23.7% [14].

5 Conclusions

A laser displacement sensor Keyence IL-S025 non-contact measuring system has been developed. The system allows for determining the material removal rate in the machining process, such as grinding, wire electrical discharge machining (WEDM), etc. In addition, the system can control the measurement head speed, evaluation, traverse lengths, cut-off, the number of working tracks, and the distance between the measured tracks. The software developed in MATLAB allows the cross-section area of the cut layer and material removal rate in the cutting by WEDM to be calculated. This will make it possible to determine similar parameters when grinding implants to determine the specific grinding energy and parameters connected with it., e.g., grinding temperature.

A non-contact laser measurement system developed for this research was used to determine the material removal rate in the different cutting processes, such as grinding the freeform surfaces, the WEDM, etc. The developed non-contact distance measurement system based on the Keyence IL-S025 laser sensor head has shown a resolution of 0.01 mm with the same standard deviation regardless of the absolute value of the height parameters in the specified height range.

It has been shown that the measured height of the standard block gauge is invariant to the speed of the laser head. Therefore, you can set the maximum speed of the laser head during the measurement, i.e., 4 mm/s.

For the measured steps from 0.01 mm to 1.60 mm, the standard deviation changes in the range of 0,01 mm, and the margin of error does not exceed 0.02526 mm.

When measuring block gauges using contact and non-contact methods, the relative error does not exceed 8.46%.

A methodology and corresponding scripts in MATLAB have been developed to determine the cut layer cross-sectional areas and the material removal rate. The technique was tested on a specially designed sample with radius grooves cut using the WEDM. For example, the cross-section area, calculated as an average value over four tracks on the specimen, is 3.5182 mm, in contrast to the theoretical one, 3.502 mm, i.e., the difference between the theoretical groove area and the experimental one is 0.4855%.

Acknowledgment. This research was carried out at the Department of Mechanical, Manufacturing, and Biomedical Engineering of Trinity College Dublin in accordance with the project "Data-driven optimization of complex-shaped parts produced by grinding and abrasive processes", funded by Enterprise Ireland and the European Commission under the Horizon 2020 Marie Skłodowska-Curie Actions.

References

1. Schöch, A., Savio, E.: High-speed measurement of complex shaped parts by laser triangulation for in-line inspection. In: Gao, W. (ed.) Metrology, pp. 307–328. Springer Singapore, Singapore (2019). https://doi.org/10.1007/978-981-10-4938-5_10
2. Savio, E., De Chiffre, L., Schmitt, R.: Metrology of freeform shaped parts. CIRP Ann. **56**(2), 810–835 (2007). https://doi.org/10.1016/j.cirp.2007.10.008
3. Yangsheng, L., Lijue, X.: Surface contour measurement using a short range laser displacement sensor. In: Proceedings of the 20th international solid freeform fabrication symposium (2009)
4. Zha, J., Zhan Li, H.: Analysis of the principle of laser displacement sensor and its application. Appl. Mech. Mater. **734**, 84–89 (2015). https://doi.org/10.4028/www.scientific.net/AMM.734.84
5. Suh, Y.S.: Laser sensors for displacement, distance and position. Sensors **19**, 1924 (2019). https://doi.org/10.3390/s19081924
6. Sun, B., Li, B.: Laser Displacement sensor in the application of aero-engine blade measurement. IEEE Sens. J. **16**(5), 1377–1384 (2016). https://doi.org/10.1109/JSEN.2015.2497363
7. Giri, P., Kharkovsky, S.: Detection of surface crack in concrete using measurement technique with laser displacement sensor. IEEE Trans. Instrum. Meas. **65**(8), 1951–1953 (2016). https://doi.org/10.1109/TIM.2016.2541358
8. Ding, D., Zhao, Z., Li, Y., et al.: Calibration and capability assessment of on-machine measurement by integrating a laser displacement sensor. Int. J. Adv. Manuf. Technol. **113**, 2301–2313 (2021). https://doi.org/10.1007/s00170-021-06676-5
9. Huang, H.-L., et al.: Development of a novel laser-based measuring system for the thread profile of ballscrew. Opt. Lasers Eng. **48**, 1012–1018 (2010). https://doi.org/10.1016/j.optlaseng.2010.05.002
10. Sandak, J., Tanaka, C.: Evaluation of surface smoothness by laser displacement sensor 1: effect of wood species. J. Wood Sci. **49**, 305–311 (2003). https://doi.org/10.1007/s10086-002-0486-6
11. Ding, D., Ding, W., Huang, R., Fu, Y., Xu, F.: Research progress of laser triangulation on-machine measurement technology for complex surface. A review. Measurement **216**, 113001 (2023). https://doi.org/10.1016/j.measurement.2023.113001

12. Brazel, E., Hanley, R., Cullinane, R., et al.: Position-oriented process monitoring in freeform abrasive machining. Int. J. Adv. Manuf. Technol. **69**, 1443–1450 (2013)
13. Lishchenko, N., O'Donnel, G.E., Culleton, M.: Contactless method for measurement of surface roughness based on a chromatic confocal sensor. Machines **11**, 836 (2023). https://doi.org/10.3390/machines11080836
14. Lishchenko, N., Piteľ, J., Larshin, V.: Monitoring of surface quality for diagnostic features in 3D printing. Machines **10**(7), 541 (2022). https://doi.org/10.3390/machines10070541
15. Hayashi, T., Mori, N., Ueno, T.: Non-contact imaging of subsurface defects using a scanning laser source. Ultrasonics **119**, 106560 (2022). https://doi.org/10.1016/j.ultras.2021.106560

Advancing Circular Economy: The Product Circularity Index as a Tool for Sustainable Design

Foivos Psarommatis[1,3(✉)], Fotios K. Konstantinidis[2], Victor Azamfirei[3], and Gökan May[4]

[1] SIRIUS, University of Oslo, 23B, Gaustadalleen, 0373 Oslo, Norway
foivosp@ifi.uio.no
[2] Institute of Communication and Computer Systems, 15772 Zografou, Athens, Greece
[3] Zerofect GmbH, Alblisbick 49, 6319 Baar, Switzerland
[4] University of North Florida, Jacksonville, FL 32224, USA

Abstract. The rise of the fast-consuming era, marked by manufacturers continuously increasing production rates, has led to the design and manufacturing of products without due consideration for sustainability aspects. Despite the overall reduction in production costs, this approach harms the environment and circumvents circularity methodologies. To bridge the gap between traditional design practices and sustainability, we propose a structural method for measuring circularity in design. The introduced Product Circularity Index (ProdCircIn) serves as a quantifiable measure to assess a product's alignment with circular economy principles and functions as a key performance indicator (KPI) for evaluating and comparing products based on their circularity attributes. Specifically, ProdCircIn evaluates products in six pillars: design philosophy, usage of materials, design for manufacturing, design for quality, design for warranty, and design for the future. These pillars are quantified through relevant questionnaires, as analytical solutions and formulas could be more practical due to the distinct characteristics of each product.

Keywords: Circularity Index · Sustainable Design · Product Design · Circularity · Sustainability · Product Innovation

1 Introduction

The concept of a circular economy (CE) has gained significant traction as a sustainable alternative to the traditional linear economy based on a 'take-make-dispose' model [1]. This linear approach leads to substantial waste and environmental degradation [2, 3]. In contrast, the circular economy aims to redefine growth, focusing on positive society-wide benefits by decoupling economic activity from the consumption of finite resources and designing waste out of the system [4]. It is underpinned by a transition to renewable energy sources and builds economic, natural, and social capital [5].

© The Author(s), under exclusive license to Springer Nature Switzerland AG 2024
V. Ivanov et al. (Eds.): DSMIE 2024, LNME, pp. 51–62, 2024.
https://doi.org/10.1007/978-3-031-61797-3_5

In the context of product design and manufacturing, Circularity refers to creating products and systems that are regenerative by design [6]. This approach aims to retain as much value as possible from products, parts, and materials [7]. In a circular system, product life cycles are extended. When products reach the end of their life, materials are kept within the economy wherever possible through strategies such as reuse, repair, refurbishment, and recycling, reducing waste [8].

A pivotal component in realizing the vision of a circular economy is the Digital Product Passport (DPP), a digital twin of a physical product that contains all relevant information about the product's lifecycle [9]. The DPP enables manufacturers, consumers, and recyclers to access crucial information, facilitating decision-making towards more sustainable and circular practices [10]. It also plays a crucial role in traceability and accountability in supply chains [11].

Sustainable product design is a cornerstone of shifting towards a circular economy [12]. It involves designing products with minimal environmental impact, considering energy efficiency, material selection, and end-of-life disposal [13]. Sustainable design focuses on extending the lifespan of products, facilitating repair and reuse, and ensuring that its materials can be easily recovered and recycled [14].

In the circular economy, the product lifecycle is viewed through a lens emphasizing longevity, renewability, and recyclability [15]. This lifecycle approach considers every stage of a product's life, from design, production, and use to end-of-life management [16]. The goal is to create a closed-loop system where products are designed for longevity, repairability, and recyclability, thereby minimizing the environmental impact and resource depletion [17].

A critical challenge in transitioning to a circular economy is evaluating product designs for their circularity [18]. Traditional design metrics focus on functionality, cost, and aesthetic appeal, often neglecting the aspect of circularity [19]. This oversight can lead to inherently unsustainable designs and contribute to the depletion of finite resources. To address this gap, there is a need for a comprehensive measure to evaluate product designs for their alignment with circular economy principles. Such a measure would assist designers and manufacturers in optimizing product designs toward circularity and more sustainable manufacturing processes.

Introducing a Product Circularity Index (ProdCircIn) could be a groundbreaking step in this direction. ProdCircIn would be a quantifiable measure to assess how well a product aligns with circular economy principles. It would guide designers in integrating circular approaches like modularity, ease of disassembly, and use of sustainable materials right from the design phase. This index would serve as a design tool and a key performance indicator (KPI) for evaluating and comparing products on their circularity attributes.

This paper introduces the concept of ProdCirIn, a novel tool designed to evaluate and enhance the circularity of product designs. We discuss the methodology behind ProdCircIn, its components, and how it can be applied in various product design and manufacturing stages. ProdCircIn aims to bridge the gap between traditional design practices and the imperative for sustainability in the modern world by providing a structured and quantifiable approach to circular design.

2 Literature Review

Transitioning to a CE necessitates a nuanced understanding of product design and lifecycle management, which have witnessed significant scholarly attention. Recent research in this domain has been diverse, focusing on developing methodologies, frameworks, and tools to facilitate this transition.

Noteworthy contributions in the realm of circular economy indicators and tools in product design have been made by [20] and [21]. Saidani and Kim identified twelve product-centric circularity indicators, each with a computational tool, and mapped them along a generic five-step design process. This approach underscores the importance of integrating circularity considerations early in the design phase. Complementing this, Ruiz-Pastor et al. introduced the CN_Con metric, which uniquely measures the circularity and novelty of conceptual design proposals, emphasizing the role of creativity in circular design.

In assessing circularity at a broader level, [22] and [23] have explored sustainability indicators and performance evaluation frameworks. Konstantinidis et al. [24] focused on evaluating machine vision systems as products, considering circularity principles. Mesa et al. (2018) proposed a set of sustainability indicators specifically for product families, focusing on material flow, reusability, and functional performance. This family-centric approach provides a unique perspective on circularity. Hapuwatte et al. (2022) extended the concept of product sustainability performance (PSP) into a dynamic measure, proposing a metrics-based framework that considers variations in demand and production over time. This work highlights the evolving nature of PSP in closed-loop productions.

Some other research works have focused on applying circularity principles in manufacturing and eco-labeling [25] and [26]. Azevedo et al. proposed a Sustainable Circular Index (SCI) for manufacturing companies, a benchmarking tool for assessing and improving sustainable practices. Lanaras-Mamounis et al. developed an Eco-Label Circularity Index (ECI) to assess the circularity level of eco-labels, addressing the gap in conveying circular economy information to consumers.

The theoretical foundations and practical tools for circular product design have been studied by [19, 27], and [28]. Corona et al. critically assessed existing circularity metrics, revealing a need for more comprehensive approaches that avoid burden shifting [19]. Shevchenko and Cluzel announced the development of a Circular Product Design Toolkit (CPD Toolkit) aimed at enhancing product circularity through redesign. Patti's work on eco-efficiency and circularity measurement provides insights into the relationships between ecosystems, resources, and circularity metrics [27].

Saidani et al. have taken a different approach by reviewing and classifying 55 sets of circularity indicators, proposing a need-driven taxonomy to clarify their purposes and usages [29]. This taxonomy provides a systematic approach to selecting appropriate indicators, addressing the diverse needs of different CE applications.

The reviewed literature collectively underlines the growing importance of circularity in product design and the need for robust metrics and tools to evaluate and enhance this circularity. These studies offer a rich tapestry of methodologies and insights, from comprehensive frameworks and taxonomies of circularity indicators to specific metrics for assessing product designs and manufacturing practices. However, a common thread in these studies is the acknowledgment of existing gaps, such as the underrepresentation

of complex cycles, the need for dynamic measures in sustainability performance, and the absence of holistic approaches to circularity evaluation.

The diversity in focus areas - from product design and manufacturing to eco-labels and product families - reflects the multifaceted nature of CE and the necessity for tools that cater to different stages and aspects of the product lifecycle. Integrating these approaches and tools into practical applications remains a critical challenge, highlighting the need for continued research and development in this field.

This summary table below, Table 1, encapsulates the core contributions of each paper, providing a quick reference for researchers and practitioners in the field of CE.

Table 1. Top 10 key contributions in Product Circularity Index.

Paper	Authors	Year	Focus Area	Key Contribution
[20]	Saidani, Kim	2021	Product Design	Identified 12 circularity indicators for design phases
[21]	Ruiz-Pastor et al	2022	Conceptual Design	Developed CN_Con metric for circularity and novelty
[22]	Mesa et al	2018	Product Families	Proposed sustainability indicators for product families
[23]	Hapuwatte et al	2022	Sustainability Performance	Metrics-based framework for dynamic sustainability evaluation
[25]	Azevedo et al	2017	Manufacturing	Sustainable Circular Index for manufacturing companies
[29]	Saidani et al	2019	Circular Economy Indicators	Taxonomy of circularity indicators
[26]	Lanaras-Mamounis et al	2022	Eco-Labels	Eco-Label Circularity Index
[19]	Corona et al	2019	Circularity Metrics	Critical assessment of circularity metrics
[27]	Shevchenko, Cluzel	2023	Product Redesign	Circular Product Design Toolkit
[28]	Patti	2023	Eco-Efficiency	Discussion on eco-efficiency and circularity metrics

Building on the foundations laid by the aforementioned studies, our paper seeks to address the critical gaps in the circular economy and product design field. While existing research has made significant strides in developing indicators, metrics, and tools for assessing circularity, a comprehensive and integrated approach that seamlessly blends

these elements into the product design and manufacturing process still needs to be discovered. Our work introduces ProdCircIn, a novel framework that quantifies the circularity of products and guides designers and manufacturers in embedding circular principles from the conception phase to end-of-life management. ProdCircIn is designed to be dynamic, acknowledging the evolving nature of products and production processes, and adaptable to various product types and manufacturing contexts. By providing a structured and quantifiable approach to a circular design, ProdCircIn aims to bridge the gap between theoretical circularity metrics and practical application in product development, offering a holistic, theoretically robust, and practically applicable tool. This approach is anticipated to catalyze a paradigm shift in evaluating and implementing product circularity, contributing significantly to advancing sustainable manufacturing practices.

3 Research Methodology

The product circularity index (ProdCircIn) is meant to be calculated during the design phase of a product, and this index will accompany the product throughout its entire lifecycle. ProdCircIn measures how circular a product is; more specifically, it indicates how easy or difficult the different circular approaches can be applied. Circular approaches are considered the reuse, repurpose, and recycling of the product [8]. Within those three circular approaches are other concepts, such as remanufacturing, repairing, etc. The ProdCircIn can be used in two ways: during the product's design process, in addition to the functional requirements, the circular requirements can also be added as a KPI for selecting the most circular design. The second way of using ProdCircIn is to compare products of the same type together as a consumer or OEM, supplier, etc. Figure 1 illustrates the sustainable/ circular product life cycle taken from [8] and the proposed additional steps in the product design to make the products more circular.

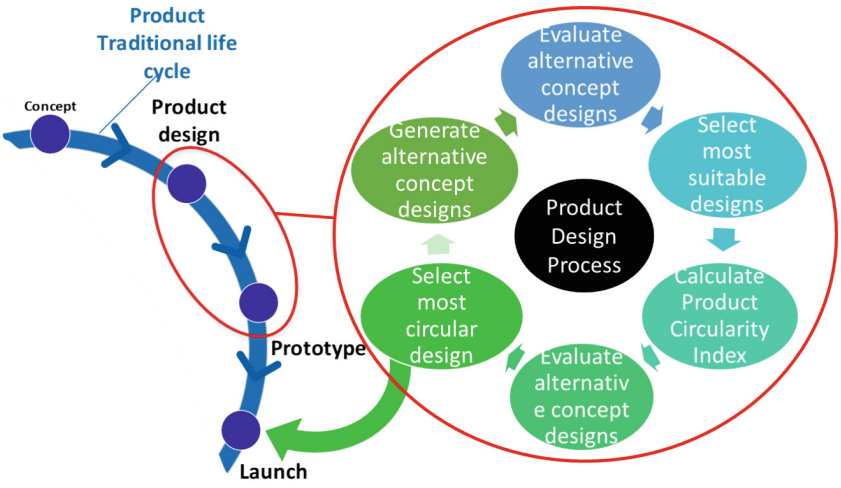

Fig. 1. Interplay between Product design and Circular product design cycles (adapted from [8]).

Once the product has been conceptualized, alternative designs are produced and evaluated according to their conformance to the product requirements. As a second phase, the product circularity is calculated to identify and improve the most circular designs if needed. Therefore, the circularity index is assessed in the following circ-disciplines based on the product life-cycle, from the design phase up to recycling.

3.1 Components of Circular-Design

The circular design is the main pillar of the circularity index as it refers to the principles used to design environmentally friendly products to be easily reused, repurposed, or recycled at the end-of-life phase. The following aspects are assessed:

- Product modularity and simplicity: Simplification of the design drives to reduce the number of components, not only simplifying manufacturing operations but also facilitating non-complex disassembly that drives to repair and recycle [30, 31] easily.
- Design philosophy: Clever and innovative design generates products without complex assembly needs with add-on substances (e.g., screws), which normally minimize the scraps and discards. In addition, these intelligent designs aim to reduce the mass and volume of products, minimizing also the packaging needs [14].
- Circular Material: Non-toxic and harmless materials offer simple recycling processes without chemical-based valorization techniques, reducing the overall environmental impact. On the other hand, renewable and bio-based materials contribute to waste segregation, while recycled materials should also be used in the design process [14].
- Manufacturing simplicity: Simpler designs without needing to be manufactured in different factories, which leads to easier manufacturing, assembly, and maintenance by the use of standardized components and processes to reduce the need for specialized tools [32].
- Upscaling philosophy: The product can be easily disassembled by employing modular design and standardized components. This allows for the reuse of specific components in manufacturing the same or other products [30, 31].
- Maintenance support: Exclusive repair services are performed by OEMs or certified service personnel authorized by the manufacturer, ensuring that repairs are conducted with the utmost expertise, adherence to quality standards, and utilization of genuine components, reducing logistics and extending the lifecycle [33, 34].

3.2 Assessing the Circularity Index

The assessment of the ProdCircIn is a challenging task. Analytical solutions and formulas cannot be applied due to the different characteristics of each product. Therefore, the questionnaire method has been employed [35]. Table 2 presents the questions developed for that scope and the generic categories each question falls into. In total, 30 questions were defined under different categories. The questions have only two possible answers: Yes and No. Each answer has a value if it is yes then it is +0.5 if it No then it is −0.5. Equation 1 presents how ProdCircIn is calculated, i represents the question and w is the weight of the answer of the question.

$$ProdCircIn = 30 + \sum_{i=1}^{30} w_i \tag{1}$$

Table 2. Questionnaire for ProdCircIn calculation.

Category	Question	Answer
Design Philosophy	-Is the product designed with scope to be reused after end of first life?	Yes/No
	-Is the product design structured to accommodate modular components?	Yes/No
	-Can individual components be easily identified and replaced without affecting the entire product?	Yes/No
	-Are there clear interfaces between different components to ensure seamless integration?	Yes/No
Materials	-Does the materials used in the product are non-toxic and harmless? -Can all the materials be recycled?	Yes/No
	-Does the choice of materials influence the ease of disassembly?	Yes/No
	-Are renewable and bio-based materials integrated into the design contributing to waste segregation?	Yes/No
	-Are recycled materials incorporated into the design of the product?	Yes/No
Design for Manufacturing	-Can the product be manufactured in a single facility?	Yes/No
	-Can highly flexible machines such as Additive Manufacturing (AM) be used to alleviate the usage of the global supply chain?	Yes/No
	-Does the design minimize the need for complex assembly processes, such as the use of add-on substances like screws?	Yes/No
	-Can the product assembly be easily understood and executed without extensive training?	Yes/No
	-Does the design minimize the number of components while maintaining functionality?	Yes/No
	-Does the design contribute to reducing the time and complexity of the assembly phase?	Yes/No
	Are there permanent assembly processes that make disassembly difficult (glue, weld, etc.)?	Yes/No
	-Can the disassembly of the product be easily performed without putting the entire product	Yes/No
Design for Quality	-Does the selected material present reflective or extremely light-absorbent properties?	Yes/No
	-Are the components easily identifiable and separable?	Yes/No

(*continued*)

Table 2. (*continued*)

Category	Question	Answer
	-Does the design use highly standardized modular pieces?	Yes/No
	-Are previous customer and operator complaints considered in the new design?	Yes/No
	-Is the cost of quality thoroughly considered?	Yes/No
Design for warranty	-Are special tools or expertise required for disassembly?	Yes/No
	-Are there any certifications/training required to become an authorized personnel member for repairs?	Yes/No
	-Does the repair service ensure the use of genuine components in the repair process?	Yes/No
	-Are there specific repair and maintenance strategies aimed at maximizing product longevity?	Yes/No
	-Are OEM repair services accessible to customers, especially in different geographic locations?	Yes/No
Design for the future	-Can components from this product be easily integrated into the manufacturing of the same product?	Yes/No
	-Has a lifecycle assessment been conducted to evaluate the product's environmental impact from production to disposal?	Yes/No
	-Has the product been designed for multiple lives and not only one?	Yes/No
	-Is compatibility with future technologies or upgrades considered?	Yes/No

4 Results and Discussion

The linear economic approach has so far led to substantial waste and environmental degradation. The transition to a circular economy, in the context of this paper, refers to creating products and systems that allow for modularity, repairability, updatability, and wasteless end-of-life. Though all these design concepts are not new-- -and may date back to the 13th century (repairability), 1965 (modularity), and 1994 (upcycling)-- -it has yet to be widely accepted by the manufacturing industry. Quality and Sustainability start from the design of the product and its respective systems.

Sustainable product design involves creative thinking, prototyping, testing, and planning for such products. Sustainability is the balance of innovation and environmental responsibility. Design tools have been historically criticized for "limiting" divergent and innovative thinking. In this paper, we argue that modern design thinking can benefit from calculating the ProCirIn before reaching the final design, which makes it faster and more environmentally friendly, as seen in Fig. 1.

In contrast to previous methods presented in Sect. 2, the proposed questionnaire for assessing the ProdCirIn assesses from cradle to cradle, from design to new life and end-of-life. First, philosophy, the design already starts with the vital CE design components. Second, materials and the finite nature of the earth force modern designers to think about energy, availability, and contamination. Third, Design for manufacturing, the global supply chain has yet to reach a level of robustness that allows for a sustainable future. Reducing the number of manufacturing facilities needed when designing new products is important. Emerging tools such as AM should be thoroughly considered early in securing the future. Fourth, Design for quality, no system is perfect or error-free. Designers should design with defects in mind, such as how they may occur during the manufacturing process or the usage of that product. Thus, Fifth, Design for warranty, Warranty is an incidental process that most manufacturers offer to maintain their reputation in case of design or manufacturing failure. This step should be avoided as the cost of appraisals is lower than customer dissatisfaction, recall of products, and repair in the warranty period. Finally, Design for the future. Designing for the future is a key requirement in CE. The human mind, extremely capable of imagining and creating new ideas all the time, is prone to underestimate future prognostics. Thus, creating processes to aid such minds in developing the best sustainable future is logical. Products should be designed not only for current environmental requirements but also for future ones and economic requirements. In other words, products should be easily repairable, updateable, repurposed, or recycled; being the last one the least desired option.

5 Conclusions

This paper presents a comprehensive measure to evaluate product designs and their alignment with CE principles. For that purpose, a questionnaire was created and discussed. Such a measure would assist designers and manufacturers in optimizing product designs toward circularity and more sustainable manufacturing processes. The questions are formulated from cradle to cradle, from the beginning of the creative process to the end-of-life and new-life assessment. It comprises addressing (1) design philosophy, (2) usage of materials, (3) design for manufacturing, (4) design for quality, (5) design for warranty, and (6) design for the future. In contrast to current frameworks, the design, manufacturing, availability of resources, and quality are treated simultaneously and not isolated, as all are part of a more extensive system, and their interplay may negatively affect the Circular Economy. Future efforts will concentrate on quantifying the proposed questions and more detailed reinterpretation in collaboration with practitioners. The digital product passport concept will be linked as it will benefit the ProdCircIn calculation. Furthermore, as design and manufacturing directly influence the CE, new emerging manufacturing concepts such as machine as a service, manufacturing as a service, and zero-defect manufacturing need to be analyzed and compared with the goal of having the lowest impact possible while maintaining economic and social leverage.

Acknowledgment. The presented work was partially supported by the projects CIRCULess, and PLOOTO, EU H2020 projects under grant agreements No 101138330 101016175, and 101092008 accordingly.

References

1. Elisha, O.: Moving beyond take-make-dispose to take-make-use for sustainable economy. Int. J. Sci. Res. Educ. **13**(3), 497–516 (2020)
2. Sariatli, F.: Linear economy versus circular economy: a comparative and analyzer study for optimization of economy for sustainability. Visegrad J. Bioecon. Sustain. Develop. **6**, 31–34 (2017). https://doi.org/10.1515/vjbsd-2017-0005
3. Konstantinidis, F.K., et al.: Multi-modal sorting in plastic and wood waste streams. Resour. Conserv. Recycl. **199**, 107244 (2023). https://doi.org/10.1016/j.resconrec.2023.107244
4. Heikkinen, A., Kujala, J., Blomberg, A.: Outlining stakeholder engagement in a sustainable circular economy. In: Kujala, J., Heikkinen, A., Blomberg, A. (eds.) Stakeholder engagement in a sustainable circular economy: theoretical and practical perspectives, pp. 1–15. Springer International Publishing, Cham (2023). https://doi.org/10.1007/978-3-031-31937-2_1
5. Khanna, M., Gusmerotti, N.M., Frey, M.: The relevance of the circular economy for climate change: an exploration through the theory of change approach. Sustainability **14**, 3991 (2022). https://doi.org/10.3390/su14073991
6. Reslan, M., Last, N., Mathur, N., Morris, K.C., Ferrero, V.: Circular economy: a product life cycle perspective on engineering and manufacturing practices. Procedia CIRP **105**, 851–858 (2022). https://doi.org/10.1016/j.procir.2022.02.141
7. Pollard, J., Osmani, M., Cole, C., Grubnic, S., Colwill, J., Díaz, A.I.: Developing and applying circularity indicators for the electrical and electronic sector: a product lifecycle approach. Sustainability **14**, 1154 (2022). https://doi.org/10.3390/su14031154
8. Psarommatis, F., May, G.: Achieving global sustainability through sustainable product life cycle. IFIP Adv. Inform. Commun. Technol. **663**, 391–398 (2022). https://doi.org/10.1007/978-3-031-16407-1_46/COVER
9. Walden, J., Steinbrecher, A., Marinkovic, M.: Digital product passports as enabler of the circular economy. Chem. Ing. Tec. **93**, 1717–1727 (2021). https://doi.org/10.1002/cite.202100121
10. Plociennik, C., et al.: Towards a digital lifecycle passport for the circular economy. Procedia CIRP **105**, 122–127 (2022). https://doi.org/10.1016/j.procir.2022.02.021
11. Digital Product Passport: the ticket to achieving a climate neutral and circular European economy?. https://circulareconomy.europa.eu/platform/en/knowledge/digital-product-passport-ticket-achieving-climate-neutral-and-circular-european-economy. Accessed 29 Nov 2023
12. Burke, H., Zhang, A., Wang, J.X.: Integrating product design and supply chain management for a circular economy. Product. Plan. Control **34**, 1097–1113 (2023). https://doi.org/10.1080/09537287.2021.1983063
13. Li, J., Li, Y., Song, H., Fan, C.: Sustainable value creation from a capability perspective: how to achieve sustainable product design. J. Clean. Prod. **312**, 127552 (2021). https://doi.org/10.1016/j.jclepro.2021.127552
14. Dumée, L.F.: Circular materials and circular design—review on challenges towards sustainable manufacturing and recycling. Circ. Econ. Sust. **2**, 9–23 (2022). https://doi.org/10.1007/s43615-021-00085-2
15. Diaz, A., Schöggl, J.-P., Reyes, T., Baumgartner, R.J.: Sustainable product development in a circular economy: Implications for products, actors, decision-making support and lifecycle information management. Sustain. Product. Consump. **26**, 1031–1045 (2021). https://doi.org/10.1016/j.spc.2020.12.044
16. Zhang, X., Zhang, L., Fung, K.Y., Bakshi, B.R., Ng, K.M.: Sustainable product design: a life-cycle approach. Chem. Eng. Sci. **217**, 115508 (2020). https://doi.org/10.1016/j.ces.2020.115508

17. van Loon, P., Diener, D., Harris, S.: Circular products and business models and environmental impact reductions: current knowledge and knowledge gaps. J. Clean. Prod. **288**, 125627 (2021). https://doi.org/10.1016/j.jclepro.2020.125627
18. Aguiar, M.F., Jugend, D.: Circular product design maturity matrix: a guideline to evaluate new product development in light of the circular economy transition. J. Clean. Prod. **365**, 132732 (2022). https://doi.org/10.1016/j.jclepro.2022.132732
19. Corona, B., Shen, L., Reike, D., Rosales Carreón, J., Worrell, E.: Towards sustainable development through the circular economy—a review and critical assessment on current circularity metrics. Resour. Conserv. Recycl. **151**, 104498 (2019). https://doi.org/10.1016/j.resconrec.2019.104498
20. Saidani, M., Kim, H.: Design for product circularity: circular economy indicators with tools mapped along the engineering design process. In: ASME 2021 International Design Engineering Technical Conferences and Computers and Information in Engineering Conference. American Society of Mechanical Engineers, Virtual, United States (2021). https://doi.org/10.1115/DETC2021-69629
21. Ruiz-Pastor, L., Chulvi, V., Mulet, E., Royo, M.: A metric for evaluating novelty and circularity as a whole in conceptual design proposals. J. Clean. Prod. **337**, 130495 (2022). https://doi.org/10.1016/j.jclepro.2022.130495
22. Mesa, J., Esparragoza, I., Maury, H.: Developing a set of sustainability indicators for product families based on the circular economy model. J. Clean. Prod. **196**, 1429–1442 (2018). https://doi.org/10.1016/j.jclepro.2018.06.131
23. Hapuwatte, B.M., Seevers, K.D., Jawahir, I.S.: Metrics-based dynamic product sustainability performance evaluation for advancing the circular economy. J. Manuf. Syst. **64**, 275–287 (2022). https://doi.org/10.1016/j.jmsy.2022.06.013
24. Konstantinidis, F.K., Myrillas, N., Tsintotas, K.A., Mouroutsos, S.G., Gasteratos, A.: A technology maturity assessment framework for Industry 5.0 machine vision systems based on systematic literature review in automotive manufacturing. Int. J. Product. Res. (2023). https://doi.org/10.1080/00207543.2023.2270588
25. Azevedo, S., Godina, R., Matias, J.: Proposal of a sustainable circular index for manufacturing companies. Resources **6**, 63 (2017). https://doi.org/10.3390/resources6040063
26. Lanaras-Mamounis, G., Tsalis, T.A., Anagnostopoulou, K., Vatalis, K.I., Nikolaou, I.E.: The development of an index for assessing the circularity level of eco-labels. Sustain. Product. Consump. **33**, 586–596 (2022). https://doi.org/10.1016/j.spc.2022.07.019
27. Shevchenko, T., Cluzel, F.: A circular product design toolkit: methodological background, basic principles and building blocks. Proc. Des. Soc. **3**, 59–68 (2023). https://doi.org/10.1017/pds.2023.7
28. Patti, Sebastiano: Eco-efficiency, circularity measurement and assessment. In: Patti, S. (ed.) Circular economy and policy: sustainability, environmental, and social perspectives, pp. 137–161. Springer International Publishing, Cham (2023). https://doi.org/10.1007/978-3-031-43324-5_7
29. Saidani, M., Yannou, B., Leroy, Y., Cluzel, F., Kendall, A.: A taxonomy of circular economy indicators. J. Clean. Prod. **207**, 542–559 (2019). https://doi.org/10.1016/j.jclepro.2018.10.014
30. Machado, N., Morioka, S.N.: Contributions of modularity to the circular economy: a systematic review of literature. J. Build. Eng. **44**, 103322 (2021). https://doi.org/10.1016/j.jobe.2021.103322
31. Pluhnau, R., Lübke, J., Nagarajah, A.: Multi-Life-Products – towards a new paradigm of product development aligning on module's multiple usage-scenarios. Proc. CIRP **119**, 873–878 (2023). https://doi.org/10.1016/j.procir.2023.03.132
32. Azevedo, S.G., Godina, R., Matias, J.C. de O.: Proposal of a sustainable circular index for manufacturing companies. Resources **6**, 63 (2017). https://doi.org/10.3390/resources6040063

33. Mishra, A., Verma, P., Tiwari, M.K.: A circularity-based quality assessment tool to classify the core for recovery businesses. Int. J. Prod. Res. **60**, 5835–5853 (2022). https://doi.org/10.1080/00207543.2021.1973135
34. Balakera, N., Konstantinidis, F.K., Tsimiklis, G., Latsa, E., Amditis, A.: IIoT network system from data collection to cyber-physical system transmission under the Industry 5.0 Era. In: Xin-She Yang, R., Sherratt, S., Dey, N., Joshi, A. (eds.) Proceedings of eighth international congress on information and communication technology: ICICT 2023, London, Volume 4, pp. 929–941. Springer Nature Singapore, Singapore (2024). https://doi.org/10.1007/978-981-99-3236-8_75
35. Psarommatis, F., May, G.: A standardized approach for measuring the performance and flexibility of digital twins. Int. J. Product. Res. 1–16 (2022). https://doi.org/10.1080/00207543.2022.2139005

Simulation-Driven Evaluation of Reward Systems for Activity-Based Manufacturing Environments

Unais Sait(✉), Marco Frego, Antonella De Angeli, and Angelika Peer

Free University of Bozen-Bolzano, 3, Piazza Domenicani, 39100 Bolzano, BZ, Italy
usait@unibz.it

Abstract. The rise of automation in the manufacturing sector and the transition from traditional role-based to activity-based shop floor management systems have brought greater flexibility and skill utilisation among shop floor workers. The vast array of task choices in activity-driven environments can overwhelm employees, potentially leading to sub-optimal decisions. Moreover, determining the optimal tasks in such a dynamic environment is complicated, and there is a risk that lower-priority tasks will be neglected. In this circumstance, it is crucial to impart knowledge to the workers about the value of a task through rewards. This study advocates for using simulations to assess the impact of various reward systems on worker performance in activity-based shop floor management systems. Simulations offer a cost-efficient and risk-averse means to explore scenarios, enabling organisations to make informed decisions about reward strategies. The paper aims to compare two reward systems based solely on worker skills and another incorporating historical skill utilisation and task unacceptance ratios. The simulation results demonstrate that the reward system considering unacceptance ratios leads to reduced unacceptance of tasks and a decrease in the number of open tasks compared to the skill-based reward system. The findings of this simulation could assist manufacturing sectors in selecting the most effective reward system for their employees and could act as a preliminary investigation to understand the reward system before testing it in the real world on the shop floor.

Keywords: Digital Manufacturing · Simulation · Automation · Reward Systems · Manufacturing Innovation

1 Introduction

With rapid advances in the automation of manufacturing processes and its widespread adoption in industrial processes, shop floor management systems are transforming from traditional role-based to activity-based practices [1]. In role-based shop floor management, workers are assigned fixed roles, leading to the under-utilisation of their skill sets and reducing flexibility [2]. New technologies have paved the way for the dynamic allocation of activities to workers, allowing them to perform a broader range of tasks in a digital shop floor management system [3]. This transformation has created workspaces characterised by an activity-based work environment, offering increased flexibility for workers in carrying out tasks [4].

© The Author(s), under exclusive license to Springer Nature Switzerland AG 2024
V. Ivanov et al. (Eds.): DSMIE 2024, LNME, pp. 63–74, 2024.
https://doi.org/10.1007/978-3-031-61797-3_6

One of the challenges posed by activity-driven shop floors is the abundance of tasks accessible to workers, unlike the limited options in role-based systems, which can overwhelm them and potentially lead to suboptimal decisions [5]. Other challenges include factors such as task procrastination, where employees tend to postpone complex tasks in favour of those that are easier to complete [6]. This study investigates the challenges of determining optimal task allocation by designing effective reward systems within activity-based shop floor systems, considering task acceptance and skill utilisation.

2 Literature Review

Digital shop floor management systems are increasingly adopted in various industries, particularly manufacturing [7]. About 17.5% of German-based industries have already adopted digital shop floor management systems, which is set to increase further as more shop floors are digitised [8]. Technological interventions such as smartwatches, mobile applications, and smart screens have been proposed to facilitate allocating activities to workers [9]. These interventions aim to provide workers with real-time information and enable them to select and perform tasks independently. The freedom to choose from larger tasks could potentially overwhelm workers [9, 10]. This situation highlights the need for assistance to support workers in making reasonable and rational decisions, both in the short and long term. However, this practice can lead to significant issues, particularly when the task with the highest priority needs to be addressed and when tasks are dependent on one another sequentially.

One approach to assist employees in selecting the most suitable tasks is by providing rewards for the task with the highest level of optimality [11]. Rewarding employees is a method to encourage the acquisition of relevant knowledge, thereby enabling them to make optimal decisions [12]. However, determining the most optimal task in a dynamic environment presents an enormous challenge [13, 14]. If only the most challenging tasks are incentivised, the less complicated tasks tend to be neglected due to their lower rewards. Consequently, accepting these less demanding tasks becomes a significant factor to consider when calculating rewards. Thus, before implementing reward systems in a real-world context, it is advisable to evaluate their effectiveness within a simulated environment [15]. Simulations provide a cost-efficient and risk-averse way to assess the impact of various reward systems on worker performance, offering precise data and scenario exploration capabilities [16]. Simulations have been employed in numerous studies to assess the efficiency of various strategies, encompassing operational-level human resource planning and improving the organisation of the factory floor [17–19]. This approach saves time and resources compared to real-world testing, enabling organisations to make informed decisions about reward strategies.

This study seeks to address the gap concerning the need to assist workers in selecting optimal tasks in dynamic environments, emphasising the importance of considering unaccepted tasks when formulating reward structures. Hence, this paper evaluates simulated scenarios in which workers experience two distinct reward systems: one based solely on worker skills and another incorporating historical skill utilisation and task unacceptance ratios.

3 Research Methodology

In this work, we consider a conventional shop floor with machine groups, which are collections of machinery and equipment arranged in groups for a particular industrial function, see Fig. 1. The composition and arrangement of these machine groups can vary widely, tailored to the company's manufacturing requirements, potentially including similar or diverse machine types. The demand for specific skills arises from these machine groups, and a worker may be assigned to multiple machine groups. Occasionally, workers may lack the necessary skills for certain tasks.

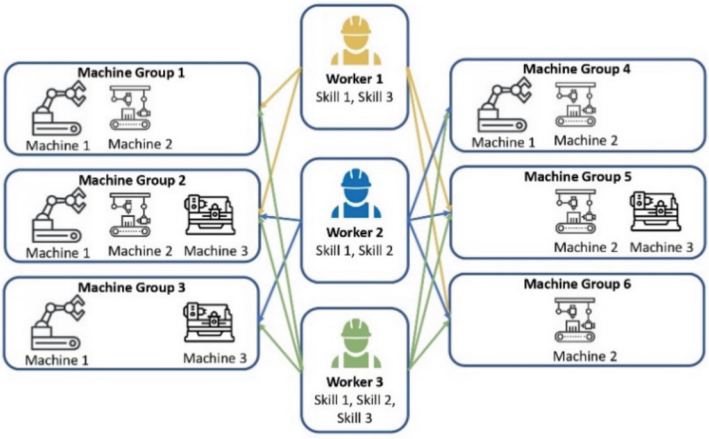

Fig. 1. Shop floor configuration.

The simulation takes input from data sourced from the organisation's Enterprise Resource Planning (ERP) and Manufacturing Execution System (MES), which are software systems used to manage and coordinate various aspects of manufacturing, including inventory control, order processing, real-time monitoring, and control of production operations. This data is supplemented by historical production information. This historical data is related to past unaccepted tasks and contains information about the duration and distribution of tasks across machine groups. Based on this data, this study defines the following input variables and computes the rewards, as shown in Fig. 2.

Fig. 2. Method for selection of reward system.

3.1 Extraction of Input Variables for Simulation

Skill Level Matrix (S): The Skill Level Matrix, denoted as S, represents the skill levels of workers. Each entry of $S_{i,w}$ corresponds to the difficulty level (x) associated with a specific skill i possessed by a worker w. The worker experience is not considered in the calculation of the skill level. This matrix remains constant unless the worker takes a new training session for a new skill they do not possess. The $\boldsymbol{S}$ matrix is represented by

$$S_{i,w} = \begin{cases} x \text{ if worker } w \text{ has skill } i, \\ 0 \text{ if worker } w \text{ has no skill } i, \end{cases} \tag{1}$$

where i represents the skill, w represents the worker, and x represents the skill difficulty level.

Worker Distribution Matrix (D): The Worker Distribution Matrix

$$D_{w,j} = \begin{cases} 1 \text{ if worker } w \text{ belongs to MG j}, \\ 0 \text{ if worker } w \text{ does not belong to MG } j, \end{cases} \tag{2}$$

defines whether a worker belongs to a specific machine group (MG). It is binary, with 1 indicating worker membership in MG j and 0 indicating non-membership. The Worker Distribution Matrix remains static unless there is a notable change in the workforce, such as adding new workers to the company or removing any worker.

Open Task Matrix (N): The Open Task Matrix, denoted as N, represents the number of open tasks for specific skills on the shop floor. Each entry of $N_{i,j}$ corresponds to the number of open tasks for a specific skill i arising from machine group j. It is dynamic and updated as workers accept tasks and skill demands change in various machine groups. For simulation purposes, a distribution of open tasks is added at regular intervals of 15 min. The open task distribution is derived from the previous distribution of probabilities for various open tasks on the shop floor. The total open tasks are denoted as O_t is the sum of all entries in the matrix N at a given time t:

$$O_t = \sum_{i=1}^{n} \sum_{j=1}^{m} N_{i,j} \tag{3}$$

Progress Time Matrix (T): The Progress Time Matrix, denoted as T, defines the average time required to complete a task for specific skills and machine groups. Similar to open tasks, this matrix is formulated from historical data. Each entry $T_{i,j}$ corresponds to the average progress time to complete a skill i on a specific machine group j.

Worker Availability Matrix (A): The Worker Availability Matrix, denoted as A_i, is a binary matrix indicating whether a worker i is available (1) or unavailable (0) for tasks. The worker's availability is updated automatically after the average task completion time has elapsed.

Unacceptance Matrix (W): The Unacceptance Matrix

$$W_{i,j} = \frac{N_{i,j}}{\text{Total Tasks}_{i,j}} \tag{4}$$

represents the unacceptance ratio for each skill level and machine group, whereby i is the skill, j models the machine group, $N_{i,j}$ is the number of open tasks for skill i in machine

group j, and Total Tasks$_{i,j}$ is the total tasks (open + accepted) for skill i in machine group j. It is derived from historical data and updated hourly by dividing the total open tasks by the total tasks over the hour. Thus, if a task remains unaccepted for over an hour, it could be assigned a higher priority. The total unacceptance ratio is denoted as U_t is the sum of all entries in the matrix W at a given time t:

$$U_t = \sum_{i=1}^{n} \sum_{j=1}^{m} W_{i,j}. \tag{5}$$

3.2 Definition of Rewards

After gathering the input variables from the shop floor's dataset, the subsequent step involves calculating rewards continuously in simulation. This process examines two distinct rewarding strategies. The reward computation operates on the premise that the worker is inclined to choose the most rewarding task. To model this behaviour, workers are considered rational agents seeking to maximize their immediate rewards. These strategies are elaborated upon in the following sections.

1. Reward computation with only skill level (R1): In this particular context of reward computation, the assumption is that the most rewarding task corresponds to the most challenging task requiring the highest skill level within the shop floor. In this scenario, reward computation primarily involves the direct calculation of the skill level value, which is then multiplied by the worker distribution to filter out workers who do not belong to the respective machine group:

$$R^W_{i,j} = D_{w,j} S^*_{i,w}. \tag{6}$$

   Here, the skill level matrix is normalised and denoted as $S^*_{i,w}$. Consequently, a zero reward signifies that the worker does not belong to the machine group or lacks the necessary skills for the task. It is important to note that the reward will range between 0 and 1, as the skill matrix is normalised, with 1 representing the most challenging task on the shop floor.
2. Reward computation with skill level and unacceptance ratio (R2): This proposed reward system operates dynamically, adjusting rewards based on task unacceptance. The reward calculation incorporates an unacceptance ratio, and the reward is updated on an hourly basis when the unacceptance ratio is computed:

$$R^W_{i,j} = D_{w,j}(S^*_{i,w} + W_{i,j}) \tag{7}$$

   where $R^W_{i,j}$ is the reward for worker w with skill i in machine group j, $D_{w,j}$ is the entry in the Worker Distribution Matrix for worker w and machine group j, $S^*_{i,w}$ is the normalised skill level of worker w for skill i, and $W_{i,j}$ is the unacceptance ratio for skill i in machine group j. Consequently, tasks that have remained unaccepted for over an hour are likely to receive a higher reward, increasing the likelihood of them being accepted.

3.3 Simulation Process

For the simulation, a study was conducted to capture the actual shop floor configuration from the industry. After extracting the data from ERP, MES, and related historical data for the one-year duration, a shop floor configuration with 6 machine groups, 3 workers, and 3 skills is considered in this study. As depicted in Fig. 1, Worker 1 lacks Skill 2 and does not belong to Machine Groups 3 and 4. Worker 2, on the other hand, lacks Skill 1 and is not a member of Machine Group 1. Worker 3 possesses all 3 skills and belongs to all machine groups. Therefore, the skill and worker distribution matrices are represented as follows:

$$S = \begin{bmatrix} 1 & 0 & 1 \\ 0 & 2 & 2 \\ 3 & 3 & 3 \end{bmatrix}, \mathrm{D} = \begin{bmatrix} 1 & 1 & 0 & 0 & 1 & 1 \\ 0 & 1 & 1 & 1 & 1 & 1 \\ 1 & 1 & 1 & 1 & 1 & 1 \end{bmatrix}, \text{and } S^* = \begin{bmatrix} 1/3 & 0 & 1/3 \\ 0 & 2/3 & 2/3 \\ 1 & 1 & 1 \end{bmatrix} \quad (8)$$

where S^* is the normalised skill matrix and is calculated by dividing all the entries in S with the highest skill value, which is 3 in the current scenario.

Task Acceptance Conflict: During the simulation, a crucial consideration involves addressing conflicts that arise when two workers are equally eligible to undertake a particular task, receiving the highest possible reward. In such instances, the simulation resolves the conflict by randomly selecting one of the available workers to assign the task. However, in a real-world scenario, this situation can be better managed by either being accepted by the most motivated worker or creating a competitive environment where the first individual to accept the task gets it. A function named *check_uniques* monitors these conflicts and prevents them.

Simulation Steps: The overall simulation consists of the following steps:

1. Calculate initial rewards based on the sample conditions.
2. Scrutinise the availability matrix to identify workers available for tasks.
3. Allocate tasks to available workers with a focus on maximizing reward points while ensuring uniqueness to prevent conflicts.
4. Dynamically update the open task matrix to reflect new task arrivals and reductions every 15 min.
5. Perform hourly updates, including recording the open tasks matrix and unacceptance calculations.
6. Monitor and plot the frequency at which workers use their highest available skill hourly.
7. Continue the simulation for eight hours.

Algorithm: Fig. 3 depicts the algorithm that models the task allocation system.

It begins by setting simulation parameters, including the total simulation duration (8 h), intervals for new tasks and unacceptance (15 min and 1 h, respectively), a reward calculation case (either 1 or 2), and the typical duration of the task is computed based on historical data comprising 3 skills each across 6 machine groups, resulting in a total of 18 task types. Next, it defines the simulation environment, including the number of workers, machine groups, and skills. The algorithm then initialises various matrices and conditions, such as skill levels, worker distribution, open tasks, progress time, skill usage, accepted tasks, allocation, and worker rewards. The core simulation logic involves

Algorithm 1 Simulation Algorithm

```
INPUT: Simulation Parameters
  total_hours ← 8
  newtask_interval ← 15                                          ▷ minutes
  unacceptance_interval ← 1                                      ▷ hour
  case ← 1                          ▷ Reward calculation case 1 for R1 and 2 for R2
  total_seconds ← total_hours × 60 × 60
Define the Environment:
  num_workers ← 3
  num_machines ← 6
  num_skills ← 3
Initialise Matrices:
  Initialize Skill_Level, Worker_Distribution, Open_Tasks, Progress_Time
OUTPUT:
  function COMPUTE_REWARDS
      Calculate reward values based on conditions
  end function
  function UPDATE_OPENTASKS(i, j)
      Update Open_Tasks and accepted_tasks
  end function
  function ACCEPT_TASKS
      Assign tasks to workers based on reward
  end function
  function CHECK_UNIQUES
      Check the uniqueness of task allocation
  end function
  for seconds in range(total_seconds) do
      seconds + = 1
      Update matrices, compute rewards, accept tasks, check uniqueness, etc.
  end for
End Simulation
```

Fig. 3. Simulation algorithm.

iterating through each second within the total duration, updating matrices, computing rewards, assigning tasks to workers based on rewards, and checking for uniqueness in task allocation. Finally, the algorithm saves the simulation data and concludes the simulation.

4 Results and Discussion

Completing the simulation yielded two sets of data corresponding to the two reward systems under investigation.

4.1 Effect of Reward Systems on Open Tasks and Unacceptance Ratio

This study analysed two primary output variables: the total unacceptance ratio and the number of open tasks. These critical variables were systematically recorded at fifteen-minute intervals during the simulation. The graphical representations of these data sets are presented for a particular simulated day in Fig. 4.

This figure illustrates a noticeable reduction in both the number of open tasks and the unacceptance ratio in the reward system that integrated the concept of unacceptance ratios. The open tasks plot begins at approximately 25 tasks. This is because, on a shop floor, there are typically ongoing tasks that carry over from previous shifts and have not

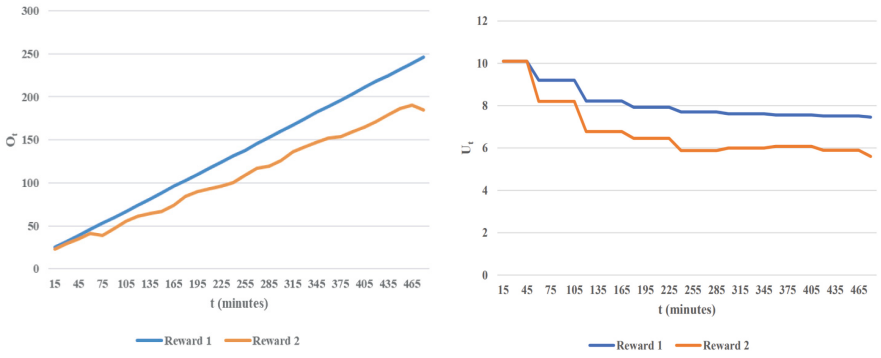

Fig. 4. Simulation of open tasks (a) and unacceptance ratio (b) for a particular simulated day.

been accepted yet, resulting in this initial task count. The open tasks data of the previous shift is extracted from the data from ERP and MES of the shop floor. After four hours of simulation, it becomes evident that both reward systems exhibit a steady-state pattern in terms of unacceptance. This phenomenon arises because open tasks are consistently added at a similar rate to task acceptance. Notably, in real-world scenarios, this steady state of unacceptance may disappear if there are fluctuations in the number of open tasks.

In reward system 2, the graph representing total open tasks exhibits fluctuations compared to reward system 1, indicating the dynamic impact of reward system 2 instead of reward system 1, where the reward for a specific skill remains constant over time. The increasing count of open tasks is attributed to the selection of a shift that is notably understaffed in this simulation. This is done to consider the situations where there is an excess of tasks available for workers, surpassing their immediate requirements. Nevertheless, shifts with reduced task allocations facilitate the completion of previously accumulated open tasks.

Within the initial 120 min of the simulations, a substantial change in the unacceptance ratio is observed, descending from 10.1 to 6.77. This transition is attributed to the simulation's initiation with a default unacceptance rate from the shop floor before implementing the reward systems. This data is captured from the unacceptance rate of the previous shifts. Consequently, the unacceptance ratio initially tends to be higher, with workers being modelled to prefer selecting the highest-rewarding tasks, as depicted in Fig. 4(b). On the other hand, there is a notable difference in the acceptance behaviour in reward system 2, particularly with an increase in skill 1, which had a lower reward in reward system 1. This is illustrated in Fig. 5. The reward system 2 is designed to consider historical unacceptance trends as a key determinant for task allocation. Such an outcome also underscores the significance of accounting for worker behaviour patterns when devising reward systems tailored for dynamic shop floor management systems.

The simulation was repeated using varying input data, encompassing data from 10 different days. This systematic approach aimed to ensure robust results, validating the reward strategy's effectiveness and confirming that the observed patterns remain consistent even when altering the input data. The Area Under the Curve (AUC) values

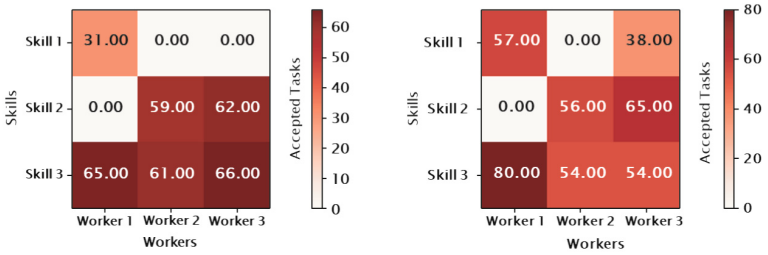

(a) Reward 1 (b) Reward 2

Fig. 5. Heatmap of accepted tasks by workers.

for both total open tasks and the unacceptance ratio are computed, and these results are depicted in Fig. 6. Upon observation of the plots, a consistent pattern emerged: there was a notable decrease in both open tasks and unacceptance ratio AUC values for reward system two compared to reward system one across all 10 days.

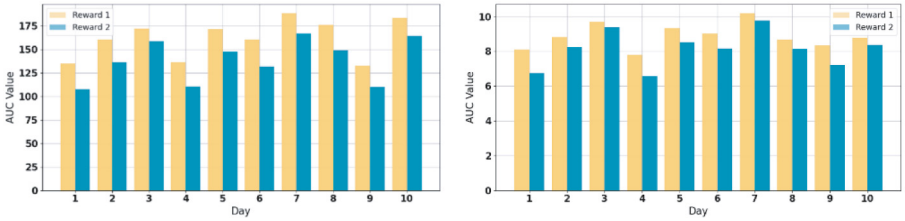

(a) Open tasks (b) Unacceptance ratio

Fig. 6. AUC plot for open tasks and unacceptance ratio.

4.2 Statistical Analysis

In this specific scenario, the workers operate under identical shop floor conditions for the two reward systems, and the measurements for both open and unaccepted tasks are taken by repeating the simulation for 10 different days. Hence, a paired t-test was employed to assess the statistical significance of these observed differences between the two reward systems. The paired t-test was conducted based on the AUC values observed over the 10 simulations (based on input data from 10 different days) for total open tasks and total unacceptance ratio within each reward system. Statistical differences between R1 and R2 were found for open tasks ($t(9) = 16.45, p < 0.05, d = 4.509$) as well as for the unacceptance ratio ($t(9) = 6.45, p < 0.05, d = 0.373$).

Applying the paired t-test revealed compelling evidence that the reward system based on a combination of worker skills and unacceptance ratios led to significantly lower unacceptance ratios and a notable reduction in the number of open tasks compared to the skill-based reward system. This statistical significance reinforces the assertion that integrating

historical unacceptance data into reward calculations substantially impacts the overall efficiency of task allocation in the context of activity-based shop floor management systems. The implications of these findings hold substantial importance for organisations navigating the transition to activity-based shop floor management systems. They provide concrete guidance on designing reward systems tailored to the specific challenges posed by dynamic task allocation scenarios. Furthermore, this study underscores the importance of data-driven decision-making and the utilisation of simulation methodologies as invaluable tools for evaluating and refining management strategies within the evolving landscape of manufacturing practices.

The simulation results convincingly advocate for adopting reward systems that integrate worker unacceptance behaviour as a pivotal factor in addressing the intricacies of dynamic task allocation within activity-based shop floor management systems. These findings offer practical insights for organisations striving to harness the full potential of their workforce in an era characterised by transformative technological advancements. It is essential to acknowledge the study's limitations. Specifically, the study does not consider irrational decisions or delve into the dynamics of interpersonal interactions among workers and how these interactions might influence their behaviour. Furthermore, the study does not account for the potential benefits of teamwork. These limitations present opportunities for future research and exploration.

5 Conclusions

In conclusion, transforming traditional role-based shop floor management systems to activity-based systems has increased workers' flexibility and skill utilisation. However, the abundance of task choices in activity-driven environments can lead to decision-making challenges and potentially sub-optimal choices. This paper has explored using simulations to assess the impact of different reward systems on worker performance in activity-based shop floor management.

This study compared two reward systems based solely on worker skills and another incorporating historical skill utilisation and task unacceptance ratios. The simulation results demonstrated that the reward system considering unacceptance ratios led to reduced unacceptance of tasks and decreased the number of open tasks compared to the skill-based reward system. The simulation was tested with varying input data across ten different days. This testing validated the consistency of observed data, affirming that the strategy's efficacy remained consistent despite variations in input data. This consistency reinforces the reliability and effectiveness of the proposed reward strategy, emphasising its stability across diverse operational scenarios.

Statistical analysis, including paired t-tests, confirmed statistically significant differences between the two reward systems, supporting the efficacy of incorporating unacceptance ratios into reward calculations. This study underscores the importance of data-driven decision-making and the use of simulations in the context of evolving manufacturing practices. As technology continues to reshape industrial processes, adapting and refining management strategies through rigorous analysis becomes increasingly vital for maintaining competitiveness and efficiency in the manufacturing sector.

Acknowledgement. This work was supported by a PhD fellowship funded under the Programma Operativo Nazionale (PON) "RICERCA E INNOVAZIONE" 2014-2020 and GKN Sinter Metals. The authors express gratitude to GKN Sinter Metals S.P.A. and special thanks to Mr. Philip Roell, Dr. Thomas Tschager, and Mr. Jakob Engl for their invaluable assistance in studying the shop floor and understanding the requirements.

References

1. Tropschuh, B., Korder, S., Dillinger, F., Bauer, H., Reinhardt, G.: Activity-based shop floor management – a concept to enhance flexibility. In: Proceedings of the Conference on Production Systems and Logistics, pp. 259–268. Publishing, Hannover (2020). https://doi.org/10.15488/9667
2. Keiser, Y., West, S., Züst, S.: Reflections from a hybrid approach used to develop a specification of a shopfloor platform for smart manufacturing in an engineered-to-order SME. In: Dolgui, A., Bernard, A., Lemoine, D., von Cieminski, G., Romero, D. (eds.) APMS 2021. IAICT, vol. 633, pp. 691–701. Springer, Cham (2021). https://doi.org/10.1007/978-3-030-85910-7_73
3. Dutta, G., Kumar, R., Sindhwani, R., Singh, R.K.: Adopting shop floor digitalization in Indian manufacturing SMEs—a transformational study. In: Phanden, R.K., Mathiyazhagan, K., Kumar, R., Paulo Davim, J. (eds.) Advances in Industrial and Production Engineering. LNME, pp. 599–611. Springer, Singapore (2021). https://doi.org/10.1007/978-981-33-4320-7_53
4. Hoendervanger, J.G., de Been, I., van Yperen, N.W., Mobach, M.P., Albers, C.J.: Flexibility in use: switching behaviour and satisfaction in activity-based work environments. J. Corp. Real Estate **18**, 48–62 (2016). https://doi.org/10.1108/JCRE-10-2015-0033
5. Shi, Z., Xie, Y., Xue, W., Chen, Y., Fu, L., Xu, X.: Smart factory in Industry 4.0. Syst. Res. Behav. Sci. **37**, 607–617 (2020)
6. Kühnel, J., Bledow, R., Feuerhahn, N.: When do you procrastinate? Sleep quality and social sleep lag jointly predict self-regulatory failure at work. J. Organ. Behav. **37**, 983–1002 (2016). https://doi.org/10.1002/job.2084
7. Clausen, P., Mathiasen, J.B., Nielsen, J.S.: Smart manufacturing through digital shop floor management boards. Wirel. Pers. Commun. **115**, 3261–3274 (2020). https://doi.org/10.1007/s11277-020-07379-y
8. Grundnig, A., Meitinger, S.: Production cockpit 4.0 as shop floor management of the future: only a customer-specific solution can adequately take organization, IT systems and processes into account. J. Econ. Factory Oper. **113**, 873–877 (2018). https://doi.org/10.3139/104.112028 (in German)
9. Ghobakhloo, M., Ching, N.T.: Adoption of digital technologies of smart manufacturing in SMEs. J. Ind. Inf. Integr. **16**, 100107 (2019)
10. Zhang, C., Chen, Y.: A review of research relevant to the emerging industry trends: Industry 4.0, IoT, blockchain, and business analytics. J. Ind. Integr. Manag. **5**, 165–180 (2020)
11. Ngwa, W.T., Adeleke, B.S., Agbaeze, E.K., Ghasi, N.C., Imhanrenialena, B.O.: Effect of reward system on employee performance among selected manufacturing firms in the Litoral region of Cameroon. Acad. Strateg. Manag. J. **18**(3), 1–16 (2019)
12. Richter, G., Raban, D.R., Rafaeli, S.: Studying gamification: the effect of rewards and incentives on motivation. In: Reiners, T., Wood, L.C. (eds.) Gamification in Education and Business, pp. 21–46. Springer, Cham (2015). https://doi.org/10.1007/978-3-319-10208-5_2

13. Liu, C., Zeng, W., Zhou, H., Cao, L., Yang, Y.: Dynamic task allocation and action coordination under uncertain environment. In: Wang, Y., Li, T. (eds.) Foundations of Intelligent Systems. AISC, vol. 122, pp. 365–369. Springer, Heidelberg (2012). https://doi.org/10.1007/978-3-642-25664-6_42
14. Bevilacqua, P., Frego, M., Palopoli, L., Fontanelli, D.: Activity planning for assistive robots using chance-constrained stochastic programming. IEEE Trans. Industr. Inf. **17**, 3950–3961 (2021). https://doi.org/10.1109/TII.2020.3012094
15. Rüßmann, M., et al.: Industry 4.0: The Future of Productivity and Growth in Manufacturing Industries, vol. 9, pp. 54–89. Boston Consulting Group (2015)
16. Ng, Y.W., Ren Jie, J.C., Kamaruddin, S.: Analysis of shop floor performance through discrete event simulation: a case study. J. Ind. Eng. **2014**, 1–10 (2014). https://doi.org/10.1155/2014/878906
17. Baron-Puda, M., Mleczko, J.: Simulation of human resources allocation in scheduling processes. Appl. Comput. Sci. **4**(2), 1–16 (2008)
18. Kanduč, T., Rodič, B.: Optimisation of factory floor layout using force-directed graph drawing algorithm. In: 2015 38th International Convention on Information and Communication Technology, Electronics and Microelectronics (MIPRO), pp. 1087–1092 (2015). https://doi.org/10.1109/MIPRO.2015.7160437
19. Mönch, L., Rose, O., Sturm, R.: A simulation framework for the performance assessment of shop floor control systems. SIMULATION **79**, 163–170 (2003). https://doi.org/10.1177/0037549703256039

Creation of a Localization Project in RTLS Studio for the Need of an Industrial Data Collection Application

Peter Trebuňa, Marek Mizerák(✉), Miriam Pekarčíková, and Jozef Trojan

Technical University of Košice, 9, Park Komenského, 04200 Košice, Slovakia
marek.mizerak@tuke.sk

Abstract. This article deals with creating a localization project in RTLS (Real-Time Locating System) Studio to optimize the process of collecting production data in an industrial enterprise. RTLS Studio is part of the innovative RTLS technology that enables real-time tracking and device location. This project aims to use RTLS to improve the efficiency and accuracy of data collection in an industrial environment. Implementing this localization project will provide accurate information about equipment location in an industrial plant, allowing better monitoring and management of production processes. This has the effect of reducing response time, minimizing errors, and optimizing the overall performance of the production facility. The article examines the creation of this project directly in a manufacturing company that deals with heavy engineering for further use in the creation of various types of analysis and technical aspects of the implementation of RTLS technology to obtain the maximum sound output. Emphasis is placed on data security and the transfer of information between devices to ensure the safe and reliable operation of the entire system. The results of this work represent potential benefits for industrial enterprises, including increased productivity, better inventory tracking, and faster response to changes in the production environment. In this way, the article benefits the industrial sector and supports further research and implementation of localization projects within RTLS systems.

Keywords: RTLS · Industry · Location · Project · Industrial Growth

1 Introduction

A real-time location system (RTLS) consists of two essential parts: hardware and software. Together, they form a multi-functional platform, serving multiple indoor surveillance use cases - from property tracking and material flow to tracking people for security reasons. The advantage of RTLS is its direct UWB (Ultra-Wide Band) technology. This technology has received comprehensive industry certification to ensure reliable and scalable performance. Sewio is a fully scalable solution that allows you to customize existing tags, add additional trackable objects, and increase coverage according to demand and need. It is possible to easily integrate third parties with an open API interface, which allows adapting the technology to the customer's vision and needs. Complete visibility

© The Author(s), under exclusive license to Springer Nature Switzerland AG 2024
V. Ivanov et al. (Eds.): DSMIE 2024, LNME, pp. 75–85, 2024.
https://doi.org/10.1007/978-3-031-61797-3_7

of all live processes enables faster assessment of projects based on Industry 4.0 principles. This led to optimizing workflows, increased production, and reduced costs. The outstanding accuracy of Sewio RTLS provides a flexible infrastructure that fits the scale of existing and future business cases. Business projects are ready for Industry 4.0 with less time to add value quickly and with lower maintenance costs, and they are within budget for widespread adoption by all stakeholders [1].

This scientific article aims to present a clear and transparent methodology for the creation and implementation of the RTLS project directly in the production company to collect and digitize production data.

2 Literature Review

There is extensive literature on developing localization projects and using RTLS (Real-Time Location System) for industrial data collection needs, which provides the basic framework and opportunities for this research project.

RTLS in an industrial environment) [1]: Smith et al. demonstrate the successful use of RTLS in a factory for process optimization and equipment movement tracking. Their work identifies the challenges and benefits of implementing RTLS in industrial scenarios.

Software tools for localization [2]: Brown and Jones present a case study Using RTLS Studio in the context of localization projects. Their research focuses on the development of software solutions for the efficient acquisition of accurate location data.

RTLS integration with data collection applications [3]: Garcia and Kim analyze ways to integrate RTLS into industry data collection applications. Their work provides insight into the technological and implementation challenges of this integration.

Use of localization projects in practice [4]: Johnson et al. provide examples of the successful deployment of localization projects in a natural industrial environment and analyze the benefits of data accuracy and increasing the efficiency of production processes.

Current challenges in localization and data collection applications [5]: White and Smith present an overview of current challenges in localization projects and point to avenues for further development, including the need for precise localization in industries.

These provide the starting point for our research project and the current direction for further development and refinement of the localization project in RTLS Studio for the needs of industrial data collection.

3 Research Methodology

The RTLS localization system from Sewio consists of three main components: hardware in the form of anchors, tags, and RTLS Studio software.

Tags are electronic devices that serve as signal transmitters in the interior to track objects, workers, or other parts of production. The principle of operation of the tags consists of sending short flashes captured by the receivers (anchors). Then, the data is sent to the localization server, which calculates the position of the tags based on this

data. Tags are used in applications such as employee security and location, asset and vehicle tracking, and material flow analysis [6].

Since each use case is different, tags also have different requirements.

Therefore, Sewio has developed three types of tags that will allow customers to choose the right one that will suit their requirements and budget. In the framework of real-time positioning of individual objects and people (RTLS), the anchor, as mentioned, is an electronic device functioning as a receiver of UWB pulses sent by smaller electronic devices. These namely tags send subsequent data to a localization server to calculate the exact position tag. In addition, anchors can receive data from tagged sensors, such as acceleration, orientation, button events, or user data. The data is further made available to users through open APIs. Each anchor has its unique IP address and is equipped with an Ethernet/Wi-Fi interface for data backhaul or power supply. It uses RTLS Studio software to configure and manage anchors. Various types of anchor brackets are available to simplify installation in any space. They are mounted above the tags, ensuring maximum coverage and minimizing obstacles blocking their communication lines [7].

Therefore, it is necessary to create a monitoring network made of anchors to measure and, therefore, to cover a larger monitored area. These anchors are mounted above the monitored area. The height is usually between 2 m and 6 m. However, this parameter is specific and depends on the specific dimensional conditions of the selected monitored space. In this way, the infrastructure is created, which is subsequently incorporated into the software environment of the RTLS Studio program. Since the network localization infrastructure is fully scalable, the system can be easily expanded by adding additional anchors (tags) to this localization network, thus increasing the monitored area [8].

4 Results and Discussion

4.1 Creation of a Localization RTLS Project in the Environment of Production Company

The initial measurement of the dimensions was carried out using a Leica Disto D510 laser distance meter, which determined the maximum distances for the most suitable location of the anchors at the workplace. For RTLS technology, the maximum anchor distances were 25 m (Fig. 1).

These anchor placement positions had to meet several requirements, namely:

- preventing the creation of an obstacle in the working and handling space,
- meeting the maximum distance between individual anchors,
- prevention of the “ghost effect” (obstruction in the direct view of the anchor from at least two positions of the stored anchors),
- safety and health protection at work.

In Fig. 2, we can see a map of the dimensions of the distribution of anchors in production in hall No. 2. As mentioned, the maximum distance for measurement when using such a system of RTLS anchors is 25 m. However, for measuring the production in the hall, an RTLS monitoring network in the dimensions shown in Fig. 3 was sufficient.

Fig. 1. Basic measurement for the correct determination of the anchor position.

Four Vista DirectFive anchors from Sewio were used for the measurement. Subsequently, they were connected by Ethernet cables with a total length of approximately 100 m. In the next preparatory step, these individual anchors were connected to a switch with an active PoE power supply, which provides the entire network of anchors with the electricity necessary for operation. This switch is characterized by a switching capacity of 10 Gb/s and a LAN port transmission speed of 1 Gbit [6, 7].

In the next step, it is necessary to connect the switch to the computer using an Ethernet cable. In this way, an internal LAN network is created. One of the advantages of this network is that it can transmit large volumes of data with relatively low power consumption. Another significant advantage is that this entire RTLS network does not need an Internet connection. This fact is an advantage in older production halls like this one, where there is no possibility of any Ethernet connection or Wi-Fi network.

By default, anchors have the same IP address 192.168.225.200. Changing the address of all anchors sharing the network individually is advisable to a different address. After changing the IP addresses, ensuring the IP connection with all anchors is working is necessary. If not, go to RTLS Manager → Anchors Summary and check that they are all online with a different address [8].

A graphical method was used to verify the functionality of the network and the UWB stability of all RTLS anchors about the mother anchor, which the software will always design according to the best and highest parameters. The stability values should be lower than 2.0; if this value is exceeded, it is necessary to change the orientation of the anchors by turning them either more into the room or the floor. In the case of this measurement, it was possible to set the stability to a value of 1.0, which is considered to be a very high-quality stability of the signal coverage of the given measured space [9, 10].

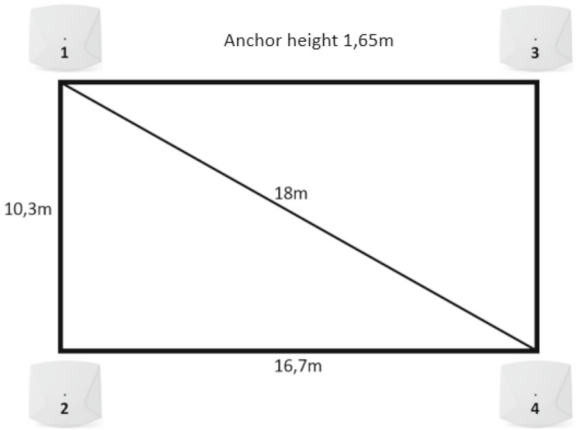

Fig. 2. Map of the dimensions of the distribution of anchors in the production hall.

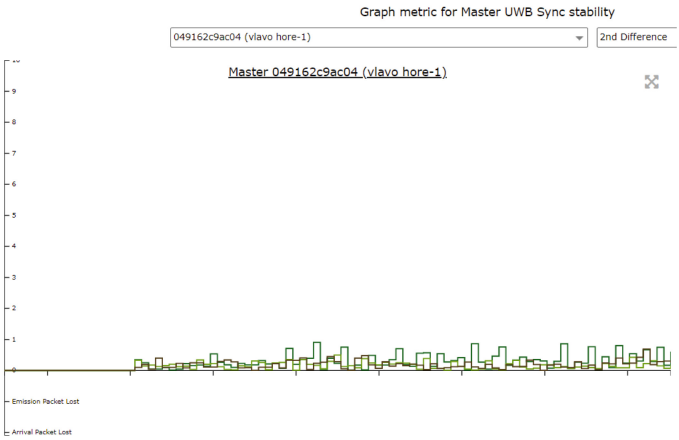

Fig. 3. Graphical representation for UWB stability of mother anchor.

In the case of values greater than 2.0, the UWB stability can be adjusted by moving the anchors to a more suitable position or by simply reorienting the direction of the anchors to the center of the measured area. These values can also be adjusted by measuring the height of the anchors and setting them to the same height as possible.

4.2 Installation of RTLS Tags on Measured Objects and Persons

The company's measurement and collection of production data was primarily focused on the movement of people and handling equipment such as pallet trucks and electric pallet trucks. The tags were attached to the handling devices using double-sided adhesive tape.

This attachment method has proven to be convenient for its easy installation on devices and easy removal after the measurement is finished.

An RTLS tag from Sewio Leonardo Asset was used for the measurement, characterized by a long battery life and resistance in a dusty industrial environment [9].

Several moving objects were monitored in the measured area. Within the pallet trucks, the tags were placed on the most visible surface, namely above the piston of the pallet truck with the already mentioned simple double-sided tape, which proved to be an adequate solution for attachment to the object, as can be seen in Fig. 4 and Fig. 5.

Fig. 4. Leonardo Asset tag on a pallet truck.

The procedure for the electric high-lift pallet truck was similar to that of the pallet truck, which was to attach it to the flattest and most visible surface of the truck. The placement of the tags was consulted with the workers to prevent possible restrictions on the work of either the worker or the handling device itself. The correct placement of these tags on the handling mentioned above means also has its justification in the collection of production data, for the reason that a tag placed incorrectly (under the cover, the roof of the truck, or others) can, in some instances send later responses to the server and thus will production data collection is distorted and thus understandably inaccurate [10].

When monitoring the workers, classic reflective vests were used, on which tags were also attached at the best possible point visually for sending a signal to the anchors and subsequent analysis of the position by the server (Fig. 6).

At this point, an experiment was carried out where the worker kept a tag in his breast pocket on his work clothes for a certain period, and his movement and activity were monitored and evaluated. After a short analysis, our assumptions were confirmed, as well as the recommendations of the manufacturer of RTLS technology, which talks about placing the tag in the most visible place of the monitored object or person.

4.3 Measurement Process

After all preparatory steps, settings, and configuration, measurement and analysis were applied in RTLS Studio software. In Fig. 7, tags marked with a blue mark are considered currently active. Tags marked with a gray mark are currently in “sleep mode”, which

Fig. 5. Leonardo Asset tag on an electric pallet truck.

Fig. 6. Leonardo Asset tag on the reflective vest.

primarily serves to save the tag's battery that is not in motion, i.e., it is inactive. The tag will automatically enter the "working" state when it is moved. We assigned tags to their designations according to the tracked object or person they were attached to.

The anchors were marked automatically by the software with a green mark, and the master anchor was marked with a signal mark.

At the next point, we decided that virtual zones would be created on the layout in the location of the machine tools, which will provide more specific information about how much time the given worker spent at the machine, what his workload was, and his exact position within the monitored space.

Fig. 7. Layout of the measured production plant with individual RTLS parts.

Based on these settings and the creation of virtual zones, material flow, and workspace inputs, we focused primarily on Heatmaps, spaghetti diagrams, and other analyses offered by the RTLS Studio software platform and its Sensmap module.

The other pictures show the graphic movements of manipulators and people.

The heat maps in Fig. 8 clearly deduce that the workers moved the most in their work positions directly in the created virtual zones. It can also be seen on the label "TAG_1-worker" that workers can control several machine tools. In this case, it was a HACO 150 folding machine.

The worker with the tag "TAG_2-worker" also operated a bending machine, HACO 150. His range of movement is extended since, at this working position, there was also an intermediate warehouse with the material in the given measured time, which the worker placed in this machine sheet metal for forming and other production operations.

The worker with the tag "TAG_3-worker" worked on the COST CUTTER 306 hydraulic shears, and his virtual zone was positionally marked as the first in the given layout. His movements also directed to the intermediate material storage for sheet metal processing. Still, the worker with this designation used a crane to pick the necessary material from the warehouse, located outside the monitored measurement area of production data collection.

In Fig. 9, the movements of these workers can be seen in a graphic representation in the form of spaghetti diagrams. During the production data collection in the production company, several shortcomings were detected with the help of RTLS technology, which can be largely corrected or optimized according to the possibilities of the production company. Understandably, not all optimization elements can be set and fixed quickly.

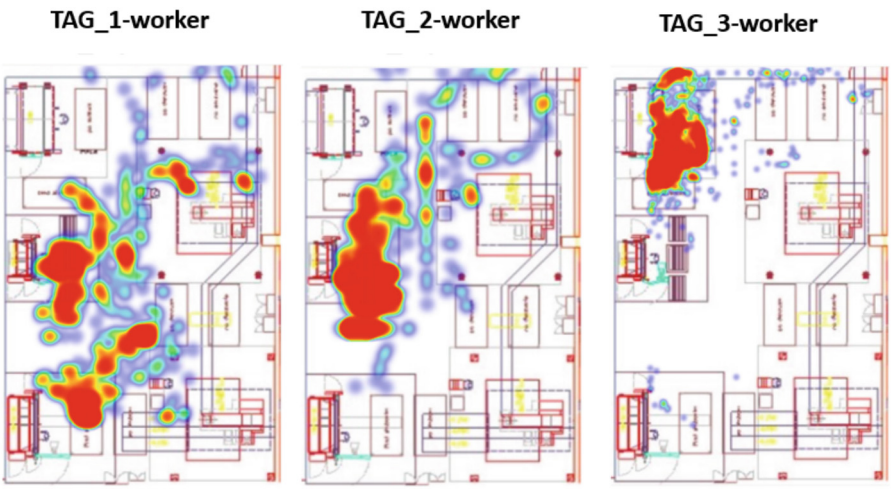

Fig. 8. Heatmaps of workers with appropriate tags (1, 2, 3).

These shortcomings were also consulted directly at these workplaces, so we can consider this as a verification that the results of the analyses were correct.

The results of the analysis revealed deficiencies. Most of these are lengthy material transportation, improperly positioned intermediate warehouses, and outdated technology without automation elements currently considered necessary in a modern company.

These aspects could be considered as the main shortcomings in the selected productions. As such, the industry faces these kinds of problems daily, so it is appropriate to label these deficiencies as conventional.

Fig. 9. Spaghetti diagram of workers with appropriate tagging.

This article clearly states its use in industrial practice, which is possible to build on in further research, which we would like to continue by adding and defining other research parameters. The RTLS system is irrevocably entering the sphere of business processes where it is used as an irreplaceable tool for monitoring and localization. In this trend, it is necessary to continue and develop either in test versions or in implemented localization system companies.

5 Conclusions

In the final phase of our research and implementation, we successfully created a localization project in the RTLS Studio environment, considering the needs of industrial data collection. This project represents a significant step forward in accurately tracking assets and resources in industrial environments. Our approach to the design and implementation of a localization system offers an effective solution for accurate positioning, thereby contributing to the optimization of production processes and the improvement of the enterprise's overall efficiency [11].

In the final phase of our research and implementation, we successfully created a localization project in the RTLS Studio environment, considering the needs of industrial gathering. This project represents a significant step forward in accurately tracking assets and resources in industrial environments. Our approach to the design and implementation of a localization system offers an effective solution for accurate positioning, thus contributing to the optimization of production processes and improving the enterprise's overall efficiency.

Considering the dynamics of modern industrial environments and the ever-growing demands for efficiency and traceability, our work will bring valuable knowledge and inspiration for further development in RTLS applications. We will continue to monitor the development of this technology and gather experience to contribute to continuous process improvement and innovation in the industrial sector.

Acknowledgment. This article was created by the implementation of the grant projects: APVV-17-0258 Digital engineering elements application in innovation and optimization of production flows, APVV-19-0418 Intelligent solutions to enhance business innovation capability in the process of transforming them into smart businesses. VEGA 1/0438/20 Interaction of digital technologies to support software and hardware communication of the advanced production system platform. KEGA 020TUKE-4/2023 Systematic development of the competence profile of students of industrial and digital engineering in the process of higher education. VEGA 1/0508/22 „Innovative and digital technologies in manufacturing and logistics processes and system".

References

1. Boulos, M.N.K., Berry, G.: Real-time locating systems (RTLS) in healthcare: a condensed primer. Int. J. Health Geogr. **101**(1), 25–32 (2012)
2. Edl, M., Rosi, B., Lerher, T.: Energy efficiency model for the mini-load automated storage and retrieval systems. Int. J. Adv. Manuf. Technol. **70**, 97–115 (2014)

3. Edl, M.: A systemic concept of the life cycle of a technical project in the environment. DP. 1. Smart Motion, Pilsen (2013). (in Czech)
4. Grznar, P., et al.: A system to determine the optimal work-in-progress inventory stored in interoperation manufacturing buffers. Sustainability **11**(14), 3949 (2019)
5. Mizerák, M., Trojan, J., Trebuňa, P., Švantner, T.: RTLS system in industrial enterprises. In: Proceeding of the InvEnt 2021: Industrial engineering – Invention for enterprise, pp. 96−99. Publishing House of the Academy of Technology and Humanities, Bielsko-Biala (2021)
6. Mizerák, M., Kliment, M., Pekarčíková, M., Kopec, J.: Location detection technologies as exponential tool of Industry 4.0. In: Proceeding of the 24th International Scientific Conference «Trends and Innovative Approaches in Business Processes 2021», pp. 67−71. Technical University of Košice, Košice (2021)
7. Masek, P., Sedlacek, P., Ometov, A., et al.: Improving the precision of wireless localization algorithms: ML techniques for indoor. In: Proceeding of the 43rd International Conference on Telecommunications and Signal Processing (TSP), pp. 589−594. Electr. Network (2020)
8. Votava, V., Ulrych, Z., Edl, M., Trkovský, V., Korecký, M.: Analysis and optimization of complex small-lot production in new manufacturing facilities based on discrete simulation. In: EMSS 2008, pp. 198−203. Diptem Universita di Genova, Genova (2008)
9. UWB Technology. https://www.sewio.net/uwb-technology/. Accessed 15 Nov 2023
10. SEWIO UWB Real-Time Location System (RTLS). https://www.sewio.net/real-time-location-system-rtls-on-uwb/. Accessed 15 Nov 2023
11. What is an Industrial RTLS?. https://www.sewio.net/rtls-in-industry/. Accessed 15 Nov 2023

Information Management Systems

Directions of IT Systems Development in Warehouses Management: Polish Practitioners Viewpoint

Ludmiła Filina-Dawidowicz[1], Piotr Trojanowski[1(✉)], Piotr Mrowiński[1], and Anastasiya Troynina[2]

[1] West Pomeranian University of Technology in Szczecin, 17, Piastów Avenue, 70-310 Szczecin, Poland
piotr.trojanowski@zut.edu.pl

[2] Odesa Polytechnic National University, 1, Shevchenko Avenue, Odesa 65044, Ukraine

Abstract. During the last two decades, a rapid development of information technology (IT) systems used by logistics companies has been observed. These systems facilitate decision-making processes, reduce operation duration, save costs, and integrate data users. Suppliers are creating and delivering systems to the market, considering the varied and stringent customers' requirements. Considering the practitioner's viewpoint, the article examines the directions of IT systems development in warehouse management. Practitioners' opinions in companies located in selected voivodeships in Poland were analyzed. The barriers to the expansion of IT systems were identified, and the directions of their development in logistics companies were investigated. It was concluded that the development of IT systems used to support operations performed in warehouses should be perceived in a complementary manner because the move towards systems integration will facilitate the execution of tasks not only in the warehouses but also within the company and consequently in the whole supply chain. The research results show the desired directions of IT systems development that may interest logistics companies, IT systems suppliers, and users.

Keywords: IT System · Development Directions · Warehouse Management · Logistics Company · Supply Chain · Cognitive System · Industrial Innovation

1 Introduction

Technological development is one of the indispensable conditions for the successful operation of modern companies in the transport and logistics (T&L) industry [1]. A company striving to be competitive in a globalized environment must use new technologies to improve its management and operation. IT systems have become essential due to the growing demands of these companies' customers and the need to reduce costs and the duration of operations.

© The Author(s), under exclusive license to Springer Nature Switzerland AG 2024
V. Ivanov et al. (Eds.): DSMIE 2024, LNME, pp. 89–99, 2024.
https://doi.org/10.1007/978-3-031-61797-3_8

Warehouses play an important role in supply chains [2] and should be designed appropriately. These facilities allow for short-term and long-term cargo storage and should enable smooth cargo flow. Warehouses are located within different links of supply chains and must be equipped with appropriate infrastructure and technical devices, particularly IT systems, allowing for efficient management of performed processes.

Analysis of the available literature revealed that much attention is paid to IT systems development and their application in the T&L industry. However, IT suppliers may face challenges identifying desired directions of IT systems development considering the customers' needs. Therefore, there is still a need to investigate current demands expressed by practitioners and their opinions on the IT systems operation and possible expansion related, i.e., to factors influencing systems implementation, barriers to their expansion in the company, and desired development directions.

The presented article examines the directions of IT systems development in warehouse management, considering the practitioners' opinions.

2 Literature Review

In the available scientific literature, great emphasis is placed on the role of digitization development in operational processes [3], including information systems used in the T&L sector. There are studies thoroughly analyzing various aspects related to information systems development in warehouse management [4], production processes, distribution [5], transport infrastructure [6], and transport processes [7]. It is worth highlighting the key issues studied in the literature involving automation [8], systems integration [9], process optimization [10], data security [11], cargo flow modeling [12], and new technology acceptance [13]. Research papers also pay attention to the impact of these issues on the overall operational efficiency of warehouses [14]. However, it should be mentioned that in the available studies, mainly individual problems of IT systems utilization in warehouses are analyzed.

Different IT systems are described in the literature [15]. These systems may facilitate the operation of selected companies and allow the process of data within the whole supply chain. Implementing these systems aims to support decision-making [16] and allow for joint optimization of activities performed by different companies [17, 18]. Transport and logistics companies may use different software. Therefore, its integration within the company and with systems used by other participants of supply chains may be required. Nafisa et al. [19] described the software integration approach.

Among the systems supporting warehouse operations is the warehouse management system (WMS) [20]. Moreover, other kinds of information systems can be applied by logistics enterprises to support their functioning, including ERP (Enterprise Resources Planning) and SAP (Systems Applications and Products in Data Processing) [21]. For example, in the available literature, the software systems for spare parts management of grain harvesting machinery were examined, and IoT-based enterprise management systems using global manufacturing were considered [22].

The attention is drawn to the need to customize warehouse services [23], which also deals with IT systems development. Modern systems should also support the sustainable development of transport and logistics [24].

Based on the available literature analysis, it could be stated that there are different directions of IT systems development in warehouses. However, while implementing IT solutions, the logistics companies' managers may face different barriers [25]. Moreover, the application of these systems is conditioned by different factors. Buyers' expectations of information systems are changing as the logistics industry evolves. This fact has prompted the need to survey warehousing companies' representatives to identify desired directions for further IT systems development.

3 Research Methodology

Based on the results of the literature analysis and the author's observations, the survey questionnaire was developed using Google Forms. The survey was carried out to receive the answers to the following research questions:

1. What problems may an IT system user face when utilizing it?
2. What are the barriers to the expansion of IT systems in the company?
3. What factors will influence the development of these systems and their broader use in the company?
4. What are the directions for developing IT systems in logistics companies involved in warehouse management?

The questionnaire contained both closed and open-ended questions, providing the opportunity to propose their answer by the respondent. The first part of the questionnaire aimed at defining the respondents' profiles (5 questions), while the second part contained thematic questions (6 questions).

An electronic version of the questionnaire was emailed to 60 warehouse employees in the West Pomeranian and Lower Silesian Voivodeships of Poland. Their significance in supply chains conditioned the selection of warehouses. The key stakeholders were identified and asked to take part in the survey. Moreover, the questionnaire was distributed using social media (Facebook), allowing practitioners from other voivodeships to participate in the survey. It was possible to complete the questionnaire from 26 May 2022 until 15 June 2022. The survey involved 51 respondents.

Then, the results obtained were analyzed, and appropriate conclusions were drawn.

4 Results and Discussion

The results analysis revealed that a greater share of respondents who filled in the questionnaire were men – 34 persons (66.7% of surveyed practitioners), while women constituted 17 interviewees (33.3%). The largest group of practitioners ranged in age from 25 to 40 years, this option was chosen by 16 respondents (31.4%), followed by 41–55-year-olds (14 persons - 27.4%), 18–24-year-olds (13 respondents - 25.5%), the smallest age group was 55+ year-olds, which was chosen by 8 practitioners (15.7%). Regarding the represented workplace, the largest group of respondents formed process management specialists. This option was selected by 14 interviewees (27.4%). It was followed by

heads of departments and procurement/distribution department staff with 13 representatives of specified workplace groups (25.5% each), logistics operators with 8 respondents (15.7%), and directors represented by 3 practitioners (5.9%). The structure of the surveyed respondents is shown in Fig. 1.

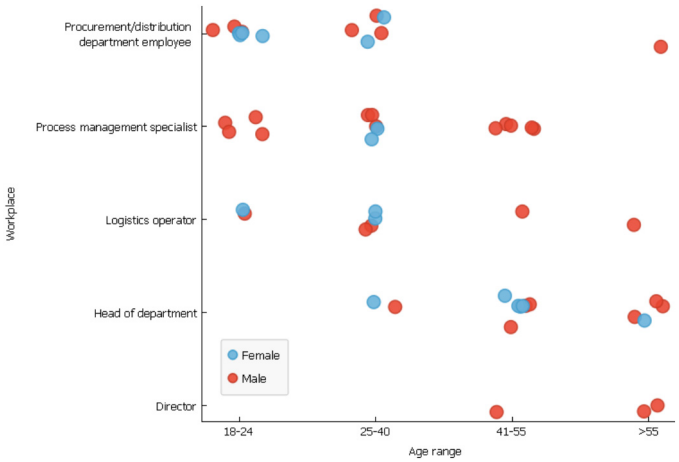

Fig. 1. Structure of respondents who took part in the survey.

The largest group of respondents were those with seniority of less than 5 years - 21 respondents (41.2%), the option of work experience between 5 and 10 years was selected by 12 practitioners (23.5%), 10 to 15 years was indicated by 10 persons (19.6%). In contrast, the smallest group of respondents was with seniority of more than 15 years - 8 respondents (15.7%). It should be noted that the work experience was related to the current position, so the person completing the survey could possess more experience in the T&L industry, albeit at a different position or in a different company. Regarding the company's location, the responses were received from the West Pomeranian Voivodeship of Poland, with 25 responses (49%), and the Lower Silesian Voivodeship, with 26 interviewees (51%). Among the thematic questions, there was a question aimed at identifying the IT systems that each respondent uses in the workplace. This was a multiple-choice question with the option to propose their suggestion of the system used (Fig. 2). It should be stated that none of the respondents took the opportunity to place their answer. Among 8 proposed systems, SAP was chosen by most of the respondents (33 practitioners – 64.7%). This was followed by systems such as ERP (27 respondents – 52.9%) and WMS (26 practitioners – 51%). It should be highlighted that the structure of respondents' workplaces influenced the results obtained.

The next question sought to investigate the level of IT systems integration in the respondents' companies (Fig. 3). This was a multiple-choice question. The highest number of responses (33 practitioners – 64.7%) was given to integrating systems "at company department level". This indicates that IT systems are used in companies represented by practitioners mainly to support the work of individual departments, as most systems are dedicated to strictly defined tasks (production, transport, warehousing, and contact with

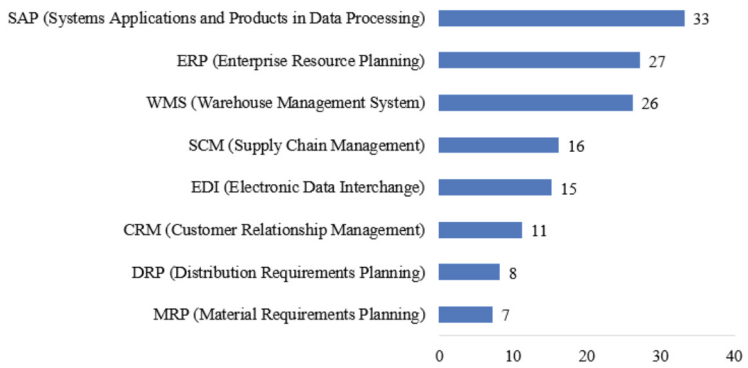

Fig. 2. Systems used by respondents in their company workplace (number of responses).

customers). The second most frequently selected answer (given by 27 respondents – 52.9%) was integrating systems at the level of the entire company. This can be related to using SAP or ERP systems that enable the entire enterprise's management. These systems consist of different modules and allow the integration of the processes and ensure efficient data flow within the company. Only 10 respondents indicated the integration of IT systems within the supply chain.

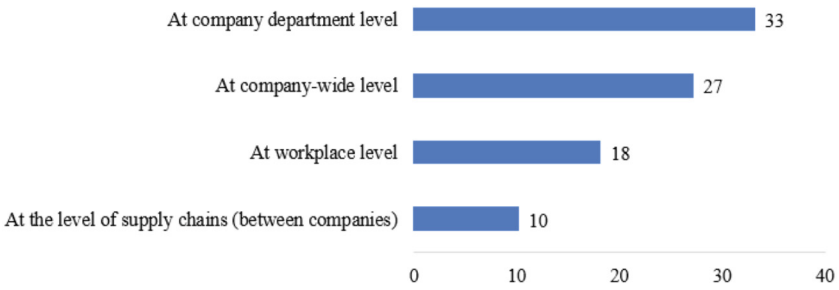

Fig. 3. Integration of IT systems in companies represented by practitioners (number of responses).

Practitioners were asked to specify the problems of utilizing IT systems in an enterprise. This was also a multiple-choice question (Fig. 4). Among the problems faced by IT systems users, the options "unintelligible messages" and "non-intuitive interface" received the highest ranks (indicated by 23 practitioners – 45.1% each). Unintelligible messages may result from imprecisely worded commands provided by the system. The non-intuitive interface may be related to an inadequately designed graphical interface that, for novice users with little experience, may pose problems in performing their duties efficiently. The graphical interface should be designed to be simple and understandable. The problem with starting up and using the system, indicated by 22 respondents (43.1%), may be related to the office hardware and the number of available systems in operation, proving excessive waiting times. In contrast, the options "outdated computer/office

equipment" and "poor internet connection" were selected by a smaller number of respondents (13 persons – 25.5% each). Newer systems often perform advanced computing processes, which require adjusting the company's hardware.

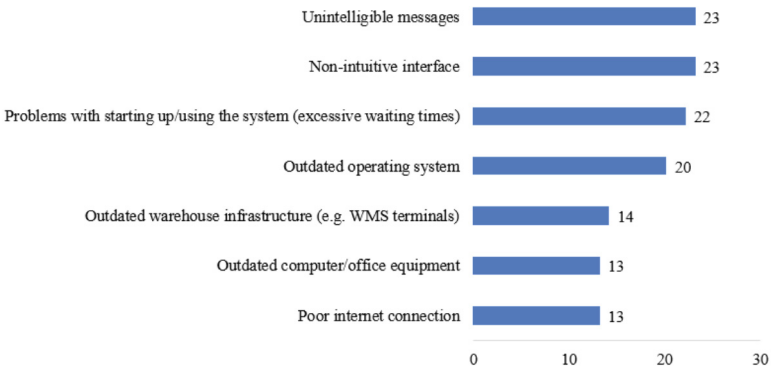

Fig. 4. Problems of using IT systems in a company (number of responses).

Respondents were asked to assess the barriers to the expansion of IT systems in a company using the Likert scale [26] from 1 to 5, where 1 means the least significant barrier, 5 - the most significant (Fig. 5). Respondents indicated the high costs of using and maintaining IT systems as the most significant barrier to the development of IT systems (with mean value 3.62). In the case of medium-sized companies, which constitute the largest group among the companies involved in warehouse management in Poland, the use of advanced systems may turn out to be too expensive, taking into account not only the costs of the system purchase but also its implementation, adaptation of the company's infrastructure, employees training, and everyday support. Investment risks and hacking attacks were assessed as the least significant barriers (with mean values of 2.83 and 2.82, respectively).

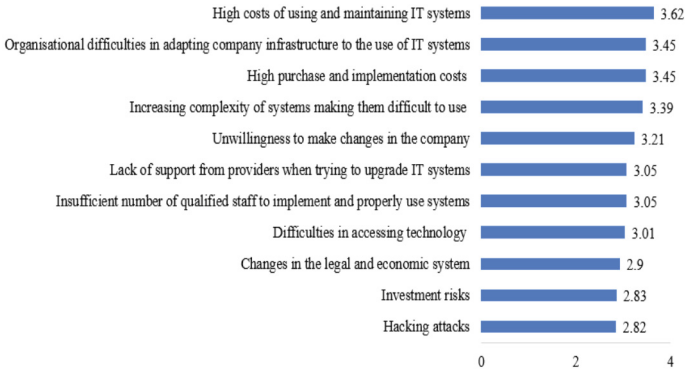

Fig. 5. Barriers to IT systems expansion in a company (mean values).

The next question concerned the factors that, according to the respondents' opinion, will affect the development of IT systems and their wider use within the company (Fig. 6). The respondents were also asked to apply the Likert scale to assess the proposed options, where 1 was the least important factor, 5 – the most important. The striving for cost savings was ranked by the practitioners as the most important factor (with a mean value of 3.6). This is reflected in the competitive T&L market environment, as every company aspires to minimize costs while maximizing profits. Therefore, the more a given system allows to reduce a company's operation costs, the more managers will be willing to implement it. Noteworthy is the need to integrate IT systems (mean value – 3.43). Combined IT solutions allow the creation of complementary systems. Integrating systems derived from different suppliers remains a challenge for different logistics companies.

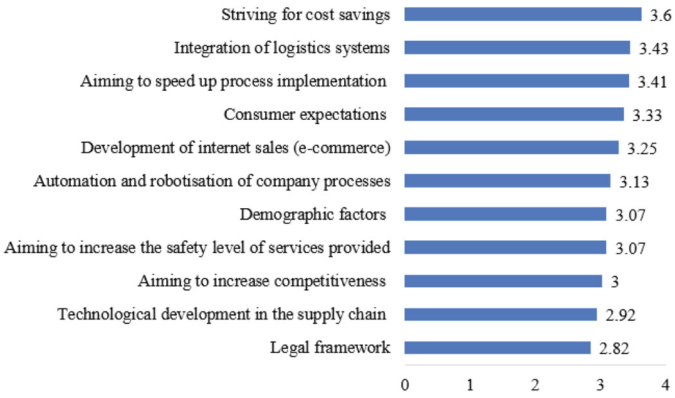

Fig. 6. Factors influencing the development of IT systems and their broader use in companies (mean values).

The last question concerned the desired directions of IT systems development (Fig. 7). According to the respondents, the most important IT systems development direction deals with decreasing implementation and operation costs. This option was chosen by 34 practitioners (66.7%). This may influence the managers' decisions on the broader use of IT systems in companies involved in warehouse management. It should be emphasized that the implementation and maintenance of IT systems include company customization, system configuration, installation, training, and servicing to use the system's full potential.

The respondents highly ranked the need to integrate various IT systems, indicating a real need to develop complementary IT systems and combine existing ones to manage the processes within the company and the entire supply chain. Systems should evolve mainly by increasing their integration and functionality, enabling effective data exchange.

Based on the research results, it could be concluded that IT systems suppliers should try to reduce the costs of systems development. In turn, IT systems purchases should look for co-financing opportunities and realize the long-term benefits of modern IT systems implementation in companies.

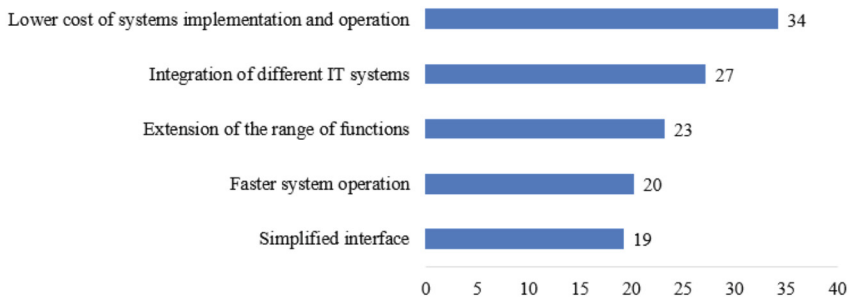

Fig. 7. Desired directions of IT systems development (number of responses).

While discussing the research results, it should be stated that the identified barriers are partly similar to those indicated in the literature (e.g., lack of government support related to the problem of high costs or lack of skilled human resources) [25]. Moreover, there is a convergence between the conclusions from the conducted research and the literature review, which shows that the development of IT systems will contribute to improving the management of warehouse processes.

Notably, the research results are limited to a small but representative sample, which may affect the results obtained. Therefore, it is essential to repeat the research and investigate the opinions of practitioners from other voivodeships in Poland and other countries, which will allow the opportunity to compare the results obtained. Moreover, besides the representatives of warehouses, the opinions of other companies involved in T&L activity (e.g., transport and manufacturing companies) should be investigated.

5 Conclusions

The article identifies and examines the desired directions of IT systems development, considering the practitioner's viewpoint. The problems and barriers to developing IT systems in logistics companies dealing with warehouse management and the factors determining their development in the enterprise were analyzed. The opinions of practitioners were obtained using a questionnaire survey.

Respondents used different systems in the company to perform tasks. Among 8 proposed systems, SAP was mentioned as the most frequently used system, followed by ERP and WMS. In enterprises represented by respondents, IT systems were integrated mostly at the department and company-wide levels. The most significant problems surveyed IT systems users faced were "unintelligible messages" and "non-intuitive interface". According to practitioners, the highest-rated barrier to developing IT systems in the company was related to the high costs of using and maintaining these systems. That fact may indicate that IT systems suppliers offer too high prices for their products, making the purchase and implementation of systems too expensive for companies involved in warehouse management. In addition, decreasing the costs of such systems implementation and operation is a desirable direction of systems development, defined by a surveyed group of practitioners.

It can be concluded that there are clear prospects for further development of IT systems supporting the warehouses' operation. These systems increase the effectiveness of activities carried out in the enterprise. However, development directions of these systems and provided improvements should consider users' needs and opinions. Systems users are striving to improve not only the comfort of their work but also the efficiency of the entire enterprise.

Based on the research carried out, it can be stressed that the development of IT systems to support warehouse management should be seen as complementary, as the move towards system integration will increase productivity and data accuracy and speed up the execution of tasks not only in the warehouse but also throughout the company. This involves the information flow between the company's departments and the possibility for employees at different management levels to use it. The development of IT systems is contingent on close cooperation between information systems users and suppliers striving for systems integration and reducing the costs of their purchase and subsequent operation. Moreover, systems integration between the companies is crucial (e.g., between warehouses and road transport companies). This should be a promising direction for their further development.

Further scientific research will focus on a more detailed analysis of the conditions for cognitive systems implementation and operation in logistics enterprises.

The research results may be of interest to IT systems suppliers and managers of transport and logistics companies operating these systems.

Acknowledgment. The research was partially supported by the International Association for Technological Development and Innovations (IATDI).

References

1. Kostrzewski, M., Filina-Dawidowicz, L., Walusiak, S.: Modern technologies development in logistics centers: the case study of Poland. Transp. Res. Procedia **55**, 268–275 (2021). https://doi.org/10.1016/j.trpro.2021.06.031
2. Szczepański, E., Jachimowski, R., Izdebski, M., Jacyna-Gołda, I.: Warehouse location problem in supply chain designing: a simulation analysis. Arch. Transp. **50**(2) (2019). https://doi.org/10.5604/01.3001.0013.5752
3. Adamczak, M., Kolinski, A., Trojanowska, J., Husár, J.: Digitalization trend and its influence on the development of the operational process in production companies. Appl. Sci. **13**(3), 1393 (2023). https://doi.org/10.3390/app13031393
4. Shmatko, A., Barykin, S., Sergeev, S., Thirakulwanich, A.: Modeling a logistics hub using the digital footprint method—the implication for open innovation engineering. J. Open Innov. Technol. Mark. Complex. **7**(1), 59 (2021). https://doi.org/10.3390/joitmc7010059
5. Pavlenko, O., Shramenko, N., Muzylyov, D.: Logistics optimization of agricultural products supply to the European Union based on modeling by Petri nets. In: Karabegović, I. (ed.) NT 2020. LNNS, vol. 128, pp. 596–604. Springer, Cham (2020). https://doi.org/10.1007/978-3-030-46817-0_69
6. Sęk, J., Trojanowski, P., Gilewicz, Ł, Gapinski, B., Evtuhov, A.: Implementation of intelligent transport systems in an urban agglomeration: a case study. In: Ivanov, V., Trojanowska, J., Pavlenko, I., Rauch, E., Piteľ, J. (eds.) DSMIE 2023. LNME, pp. 152–161. Springer, Cham (2023). https://doi.org/10.1007/978-3-031-32767-4_15

7. Yazdani, M., Pamucar, D., Chatterjee, P., Chakraborty, S.: Development of a decision support framework for sustainable freight transport system evaluation using rough numbers. Int. J. Prod. Res. **58**(14), 4325–4351 (2020). https://doi.org/10.1080/00207543.2019.1651945
8. Jaghbeer, Y., Hanson, R., Johansson, M.I.: Automated order picking systems and the links between design and performance: a systematic literature review. Int. J. Prod. Res. **58**(15), 4489–4505 (2020). https://doi.org/10.1080/00207543.2020.1788734
9. Ju, Y., Hou, H., Yang, J.: Integration quality, value co-creation and resilience in logistics service supply chains: moderating role of digital technology. Ind. Manag. Data Syst. **121**(2), 364–380 (2021). https://doi.org/10.1108/IMDS-08-2020-0445
10. Adi, T.N., Iskandar, Y.A., Bae, H.: Interterminal truck routing optimization using deep reinforcement learning. Sensors **20**(20), 5794 (2020). https://doi.org/10.3390/s20205794
11. Sergi, I., Montanaro, T., Benvenuto, F.L., Patrono, L.: A smart and secure logistics system based on IoT and cloud technologies. Sensors **21**(6), 2231 (2021). https://doi.org/10.3390/s21062231
12. Pavlenko, O., Muzylyov, D., Shramenko, N., Cagáňová, D., Ivanov, V.: Mathematical modeling as a tool for selecting a rational logistical route in multimodal transport systems. In: Cagáňová, D., Horňáková, N. (eds.) Industry 4.0 Challenges in Smart Cities. EAI/Springer Innovations in Communication and Computing, pp. 23–37. Springer, Cham (2022). https://doi.org/10.1007/978-3-030-92968-8_2
13. Kapser, S., Abdelrahman, M.: Acceptance of autonomous delivery vehicles for last-mile delivery in Germany-Extending UTAUT2 with risk perceptions. Transp. Res. Part C: Emerg. Technol. **111**, 210–225 (2020). https://doi.org/10.1016/j.trc.2019.12.016
14. Halawa, F., Dauod, H., Lee, I.G., Li, Y., Yoon, S.W., Chung, S.H.: Introduction of a real time location system to enhance the warehouse safety and operational efficiency. Int. J. Prod. Econ. **224**, 107541 (2020). https://doi.org/10.1016/j.ijpe.2019.107541
15. Kihel, Y.E.: Digital transition methodology of a warehouse in the concept of sustainable development with an industrial case study. Sustainability **14**(22), 15282 (2022). https://doi.org/10.3390/su142215282
16. Duque, J., Moreira, J.J., Costa, J.: Data mining to support decision-making—a research approach. In: Nagar, A.K., Singh Jat, D., Mishra, D.K., Joshi, A. (eds.) Intelligent Sustainable Systems. LNNS, vol. 578, pp. 553–563. Springer, Singapore (2023). https://doi.org/10.1007/978-981-19-7660-5_48
17. Qin, J., Yang, S., Dai, B.: Joint optimization of order allocation and path planning in e-commerce robotic mobile fulfillment system. J. Railway Sci. Eng. **20**(1), 116–126 (2023)
18. Hricova, R., Madzinova, R.: Innovations in a modern engineering enterprise in the context of Industry 4.0 strategy. J. Eng. Sci. (Ukraine) **10**(2), A1–A9 (2023). https://doi.org/10.21272/jes.2023.10(2).a1
19. Nafisa, Y., Gulnara, V., Rustem, Z.: Approach to software integration of heterogeneous sources of medical data based on microservice architecture. Inform. Autom. **21**(5), 881–915 (2022). https://doi.org/10.15622/ia.21.5.2
20. Kellermayr-Scheucher, M., Niedermeier, M., Brandtner, P.: Applications and perceptions of workforce management systems for warehouse operation-results and findings from expert interviews. Procedia Comput. Sci. **219**, 255–262 (2023). https://doi.org/10.1016/j.procs.2023.01.288
21. Belkacem Bouzida, I., Merzoug, S.: Impact of logistics information systems on supply chain optimization: case of Group Bachir Rachid. J. Sustain. Dev. Transp. Logist. **6**(2), 60–80 (2021). https://doi.org/10.14254/jsdtl.2021.6-2.4
22. Alsudani, M.Q., et al.: Smart logistics with IoT-based enterprise management system using global manufacturing. J. Comb. Optim. **45**(2), 57 (2023). https://doi.org/10.1007/s10878-022-00977-5

23. Khan, N., Solvang, W.D., Yu, H.: Customizing smart warehouse management for large scale production industries. In: 2023 IEEE Conference on Technologies for Sustainability. SusTech 2023, pp. 199–204. IEEE (2023). https://doi.org/10.1109/SusTech57309.2023.10129595
24. Scurt, F.B., Beles, H., Vesselenyi, T., Lehel, C.: Driver alertness monitoring system in the context of safety increasing and sustainable energy use. Cogn. Sustain. **2**(1) (2023). https://doi.org/10.55343/cogsust.49
25. Kumar, S., Raut, R.D., Narwane, V.S., Narkhede, B.E., Muduli, K.: Implementation barriers of smart technology in Indian sustainable warehouse by using a Delphi-ISM-ANP approach. Int. J. Product. Perform. Manag. **71**(3), 696–721 (2022). https://doi.org/10.1108/IJPPM-10-2020-0511
26. Likert, R.: A technique for the measurement of attitudes. Arch. Psychol. (1932). 1933-01885-001

Generative AI in Agile, Project, and Delivery Management

Bohdan Haidabrus[1,2,3](✉)

[1] Accenture Baltics, 214, Brivibas Street, Riga 1039, Latvia
haidabrus@gmail.com
[2] Riga Technical University, 6A, Kipsalas Street, Riga 1048, Latvia
[3] University of Applied Science, 3, Meza Street, Riga 1048, Latvia

Abstract. Generative Artificial Intelligence (AI) is poised to revolutionize Agile delivery by introducing unprecedented levels of efficiency, innovation, and adaptability. As Agile methodologies emphasize iterative progress, customer collaboration, and response to change, Generative AI offers a suite of tools that align with these principles by automating and creating tasks, generating a wealth of potential solutions to complex problems, and facilitating rapid prototyping. This article explores the intersection of Generative AI with Agile practices, identifying the enhancements and challenges this integration presents. The discussion is grounded in current trends, practical case studies, and strategies for implementation. The potential benefits and limitations of incorporating Generative AI into Agile frameworks are weighed, with considerations of technical and ethical nature. The article concludes by considering future directions for both Generative AI advancements and the evolution of Agile methodologies. The implications for teams, project management, and overall delivery of products and services are substantial, signaling a transformative phase in the Agile culture, especially for Information Management Systems delivery.

Keywords: GenAI · Agile Framework · Delivery Management · Artificial Intelligent · Industry · Innovation · Infrastructure · Data Science · Machine Learning · Product Innovation

1 Introduction

The landscape of software development and project management has evolved significantly over the past few decades, moving from rigid, linear approaches to more flexible, iterative methodologies. The introduction of Agile has been a game-changer in this evolution, promoting adaptive planning, evolutionary development, early delivery, and continual improvement. Alongside this, advancements in AI, particularly Generative AI, have opened new avenues for innovation. This section provides a foundational understanding of Agile delivery and Generative AI, setting the stage for their convergence [1].

© The Author(s), under exclusive license to Springer Nature Switzerland AG 2024
V. Ivanov et al. (Eds.): DSMIE 2024, LNME, pp. 100–110, 2024.
https://doi.org/10.1007/978-3-031-61797-3_9

Agile delivery is an approach to software development that values customer collaboration, flexibility, and rapid value delivery. Emerging from the Manifesto for Agile Software Development in 2001, Agile methodologies such as Scrum, Kanban, and Extreme Programming (XP) have transformed the way organizations approach project management and product development [2, 3]. Agile's core principles emphasize cross-functional teams, adaptability to changing requirements, and a focus on delivering working software frequently.

Generative AI refers to the subset of AI technologies that can generate new content after learning from a dataset. This includes technologies like Generative Adversarial Networks (GANs), which can produce images, text, and other forms of media that are often indistinguishable from human-generated content. Beyond GANs, other forms of Generative AI include natural language processing (NLP) models, such as GPT-4, which are capable of writing code, composing music, and more after being trained on vast amounts of data (Fig. 1) [4].

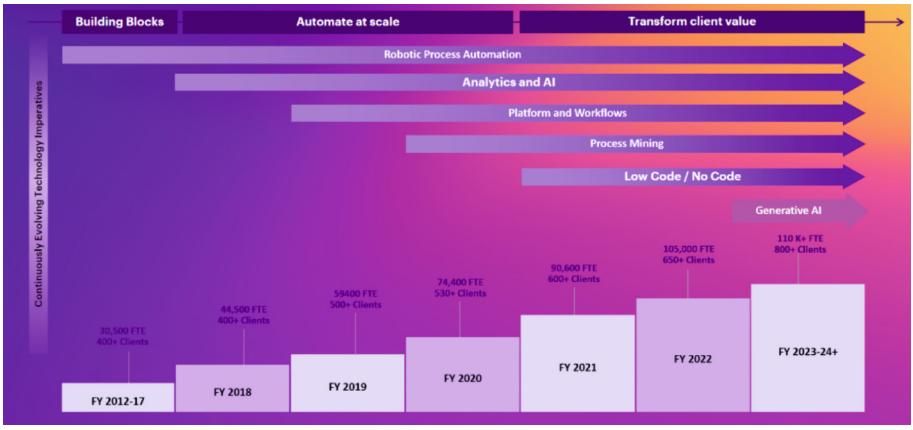

Fig. 1. Generative AI to augment the Intelligent Automation Journey across the areas.

Generative AI can enhance Agile delivery by automating and optimizing various facets of the development process and building necessary competencies to improve Manufacturing Engineering Management and Information Management Systems Delivery [5, 6]. As shown in Fig. 1, there is an evolution from Robotic Process Automation through Analytics, AI, and Process Mining to Generative AI. From generating code to assisting in designing user interfaces, the application of GenAI within Agile teams could significantly alter the velocity and quality of development cycles.

Integrating specific AI technologies within Agile frameworks can significantly enhance various aspects of the Agile process, from project planning to execution, monitoring, and controlling. This paper is based on a detailed look at some key AI technologies relevant to project management and Agile framework, such as [7] Machine Learning and Predictive Analysis, Natural Language Processing, AI-powered code Generation and Assistance, Automated Testing and Quality Assurance; Data Visualization and Reporting Tools; Decision Support Systems; Sentiment Analysis; Deep Learning.

This paper aims to provide research results for implementing GenAI solutions to Agile projects, how it helps increase stakeholder value, and how to start implementing Generative AI tools and techniques.

2 Literature Review

The union of Generative AI and Agile methodologies represents a symbiotic relationship where AI's innovative and efficiency-driven aspects complement Agile's dynamic and iterative nature. This section delves into how this convergence reshapes project management and software development [1, 15].

Adopting AI in Agile environments is not just theoretical but is rapidly becoming a norm. A study by VersionOne's 14th Annual State of Agile Report indicates an increasing trend of integrating AI and machine learning into Agile practices. For example, AI-driven analytics for project data enables Agile teams to predict bottlenecks and improve sprint planning. Generative AI is taking this a step further by analyzing data and generating actionable insights and elements of the development process itself, such as code and test cases [2, 4, 16].

Practical examples of Generative AI in Agile delivery can be seen in companies like GitHub, with their Copilot feature powered by OpenAI's Codex, which suggests real-time code snippets and entire functions to developers. Another example is the use of AI in automated testing, where AI algorithms are used to generate test scenarios, improving the coverage and efficiency of the testing phase in Agile cycles [7, 18].

The intersection of Generative AI and Agile is challenging. While AI can dramatically speed up specific processes, it also introduces complexities in integration, a need for new skills, and raises ethical questions around decision-making and creativity.

Implementation of Generative AI within Agile frameworks must be strategic to maximize benefits while mitigating potential disruptions. This section outlines the approaches for integrating these technologies into Agile workflows effectively [8, 22]. The introduction of Generative AI tools into Agile teams should follow Agile's principles – an iterative approach with regular feedback loops. Integration strategies should include [9, 21]:

- Incremental Adoption: gradually introducing AI tools to the team to manage the learning curve and adjust to the changing dynamics.
- Continuous Training: investing in ongoing training and development to build the team's competency in working alongside AI.
- Cross-functional Collaboration: encouraging collaboration between data scientists, AI experts, and Agile team members to facilitate knowledge exchange and joint problem-solving (Fig. 2) [4].

Total Enterprise Reinvention is made possible when companies:

- Build a strong digital core.
- Invest in new technologies.
- Change how collaboration works across the C-level.

Choosing the right tools and platforms is critical for successful implementation. Open-source frameworks such as TensorFlow and platforms like Google's AI Platform can be valuable for teams to experiment with and adopt AI capabilities. Project management tools with integrated AI features can also help forecast project timelines and allocate resources.

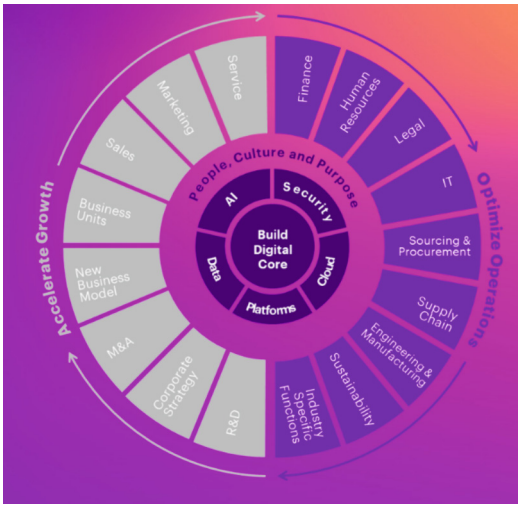

Fig. 2. Generative AI to augment the Intelligent Automation Journey across the areas.

The impact of Generative AI on Agile processes should be assessed regularly. Metrics such as sprint velocity, defect rates, and time to market can provide insights into the effectiveness of AI integration [10]. Continuous assessment helps understand the ROI of Generative AI tools and guides further investment and scaling decisions [11].

3 Research Methodology

The adoption of Generative AI technologies promises numerous benefits for Agile teams. This section explores our methodology of how Generative AI can enhance Agile delivery across various dimensions.

Generative AI can automate routine and complex tasks, leading to significant efficiency gains. For instance, AI-powered code completion tools can reduce developers' time writing standard code, allowing them to focus on solving more complex problems [12]. Moreover, AI can process and analyze large volumes of data faster than any human team, leading to quicker insights and decision-making (Fig. 3) [4].

Generative AI does not only execute tasks but can also generate novel ideas and approaches. By handling the more mundane aspects of design and development, AI frees human team members to engage in more creative and strategic activities [13–15].

For instance, AI can suggest several designs for a user interface, which the team can refine and iterate upon, potentially leading to more innovative outcomes.

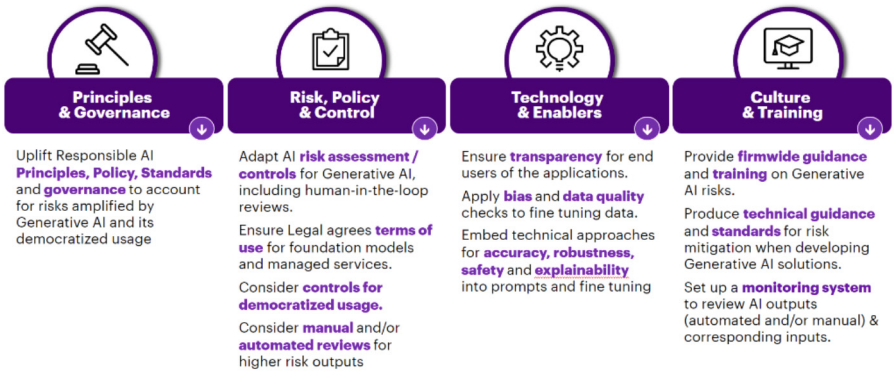

Fig. 3. Both Technical and Governance approaches as a mitigation of the responsible AI Risks of Generative AI.

3.1 Technical and Ethical Considerations

While the benefits are significant, the integration of Generative AI into Agile teams also presents challenges and limitations that need to be acknowledged and managed.

The technical complexity of AI models can make them appear as 'black boxes,' which can be a barrier to trust and adoption among Agile team members. Ethical considerations must be rigorously addressed, especially around data privacy and potential biases in AI-generated outputs.

Exploring the ethical considerations of incorporating Generative AI into Agile environments is crucial, especially as these technologies become increasingly integral to various processes [4]. Key concerns include potential biases in AI-generated outputs and data privacy issues:

Potential Biases in AI-Generated Outputs. AI systems, including Generative AI, learn from data sets that may contain biases. These biases can be based on gender, race, socioeconomic status, or other factors. Biases can manifest in various forms, such as code generation, automated decision-making, content creation, or data analysis. In terms of impacting agile environments in software development, biased AI could lead to the creation of products that don't adequately serve a diverse user base. In decision-making, biased AI might favor specific project directions or solutions, ignoring potentially valuable and diverse perspectives. Using diverse and inclusive data sets for training AI models, regularly auditing and reviewing AI outputs for biases, involving diverse teams in this process, and implementing ethical AI guidelines and frameworks within the Agile environment are the mitigation strategies for potential biases in AI-generated outputs.

Data Privacy. Generative AI often requires access to large amounts of data, including potentially sensitive information, to learn and generate outputs. In Agile environments, this might include proprietary project information, team members' personal data, or customer data. These impact the risk of unintentional exposure or misuse of sensitive data, and compliance with data protection regulations (like GDPR) can become more complex. Mitigation of the data privacy concerns issues might based on implementing strict data governance policies, ensuring that AI systems are only fed data that is appropriate and has been obtained with consent, using data anonymization and encryption to protect

sensitive information, and ensuring compliance with relevant data protection laws and industry standards.

Ethical Decision-Making. AI might be used to make or influence decisions in Agile processes. If not correctly overseen, this can lead to ethical issues, such as over-reliance on AI without considering human judgment. To avoid these, a project team must maintain a clear boundary between AI suggestions and human decision-making and foster an organizational culture that values ethical considerations and human judgment alongside AI insights.

3.2 Case Studies of the Practical Application of Generative AI

There are several notable examples and hypothetical case studies that demonstrate the practical application of Generative AI in Agile environments. This research explores how digital organizations might leverage Generative AI in various Agile contexts.

Case Study 1: Automation Documentation in Digital Software Development
Scenario: A software development company uses Agile methodologies for its projects.

Application of Generative AI: The company integrates a Generative AI tool to automate the creation of technical documentation, user manuals, and API documentation.

Outcome: This automation significantly reduces the time developers spend on documentation, allowing them to focus more on coding and innovation. The AI-generated documentation is also consistently updated with each iteration, ensuring accuracy and relevancy.

Case Study 2: Enhancing User Story Creation and Backlog Refinement
Scenario: An Agile team needs help creating detailed and precise user stories for their product backlog.

Application of Generative AI: The team employs a Generative AI system to refine and elaborate user stories. The AI tool analyzes existing stories, suggests enhancements, and identifies gaps based on user feedback and product data.

Outcome: The enriched user stories lead to better-developed features and a more streamlined development process, as developers have a clearer understanding of what needs to be built.

Case Study 3: Predictive Analytics in Project Management
Scenario: A project management team in digital development uses Agile ways of working for their software development.

Application of Generative AI: The team uses an AI tool for predictive analytics, assessing risks, forecasting project timelines, and predicting potential roadblocks.

Outcome: Early identification of risks and predictive insights enable the team to proactively address issues, leading to more successful project completions and reduced time and cost overruns.

Case Study 4: Personalized Learning for Continuous Improvement
Scenario: An Agile team at a large corporation continuously seeks to improve its skills and knowledge.

Application of Generative AI: The corporation implements an AI-driven learning platform that analyzes each team member's performance, suggesting personalized learning resources and training modules.

Outcome: Team members receive tailored learning experiences that enhance their skills in areas most relevant to their work, leading to improved performance and innovation in projects.

Case Study 5: AI-Assisted Code Review and Quality Assurance
Scenario: A software development team following Agile practices must maintain high code quality while meeting rapid release schedules.

Application of Generative AI: The team uses an AI tool that assists in code reviews by analyzing code submissions, identifying potential errors, suggesting optimizations, and ensuring coding standards are met.

Outcome: The AI-assisted code review process speeds up the review time, improves code quality, and reduces the number of bugs in production.

These examples and case studies illustrate the potential of Generative AI in enhancing the efficiency, effectiveness, and innovation capacity of teams operating in Agile environments, especially regarding quality control, ethical considerations, and skills adaptation [4]. The successful use of Generative AI requires specific skills and knowledge, which may only be present in some Agile teams. Bridging this skill gap requires significant investment in training and may also necessitate hiring new talent with expertise in AI.

4 Results and Discussion

As we look towards the horizon, it is evident that the convergence of Generative AI and Agile methodologies will continue to evolve. This section speculates on future developments in this field and how they may further impact Agile delivery. During our research, we assessed the impact of the ecosystem and enterprise platforms embedding Generative AI [4] (see Fig. 4).

4.1 Prediction of Advancements in AI and Evolving Agile Practices

The field of AI is progressing at a rapid pace. We can anticipate more sophisticated Generative AI models that are more accessible and easier to integrate into existing development pipelines [16]. As these tools become more refined, they will likely be capable of undertaking more complex tasks with less human intervention, further expediting the Agile process.

As Agile teams become more accustomed to working with Generative AI, Agile methodologies themselves may evolve. We could see the emergence of new frameworks and practices specifically designed to maximize AI's advantages, such as AI-driven decision-making and automated backlog refinement sessions.

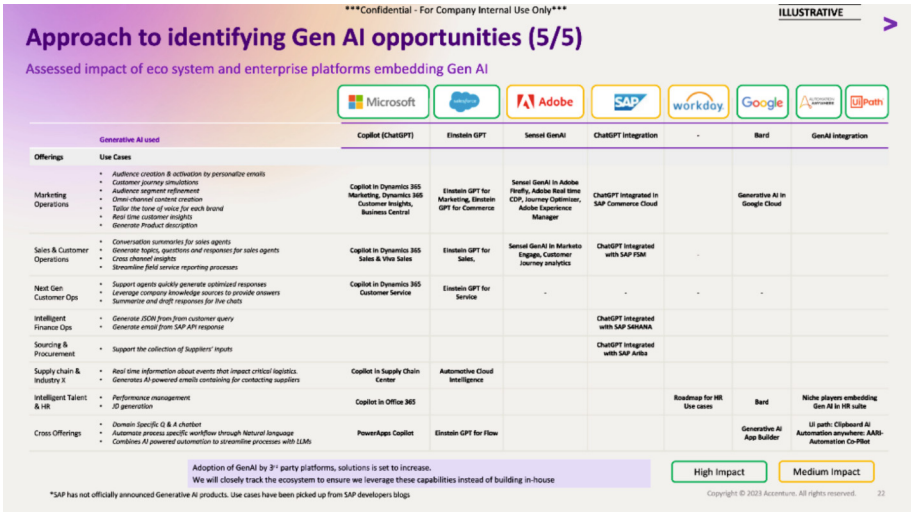

Fig. 4. Approach to identifying Gen AI opportunities.

4.2 Enhanced Collaboration Between Humans and AI

Looking forward, the focus will likely be on enhancing the collaboration between humans and AI, ensuring that AI tools are supportive, intuitive, and aligned with human creativity and strategic thinking [17–24]. This could lead to the development of new roles and responsibilities within Agile teams dedicated to managing and directing AI resources.

Comparing traditional Agile methodologies with those that integrate Generative AI highlights significant differences in approach, capabilities, and potential outcomes with additional discussion (Table 1).

Integrating AI into Agile frameworks offers advantages in efficiency and innovation but also introduces new challenges and complexities. It requires balancing AI capabilities with human insights and ethics.

It is necessary to mention that Generative AI can potentially transform business functions across Industries, thereby accelerating Total Enterprise Reinvention. Total Enterprise Reinvention Is made possible when companies build a strong digital core, invest in new technologies, and change how collaboration works across the C-level. But, making this happen with speed and scale across multiple functions requires compressed transformation, which is only possible with additional scientific and industrial research.

Table 1. Comparison of Agile framework to Generative AI integration.

Criteria	Tradition Agile	GenAI Agile
Efficiency and Speed	Agile relies on human resources for every aspect	Can automate routine tasks, significantly speeding up the development process
Decision Making and Planning	Relies on team expertise for decision-making	Can provide predictive insights for better planning
Scope of Innovation	Limited by the team's collective knowledge	Can suggest innovative solutions beyond the team's knowledge base
Risk Management	Manages risks based on experience, tools, and technics	Can predict potential risks using data analysis
Personalization and User Focus	Both methodologies focus on user needs, but Agile with Generative AI can analyze user data for deeper insights	
Learning and Adaptation	Relies on feedback loops for learning	Can facilitate rapid learning through data analysis
Communication and Collaboration	Emphasizes human interaction	Can automate communication While potentially impacting team dynamics
Skill Requirements	Requires a range of technical and soft skills	Demands understanding AI tools and data literacy
Quality and Reliability	Both approaches focus on quality, but Agile with Generative AI can introduce new types of errors requiring human oversight	
Ethical Considerations	Focuses on product and team ethics	Adds considerations around data privacy and AI bias

5 Conclusions

Generative AI can be a transformative force in Agile delivery, offering enhancements in efficiency, productivity, and potential for innovation to improve such related projects, Intelligent Manufacturing Systems, Robotics and Automation, Smart and Lean Manufacturing, Logistics, and Supply Chain with management and delivery. The journey towards fully integrating these technologies has challenges, yet the rewards promise to be substantial. As we continue to navigate the technical, ethical, and practical complexities, the Agile landscape is poised to evolve significantly, with Generative AI as a central driving force.

Integrating AI technologies into Agile frameworks offers significant potential to enhance efficiency, innovation, and decision-making. However, careful planning, training, and consideration of ethical implications are required to be truly effective. The paper shows that a careful balance between leveraging AI capabilities and maintaining essential human insights and ethics in the development process is required.

Acknowledgment. The research was partially supported by the International Association for Technological Development and Innovations (IATDI).

References

1. Boden, M.A.: Creativity and artificial intelligence. Artif. Intell. **103**(1–2), 347–356 (1998). https://doi.org/10.1016/S0004-3702(98)00055-1
2. Hoelbeche, L.: Designing sustainably agile and resilient organizations. Syst. Res. Behav. Sci. **36**(5), 668–677 (2019). https://doi.org/10.1002/sres.2624
3. Nguyen, D.: Success factors that influence agile software development project success. Am. Sci. Res. J. Eng. Technol. Sci. **17**(1), 172–222 (2016)
4. Generative AI Technology Services. https://www.accenture.com/cn-en/services/applied-intelligence/generative-ai. Accessed 01 Dec 2023
5. Ivanov, V., Vashchenko, S., Rong, Y.: Information support of the computer-aided fixture design system. In: CEUR Workshop Proceedings, vol. 1614, pp. 73−86 (2016)
6. Haidabrus, B., Grabis, J., Protsenko, S.: Agile project management based on data analysis for information management systems. In: Ivanov, V., Trojanowska, J., Pavlenko, I., Zajac, J., Peraković, D. (eds.) DSMIE 2021. LNME, pp. 174–182. Springer, Cham (2021). https://doi.org/10.1007/978-3-030-77719-7_18
7. Grabis, J., Haidabrus, B., Protsenko, S., Protsenko, I., Rovna, A.: Data science approach for it project management. ETR **2**, 51–55 (2019). https://doi.org/10.17770/etr2019vol2.4163
8. Kischelewski, B., Richter, J.: Implementing large-scale agile – an analysis of challenges and success factors. In: ECIS 2020 Research Papers, vol. 176, pp. 1−16 (2020)
9. Abadi, M., et al.: TensorFlow: a system for large-scale machine learning. In: 12th USENIX Symposium on Operating Systems Design and Implementation (OSDI '16), pp. 265−283 (2016). https://doi.org/10.48550/arXiv.1605.08695
10. Conforto, E.C., Salum, F., Amaral, D.C., Da Silva, S.L., De Almeida, L.F.M.: Can agile project management be adopted by industries other than software development? Proj. Manag. J. **45**(3), 21–34 (2014). https://doi.org/10.1002/pmj.21410
11. Rigby, D.K., Sutherland, J., Takeuchi, H.: Embracing Agile: how to master the process. That's transforming management. Harv. Bus. Rev. **94**(5), 40–50 (2016)
12. Kuric, I., Kandera, M., Klarák, J., Ivanov, V., Więcek, Da.: Visual product inspection based on deep learning methods. In: Tonkonogyi, V., et al. (eds.) InterPartner 2019. LNME, pp. 148–156. Springer, Cham (2020). https://doi.org/10.1007/978-3-030-40724-7_15
13. Heikkilä, V.T., Paasivaara, M., Lasssenius, C., Damian, D., Engblom, C.: Managing the requirements flow from strategy to release in large-scale agile development: a case study at Ericsson. Empir. Softw. Eng. **22**(6), 2892–2936 (2017). https://doi.org/10.1007/s10664-016-9491-z
14. Hricova, R., Madzinova, R.: Innovations in a modern engineering enterprise in the context of Industry 4.0 strategy. J. Eng. Sci. (Ukraine) **10**(2), A1–A9 (2023). https://doi.org/10.21272/jes.2023.10(2).a1
15. Pavlenko, I., et al.: Using regression analysis for automated material selection in smart manufacturing. Mathematics **10**(11), 1888 (2022). https://doi.org/10.3390/math10111888
16. Denning, S.: How Agile can transform manufacturing: the case of Wikispeed strategy and leadership, **40**(6), 22−28 (2012). https://doi.org/10.1108/10878571211278859
17. Hofman, M., Grela, G.: Project portfolio risk identification – application of Delphi method. J. Bus. Econ. **6–11**, 1857–1867 (2015). https://doi.org/10.15341/jbe(2155-7950)/11.06.2015/004

18. Cohen, D., Lindvall, M., Costa, P.: An introduction to agile methods. Adv. Comput. **62**(C), 1−66 (2004). https://doi.org/10.1016/S0065-2458(03)62001-2
19. Gandomani, T.J., Tavakoli, Z., Zulzalil, H., Farsani, H.K.: The role of project manager in agile software teams: a systematic literature review. IEEE Access **8**, 117109–117121 (2020). https://doi.org/10.1109/ACCESS.2020.3004450
20. Gren, L., Torkar, R., Feldt, R.: The prospects of a quantitative measurement of agility: a validation study on an agile maturity model. J. Syst. Softw. **107**, 38–49 (2015). https://doi.org/10.1016/j.jss.2015.05.008
21. Ivanov, V.: Process-oriented approach to fixture design. In: Ivanov, V., et al. (eds.) DSMIE 2018. LNME, pp. 42–50. Springer, Cham (2019). https://doi.org/10.1007/978-3-319-93587-4_5
22. Muzylyov, D., Shramenko, N., Ivanov, V.: Management decision-making for logistics systems using a fuzzy-neural simulation. In: Cagáňová, D., Horňáková, N., Pusca, A., Cunha, P.F. (eds.) Advances in Industrial Internet of Things, Engineering and Management. EICC, pp. 175–192. Springer, Cham (2021). https://doi.org/10.1007/978-3-030-69705-1_11
23. Vedal, H., Stray, V., Berntzen, M., Moe, N.B.: Managing dependencies in large-scale agile. In: Gregory, P., Kruchten, P. (eds.) XP 2021. LNBIP, vol. 426, pp. 52–61. Springer, Cham (2021). https://doi.org/10.1007/978-3-030-88583-0_6
24. Luscinski, S., Ivanov, V.: A simulation study of industry 4.0 factories based on the ontology on flexibility with using Flexim Software. Manag. Product. Eng. Rev. **11**(3), 74−83 (2020). https://doi.org/10.24425/mper.2020.134934

Management of Information Resources at Industrial Companies

Dmytro Gorovyi[1], Yevheniia Basova[1], Olena Lynnyk[1], Ivan Pavlenko[2,3](✉), and Justyna Trojanowska[4]

[1] National Technical University "Kharkiv Polytechnic Institute", 2, Kyrpychova Street, Kharkiv 61002, Ukraine
[2] Sumy State University, 116, Kharkivska Street, Sumy 40007, Ukraine
i.pavlenko@cm.sumdu.edu.ua
[3] Technical University of Košice, 1, Bayerova Street, 080 01 Prešov, Slovak Republic
[4] Poznan University of Technology, 5, M. Skłodowska-Curie Square, 60-965 Poznan, Poland

Abstract. Information became the third critical issue for the company with material and labor resources. Therefore, its role is significant, but the features of information as an industrial resource are still not pointed out. They do not have a specific methodology for their valuation. The paper examines the role and specific features as a part of their management at the company. The study compares information resources with other companies' resources, highlighting the unique features of information resource descriptions. It also helps close the research gap regarding the management of information resources at the company in the field of their unique features determination, synergistic effect influence, and methods of their estimation and assessment. A fundamental feature of information is its replication. As a result, the need to organize a system of protecting and ensuring information security at the company becomes urgent. However, these measures are not always relevant for companies due to the small use of electronic document management and the traditional paper bureaucracy of processes. In addition, the question of information value is clarifying. Mainly, score methods were applied previously. As a result of the research, the estimation methods of profit on informational resource values were developed using the entropy method. The results highlight the influence of the value of information resources on the company's profit.

Keywords: Information Management System · Small and Medium-sized Companies · Estimation Theory · Synergy · Entropy · Value of Information · Sustainable Manufacturing

1 Introduction

Managing information resources at an industrial company is critical for efficient operability, decision-making, and competitiveness in the global market [1]. The key strategies in effectively managing information resources at an industrial company include the following aspects. Data collection and integration ensure data reliability from various

© The Author(s), under exclusive license to Springer Nature Switzerland AG 2024
V. Ivanov et al. (Eds.): DSMIE 2024, LNME, pp. 111–123, 2024.
https://doi.org/10.1007/978-3-031-61797-3_10

sources (e.g., production processes, supply chain, and customer interactions). It should be collected and integrated into a comprehensive database [2]. As a result, this makes it possible to view the entire industrial operation comprehensively. Data security and privacy allow robust security measures to safeguard sensitive information from breaches, unauthorized access, and cyber threats. This aspect includes encryption, firewalls, access controls, and regular security audits [3].

Also, data analysis and interpretation are needed to provide valuable insights into production trends, market demands, and customer preferences, enabling informed decision-making and proactive planning [4]. Implementing company resource planning systems allows for streamlining production planning, inventory management, and resource allocation for better coordination among different departments [5].

Investment in technology and infrastructure, training and skill development, and compliance with industry standards and regulations are essential to implementing advanced automation systems and decision-making approaches [6, 7] and contributing to the overall data management process [8].

Risk management and contingency planning also allow for addressing potential data-related risks (e.g., data loss, system failures, natural disasters) to minimize the impact of unforeseen events. Moreover, regular performance evaluation, optimization, and adoption of cloud computing and big data solutions also play a significant role in flexibility, cost-effectiveness, and information resource management [9, 10].

By incorporating these strategies, an industrial company can manage its information resources effectively, improve operational efficiency, and make well-informed strategic decisions for sustainable growth and success [10].

Information is now the least researched and most invaluable component of a company's capital. Today, information is almost equal in price to material and labor resources, and it has become the third most crucial resource of the company [11]. After all, with increased production volumes, the necessary information to ensure new production volumes increases significantly [12]. With the economy's transition to the post-industrial informational stage, its role will grow more and more because even now, the amount of information used at any company has increased significantly compared to the end of the 20th century.

The research aims to find the features of information resources and to divide them into general with other resources and unique ones, to propose the ways for information protection measures at the company, and to propose the methodology to calculate the value of information which will maximize the company's profit.

The paper consists of the following parts: Literature Review, Research Methodology, Results and Discussion, and Conclusions.

2 Literature Review

Recently, the role of information as a specific resource in the company's activity has grown immeasurably.

It has been proven that the main features of information resources, which differ from the rest of the company's resources, are inexhaustibility (its quantity at the producer does not decrease when it is exchanged or transferred to another company or person) and

replication (repeated use). These features create a potential threat in the form of a possible leak of information from the company, which causes significant negative consequences for the company: a change in its reputation in the eyes of partners, causing moral or financial damage, conflict with state authorities, dependence on criminal structures, and raider grab. The information itself, sold or stolen by a competitor, remains in the possession of the source only if the market situation changes.

The process of production and consumption of information is characterized by uncertainty. This is manifested, first, in the uncertainty of specific work on applying this information. The costs of overcoming this uncertainty exceed the income from using new information [13].

It should also not be forgotten that the primary carrier of information receiving and processing in production for a long time was a person who directly participates in the technological process and manages it [14]. Therefore, despite the existing significant shortcomings of human capital assessment methods, as well as a significant number of examples not of underestimation but on the contrary of overestimation of the role and value of human capital in world practice [15], to prevent the latter (in the first place) one should also stop at the assessment of human capital modern companies.

Modern scientific works prove that this happens because of the development of information technologies and the spread of the Internet use as a particular source of knowledge and exchange of experience [16] and the approval of information as a product for purchase and sale, and the creation of companies that produce information or provide information services [17].

In the economic interpretation, information is data about product production, distribution, exchange, and consumption [18]. This interpretation allows the company to respond adequately to external and internal changes to organize and carry out its business activities effectively.

Information is a summary of knowledge that reduces uncertainty, considering information as something that reduces the risk of decision-making that is not entirely correct [19].

Therefore, the information itself carries a few qualitative differences. In general, information as something that contributes to reducing the degree of risk from deciding has an ambiguous character. This ambiguity lies in the fact that information alone, which reflects objectively existing facts, is not enough to decide, and their appropriate interpretation is also required, that is, the creation and correction of a model of the behavior of the company and its environment according to this information. Additional information is also needed for the specified interpretation to reflect the actual situation and be useful for practical decision-making.

Overall, if information is an industrial resource, it is necessary to determine its features that are general to all types of resources and their unique ones. In addition, it is necessary to provide managerial decisions for information on a particular industrial resource and to propose methods for its valuation and increasing its profitability, as previously only score methods were proposed.

The review shows the lack of investigations on information features as a specific resource and the lack of ideas for its actual valuation compared to other resources.

3 Research Methodology

A research flowchart is presented in Fig. 1. It includes three stages (initial, methodological, and resulting), from analyzing information sources to finalizing by parameter identification and evaluating the value of information and net profit.

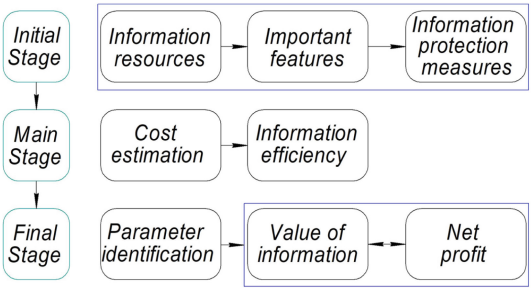

Fig. 1. The flowchart of the research methodology.

In contrast to material production resources (as elements of the total capital of the company), informational resources have specific properties summarized in Table 1.

Table 1. Features of information as the company's resources.

General resource features of a company	Unique information resource features
Meaningfulness	Inexhaustibility
Achievement of the company's goals	Difficult volume controllability
Limitation	Potential effectiveness
Cost	Reproducibility
Possibility of transfer	Existence without material carriers
An increase in the production cost	Synergy
Life cycle	Uniqueness
Ability to be accumulated and transformed	Operational efficiency

The most important feature of information resources and the main difference from the rest of the company's resources is their inexhaustibility. After all, the accumulated data is not wasted under the condition of correct use of information [20]. Therefore, its quantity at the company does not decrease when exchanged or transferred to another company [21]. It is also necessary to determine two more specific interrelated properties: potential efficiency and reproducibility (repeated use).

The potential effectiveness of information resources does not disappear, even after repeated use of the same information, since a decrease in effectiveness can only be associated with its moral wear.

Another special feature of the company's information resources is synergism. In general, it is a property of the system, which consists of the fact that the joint interaction of elements ensures an increase in their overall effect to a value greater than the sum of the effects of the same subsystems acting independently. From the point of view of information, synergism is the ability to use it with other information or resources to achieve different goals based on the principle that the whole is greater than the sum of its parts. Synergism means exceeding the total result of the sum of the factors that make it up.

Thus, in the case of information, the revenues from the joint use of such resources exceed the sum of revenues from the use of the same resources separately, e.g., as follows. Firstly, potential synergy is revealed by the joint use of several sources of information and the simultaneous conducting of surveys. Secondly, a merger of information and client bases of several companies for joint solutions of scientific, technical, commercial, social, production, and other tasks. The functioning of these companies as a part of the created association determines the effective use of investments for the implementation of large-scale measures, which are equally beneficial to all companies but are beyond the reach of each of them individually.

Finally, joint use of design, the latest developments by several economic entities within the framework of the production system in which they are part. This makes it possible to reduce forced downtime of equipment significantly, and it turns out to increase the efficiency of its use to a value greater than the autonomy of economic entities. Thus, synergism allows companies to accelerate the introduction of new products, increase sales volume, and reduce costs and management costs.

However, it remains unclear from these studies how exactly to calculate the added value of information from a financial point of view caused by the synergistic effect. After all, unlike physical systems, for which there are units of energy measurement and methods of assessing the energy potential, for the economy of companies, there are still no methods of objective assessment of the level of internal synergy. In addition, it is worth determining that the synergistic effect of capital itself is not homogeneous, so it is necessary to classify these effects and determine the factors that cause them. In addition, the issue of the anti-synergistic effect, i.e., the reduction of the actual value of capital when different types of it are combined, remains unexplained.

Moreover, it is essential to understand that not every combination of information resources is accompanied by positive synergy, and often, on the contrary, a negative synergistic effect can occur. For example, conflicts occur due to differences in corporate culture, rules of conduct, and rejection of the new management style. Such performance results are examples of anergic (anti-synergistic) effect.

Another fundamental feature of information is its replication. For the company to accumulate material gains in the conditions of modern production, the difficulties of manufacturing one copy of the product by the manufacturer are much smaller than the difficulties of copying by the consumer or competitor. In contrast to material resources (e.g., raw materials, production of products), when replicating information, mental work is no longer spent on its creation, and physical work spent on the reproduction of information is insignificant and, as a rule, can be neglected when evaluating the effectiveness of information use. That is, the creation of information is much more complicated than

the cost of copying it. Therefore, the right to ownership of information is a particular entity's exclusive right for copying and distributing information. That is, the buyer in the act of exchange on the information market does not buy the right to copy information, but only the right to use this information, and even only for a limited period.

Failure to comply with this condition may lead to significant losses in the future for the producer of the information resource. Such a property of information as its simple replication creates another potential threat: a possible information leakage from the company. Information leakage, as a rule, causes significant negative consequences for the company: it can significantly change its reputation with partners, cause significant moral or financial damage, bring conflict with state entities, put dependence on criminal structures, and become the cause of raider attacks. The information itself, whether sold or stolen by a competitor, remains in the possession of the source; only the market situation changes [22].

As a result, the need to organize a system of protecting and ensuring information security at the company becomes urgent. For the protection of information of the company, as a way of managing its capital, a system of measures is needed, the goals of which are: prevention of leakage, theft, loss, distortion, and forgery of information due to its duplication; prevention of threats to the security of an individual, company, society, state as a result of disclosure or distortion of information; prevention of unauthorized actions to destroy, modify, copy, block information, which may lead to a decrease in its potential effectiveness; prevention of various forms of illegal interference in the company's information resources and systems; ensuring legal protection of information as an object of ownership; protection of the constitutional rights of citizens to preserve personal privacy and confidentiality of personal data available in company information systems; preserving the confidentiality of documented information according to the law (e.g., confidentiality, rights of access and distribution).

Based on this, it is proposed that the company implement such measures to ensure information protection (Table 2).

Table 2. Information protection measures at the company.

Activity	Information protection measures
Information safety	Audit of used information and information flow
	Grouping and ranking of information by degree of confidentiality
	Forecast threats to the security of information resources
	Protection of the information using special software
Risk reduction	Reduction of access points from the external environment
	Description of the rules to access information and rights
	Localization of damage from illegal actions
	Generation of positive information about the company
	Implementation of the data loss prevention (DLP) systems

However, the latter measure is not always relevant for domestic companies due to the small use of electronic document management and traditional paper bureaucracy.

Rumors are an essential type of marketing information for a company, the creation of which also costs financial, material, human, and time resources. They affect the popularity of a particular product or the overall result of the company's work. On the one hand, when a favorable result is achieved, it represents an intangible achievement that forms a positive company image. On the other hand, with negative consequences for the company, it is a factor that destroys the image of the company and forces the company to spend resources (e.g., financial, material, human, and time) to refute these rumors, even if there were no reasons for them, and reduces the market value of the company due to the devaluation of its brand (decrease in the value of the company's shares).

In the optimal version, the source of rumors about the company and its activities should be the company itself, directing them to the necessary contact audiences and achieving a positive image of the company. However, in most cases, the source of rumors is outside the company, which means that the PR department (the department of communications, information, public relations, and press service) needs to develop a system of forming its image within the framework of its information activities.

The next step in managing the company's information resources is the development of a methodology for the cost estimation of information resources and the search for a compromise between the actual value of information and its costs.

Unfortunately, modern companies have not yet developed unified principles for economic evaluation and management of information flows. With the variety of types and forms of information resources, the problem of their assessment seems practically insoluble. Using the traditional value approach to evaluate the effectiveness of information resources is considered practically impossible. After all, the principles inherent in evaluating material resources (by cost and analogs) do not work when evaluating information.

When determining information efficiency, one often should deal with indicators that are difficult to consider in specific measurement units. A possible simplification of efficiency assessment is the creation of classification tables in which each efficiency indicator corresponds to a certain number of points. Point assessment can play an essential role in comparing the functional efficiency of different systems.

In addition, the survey of information needs can be carried out by probabilistic and statistical methods. Then, assessing the effectiveness of using information resources can be considered as assessing the degree of their influence on realizing the company's goals. For such an assessment, it is necessary the following. Firstly, to estimate the probability that this information resource will be used to achieve the goal. Such assessments can be obtained from the relative importance of an information resource in implementing the corresponding goal. However, a problem arises because the same information can affect multiple sub-goals. Secondly, assessing the information potential allows for considering the probability of achieving the sub-goal.

Evaluating the effectiveness of information use, it is also worth considering another of its fundamental features: the created information arrays only become factual information, and accordingly, information resources, when they find their user. This is because

receiving information late due to its aging leads to a decrease in practical benefits proportional to the delay period. Such a decline in the value of information over time can be due to the following reasons: the appearance of new information, which includes a particular part of the data; change in the need for information; because the lively and objectified work spent in the process of the previous stages of scientific research does not give the company a helpful effect for a long time. It can be obtained because of the next period of production use of information.

Thus, time becomes a complex indicator for evaluating information efficiency. The time factor as an economic category is covered quite fully in literature and can be used for practical calculations of the economic efficiency of information use. When calculating efficiency, it should be considered that reducing the circulation of information will lead to an accelerated return on funds spent on the direct implementation of new technical solutions in production and, equivalently, to the company receiving additional savings.

Information is also a limited resource: material, labor, and financial resources are spent on its production and use. Nevertheless, the consumption of energy and physical work to produce a given amount of information resource is generally less than the saving of material and energy resources that is achieved in the system with a given amount of information due to the reduction of uncertainty and the selection of better ways of system development, i.e., due to saving time. In modern conditions of struggle against entropy for national economic systems, the mode of economy often turns out to be more critical for further growth than the additional involvement of material and energy resources in the economic circulation.

In this case, the principles used in cybernetics should be considered fundamental. Entropy is used to measure the uncertainty of the system's behavior under given conditions to characterize the volume of information.

According to Shannon's formula [23], the amount of information H is as follows:

$$H = -E = -\sum_{i=1}^{n} \left[p_i \cdot log_2(p_i) \right], \tag{1}$$

where E – entropy (a measure of uncertainty of any experience); i – integer number ($i \in [1, n]$); pi – the probability of realization of each variant n of an information event ($p_i \in [0, 1]$, $\sum_{i=1}^{n} p_i = 1$).

In this case, if $p_1 = 1$, the rest $p_i = 0$, and the entropy of the system $E = 0$. If all probabilities are equal to $p_i = \frac{1}{n}$, the amount of information H acquires the most significant value $H = log_2(n)$.

From an economic point of view, each piece of information can be used for profit with varying degrees of probability of this event. In this case, the information that provides the largest value H is more valuable because it will provide the required result under any circumstances (e.g., the probability of events is equal). To convert information into monetary form, the modified Shannon's formula [24] can be applied:

$$W = K \cdot H = -K \cdot \sum_{i=1}^{n} \left[p_i \cdot log_2(p_i) \right], \tag{2}$$

where W – the value of information; K – a constant for converting the volume of information into monetary units.

Since entropy is a physical quantity that characterizes the uncertainty of a system, in the considered case study, it is assumed that, depending on the state of certainty or

uncertainty, companies can have a positive profit (or negative loss) from financial results. In this case, if $p_1 = 1$, then the rest $p_i = 0$, and the system's entropy tends to 0, i.e., $H \to 0$.

If all the events are equally probable ($p_i = \frac{1}{n}$), then H takes its highest value: $H = 1$. In this case, $W = K$. However, if the probability of events is also small ($p_i \approx 0$, although $\sum_{i=1}^{n} p_i = 1$), then $H \to 0$.

Therefore, the relationship between the amount of information H and the probability of events occurring, depending on its acquisition, is like that of the normal distribution.

4 Results and Discussion

According to the law of diminishing marginal utility, there is an inverse quadratic dependence between the profit P of the company and the value of its information W. Therefore, the following dependence can be applied:

$$P = -a \cdot W^2 + b \cdot W + c, \tag{3}$$

where a, b, c – parameters of the system.

The parameters mentioned earlier can be evaluated by finding the value of the information at which the profit will be maximized:

$$\frac{dP}{dW} = -2a \cdot W + b = 0. \tag{4}$$

Therefore, considering the maximum value of $W = K$ for the case of equally probable events ($p_i = \frac{1}{n}$), the following formula for evaluating the parameter K can be applied:

$$K = \frac{b}{2a}. \tag{5}$$

However, to find the coefficients a and b values, the data on net profit and the value of information from several companies can be used (Table 3).

Table 3. Comparison of information value and net profit, 10^6 UAH (the exchange rate is 100 EUR = 4135 UAH).

Parameter	PJSC "KharP"	PJSC "KhTZ"	PJSC "Avtramat"	PJSC "Pivdenkabel"
Net profit	–38.0	–24.8	–19.4	+ 37.4
Value of information	0.0	0.9	25.8	147.6

The value of information was evaluated approximately using the score method [25].

The corresponding correlation field was obtained (Fig. 2) to find the dependence between the net profit and the value of information.

(the exchange rate is 100 EUR = 4135 UAH).

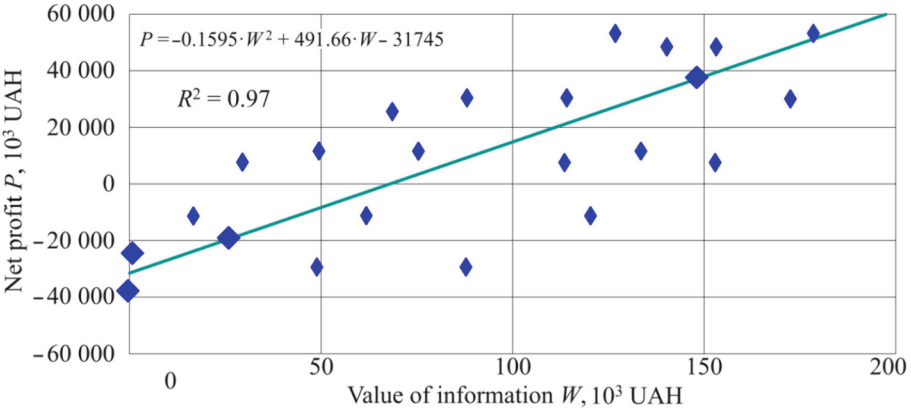

Fig. 2. The dependence of net profit P on the value of information W by the companies

Larger marks indicate the data of the enterprises from Table 1. Smaller marks indicate the data of the other enterprises in the study.

The approximation reliability coefficient's relatively high value confirms the calculated function's correctness.

As a result, the following coefficients in formula (3) were evaluated: $a = -0.160$, $b = 491.660$, and $c = 31.745$, and $P = -0.16 \cdot W^2 + 491.66 \cdot W + 31.745$ with a correlation coefficient of 0.97.

Therefore, according to formula (5), the parameter of formula (4) is as follows: $K = 1.541 \cdot 10^6$ UAH (37 268 EUR).

Thus, it is only necessary to rank information events at each company to determine the minimum profit from which it is necessary to evaluate and spread the probability of these events, which will be an object of further research.

The further processing and management of information flows of the company can be built with the probability indicator p. It can also be evaluated based on the mathematical apparatus of the chaos theory [26], as chaos is an unforeseen state that arises in the system due to great sensitivity to initial conditions. The adequacy of the considered model can be proven by a relatively high value of the correlation coefficient of 0.97 for the used regression dependence (3).

Despite the study being limited to Ukrainian enterprises, it can be extended by enterprises from the Slovak Republic, Poland, and other European countries. Moreover, it allows for improvements in the available approaches presented in other empirical studies [27–29] worldwide.

Further, this will help to improve the developed reliable methodology for evaluating information resources based on decreasing the company's entropy.

Since it is necessary and enough information contributes to reducing the chaotic nature of the production process, a more rational volume of information (in terms of content and quantity at the beginning of the production cycle) leads to less entropy, meaning a more predictable production process.

The novelty of the research is in the following. Firstly, the unique features of information resources, general to all the resource types, were determined. Secondly, the influence

of different synergistic effects when combining information resources was highlighted. Also, the impact of anergic effects from the combination of information resources was highlighted. Moreover, the company's information protection measures were compiled. Finally, an approach for information valuation was developed using the probabilistic approach.

5 Conclusions

During the research, it was determined that information became the third critical issue for the company with material and labor resources. Therefore, its role is significant, but the features of information as an industrial resource are still not pointed out.

Information is similar to other resources. It has general features for all companies' resources. On the other hand, information is also a limited resource: material, labor, and financial resources are spent on its production and use. That is why there were pointed unique information resource features. The most important feature of information resources and the main difference from the rest of the company's resources is inexhaustibility. Due to this, protection measures at the company were proposed.

Another special feature of the company's information resources is synergism. This happens because of similarity and compatibility or automatic advantages when combining capitals. Also, it was proven that not every combination of information resources is accompanied by positive synergy. On the contrary, a negative synergistic (anti-synergistic or anergic) effect can often arise, associated with the incompatibility of the combination of assets, overestimation of their value, or excessive expectations from these assets.

It was also determined that from an economic point of view, each piece of information can be used for profit with a different degree of probability of this event. In this case, the information that decreases entropy is more valuable because it will provide the desired result under any circumstances. It was proposed to calculate the value of information on the basis of Shannon's formula.

The dependence of companies' net profit on their information value was proposed and calculated based on the corresponding correlation of more than 30 Ukrainian companies. Due to these calculations, the ratio $1.541 \cdot 10^6$ UAH (37 268 EUR), as a constant for converting the volume of information into monetary units in Shannon's formula, was calculated.

Acknowledgment. The research was partially funded by the Polish National Agency for Academic Exchange within the project "Digitalization in Mechanical Engineering" (agreement no. BNI-UE-2023-2), the EU NextGenerationEU through the Recovery and Resilience Plan for Slovakia under the project No. 09I03-03-V01-00093, Ministry of Education and Science of Ukraine (State Reg. No. 0122U200875). The authors appreciate the support of the International Association for Technological Development and Innovations (IATDI) and Research and Educational Center for Industrial Engineering (Sumy State University).

References

1. Hricova, R., Madzinova, R.: Innovations in a modern engineering enterprise in the context of Industry 4.0 strategy. J. Eng. Sci. **10**(2), A1–A9 (2023). https://doi.org/10.21272/jes.2023.10(2).a1
2. Alshurideh, M., Alsharari, N.M., Al Kurdi, B.: Supply chain integration and customer relationship management in the airline logistics. Theor. Econ. Lett. **9**(2), 392–414 (2019). https://doi.org/10.4236/tel.2019.92028
3. Navigating Cybersecurity in 2023–2024: Practical Tips for Enterprise Security. https://www.infopulse.com/ebooks-reports/enterprise-cybersecurity-ebook. Accessed 11 Nov 2023
4. Rosário, A.T., Dias, J.C.: How has data-driven marketing evolved: challenges and opportunities with emerging technologies. Int. J. Inf. Manag. Data Insights **3**(2), 100203 (2023). https://doi.org/10.1016/j.jjimei.2023.100203
5. Gupta, M., Kohli, A.: Enterprise resource planning systems and its implications for operations function. Technovation **26**(5–6), 687–696 (2006). https://doi.org/10.1016/j.technovation.2004.10.005
6. Pavlenko, I., et al.: Using regression analysis for automated material selection in smart manufacturing. Mathematics **10**(11), 1888 (2022). https://doi.org/10.3390/math10111888
7. Ivchenko, O., et al.: Method for an effective selection of tools and cutting conditions during precise turning of non-alloy quality steel C45. Materials **15**(2), 505 (2022). https://doi.org/10.3390/ma15020505
8. Dwivedi, Y.K., Hughes, L., Baabdullah, A.M., et al.: Metaverse beyond the hype: multidisciplinary perspectives on emerging challenges, opportunities, and agenda for research, practice and policy. Int. J. Inf. Manag. **66**, 102542 (2022)
9. Golightly, L., Chang, V., Xu, Q.A., Gao, X., Liu, B.S.: Adoption of cloud computing as innovation in the organization. Int. J. Eng. Bus. Manag. **14** (2022). https://doi.org/10.1177/18479790221093992
10. Tigariev, V., Lopakov, O., Rybak, O., Kosmachevskiy, V., Cioată, V.G.: Design in modern information systems by applying cloud technologies. J. Eng. Sci. (Ukraine) **10**(1), E8–E13 (2023). https://doi.org/10.21272/jes.2023.10(1).e2
11. Martínez-Peláez, R., et al.: Role of digital transformation for achieving sustainability: mediated role of stakeholders, key capabilities, and technology. Sustainability **15**(14), 11221 (2023). https://doi.org/10.3390/su151411221
12. Javaid, M., Haleem, A., Singh, A.P., Suman, R., Gonzalez, E.S.: Understanding the adoption of Industry 4.0 technologies in improving environmental sustainability. Sustain. Oper. Comput. **3**, 203–217 (2022). https://doi.org/10.1016/j.susoc.2022.01.008
13. Jun, L., Qiuzhen, W., Qingguo, M.: The effects of project uncertainty and risk management on IS development project performance: a vendor perspective. Int. J. Project Manag. **29**(7), 923–933 (2011). https://doi.org/10.1016/j.ijproman.2010.11.002
14. Li, C., Chen, Y., Shang, Y.: A review of industrial big data for decision making in intelligent manufacturing. Eng. Sci. Technol. Int. J. **29**, 101021 (2022). https://doi.org/10.1016/j.jestch.2021.06.001
15. Ma, L., Zhai, X., Zhong, W., Zhang, Z.-X.: Deploying human capital for innovation: a study of multi-country manufacturing firms. Int. J. Prod. Econ. **208**, 241–253 (2019). https://doi.org/10.1016/j.ijpe.2018.12.001
16. Plekhanov, D., Franke, H., Netland, T.H.: Digital transformation: a review and research agenda. Eur. Manag. J. **41**(6), 821–844 (2023). https://doi.org/10.1016/j.emj.2022.09.007
17. Cai, X., Cebollada, J., Cortiñas, M.: Impact of seller- and buyer-created content on product sales in the electronic commerce platform: the role of informativeness, readability, multimedia richness, and extreme valence. J. Retail. Consum. Serv. **70**, 103141 (2023). https://doi.org/10.1016/j.jretconser.2022.103141

18. Haidabrus, B., Grabis, J., Ivanov, V., Druzhinin, E., Psarov, O.: Improving Agile teams effectiveness through the metrics. In 2023 IEEE 64th International Scientific Conference on Information Technology and Management Science of Riga Technical University (ITMS 2023), pp. 1–5 (2023). https://doi.org/10.1109/ITMS59786.2023.10317789
19. Zhu, T., Haugen, S., Liu, Y.: Risk information in decision-making: definitions, requirements and various functions. J. Loss Prev. Process Ind. **72**, 104572 (2021). https://doi.org/10.1016/j.jlp.2021.104572
20. Gandomi, A., Haider, M.: Beyond the hype: big data concepts, methods, and analytics. Int. J. Inf. Manag. **35**(2), 137–144 (2015). https://doi.org/10.1016/j.ijinfomgt.2014.10.007
21. Chung, D.Y., Hrazdil, K., Novak, J., Suwanyangyuan, N.: Does the large amount of information in corporate disclosures hinder or enhance price discovery in the capital market? J. Contemp. Account. Econ. **15**(1), 36–52 (2019). https://doi.org/10.1016/j.jcae.2018.12.001
22. Handoyo, S., Suharman, H., Ghani, E.K., Soedarsono, S.: A business strategy, operational efficiency, ownership structure, and manufacturing performance: the moderating role of market uncertainty and competition intensity and its implication on open innovation. J. Open Innov. Technol. Mark. Complex. **9**(2), 100039 (2023). https://doi.org/10.1016/j.joitmc.2023.100039
23. Beisel, J.-N., Moreteau, J.-C.: A simple formula for calculating the lower limit of Shannon's diversity index. Ecol. Model. **99**(2–3), 289–292 (1997). https://doi.org/10.1016/S0304-3800(97)01954-6
24. Ma, J.: Modified Shannon's capacity for wireless communication [speaker's corner]. IEEE Microwave Mag. **22**(9), 97–100 (2021). https://doi.org/10.1109/MMM.2021.3086386
25. Gorovyi, D.A.: Formation and Development of Virtual Capital of an Industrial Enterprise. Kharkiv National Automobile and Highway University, Kharkiv, Ukraine (2013)
26. Guégan, D.: Chaos in economics and finance. Annu. Rev. Control. **33**(1), 89–93 (2009). https://doi.org/10.1016/j.arcontrol.2009.01.002
27. Mithas, S., Tafti, A., Bardhan, I., Goh, J.M.: Information technology and firm profitability: mechanisms and empirical evidence. MIS Q. **36**(1), 205–224 (2012). https://doi.org/10.2307/41410414
28. Altaf, N.: Economic value added or earnings: what explains market value in Indian firms? Future Bus. J. **2**(2), 152–166 (2016). https://doi.org/10.1016/j.fbj.2016.11.00
29. Albart, N., Purnomo, H., Suherman, U., Hermuningsih, S.: The effects of net profit margin, debt ratio, total assets turnover, and current ratio on the stock prices of IDX 30 companies within 2018–2022. Int. J. Sci. Soc. **5**(5), 499–506 (2023). https://doi.org/10.54783/ijsoc.v5i5.907

Deployment and Release Management Process in Agile Digital Projects

Janis Grabis[1], Bohdan Haidabrus[1,2,3](✉), Evgeniy Druzhinin[4], and Kateryna Kolesnikova[5]

[1] Riga Technical University, 6A, Kipsalas Street, Riga 1048, Latvia
haidabrus@gmail.com
[2] Accenture Baltics, 214, Brivibas Street, Riga 1039, Latvia
[3] University of Applied Science, 3, Meza Street, Riga 1048, Latvia
[4] National Aerospace University, 17, Chkalov Street, Kharkiv 61000, Ukraine
[5] International IT University, 34/1, Manasa, 050000 Almaty, Kazakhstan

Abstract. This article explores the multifaceted dimensions of executing technical and commercial go-live phases in digital projects, specifically within Agile frameworks. Agile methodologies have become pivotal in managing complex project lifecycles in the rapidly evolving digital technology landscape. The go-live phase, a critical juncture in project deployment, presents unique challenges and opportunities, particularly in Agile environments. A scientific novelty of the research is to provide a comprehensive analysis by integrating empirical evidence and theoretical models, offering insights into best practices, strategies, and common pitfalls associated with these pivotal phases. Drawing on a blend of case studies, academic research, and industry reports, the paper provides a nuanced understanding of the Agile go-live process, offering valuable insights for practitioners and scholars in project management. Ultimately, this article contributes to the broader discourse on Agile methodologies, underscoring their transformative impact on the planning and executing technical and commercial go-live phases in digital projects. It aims to guide project managers, Agile practitioners, and organizational leaders in navigating these complex but critical stages of project deployment.

Keywords: Agile Framework · Delivery Management · Scrum · Go-Live Process · Project Management · Decent Work · Economic Growth · Industrial Growth

1 Introduction

Through a comparative analysis of Agile and traditional project management approaches, this article sheds light on the effectiveness and efficiency of Agile practices in managing go-live events. It also discusses the implications of these approaches on key project metrics such as time-to-market, return on investment, and customer satisfaction. Drawing on a blend of case studies, academic research, and industry reports, the paper provides a nuanced understanding of the Agile go-live process, offering valuable insights for practitioners and scholars in project management [1].

© The Author(s), under exclusive license to Springer Nature Switzerland AG 2024
V. Ivanov et al. (Eds.): DSMIE 2024, LNME, pp. 124–136, 2024.
https://doi.org/10.1007/978-3-031-61797-3_11

This research aims to dissect the intricacies of executing technical and commercial go-live phases in digital projects within Agile frameworks. It seeks to integrate both empirical evidence and theoretical models to provide a holistic view of best practices and common challenges faced during these critical project phases through the [2]:

- Examining existing literature on Agile project management, focusing on the go-live phase.
- Analysis of case studies and empirical data on successful and challenging go-live scenarios in Agile environments.

Authors delve into the specificities of technical go-live processes, examining how Agile practices like continuous integration, automated testing, and frequent iterations contribute to a seamless transition from development to production. The commercial go-live phase is scrutinized, highlighting how Agile methodologies can be harmonized with market launch strategies to optimize product release and customer engagement.

2 Literature Review

In the rapidly evolving digital technology landscape, adopting Agile methodologies has marked a significant shift in project management practices [1, 2]. Agile, characterized by its flexibility, iterative processes, and emphasis on collaboration, has become a cornerstone methodology for managing complex digital projects [3]. Within this Agile framework, the go-live phase—wherein a project transitions from development to production—stands as a critical milestone [4, 5]. This phase marks the culmination of development efforts and serves as a gateway to the project's operational life and market interaction [6].

This article dissects and analyzes the nuances of executing the technical and commercial go-live phases in digital projects managed under Agile methodologies. Given the dynamic nature of Agile projects, where requirements and solutions evolve through collaborative efforts, the go-live phase presents unique challenges and opportunities [7–9]. This article aims to bridge the gap in the literature by providing an in-depth examination of how Agile practices influence the preparation, execution, and outcome of go-live events [10].

The scope of this article extends to various aspects of the go-live process in Agile environments. It includes an exploration of technical go-live, where the focus is placed on ensuring that the product or system is functionally ready and stable for production use [9, 10]. This involves examining Agile-specific practices such as continuous integration, automated testing, and sprint reviews and their impact on technical readiness. Additionally, the article delves into the commercial go-live phase, focusing on strategies for market launch and customer engagement within Agile frameworks [6, 11].

This exploration is particularly relevant as digital projects increasingly adopt Agile methodologies, necessitating a deeper understanding of how these frameworks can be effectively leveraged during critical project phases [12]. Through this article, the authors aim to provide practitioners, scholars, and organizational leaders with comprehensive insights into the Agile go-live process, highlighting best practices, challenges, and strategies for success. Doing so needs to contribute to the evolving discourse on Agile project management and its practical applications in the digital domain [13–15].

3 Research Methodology

In the dynamic landscape of digital solution development, Agile deployment emerges as a critical methodology that fundamentally transforms the velocity and quality of deploying software products. Agile, as a disciplined project management process that adheres to the iterative and incremental delivery of products, significantly shortens the cycle time to go live. This approach embraces change, even in the later stages of development, ensuring that the end product is closely aligned with customer needs and market demands.

Before the go-live of any digital solution, a comprehensive set of preparations is paramount to ensure a smooth transition and deployment. These preparations include technical readiness, stakeholder alignment, and operational readiness. As outlined in Table 1, the Agile readiness checklist encompasses a broad spectrum of critical considerations, from code stability and performance benchmarks to training and support structures. An Agile readiness checklist is a key to our deployment and release management methodology (Table 1).

Table 1. Agile Readiness Checklist.

Readiness Aspect	Description	Status (Ready/Not ready)
Code stability	Ensure the codebase is robust and fully tested	
Performance Benchmarks	Validate that the solution meets performance criteria	
Stakeholder Alignment	Confirm that all stakeholders are informed and prepared for go-live	
Operational Training	Guarantee that teams are trained for support and operations	
Rollback Procedures	Have clear procedures in place for rolling back changes if necessary	

Release management within Agile frameworks is characterized by a high frequency of smaller and more manageable releases, unlike the traditional models that aim for less frequent, larger deployments. The result of the proposed research allows for a smoother transition into production with fewer disruptions and a structured method for tracking and managing changes. The Agile release process typically involves stages such as planning, scheduling, coordination, and deployment, each intertwined with Agile ceremonies like sprints and retrospectives. A comprehensive outline of the release management process, tailored to the Agile ways of working, ensuring a streamlined deployment and subsequent operational tranquility.

On-call support during deployment is a linchpin of the Agile framework and proposed methodology. It involves the availability of a dedicated team that can quickly respond to issues as they arise during and immediately after the Go-Live Phase. This support system not only rectifies live incidents but also provides a feedback loop to development teams, thereby embodying the Agile tenet of continuous improvement.

4 Results and Discussion

4.1 A Go-Live Phase

The Go-Live phase, as one of the key results of our approach, is a pivotal juncture in the Agile deployment process, marking the transition of digital solutions from a controlled, pre-production environment to a live, user-accessible environment. Preparing for this phase involves a comprehensive assessment and readiness check to ensure seamless deployment, minimal disruptions, and effective operation post-deployment. This article explores the crucial aspects of Go-Live preparation and readiness for digital solutions in Agile frameworks, backed by scientific data and industry practices.

Go-Live preparation in Agile environments entails a blend of technical and organizational readiness. It encapsulates a series of activities to validate the stability, performance, and functionality of digital solutions, ensuring that teams and stakeholders are well-prepared for the transition (see Fig. 1).

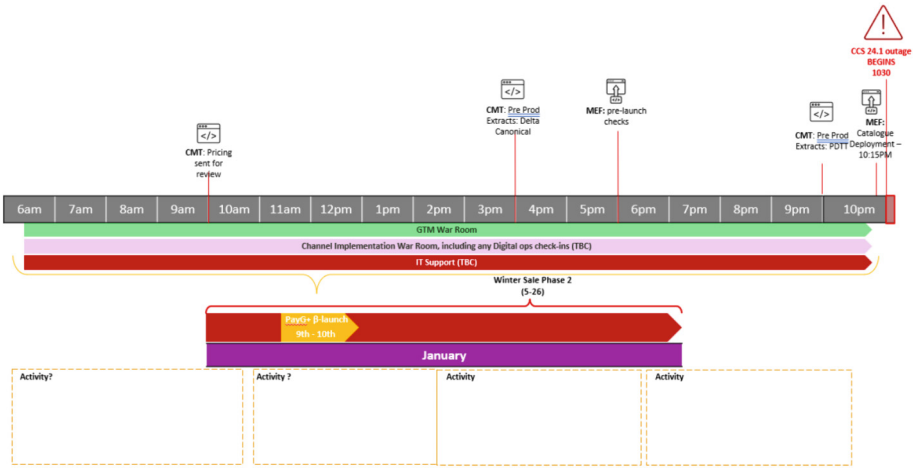

Fig. 1. Hourly Deployment timeline.

In our approach, Go-Live Readiness consists of Technical and Organizational Readiness, Risk Assessment, and Mitigation [13, 16].

Technical Readiness by environment preparation ensures that the production environment is set up correctly, including configurations, server resources, and network settings. The next step is Data Migration and Validation by migrating necessary data to the production environment and validating its integrity. Conducting performance acceptance testing by the quality assurance team as a part of development needed to ensure the system can handle the expected load and traffic.

Under the Organizational Readiness, there are:

- training by providing necessary training to end-users and support teams to ensure they are well-acquainted with the new system;
- communicating the Go-Live plan, including schedules, roles, and responsibilities, to all stakeholders;
- support plan by establishing a support plan to address any issues or inquiries post-deployment promptly.

The Go-Live readiness checklist is invaluable in orchestrating a seamless transition to a production environment. A systematic checklist can significantly aid in ensuring comprehensive readiness. It can encompass various aspects like system and integration testing results, performance testing results, data migration validation, training completion, support, and rollback plans.

4.2 Commercial and Technical Go-Live

Extending the comparison between commercial and technical go-live phases in Agile projects involves a deeper examination of the distinct characteristics, challenges, and approaches within each phase, and how Agile methodologies influence them differently; in Table 1, there is a detailed comparison.

This comparative analysis illustrates how the commercial and technical go-live phases in Agile projects, while interconnected, require distinct approaches and considerations. Understanding these differences is crucial for Agile teams to navigate these critical stages of a project's lifecycle effectively.

4.3 Final Mobile Marketing Review Process

The process of a Final Mobile Marketing Review is a critical step in ensuring the effectiveness and readiness of a mobile marketing project before its launch. This review is essential in validating that the project aligns with the overall marketing strategy, targets the intended audience effectively, and utilizes mobile platforms optimally. Here's a step-by-step description of this process:

1. Review of Project Objectives and Strategy. It is essential to revisit the primary goals and objectives of the mobile marketing project. Ensure they align with the broader marketing strategy and business objectives and confirm that the project's strategy is appropriate for reaching the target audience through mobile channels.
2. Content and Creative Evaluation. In this step, a delivery team should examine all creative elements, including ad copy, graphics, videos, and interactive components, to ensure they are engaging, on-brand, and optimized for mobile devices. Considering the limited screen space and user attention on mobile devices, the team must check for clarity, brevity, and messaging effectiveness.

Category	Technical Go-Live	Commercial Go-Live
Objectives and Focus	The primary focus is on the technical readiness of the product. This includes ensuring the software or digital product is free from critical bugs, performs efficiently under load, and integrates seamlessly with existing systems	Here, the focus shifts to market readiness. It encompasses marketing strategies, sales enablement, customer engagement, and market penetration tactics. The aim is to ensure the product is well-received in the market and achieves its commercial objectives
Key Activities	Activities include final rounds of testing such as performance and security testing, data migration, and environment setup. Emphasis is placed on technical aspects like deployment pipelines, rollback strategies, and monitoring systems	This phase involves activities like market research, customer outreach, promotional projects, pricing strategies, and sales channel preparation. The focus is on creating market buzz and ensuring customer readiness
Agile Practices	Agile practices in this phase include continuous integration/continuous deployment (CI/CD), sprint reviews focusing on technical deliverables, and rapid iterations for bug fixes. Agile teams prioritize flexibility in responding to technical challenges that arise during this phase	Agile practices include cross-functional teams involving marketing and sales, iterative feedback loops with potential customers, and adaptive marketing strategies. Agile principles support rapid response to market feedback and adjustments in commercial strategies
Challenges	Technical Go-Live: Challenges often involve managing technical debt, ensuring system stability and performance, and addressing last-minute bugs. Managing various environments and configurations in an Agile setting is also complex	Challenges include aligning the product launch with market expectations, timing the launch to gain maximum traction, and effectively communicating the product's value proposition. Agile teams may need help with rapidly changing market conditions and customer preferences
Success Metrics	Success is typically measured by system performance metrics, bug counts, uptime statistics, and user feedback on system functionality	Success metrics revolve around market acceptance measures such as sales figures, market share, customer satisfaction scores, and brand engagement metrics

(*continued*)

(*continued*)

Category	Technical Go-Live	Commercial Go-Live
Post-Go-Live Activities	Involves monitoring system performance, addressing any emerging technical issues, and iterating on feedback to improve system stability and performance	Focuses on analyzing market response, adjusting marketing strategies, enhancing customer support, and collecting insights for future product development

3. Technical Review and Compatibility Check. The following steps are testing the project on various mobile devices and operating systems to ensure compatibility and optimal performance and verifying that all links, buttons, and interactive elements function correctly and that landing pages are mobile-friendly.
4. Compliance and Legal Review. A compliance validation team ensures the project adheres to all relevant regulations and legal requirements, including privacy laws, data protection standards, and advertising guidelines. It is important to check for proper usage of trademarks, copyrights, and permissions for any third-party content.
5. Targeting and Segmentation Review. Reviewing the targeting parameters to ensure the project reaches the intended demographic, geographic, and psychographic audience segments is necessary. Assess the level of personalization and relevance in the project, ensuring that messages are tailored to the audience's preferences and behaviors.
6. Analytics and Measurement Setup. A delivery team is working with the stakeholders to confirm that the mobile marketing project is well integrated with other marketing channels and touchpoints, providing a cohesive experience across all platforms. Ensure consistency in messaging and branding across different channels.
7. Budget and ROI Review. The finance and operations team reviews the budget allocation for the project, ensuring it aligns with expected outcomes and ROI projections. Confirm that tracking mechanisms are in place for monitoring project performance and measuring success against key performance indicators (KPIs).
8. Feedback and Approval from Stakeholders. A delivery and release management team needs to gather feedback from various stakeholders, including marketing teams, creative teams, technical staff, and leadership. Make necessary adjustments based on feedback and obtain final approval from decision-makers.
9. Launch Preparedness and Contingency Planning. This step is important to ensure that all teams are prepared for the project launch, with clear roles and responsibilities. Develop contingency plans for potential issues such as technical glitches, unexpected user feedback, or changes in market conditions.
10. Final Approval and Launch. Document the final project plan, including strategies, creatives, targeting details, and expected outcomes. Keep records of all compliance checks, approvals, and stakeholder feedback for future reference.

The order of these steps follows a natural progression from broad planning to specific details and from internal preparation to external execution. Each step builds upon the previous one, ensuring that all aspects of the campaign are thoroughly vetted and optimized before launch. This systematic approach helps identify and address potential issues early,

thereby enhancing the overall effectiveness of the project. By carefully executing each step, you can ensure that the mobile marketing project is well-prepared to achieve its objectives, engage effectively with the target external and internal stakeholders, and deliver a positive return on investment.

4.4 Design Verification Testing

Design Verification Testing (DVT) is a crucial phase in product development, particularly in fields like electronics, engineering, and manufacturing. The primary goal of DVT is to verify that the design of a product meets the specified requirements and performance criteria. Here's a general overview of what DVT entails:

1. Defining Test Criteria and Requirements: Before DVT begins, it's essential to clearly define the criteria and requirements that the product must meet. These are typically based on the product's design specifications, industry standards, and any regulatory compliance needs.
2. Developing Test Plans: A comprehensive test plan is developed, detailing how each aspect of the product will be tested to meet the defined criteria. This plan includes the methods, equipment, procedures, and schedules for testing.
3. Setting Up Test Environments: The appropriate testing environments and setups are created. This may involve specialized equipment and facilities, especially for products that require testing under various environmental conditions.
4. Conducting Tests: The DVT phase involves conducting a series of tests on the product prototype(s). These tests can be extensive and include performance testing, durability testing, environmental testing (like temperature and humidity conditions), electrical testing, and more, depending on the product type.
5. Data Collection and Analysis: Data from the tests is collected and analyzed to assess whether the product meets the design specifications and performance criteria. This analysis is critical in identifying any design issues or areas for improvement.
6. Documentation and Reporting: All results from the DVT are thoroughly documented and reported. This documentation is crucial for internal review and compliance with external regulatory standards.
7. Feedback and Iteration: Based on the test results, feedback is provided to the design team. If the product does not meet specific criteria, it may return to the design phase for modifications. This iteration continues until the product meets all the specified requirements.
8. Final Verification: Once the product successfully passes all the DVT tests, it is verified as meeting the design requirements. This verification is essential for the product to proceed to the next development phase, such as production or market release.

DVT is a rigorous process that ensures product quality, reliability, and compliance with necessary standards. It helps identify potential issues early in the development cycle, thereby reducing the risk of costly changes or recalls after the product is launched in the market (see Fig. 2).

Identify potential risks associated with the Go-Live process and devise mitigation strategies to address them. In the context of a commercial go-live for a digital project, analytics reporting framework, and dashboards are critical components for monitoring,

evaluating, and optimizing the performance of the project post-launch. This framework typically includes tools and methodologies designed to capture, analyze, and present data meaningfully. Digital Launch Risk Management consists of [13]:

- Risk Assessment: Identify potential risks in the DVT process, such as equipment failure or delays in testing.
- Mitigation Strategies: Develop strategies to mitigate identified risks, such as having backup equipment or additional personnel training.

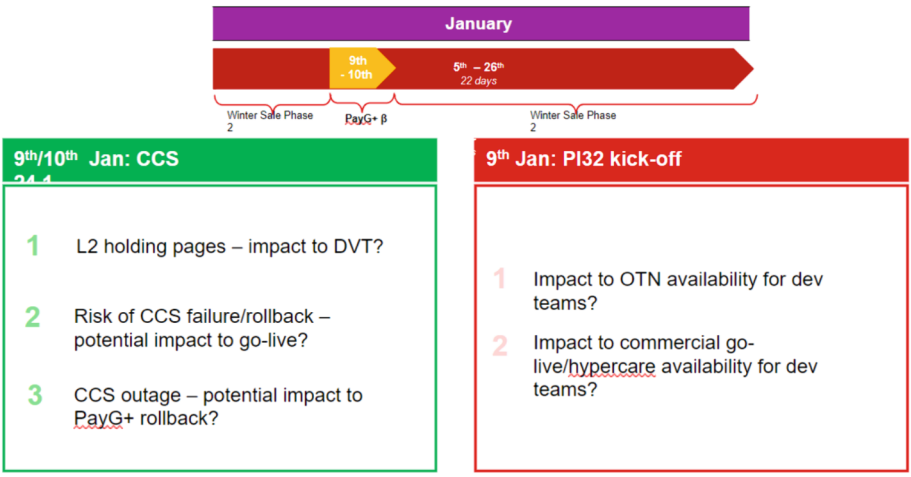

Fig. 2. Digital Launch Risks.

4.5 Analytics Reporting Framework and Dashboards

Here's an overview of how such a framework and dashboards might be developed and utilized:

1. Defining Key Performance Indicators. Identifying critical metrics by establishing key performance indicators aligning with the commercial go-live business objectives is important. These could include metrics like user engagement, conversion rates, revenue, customer acquisition cost, churn rate, etc. Set specific goals for each KPI and establish benchmarks based on industry standards or historical data as a part of Goals and Benchmarks.
2. Data Collection and Integration. The delivery team should identify various data sources such as web analytics tools, CRM systems, marketing platforms, and financial systems. Ensure these tools are integrated to allow for seamless data collection and aggregation. This might involve using APIs, data warehousing solutions, or ETL (Extract, Transform, Load) processes.
3. Dashboard Design and Development. It is important to have a User-Friendly Interface as a design dashboard that is easy to navigate and understand. It should present data

in an intuitive format, suitable for the intended audience (e.g., executives, marketing teams, product managers). Real-Time Data Visualization utilizes tools that allow for the real-time visualization of KPIs. This might include graphs, charts, and heat maps. Customization and Filters incorporate customization and filtering features, enabling users to drill down into specific data segments or timeframes.

4. Reporting and Analysis. The next step is automated reporting, setting up automated reporting mechanisms to generate regular updates on key metrics. In-depth Analysis Tools for more in-depth analysis include cohort analysis, customer segmentation, or trend analysis. Implementing alert and notification systems for critical metrics that require immediate attention is necessary.
5. Accessibility and Distribution. Access Controls to ensure that the dashboards and reports are easily accessible to relevant stakeholders while maintaining data security and privacy. Optimize dashboards for mobile devices if stakeholders need to access data on the go.
6. Continuous Monitoring and Optimization. Stakeholders use the dashboards to monitor trends and patterns in the data continuously. Establish a feedback loop where insights from the data are used to make informed decisions and optimize marketing strategies, product features, customer experience, etc.
7. Scalability and Evolution. Scalable Solutions can be achieved by choosing tools and platforms that can scale with the growth of the business and the increasing complexity of data. Release management team regularly update and evolve the analytics framework and dashboards to accommodate new data sources, changing business needs, and technological advancements.
8. Compliance and Data Governance. The compliance team should ensure that the collection and use of data comply with data privacy laws and regulations. Implement strong data governance policies to maintain the integrity and accuracy of the data as part of data governance.

Under discussion, analytics reporting framework and dashboards for a commercial go-live are essential for capturing the correct data, deriving actionable insights, and driving informed decision-making. They provide a comprehensive view of the project's performance and are instrumental in guiding strategic adjustments and improvements post-launch. Our project experience, highlighted in this paper, shows that the deployment and release management process is an integral part of delivering digital projects. This process ensures that software is deployed and released in a way that aligns with Agile principles, such as iterative development and continuous integration, automated testing and deployment, release planning and scheduling, feature flags and canary releases, collaboration and communication, feedback loops and continuous improvement, risk management and compliance [17–20].

In continuous integration, developers frequently merge their changes into a shared repository. Automated builds and tests verify each integration to detect integration errors as quickly as possible. Automation is key in Agile release management. Automated testing ensures that new changes stay within the existing functionality, and automated deployment tools enable teams to deploy software frequently and reliably. Unlike traditional methods, Agile release planning is flexible and adaptive. Release schedules are

often aligned with the end of sprints, but they can be adjusted based on feedback and project progress. This flexibility allows teams to respond to changes quickly.

Agile teams often use feature flags to roll out new features gradually. Canary releases, where new features are rolled out to a small subset of users before a full release, are also common. These techniques allow teams to test in production environments and quickly roll back changes if issues arise. After a release, Agile teams gather feedback to inform future development. This feedback loop is essential for continuous improvement, ensuring the product evolves according to user needs and market demands. Agile release management also involves managing risks and ensuring compliance with relevant standards and regulations, including security testing, compliance checks, and risk assessments [12, 13].

These elements of Agile release and deployment management underscore its focus on rapid, reliable, and flexible delivery, essential in the dynamic landscape of digital projects. Agile methodologies enable organizations to adapt quickly to changing requirements and market conditions, delivering value to customers faster.

Defect rates per release or per function point can be a useful metric. Agile projects might show a lower defect rate due to continuous testing and integration. For example, a study by QSM Associates found that Agile projects had 75% fewer defects than traditional projects [9, 21].

5 Conclusions

To encapsulate, Agile deployment is a potent paradigm that accelerates the deployment of digital solutions, facilitating a competitive edge in rapidly evolving markets. It necessitates thorough preparation, robust on-call support, and meticulous release management. The interplay between these elements underscores the essence of Agile - adaptability, responsiveness, and quality - in fostering successful digital solution deployment.

To perform a comparative analysis of the achieved results of Agile release and deployment management to previous results and in contrast to more traditional release management approaches, there are key differences lie in several areas: speed of delivery, adaptability to change, quality and reliability, stakeholder engagement and feedback, risk management, resource utilization, customer satisfaction.

As authors proceed with the article, confirmation of each completed section will ensure that alignment is maintained and address any further details needed for each step. By meticulously addressing each aspect of technical and organizational readiness, teams can significantly reduce the likelihood of issues during the Go-Live process, paving the way for a successful deployment of digital solutions in an Agile framework as a highlighted scientific novelty of the research.

The Go-Live readiness checklist ensures that every aspect, from technical configurations to organizational coordination and risk mitigation, is accounted for, thereby facilitating a structured and well-prepared approach toward deploying digital solutions.

References

1. Conforto, E.C., Salum, F., Amaral, D.C., Da Silva, S.L., De Almeida, L.F.M.: Can agile project management be adopted by industries other than software development? Proj. Manag. J. **45**(3), 21–34 (2014). https://doi.org/10.1002/pmj.21410
2. Gandomani, T.J., Tavakoli, Z., Zulzalil, H., Farsani, H.K.: The role of project manager in agile software teams: a systematic literature review. IEEE Access **8**, 117109–211712 (2020). https://doi.org/10.1109/ACCESS.2020.3004450
3. Nguyen, D.S.: Success factors that influence agile software development project success. Am. Sci. Res. J. Eng. Technol. Sci. **17**(1), 172–222 (2016)
4. Hoelbeche, L.: Designing sustainably agile and resilient organizations. Syst. Res. Behav. Sci. **36**(5), 668–677 (2019). https://doi.org/10.1002/sres.2624
5. https://www.scaledagileframework.com/pi-planning., Accessed 15 Aug 2023
6. Cohen, D., Lindvall, M., Costa, P.: An introduction to agile methods. Adv. Comput. **62**(C), 1−66 (2004). https://doi.org/10.1016/S0065-2458(03)62001-2
7. Denning, S.: How Agile can transform manufacturing: the case of Wikispeed. J. Strateg. Leadersh. **40**(6), 22–28 (2012). https://doi.org/10.1108/10878571211278859
8. Gren, L., Torkar, R., Feldt, R.: The prospects of a quantitative measurement of agility: a validation study on an agile maturity model. J. Syst. Softw. **107**, 38–49 (2015). https://doi.org/10.1016/j.jss.2015.05.008
9. Heikkilä, V.T., Paasivaara, M., Lasssenius, C., Damian, D., Engblom, C.: Managing the requirements flow from strategy to release in large-scale agile development: a case study at Ericsson. Empir. Softw. Eng. **22**(6), 2892–2936 (2017). https://doi.org/10.1007/s10664-016-9491-z
10. Kischelewski, B., Richter, J.: Implementing large-scale agile – an analysis of challenges and success factors. In: ECIS 2020 Research Papers, vol. 176, pp. 1−16 (2020)
11. Rigby, D.K., Sutherland, J., Takeuchi, H.: Embracing Agile: how to master the process. That's transforming management. Harv. Bus. Rev. **94**(5), 40–50 (2016)
12. Haidabrus, B., Grabis, J., Psarov, O., Druzhinin, E.: Agile framework as a key to information management systems delivery. In: Ivanov, V., et al. (eds.) DSMIE 2023. LNME, vol. 1, pp. 113–120. Springer, Cham (2023). https://doi.org/10.1007/978-3-031-32767-4_11
13. Grabis, J., Minkēviča, V., Haidabrus, B., Popovs, R.: Is team always right: producing risk aware effort estimates in agile development. In: Buchmann, R.A., Polini, A., Johansson, B., Karagiannis, D. (eds.) BIR 2020. LNBIP, vol. 398, pp. 101–110. Springer, Cham (2020). https://doi.org/10.1007/978-3-030-61140-8_7
14. Pavlenko, I., et al.: Using regression analysis for automated material selection in smart manufacturing. Mathematics **10**(11), 1888 (2022). https://doi.org/10.3390/math10111888
15. Ivchenko, O., et al.: Method for an effective selection of tools and cutting conditions during precise turning of non-alloy quality steel C45. Materials **15**(2), 505 (2022). https://doi.org/10.3390/ma15020505
16. Vedal, H., Stray, V., Berntzen, M., Moe, N.B.: Managing dependencies in large-scale Agile. In: Gregory, P., Kruchten, P. (eds.) XP 2021. LNBIP, vol. 426, pp. 52–61. Springer, Cham (2021). https://doi.org/10.1007/978-3-030-88583-0_6
17. Hofman, M., Grela, G.: Project portfolio risk identification – application of Delphi method. J. Bus. Econ. **6–11**, 1857–1867 (2015). https://doi.org/10.15341/jbe(2155-7950)/11.06.2015/004
18. Ivanov, V.: Process-oriented approach to fixture design. In: Ivanov, V., et al. (eds.) DSMIE 2018. LNME, pp. 42–50. Springer, Cham (2019). https://doi.org/10.1007/978-3-319-93587-4_5

19. Luscinski, S., Ivanov, V.: A simulation study of industry 4.0 factories based on the ontology on flexibility with using Flexim Software. Manag. Product. Eng. Rev. **11**(3), 74−83 (2020). https://doi.org/10.24425/mper.2020.134934
20. Ivanov, V., Vashchenko, S., Rong, Y.: Information support of the computer-aided fixture design system. IN: CEUR Workshop Proceedings, vol. 1614, pp. 73−86 (2016)
21. Hricova, R., Madzinova, R.: Innovations in a modern engineering enterprise in the context of Industry 4.0 strategy. J. Eng. Sci. (Ukraine) **10**(2), A1–A9 (2023). https://doi.org/10.21272/jes.2023.10(2).a1

Manufacturing Technologies

An Increase in the Vibration Resistance of Finishing and Boring Machines when Cutting Ends Using the Plunge-In Method

Olexandr Badovskyi[1], Anna Balaniuk[1(✉)], Gennadii Oborskyi[1], Alexandr Orgiyan[1], and Milan Edl[2]

[1] Odesa Polytechnic National University, 1, Shevchenko Avenue, Odesa 65044, Ukraine
annabalanyuk24@gmail.com
[2] University of West Bohemia, 2732/8, Univerzitní, 301 00 Pilsen, Czech Republic

Abstract. The article examines the operation of trimming the free end using the cutting-in method. This operation is widely used in the technological process of manufacturing parts. The vibration resistance of the delicate tuning process during the finishing trimming of solid ends has been studied. The experiments were carried out on a special stand with the ability to change the parameters of the elastic system. Inductive and inductive sensors were used to measure vibrations. A method has been developed for calculating the maximum cutting width with a cutter shovel when changing the rigidity of the part-device subsystem, feed, and workpiece material. It has been established that the rigidity of the part-device subsystem largely determines the occurrence of vibrations. The article mainly examines vibrations along the axial coordinate in the feed direction, which determines the cleanliness of the machined surface and the feasibility of the end-trimming operation. A calculation model of the operation has been developed. In this model, the cutting process is described by a dynamic characteristic reflecting the inertial properties of the process. The stability of the cutting process is determined by the Routh-Hurwitz criterion. Calculations make it possible to determine the dimensions of a given device's maximum permissible width of the machined end. The experiment and corresponding calculations were done using a device with variable parameters. The results of the work are presented in the form of tables and graphs.

Keywords: Vibration Resistance · Cutting of Solid Ends · Rigidity · Vibration Amplitude · Frequency · Cutting Method · Industrial Growth · Process Innovation

1 Introduction

The technology of combining operations on finishing boring machines (FBM) provides for two fundamentally different methods for performing the end trimming operation: the radial feed method and the axial feed method. The main requirement for this operation is the high quality of processed surfaces and optimal productivity. Fine trimming of ends is often performed using the radial feed method. This ensures the production of an accurate end with a high surface finish, but the productivity of this processing method could be

© The Author(s), under exclusive license to Springer Nature Switzerland AG 2024
V. Ivanov et al. (Eds.): DSMIE 2024, LNME, pp. 139–151, 2024.
https://doi.org/10.1007/978-3-031-61797-3_12

much higher. Developing and assembling a cutting head for a radial cutter feed could be improved. The presence of a radial feed mechanism makes it difficult to produce a compact and well-balanced head. A simpler (in terms of kinematics) and more productive method is the axial feed method (plunging method), that is, trimming with a wide-blade cutter knife. This finishing trimming of the ends is still a relatively new technological operation. Because the capabilities of this method have yet to be sufficiently studied, this work carried out experimental and theoretical studies of the technological possibilities of trimming solid ends on finishing and boring machines based on studying the dynamics of fine turning.

This work aims to increase the vibration resistance of a boring machine when finishing the ends of parts using the tapping method.

To achieve this goal, the following tasks should be solved:

1. Determine the parameters of the elastic-dissipative-inertial system and the cutting process, ensuring the feasibility of the trimming operation, as well as the vibration resistance of the finishing and boring machine.
2. Determine the differences in vibrations when trimming ends of different diameters.
3. Develop a calculation method for determining the maximum cutting width when changing the parameters of machine subsystems, cutting modes, and characteristics of the material being processed.

2 Literature Review

It should be noted that there is a fairly large number of published works on predicting cutting forces during transverse and longitudinal (plunge) turning (Fig. 1) [1, 2].

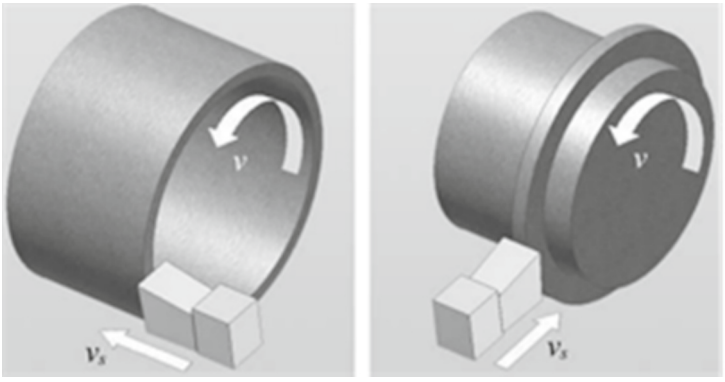

Fig. 1. Schemes of orthogonal cutting for longitudinal and transverse turning.

In this case, the feed direction coincides with the perpendicular in the direction of the machined surface. A procedure is used to test the proposed analytical models of the chip formation process, tool failure detection, etc., to determine forces and cutting coefficients based on creating special measuring devices [3, 4]. Cutting and chip formation coefficients are determined experimentally for each combination of tool and workpiece

materials [5, 6]. Using the simplest model of orthogonal cutting (Fig. 2), cutting coefficients, components of forces during chip formation, deformation of chip elements, friction coefficients, etc., were determined.

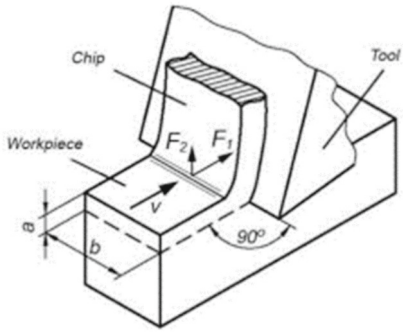

Fig. 2. Orthogonal cutting scheme.

The elements of the chip and the mechanisms of formation of cutting forces when the thickness of the chip changes are also considered. The influence of tool geometry on the orthogonal cutting process was studied. The deformation of chip elements during radial and plunge turning was studied using special digital microscopes to determine the thickness, length, and shrinkage, as well as the mass of the cut layer [7, 8].

Oscillograms of vibrations of the cutting wedge are presented. Note that in these calculations, the parameters of the elastic system of the spindle and device for ensuring stable cutting were not studied. Also, the patterns of vibrations when trimming ends of different diameters have yet to be studied. In foreign publications, the process of removing part of the material from the workpiece is called machining. Difficulties in the machining process change the quality and productivity of the cutting process. They are directly reflected in surface integrity (surface roughness and other surface topographic features) and mechanical properties (residual stresses, hardness, microstructure) [9, 10]. This is reflected both in the surface layer and at specific depths of part [11]. Surface integrity defines residual stress as the most critical parameter for assessing the quality of the machined surface and achieving a high level of reliability [12]. Many studies aim to establish an accurate numerical model to predict the residual stress in the machined workpiece. For this purpose, the finite element method is often used [13]. Many publications reflect the features of machining during orthogonal and inclined cutting. The features of three deformation zones during chip formation were studied [14]. It has been established that the friction coefficient decreases with increasing cutting speed [15, 16]. Special lubricants have been proposed for cooling the cutting zone [17].

The main requirements for the development of mechanical engineering technology are two factors - increasing efficiency (productivity) and quality. Significant improvement of these two factors seems impossible. However, scientific research and the development of dynamic models are becoming valuable tools for solving technological problems [18, 19].

In [20–22], the excitation of vibrations during end cutting is explained by the presence of a regenerative effect (cutting along the mark) and dissipation of the cutting process (Fig. 3).

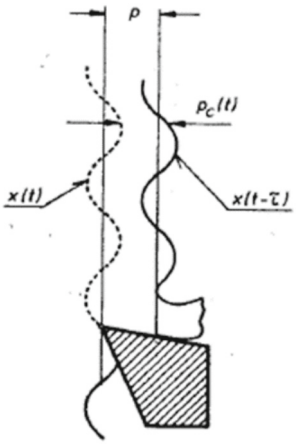

Fig. 3. Scheme of changing the cutting force with the regenerative effect

Dynamic models are presented, based on which the equations of motion with one and two degrees of freedom are studied, describing the effects of cutting along the mark when trimming solid ends (Fig. 4).

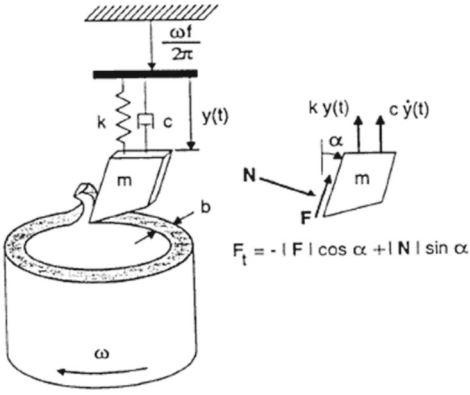

Fig. 4. Scheme of changing the cutting force with the regenerative effect

The authors consider the regenerative effect to be the most crucial dissipative factor. Measuring stands have been proposed for calculating roughness [23].

Analyzing the primary studies on the final cutting of solid ends using the plunge-in method, we note that several features of this operation on finishing and boring machines

need to be reflected in publications. Potentially unstable vibration modes of the spindle-boring-bar and workpiece-device subsystems have not been identified. The maximum cutting width of the end of different materials has yet to be studied when the rigidity of the device changes. Methods for calculating vibration resistance for precise trimming of solid ends are not reflected in publications. The features of the excitation of vibrations when trimming ends of different diameters on finishing boring machines and the dynamic interactions of machine subsystems that ensure the feasibility of the trimming and curing operation have yet to be studied.

3 Research Methodology

An experimental study of stability conditions when trimming an end was carried out according to the scheme (Fig. 5): the scoring cutter 6 was installed on a rotating mandrel 7, and the workpiece 5 was fixed in the hole of the device. The rigidity can vary within wide limits.

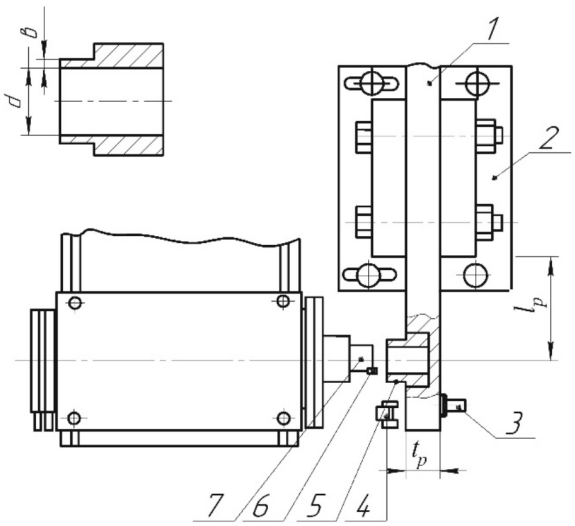

Fig. 5. Experiment to measure vibrations during end trimming

The retractable plate 1, fixed between the posts 2, was made in two versions in terms of thickness (t_p) and height (h_p) of the cross-section: the first –t_p = 20 mm, h_p = 90 mm, the second –t_p = 35 mm, h_p = 120 mm. In both variants, the value (l_p) of the plate's overhang of the cantilever part varied from 40 to 250 mm. The location of the sample being processed and the mandrel was aligned by moving the slide in the transverse direction, on which the device racks were attached. Oscillations in the direction of the processing axis were measured at idle and during cutting with an induction sensor 3 mounted on the plate and an inductive sensor 4 (low-frequency component). When cutting steel C45 [24], cutters with plates made of P01 alloy with the following geometry

were used: $\alpha = 9°$, $\gamma = 15°$, $\lambda = 0°$ at cutting speed $\nu = 100$ m/min, cutting width b = 1 mm; cutting depth t = 0.02 mm; feed per revolution $s_o = 0.02$ mm. When trimming the ends of samples made of EN-GJL-150 (EN), cutters made of K01 alloy were used, the sharpening angles of which were $\alpha = 9°$, $\gamma = 5°$.

4 Results and Discussion

The characteristics of the elastic system of the fixture model for both versions of the plate were obtained by changing l_p in increments of 10 mm (Fig. 6).

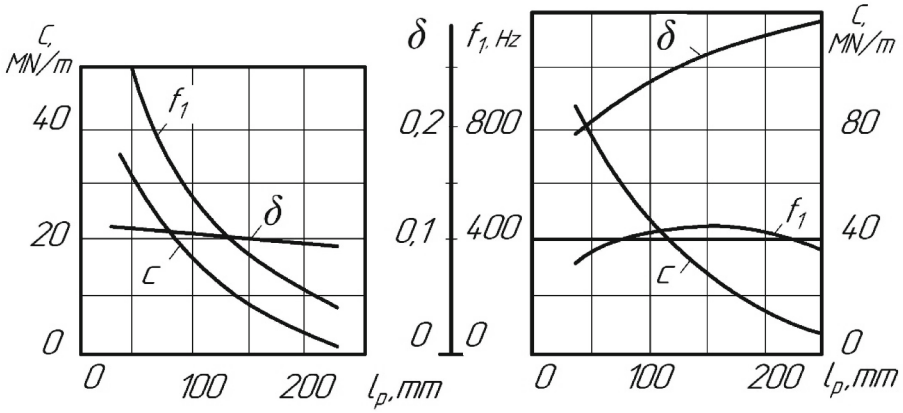

a) b)

Fig. 6. Characteristics of the elastic device system: a - $t_p = 20$ mm; b – $t_p = 35$ mm

Rigidity C is measured in the direction of the machining axis, and the natural frequency f_1 and the logarithmic decrement of vibrations δ are determined from the oscillograms of damped vibrations excited by the impact.

The study of the stability limit of processing when trimming the ends of steel samples was carried out with values of end width b = 1, 2, and 4 mm. The ratio of vibration amplitudes determined the stability limit during cutting and during idle. The value of this ratio corresponding to the beginning of the region of sharp increase in oscillation amplitudes ($a_{cut}/a_{id} \cong 1.5$) is taken as the boundary value. According to the measurement data (Fig. 7) the limit values of the overhang l_p for a plate with $t_p = 35$ mm, have been established.

The values of the maximum end width when processing EN-GJL-150 (EN) cast iron under the same conditions are 9 mm, and when processing CuSn5Zn5Pb5-C (EN) bronze and aluminum - at least 10 mm ($t_p = 20$ mm).

Several patterns that are important for the practical assessment of vibration resistance, arising due to the variability of parameters, are discovered in experiments on the model and on real devices. When trimming ends of a small diameter (about 15 mm), approaching the stability boundary, oscillations develop with a frequency close to the

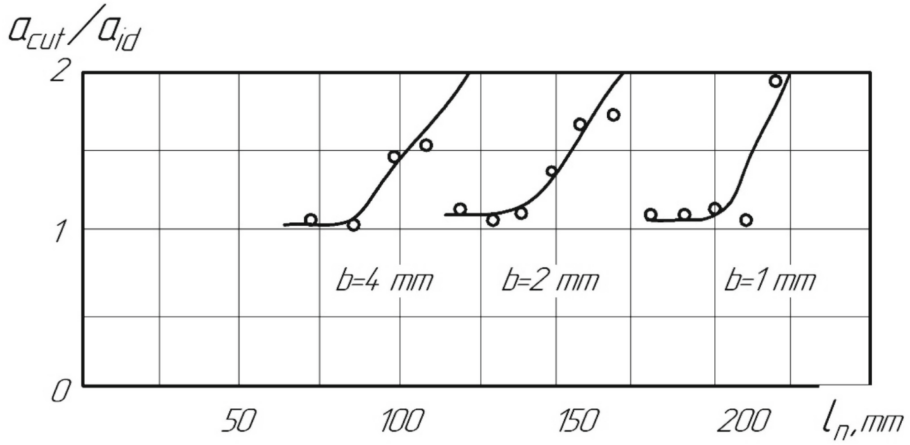

Fig. 7. The influence of the overhang of the device console on the amplitude of vibrations at three values of the width of the cut end: ⬭- experiment; ⌒- approximating curve

natural frequency f_1 of the elastic system. Moreover, the level of these vibrations almost does not change within one revolution, and traces of vibrations are evenly distributed over the treated surface. When processing ends with a diameter of 40 mm or more under the same conditions, fluctuations of a variable level are observed, the maximum of which occurs at the greatest distance of the cutter from the embedding of the device (Fig. 8). In the corresponding areas of the machined end, significantly more intense traces of vibrations are found. In addition, when machining large-diameter ends, low-frequency oscillations develop at a spindle rotation frequency f_{rot}, the range of which near the stability limit does not exceed 0.5 μm.

In this work, we consider only fluctuations along the coordinate x, which determine the cleanliness of the machined surface and the feasibility of the end trimming operation. The parameters characterizing the elastic system must correspond to the parameters of the part-device subsystem when oscillating along the lowest form in the direction of the axis x. The cutting process in vibration resistance calculations is described by a dynamic characteristic.

The characteristic establishes a connection between vibration movements and corresponding changes in cutting force. The dynamic characteristic reflects the inertial properties of the process, manifested in the phase shifts (lag) of the force P_z from the movement in the x direction.

The simplest form of the dynamic characteristic in operator form is written as:

$$P_z = \frac{K_p}{T_p p + 1} x,$$

where: K_p- cutting coefficient equal to. $K_p = 1.5\sigma_t \xi_o b$; σ_t- temporary resistance of the processed material; ξ_o - shrinkage of chips; b - cutting width; T_p -chip formation time constant ($T_p = 1.5\frac{a_0 \xi_0}{V}$); a_0-cut thickness; V-cutting speed, $p = \frac{d}{d\tau}$ - operator of differentiation with respect to time.

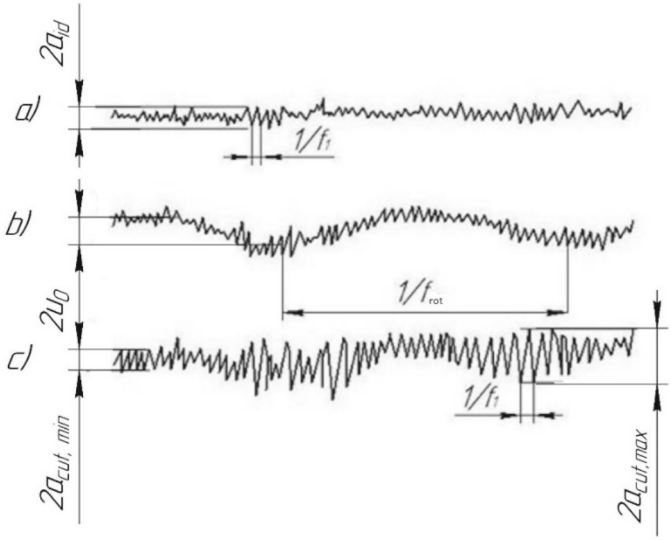

Fig. 8. Oscillations of the device model: a - idle; b - reliably stable cutting; c - cutting near the stability boundary, where 2a – range of oscillations.

The closed system is described by the equations:

$$\begin{aligned} T_1^2\ddot{x} + T_2\dot{x} + x &= kP_x, \\ T_p\dot{P}_z + P_z &= -k_p x, \end{aligned} \tag{1}$$

where: $T_1^2 = \frac{m}{c}$; $T_2 = \frac{h}{c}$; $k = \frac{1}{c}$; h- damping coefficient; m - is the reduced mass of the part-device subsystem (Eq. (1)).

Considering that approximately $P_x = \mu P_z$, where μ is the coefficient of friction of the chips on the front face, we write the equations of motion in the form:

$$\begin{aligned} T_1^2\ddot{x} + T_2\dot{x} + x &= k\mu P_z, \\ T_p\dot{P}_z + P_z &= -k_p x. \end{aligned} \tag{2}$$

Let us consider the conditions for the system's stability Eq. (2). The characteristic equation of the system has the form:

$$\begin{vmatrix} T_1^2p^2 + pT_2 + 1 & -k\mu \\ k_p & T_p p + 1 \end{vmatrix} = 0.$$

Expanding the determinant, we get (Eq. (3)):

$$\left(T_1^2p^2 + T_2p + 1\right)\left(T_p p + 1\right) + k_p k\mu = 0. \tag{3}$$

The p coefficients of the characteristic equation in decreasing powers are equal:

$$p^3 \to a_0 = T_1^2 T_p;$$
$$p^2 \to a_1 = T_1^2 + T_2 T_p;$$
$$p^1 \to a_2 = T_2 + T_p;$$
$$p^0 \to a_3 = 1 + k_p k \mu.$$

The system is stable if the coefficients a_0, a_1, a_2, a_3 and the Hurwitz determinant are positive, having the form:

$$\Delta = \begin{vmatrix} a_1 & a_0 \\ a_3 & a_2 \end{vmatrix} = a_1 a_2 - a_0 a_3.$$

The first condition is always satisfied. The second condition ($\Delta \succ 0$) is satisfied at specific values of the parameters of the elastic system and the cutting process. To analyze stability, we will reveal the value of the Hurwitz determinant:

$$\Delta = T_1^2 T_2 + T_2^2 T_p + T_2 T_p^2 - T_1^2 T_p k_p k \mu \succ 0.$$

Writing this condition in the cutting process parameters and moving to the maximum value of the cut width $b_{\max}$, we find

$$b_{\max} \leq \frac{T_2\left(T_1^2 + T_2 T_p + T_p^2\right)}{k_p T_1^2 T_p k \mu}. \tag{4}$$

The resulting expression makes it possible to calculate the maximum permissible width of the cut end for a given rigidity of the device, as well as known parameters of the material being processed and the cutting mode (Eq. (4)).

The following calculations were taken: the material being processed is steel C45 (EN), $\sigma_t = 700\ N/mm^2$, cutting speed $V = 100\,m/min = 1.67 \cdot 10^3\ mm/sek$, feed s = 0.02 mm/r (cut thickness $a_0 = 0.02$ mm), chip shrinkage $\xi = 5$. Coefficient of friction between chips and cutter $\mu = 0.8$.

The results of stability calculations when changing the rigidity of the device are given in the Table 1.

In accordance with the set goal and objectives, this work has investigated the oscillations of a dynamic system with variable parameters, such as the operation of trimming the free end using the plunge method. The experimental determination of stability conditions has been carried out using a particular device whose rigidity varies widely. In the experiments, the processing stability boundary was studied based on the ratio of the vibration amplitudes during cutting and idle operation.

It has been established that, both in the model of the device and in real devices, the patterns of change in vibration resistance are determined by the variability of the parameters of the elastic system. Thus, when trimming ends of small diameter (about 15 mm), the level of vibrations within one revolution practically does not change, and when processing ends of more than 40 mm, low-frequency vibrations of a variable level

Table 1. Results of calculations of the maximum width of the ends for normalized devices.

Width of cut end, mm		2	4	6	8	10	12	End diameter, mm	Roughness Ra, μm
Trimming device rigidity (without maintenance), N/μm	cast iron EN-GJL-150 (EN)	40	60	80	95	110	120	60 90 120 140	1.25 1.25 1.25 2.5
	steel C45 (EN)	70	95	120	135	150	160	60 90 120 140	1.0 1.25 1.25 1.25

occur with intense traces at the ends (Fig. 8). To determine the amplitudes of low-frequency forced vibrations excited parametrically, it is necessary to develop a design diagram of a rigid device with compliant embedding, which also reflects the increment in the arm of the bending moment of the cutting force P during rotation of the cutter. When cutting steel samples with a diameter of 40 mm on a model of a fixture, using the values of the rotation frequency $f_{rot} = 13$ Hz and the natural frequency of the elastic system $f_1 > 300$ Hz, we calculate the dimensionless frequency of the parametric disturbance $\nu = f_{rot}/f_1 \prec 0.05$ at such values ν one cannot expect the appearance of parametric instability, since high-order parametric resonances are not excited.

Changes in the level of high-frequency forced oscillations are associated with the dependence of the system's stability on its changing parameters. However, the peculiarities of the dynamic system under consideration do not allow the use of a design scheme with periodically varying stiffness. Movements of the scoring cutter relative to the compliant element of the elastic system do not affect the parameters of the reduced oscillator but only change the position of the cutting zone relative to the reduction point. In this case, the elastic movements of the point of reduction of the parameters of the elastic system are caused by the cutting force, change, and the increments of the cutting force caused by the movements of this point. Thus, variable design coefficients appear in the design scheme of a dynamic system.

The devices used in finishing and boring machines for basing the parts on which the ends are cut are often box-shaped structures reinforced with stiffeners (Fig. 9).

When calculating the relative movements of the scoring cutter and the workpiece, one must pay attention to the fixtures' inherent compliance and consider only the contact movements at the junction of the fixture with the Table. 1

The limit values of the end width for cast iron and steel are shown in Fig. 10. Comparison of the calculated curve with experimental data leads to a discrepancy within 10–15%. Using devices with increased rigidity ensures the roughness of the processed surface within the range of Ra = 1.25–1.0 microns, depending on the diameter of the end.

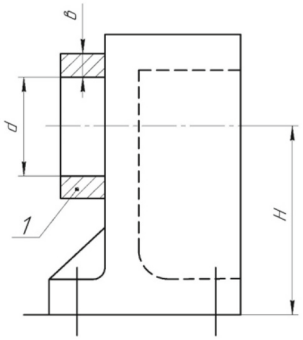

Fig. 9. Normalized adaptation to finishing and boring machine: 1 – workpiece.

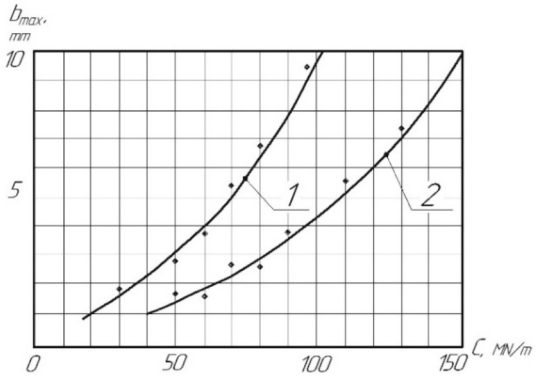

Fig. 10. Limit values of cut width for normalized devices: 1 – EN-GJL-150 (EN); 2 – steel C45 (EN), points – experiment, curve – calculation.

5 Conclusions

Analysis of the parameters of normalized devices used when cutting ends with wide-blade cutters on finishing and boring machines allows us to propose simple evaluation criteria for the feasibility of this operation based on the above experimental and calculation data.

The rigidity of the fixtures, measured in the feed direction (50–150 MN/m), is 3–4 times less than the axial rigidity of the spindle units used for trimming ends. (300–500 MN/m), and the natural frequency of the fixtures is approximately half as low: 100–180 Hz compared to 300–400 Hz. The oscillation decrement of spindle units is approximately the same as that of fixtures, $\delta \cong 0.1 - 0.2$. With such a relationship between the parameters of the subsystems, the mutual movement of the part and the tool is determined mainly by the movements of the "part-device" subsystem.

When carrying out a dynamic calculation to determine vibration resistance and find dependencies between the parameters of the elastic system and the cutting process,

we consider a single-circuit system consisting of two elements: an equivalent elastic system and the cutting process. This allows you to apply the design scheme of a one-dimensional elastic-dissipative-inertial system and impose restrictions only on the device's parameters.

In conclusion, the following recommendations are given to ensure vibration resistance of finishing and boring machines when trimming solid ends:

- The rigidity of the device is determined in the feed direction for the point of the machined end furthest from the table plan;
- the minimum permissible values of rigidity when processing the ends of parts made of cast iron EN-GJL-150 (EN) and steel C45 (EN), depending on the width of the free end, are determined according to the developed method and Fig. 10;
- If the trimming operation includes maintenance, the minimum permissible rigidity should be increased by 1.5–2 times;
- When using finishing and boring machines on which the end trimming operation is performed with a wide-blade cutter, devices with normalized bodies of increased rigidity should be used.

References

1. Altintas, Y., Brecher, C., Weck, M., Witt, S.: Virtual machine tool. CIRP Ann. Manuf. Technol. **2**(54), 115–138 (2005)
2. Altintas, Y.: Manufacturing Automation: Metal Cutting Mechanics, Machine Tool Vibrations, and CNC Design. Cambridge University Press, Cambridge, UK (2012)
3. Kaymakci, M., Kilic, Z.M., Altintas, Y.: Unified cutting force model for turning, boring, drilling and milling operations. Int. J. Mach. Tools Manuf **54–55**, 34–45 (2012)
4. Qi, Z., Zhang, K., Cheng, H., Wang, D., Meng, Q.: Microscopic mechanism based force prediction in orthogonal cutting of unidirectional CFRP. Int. J. Adv. Manuf. Technol. **79**(5–8), 1209–1219 (2015). https://doi.org/10.1007/s00170-015-6895-7
5. Popovic, M.R., Tanovic, L., Ehmann, K.E.: Cutting forces prediction: the experimental identification of orthogonal cutting coefficients. Trans. FME Trans. **4**(45), 459–467 (2017). https://doi.org/10.5937/fmet1704459P
6. Chalyj, V., Moroz, S., Tkachuk, A., Zablotskyi, V., Trokhymchuk, I., Stelmakh, A.: Formation of bearings parts waviness in centerless mortise grinding on rigid supports. J. Eng. Sci. **10**(1), A15–A21 (2023). https://doi.org/10.21272/jes.2023.10(1).a3
7. Moufki, A., Dudzinski, D., Le Coz, G.: Prediction of cutting forces from an analytical model of oblique cutting, application to peripheral milling of Ti-6Al-4V alloy. Int. J. Adv. Manuf. Technol. **1**(81), 615–626 (2015)
8. Adem, K.A.M., Fales, R., El-Gizawy, A.S.: Identification of cutting force coefficients for the linear and nonlinear force models in end milling process using average forces and optimization technique methods. Int. J. Adv. Manuf. Technol. **79**(9–12), 1671–1687 (2015)
9. Maikopoulos, AP, Karkalos, N.E., Vaxevanidis, N.M., Manolakos, D.E.: Friction in orthogonal cutting finite elements models with large negative rake angle. Tribol. Ind. **38**(2), 214–220 (2016)
10. Pavlenko, I., et al.: Using regression analysis for automated material selection in smart manufacturing. Mathematics **10**(11), 1888 (2022). https://doi.org/10.3390/math10111888

11. Sharma, V.S., Dhiman, S., Sehgal, R., et al.: Estimation of cutting forces and surface roughness for hard turning using neural networks. J. Intell. Manuf. **19**, 473–483 (2008). https://doi.org/10.1007/s10845-008-0097-1
12. Hurey, I., et al.: Resistance to wear during friction without lubrication of steel-cast iron pairing with nanocrystalline structure-reinforced surface layers. Lubricants **11**, 418 (2023). https://doi.org/10.3390/lubricants11100418
13. Alajmi, M.S., Alfares, F.: Prediction of cutting forces in turning process using de-neural networks. In: Proceedings Artificial Intelligence and Applications, Innsbruck, Austria (2007)
14. Haci, S., Faruk, U., Yaldiz, S.: Investigation of the effect of rake angle and approaching angle on main cutting force and tool tip temperature. Int. J. Mach. Tools Manuf **46**(2), 132–141 (2006)
15. Petrakov, Y.V., Ohrimenko, O.A., Sikailo, M.O., Myhovych, A.V.: Cutting forces simulation for end milling. J. Eng. Sci. **10**(2), A27–A33 (2023). https://doi.org/10.21272/jes.2023.10(2).a4
16. Markopoulos, A.P.: Machining processes. In: Finite Element Method in Machining Processes. SpringerBriefs in Applied Sciences and Technology. Springer, London (2013). https://doi.org/10.1007/978-1-4471-4330-7_1
17. Banerjee, N., Sharma, A.: Development of a friction model and its application in finite element analysis of minimum quantity lubrication machining of Ti-6Al-4V. J. Mater. Process. Technol. **238**, 181–194 (2016)
18. Oborskyi, G., Orgiyan, A., Ivanov, V., Balaniuk, A., Pavlenko, I., Trojanowska, J.: Improvement of the dynamic quality of cantilever boring bars for fine boring. Machines **11**(1), 7 (2023). https://doi.org/10.3390/machines11010007
19. Jablonski, W.: Simulation of cutting process – modeling and applications. In: Dudas, L. (ed.) Engineering the Future. IntechOpen, UK (2010). https://doi.org/10.5772/10374
20. Karayel, D.: Prediction and control of surface roughness in CNC lathe using artificial neural network. J. Mater. Process. Technol. **209**, 3125–3137 (2009). https://doi.org/10.1016/j.jmatprotec.2008.07.023
21. Göloğlu, C., Arslan, Y.: Zigzag machining surface roughness modelling using evolutionary approach. J. Intell. Manuf. **20**(2), 203–210 (2009). https://doi.org/10.1007/s10845-008-0222-1
22. Öktem, H.: An integrated study of surface roughness for modelling and optimization of cutting parameters during end milling operation. Int. J. Adv. Manuf. Technol. **43**, 852–861 (2009). https://doi.org/10.1007/s00170-008-1763-3
23. Suresh Kumar Reddy, N., Venkateswara Rao, P.: Selection of optimum tool geometry and cutting conditions using a surface roughness prediction model for end milling. Int. J. Adv. Manuf. Technol. **26**, 1202–1210 (2005). https://doi.org/10.1007/s00170-004-2110-y
24. Ivchenko, O., et al.: Method for an effective selection of tools and cutting conditions during precise turning of non-alloy quality steel C45. Materials **15**(2), 505 (2022). https://doi.org/10.3390/ma15020505

Use of the Processing Arrays Theory of Experimental Data for the Analysis of the Technological Scheme in the Rolled Metal Production – Controlled Rolling

Oleksandr Beketov[1], Dmytro Laukhin[2], Nataliia Rott[2(✉)], Eugene Babenko[1], and Valentyn Kozechko[2]

[1] Prydniprovsk State Academy of Civil Engineering and Architecture, 24A, Chernishevskogo Street, Dnipro 49005, Ukraine

[2] Dnipro University of Technology, 19, D. Yavornytsky Avenue, Dnipro 49005, Ukraine

rott.n.o@nmu.one

Abstract. Formulation of the problem. Establishing a quantitative relationship between the temperature parameters of the traditional controlled rolling scheme and the mechanical properties of thick-rolled metal is an urgent problem. It can significantly affect the production of domestic rolled products with increased operational properties due to the formation of a given structural state of the finished thin-rolled product by adjusting the temperature-deformation parameters of rolling in the cleaning cage. The article aims to build mathematical models of the relationship between the parameters of the controlled rolling technology at the final rolling stage and the main mechanical properties of rolled metal. Conclusion. Mathematical models of the relationship between temperature parameters of controlled rolling and basic mechanical properties of rolled metal from low-carbon low-alloy steel 10Mn2VNb. At the same time, it is shown that the temperature increase at the beginning of the finishing process rolling will lead to an increase in the level of strength characteristics. The analysis of the results of the conducted research showed the perspective of correcting the formation of structural and substructural components based on reduction to a minimum of the cooling period on the bypass roller conveyor and further continuous deformation in the intercritical temperature interval. Simultaneously, lowering the temperature of the end of hot rolling to the lower limit of the intercritical interval will allow further improvement and stabilize the set of mechanical characteristics of rolled steel for building structures.

Keywords: Controlled Rolling · Low-Carbon Low-Alloy Steel · Mechanical Properties · Industrial Growth

© The Author(s), under exclusive license to Springer Nature Switzerland AG 2024
V. Ivanov et al. (Eds.): DSMIE 2024, LNME, pp. 152–163, 2024.
https://doi.org/10.1007/978-3-031-61797-3_13

1 Introduction

Traditional controlled rolling is a type of thermomechanical processing of steels, characterized by regulated (depending on the chemical composition) temperature and deformation parameters of the process, given by the metal cooling regimes at different stages of plastic processing.

From the point of view of structure formation, the process of controlled rolling aims to achieve the main goal - ferrite grain grinding by combining plastic deformation and controlling the processes of microstructure formation [1]. By controlling the conditions of hot rolling in austenite, a high density of nucleation centers of the ferrite phase is created, which makes it possible to achieve significant grinding of the ferrite grain size after the $\gamma \rightarrow \alpha$ transformation [2].

Thus, the work aims to obtain increased operational characteristics in rolled metal for welded building structures by developing an improved technological scheme to produce high-strength rolled steel from low-carbon, low-, micro-, and unalloyed steel.

2 Literature Review

According to the technological scheme of controlled rolling, most common in domestic enterprises, slabs are heated to 1250…1140 °C before rolling. The temperature at the end of rolling can be from 900 to 700 °C with relative compressions in the last passes up to 15%. In order to ensure the required temperature of finishing rolling, the workpieces are kept on a bypass roller conveyor (bypass).

Simultaneously, it should be noted that if the release of the carbide phase is suppressed by the cooling rate of the thick sheet, then the increase in mechanical properties is not only related to the formation of the dislocation substructure of ferrite. Subsequently, in further slow cooling, the carbide phase is separated [3]. Thus, above 900…950 °C, austenite recrystallizes after hot deformation at a rate dependent on the degree of deformation and temperature. If the rolling temperature is below the austenite recrystallization temperature range, the ferrite grain size decreases due to the preservation of the developed austenite substructure. If deformation during rolling occurs at temperatures below the recrystallization threshold of austenite, the austenite grain is elongated, and the length of grain and subgrain boundaries increases, which leads to an increase in the number of ferrite nucleation sites. Deformed crushed austenite disintegrates into fine-grained ferrite. This effect increases with the degree of deformation below the austenite recrystallization temperature. The accelerated cooling of non-recrystallized austenite forms a more dispersed final ferrite grain. On the other hand, accelerated cooling of non-recrystallized austenite can lead to numerous centers of ferrite nucleation inside the austenite grain at additional centers of heterogeneous nucleation of the new phase and deformation bands. All these factors grind the final ferrite grain.

The analysis of the processes of structure formation during hot plastic deformation shows that the effective and stable influence of deformation on the steel structure is determined by the presence and magnitude of three temperature intervals, limited by the critical transformation points and recrystallization temperatures of the deformed austenite of this steel [4–6] (see Fig. 1).

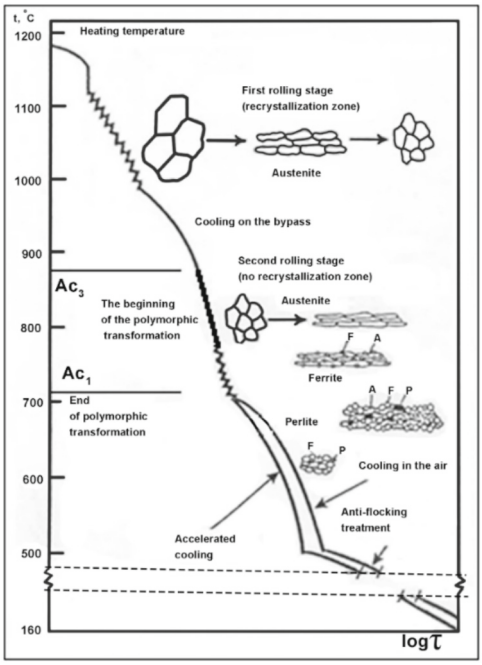

Fig. 1. Scheme of controlled rolling.

On the other hand, the analysis of the data given in [7] shows the possibility of forming the structural state of the finished rolled metal by adjusting the temperature and deformation parameters of rolling in the finishing cage. Thus, this work aims to build mathematical models of the relationship between the parameters of the controlled rolling technology at the final rolling stage and the main mechanical properties of rolled metal.

3 Research Methodology

As a material for this study, 10Mn2VNb steel with a thickness of 20 mm was chosen, which was produced according to the technological scheme of controlled rolling schematically shown in Fig. 2a). The chemical composition of 10Mn2VNb steel is presented in Table 1, and the corresponding complex of mechanical properties is presented in Table 2.

After controlled rolling, 10Mn2VNb steel has the structure shown in Fig. 2b, c.

Analysis of the data in Fig. 2 shows the structure has a mixed polyhedral type according to the general classification of structure types. Ferrite and cementite form in austenite at relatively low supercooling. Austenite in equilibrium with ferrite has one composition and with cementite another. The difference in carbon concentrations at the boundaries of austenite with ferrite and cementite determines the diffusion of carbon and the subsequent formation of ferrite and cementite. The formation of polyhedral ferrite occurs by the diffusion mechanism in conditions of significant mobility of atoms

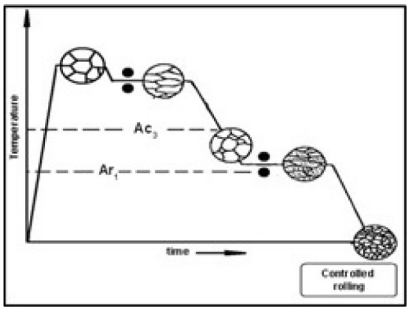

a)

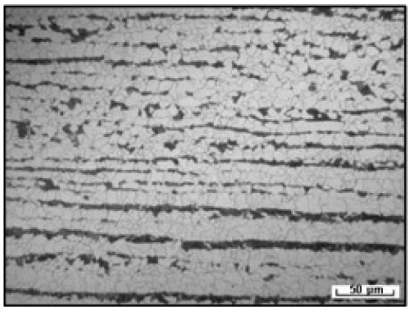

b)

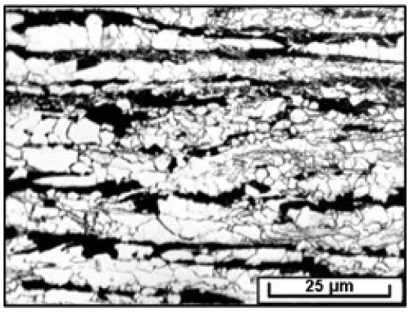

c)

Fig. 2. Technological scheme of controlled rolling (a); microstructure of steel 10Mn2VNb in the state of delivery (b, c).

Table 1. Chemical composition of steel 10Mn2VNb.

Steel	The mass fate of the element, %									
	C	Mn	Si	S	P	N	Cr	V	Nb	Fe
10Mn2VNb	0.10	1.58	0.18	0.005	0.015	0.008	–	0.088	0.022	balance

Table 2. Mechanical properties of steel 10Mn2VNb.

Steel	Strength limit, MPa	Yield strength, MPa	Relative elongation, %	Impact viscosity KCV + 20, J/ $m^{2*}10^{-4}$
10Mn2VNb	545	445	30	151

when there are no internal stresses, and the crystals that are formed seek to obtain the thermodynamically most advantageous form.

To obtain appropriate mathematical models, the following stages of statistical processing of the analyzed parameters were applied:

– preliminary statistical processing;
– correlation analysis;
– multivariate dispersion analysis;
– multivariate regression analysis.

Preliminary statistical processing was performed according to the recommendations [8].

Multivariate variance analysis is a statistical method of analyzing the results of observations that depend on various simultaneously acting factors, selecting the most important of them, and evaluating their impact. Multifactor analysis allows for checking the influence of several factors on the dependent variable and evaluating the influence of each factor and their interaction separately [9].

In this paper, the method of multivariate variance analysis was applied as follows:

– a null hypothesis was formulated (the studied factors do not have any influence on the value of the resulting characteristic, and the obtained differences are random);
– the probability of obtaining the observed (or stronger) differences under the condition of validity of the null hypothesis was determined;
– if this probability was small (the maximum acceptable probability was rejected, the true null hypothesis was marked with a significance level of $\alpha = 0.05$), then the null hypothesis was rejected. As a result, it was assumed that the results were statistically significant.

In the multiple regression study, graphical interpretation (according to recommendations [10]) of the multivariate space was not used. In this paper, the task of linear multiple regression was to construct a hyperplane in $(k + 1)$-dimensional space, the deviation of the observation results from which would be minimal when using the least squares method. The procedure for determining the coefficients does not differ from the one-dimensional case [11].

The following assumptions were made during the regression analysis:

– the input parameter was measured with a small error;
– the results of observations of the initial value are independently normally distributed random variables;
– when experimenting with a sample size, provided that each experiment is repeated a certain number of times, the sample variances must be homogeneous (this means that the experimental data belong to the same general population).

After obtaining the regression equation, a statistical analysis of the results was carried out. This analysis consisted of checking the significance of all the coefficients and establishing the equations' adequacy [11].

The adequacy of the model was tested under the assumption that the random errors of observations are independent, normally distributed random variables with zero mean values and equal variances. Mathematically, the verification was done using the quasi-Newton method – a nonlinear estimation procedure that calculates the value of the

function at different points for estimating the first and second derivatives at each step [12].

The computing operations were performed on a personal computer using the package of example programs for statistical processing Statistica [13].

4 Results and Discussion

The relationship between the parameters of the controlled rolling technology and the main mechanical properties of rolled metal was established based on data obtained during the production of low-carbon low-alloy steel 10Mn2VNb.

The arrays of data subjected to statistical processing are shown in Table 3. Simultaneously, the temperature at the beginning of finishing rolling (Ts) and the temperature at the end of finishing rolling (Tf) were chosen as the independent variables, and the yield strength (YS) was chosen as the criteria of the model (response functions), strength limit (σ_B), relative elongation (δ_5).

Table 3. Data arrays for preliminary statistical processing.

Strength limit, MPa	Yield strength, MPa	Relative elongation, %	Ts	Tf
380	520	29.5	785	745
351	505	29.0	785	745
403	560	27.5	782	742
384	540	32.0	782	742
389	541	27.0	783	743
371	533	27.5	784	744
380	520	29.5	784	744
351	505	29.0	780	740
403	560	27.5	788	748
384	540	32.0	785	745
389	541	27.0	783	743
371	533	27.5	797	757

The main statistical indicators are presented in Table 4. The verification of the adequacy of the distribution of data arrays to the normal law is shown in Fig. 3.

Joint analysis of the given data showed that all variables have a distribution of values close to the law of normal distribution (Gaussian distribution). The main statistical indicators are within the limits that satisfy the regulatory requirements (see, for example, [14]). Thus, all arrays of values can be subjected to further statistical analysis without additional operations of mathematical transformation.

To build the appropriate mathematical models, we will analyze the type, closeness, and strength of the connection between the variables. According to the recommendations

Table 4. Main statistical indicators.

Variables	Number	Average value	Minimum	Maximum	Scope	Dispersion	Mean square deviation	Standard error	Asymmetry coefficient	Excess
YS, MPa	12	380	351	403	52	30.00	17.59	−0.58	0.85	0.95
$\sigma_в$, MPa	12	533	505	560	55	35.60	18.95	−0.20	0.85	0.18
δ5, %	12	29	27	32	5	3.48	1.86	1.18	0.85	1.06
Ts, °C	12	785	780	797	17	18.69	4.32	1.25	2.24	6.2
Tf, °C	12	745	740	757	17	18.69	4.32	1.25	2.24	6.2

[11], the multiple correlation coefficient should be used to determine the closeness of the relationship between the response function and several independent changes. However, the correlation coefficients were used to estimate tightness based on the assumption that there would be a stochastic relationship between the response functions and the independent variables.

These coefficients make it possible to determine the degree of influence of one of the independent variables on the response function, provided that other independent changes can be considered constant. The results of the analysis are presented in Table 5.

The obtained data show that the "yield limit" and "strength limit" are most dependent on the "Ts" variable. The correlation between these parameters has a direct and close connection. Therefore, as the temperature of the start of rolling increases, the indicators of strength properties increase.

To analyze the influence of two independent variables (Ts, Tf) on each of the response functions (YS, σ_B, and δ_5), the mathematical apparatus of multivariate dispersion analysis was applied. The results are shown in Table 6 and Fig. 4.

$$y = b_0 + b_1 \cdot x_{ij} + \ldots + b_j \cdot x_{ij} + b_k \cdot x_{ik} + e_i \quad (1)$$

The results of the calculation and nonlinear estimation of the coefficients of the regression equation are presented in Table 7.

All coefficients satisfy the requirements, and the significance of the null hypothesis is confirmed. To check the adequacy of the obtained models, residual graphs were drawn on normal probability paper. The results are presented in Fig. 5a–c. The obtained results make it possible to present the studied dependencies graphically. For this purpose, response function surfaces were constructed considering the specified temperatures of rough rolling intervals. The results are presented in Fig. 5(d-e).

The analysis of the results of the conducted research showed the perspective of correcting the processes of formation of structural and substructural components based on the reduction to a minimum of the cooling period on the bypass roller conveyor and further continuous deformation in the intercritical temperature interval. At the same time, lowering the temperature of the end of hot rolling to the lower limit of the intercritical interval will allow for further improvement and stabilization of the set of mechanical characteristics of rolled steel for construction.

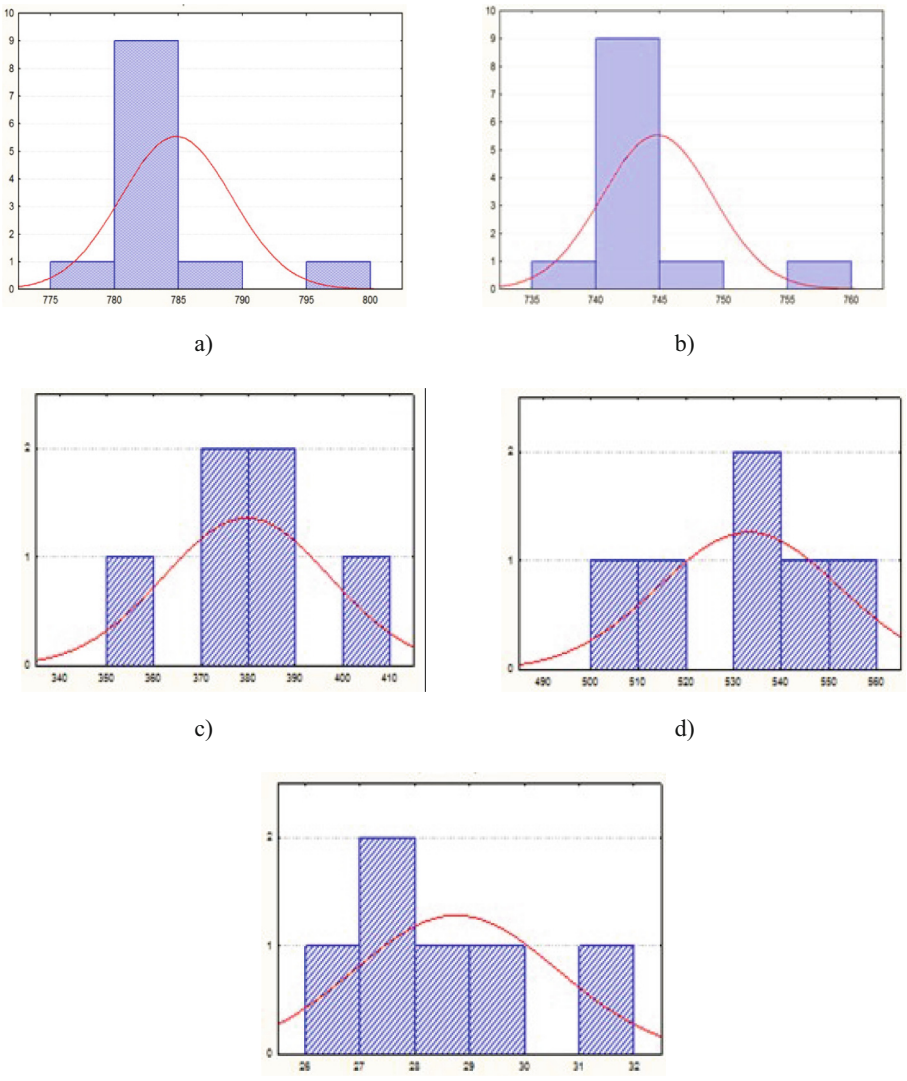

Fig. 3. Checking the adequacy of the distribution of data arrays to the normal distribution law: a – the temperature of the start of finishing rolling (Ts); b – temperature at the end of finishing rolling (Tf); c – yield strength (YS); d – strength limit (σ_B); e – relative elongation (δ_5).

Table 5. Correlation analysis data for 10Mn2VNb/

Variable	Yield strength, MPa	Strength limit, MPa	Relative elongation, %
Ts	0.77	0.89	−0.10
Tf	−0.35	−0.24	0.57

Table 6. Results of multivariate variance analysis.

Yield strength					
Effect	Value	F	Influence df	Error df	p
Crossing	0.000045	44511.42	2	4	0
Yield strength	0.248792	0.67	12	8	0.743707
Strength limit					
Crossing	0.000032	46529.39	2	3	0
Strength limit	0.016247	2.93	14	6	0.096297
Relative elongation					
Crossing	0.00001	196645.8	2	4	0
Relative elongation	0.051576	2.3	12	8	0.125648

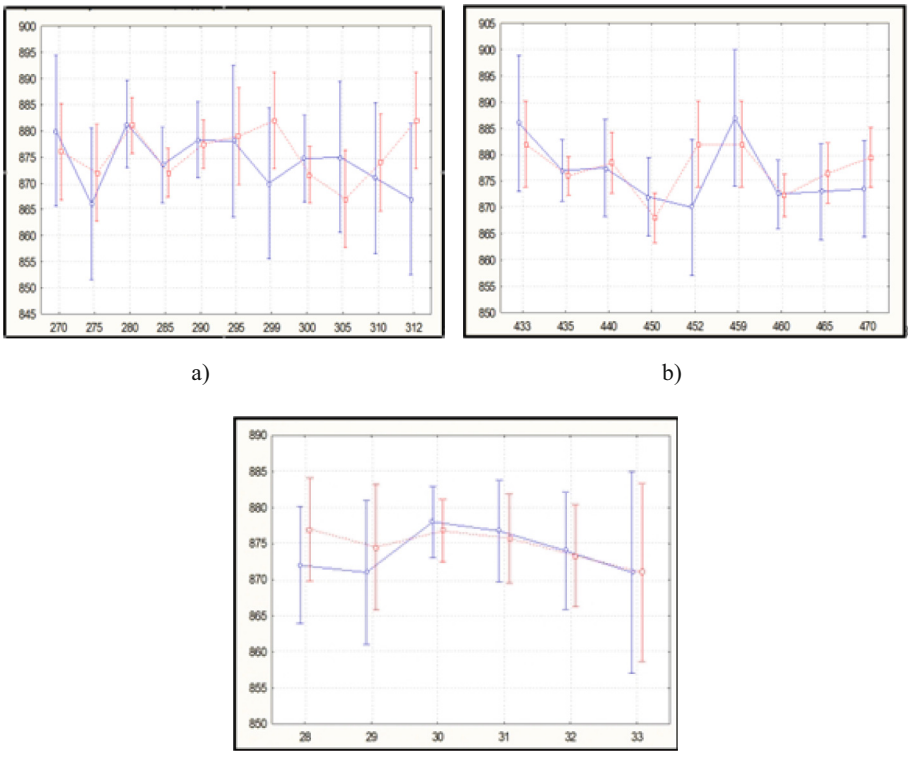

a) b)

c)

Fig. 4. Graphic display of the influence of independent variables: a – to the limit of fluidity; b – to the limit of strength; c – on relative elongation.

Table 7. Nonlinear estimation of the coefficients of the regression Eq. (1).

	The coefficients of Eq	The coefficients of Eq	The criterion for estimating the coefficient of the regression equation	The probability of the 0th hypothesis for the coefficients of the regression equation	Tolerance
Yield strength					
Ts	−0.76	−5	−1.85	0.16	0.81
Tf	0.03	0	0.07	0.95	0.81
Strength limit					
Ts	−0.97	−10	−3.57	0.04	0.81
Tf	−0.17	−2	−0.64	0.57	0.81
Relative elongation					
Ts	0.16	0.0	0.31	0.78	0.81
Tf	0.64	0.0	1.24	0.30	0.81

5 Conclusions

Mathematical models of the relationship between temperature parameters of controlled rolling and the main mechanical properties of rolled metal from low-carbon low-alloy steel 10Mn2VNb were obtained.

Applying the mathematical apparatus of the theory of processing arrays of experimental data made it possible to establish a relationship between the temperature parameters of the traditional controlled rolling scheme and the mechanical properties of thick sheet metal rolling. The conducted correlation analysis showed the presence of dependencies between response functions (mechanical characteristics) and variables (temperatures at the beginning and end of finishing rolling).

The application of multivariate variance analysis made it possible to establish the influence of each variable on each response function. At the same time, it is shown that a change in the temperature interval of finishing rolling leads to a change in the strength characteristics.

Applying the mathematical apparatus of multiparametric regression analysis made it possible to build mathematical models of the relationship between mechanical characteristics and temperatures at the beginning and end of finishing rolling. Graphical methods verified the adequacy of the obtained models and showed a high convergence of the obtained results. Analysis of the models showed that an increase in the temperature at the start of finishing rolling would increase the level of strength characteristics.

Based on the obtained results, an adjusted technological scheme is recommended for the industrial production of rolled products from low-carbon, low-, micro-, and unalloyed steels, which includes continuous deformation of the polygonal structure of austenite and, due to the adjustment of the temperature parameters of rolling, ensures the formation of a developed ferrite-pearlite structure with a given type of cementite framework of the

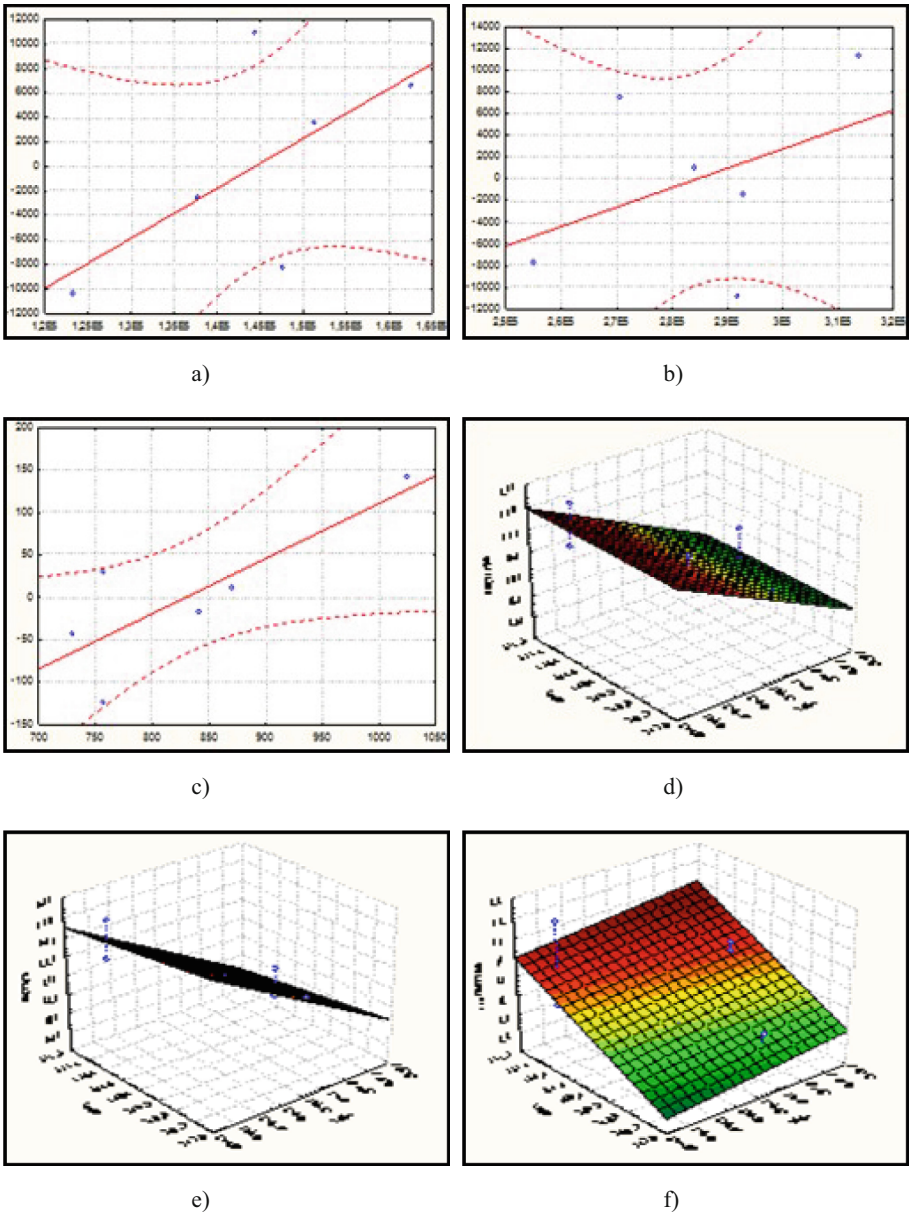

Fig. 5. Checking the adequacy of the received models (a–c) and graphical interpretation of the received models (d, e): a, d – σ_t = f(Ts, Tf); b, d – σ_B = f(Ts, Tf); c, e – δ_5 = f(Ts, Tf).

pearlite phase. This technological scheme can also be used in the production of rolled metal for steels that contain carbide-forming elements and materials without additional alloying.

References

1. Hu, J., Du, L.-X., Wang, J.-J., Xie, H., Gao, C.-R., Misra, R.D.K.: Structure–mechanical property relationship in low carbon microalloyed steel plate processed using controlled rolling and two-stage continuous cooling. Mater. Sci. Eng. A **585**, 197–204 (2013). https://doi.org/10.1016/j.msea.2013.07.071
2. Pogrebna, N.E., Kutsova, V.Z., Kotova, T.V.: Methods of Strengthening Metals. NMetAU, Dnipro, Ukraine (2021)
3. Deyneko, L.N., Kripak, I.Y., Nikitchenko, V.S., Nazarets, A.S., Litvinenko, E.I.: Effective technology for strengthening heat treatment of products made from tool and structural steel grades. Equipment and technologies for heat treatment of metals and alloys. Part 1, 62–66 (2003)
4. DeArdo, A.J.: Modern termomechanical processing of microalloyed steel. In: Proceedings of the International Conference "Microalloying 95", pp. 15–35 (1995)
5. Tamura, L., Ouchi, C., Tanaka, T., Seikine, H.: Termomechanical Processing of High Strength Low Alloy Steels. Robert Hartnoll Ltd., Bodmin (1998)
6. Bolshakov, V.I.: Substructural Hardening of Structural Steels. Basilian Press, Kanada (1998)
7. Laukhin, D., Pozniakov, V., Beketov, O., Rott, N., Shchudro, A.: Analysis of the effects of welding conditions on the formation of the structure of welded joints of low-carbon low-alloy steels. Key Eng. Mater. **844**, 146–154 (2020). https://doi.org/10.4028/www.scientific.net/KEM.844.146
8. Mandel, J.: The statistical Analysis of Experimental Data. Courier Corporation, New York, NY, USA (2012)
9. Zhiltsov, O.B.: Probability Theory and Mathematical Statistics in Examples and Problems. University named after B. Hrinchenko, Kyiv, Ukraine (2015)
10. Kushlyk-Dyvulska, O.I., Polishchuk, N.V., Orel, B.P., Shtablyuk, P.I.: Probability Theory and Mathematical Statistics. NTUU "KPI", Kyiv, Ukraine (2014)
11. Beketov, A.V., Bolshakov, V.I., Sukhomlin, G.D., Laukhin, D.V., Murashkin, A.V., Gerasenko, K.M.: Method of regression modeling of dependence of basic mechanical properties of low-carbon micro alloyed iron plates on hot rolling finishing temperatures. In: 10th International Student's Day of Metallurgy, pp. 25−28. Freiberg, Germany (2012)
12. Zholdak, M.I., Kuzmina, N.M., Berlinska, S.Y.: Theory of Validity and Mathematical Statistics with Elements of Information Technology. Vishcha School, Kyiv, Ukraine (1995)
13. Ivanyuta, I.D., Ribalka, V.I., Rudomino-Dusyatska, I.A.: Elements of the Theory of Variables and Mathematical Statistics. Slovo, Kyiv, Ukraine (2003)
14. Barkovsky, V.V., Barkovska, N.V., Lopatin, O.K.: The Theory of Variables and Mathematical Statistics. TsUL, Kyiv, Ukraine (2002)

Research of Static Stiffness of Flexible Fixtures for Y-Type Fork Parts

Ivan Dehtiarov[1], Vitalii Ivanov[1,2(✉)], Artem Evtuhov[1], Ruslan Ostroha[1], and Olaf Ciszak[3]

[1] Sumy State University, 116, Kharkivska Street, Sumy 40007, Ukraine
ivanov@tmvi.sumdu.edu.ua
[2] Technical University of Kosice, 1, Bayerova Street, 08001 Presov, Slovakia
[3] Poznan University of Technology, 5, M. Sklodowska-Curie Square, 60-965 Poznan, Poland

Abstract. Modern machining centers with broad technological capabilities require the development of flexible fixtures that ensure one-setup machining with high-performance cutting modes and maximum tool accessibility. It is especially crucial for multiproduct and batch manufacturing. The article experimentally proves the scientific approach based on the machining Y-type forks using fixtures with incomplete locating and clamping on unmachined surfaces in one setup, which ensures machining accuracy. The research presents an improved fixture configuration and theoretical substantiation. The experimental studies of the stress-strain state in the static mode were performed. The obtained values of stresses and displacements proved the advantages of the proposed approach. It was experimentally proven for the first time that the design of the improved fixture for machining Y-type forks provides the necessary machining accuracy under static load and, simultaneously, has a margin of accuracy that exceeds the value of deformations by 1.2…2.3 times. Theoretically and experimentally, it has been proven that the scientific approach to designing fixtures with incomplete locating allows the specified machining accuracy to be obtained while ensuring the necessary stable position exclusively by clamping forces.

Keywords: Accuracy · Deflection · Stress · Numerical Simulation · Error · Industrial Growth · Process Innovation

1 Introduction

In today's conditions of active development of the machine-building industry and on the threshold of the already outlined boundaries of Industry 5.0, manufacturers of products for cars, tractors, and other machinery face significant challenges. It is essential to follow the market needs [1], rapid manufacturing of a wide range of high-quality products, as required by the ISO 9001 standard [2], interdisciplinary approach [3], and evaluate possible risks [4]. Also, the finished part's quality must first meet the requirements specified by the designer on the drawing. Therefore, it is necessary to modernize and apply the newest equipment, manufacturing technologies, and production processes to obtain

© The Author(s), under exclusive license to Springer Nature Switzerland AG 2024
V. Ivanov et al. (Eds.): DSMIE 2024, LNME, pp. 164–177, 2024.
https://doi.org/10.1007/978-3-031-61797-3_14

competitive products [5]. Also, with the transition to modern machines, the approaches to fixture design remained traditional. Specifically, large-sized rigid fixtures are used as special mandrels located on a body or fixture installed on standard rotary tables and dividing heads. At the same time, it is challenging to implement tool accessibility fully in some practical cases. It is also unnecessary because a modern machining center provides all these provisions solely due to its technical characteristics. Considering those mentioned above, it is worth designing fixtures with as much tool accessibility as possible, ensuring the primary condition for the stability of the workpiece during machining. The research was performed based on the Y-type forks [6] that are widely used in the automotive industry.

Therefore, this research aims to experimentally determine the static stiffness and prove the possibility of manufacturing Y-type forks in a flexible fixture in one setup, meeting the design and technological documentation requirements.

2 Literature Review

For more than four hundred years, the construction of a transmission mechanism of the cardan type has been known [7]. In automotive equipment, agricultural machines, and devices, cardan transmission has been actively used for more than a hundred years. It remains relevant for all-wheel drive, rear-wheel drive, trucks, and other heavy equipment. In today's world, the range of cars is being updated very quickly, and the time it takes for products to enter the market is decreasing, which is also reflected in the approach to the production of spare parts, specifically in terms of materials and technologies for obtaining parts. However, the latest composite materials and their processing technologies are currently quite expensive.

Cardan transmissions will generally remain relevant for a long time due to their versatility and operational performance. Therefore, many scientists worldwide are engaged in research, design, strength calculations, and improving existing structures regarding material consumption. Thus, in [8], a dynamic study of the vibrations of a heavy cardan shaft on U-like joints was carried out using numerical modeling methods, and it was established that with a sizeable parallel shift between the input and output shafts occurs the Sommerfeld effect, with resonance frequencies.

Cardoso et al. [9] analyzed the fatigue resistance of several universal cardan joints for the control column in trucks using finite element methods and experimental mechanical tests on torsion, which made it possible to establish the permissible number of inclusions in the material of the connection parts and parameters of roughness to obtain acceptable fatigue strength indicators. Research works [10, 11] are devoted to identifying cardan shaft imbalance in a high-speed train. From the results, it was possible to establish that the imbalance occurs due to misalignment of the cardan shaft. It allows practical recommendations [10] for eliminating the imbalance by establishing a reasonably permissible misalignment deviation during assembly. The study [11] proposes a new method for diagnosing imbalance, of which 15% has a smaller margin of error than the existing ones.

Authors Kuo and Wu [12] proposed a device for balancing cardan shafts based on compression and tension springs. In the research work [13], the authors performed an

experimental-analytical study of the cardan shaft cross-piece. They established the most dangerous intersections of the cross-pieces and forks of the hinge under alternating-sign loads.

The results of numerous works confirm the focus on reducing the weight of cardan mechanisms. Namely, in the study [14], a methodology for laying carbon fibers was proposed using the example of a Y-type fork and was checked using numerical simulation in the ABAQUS environment. In the study [15], the cardan shaft of a passenger car was analyzed and optimized according to the minimum weight criterion.

Authors of the research work [16] considered designing and improving fork-type parts using optimization methods according to the fatigue strength and metal consumption criteria. The results showed a 24% reduction in mass and reduced maximum stresses by 9%. Also, simulation modeling improved stiffness by 37% compared to the original fork-type configuration. Using materials with predefined properties can be an efficient solution for designing and manufacturing engineering products [17, 18].

Enterprises manufacturing spare parts are actively intensifying production processes to reduce the cost of the final product by reducing the time it takes to produce finished parts and assemble them. Enterprises are ready to invest money in purchasing progressive metal-cutting machines, which reduce or eliminate the worker's labor. Developing and implementing new technical solutions to direct the technological process toward the concentration of mechanical operations is also necessary. A significant increase in the technological capabilities of modern metal-cutting machines is associated with the appearance of functions of automatic binding to the position of the coordinates of each workpiece [19]. Modern machining centers are equipped with the function of automatic recalculation of the coordinates of the reference points of the contour of the workpiece in the machine tool coordinate system, which allows you not to apply to locate in the classical form but to install the parts in a way that it is fast and convenient and does not require high qualification of the worker or would allow you to completely abandon participation of workers at the stage of machining, i.e., maximum use of unmanned technologies.

In this regard, flexible fixture design is an urgent task for up-to-date manufacturing. Flexible fixtures should have sufficient rigidity to maximize the machine tool's power and tool accessibility to the machining area. At the same time, the fixtures should have the minimum possible number of components. Dimensional and mass characteristics should also be tending to the minimal values. At one time, fixtures should allow the installation of parts of a similar configuration in a specific range of sizes according to their characteristics. Dedicated fixtures need to meet the conditions for installing parts of a complex geometric shape with maximum tool accessibility and are also characterized by relatively large overall dimensions and weight. At the same time, locating requires a high worker qualification and a significant expenditure of auxiliary time, so their use is impractical for solving the tasks, as mentioned earlier. Dedicated and modular fixtures have a limited scope of application from an economic point of view [20].

In the study [21], scientists proposed an algorithm for automated fixture design to fix complex profile parts of cars based on optimizing the number of clamping places and their locations. Also, in the scientific work [22], a review of the created methodology of end-to-end design of fixtures according to all currently existing algorithms, such as

locating planning, clamping planning, design and verification of fixtures based on the integration of several segmented methodologies into one integrated one, was performed.

Analysis of the latest research and publications showed that introducing means of production, namely fixtures, which ensure increased productivity and reduced cost of finished products, is relevant.

3 Research Methodology

It is proposed the following steps to achieve the set goal: 1) to develop a structure of fixture for machining Y-type forks in one step; 2) to research the stress-strain design of the fixture for machining Y-type forks using numerical simulation methods; 3) to perform experimental studies using the novel fixture configuration and compare them with the numerical simulation results.

Y-type forks are the main element of any cardan transmission and differ mainly only in overall dimensions and some minor design features, such as parameters or type of spline connection. The Y-type fork (also called the Hook joint) is a connecting part between the cross and another fixed fork, which is attached to the output shaft of the mechanism. Y-type forks for cardan transmissions, as a rule, have a spline hole to ensure the possibility of axial movement of the cardan when the car is moving on the terrain or a slight adjustment of the distance between the mechanisms that must transmit torque to each other not in direct communication, but through the cardan shaft. In this way, the fork moves slidingly and rotates in the hinged joint, which is why the requirements for the imbalance of this unit are pretty high. Also, by this, minimum tolerances of symmetry and runout are assigned to all connection parts, which must be achieved during the operations of the technological process of machining.

Y-type forks were chosen as the research object. The most common design variants of forks of steering mechanisms (Fig. 1a, b) and wheel drive mechanisms (Fig. 1c, d) have the following parameters:

- overall dimensions: $l \times b \times h = 100 \times 60 \times 30 \ldots 120 \times 85 \times 40$ mm;
- weight: $m = 0.9 \ldots 1.5$ kg;
- accuracy of the main holes in the ears: IT 7…IT9;
- roughness of holes and contact surfaces: R_a (1.6…3.2) μm.

Of all the designs of the specified fork-type parts, in this article, we will consider the most common design of the fork with a long shank (Fig. 1c), which is widely used in power transmission mechanisms from the gearbox to the rear axle reducer of trucks and heavy machinery.

Currently, a wide variety of cars, tractors, special equipment, and other machines include cardan transmissions. However, the designs of the fork-type parts are very similar (Fig. 1). Their standard sizes and design parameters are also quite similar. Accordingly, the concept of machining a specific nomenclature and standard size of parts in one flexible fixture can be implemented. Using modern progressive machines, it is possible to deviate from the principle of complete orientation of the workpiece in the fixture and to ensure only its reliable fixing, excluding any displacement during the machining process.

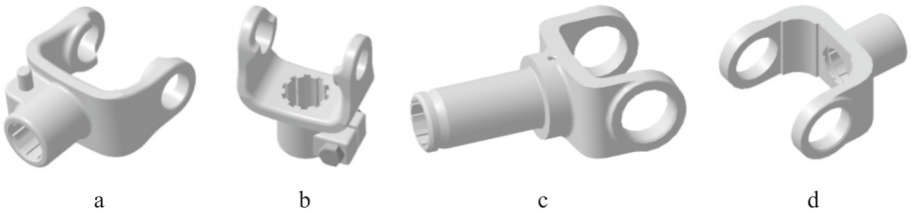

Fig. 1. Examples of Y-type forks in the automotive industry: a – Peugeot Partner; b – Dacia Logan MCV; c – Mercedes Sprinter; d – Renault Master.

In the study [6], a progressive technological process of machining Y-type forks was proposed for one-setup machining in fixtures with an incomplete type of locating, for which a patent was obtained. The methods of finite element analysis investigated the proposed design of the fixture. The research results presented in [6] from the point of view of maximum stresses, displacements, and natural frequencies of oscillations were satisfactory. It makes it possible to discuss the prospects of this research direction and develop fixtures based on the principle of incomplete locating. Figure 2 shows the workpiece location chart in the fixture [6].

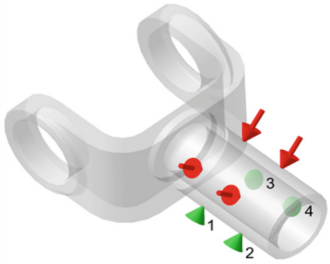

Fig. 2. The locating-and-clamping chart in a flexible fixture for Y-type forks.

It assumes the presence of only a double guide base on the outer cylindrical surface, which occurs when the shank of the fork comes into contact with the prism and deprives, by definition, of four degrees of freedom (datums are represented by contact points in the form of green cones). In this way, two degrees of freedom remain free, namely the rotation of the fork around the axis of the shank and the axial movement along the V-block. Workpiece clamping is carried out by applying force to the outer cylindrical surface (red arrows represent clamping positions). The proposed fixture is intended for the setup of Y-type forks in the range of length 80–120 mm, the distance between the outer ends of the lugs 60–90 mm, and the diameter of the shank 25–40 mm, which is carried out by adjusting the screws that provide a change in the distance between the locating element of the fixture is a V-block and the clamping element of the fixture [6].

However, as a result of studies of the stress-strain state [6], it was found that the contact stresses in the zone of the axes established in the V-block during the tightening of the screws with force necessary for the stable position of the workpiece during the

machining process are at the limit of permissible values. When applying maximum loads during the simulation of the machining of fork-type parts with the maximum standard sizes, the contact stresses generally exceed the limit of allowable values. That is, crumpling of the axle surfaces occurs. This does not allow you to utilize the maximum clamping force that screws in tension fully could withstand.

In this way, the design of the improved fixture (Fig. 3) is proposed, which allows minimizing of the effect of elastic deformations and contact stresses during screw tightening to increase the surface area for clamping the fixture [6] and to increase the stiffness of the grip. At the same time, the locating chart is similar to the previous fixture design [6]. The improved fixture was studied using numerical simulation of the stress-strain state in the Static Structural module of the ANSYS Workbench calculation complex. The movements of the machined surfaces (marked in red, Fig. 3) relative to their initial position will also be determined.

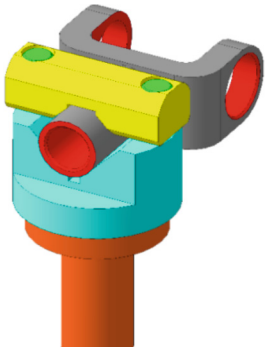

Fig. 3. 3D model of an advanced flexible fixture with an incomplete location for Y-type forks.

During the simulation, the boundary conditions shown in Table1 were set, and the fixture material and workpiece properties are similar to those in [6]. This model also considers the Coulomb friction between the contact surfaces of the fixture with a coefficient of 0.1 since they have approximately the same roughness within Ra (1.6…3.2) μm. The datum surface for clamping is the fixture shank (surface A, Table 1), which is rigidly fixed in the chuck on the machine table using the Fixture Support contact type, which implies its complete immobility (in this case, not the entire technological system is researched, but only the "fixture–workpiece' system).

During the simulation, cutting forces and torques were applied to each surface to be machined because single-tool machining is usually implemented on CNC machines. The force value at different machining transitions varied within 128…1105 N and torques 1275…3560 N·mm, depending on the method and stage of machining. At the same time, a clamping force of 2000 N was transmitted to the clamp from each of the screws.

Table 1. Contact pairs of improved fixtures for forks.

Contacts locating chart in the "fixture-workpiece" system

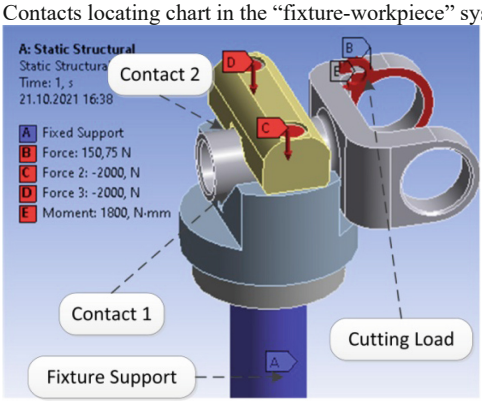

Parameters of implemented connection groups

Contact	Contact surfaces	Contacting surfaces	Coefficient of friction f [6]
1	the working surface of the prism / cylindrical surface of the fork shank	smooth/unmachined	0.2
2	the working surface of the clamp / cylindrical surface of the fork shank	corrugated/unmachined	0.7

4 Results and Discussion

Setting these boundary conditions allowed the implementation of the maximal naturality process simulation during the fixture static loading with forces and moments. The values of the maximum equivalent stresses according to the IV hypothesis of Mises's strength and maximum displacements of the elements of the "fixture-workpiece" system were obtained and compared with similar indicators of the fixture (Table 2).

The results of numerical simulating of the main steps of mechanical processing in the improved fixture showed that it is possible to achieve the required accuracy specified by the designer because the displacements, in this case, do not exceed the absolute permissible values, and the values along the coordinate axes. The static stresses during the application of the load in the improved fixture are also within the permissible limits according to the characteristics of the corresponding materials. Also, tensions and displacements in the improved fixture are minor compared to similar indicators [6]. From the nature of the stresses, it is clear that the most stressed element in the system is the workpiece, where the lugs are attached to the fork shank. The obtained positive simulation results allow experimental studies of the stress-strain state of the "fixture–workpiece" system to be conducted for an improved fixture.

Table 2. Comparison of the numerical simulation results of flexible fixture with incomplete location and improved fixture for Y-type forks.

Manufacturing step with a maximum loading	Maximum displacements of the fixture elements, mm				Admissible displacements, mm	Maximum stresses, MPa		Admissible stresses, MPa
	improved fixture		[6] (Fig. 3)					
	axial	total	axial	total		improved fixture	[21] (Fig. 3)	
Milling of the inner end face of the ear	0.019	0.022	0.019	0.024	0.1	385	396	600
Drilling of the hole (diameter 15.5 mm) in the backend	0.121	0.147	0.139	0.172	0.2	335	497	600
Drilling out of the hole (diameter 24.5 mm) in the ear	0.074	0.082	0.081	0.093	0.2	398	542	600

Experimental studies of the stress-strain state of the "fixture–workpiece" system act as an intermediate stage between numerical simulation and dynamic tests in the machining process. A static experiment is also necessary to verify the adequacy of the finite element analysis results by comparing them with the results of physical experiments for the improved fixture. The fixture for experimental studies was made according to the nominal dimensions, similar to the dimensions in the model (Fig. 3). As an experimental sample, a Y-type fork was taken from the cardan shaft of the RUTA 25 minibus, which the drawing with the main dimensions is shown in Fig. 4. Also, Fig. 5 presents an experimental sample of an improved fixture for Y-type forks.

For machining Y-type forks.

Static experimental studies involved the application of loads to the places of the machined surfaces of the part and the measurement of displacements at the point of application of the load. It was realized by creating an experimental setup (Fig. 6) for fixing the fixture and applying loads based on the milling machine model 676P.

In the photo of the experimental setup (Fig. 6), the improved fixture 1 was fixed in the three-jaw chuck 2, which, in turn, was installed on the machine table. The force acting on the workpiece was applied through the mandrel installed in machine spindle 3. Also, mandrels 4 were alternately installed in each of the fork lugs to locate the mechanical dynamometer 5. The dynamometer of the Mohr & FEDERHAFF MANNHEIM is a tared spring clip, the stiffness of which is known to be 6 N/μm. The dynamometer is equipped with a watch-type indicator of the MIG1 GOST 9696–82 model, the scale interval of which is 1 μm. The displacement of the device elements was recorded using

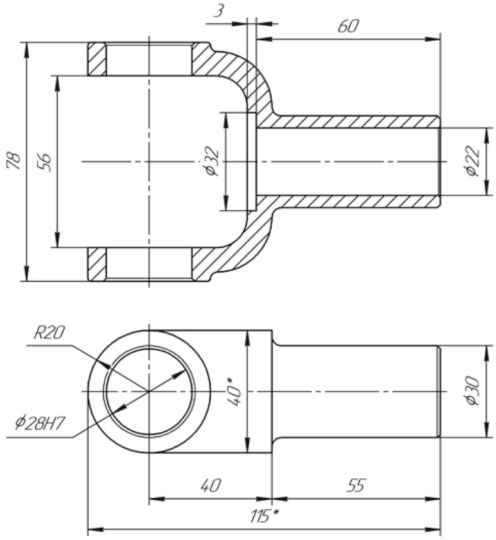

Fig. 4. Drawing by Y-type fork of the RUTA 25 minibus.

Fig. 5. An experimental sample of an improved fixture with an incomplete locating

indicator 6, also of the MIG1 GOST 9696–82 model, which is installed in the indicator stand on the machine table and contacts its measuring surface with the end face of the head, which is opposite to the end face to which the force is applied. The loads' values corresponded to those set during the numerical simulation.

As a result of experimental studies, we obtained the ten values of displacements at each of the studied stages of mechanical processing (Fig. 7). We determined the arithmetic mean values of displacements. These values are summarized in Table 3, and a numerical comparison of the corresponding values was performed. Absolute and relative deviations of experimental data and data obtained from numerical simulation were determined.

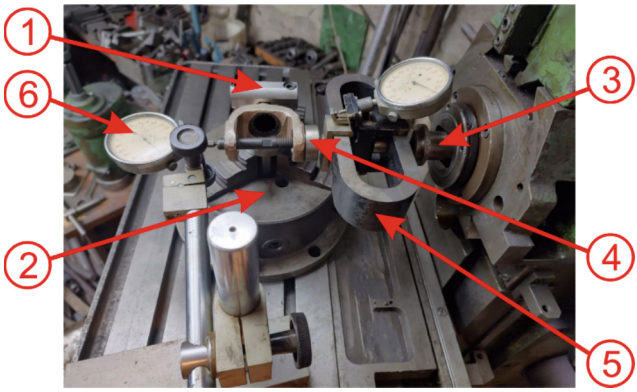

Fig. 6. Experimental setup for determining the displacements of the fixture elements for machining Y-type forks.

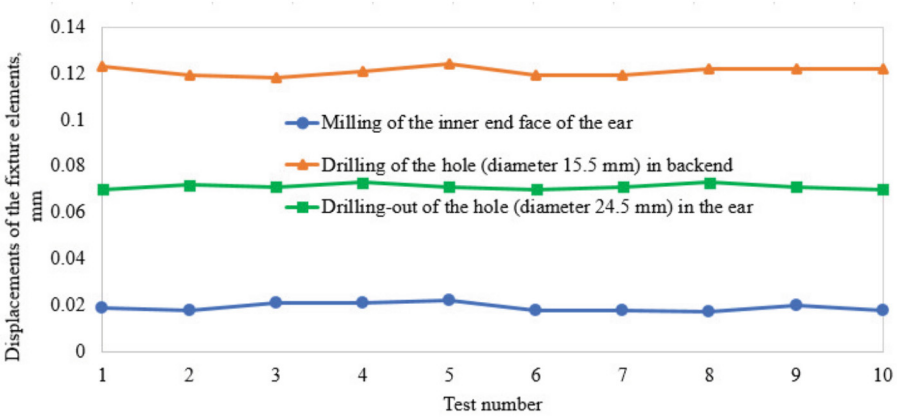

Fig. 7. The results of experimental tests for determining fixture displacements at stages.

The results presented in Table 3 show that the values of displacements obtained experimentally do not exceed the permissible values of these parameters, although they are higher than during numerical modeling in the range of 4.7…13.7%, depending on the machining stage. This can be explained by the natural conditions of the experiment and the errors that occur during the manufacture and measurements. However, in this case, the maximum relative error was less than 20%, despite the size of the margin to the permissible values of displacements being quite significant compared with the actual values of displacements at specific stages.

Based on numerical simulation of the magnitudes of stresses and displacements in the improved fixture, which was developed using the principles of incomplete location, it is theoretically proven that the stress values in the structural elements of the fixture do not exceed the allowable values according to the characteristics of the materials of the "fixture–workpiece" system. At the same time, the magnitude of the stresses is 27…32%

Table 3. Comparison of numerical simulation results of a flexible fixture with an incomplete location and an improved fixture for Y-Type forks.

Manufacturing step with a maximum loading	Maximum displacements of the improved fixture elements in the direction of the measuring axis, mm		Admissible displacements, mm	Value of the admissible margin of the displacements, mm	Absolute error, mm	Relative error, %
	for numerical simulation	for natural experiment				
Milling of the inner end face of the ear	0.019	0.022	0.1	0.078	0.003	13.7
Drilling of the hole in the backend	0.121	0.127	0.2	0.073	0.006	4.7
Drilling out of the hole in the ear	0.074	0.080	0.2	0.12	0.006	7.5

less than the values at the corresponding stages in the compared fixture, except for the step of milling the inner end face of the ear, where the stresses in the two fixtures are almost the same. This is because, at this machining stage, when the part is cantilevered in both fixtures, they are determined only by the stiffness of the workpiece itself but do not exceed the permissible values. It was also established that the values of the total displacements of the processed surfaces in the improved fixture, which was developed based on the previously investigated technical solution, do not exceed the tolerances on the machined surfaces and are 8…15% smaller than the corresponding values with the compared device. The values of displacements along the coordinate axes along which the load was applied also do not exceed the values allowed by the designer and are 9…13% smaller than the corresponding indicators with the compared fixture.

From the experimental results, it can be seen that the design of the improved fixture for machining Y-type forks can provide the necessary accuracy of machining under static load because the magnitudes of displacements are even more significant than during numerical simulation by 3…6 μm which in relative terms is 4.7…13.7% depending on the stage of machining, but do not exceed the permissible values.

As for the comparison with the works of other authors in this area, in particular, in the article [23], the authors developed and researched a locating and clamping fixture that allows changing the position of the clamping elements depending on the deformation at the clamping point. This made it possible to minimize the impact of clamping forces on the workpiece by 12%. Still, in this work, the static deformations of the "fixture–workpiece" system as a whole under the influence of loads that will occur during machining were not investigated.

In the study [24], the authors developed an adaptive fixture for fixing thin-walled casings and a system for controlling cutting modes depending on the deformation of the workpiece. Thus, it allowed for reduced deformations in the machining zone. However, in this work, the fixture's design is rather complicated and bulky, and at the same time, the tool accessibility is limited. However, the results of this study will be used during future studies of fixtures in dynamic mode.

The research [25] is focused on modeling contact stresses between the surfaces of the workpiece and the fixture and experimental measurements of Coulomb friction. However, a rigid parallelepiped was chosen as the studied workpiece, which cannot describe all types of interaction between the workpiece and the fixture elements, and only deformations due to clamping forces generated by the clamping device were determined, in turn, deformations caused by loads during machining were not considered. Also, the research results correspond to the main statements of the scientific study [26], which focused on the cutting forces simulation during the end milling.

Based on the results of theoretical and experimental studies, it was established that the proposed scientific approach of the fixture design with incomplete locating and ensuring the necessary stable position by clamping forces allows obtaining the specified machining accuracy. It proves the correctness of the research hypothesis [6] that fixtures with incomplete locating can ensure the specified accuracy of machining, and this article is a logical continuation of previous research in this area and confirms this hypothesis experimentally.

5 Conclusions

Numerical simulation methods have theoretically proven that fixtures with incomplete locating for Y-type forks provide sufficient machining accuracy, and the "bottleneck" at certain stages of processing with this type of locating is the stiffness of the cantilever part of the workpiece because the magnitude of stresses at the stage of milling the inner end face of the lug in of the compared fixtures are almost the same. At other stages, the stresses in the improved fixture are 27…32% lower, making it possible to proportionally intensify the machining modes at these stages when using the improved fixture.

It was established that the value of the allowable margin for displacements at individual stages varies from 0.073 mm to 0.12 mm, which will allow the calculation of the maximum permissible error of machining and bring it to acceptable limits by selecting appropriate technological methods.

For the first time, it was experimentally proven that the proposed design of the improved fixture for machining Y-type forks can provide the necessary machining accuracy under static load because the displacements do not exceed the permissible values. However, they are more extensive than during numerical simulation, in the worst case, by 13.7%. It allows consideration of the prospects of introducing fixtures with incomplete locations for machining in one step for other parts of a complex shape, for example, brackets, rockers, etc.

It has been experimentally proven that a scientific approach to the fixture design with incomplete location allows you to obtain the specified machining accuracy while ensuring the necessary stable position exclusively by clamping forces.

Further research will focus on the experimental determination of fixtures' accuracy and stiffness characteristics for machining Y-type forks in dynamic mode during the machining process.

Acknowledgment. The research was partially supported by the Polish National Agency for Academic Exchange within the project "Digitalization in mechanical engineering" (agreement no. BNI-UE-2023–2), The NAWA Ulam Programme (grant number BPN/ULM/2022/1/00045), EU NextGenerationEU through the Recovery and Resilience Plan for Slovakia under the project No. 09I03–03-V01–00094, International Association for Technological Development and Innovations, Research and Educational Center for Industrial Engineering (Sumy State University), and Ministry of Education and Science of Ukraine (State Reg. No. 0122U200875).

References

1. Haidabrus, B., Protsenko, S., Rosenberger, P., Grabis, J.: Data analysis of readiness programs of machine-building enterprises. In: Ivanov, V., Trojanowska, J., Pavlenko, I., Zajac, J., Peraković, D. (eds.) DSMIE 2020. LNME, pp. 128–136. Springer, Cham (2020). https://doi.org/10.1007/978-3-030-50794-7_13
2. Hys, K.: ISO 9001 standard management system certification – data analysis for sectors by country. QPI **1**, 162–169 (2019). https://doi.org/10.2478/cqpi-2019-0022
3. Haidabrus, B., Druzhinin, E., Elg, M., Jason, M., Grabis, J.: Programs to boost IT-readiness of the machine building enterprises. In: Ivanov, V., Trojanowska, J., Machado, J., Liaposhchenko, O., Zajac, J., Pavlenko, I., Edl, M., Perakovic, D. (eds.) DSMIE 2019. LNME, pp. 75–84. Springer, Cham (2020). https://doi.org/10.1007/978-3-030-22365-6_8
4. Pohudina, O., Morikova, A., Haidabrus, B., Kiyko, S., Druzhinin, E.: Comparison of metoheuristic search methods for the task of choosing a rational set of measures to risks' Respond. In: Nechyporuk, M., Pavlikov, V., Kritskiy, D. (eds.) ICTM 2020. LNNS, vol. 188, pp. 657–666. Springer, Cham (2021). https://doi.org/10.1007/978-3-030-66717-7_56
5. Cevhanova, V., Perevertaylo, T.: Competitiveness of machine building products: realities and opportunities. Mod. Econ. **14**, 279–284 (2019). https://doi.org/10.31521/modecon.V14(2019)-43
6. Ivanov, V., Dehtiarov, I., Evtuhov, A., Pavlenko, I., Ruban, A.: Multiaxis machining of fork-type parts: fixture design and numerical simulation. In: Karabegović, I. (ed.) NT 2021. LNNS, vol. 233, pp. 142–152. Springer, Cham (2021). https://doi.org/10.1007/978-3-030-75275-0_17
7. History behind the universal joint. https://www.machineservice.com/products/universal-joints/history-behind-the-universal-joint/. Accessed 20 Nov 2023
8. Bharti, S.K., Samantaray, A.K.: Resonant capture and sommerfeld effect due to torsional vibrations in a double cardan joint driveline. Commun. Nonlinear Sci. Numer. Simul. **97**, 105728 (2021). https://doi.org/10.1016/j.cnsns.2021.105728
9. Cardoso, A.S.M., et al.: Fatigue resistance performance of universal cardan joint for automotive application. Eng. Fail. Anal. **135**, 106128 (2022). https://doi.org/10.1016/j.engfailanal.2022.106128
10. Hu, Y., Tan, A.C., Liang, C., Li, Y.: Failure analysis of fractured motor bolts in high-speed train due to cardan shaft misalignment. Eng. Fail. Anal. **122**, 105246 (2021). https://doi.org/10.1016/j.engfailanal.2021.105246

11. Zheng, Z., Lin, J., Hu, Y., Zhou, Q., Yi, C.: Dynamic unbalance identification and quantitative diagnosis of cardan shaft in high-speed train based on improved TQWT-RBFNN-NSGA-II method. Eng. Fail. Anal. **136**, 06226 (2022). https://doi.org/10.1016/j.engfailanal.2022.106226
12. Kuo, C., Wu, Y.: Perfect static balancing using cardan-gear spring mechanisms. Mech. Mach. Theory **181**, 105229 (2023). https://doi.org/10.1016/j.mechmachtheory.2023.105229
13. Avrigean, E., Pascu, A.M., Oleksik, V.S.: Study of the cardan cross using the experimental and analytical method. Procedia Eng. **100**, 499–504 (2015). https://doi.org/10.1016/j.proeng.2015.01.396
14. Zhang, L., Wang, X., Zhang, D., Qian, J., Wang, S.: Mechanism for wrapping fiber around the Y fork. Compos. Struct. **275**, 114480 (2021). https://doi.org/10.1016/j.compstruct.2021.114480
15. Singh, U., Yadav, P.K., Vidya, S., Srikanth, K.S.: Finite element analysis of vehicle compo-site propeller shaft. Mater. Today Proc. **56**(1), 395–399 (2022). https://doi.org/10.1016/j.matpr.2022.01.228
16. Kaya, N., Karen, I., Öztürk, F.: Re-design of a failed clutch fork using topology and shape optimisation by the response surface method. Mater. Des. **31**(6), 3008–3014 (2010). https://doi.org/10.1016/j.matdes.2010.01.002
17. Pavlenko, I., et al.: Using regression analysis for automated material selection in smart manufacturing. Mathematics **10**(11), 1888 (2022). https://doi.org/10.3390/math10111888
18. Ivchenko, O., et al.: Method for an effective selection of tools and cutting conditions during precise turning of non-alloy quality steel C45. Materials **15**(2), 505 (2022). https://doi.org/10.3390/ma15020505
19. Corrado, A., Polini, W.: Tolerance analysis tools for fixture design: a comparison. Procedia CIRP **92**, 112–117 (2020). https://doi.org/10.1016/j.procir.2020.05.174
20. Ivanov, V., Dehtiarov, I., Zaloga, V., Kosov, I., Savchuk, V.: Increasing productivity of connecting rods machining. In: Ivanov, V., Trojanowska, J., Pavlenko, I., Zajac, J., Peraković, D. (eds.) DSMIE 2020. LNME, pp. 264–275. Springer, Cham (2020). https://doi.org/10.1007/978-3-030-50794-7_26
21. Fritzsche, R., Voigt, E., Schaffrath, R., Todtermuschke, M., Röber, M.: Automated design of product-flexible car body fixtures with software-supported part alignment using particle swarm optimization. Procedia CIRP **88**, 157–162 (2020). https://doi.org/10.1016/j.procir.2020.05.028
22. Kamble, V.D., Mathew, A.T.: Brief review of methodologies for creation of cohesive fixture design. Mater. Today Proc. **22**(4), 3353–3363 (2020). https://doi.org/10.1016/j.matpr.2020.04.285
23. Gonzalo, O., et al.: A method to minimize the workpiece deformation using a concept of intelligent fixture. Robot. Comput. Integr. Manuf. **48**, 209–218 (2017). https://doi.org/10.1016/j.rcim.2017.04.005
24. Chai, S., Ouyang, L., Bi, Q., Yu, J., Zhang, Y.: An adaptive fixture for suppress vibrations and measuring workpiece deformation of thin-walled casings. Procedia CIRP **101**, 322–325 (2021). https://doi.org/10.1016/j.procir.2020.05.269
25. Feng, Q., Maier, W., Braun, S., Möhring, H.C.: Dynamic modeling of the workpiece-fixture contact behavior for intelligent fixture design. Procedia CIRP **119**, 58–65 (2023). https://doi.org/10.1016/j.procir.2023.02.126
26. Petrakov, Y.V., Ohrimenko, O.A., Sikailo, M.O., Myhovych, A.V.: Cutting forces simulation for end milling. J. Eng. Sci. **10**(2), A27–A33 (2023). https://doi.org/10.21272/jes.2023.10(2).a4

Surface Hardness Improvement of AISI D2 Tool Steel by Laser Transformation Hardening Process Using High-Power Disk Laser

Vitaliy Dzhemelinskyi[1], Matej Hruska[2], Bohdan Mordyuk[3,4], Daniel Grochala[5], and Dmytro Lesyk[1,3,6(✉)]

[1] National Technical University of Ukraine "Igor Sikorsky Kyiv Polytechnic Institute", 37, Prospect Beresteiskyi, Kyiv 03056, Ukraine
lesyk_d@ukr.net
[2] University of West Bohemia, 2732/8, Univerzitní, 30100 Pilsen, Czech Republic
[3] G.V. Kurdyumov Institute for Metal Physics of the NAS of Ukraine, 36, Academician Vernadsky Boulevard, Kyiv 03142, Ukraine
[4] E.O. Paton Electric Welding Institute of the NAS of Ukraine, 11, Kazymyr Malevych Street, Kyiv 03150, Ukraine
[5] West Pomeranian University of Technology, 17, Al. Piastów, 70-310 Szczecin, Poland
[6] University of the Basque Country, 1, Plaza Ingeniero Torres Quevedo, 48013 Bilbao, Spain

Abstract. The remote laser phase transformation hardening process is an effective and fast self-quenching method of surface modification to provide a uniform hardening depth over the treated surface. To enhance the surface integrity of the AISI D2 tool steel, a robot-assisted laser hardening process using a high-power disc laser was applied in this work. Using a constant power strategy, the D2 steel flat specimens were selectively processed by a laser phase transformation hardening technique. The effects of laser power and scan speed on the surface roughness, hardness, and hardening intensity were studied. The scan speed from 9 to 15 mm/s and laser power from 1050 to 2550 W were selected to estimate the influence of the related effective parameters on surface hardness improvements. The results indicated that the hardness HV values in the subsurface layer achieved 550–670 HV by the optimized laser heat treatment parameters.

Keywords: Advanced Technology · Remote Laser Surface Hardening · High-Power Disc Laser · Robot-Assisted 3D Scanning · AISI D2 Tool Steel

1 Introduction

Paying attention to the need for modernization of existing production processes to selectively enhance the properties of operations of metal products and developing new surface modification techniques is an urgent issue in mechanical engineering for critical applications. The performance of critical metal parts largely depends on the quality/integrity of their surfaces. Conventional technologies for surface treatment often need to satisfy the required industrial conditions fully. Much attention is now being paid to the research

© The Author(s), under exclusive license to Springer Nature Switzerland AG 2024
V. Ivanov et al. (Eds.): DSMIE 2024, LNME, pp. 178–187, 2024.
https://doi.org/10.1007/978-3-031-61797-3_15

of advanced manufacturing techniques for surface finishing/hardening using highly concentrated energy sources. This work aims to assess the influence of a robot-assisted laser hardening method on the surface integrity of high-alloy steel.

2 Literature Review

Currently, both the development and improvement of surface modification methods are urgent tasks in manufacturing processes to enhance the surface integrity of metal products. Improving the surface morphology parameters and physical-mechanical properties in the subsurface increases resistance to wear and corrosion. Additionally, the fatigue strength of the modified surfaces of the parts is increased.

Currently, AISI D2 steel material contains high alloying elements, which is cold work die steel that is commonly applied in industrial applications, such as stamping tools and forming tools that require high reliability and hardenability [1]. It is well-known that AISI D2 tool steel has good protection against oxidation and wear at elevated temperatures owing to its high chromium content [2]. However, the high chromium content needs to be increased to ensure corrosion resistance of this steel because a significant part of the chromium is included in alloy carbides [3].

Various surface modification treatments were proposed to improve the surface quality and operational characteristics of the AISI D2 tool steel using an advanced thermochemical surface hardening process, such as electrochemical boriding [4], gas nitriding [5], plasma/ion nitriding [6], plasma nitriding followed by post-oxidation [7] or pack siliconizing followed by plasma nitriding [8]. Kim et al. [4] found that the borided D2 steel specimens provided the average thickness of boride layers of ~ 60 μm (hardness is ~ 1700 HV) at 950 °C after a boriding time of 60 min. Compared to the most common conventional pack boriding process (~9 h to obtain 45 μm thick layers), the process duration was significantly reduced by the electrochemical boriding method. Sista et al. [5] revealed that the average hardness of the nitrided D2 steel achieved ~ 1250 HV at 520 °C and the nitriding potential below 5 $atm^{-1/2}$. Díaz-Guillén et al. [7] analyzed the impact of the plasma nitriding combined with the oxidation on corrosion performance. They concluded that the surface microhardness values of the nitrided layers are increased (~1400 HV) by plasma nitriding at 470 °C, but then slightly reduced with the final oxidation treatment (~1250 HV) due to the iron oxides formation. Nevertheless, the plasma nitriding treatment leads to an essential increase in the roughness of the treated surface parts, which is not undesirable for responsible components, including stamping/forming tools [9].

Another solution for improving the hardness and roughness of the die steels is the application of mechanical surface treatments using a mono-pin ultrasonic tool [10] or a multi-pin ultrasonic tool [11]. This technology increases the surface hardness due to the nanocrystalline modification of the near-surface layers without a change in chemical compositions. The surface hardness increased to about 15% after mono-pin ultrasonic treatment, providing a hardening depth of 150 μm and compressive residual stress of ~ 800 MPa in the subsurface layer [10]. The surface roughness magnitudes can be ranged from 0.1 to 0.4 μm [11]. Given the favorable stress state and surface quality/nanostructure, the hardness of the AISI D2 high-alloy steel is insufficient.

One of the effective methods of surface treatment of steel parts is a remote laser phase transformation hardening process, which significantly enlarges the hardness in the subsurface layer [12] and has a negligible effect on the surface texture [13]. The laser phase transformation hardening of steels consists of the formation of an austenitic microstructure during high-speed heating and its subsequent transformation to a fine martensitic microstructure during cooling by absorbing and transferring the high-concentration energy to a thin surface layer [14]. The hardened near-surface layer consists of martensite and carbide precipitates. It should also be noted that the environmentally friendly laser hardening process can be applied locally to treat surfaces and induce homogenous hardness to a depth of 0.2–2 mm in contrast to thermo-chemical surface hardening processes. The influence of laser treatment parameters on the structural and phase composition, hardening depth, and operation properties of the steels processed by the high-power CO_2 [15], diode [16], and fiber [17] lasers is studied and compared in detail. In particular, Tobar et al. [15] obtained the hardened surface layer of ~ 0.3 mm depth and hardness of ~ 500 HV by the CO_2 laser. Advanced laser hardening systems using a diode laser (rectangular beam shape) or fiber laser in combination with scanning optics resulted in an essential improvement in the hardness (> 650 HV) [16], generating compressive residual stress on the surface [18]. The laser transformation hardening in a controlled atmosphere leads to a higher surface hardness value [16]. At the same time, studying the effects of the laser heat treatment parameters using a high-power disk laser on the surface properties of the D2 high-chromium steel is relevant today. Wear-resistant D2/D3 steels are one of the most common types of air-hardening materials designed to manufacture dies, stamps, and other tools that must have high strength to withstand high loads and not deform when working with metal. Therefore, during the manufacture of forming dies from D2/D3 steel, it is necessary to develop a new method of surface hardening and finishing to improve the quality of the working surfaces of the forming dies.

In this study, the AISI D2 tool steel parts were locally treated by a robot-assisted 3D scanning laser hardening system to improve surface integrity. This work aims to study the influence of laser phase transformation hardening using a disc laser and scanning optics on the surface hardness, strengthening intensity, and roughness of high-carbon and high-chromium tool steel.

3 Research Methodology

The high-alloy tool steel with an average carbon content of ~ 1.5%, chromium content of ~ 12%, and molybdenum content of ~ 0.8% was selected in this research. The nominal chemical composition of the AISI D2 tool steel in weight percent is listed in Table 1.

Table 1. Chemical composition of AISI D2 steel (% by a mass fraction).

Chemical element	C	Cr	Mo	V	Mn	Si	Fe
ASTM standard	1.55	11.8	0.8	0.8	0.4	0.3	Balance

The initial surface hardness of the specimens was ~ 229 HV_5. The studied specimens were polished before experiments on the laser surface hardening (the initial surface roughness *Ra* parameter was ~ 0.55 μm).

The flat specimens with the dimensions of 100 mm × 400 mm × 15 mm were subjected to single-passes laser heat treatment (LHT) using a Fanuc M 710iC robot-assisted 3D scanning laser hardening system with a Trudisk 8002 solid state disk laser and SCANLAB intelliWELD 30 FC V scanning optics (Fig. 1).

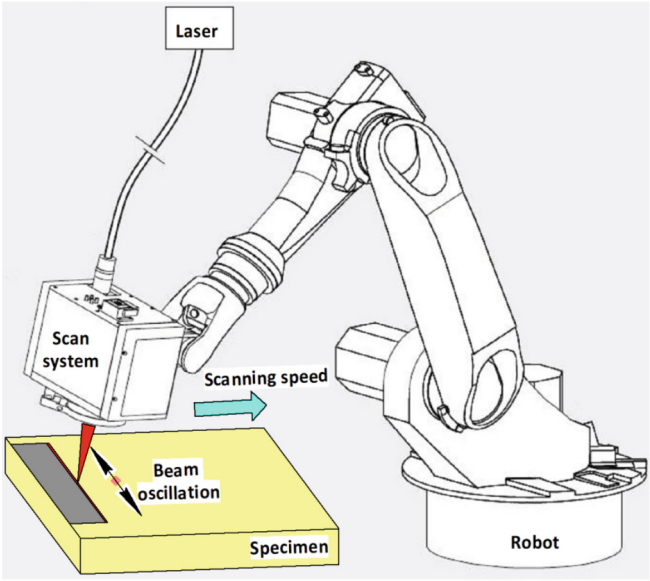

Fig. 1. Robot-assisted laser hardening process.

A 5 kW multi-mode Yb:YAG continuous-wave disk laser of 1030 nm with a laser spot size of 10 mm × 0.8 mm (width x length) was applied to laser treat processing of the studied die steel. The maximum laser power can be achieved at 8 kW on the working surface with a specified cooling. The laser was connected to the scanner with a 200 μm fiber, providing a maximum laser beam deflection speed of 21.5 m/s. The laser power from 1050 to 2550 W, scan speed from 9 to 15 mm/s, and scan velocity (beam oscillation) from 15000 to 20000 mm/s were used in the study (Table 2). The LHT tests were carried out using the RobotSyncUnit software, while the laser scanning parameters were implemented by the SAMLight software.

The laser-hardened surfaces were analyzed using a Hommelwerke T2000 contact profilometer. The averaged surface roughness parameters within a sampling length of 0.8 mm were defined by the standard ISO 4287–97. Each laser selectively hardened area was estimated at least three times.

The surface hardness was measured using a LV700AT macro-Vickers hardness tester with a load on the indenter of 5 kgf for a holding time of 15 s. In all cases, a total number of about 5 measurements were implemented at various areas in the center of the laser passes.

Table 2. Laser processing parameters.

No. LHT test	Power (W)	Scan speed (mm/s)	Scan velocity (mm/s)	Laser beam spot size (mm^2)
LHT1	1050	11	20000	10 × 0.8
LHT2	1350	9	15000	10 × 0.8
LHT3	1350	11	20000	10 × 0.8
LHT4	1350	15	20000	10 × 0.8
LHT5	1950	9	15000	10 × 0.8
LHT6	1950	11	20000	10 × 0.8
LHT7	1950	15	20000	10 × 0.8
LHT8	2250	11	20000	10 × 0.8
LHT9	2550	9	15000	10 × 0.8
LHT10	2550	11	20000	10 × 0.8
LHT11	2550	15	20000	10 × 0.8

The strengthening intensity was evaluated by the HRC hardness magnitudes of the unprocessed and laser-hardened specimens using such as an expression $I_{\text{hard}} = (\text{HRC}_{\text{LHT}} - \text{HRC}_{\text{in}})/\text{HRC}_{\text{in}} \cdot 100\%$.

4 Results and Discussion

4.1 Surface Hardness

The hardness in the hardened area depends on the amount of laser energy density (processing speed (mm/s) and laser power (W)). The surface hardness experiments show that the surface hardening of the selected steel does not occur sufficiently (HV ~ 230) at the laser power of 1050 W / 1350 W and scan speed of 9–15 mm/s (LHT1–LHT4). The laser power is further increased, which increases the hardness of the hardened near-surface layer but to a different extent (Figs. 2 and 3).

The surface hardness values are dramatically increased at the LHT6 (Fig. 2) and LHT11 (Fig. 3) modes. The effects of laser power (1050–2550 kW) at constant scanning speed (11 mm/s) on the HV values of the LHT-processed D2 steel is presented in Fig. 3. The results show that the highest hardness can be achieved at the laser power of 1950 W and scan velocity of 11 mm/s (LHT6 mode). A further increase in laser power leads to a decrease in surface hardness. The surface hardness ranges between 434 HV and 557 HV at 2550 W.

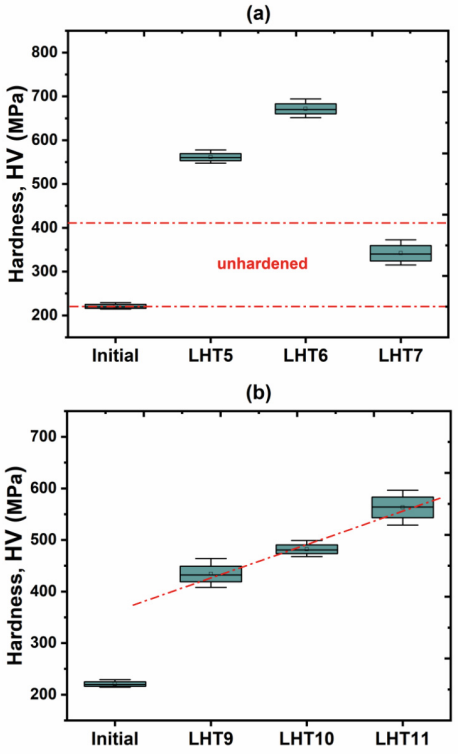

Fig. 2. Values of the surface hardness of the AISI D2 steel specimens processed by LHT at the laser power of 1950 W (a) and 2550 W (b).

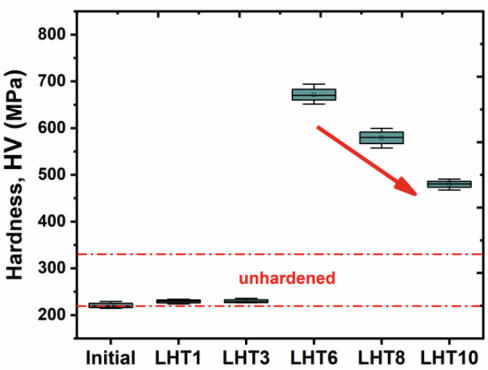

Fig. 3. Change in surface hardness depending on laser power and scanning speed of the LHT-processed AISI D2 steel.

In comparison with the unhardened specimens (~229 HV), the surface hardness is respectively increased by about 2 times, 2.5 times, and 3 times after the LHT10, LHT8/LHT11, and LHT6 modes. The increase in hardness is associated with a phase transformation that occurs due to rapid heating followed by rapid cooling. The structure of the hardened D2 steel consists of the fine-grained martensite and residual austenite with the dispersed many fine secondary carbides (Cr2.5Fe4.3Mo0.1)C3 and some primary carbides (Cr,Fe)7C3 on the grains boundaries in the subsurface layer while the fine ferrite-carbide structure is formed in the lower layer [11, 13]. A similar study showed that grain size and carbon content values fluctuated in the heat-affected zone [19]. As a result, the selective LHT-induced phase transformation hardening of the surface is defined by the solid solution/grain-boundary and dislocation/dispersion strengthening mechanisms. In particular, laser hardening of the tool steel due to dislocation density in martensite structure contributes to the higher yield strength and softening resistance for a longer time [20].

4.2 Hardening Intensity

The extent of the hardening intensity induced by different LHT parameters can be illustrated in Fig. 4. In the previous section. It was found that the LHT1–LHT4 modes are ineffective for surface hardening of the high-alloy steel. Among other LHT modes applied, a smaller extent of the hardening intensity increase (Ihard. = 78.5%) is observed in the case of the LHT7 test (P = 1950 W, S = 15 mm/s). In comparison, the highest extent of the hardening intensity increase (Ihard. = 232.3%) is found after the LHT6 test (P = 1950 W, S = 11 mm/s). The strengthening intensity magnitudes are presented in Fig. 4.

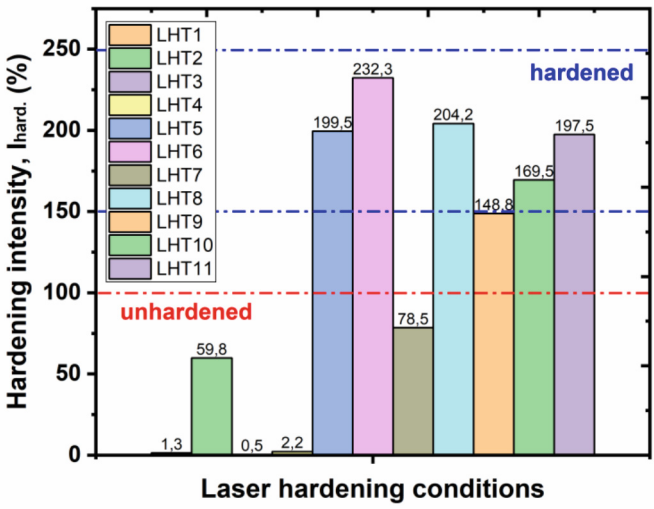

Fig. 4. Effects of laser hardening conditions on the hardening intensity of AISI D2 steel.

Considering the extent of hardening intensity, the LHT5, LHT6, and LHT8–LHT11 modes may be selected for the surface hardening of the die steels. Nevertheless, the required mode of laser processing should be selected considering the change in the surface roughness values addressed in the following section.

4.3 Surface Roughness

The surface roughness values of the laser-hardened AISI D2 steel specimens are shown in Fig. 5. The average surface roughness magnitudes of the laser transformationally hardened specimens are varied to different extents as compared to the initial parts (Ra = ~ 0.55 μm). The surface roughness parameters after the LHT1–4, LHT7, and LHT10 conditions are close to the unprocessed surface. The surface roughness parameters may be slightly changed/increased due to the formation of the oxide layer (Fe_2O_3) due to the lack of protective gas. The results obtained correlated with the previous works [11, 16].

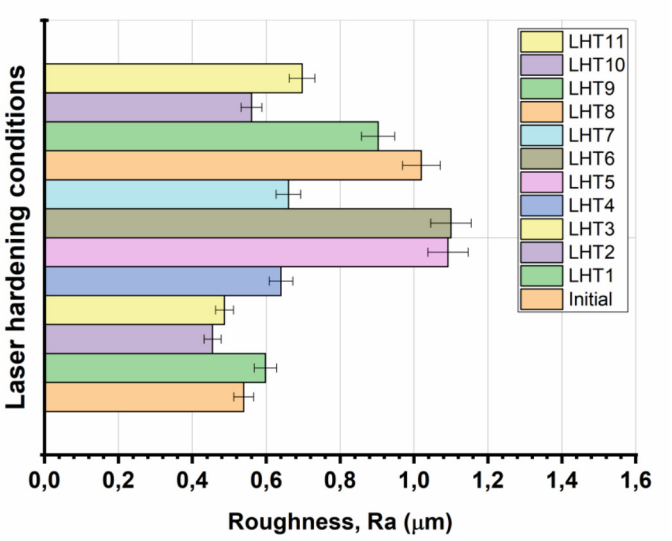

Fig. 5. Surface roughness of the unhardened and LHT-hardened AISI D2 steel specimens.

It should also be noted that the LHT treatment under the following LHT5/LHT6 and LHT8/LHT9 laser hardening conditions resulted in a significant increase in the surface roughness parameters due to the increasing of the amount of heat input (6.4–8.5 J/mm^2). In particular, the roughness *Ra* parameter was increased by ~ 50% after LHT5, LHT6, and LHT8 as compared to the untreated state. At the same time, a partial melting of micro-irregularities of the surface profile can be expected. Therefore, the 3D surface texture analysis should be performed to identify the surfaces with a partial melting that is undesirable for surface hardening of the responsible components, affecting tolerances.

Considering the obtained magnitudes of the surface hardness (strengthening intensity) and roughness, the defined LHT10 and LHT 11 modes may be used for the surface

hardening of AISI D2 tool steel by the high-power disk laser. The surface hardness of 480–550 HV is achieved using the proposed LHT modes. Today, the width of the laser spot can be enlarged up to 10 cm using high-power disk lasers, avoiding a softened area in the overlap section. Schuöcker et al. [21] used a disc laser with a laser power of 6 kW, generating the laser-hardened tracks with a width of 20 mm and depth of 3 mm and providing the surface hardness (~58 HRC) without melting at the edges. As a result, the laser heat treatment technology using high-power disk lasers can be effectively applied for surface hardening of large-sized steel products, including tool and die-making equipment.

5 Conclusions

The advanced laser surface hardening technique was applied in this research to increase the surface hardness of high-alloy steel. The following conclusions can be drawn.

Compared to the unprocessed specimens (~229 HV), HV values are increased by about 2 times, 2.5 times, and 3 times after the LHT10, LHT8/LHT11, and LHT6 modes, respectively. The smaller extent of the hardening intensity increase is observed in the case of the LHT7 test ($P = 1950$ W, $S = 15$ mm/s), while the highest extent of the hardening intensity increase is identified after the LHT6 test ($P = 1950$ W, $S = 11$ mm/s).

A significant increase in the average surface roughness values was found after the laser power increase and the scan velocity decrease (LHT5/LHT6 and LHT8/LHT9). Therefore, it is recommended to use the LHT10 and LHT 11 modes (2550 W and scan speed of 11–15 mm/s) for the laser heat treatment by the laser spot of 10×0.8 mm and scan speed of 15000–20000 mm/s, providing the surface hardness of 480–550 HV.

The study of the surface morphology using a laser profilometer on the one hand, as well as near-surface microstructure and X-ray diffraction analysis, microhardness distribution, and corrosion performance of the disk, laser-treated D2 tool steel, on the other hand, is planned for further study.

Acknowledgements. The authors acknowledge the Ministry of Education, Youth and Sports of the Czech Republic and the Ministry of Education and Science of Ukraine (agreement No. 0121U113829 and 0122U002389) and the Ulam NAWA program (Grant Number BPN/ULM/2021/1/00153) for their support. The research was also partially supported by the International Association for Technological Development and Innovations (IATDI).

References

1. Mallick, R., et al.: Performance characteristics of hardened AISI D2 steel turning: a review. Mater. Today Proc. **26**, 2685–2690 (2020). https://doi.org/10.1016/j.matpr.2020.02.565
2. Kumar, S., et al.: Parametric optimization and wear analysis of AISI D2 steel components. Mater. Today Proc. (2023). https://doi.org/10.1016/j.matpr.2023.01.247[Inpress]
3. Mochtar, M.A., et al.: Effect of tempering temperature and subzero treatment on microstructures, retained austenite, and hardness of AISI D2 tool steel. Mater. Res. Express **10**, 056511 (2023). https://doi.org/10.1088/2053-1591/acd61b

4. Sista, V., et al.: Electrochemical boriding and characterization of AISI D2 tool steel. Thin Solid Films **520**, 1582–1588 (2011). https://doi.org/10.1016/j.tsf.2011.07.057
5. Kim, K.-H., et al.: Microstructure and fracture toughness of nitrided D2 steels using potential-controlled nitriding. Metals **12**, 139 (2022). https://doi.org/10.3390/met12010139
6. Cho, K.T., et al.: Enhanced surface hardening of AISI D2 steel by atomic attrition during ion nitriding. Surf. Coat. Tech. **251**, 115–121 (2014). https://doi.org/10.1016/j.surfcoat.2014.04.011
7. Díaz-Guillén, J.C., et al.: Duplex plasma treatment of AISI D2 tool steel by combining plasma nitriding (with and without white layer) and post-oxidation. Surf. Coat. Tech. **385**, 125420 (2020). https://doi.org/10.1016/j.surfcoat.2020.125420
8. Najafizadeh, M., et al.: Characterization of tribological and mechanical properties of the Si3N4 coating fabricated by duplex surface treatment of pack siliconizing and plasma nitriding on AISI D2 tool steel. Metall. Mater. Trans. A **52**, 4753–4766 (2021). https://doi.org/10.1007/s11661-021-06410-6
9. Singh, G.P., et al.: Effect of surface roughness on the properties of the layer formed on AISI 304 stainless steel after plasma nitriding. Surf. Coat. Tech. **200**, 5807–5811 (2006). https://doi.org/10.1016/j.surfcoat.2005.08.149
10. Pyun, Y., et al.: Development of D2 tool steel trimming knives with nanoscale microstructure. AISTech 2005 Proc. **2**, 465–475 (2005)
11. Lesyk, D., Martinez, S., Mordyuk, B., Dzhemelinskyi, V., Danyleiko, O.: Effects of the combined laser-ultrasonic surface hardening induced microstructure and phase state on mechanical properties of AISI D2 tool steel. In: Ivanov, V., Trojanowska, J., Machado, J., Liaposhchenko, O., Zajac, J., Pavlenko, I., Edl, M., Perakovic, D. (eds.) DSMIE 2019. LNME, pp. 188–198. Springer, Cham (2020). https://doi.org/10.1007/978-3-030-22365-6_19
12. El-Batahgy, A.-M., et al.: Laser surface hardening of tool steels – experimental and numerical analysis. Surf. Coat. Tech. **3**, 146–153 (2013). https://doi.org/10.4236/jsemat.2013.32019
13. Liu, Z., et al.: A comparative study on surface topography and microhardness of laser polished-hardened AISI D2 tool steel. J. Adv. Manuf. Technol. **122**, 499–512 (2022). https://doi.org/10.1007/s00170-022-09361-3
14. Karmakar, D.P., et al.: Effect of tempering on laser remelted AISI H13 tool steel. Surf. Coat. Tech. **361**, 136–149 (2019). https://doi.org/10.1016/j.surfcoat.2019.01.022
15. Tobar, M.J., et al.: Laser transformation hardening of a tool steel: Simulation-based parameter optimization and experimental results. Surf. Coat. Tech. **22–23**, 6362–6367 (2006). https://doi.org/10.1016/j.surfcoat.2005.11.067
16. Muthukumaran, G., Babu, P.D.: Laser transformation hardening of various steel grades using different laser types. J. Braz. Soc. Mech. Sci. Eng. **43**, 103 (2021). https://doi.org/10.1007/s40430-021-02854-4
17. Lesyk, D., Martinez, S., Mordyuk, B., Dzhemelinskyi, V., Lamikiz, A.: Wear characteristics of carbon and tool steels hardened by combined laser-ultrasonic surface treatment. In: Ivanov, V., Trojanowska, J., Pavlenko, I., Zajac, J., Peraković, D. (eds.) DSMIE 2021. LNME, pp. 62–72. Springer, Cham (2021). https://doi.org/10.1007/978-3-030-77719-7_7
18. Frerichs, F., et al.: Process signature for laser hardening. Metals **11**, 465 (2021). https://doi.org/10.3390/met11030465
19. Lu, Y., et al.: Influence of multi-pass laser hardening of normalized AISI 4140 on the grain size. Surf. Coat. Tech. **421**, 127434 (2021). https://doi.org/10.1016/j.surfcoat.2021.127434
20. Telasang, G., et al.: Structure–property correlation in laser surface treated AISI H13 tool steel for improved mechanical properties. Mater. Sci. Eng. A **599**, 255–267 (2014). https://doi.org/10.1016/j.msea.2014.01.083
21. Schuocker, D., et al.: Improved laser hardening process with temperature control avoiding surface degradation. In: Proceedings of the Materials of the 8th International Conference on Photonic Technology, LANE 2014, p. 210969709 (2014)

Ensuring Tool Run-In When Milling AISI321 Steel in Various Technological Environments

Eshreb Dzhemilov[1], Alper Uysal[2], Orhan Çakir[2], Ruslan Dzhemalyadinov[1(✉)], and Eldar Vaniev[1]

[1] Crimean Engineering and Pedagogical University named after Fevzi Yakubov, Simferopol 295015, Ukraine
rus.dzhemalyadino@gmail.com
[2] Yildiz Technical University, Beşiktaş, 34349 Istanbul, Turkey

Abstract. The article shows the results of various process fluids used in production and alternative environmentally friendly options on the durability of cutting tools during the milling process. In addition, the influence of the running-in process on the wear resistance of the cutting tool was taken into account. Considering the process of cylindrical milling with counter feed, dependencies were obtained based on the analysis of the horizontal component of the cutting force to find optimal running-in conditions. The article aims to evaluate the conditions for tool break-in when lubricating and cooling liquids of various compositions are supplied to the cutting zone to ensure tool durability. The task of constructing mathematical models of power characteristics Ph for various running-in conditions was formulated to establish a functional relationship between the variable and horizontal cutting force for various running-in conditions. The influence of coolant on the strengthening and formation of wear-resistant structures has been established, providing an almost 4-fold reduction in the wear rate of the tool concerning predetermined structures formed in the air. It is shown that the running-in of a cutting tool depends on the environment in which it occurs. Based on the data analysis, practical recommendations were determined for the selection of compositions of cutting fluids and running-in modes for specific milling conditions when processing AISI 321 stainless steel with subsequent transition to production cutting modes.

Keywords: Run-In · Tool Wear · Milling · Technological Environments · Stainless Steel · Process Innovation

1 Introduction

The use of technological media during machining is one way to increase the tool's efficiency when cutting various materials. Technological fluids are used during cutting to reduce the cutting tool's wear rate, improve the machined surface's quality, and increase labor productivity. This goal is achieved through the complex influence of physical and chemical effects accompanying the cutting fluids, consisting of many parallel processes concentrated on the contact surfaces of the tool in the chip formation zone.

© The Author(s), under exclusive license to Springer Nature Switzerland AG 2024
V. Ivanov et al. (Eds.): DSMIE 2024, LNME, pp. 188–199, 2024.
https://doi.org/10.1007/978-3-031-61797-3_16

The influence of cutting oil on the cutting process is mainly determined by the properties of the processed and tool materials, the nature and method of supplying the lubricating-cooling technological environment, the cutting regimes, the type of processing, and the constructive and geometric parameters of the cutting tool.

In this connection, the problem arises of determining the running-in regimes at which reinforced secondary structures are formed on the tool's working surfaces using different media.

2 Literature Review

Tool life has a significant impact on the productivity of the machining process. Despite numerous studies, increasing tool life is a fundamental manufacturing goal. Solving problems to achieve this goal mainly involves reducing wear on tool surfaces during cutting. One of the most common methods for reducing the coefficient of friction, thermal load in the cutting zone, adhesive, and abrasive wear is using various lubricating and cooling technological media. The authors in [1] examined the effect of naphthenic and tall oil on the end mill's durability and the machined surface's quality when machining an aluminum alloy.

To improve processing conditions, fluid compositions can be modified with various additives. Work [2] shows the effect of the activation of process fluid compositions by carbon nanotubes during the turning of stainless steel. Such additives help reduce cutting forces and wear of the cutting tool. In [3], in addition to the positive effect of activation by carbon nanotubes, the authors note the contribution of finely dispersed aluminum oxide additives during the milling of the AA6082 aluminum alloy. Coconut oil was used as the primary technological medium. The results of the experiments presented in article [4] show a change in the thermophysical and tribological properties of process fluids, including plant-based ones, due to the introduction of graphene sheets into the composition. During the milling process, a decrease in the coefficient of friction and tool wear is observed. In [5], the authors proposed a composition of a cutting fluid based on boric acid, ethylene glycol, and silver nanoparticles for milling aluminum alloy AA7075-T6. At the same time, depending on the composition of the suspension, a decrease in cutting forces and roughness of the resulting surface and a significant increase in tool life were observed [6].

The authors are also actively exploring the issue of finding alternative, environmentally friendly technological environments [7]. Katna et al. showed the effect of non-edible oils such as karanja and castor oil on tool durability and surface quality. It has been shown that such oils reduce tool wear by up to 20% compared to petroleum oils [8]. In [9], the authors propose a single-point milling method for machining difficult-to-cut Inconel 718 alloy to evaluate cutting fluids of different chemical reactivity. D'Amato et al. studied Jatropha vegetable oil as a water emulsion base for milling AA2030 aluminum alloy and AISI 1050 carbon steel [10]. There was a positive effect on cooling the working area, reducing cutting forces and the height of microroughness compared to dry processing and in a mineral oil-based emulsion environment [11].

Also, one of the ways to increase durability can be pre-treatment of the tool, which changes the surface structure of the tool. Most often, this is achieved by applying wear-resistant coatings [12]. Another method is to run-in the tool. The essence of the method

is to create conditions on the tool surface to change the morphology of the surface layer at the initial stages of tool operation.

3 Research Methodology

The measurement of the cutting force P_z when milling with cylindrical cutters with a given angle of incidence of the cutting edges and the geometry of their cutting parts, depending on the processing conditions, is characterized by the resultant P_{xz}. The resulting P_{xz} is distributed into components: horizontal P_h (feed resistance force) and vertical P_v.

This article discusses the process of up-milling. Considering that, in this case, the horizontal force $P_h = (1.1 \ldots 1.2)\, P_z$ significantly exceeds the vertical force $P_v = (0.1 \ldots 0.25)\, P_{xz}$, we choose the horizontal force P_h as the modeling parameter.

The experiments were carried out to construct a matrix of experimental data for constructing models based on them in the form of dependences of P_h on running-in modes using various technological environments. For this purpose, a workpiece blank was used (Fig. 1), on the surface of which grooves were cut to form ledges.

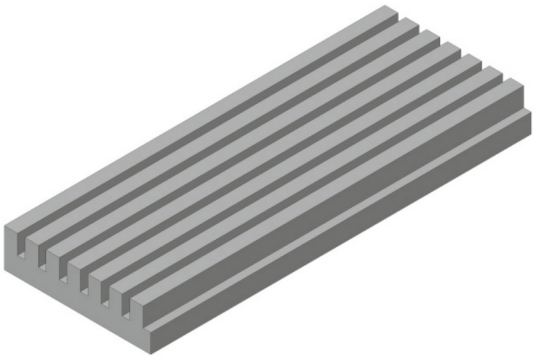

Fig. 1. Workpiece blank.

For down milling, all-disk cutters made of high-speed steel with a diameter of 100 mm with multi-directional teeth ($Z = 14$) were used, the design and geometric parameters of which are shown in Fig. 2. Only two teeth of the cutter took part in cutting (2nd and 8th). The remaining teeth were underestimated to Ø95mm.

A computer complex was used to measure the cutting forces. It consisted of a force-measuring sensor, an interface unit with a personal computer, and an analog converter. The complex used special programs to work with the interface block and measurement results files.

A two-tooth disc-milling cutter, mounted on a mandrel in the spindle of the horizontal head of the machine 6B75VF1, alternately processed the ledges on the workpiece with the specified run-in conditions. The cutting oil was fed with the help of the Noga "Minicool" device, which was intended to implement the minimum lubrication technique.

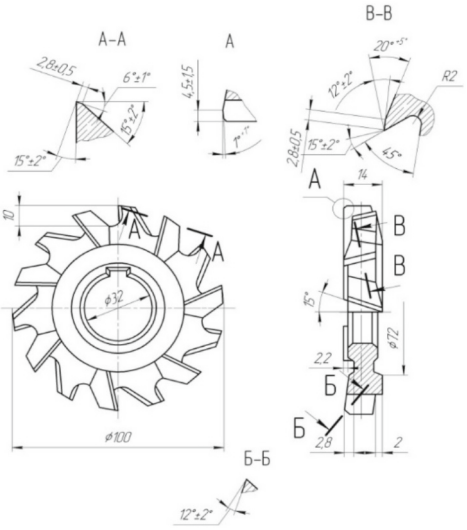

Fig. 2. Design and geometric parameters of the milling cutter.

During the processing of each ledge, the horizontal force P_h and the tool wear face were measured using the MBS-1 microscope mounted on the table.

The problem of constructing mathematical models of the power characteristics of P_h for various run-in conditions can be formulated as the problem of establishing a functional connection between the variables and the horizontal cutting forces (parameters) for different run-in conditions.

The parameters under study are random variables that depend on many factors of the functioning of the technological system, which cannot be taken into account even in an experiment conducted in the laboratory. Therefore, in simulation, each of the output parameters is described by the mathematical expectation of the parameter under consideration, considering the selected scale space.

Each of the vectors, at each stage of model building, includes variables:

$$\overline{X} = \|x_1, x_2, ..., x_n\| \tag{1}$$

$$\ln\overline{X} = \|\ln x_1, \ln x_2, ...\ln x_n\| \tag{2}$$

Thus, the problem of model synthesis using the regression analysis [13] was reduced to constructing the following function:

$$M\left(\ln Y/\overline{X}, \ln\overline{X}\right) = F\left(\ln Y/\overline{X}, \ln\overline{X}, \overline{\Theta}\right) \tag{3}$$

where $M\left(\ln Y/\overline{X}, \ln\overline{X}\right)$ mathematical expectation of the average value for the values of controlled variables in a given range from the change;

$F\left(\ln Y/\overline{X}, \ln\overline{X}\right)$ unknown in form and structure operator (functional connection);

$\Theta = \|\Theta_0, \Theta_1,\ldots,\Theta_n\|$ unknown vector of estimated parameters;

The parameter under study is the horizontal component of the resulting cutting force $P_h(H) - y$.

As the variables, the run-in speed.

The limits of change are indicated in Table 1:

Table 1. Limits of change in variable factors.

Limits of change in variable factors	Variables		
	Run-in speed Vr, $^{m}/_{min.}$ (x_i)	Feed Sz, $^{mm}/_{tooth}$ (x_2)	Depth of cut t, mm (x_3)
Lower	12	0.1	0.4
Higher	18	0.3	2.0

18 experiments were performed to obtain the models (3 parallel experiments in each). As a result of the simulation, the following dependences of the horizontal force on the run-in conditions in the medium of different technological media were obtained (Table 2).

Table 2. $P_h = f(V_r, S_z, t_r)$.

Process environment	Type of addiction
Without cutting oil	$\ln P_h(t) = 5.5 - 5.8 \cdot 10^4 \ln t \cdot \ln S_z + 3.06 \cdot S \ln S_z \ln t - 5.65 \cdot 10^{-3} Vt \ln t \ln S_z - 3.56 \cdot 10^{-1} \ln V_r + 2.38 \cdot 10^{-2} (\ln S)^3 \ln t$
Rape oil	$\ln P_h(t) = 3.82 - 4.3 \cdot 10^{-1} t \ln t - 4.41 \cdot 10^{-1} \ln S_z \cdot t \ln t + 1.69 \cdot 10^{-1} \ln V$
MR-99 (Shell Garia 402 F-15)	$\ln P_h(t) = 4.1 + 2.74 \cdot 10^{-2} \ln t \cdot V_r + 7.1 S_z^2 + 2.58 \cdot 10^{-1} \ln t^2$
Castor oil	$\ln P_h(t) = 3.98 + 3.63 S_z \cdot t - 5.47 \cdot 10^{-2} \cdot S_z \cdot V_r$
I-20 (Mobil DTE Oil 24)	$\ln P_h(t) = 4.28 + 1.38t + 1.42 \cdot 10^{-1} \ln S_z \cdot \ln V_r + 3.96 \cdot 10^{-2} S_z$

Analysis of the obtained models for P_h shows that the feed per tooth significantly influences the horizontal force for each cutting oil within the selected limits of the variable variation.

To determine rational running-in modes by considering the loading of contact surfaces, we will determine the influence of cutting modes on the horizontal component of the cutting force. In Fig. 3, graphical dependences of the horizontal component of the cutting force, constructed using models (Table 2), on the running-in speed Vr, feed per tooth Sz, and depth of cut t mm are shown.

From the graphical dependencies, it follows that the type of technological environment affects the value of the horizontal component of the cutting forces differently for different combinations of cutting conditions.

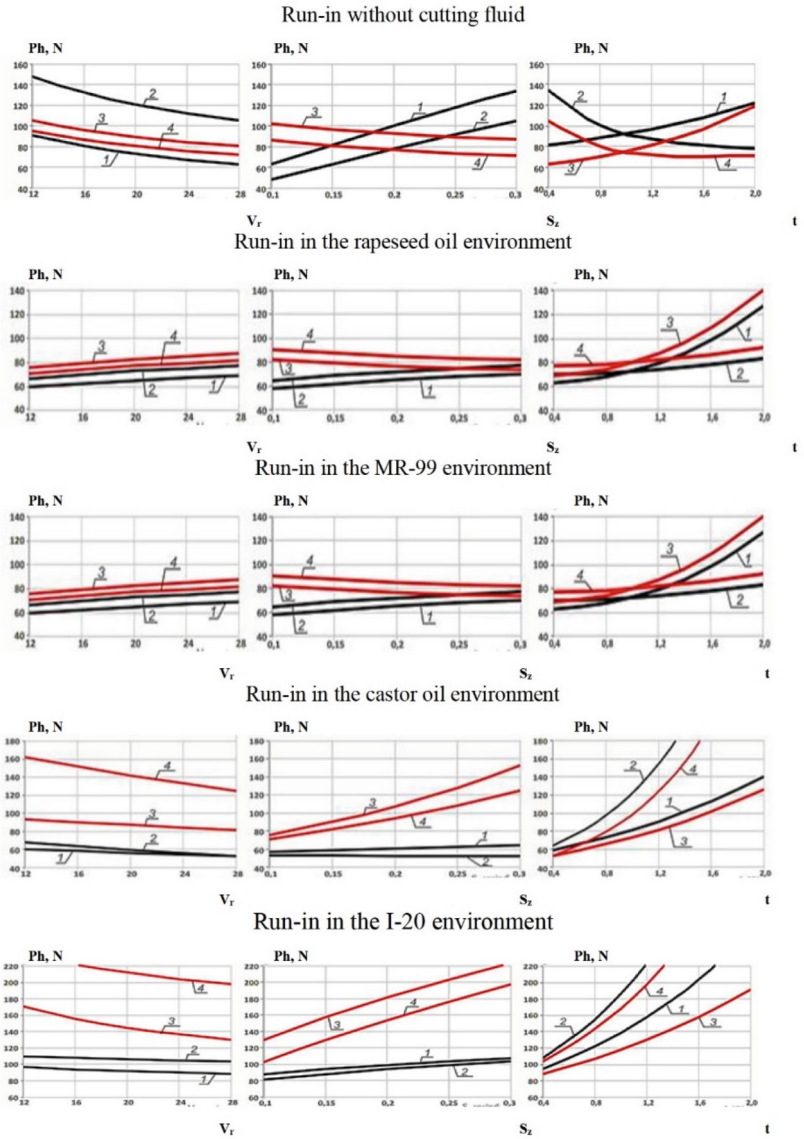

Fig. 3. The influence of the running-in regimes on the value of the horizontal component of the cutting force.

Note that the preliminary run-in, regardless of the technological environment used, was carried out at the exact value of the running-in rate. In addition, run-in was carried out at feed and depth values corresponding to dry processing. At the same time, the results of the simulation show that, depending on the technological environment, the exact values

of the run-in modes have different effects on the force that indirectly determines the level of contact stresses and, consequently, the wear rate.

4 Results and Discussion

Considering that under the same run-in regimes, their influence on the horizontal component P_h depends on the technological environment, let us consider how this affects the resistance of cutting by the attached tool. This makes it possible to determine the run-in modes, which ensure the lowest intensity of tool wear in the temperature range of 200–400 °C.

Milling of AISI321 steel was carried out in the environment of various cutting fluids and during dry cutting. When cutting with a standard tool (without preliminary running-in) at production cutting conditions (speed Vz = 40 m/min, feed Sz = 0.3 mm/tooth and depth t = 1.2 mm), in the absence of cutting fluid, tool life was T = 41 min. The criterion for performance was the wear of the rear surface of the tool by the value of lr = 0.3 mm.

In this paper, to determine the influence of the running-in regimes on resistance, the following operating modes were adopted:

- V_r = 12 m/min; 16 m/min and 28 m/min.
- S_z = 0.1 mm/tooth; t = 0.4 mm (1)
- S_z = 0.1 mm/tooth; t = 0.6 mm (2)
- S_z = 0.15 mm/tooth; t = 0.4 mm (3)
- S_z = 0.15 mm/tooth; t = 0.6 mm (4)

Run-in in these modes was carried out until wear on the rear surface l_r = 0.08 mm, after which milling continued in production cutting modes. Run-in modes allow you to stay within the required temperature range (200–400 °C), and the time required for run-in in various environments ranges from 5 to 10 min.

Figure 4 (a, b, c) shows the effect of tool running-in modes without coolant on tool life (T).

Considering the process of milling steel AISI321T with a pre-processed high-speed steel tool without coolant (Fig. 4), it can be noted that the run-in speed and higher feed speed have a minor influence on the range of operating modes.

The tool life varies slightly when changing speed from 12 m/min to 28 m/min in modes 1 and 2. When the feed increases to $S_z > 0.15$ mm/tooth (regardless of the change in the depth of cut in the range under study), tool life decreases by 25%.

Thus, to achieve the maximum value of tool life and maintain processing performance, tool running-in without coolant should be carried out at a speed of V_r = 28 m/min and a feed of 0.1 mm/tooth.

Comparing the influence of the run-in modes in the rapeseed oil environment (Fig. 5, a, b, c) with running-in without cutting fluid, it is clear that they have the same character.

Run-in in the rapeseed oil media, as compared with milling without coolants while increasing the running speed from 12 m/min to 28 m/min, reduces tool life by 10%. The tool life is also reduced at run-in with feeding Sz > 0.15 mm/tooth.

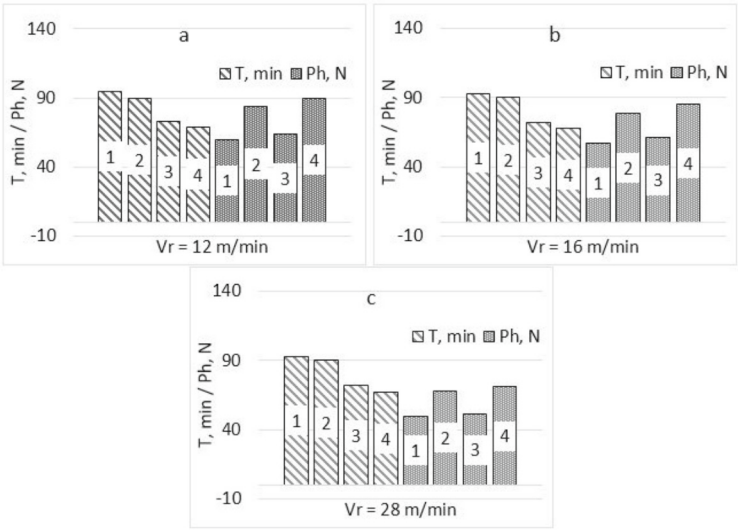

Fig. 4. Effect of run-in modes without cutting fluids.

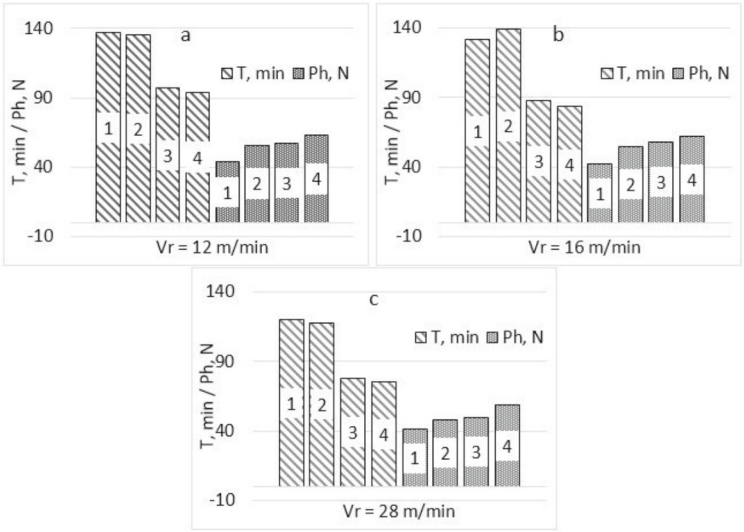

Fig. 5. Effect of run-in modes in the rapeseed oil environment.

As can be seen from Fig. 6, the bedding tool during milling AISI 321 steel at a rate of 40m/min in the MR-99 cutting fluid in the test mode between the run-in practically does not increase tool life in comparison with the run-in without coolant.

It is found that among castor oil, the most extensive tool life observed run-in at maximum speed (Vr = 28 m/min) and minimum values from consideration, S_z = 0.1 mm/tooth and t = 0.4 mm (Fig. 7 a, b, c).

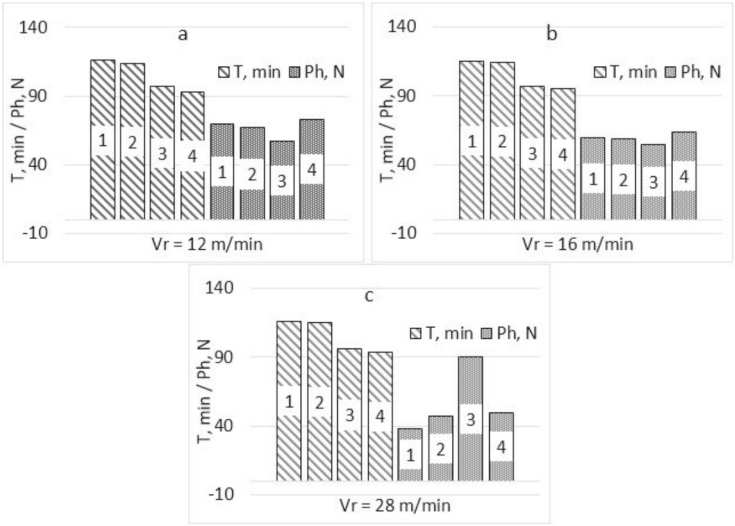

Fig. 6. Effect of run-in modes in the MR-99 cutting fluid environment.

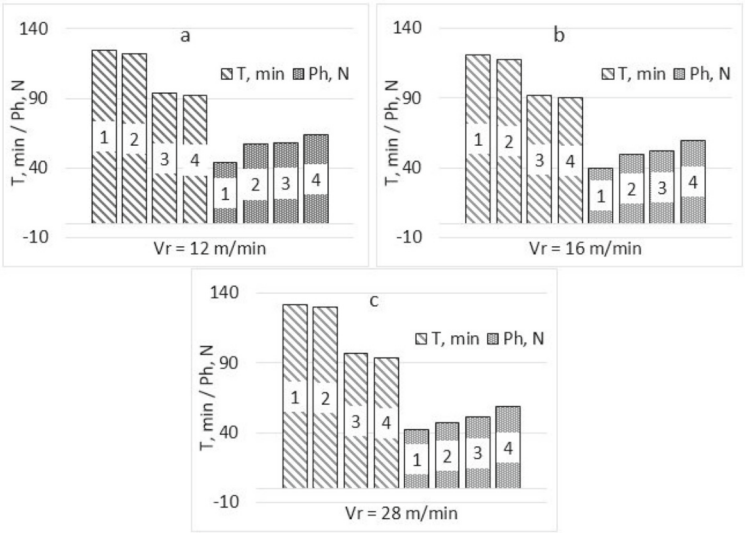

Fig. 7. Effect of run-in modes in the castor oil environment.

Increasing the running-in speed from 12 m/min to 28 m/min reduces the tool life, regardless of the values of S_z and t, in the investigated range of their variation, almost 2 times.

A similar picture is observed with an increase in Sz. In comparison with run-in without cutting oil, run-in in the presence of I-20 increases the resistance by 80% (Fig. 8).

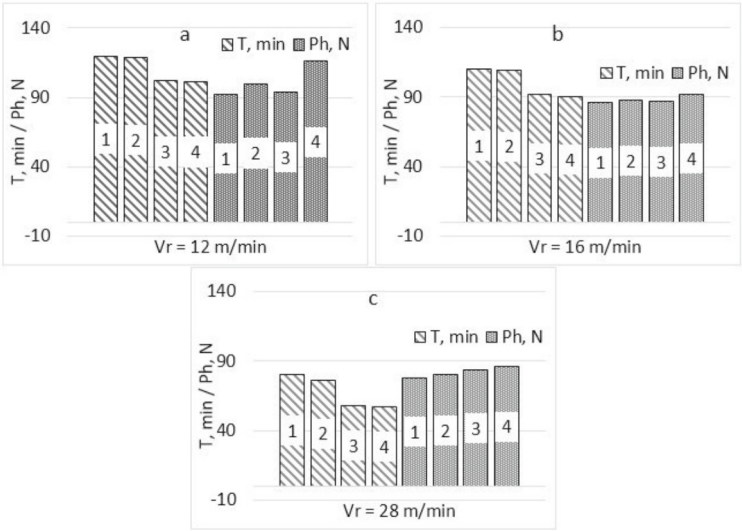

Fig. 8. Effect of run-in modes in the I-20 oil environment.

According to the results of the analysis of the tool life of the tool during milling of AISI 321 steel at a speed of V = 40 m/min, it was established that the run-in modes ensuring maximum resistance depend on the technological environment.

So, the recommended run-in modes in different environments will be:

– without cutting oil - $V_r = 12 \div 28$ m/min; $S_z = 0.1$ mm/tooth; t = 0.4–0.6 mm;
– in rape oil medium - $V_r = 12 \div 28$ m/min; $S_z = 0.1$ mm/tooth; t = 0.4–0.6 mm;
– in the MR-99 cutting fluid - $V_r = 12 \div 28$ m/min; $S_z = 0.1$ mm/tooth; t = 0.4–0.6 mm;
– in castor oil medium - $V_r = 28$ m/min; $S_z = 0.1$ mm/tooth; t = 0,4 mm;
– in the medium I-20 - $V_r = 12$ m/min; $S_z = 0.1$ mm/tooth; t = 0.4–0.6 mm.

Along with studies of the effect of run-in regimes in various environments on the tool's durability, a change in the horizontal component of the cutting force corresponding to these running-in conditions was considered.

When working the tool without cutting oil, the same run-in regimes are recommended in the environment of vegetable oil and MR-99.

The optimum run-in conditions in the castor oil medium are characterized by the maximum running-in rate ($V_r = 28$ m/min) and the minimum value of S_z ($S_z = 0.1$ mm/tooth) and t (t = 0.4 mm). The decrease in the run-in rate and the increase in Sz and t led to a significant decrease in tool life. At the same time, an insignificant change in P_h is observed in the range of variation in the run-in regime under study. This is explained by the fact that the state of the contacting layers of the instrument with the tool being processed differs from other cutting oils by the presence of upper, loosened, and underlying more passivated, increased hardness. They carried out research asserting that tool run-in in the environment of castor oil is most effective at final milling operations.

The results indicate that running-in can be used to increase the performance of a cutting tool along with those already traditionally used, such as high-speed processing,

the use of various cutting fluids, etc. The disadvantage of this method is the need to ensure the tool's operation in running-in modes is up to specific wear values. These modes are lower than recommended, which reduces processing productivity. In addition, subsequent adjustment of the machine to stationary cutting modes is necessary after the completion of the running-in period.

Future research will focus on assessing the combined effects of tool run-in, cutting fluids, and tool coatings on cutting tool life.

5 Conclusions

In the I-20 medium, the tool is most effective at speed $V_r = 12$ m/min, with the same tooth feeds and cutting depths as the cutting without technological media, in rapeseed oil and MR-99. Thus, when using the I-20, the time for run-in increases in comparison with the use of other technological media by a factor of two, and the value of the horizontal component of the force P_h of the force also increases.

It is shown that regardless of the medium used at $S_z > 0.1$ mm/run-in tooth, the tool life is significantly reduced, and the depth of cutting (except castor oil) in the test range practically does not affect the resistance.

Based on the research carried out in this work, vegetable oil, which provides the most significant effect in increasing tool life, should be recommended as a cutting (hardening) medium when cutting AISI321 stainless steel.

References

1. Pang, S., et al.: Effect of cutting fluid on milled surface quality and tool life of aluminum alloy. Materials **16**, 2198 (2023). https://doi.org/10.3390/ma16062198
2. Touggui, Y., Uysal, A., Emiroglu, U., Dzhemilov, E., Belhadi, S.: Improvement of the MQL efficiency in machining stainless steel by adding nanoparticles to the cutting fluid. In: Tonkonogyi, V., Ivanov, V., Trojanowska, J., Oborskyi, G., Pavlenko, I. (eds.) Advanced Manufacturing Processes III. InterPartner 2021. LNME, pp. 219–228. Springer, Cham (2022). https://doi.org/10.1007/978-3-030-91327-4_22
3. Saminathan, V., Iqbal, M., Ghani, J.A.: A study on the effects of hybridized metal oxide and carbonaceous nano-cutting fluids in the end milling of AA6082 aluminum alloy. Lubricants **11**(2), 87 (2023). https://doi.org/10.3390/lubricants11020087
4. Baldin, V., et al.: Influence of graphene nanosheets on thermo-physical and tribological properties of sustainable cutting fluids for MQL application in machining processes. Lubricants **10**, 193 (2022). https://doi.org/10.3390/lubricants10080193
5. Kilincarslan, S.K., Cetin, M.H.: Improvement of the milling process performance by using cutting fluids prepared with nano-silver and boric acid. J. Manuf. Process. **56**, 707–717 (2020)
6. Petrakov, Y.V., Ohrimenko, O.A., Sikailo, M.O., Myhovych, A.V.: Cutting forces simulation for end milling. J. Eng. Sci. (Ukraine) **10**(2), A27–A33 (2023). https://doi.org/10.21272/jes.2023.10(2).a4
7. Deshpande, V., Jyothi, P.N.: A review on sustainable eco-friendly cutting fluids. **1**(2), 306–320 (2020)
8. Katna, R., Suhaib, M., Agrawal, N.: Performance of non-edible oils as cutting fluids for green manufacturing. Mater. Manuf. Process. **38**(12), 1531–1548 (2023). https://doi.org/10.1080/10426914.2022.2136388

9. Taylor, C.M., Secker, J., Sajid, S.A., Curtis, D., Liskiewicz, T., Khan, T.: Resource-efficient performance testing of metalworking fluids utilizing single-point milling. Tribol. Mater. Surf. Interfaces **17**(1), 34–47 (2023). https://doi.org/10.1080/17515831.2022.2142925
10. Ivchenko, O., et al.: Method for an effective selection of tools and cutting conditions during precise turning of non-alloy quality steel C45. Materials **15**(2), 505 (2022). https://doi.org/10.3390/ma15020505
11. D'Amato, R., Wang, C., Calvo, R., Valášek, P., Ruggiero, A.: Characterization of vegetable oil as cutting fluid. Procedia Manuf. **41**, 145–152 (2019). https://doi.org/10.1016/j.promfg.2019.07.040
12. Wurood, A.M., Haydar, Al-E., Shaimaa, J.K.: Surface modification of cutting tool by multilayer coatings a-review. In: 4th International Conference on Materials Engineering & Science: Insight on the Current Research in Materials Engineering and Science, p. 020093. AIP Conference Proceedings, Duhok (2022). https://doi.org/10.1063/5.0107996
13. Pavlenko, I., et al.: Using regression analysis for automated material selection in smart manufacturing. Mathematics **10**(11), 1888 (2022). https://doi.org/10.3390/math10111888

Empirical Data-Based Failure Rate Assessment Methodology for Metal-Cutting Tools

Mykhaylo Frolov(✉), Volodymyr Tsyganov, and Vasyl Solokha

National University "Zaporizhzhia Polytechnic", 64, Zhukovsky Street, Zaporizhzhia 69063, Ukraine
mfrolov@zp.edu.ua

Abstract. The type of distribution law and its parameters reflect the physical essence of the technical object failure. Simultaneously, the failure rate is the leading component of this process as it solely defines the type of distribution law. The paper analyzes the nature of the failure rate function in the context of research and assurance of technical object reliability. It was shown that several approaches exist to determine the failure rate based on empirical data. Still, assessment of these approaches from the point of view of their adequacy is absent. No attention was paid to analyzing distribution laws from the point of view of failure rates compliance with empirical data. A criterion based on the maximum likelihood method was proposed for evaluating the empirical failure rate compared with the one obtained based on the theoretical distribution laws. It was shown that the most plausible estimate of empirical failure rate can be obtained using the average number of operational objects in a specific time interval, compared to its theoretical value obtained based on theoretical distribution law as a function of the middle of the same interval. It was shown that the proposed criterion can be used as an additional argument when choosing a theoretical distribution law based on empirical data when the goodness-of-fit criteria do not allow for drawing an unambiguous conclusion. In this case, the correspondence of the theoretical distribution law to the physical processes causing the failure of the technical object will be ensured.

Keywords: Weibull Distribution · Gamma Distribution · Maximum Likelihood Method · Chi-squared Distribution · Industrial Growth

1 Introduction

One of the main indicators when modeling the reliability of technical objects is the failure rate $\lambda(t)$. It reflects the instantaneous probability of failure of time t, related to the number of objects in good condition. It predicts the number of object failures of time t from those that "survived" at that moment. In addition, any integral distribution law can be represented as an exponent of the failure rate function:

$$F(t) = 1 - exp\left(-\int_0^t \lambda(\tau)d\tau\right) \quad (1)$$

In the theory of reliability, different distribution laws are used to describe failures of technical objects [1], the choice of which is determined both by formal goodness-of-fit

© The Author(s), under exclusive license to Springer Nature Switzerland AG 2024
V. Ivanov et al. (Eds.): DSMIE 2024, LNME, pp. 200–211, 2024.
https://doi.org/10.1007/978-3-031-61797-3_17

criteria - for example, the Pierson Chi-squared criterion and the Kolmogorov-Smirnov type criterion and the physical interpretation of the laws [2], which is mainly due to the failure rate. Having considered some distribution laws that are most often used to describe the failures of metal-cutting tools and other technical objects, the following properties of the failure rate function are noted:

- The Normal distribution reflects failures when neither the technical object's element nor its operation conditions have a key influence on the failure of the object. In this case, the failure rate is always an increasing concave function. Therefore, the first and second derivative functions of the failure rate are always positive:
  $\lambda'(t) > 0; \lambda''(t) > 0;$
- Exponential distribution characterizes sudden failures when $\lambda(t) = const$ and, accordingly $\lambda'(t) = 0$
- Gamma distribution describes failures caused by accumulated damages and characterized by an increasing convex, constant, or decreasing concave function of failure rate. Thus, one of the following versions is possible:

  – $\lambda'(t) > 0\, \lambda''(t) < 0$
  – $\lambda'(t) = 0$
  – $\lambda'(t) < 0\, \lambda''(t) > 0$

- The Weibull distribution describes the most comprehensive range of failure causes and includes all the above options.

The nature of the failure intensity function uniquely determines the stage of the object's lifecycle, which is widely known as the bath-tub curve (Fig. 1).

- In the first wear-in stage, the failure rate function is decreasing and concave. Thus, $\lambda'(t) < 0; \lambda''(t) > 0$
- The second stage, or normal operation, is usually characterized by the constant value of the failure rate function. Nevertheless, it is only possible if the wear is not a reason for failure. It's not a usual case of metal-cutting tools and any technical object worn. If it happens, something is wrong with the object (cutting tool): operator's mistakes, poor condition of the machine and/or its accessories, low quality of the object itself with a considerable variation of vital properties. Therefore, it is assumed that the failure rate is an almost linear increasing function the more this corresponds to the classical regularity of tool wear - the Taylor curve.
- The third stage – wear-out, is characterized by a rapidly increasing failure. Thus, the failure rate curve will be increasing and concave:

  $\lambda'(t) > 0; \lambda''(t) > 0$

After summarizing those mentioned above, it is concluded that failures of metal cutting tools can be described as:

- On stage I - by Gamma or Weibull distributions;
- On stage II – by Weibull or Normal distributions;
- On stage III – by Weibull distribution.

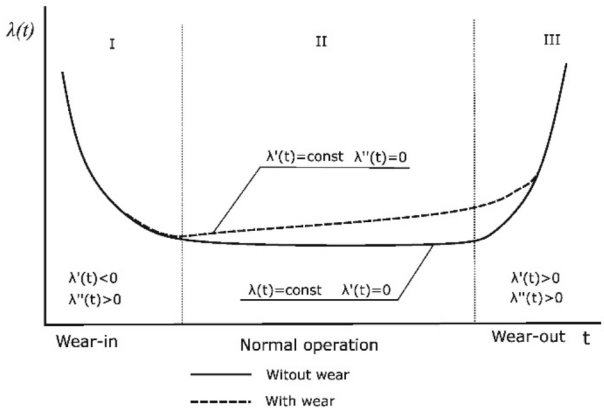

Fig. 1. Bath-tub curve of the object's life cycle.

As seen from the above, the Gamma and the Weibull distributions provide a variety of forms, which, as stated in [3], can be competing. The specified shapes are saved over the entire range of the definition area. Besides, the exponential distribution is a special case of both the Gamma and the Weibull distributions, and the Normal distribution in some cases, is close to that of Weibull [1]. Thus, under certain conditions, these distributions may be difficult to distinguish. Based on this, all three above distributions will be considered.

2 Literature Review

The above considerations relate to the theoretical distribution laws. The nature of the failure rate must be considered when choosing a theoretical distribution that describes object failures based on empirical data. This allows the physical processes that occur in the object and lead to its failure to be considered [2].

Based on the known theoretical integral and differential distribution laws – *F(t)* and *f(t)*, respectively, the theoretical failure rate is determined by the formula:

$$\tilde{\lambda}(t) = \frac{f(t)}{1 - F(t)} \tag{2}$$

Formula (2) determines the failure rate with a known theoretical distribution law. However, when the distribution law has not yet been established, and even more so if the agreement criteria specified above allow for multivariance and do not give an unequivocal answer about the type of distribution, the failure rate, estimated from empirical data, is the sole factor to make the decision. For this purpose, it is necessary to pay attention to one key point: the failure rate determined by Eq. (2) refers to a specific moment of time t, while sample data are defined for the time intervals Δt. Hence, the time within the above interval should be designated to compare theoretical and empirical values. Intervals appear because the range of sampling time until failure T is divided into k

equal intervals by one of the methods [4]:

$$\Delta t = \frac{T_{max} - T_{min}}{k} \tag{3}$$

In this case, the beginning of the *i-th* time interval is determined by:

$$t_i = T_{min} + \Delta t \cdot (i - 1) \tag{4}$$

To determine the boundaries of the intervals, i changes from *1* to $k + 1$. The existing approaches to the empirical assessment of the failure rate are as follows.

Typically, as indicated for instance, in [5], the number of products $\Delta m(t) = \Delta m_i$ that failed over the time interval Δt in the period from t_i *to* $t_i + \Delta t$ is estimated, and then the empirical evaluation of the failure rate is:

$$\hat{\lambda}(t) = \frac{\Delta m(t)}{N(t) \cdot \Delta t} \tag{5}$$

Here, *N(t)* is the number of products that are serviceable at the time t_i. Thus, the resulting estimate of the failure rate correlates with the time of the beginning of the interval $t = t_i$. In [6], an approach is demonstrated when the empirical estimation (5) correlates with the time t, which is inside the corresponding interval: $t_i < t \leq t_i + \Delta t$ but without indication of the exact one.

Another approach is demonstrated in [7]. The interval Δt is set not from time t_i, but symmetrically to the middle of the interval t_{mi}, i.e., from $t_{mi} - \Delta t/2$ to $t_{mi} + \Delta t/2$. Here:

$$t_{mi} = \frac{t_i + t_{i+1}}{2} = t_i + \frac{\Delta t}{2} \tag{6}$$

With this approach, the theoretical failure rate, its empirical assessment, and the number of serviceable products are correlated with the time of the middle of the interval. The form of Eq. (2) does not change, except that $t = t_{mi}$ and *N(t)* is now the average number of products that are serviceable in the interval *i* - N_{mi}:

$$N(t) = N_{mi} = \frac{N(t_i) + N(t_i + \Delta t)}{2} = \frac{N(t_i) + N(t_{i+1})}{2} \tag{7}$$

Taking into account that $\Delta m(t) = N(t_i) - N(t_{i+1})$, Eq. (6) and the above considerations, Eq. (5) can be rewritten in the following forms:

$$\hat{\lambda}(t) = \frac{N(t_i) - N(t_{i+1})}{N(t_i) \cdot \Delta t} \; for \; t = t_i \tag{8}$$

$$\hat{\lambda}(t) = \frac{2 \cdot \left[N(t_i) - N(t_{i+1})\right]}{\left[N(t_i) + N(t_{i+1})\right] \cdot \Delta t} for \, t = t_{mi} \tag{9}$$

At the same time, the lack of methods that analyze distribution laws from the failure rate point of view leads to the fact that distribution laws are often selected based on formal goodness-of-fit criteria. For example, lognormal distribution is sometimes used to describe failures of objects subject to wear and aging, like metal cutting tools [8], even though the failure rate of lognormal distribution decreases over time, which is impossible for this case.

Based on the foregoing, this work aims to propose a criterion for evaluating the above approaches and for empirical distribution analysis in the context of failure rate.

3 Research Methodology

The research methodology employed in this paper involves mathematical and statistical analysis based on elements of the reliability theory. The validity of the resulting relationships is assessed through the following approaches:

– Conducting simulation experiments that are widely used in engineering practice. In this experiment, a random sample of size N is generated to simulate the time until failure of a specific technical object or the tool life of a metal-cutting tool, denoted as "*ti*." The samples adhere to the Weibull and Gamma distribution laws, with shape and scale parameters α and β, respectively. The sample generation is carried out using the built-in functions of *Microsoft Excel*, respectively, for Gamma – Eq. (10) and Weibull – Eq. (11) distributions [1].

$$\langle t_i \rangle = GAMMA.INV((1 - RAND()); \langle \alpha \rangle; \langle \beta \rangle) \tag{10}$$

$$\langle t_i \rangle = \langle \beta \rangle * LN(RAND()) \wedge (1/\langle \alpha \rangle) \tag{11}$$

– Evaluating the outcomes from the established relationships by comparing them with the findings from comprehensive real-world, independent experiments focused on investigating metal-cutting tools' tool life and reliability.

4 Results and Discussion

4.1 Criterion for Evaluating Approaches to Empirical Failure Rate Assessment

The following facts should be considered to formulate a criterion for evaluating approaches to determining sample failure rate. Since the empirical failure rate is also a random value and it has its confidence interval and distribution f_λ, the approach that will provide the maximum probability of the failure rate theoretical values will be considered preferable. In other words, the above is the maximum likelihood criterion for the failure rate, which is graphically presented in Fig. 2.

Mathematically, following the maximum likelihood principle, this will be written:

$$L = \prod_{i=1}^{k} f_{\lambda i} \rightarrow max \tag{12}$$

To avoid the product and negative values, Eq. (10) is represented as a sum of logarithms:

$$L_f = -ln(L) = -\sum_{i=1}^{k} \ln(f_{\lambda i}) \rightarrow min \tag{13}$$

In Eqs. (12), and (13) f_λ is the failure rate distribution density determined for each of the intervals at the reference point *Pi* (see Fig. 2) corresponding to the value of the theoretical failure rate $\tilde{\lambda}(t)$.

In the papers [9, 10] concerning the Epstein method (B. Epstein), dependences on the distribution of the failure rate are given, mainly to determine its confidence interval, including that for the Weibull distribution, which significantly expands its scope and is

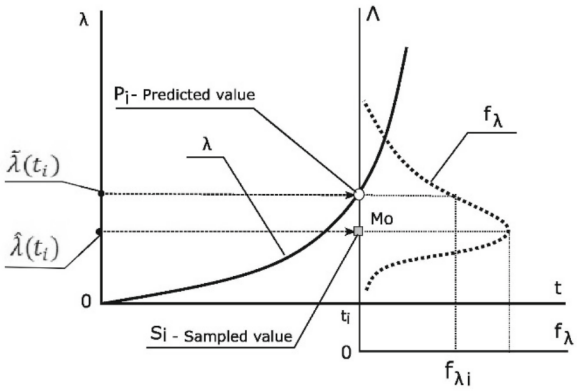

Fig. 2. Failure rate distribution.

extremely important for analyzing the reliability of a wide range of technical objects that are subjected to aging and wear processes.

In general terms, it is indicated that the variable Λ has the Pearson distribution χ^2 with the number of degrees of freedom ν:

$$\Lambda = 2 \cdot N(t) \cdot \Delta t \cdot \lambda(t) \tag{14}$$

$$\Lambda = \chi^2[\gamma, \nu] \tag{15}$$

where $\chi^2(\gamma, \nu)$ is the reciprocal of the left-handed Pearson Chi-squared distribution for the probability γ. Taking that $\lambda(t) = \lambda_\gamma(t)$- where the γ-quantile of the distribution, from (14) and (15), the confidence interval of the failure rate is determined [9]. Symbols "L" and "U" denote, respectively, its lower and upper limits:

$$\lambda_L(t) = \frac{\chi^2\left[\frac{1-\alpha}{2}, 2 \cdot \Delta m(t)\right]}{2 \cdot N(t) \cdot \Delta t} \tag{16}$$

$$\lambda_U(t) = \frac{\chi^2\left[\frac{1+\alpha}{2}, 2(\Delta m(t) + 1)\right]}{2 \cdot N(t) \cdot \Delta t} \tag{17}$$

Here α is the confidence factor. Thus, for example, at a confidence level of 0.9, the lower and upper limits of the confidence interval will be determined for probabilities γ of 0.05 and 0.95, respectively. In this case, the probability of the failure rate falling into the range from $\lambda_L(t)$ to $\lambda_U(t)$ and will be equal to α [9]:

$$Pr[\lambda_L(t) \le \lambda(t) \le \lambda_U(t)] = \alpha \tag{18}$$

The distribution density for each of the k intervals i will be determined:

$$f_{\lambda i} = f_{\chi^2}(\Lambda_i, \nu_i) \tag{19}$$

Here, the argument Λ will be calculated from (14) for the condition $\lambda(t) = \tilde{\lambda}(t)$ which corresponds to the theoretical failure rate value determined by the Formula (2). The

number of degrees of freedom will be defined from the condition that the mode of Λ Chi-squared distribution corresponds to the empirical value of the failure rate - the point *Si* in Fig. 2, which is generally determined by Eq. (5), and which will be written as

$$Mo = \Lambda \tag{20}$$

It is known that for the Chi-squared distribution:

$$Mo = \nu - 2 \tag{21}$$

Then, from Eqs. (5), (14), (15), (21) is obtained:

$$\nu - 2 = \frac{2 \cdot N(t) \cdot \Delta t \cdot \Delta m(t)}{N(t) \cdot \Delta t} \tag{22}$$

whence:

$$\nu = 2[\Delta m(t) + 1], \tag{23}$$

which corresponds to the number of degrees of freedom of the confidence interval upper limit (see Eq. (17)).

Samples with predefined characteristics were generated to test the proposed criterion. One of the typical results obtained for a sample following the Weibull distribution with the shape parameter $\alpha = 6.5$ corresponding to failures because of long-term operation [2] and the scale parameter or characteristic time $\beta = 120$, with a sample volume of $N = 100$, is shown in Fig. 3. The sample for analysis was divided into 7 intervals per the Sturges formula. Verification of the match to a given distribution law was carried out per both Pearson Chi-squared and Kolmogorov-Smirnov type criteria [11].

Figure 3 shows the failure rate's empirical values and the confidence interval's boundaries. For the generated sample, not only the failure rate of the Weibull distribution was determined, but also that of the Gamma distribution to demonstrate the fundamental difference in the nature of the failure rate.

It should be noted that for every hundred generated samples corresponding to the Weibull distribution according to goodness-of-fit criteria – Chi-squared and Kolmogorov-Smirnov type, a similar result was obtained in 94–97 cases. Results demonstrate statistical inequality according to the Student's test of L_f mean values, with a confidence factor of 0.95, is acceptable for technical objects.

4.2 Using the Criterion of the Maximum Likelihood of the Empirical Failure Rate for the Selection of the Theoretical Distribution Law

In the case when several theoretical distributions according to the goodness-of-fit criteria correspond to empirical data, an additional argument for choice, according to the obtained data, is the assessment of the failure rate as per the L_f criterion by Eq. (13). One of the typical results is the following. There were generated 30 samples subject to Weibull distribution [12] with the shape parameter $\alpha = 3$ corresponding to fatigue failure because of cyclic loads [2] and the scale parameter $\beta = 100$ of the volume $N = 100$.

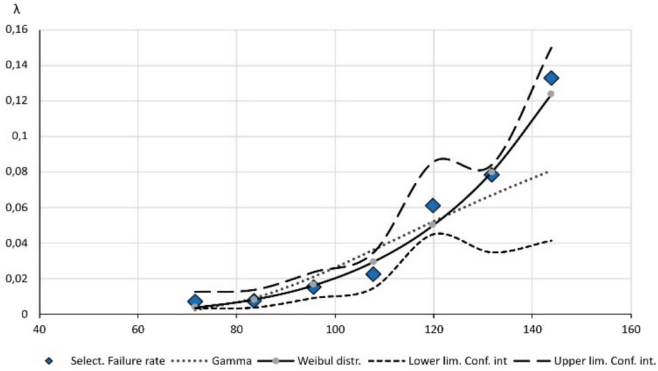

Fig. 3. Empirical and theoretical failure rates relatively confidence interval.

For all samples, goodness-of-fit tests were satisfied for both the Weibull and Gamma distributions. In this case, the criterion L_f was the sole additional argument to choose the proper distribution based on the character of the failure rate function. The following Student's test defined the inequality of mean values:

$$t = \frac{\left|\overline{L}_{fW} - \overline{L}_{fG}\right|}{\sqrt{\frac{(n-1)\left(S_w^2+S_G^2\right)}{n^2}}} > t_{\alpha,(2n-1)} \tag{24}$$

The following equation defines confidence intervals:

$$\Delta L_{fj} = \pm t_{\alpha,n-1}\sqrt{\frac{S_j^2}{n}} \tag{25}$$

where $\overline{L}_{fW}$, $\overline{L}_{fG}$ – mean values of criteria for Weibull and Gamma distributions, respectively; S_w^2 *and* S_G^2 - variances of L_f for Weibull and Gamma distributions respectively; n – number of samples; $t_{\alpha,\nu}$ – the critical value of Student's test for confidence factor α and ν degrees of freedom; j – takes a value W or G for Weibull and Gamma distributions respectfully.

The result of the simulation experiment (See Table 1) shows that having homogenous variances, L_f criteria for Weibull and Gamma distributions are significantly different with confidence factors 0.95 and up to 0.99. Comparison of mean values of L_f for both distributions indicates the belonging of samples to the Weibull distribution.

To define the adequate empirical failure rate evaluation, the following approaches, based on analysis from Sect. 2 of this paper, were examined:

- "BB" as a simulation of approach, described in [5] – both the number of serviceable items and the theoretical value of failure rate are taken for the interval's start time; thus, the empirical failure rate is found by Eq. (8);
- "BM" as a simulation of approach is described in [6] - the number of serviceable items is taken for the beginning of the interval while a theoretical value of failure rate

Table 1. Conditions and results of simulation experiments.

Distribution Law	n	$\overline{L}_{fj}$	S_j^2	$t_{0.95,29}$	ΔL_{fj}	t	$t_{0.95,59}$
Weibull (W)	30	19.4	2.73	1.699	$\pm$ 0.512	6.14	1.671
Gamma (G)	30	21.9	2.55		$\pm$ 0.495		

is for the time of the middle of the interval. The empirical failure rate is found by Eq. (8).

- "MM" as a simulation of approach, described in [7] – both the number of serviceable items and theoretical value of failure rate is taken for the time of the middle of the interval, and the empirical failure rate is found by Eq. (9).

The comparison of results is shown in Fig. 4. As can be seen from the figure, based on L_f criterion (13), the "MM" approach demonstrates the lowest value and thus the best result. A simple comparison of the relative deviation of empirical and theoretical failure rate values shows that the "MM" approach has the lowest level at 60%–70% intervals. Moreover, the difference with the rest of the approaches is sufficient – on average up to 1.75 times or more. The difference is insufficient for the rest, 30–40% of intervals,

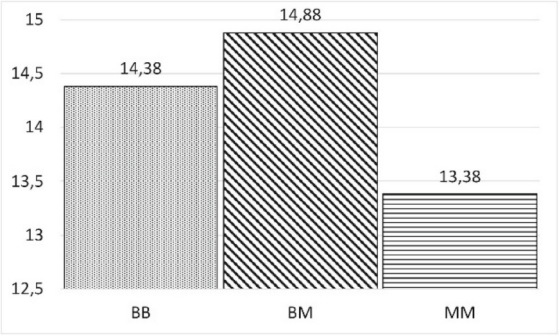

Fig. 4. Comparison of empirical failure rate evaluation approaches by L_f criterion.

Thus, as can be seen from the results, the most adequate result gives an approach when empirical and theoretical values refer to the middle of an interval [7].

As an additional argument for discussion, the developed approach has been tested using independent real-life experimental data, a reference given in [1]. The research is based on carbide cutters' tool life data selection of the volume $N = 207$ when machining alloy-bearing steel. The sample is defined as corresponding to Normal distribution characterized by the mean time to failure $\overline{T} = 65$ minutes and standard deviation $S = 16$ min. Figure 5a shows a histogram of the empirical distribution. According to the goodness-of-fit Pearson test, all three theoretical distributions – Normal, Weibull, and Gamma can describe this empirical data, though, for the Normal distribution, the test level is lowest. The result of the additional test by L_f criterion, shown in Fig. 5b, resolves this issue

and defines distribution as Normal according to the failure rate character. Moreover, it shows the principal difference between the three distributions in the nature of the failure rate. This difference regarding empirical values and confidence boundaries is shown in Fig. 6. The Gamma distribution failure rate decreases with time while Normal and Weibull increase and the Weibull distribution failure rate grows faster. This fact means that Normal distribution best fits empirical failure rate data. In this way, the prior conclusion that failures in the period of normal operation can be described by the Normal distribution along with the Weibull one is also supported.

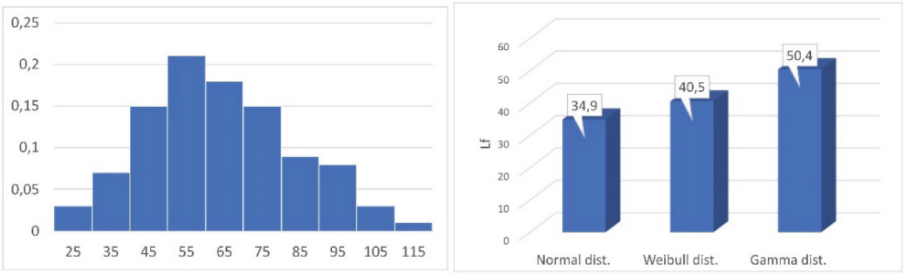

a) b)

Fig. 5. Results of carbide cutters reliability analysis: a) empirical frequency (differential distribution) of carbide cutters tool life; b) assessment of theoretical distributions by L_f criterion.

On top of that, based on data represented in Fig. 3 and Fig. 6, a conclusion different from the one made in [3] and already mentioned above can be drawn - similar in form Gamma and Weibull distributions cannot be competing in general – only under certain limited conditions. The same applies to the Normal distribution. The nature of the failure rate should not be ignored when choosing the appropriate distribution law for reliability modeling, especially for objects that are subject to wear and aging.

Though the proposed approach is of essential importance for reliability analysis and has been validated by both simulation and real-life tests, this fact does not remove some of its limitations for adequate assessment of research results associated with the current insufficiency of statistical data on failures of different nature and of a wide range of technical objects. Further development of the methodology is related to their collection and analysis based on the L_f criterion, and the study of the behavior on large and small samples. Besides, it makes sense to consider the behavior of the failure rate function concerning the confidence interval (see Fig. 6) and how informative it is when its points fall outside of it.

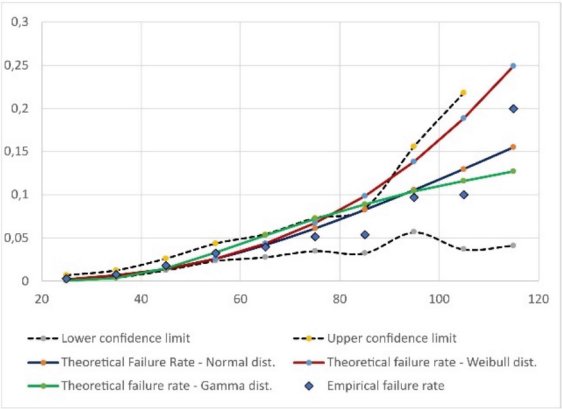

Fig. 6. Comparison of empirical and theoretical failure rate data concerning confidence boundaries for carbide cutters when machining alloy-bearing steel.

5 Conclusions

The failure rate, connected with specific failure distribution law, reflects a physical process that leads to the failure.

The failure rate function's character must be considered when choosing theoretical distribution law corresponding to empirical data.

Based on the maximum likelihood method, the criterion is proposed for the intercomparison of theoretical and empirical failure rate values at a specific time.

Following the proposed criterion, the best result for an empirical assessment of the failure rate is given by using the average number of serviceable products in a given time interval, which correlates with the theoretical value found for the same interval.

The proposed criterion L_f makes it possible to evaluate the nature of the dependence of the failure rate on time per the sample data.

The proposed L_f criterion is an additional factor for choosing a theoretical distribution law based on sample data, while goodness-of-fit criteria for several theoretical distribution laws are within acceptable limits for the same sample.

References

1. Frolov, M.: Variation coefficient and some distribution laws in the context of cutting tools and other technical objects reliability modeling. In: Ivanov, V., et al. (eds.) Advances in Design, Simulation and Manufacturing. DSMIE 2019. LNLME, pp. 13–22. Springer, Cham (2019). https://doi.org/10.1007/978-3-319-93587-4_2
2. Abernethy, R.B., Breneman, J.E., Medlin, C.H., Reinman, G.L.: Weibull Analysis Handbook. Pratt & Whitney Aircraft, West Palm Beach (1983)
3. Gamma Distribution Fitting. NCSS Statistical Software. https://ncss-wpengine.netdna-ssl.com/wp-content/themes/ncss/pdf/Procedures/NCSS/Gamma_Distribution_Fitting.pdf. Accessed 27 Aug 2023

4. Jamieson, A.: Computer Search for the Ideal Histogram. In: Annual Quality Congress Transactions, vol. 43, pp. 277–283. ASQ, Milwaukee (1989)
5. Jurgensen, J.H.: Individual Failure Rate Modelling and Exploratory Failure Data Analysis for Power System Components. KTHб Stockholm, Sweden (2018)
6. Iyer, R.K.: Hazard and Reliability Functions. Failure Rates. University of Illinois. https://courses.engr.illinois.edu/ece313/fa2013/SectionB/Lectures/lec_20.pdf. Accessed 27 Aug 2023
7. Barlow, R.E., Proschan, F.: Mathematical Theory of Reliability. SIAM. Philadelphia (1996)
8. Deng, Y.-H., Zhu, H.-P., Zhang, G.-J., Yin, H.: Optimal tool replacement decision method based on cost and process capability. In: Advances in Intelligent and Soft Computing. 125 AISC, pp. 9–14. Springer, Heidelberg (2012)
9. Berquo, J.E.: Refinement of Failure Rate: Confidence Intervals. DCA-BR. http://www.dcabr.org.br/download/artigos/iyk_24.pdf. Accessed 27 Aug 2023
10. Calculating MTTF When You Have Zero Failures. Technical Brief from Relex Software Corporation. Semantic Scholar. https://pdfs.semanticscholar.org/6b84/789a598b96dc55087130f726ff44adb712f5.pdf, last accessed 2023/08/27
11. Steele, M.C., Chaseling, J.: A comparison of the powers of the Chi-Square test statistic with the discrete Kolmogorov-Smirnov and Cramer-von Mises test statistics. In: COMPSTAT Proceedings in Computational Statistics, pp. 615−621. Physica, Heidelberg (2006)
12. Pylypchuk, M.I., Dziuba, L.F., Mayevskyy, V.O., Kopynets, Z.P., Taras, V.I.: The distribution pattern of machining errors on woodworking machine tools. J. Eng. Sci. (Ukraine) **10**(2), A34–A42 (2023). https://doi.org/10.21272/jes.2023.10(2).a5

Spindle Vibration Prediction for the CNC Machining Center Using ANFIS System

Pichai Janmanee and Suthep Butdee(✉)

Rajamangala University of Technology Krungthep, 2, Nang Linchi Road, Sathorn, Bangkok 10120, Thailand
suthep.b@mail.rmutk.ac.th

Abstract. Machining requires high precision and accuracy, whereas the machined parts rely on the machine's quality as its stability. Unbalanced and eccentric components cause machine vibration, which is a significant problem with machining. However, such problems should be detected early in process design. This paper proposes the spindle vibration of CNC machining center prediction by simulation using the ANFIS system. Three main parameters are concerned: working load, bearing life, and spindle speed. Membership functions are designed and created using machine capability. The case studies are illustrated by mainly emphasizing the workload analysis of each cutting path and feature. Cutter loads are calculated, and determined the stress occurrence using FEM. The contributions are spindle vibration estimation related to the workloads and spindle speed usage. Adjudgment data based on vibration prediction can assist machinists in controlling the quality of the machine part and utilizing the longer machine life.

Keywords: Spindle Vibration Prediction · CNC Machining Center · ANFIS System · Process Innovation · Industrial Growth

1 Introduction

CNC machines are used to cut metal parts for various industrial sectors. The quality of the machined part is mainly considered by the capability of the cutting parameters, machines, and cutting tools. Workpiece material is another variable of the machinability. The quality of the machined part is relatively dependent on machine efficiency and stability. Vibration is a critical factor in machine deficiency. It is measured by oscillations and equilibrium point [1]. Vibration can be determined by random or patterns of machined components and can be analyzed by the mathematical model using the Fourier transform, converting time wave to frequency wave. Vibration is monitored to determine machine health caused by unbalanced shaft alignment, cavitation, and bearing life [2, 3]. This paper proposes developing a prediction model for CNC spindle vibration with a working load variable before using the vibration sensor to collect data and detect real-time data. CNC Spindle is the most important mechanical component in removing metal during machining operations. The CNC Spindle is a rotating axis of the machine, which is frequently used and has a shaft at its heart. The shaft itself is called

© The Author(s), under exclusive license to Springer Nature Switzerland AG 2024
V. Ivanov et al. (Eds.): DSMIE 2024, LNME, pp. 212–222, 2024.
https://doi.org/10.1007/978-3-031-61797-3_18

the spindle; it includes three bearings in the front and two bearings in the rear of the spindle. Machine tool spindles lead to unstable chatter vibrations, cutting forces, and uneven tensions in the belt and pulleys. Vibration from the bearing of the CNC machine generates forces [4] that relate to all of the rotating elements [5, 6]. Spindle vibration can be measured by using displacement sensors, velocity sensors, and acceleration sensors via fault characteristic order (FCO) analysis [6–8]. Bearing faults are caused by failure in rotating machines [9] and include pitting, spalling, electro-erosion, and wear. Various alternative ways to analyze and predict bearing capability and component vibration. It can use experimental study, acoustic emission measurements [10], simulation, principal component analysis, fuzzy logic [11, 12], and ANFIS system [13, 14].

2 Literature Review

This section reviews the vibration modeling and prediction quality of machined parts using CNC machining centers. The vibration can worsen the machine's health, which moves in a high revolution. For example, the machine's spindle is mainly operated at 5,000 rpm to 15,000 rpm. Vibration can estimate machine efficiency based on stability and accuracy as well as defect levels of working operations, which are defined by frequencies. The vibration can be used for predicting and evaluating machine conditions and faults [15] caused by the machine's components, such as bearing [16] and bearing defects [17], inferring by the frequency vibration signals generated at the entry and exit moving elements. In addition, the bearing defect may be caused by faulty installation, poor maintenance and handling practices [18], or surface fatigue [19], which eventually leads to the formation of various types of defects [20], including spalls [21] and stress contact [22]. A theoretical model to predict the effect of localized defects on vibrations associated with ball bearings is defined by the acceleration of vibration components of the bearing [23–25]. The bearing's vibration analysis can be used for outer raceway defects [26]. Besides, the diagnosis of distributed bearing vibration analysis can be modeled by incorporating the geometrical imperfections of the bearing components [27, 28]. The designed fault diagnosis system can use both time-domain and frequency-domain signals to diagnose motor-bearing faults [28, 29]. Since most bearing vibrations are periodical movements, it is easy to extract vibration features from the frequency-time technique [30, 31]. Standard shapes of rolling elements include the ball, cylindrical roller, tapered roller, needle roller, and symmetrical and unsymmetrical barrel roller [32, 33]. Five basic motions describe the dynamics of bearing elements, with each movement having a corresponding frequency [34, 35].

3 Research Methodology

The research methodology is designed with various parts, including the ANFIS system, the finite element method for deterring the strength of the cutter, and the cutting force of the machining feature. The main objective is to estimate and predict the spindle vibration. Variables used in the ANFIS model to detect vibration of the CNC machining center are spindle speed, working hours of the bearing, and the machine loads that all impact vibration. The case study is illustrated in Fig. 1.

Fig. 1. ANFIS conceptual model for CNC machine vibration prediction.

Figure 1 shows the ANFIS conceptual model for bearing vibration prediction of the CNC machining center. Spindle speed is critical to impact the spindle vibration, too. It varies from low speed to high speed depending on the machine type, starting from 1,000 rpm to 12,000 rpm. The spindle speed relates to cutting speed, which affects tool life and wear on different cutting conditions, including feed rate and depth of cut. Bearing life measures how long the bearings have been used for both sides of the spindle: the top and the bottom. In addition, the bearings are calculated their life by working time in hours and compared to the bearing manufacturing guide. Machine tables are related to the spindle speed because they are moved synchronously. The machine table is driven by motors and ball screws. There are three components based on the machine axes: X, Y, and Z. The machine table mainly supports and holds the workpiece via machine vise. The machinist expert recommended that vibration is critical to machining part quality. Therefore, the prediction and prevention of machine failure is gainful. This model is implemented by MATLAB, and the results are tested, validated, and adjusted to fit with the expert decision and recommendation by fuzzy rules.

Table 1 shows the membership functions of inputs: spindle speed, bearing life, and machine load, whereas the vibration level is the output from prediction. The variables are divided into 5 levels: very low, low, medium, high, and very high. The ranges are derived from the standard data from the manufacturer's guide.

Table 1. Linguistic variables for the fuzzy membership input and output function.

Variables	Very low	Low	Medium	High	Very high
Spindle speed (rpm)	1,000	3,000	6,000	9,000	12,000
Bearing life (hours)	10,000	15,000	20,000	25,000	30,000
Machine load (Kw)	6.0	10	14	18	22.0
Vibration level (mm/s)	0.20	0.71	2.80	7.10	45.0

The spindle speed is driven by a motor. The spindle is supported by bearings on the vertical axis. Figure 2 shows the section view of the spindle part. There are angular bearings located on the top and bottom, which control the spindle's concentricity while it moves and is caused by vibration. The spindle speed is ranged from 1,000 rpm to

12,000 rpm. Bearing life is measured by working hours. The recommended guide ranges between 10,000 h to 30,000 h. Machine loads are the maximum value based on the maximum power of the servo on each axis: the X axis, the Y axis, and the Z axis on the workpiece table. The vibration level is set based on the input rank for training in the fuzzy inference engine and fuzzy rules. Vibration severity is recognized by the international standard ISO 10816, which is classified into four classes: class 1 for small machines, class 2 for medium machines, class 3 for large rigid foundations, and class 4 for large soft foundations. The criteria are divided into four categories: good, satisfactory, unsatisfactory, and unacceptable. The vibration is ranged from 0.28 mm/s to 45 mm/s.

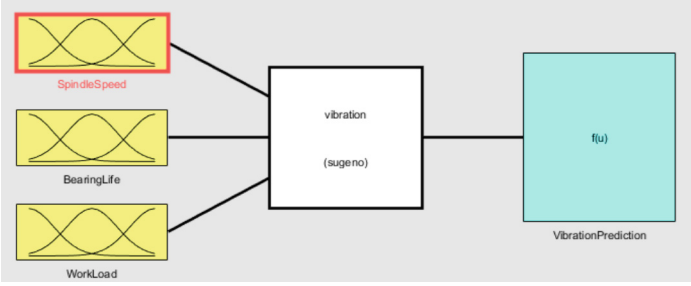

Fig. 2. ANFIS system on the MATLAB platform.

Figure 2 shows the ANFIS system on the MATLAB platform. Three membership functions are spindle speed, bearing life, and workload. The fuzzy rules for vibration decisions are created with the membership function relation at the first stage before they are trained in the ANFIS system. The output is carried out by predicting the vibration of the CNC spindle speed. However, different machines have different capabilities, efficiency, and rules. Therefore, the results may be different from this model, but it can be modified by the current cases. The membership functions are created based on the machine capability scope referred to in Table 1, as shown in the following sessions.

Figure 3 shows the membership function for the spindle speed of the CNC machining center. The range is between 1,000 rpm to 12,000 rpm. The speed is divided into 5 levels: very low, low, medium, high, and very high.

Figure 4 shows the membership function of the bearing's life that infers the efficiency of the bearing and spindle performance. The range is set between 10,000 h to 30,000 h according to the manufacturer's guide. They are divided into five levels of life: very low, meaning the new bearing, low, medium, high, and very high. The expert expressed that if the bearing's life is low. It is then that the spindle vibration is low. On the other hand, if the life is high, the spindle vibration is relatedly high.

Figure 5 shows the membership function of the CNC machining workload. It is measured by the machine power in KW. The machine user's guide recommends the machine power range from 6 KW to 22 KW. It is divided into five levels: very low, low, medium, high, and very high. The workload in this study is considered as the combination force in every dimension and loaded by the motors of the X axis, the Y axis, and the Z axis.

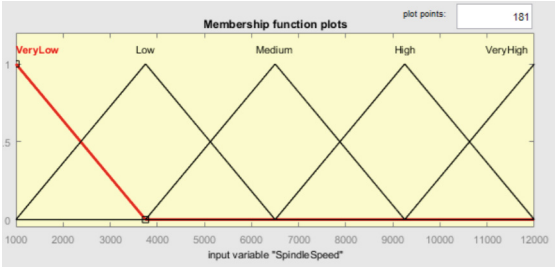

Fig. 3. Membership function for the spindle speed.

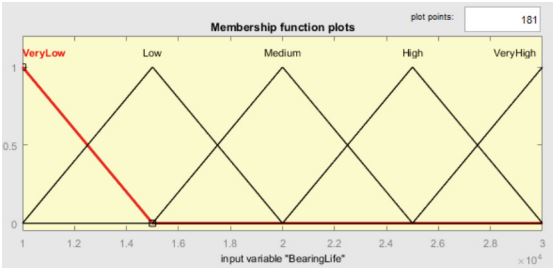

Fig. 4. Membership function of bearing's life.

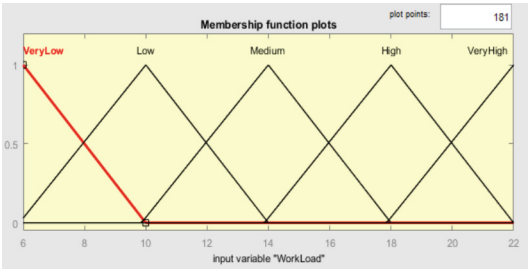

Fig. 5. The membership function of the CNC machining center's workload.

Figure 6 shows the workload region in the CNC machining center, which depends on the cutting parameters, including cutting speed, feed rate, and depth of cut. Those parameters are influenced by the machine workload, which is represented by cutting force and machine power. The cutting force is also separated by the three axes, including six directions such as X+, X−, Y+, Y−, Z+, and Z−. The figure also shows the spindle and its revolution.

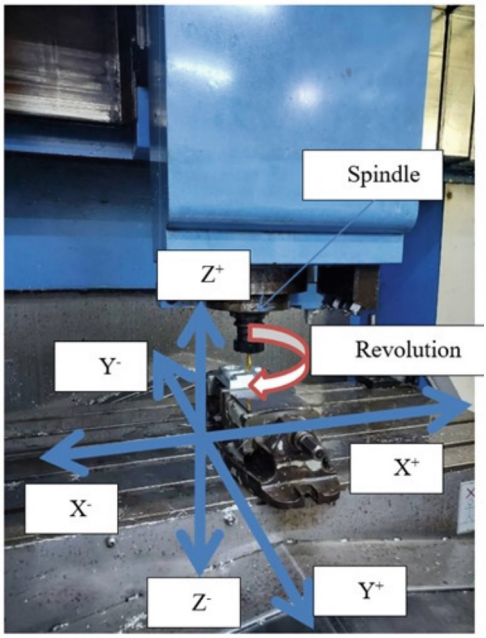

Fig. 6. The workload region in the CNC machining center.

4 Results and Discussion

The results from the ANFIS modeling are tested, discussed, verified by the expert opinion, and modified to match the acceptable level of reality.

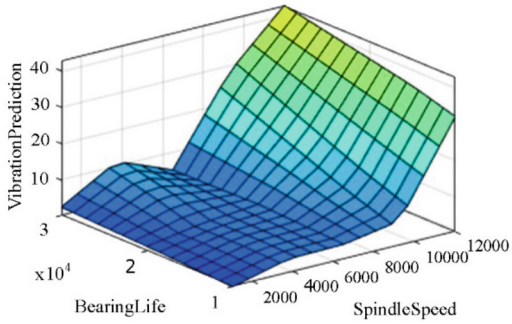

Fig. 7. The relation of bearing's life and spindle speed to impact the spindle vibration.

Figure 7 shows the relation of the bearing's life and spindle speed to impact the spindle vibration. It is shown that vibration is related to the life of the bearing. If the bearing's life is low, then the vibration is low. On the other hand, if the spindle speed is

higher, the vibration will increase until it is very high. The graph is related to the expert recommendation. The feasible region is set the spindle between 400 rpm and 8000 rpm.

Figure 8 shows the bearing's life and workload impacting the spindle vibration. The vibration is low if the bearing life is low and the workload is medium. It is found that the workload is linear compared to vibration, where the bearing life is dramatically increased. The graph infers that bearing life should be set up to 20,000 h. Spindle speed is directly related to cutting speed, whereas depth is extremely impacted by cutting force and machine power.

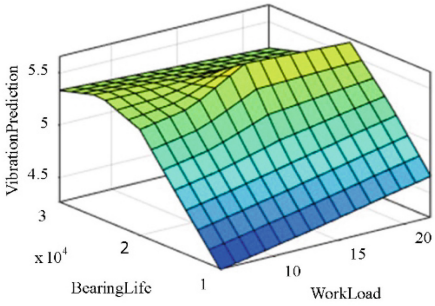

Fig. 8. The relation of bearing's life and workload to impact spindle vibration.

Table 2 shows the case study of the vibration prediction obtained from the ANFIS system. Cases 1, 6, and 10 are studied for rough cutting, whereas cases 2, 5, and 9 are studied for semi-finish cuts, and cases 1, 4, and 7 are the cases studied for finishing. Those three cutting conditions are varied by the spindle speed, which is related to the cutting speed. This study assumes that medium efficiency is sometimes used. This means that the bearing life is approximately 10,000 h of usage. The cutting force and workload are calculated by the cutting parameters.

The case study starts with the component design and conditions. Figure 9 shows the aluminum alloy (AL6061) design with a material hardness of 95 HB. The cutting tool is set by end mill ϕ 6 mm and ϕ mm, and the tool material is high-speed steel (HSS). The machined component is required by dimensional accuracy of tolerances and finished surfaced roughness. In addition, the cutting tool must be safe, meaning that it is not broken. Cutting force is a significant concern of the study for workload estimation. It involves cutting parameters such as cutting speed, feed rate, and depth of cut. The given parameters for machining consist of the machine's capability for motor sizes. This case study uses the machining center HASS-FV2 model. The spindle motor is 22.4 kW.

The result of spindle vibration shown in Table 2 of the case study can be described as the vibration being ranked between 4.01 mm/s^2 and 4.60 mm/s^2 when the spindle speed is set by 4,500 rpm and 6,000 rpm. The vibration is predicted to be very high when the spindle speed is set at a high speed of 10,000 rpm. However, it is found that the cutting force is low (4,500) when the spindle is high (10,000 rpm). The limitation of the model is that it is not flexible to various spindles of varieties of CNC machining. It should be developed as a generic method and validated with a specific case of the CNC model.

Table 2. The case study of the vibration prediction obtained from the ANFSI system.

case	Spindle speed (rpm)	Feed rate (mm/min)	Depth of cut (mm)	Bearing life (hours)	Cutting force (kg)	Workload (kw)	Vibration Prediction (mm/s^2)
1	4500	840	3	10.000	4.14	0.1	4.01
2	4500	840	6	10.000	15.3	0.34	4.26
3	4500	840	10	10.000	42.02	0.96	4.41
4	6000	840	3	10.000	2.84	0.09	4.20
5	6000	840	6	10.000	11.35	0.34	4.33
6	6000	840	10	10.000	31.52	0.96	4.60
7	10.000	840	3	10.000	1.7	0.09	13
8	10.000	840	6	10.000	6.22	0.31	13
9	10.000	840	10	10.000	7.05	0.34	13.1

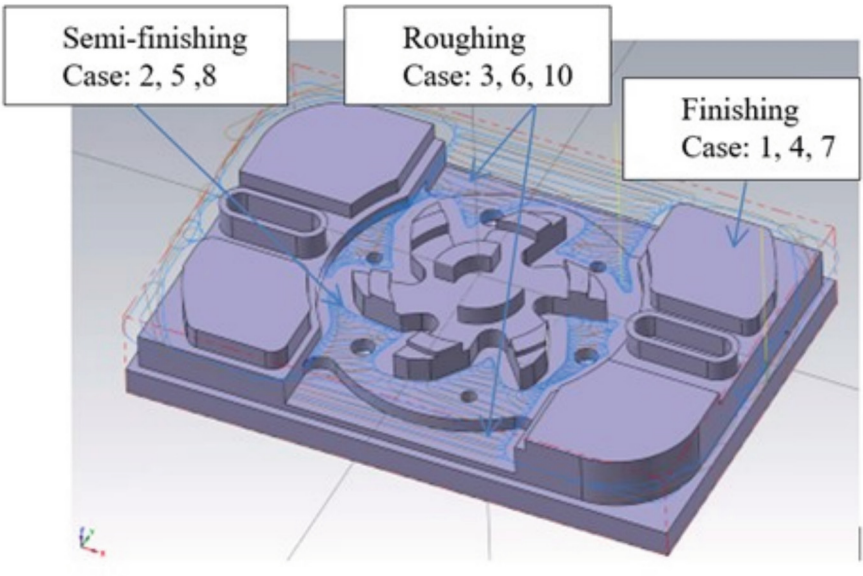

Fig. 9. The component design for testing the ANFIS prediction of the CNC machining spindle vibration.

5 Conclusions

The paper presents the CNC machining center vibration prediction occurring on the spindle vibration, which causes the machined part to have a lower quality. With the industrial and factory knowledge of CNC machining, the experts recommended that the machine vibration occurred in the spindle component while it was rotated at high speed.

In addition, the spindle vibration is also caused by the bearing's life and workload, which are referred to as cutting parameters and cutting conditions. Instead of using expert opinions or experimental studies preceded by several processes, this paper presents mathematical modeling using the ANFIS model by taking those three parameters as input membership functions. In contrast, the spindle vibration prediction is the modeling output. The input and output data relation is prepared to be set up initially before the rules are automatically generated in the fuzzy inference system. The data sets are trained to generate the output of the system prediction. The developer tests verify the system modeling and modifies it according to the expert's recommendation. The contribution is that the model development can help engineering find the optimized cutting parameters for the safety of machines, cutting tools, and good machining conditions. In addition, it is a utility knowledge-based method for cutting parameters, recommended by industrial experts with actual cases. However, the study is based on the ISO standard acceptance, in which the acceptable level for the machine class III should be less than 4.5 mm/s.

References

1. Ghazali, M.H.M., Rahiman, W.: Vibration analysis for machine monitoring and diagnosis: a systematic review. Shock Vib. **2021**, 9469318 (2021). https://doi.org/10.1155/2021/9469318
2. de Sá Só Martins, D.H.C., Viana, D.P., de Lima, A.A., et al.: Diagnostic and severity analysis of combined failures composed by imbalance and misalignment in rotating machines. Int. J. Adv. Manuf. Technol. **114**, 3077–3092 (2021). https://doi.org/10.1007/s00170-021-06873-2
3. Chavan, N.P., Kale, M.S., Deshmukh, S.P., Thakar, C.M.: A review on development and trend of condition monitoring and fault diagnosis. ECS Trans. **107**, 17863–17870 (2022). https://doi.org/10.1149/10701.17863ecst
4. Huang, H., Baddour, N.: Bearing vibration data collected under time-varying rotational speed conditions. Data Brief **21**, 1745–1749 (2018). https://doi.org/10.1016/j.dib.2018.11.019
5. Huang, H., Baddour, N., Liang, M.: Bearing fault diagnosis under unknown time-varying rotational speed conditions via multiple time-frequency curve extraction. J. Sound Vib. **414**, 43–60 (2018). https://doi.org/10.1016/j.jsv.2017.11.005
6. Wang, T., Liang, M., Li, J., Cheng, W.: Rolling element bearing fault diagnosis via fault characteristic order (FCO) analysis. Mech. Syst. Signal Process. **45**(1), 139–153 (2014). https://doi.org/10.1016/j.ymssp.2013.11.011
7. Safizadeh, M.S., Latifi, S.K.: Using multi-sensor data fusion for vibration fault diagnosis of rolling element bearings by accelerometer and load cell. Inf. Fusion **18**, 1–8 (2014). https://doi.org/10.1016/j.inffus.2013.10.002
8. Valero, M., Li, F., Zhao, L., Zhang, C., Garrido, J., Han, Z.: Vibration sensing-based human and infrastructure safety/health monitoring: a survey. Digit. Signal Process. **114**, 103037 (2021). https://doi.org/10.1016/j.dsp.2021.103037
9. Ho, D., Randall, R.B.: Optimisation of bearing diagnostic techniques using simulated and actual bearing fault signals. Mech. Syst. Signal Process. **14**(5), 763–788 (2000). https://doi.org/10.1006/mssp.2000.1304
10. Shiroishi, J., Li, Y., Liang, S., Kurfess, T., Danyluk, S.: Bearing condition diagnostics via vibration and acoustic emission measurements. Mech. Syst. Signal Process. **11**(5), 693–705 (1997). https://doi.org/10.1006/mssp.1997.0113
11. Boutros, T., Liang, M.: Mechanical fault detection using fuzzy index fusion. Int. J. Mach. Tools Manuf. **47**(11), 1702–1714 (2007). https://doi.org/10.1016/j.ijmachtools.2007.01.001

12. Tung, P.-C., Tsai, M.-T., Chen, K.-Y., Fan, Y.-H., Chou, F.-C.: Design of model-based unbalance compensator with fuzzy gain tuning mechanism for an active magnetic bearing system. Expert Syst. Appl. **38**(10), 12861–12868 (2011). https://doi.org/10.1016/j.eswa.2011.04.078
13. Chen, L., Ma, Y., Hu, H., Khan, U.S.: An effective fault diagnosis approach for bearing using stacked de-noising auto-encoder with structure adaptive adjustment. Measurement **214**, 112774 (2023). https://doi.org/10.1016/j.measurement.2023.112774
14. Chen, K.-Y., Tung, P.-C., Tsai, M.-T., Fan, Y.-H.: A self-tuning fuzzy PID-type controller design for unbalance compensation in an active magnetic bearing. Exp. Syst. Appl. **36**(4), 8560–8570 (2009). https://doi.org/10.1016/j.eswa.2008.10.055
15. Kandianis, F.: Novel laplace transform techniques in structural dynamic analysis. J. Sound Vib. **36**(2), 225–252 (1974). https://doi.org/10.1016/S0022-460X(74)80296-8
16. Dolenc, B., Boškoski, P., Juričić, Đ: Distributed bearing fault diagnosis based on vibration analysis. Mech. Syst. Signal Process. **66–67**, 521–532 (2016). https://doi.org/10.1016/j.ymssp.2015.06.007
17. Choudhury, A., Tandon, N.: A theoretical model to predict vibration response of rolling bearings to distributed defects under radial load. J. Vib. Acoust. **120**(1), 214–220 (1998). https://doi.org/10.1115/1.2893808
18. Mohammed, O.D., Rantatalo, M., Aidanpää, J.-O., Kumar, U.: Vibration signal analysis for gear fault diagnosis with various crack progression scenarios. Mech. Syst. Signal Process. **41**(1–2), 176–195 (2013). https://doi.org/10.1016/j.ymssp.2013.06.040
19. Lu, H., Wang, J., Wen, Z., Liu, T., Lian, Y., Yue, Z.: Vibration fatigue behavior and life prediction of directionally solidified superalloy based on the phase transformation theory. Eng. Fract. Mech. **282**, 109184 (2023). https://doi.org/10.1016/j.engfracmech.2023.109184
20. Saruhan, H., Sandemir, S., Çiçek, A., Uygur, I.: Vibration analysis of rolling element bearings defects. J. Appl. Res. Technol. **12**(3), 384–395 (2014). https://doi.org/10.1016/S1665-6423(14)71620-7
21. Wang, Q., Li, M., Xu, S.: Experimental study on vortex induced vibration (VIV) of a wide-D-section cylinder in a cross flow. Theor. Appl. Mech. Lett. **5**(1), 39–44 (2015). https://doi.org/10.1016/j.taml.2015.01.002
22. Kıral, Z., Karagülle, H.: Vibration analysis of rolling element bearings with various defects under the action of an unbalanced force. Mech. Syst. Signal Process. **20**(8), 1967–1991 (2006). https://doi.org/10.1016/j.ymssp.2005.05.001
23. Avellan, K., Belopotocanova, E., Puurunen, M.: Measuring, monitoring and prediction of vibration effects in rock masses in near-structure blasting. Procedia Eng. **191**, 504–511 (2017). https://doi.org/10.1016/j.proeng.2017.05.210
24. Keshtegar, B., Piri, J., Asnida Abdullah, R., Hasanipanah, M., Muayad Sabri Sabri, M., Nguyen Le, B.: Intelligent ground vibration prediction in surface mines using an efficient soft computing method based on field data. Front. Public Health **10**, 1094771 (2023). https://doi.org/10.3389/fpubh.2022.1094771
25. Hosseini, S., Pourmirzaee, R., Armaghani, D.J., Sabri Sabri, M.M.: Prediction of ground vibration due to mine blasting in a surface lead–zinc mine using machine learning ensemble techniques. Sci. Rep. **13**(1), 6591 (2023). https://doi.org/10.1038/s41598-023-33796-7
26. Dhamande, L.S., Bhaurkar, V.P., Patil, P.N.: Vibration analysis of induced draught fan: a case study. Mater. Today Proc. **72**, 657–663 (2023). https://doi.org/10.1016/j.matpr.2022.08.329
27. Andretta, M., Birgin, E.G., Raydan, M.: An inner–outer nonlinear programming approach for constrained quadratic matrix model updating. Mech. Syst. Signal Process. **66–67**, 78–88 (2016). https://doi.org/10.1016/j.ymssp.2015.05.002
28. Marconnet, P., Pottier, B., Rasolofondraibe, L., Dron, J.P., Kerroumi, S.: Measuring load distribution on the outer raceways of rotating machines. Mech. Syst. Signal Process. **66–67**, 582–596 (2016). https://doi.org/10.1016/j.ymssp.2015.04.030

29. Wang, J., He, Q., Kong, F.: A new synthetic detection technique for trackside acoustic identification of railroad roller bearing defects. Appl. Acoust. **85**, 69–81 (2014). https://doi.org/10.1016/j.apacoust.2014.04.005
30. Seo, D.-H., Choi, J.-W., Kim, Y.-H.: Impulsive sound source localization using peak and RMS estimation of the time-domain beamformer output. Mech. Syst. Signal Process. **49**(1–2), 95–105 (2014). https://doi.org/10.1016/j.ymssp.2014.03.013
31. Song, Y.-Z., et al.: Non-invasive damage detection in beams using marker extraction and wavelets. Mech. Syst. Signal Process. **49**(1–2), 13–23 (2014). https://doi.org/10.1016/j.ymssp.2013.12.011
32. Qiu, L., Liu, S., Chen, X., Wang, Z.: Lubrication and loading characteristics of cylindrical roller bearings with misalignment and roller modifications. Tribol. Int. **165**, 107291 (2022). https://doi.org/10.1016/j.triboint.2021.107291
33. Liu, Y., Chen, Z., Tang, L., Zhai, W.: Skidding dynamic performance of rolling bearing with cage flexibility under accelerating conditions. Mech. Syst. Signal Process. **150**, 107257 (2021). https://doi.org/10.1016/j.ymssp.2020.107257
34. Leavens, D.H.: Frequency distributions corresponding to time series. J. Am. Stat. Assoc. **26**(176), 407–415 (1931). https://doi.org/10.1080/01621459.1931.10502227
35. Yang, M.: Analysis on frequency domain corresponding of steering system. In: Proceedings of the 2019 2nd International Conference on Mathematics, Modeling and Simulation Technologies and Applications (MMSTA 2019). Atlantis Press, Xiamen (2019). https://doi.org/10.2991/mmsta-19.2019.48

Adaptive Fluid Jet Support Technique for Variable Stiffness Thin-Walled Parts End Milling

Serhii Kononenko, Sergey Dobrotvorskiy, Yevheniia Basova(✉), Oleksandr Kharchenko, and Dmytro Trubin

National Technical University "Kharkiv Polytechnic Institute", 2, Kyrpychova Street, Kharkiv 61002, Ukraine
e.v.basova.khpi@gmail.com

Abstract. To reduce machining errors in thin-walled parts manufacturing, the adaptive fluid jet support technique for variable stiffness thin-walled parts during the milling process was presented. The analysis of existing methods to avoid deflections in milling thin-walled parts was made. Along the tool path in the milling process, the stiffness of the thin-walled parts varies. The technique proposed was a single-point fluid jet support and implied variable impact force that considers the complex curvature of the part geometry. The behavior and the efficiency of the supporting fluid jet provided by the flow surface, including the flow features around different surface cross-section profiles and the concave and convex sides, were considered. An iterative algorithm of the adaptive adjustment of fluid jet support impact during milling considering variable stiffness of the thin-walled part was developed. The analytical errors prediction model was presented. The smoothed-particle hydrodynamics (SPH) method was applied to model the fluid jet flow. The finite element method was applied to model the thin-walled part's cutting forces and stresses under fluid jet impact. The comparison between applications of fluid jet support at different tool positions is performed. The technology is helpful from the point of view of uniform stabilization of allowance removal and approximates the machining of thin-walled low-rigid parts to the machining of completely rigid ones. The result data of sample parts showed that fluid jet support meets the requirements of thin-walled parts machining with decreased processing errors.

Keywords: Thin-Walled Parts · End Milling · Fluid Jet Support · SPH Method · Machining Errors · R&D Investment

1 Introduction

In the machining of thin-walled parts, the forces and stresses are the major factors of the part deflection that can significantly decrease the machining performance by affecting both the geometrical accuracy and the surface finish.

The deflection of the part can have various undesirable consequences for machining performance. It can result in a loss of accuracy in the machined dimensions of the part.

© The Author(s), under exclusive license to Springer Nature Switzerland AG 2024
V. Ivanov et al. (Eds.): DSMIE 2024, LNME, pp. 223–239, 2024.
https://doi.org/10.1007/978-3-031-61797-3_19

With the deflection of the part, the milling tool is not cutting in the predetermined location, resulting in an indentation from the required dimensions. This can be particularly problematic in the machining of parts with tight tolerances.

Additionally, the deflection of the part can cause variations in the surface finish of the machined part. As the tool encounters different deflection levels, it will produce different amounts of material removal, resulting in variations in the surface roughness of the machined part.

The low rigidity thin-walled part is more susceptible to vibration that can lead to tool breakage or wear [1]. The tool may experience sudden changes in loading, leading to increased stresses and the potential for tool failure. Moreover, as the tool encounters variations in the surface finish, it may experience increased wear, reducing its lifespan and further impacting machining performance. As the stiffness of the part changes along its length, the natural frequencies of the part may also change, making it more susceptible to chatter or resonance, especially when cutting forces vary.

Machining processes often rely on stable cutting conditions to maintain quality and efficiency. Meanwhile, variable stiffness can make it more challenging to maintain stable cutting conditions, leading to the need to reduce achievable cutting speeds and feeds or adaptive machining strategies.

Adaptive machining can be implemented as real-time measurements but requires sophisticated sensors and signal processing, probe hardware and integration, programming time and CAM integration, and cycle time increase to include probing operations. Another approach in adaptive machining is the preliminary adaptation of production technology to accommodate part-to-part variation, enabling more consistent and stable formation of complex geometries. A production process can be set and left to run with minimal operator input using a repeatable machine, stable fixture, and consistent material supply conditions. However, this level of input stability is essential to maintain. Variation in stock material from part to part may result in inconsistent loading that is difficult to accommodate by the machining process.

Combining adaptive machining technology, such as preliminary adjustments based on process-time data and the well-designed part fixture technique, can help stabilize the part during machining, reducing the undesirable impact of its variable stiffness.

The research objective is to develop an adaptive single-point fluid jet support technique for thin-walled parts during end milling. The novelty of the technology lies in the non-solid contact approach for the overall error reduction and alignment for variable thin-walled geometry at the different end mill tool positions.

2 Literature Review

From the literature analysis, it has been found that many studies are devoted to the adaptive control mechanisms of machining, taking into account either the parameters of cutting modes or the parameters of the thin-walled part.

The approach for predicting static surface errors in milling thin-walled parts [2] represents a virtual compensation strategy for industrial applications. It was empirically proven by matching prognosticated error profiles with the optically measured surface of the varying process parameters sample part. After applying the offered numerical model,

the error was directly determined for small radial cutting depths where the existence of tool runout affects the formation of the surface. The virtual strategy included the adaptive control of the immersion angle to compensate for the deflection of the part during processing. However, it can cause an additional deviation from the given nominal shape. In the case of a decrease in the rigidity of the part, if the immersion angle is significantly increased (to compensate for the cutting efficiency drop, namely undercut), another undesirable effect appears as an uneven allowance removal due to severe bending of the part.

Previous research on fluid jet support [3] for a thin-walled part during end milling [4] presented the fluid jet's impact on the part oscillation characteristics. As a result, the theoretical possibility of reducing the maximum oscillation amplitude of a part and shifting its oscillation characteristics to the region of higher machining frequencies was established. However, the relationship between the jet velocity and force impact with the part variable stiffness was not provided, i.e., the supporting technique for the machining process relied on a constant fluid flow.

A fast deformation calculation approach predicated on stiffness matrix reduction was suggested [5]. An iterative cutting force-induced inaccuracy prediction model was shown considering the tool-workpiece dynamic interaction, which reduced each cutting force-induced error forecasting time. The compensation experiment data showed that the provided model decreased the machining error by more than 53% with high real-time efficiency. The suggested iterative approach showed the engineering capacity to improve the machining accuracy. Nonetheless, distinct error sources, like geometric deflections or thermal deviations, were not compensated, restricting the increased machining accuracy. Moreover, considering the calculation efficiency, the material removal was not included. Another method [6] involves an approach for calculating the stiffness of the material removed by the end mill from the overall stiffness of the part to define the changing stiffness of the part, which in turn is used to determine the deflection that occurs.

A realistic 3D thermo mechanical finite element model has been developed to calculate the complicated physical interaction of a helical milling tool and the thin wall of an aluminum alloy material [7]. Lagrangian formulation with an explicit solution scheme was used to calculate the interaction between the helical milling cutter and the part. Johnson–Cook material constitutive model defined the material's behavior at high strain, strain rate, and temperature. The Johnson–Cook's damage and friction law were used to provide contact interaction and separation of the chip. The form error due to uncut material was presented. However, the analysis is time-consuming as it was stated that for 4 GB RAM and a 3.9 GHz computer, a typical material removal simulation during a complete pass of the tool along the 50 mm wall took about 340–350 h. Another research [8] provides the advantage of accurately predicting chatter stability in milling thin-walled parts, considering the force-induced deformation effect and revealing its significant impact, especially when dealing with low rigidities. However, the surface location error and process damping at low-speed cutting remain to be investigated in an interactive static and dynamic system. Another study [9] in search for optimal cutting conditions and strategies for controlling flatness error during the end milling of thin-walled components underscores the significant contribution of static deflections of the

end mill to flatness error at lower axial depth of cut (ADOC) values, while the contribution from tool deflections diminishes considerably at higher ADOC, in contrast to conventional expectations.

The multi-pass tool path generation method [10] reduces the total machining time, with a demonstrated saving of over 20%. This is achieved by variable feed rates and depth-of-cut in each pass while maintaining part and tool deflection within specified limits. However, there is room for improvement in achieving smoother tool paths and feed rates, and further research is needed to consider the dynamic characteristics of thin-walled parts for enhanced machining.

The 5-axis adaptive flank milling of thin-walled parts [11] with on-machine measurement can reduce machining errors by at least 70% compared to conventional machining, demonstrating high-precision machining. However, the accuracy of the on-machine measurement (OMM) system may be influenced by various machine tool-related error sources, such as geometric and thermal errors. Another model toward service-oriented continuous-discrete hybrid adaptive milling system based on rapid process planning by packing typical operations as services [12] demonstrates a reduction of chatter and errors in experimental results. It should be considered that unlike the preliminary data analysis approach for processing [13–16], the production applicability may require sophisticated sensors and signal processing.

A number of studies provide optimization of the milling path as an efficient way to increase the thin-walled machining stability [17–20]. A similar approach [21] is based on the finite element method (FEM), which optimizes cutting velocity to reduce deflections and vibrations during machining. It seamlessly imports G-code, efficiently analyzes complex parts with tooltip dynamics, predicts non-linear workpiece behavior, and continuously adjusts spindle speed along the tool path.

The thin-walled part-supporting technique [22] enhances milling stability by a tuneable clamping table (TCT) that allows dynamic stiffness control without interference in the cutting zone. The concept demonstrated increased stability compared to regular clamping, providing a potential solution of regenerative chatter. For industrial applications, further design improvements to reduce the moving mass of the table while maintaining high clamping stiffness and targeting higher natural frequencies may be necessary.

The cutting sequence optimization algorithm to reduce the part deformation approach [23] showed the advantage of reducing the maximum workpiece deformation during the milling process, with predicted reductions of about 20% and 63% compared to other strategies. However, there are quantitative differences between simulated and measured surface profiles, potentially due to factors like variations in material selection [24, 25], cutting force, and material removal as a “spring-back” effect, i.e., the geometric change made to a part at the end of the machining when the part has been released from the forces of the milling tool.

The simulation of low rigidity part machining study [26] offers the advantage of predicting cutting forces and vibrations in the machining of thin-walled parts, with a correlation between simulation and experimental results in cases of low vibration amplitudes and chatter-free operations. The limits in predicting amplitudes in unstable

milling, particularly when high vibration levels are involved, were concluded due to the influence of the ploughing effect.

3 Research Methodology

The mechanistic model can provide the cutting forces in milling. The basis for the forces modeling is the rigid model proposed by Altintas [27], with the thin-walled parts' features related to additions. The theoretical adaptive iterative fluid jet support technique (Fig. 1) consists of adapting jet parameters to a specified tolerance that can be set to control the processing until convergence is reached.

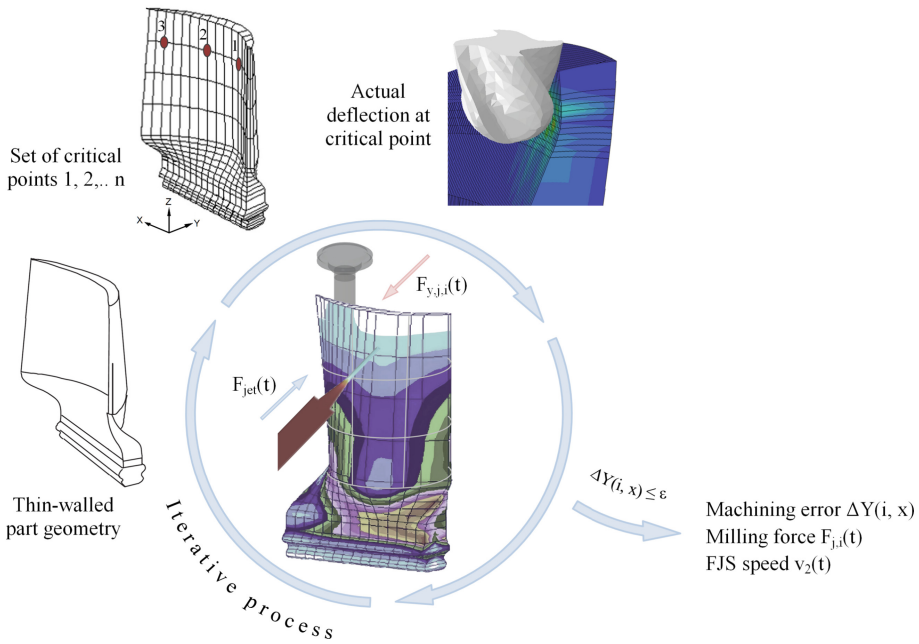

Fig. 1. An overview of an adaptive theoretical fluid jet support technique for end milling methodology.

The actual machining deflection modeling is performed to calculate the actual start immersion angle of the flexible part. It could be performed only once for the most critical region of the part. However, the number of calculation iterations application of the force depends on the number of critical points set. The more points, the more accurate the input, so the less reducibility gap to achieve the appropriate tolerance and the less computational cost of an iterative process.

3.1 Flexible Milling Force and Fluid Jet Support Force Model

Cutting forces are one of the key characteristics of the cutting process and are considered in the calculations for the strength of fixtures and cutting tools. The indicators and patterns

of cutting force variations determine the necessary power of metal cutting machines. Managing these indicators allows for addressing issues of precision and processing quality, considering tool and workpiece deformation, and influencing the processes of vibration excitation and damping.

In machining, cutting forces can induce significant stress in low-stiffness parts, leading to dimensional inaccuracies, surface defects, and even a loss of cutting process stability. Precise force calculations enable the optimization of machining parameters such as cutting speed, feed rate, cutting depth, and others to reduce the load on the workpiece and minimize the risk of damage.

Cutting forces depend on several factors, including the geometry and material of the cutting tool, processing parameters such as cutting speed, feed rate, and depth, and the properties of the workpiece material, such as hardness, plasticity, and strength.

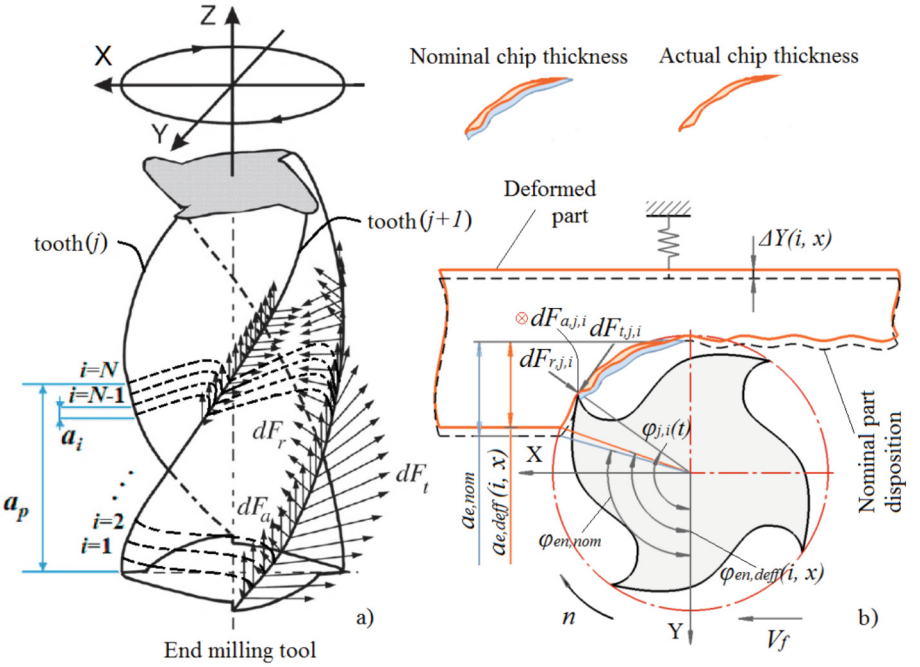

Fig. 2. Model of cutting forces in the thin-walled part machining.

To calculate the milling force in the process of machining, the spiral cutter and the part are divided into a finite number of integration segments and discrete flat elements (Fig. 2). Changes in the depths of cut at a particular axial height due to the force-induced deformation during cutting are represented by different immersion angles, namely the nominal immersion angle $\varphi_{en,nom}$ – under nominal conditions as if the workpiece had absolute rigidity, and $\varphi_{en,deff}(i, x)$ – under the deformed position, which is modeled in the contact zones of the tool and part. Accordingly, the cutting depths are $a_{e,nom}$ and

$a_{e,deff}(i, x)$. The cutting force at a time t for the N_j cutting teeth, i-th segment for a static component can be expressed as:

$$F_i(t) = \sum_{j=1}^{N_j} F_{s,j,i}(t). \tag{1}$$

According to the classical circular model of the cutting edge trajectory of the milling cutter, based on the rotation matrix in three-dimension, for the j-th cutting surface of the i-th segment, the instantaneous components of the cutting force in a general form can be expressed as follows:

$$F_{j,i}(t) = \begin{bmatrix} F_{x,j,i}(t) \\ F_{y,j,i}(t) \\ F_{z,j,i}(t) \end{bmatrix} = g_{j,i}(t) \cdot \begin{bmatrix} -\cos\phi_{j,i}(t) & -\sin\phi_{j,i}(t) & 0 \\ \sin\phi_{j,i}(t) & -\cos\phi_{j,i}(t) & 0 \\ 0 & 0 & -1 \end{bmatrix} \cdot \begin{bmatrix} F_{t,j,i}(t) \\ F_{r,j,i}(t) \\ F_{a,j,i}(t) \end{bmatrix}, \tag{2}$$

where $\varphi_{j,i}(t) = (2\pi n/60)t - i - (j-1)(2\pi/N_j)$ is the immersion angle into the material for the j-th cutting surface of the i-th segment;

n – the milling cutter's rotation frequency;

$g(\varphi_{j,i})$ – a function determining whether the j-th cutting surface of the i-th segment is engaged in the cutting process:

$$g(\phi_{j,i}) = \begin{cases} 1, & \text{if } \phi_{en,deff}(i,x) \le \phi_{j,i} \le \phi_{ex,deff}(i,x) \\ 0 & \text{otherwise} \end{cases}, \tag{3}$$

where $\varphi_{en,deff}(i, x)$, $\varphi_{ex,deff}(i, x)$ – are the entry immersion and exit angles of the milling cutter's cutting edge, defining the boundary of the contact zone between the tool and the workpiece in the i-th segment at position x; $F_{t,j,i}(t)$, $F_{r,j,i}(t)$, $F_{a,j,i}(t)$ – are the forces acting in the tangential, radial, and axial directions on the j-th cutting surface of the i-th segment at time t:

$$\begin{bmatrix} F_{t,j,i}(t) \\ F_{r,j,i}(t) \\ F_{a,j,i}(t) \end{bmatrix} = \begin{bmatrix} K_{tc} \\ K_{rc} \\ K_{ac} \end{bmatrix} \cdot h_{s,j,i}(t)dz + \begin{bmatrix} K_{te} \\ K_{re} \\ K_{ae} \end{bmatrix} dz, \tag{4}$$

where K_{tc}, K_{rc}, K_{ac} – are coefficients related to the cutting process in the tangential, radial, and axial directions; K_{te}, K_{re}, K_{ae} – are coefficients related to the cutting edge; $h_{s,j,i}(t) = fz\ sin\varphi_{j,i}(t)$ – is the static instantaneous thickness of the uncut chip for the j-th cutting surface of the i-th segment; fz – is the feed per tooth.

The force impact on a low-stiffness part during machining inevitably leads to the reaction of the elastic system. Consequently, this results in the deflection to the actual radial depth of cut (RDOC) $a_{e,deff}(i, x)$ from its nominal value $a_{e,nom}$ (Fig. 2, b). As a result, the actual immersion angle $\varphi_{en,deff}(i, x)$ also differs from the nominal value $\varphi_{en,nom}$. Thus, the actual RDOC and the boundaries of the immersion angle are different for each position of the contact zone height i and each feed position x. Considering that the process is specifically climb milling, the actual RDOC $a_{e,deff}(i, x)$ and the resulting

actual immersion angle of the milling cutter's edge $\varphi_{en,deff}(i, x)$ with a diameter D are as follows:

$$a_{e,deff}(i, x) = a_{e,nom} - \Delta Y(i, x), \tag{5}$$

where $\Delta Y(i, x)$ – actual deflection of the part which is obtained using finite element analysis (FEA);

$$\phi_{en,deff}(i, x) = \pi - \arccos(1 - \frac{2a_{e,deff}(i, x)}{D}). \tag{6}$$

To assess the intensity of the action of a fluid jet on an elastic system of a thin-walled part and further modeling, it is necessary to determine the force acting on the surface and the velocity of the liquid jet. Under the considered boundary conditions of laminar flow and ideal incompressible fluid, Bernoulli's principle and the continuity equation are applied. The continuity equation asserts that under constant flow (steady flow), with the same mass entering the system as leaving it, the law of conservation of mass is applied. Regarding the fluid flow rate – $Q = A \cdot v_2$, where $A = \pi d^2/4$ is the cross-sectional area of the nozzle, v_2 is the velocity of the flow at the nozzle exit. Based on the definition of momentum in classical mechanics as the product of the mass of an object and its velocity, the force of the jet $F_{jet}(t)$ is given by:

$$F_{jet}(t) = \frac{1}{2}\pi d^2 p_1 = \rho Q \cdot v_2(t) = \rho \frac{1}{4}\pi d^2 \cdot v_2^2(t), \tag{7}$$

where p_1 – pressure inside the nozzle; ρ – density of the liquid. It's important to note that this equation assumes ideal boundary conditions for modeling and may need to be adjusted for real-world factors such as viscosity, friction, turbulence, and losses in the system.

The iterative adaptive algorithm is presented in order to combine the flexible milling force model and the fluid jet support impact.

3.2 Iterative Algorithm for Deflection Error Reduction Using Adaptive Fluid Jet Support

An adaptive iterative approach defines the part deflection based on cutting forces and jet velocities. Due to the relation between milling force and variable part deflection, the actual immersion angle (6) does not remain constant.

The immersion start angle should correspond to the variable geometry to achieve the required accuracy in milling complex thin-walled parts. In milling, the immersion angle is crucial in the cutter's entry into the material. This angle significantly affects the quality and precision of the finished part, especially parts with low rigidity.

Choosing the smallest immersion angle is essential to minimize the force on the part and reduce the risk of deformation. According to this, the algorithm (Fig. 3) can be broken down into sequential steps:

- preprocess of input parameters and boundary conditions for mesh generation of the thin-walled part and tool to perform further iterative computation;

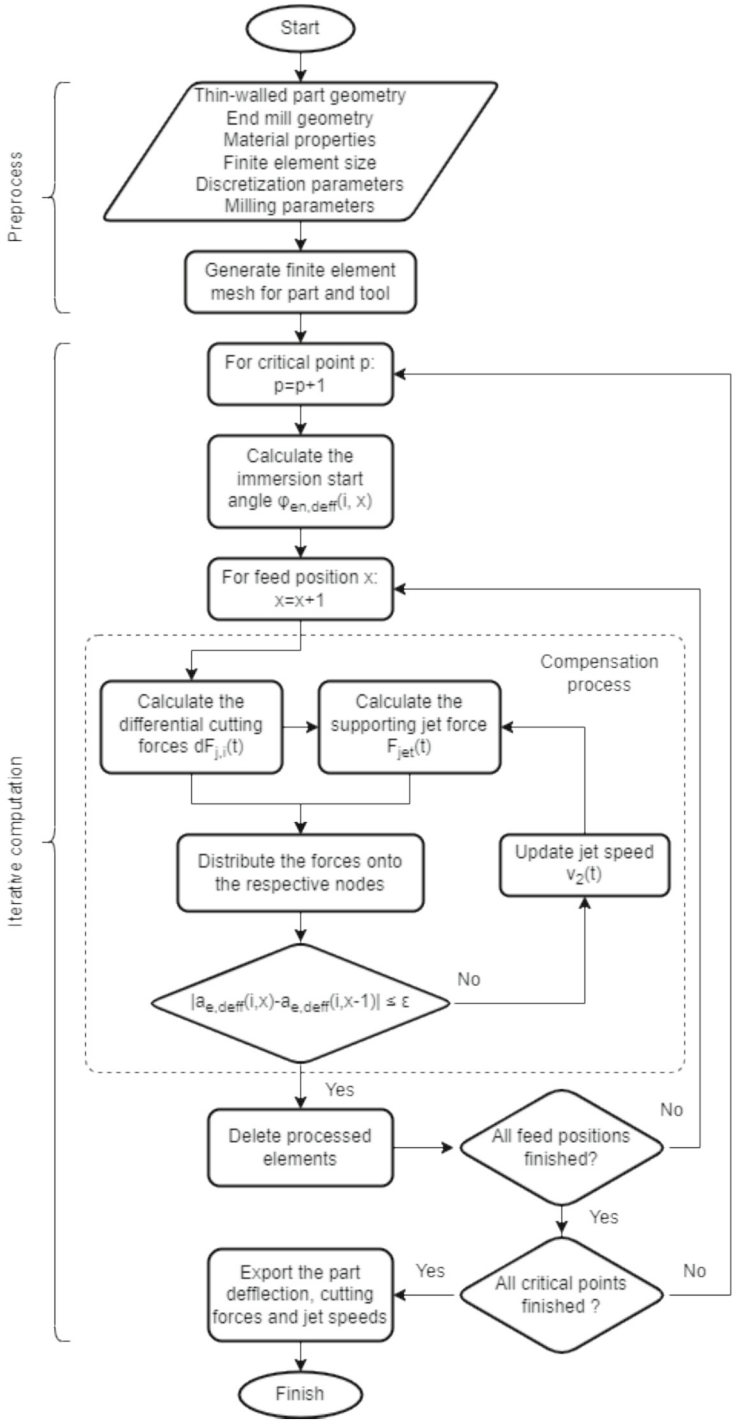

Fig. 3. An adaptive theoretical algorithm for deflection reduction by fluid jet support technique.

- design the set of critical points along the end mill pass. At each point the actual deflection $\Delta Y(i, x)$ is defined using FEA to calculate the actual RDOC (5) and immersion start angle $\varphi_{en,deff}(i, x)$ (6) for the region of that point;
- compensation process based on calculation and distribution onto the respective nodes of the differential cutting forces $dF_{j,i}(t)$ (2) and supporting jet forces $F_{jet}(t)$ (7). Subsequently, the fluid jet support velocity $v_2(t)$ is updated according to the condition of accuracy ε:

$$|a_{e,deff}(i, x) - a_{e,deff}(i, x - 1)| \leq \varepsilon. \tag{8}$$

The process repeats until convergence is achieved before the evaluation moves to the next step;

- completion of computation, deleting processed elements for the following position and critical point;
- export of data: a pass through all critical points should be completed to get the part deflection, cutting forces, and fluid jet velocities.

4 Results and Discussion

In order to verify the proposed approach, the axial turbine blade, as shown in Fig. 4, is used. Such components play a pivotal role in the efficiency and performance of various mechanical systems.

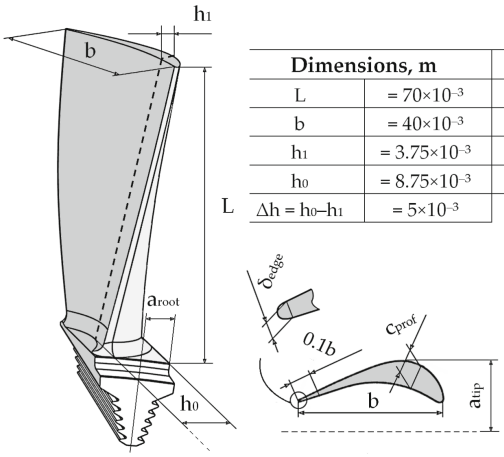

Dimensions, m		Tolerances, m	
L	$= 70\times10^{-3}$	a_{tip}	$\pm 0.3\times10^{-3}$
b	$= 40\times10^{-3}$	a_{root}	$\pm 0.2\times10^{-3}$
h_1	$= 3.75\times10^{-3}$	c_{prof}	$\pm 0.24\times10^{-3}$
h_0	$= 8.75\times10^{-3}$	δ_{edge}	$+0.15{-}0.1\times10^{-3}$
$\Delta h = h_0 - h_1$	$= 5\times10^{-3}$		

Fig. 4. The geometrical parameters of the axial turbine blade.

The part's material is AISI 4340 with density $\rho = 7850$ kg/m3, Young's modulus $E = 2.1{\cdot}10^{11}$ Pa, Poisson's ratio $\nu = 0.28$. The milling tool diameter is 8 mm with the number of flutes $z = 4$ and helix angle $\alpha = 30^{\circ}$. The boundary conditions were applied

to the shank. The jet diameter is 2 mm, the water density is 997 kg·m^{-3}, and the speed of sound in water is 1400 m·s^{-1}.

High-speed milling parameters:

- speed, n: 5593 rpm, v_c: 121.7 m/min;
- feed, v_f: 129 mm/s;
- tooth feed, f_z: 0.3458 mm;
- ADOC, a_p: 2 mm;
- RDOC, a_e: 0.3 mm.

Numerical simulations have been performed using the Abaqus/Explicit for milling operation (Fig. 5) and fluid jet support. Analyzing the machining of structural materials and their responses poses a challenging task due to the elevated strain rates involved. The complexity arises from the concurrent increase in temperature and consequential alterations in material properties, microstructure, and deformation processes. Consequently, selecting a material behavior model becomes crucial, one that comprehensively incorporates these dynamic factors to accurately capture the intricacies of the machining process under high strain rate conditions.

It is important to note that modeled and predicted forces by calculation do not rely on experimental studies data and assume limited boundary conditions. According to this, the analysis may need to be improved for real-world factors: the plough force, which is a parasitic force produced in contact with the blunt edge of the cutter and the flank face; the elastic deformation of the end mill tool in actual machining, which could lead to additional machining errors due to static deflections and dynamic vibration impact; models assume uniform material properties, but real-world materials can exhibit variations in hardness, thermal conductivity, and other properties, which can also lead to the impact of the residual stress in thin-walled structures; imperfections in the execution of equipment parts, real machines have inherent vibrations, dynamic stiffness which can lead to additional errors.

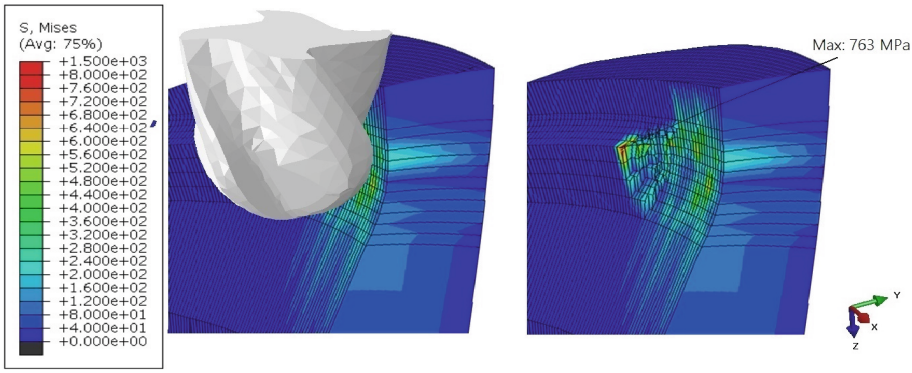

Fig. 5. FEM of the part machining based on the Johnson-Cook model.

The Johnson-Cook model is used for the fracture and plastic behavior of the material [28]. The model considers the influence of hardening, temperature variations, and

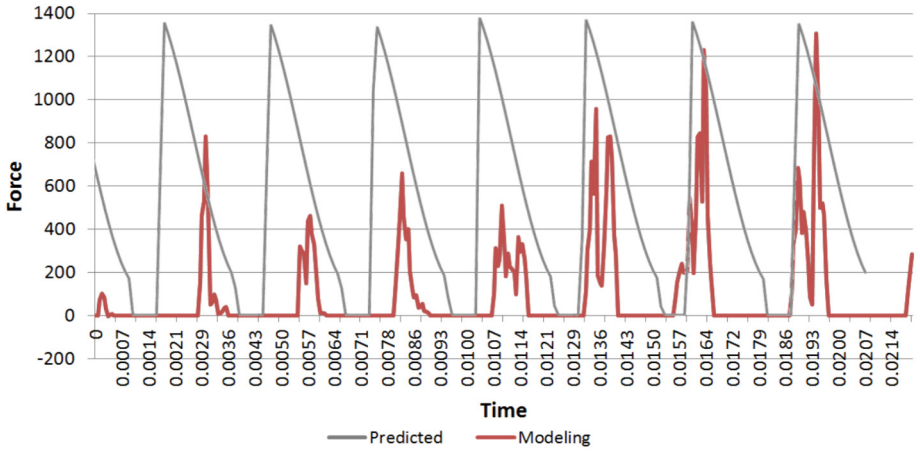

Fig. 6. Modeled and predicted cutting forces in the *Y* direction.

the corresponding alterations in strain rate. This model is extensively employed to predict cutting forces, chip morphology, residual stresses, and temperatures within the machining zone. The constants in Table 1 are presented.

Table 1. Steel alloy AISI 4340 Johnson-Cook model material constants.

Model	Material constant				
J.-C. plasticity	A, MPa	B, MPa	n	C	m
	792	510	0.26	0.014	1.03
J.-C. damage	d1	d2	d3	d4	d5
	0.05	3.44	-2.12	0.002	0.61

The F_y component of the cutting force that acts toward the minimum stiffness is the main factor to consider in thin-walled parts machining. As a result of cutting with a 4-flute end mill, 8 force bursts were obtained (Fig. 6, Table 2). The modeling results and prediction differ at the initial stages of cutting. This is caused by the fact that the analytical model does not consider the variability of the amount of allowance removed at the beginning of the cutting process and in the middle. However, when reaching the nominal depth, the magnitudes of the forces start to coincide.

The deviation of the predicted calculation model of the cutting force at the full cutting depth with the modeled one is 6%.

Smoothed Particle Hydrodynamics (SPH) particles have been employed for fluid flow modeling. The SPH method is particularly well-suited for scenarios characterized by intricate boundary dynamics, especially when dealing with freely flowing surface currents and substantial boundary displacements. The computational efficiency associated with the SPH method per particle quantity is lower than that of grid-based methods per

Table 2. The cutting forces and stresses from FEM results.

Parameter	Value							
Step time, s	6,e-4	0,003	0,005	0,008	0,011	0,014	0,017	0,021
Fy, N	101	831	463	658	508	957	1231	1306
Stress, MPa	548	551	680	703	711	747	755	763

cell quantity, particularly in cases where the metric of concern pertains to fluid density. The method enhances computational efficiency and facilitates the accurate simulation of fluid behavior in scenarios with complex boundary interactions.

The two case studies are provided. The first case study considers the application of the fluid jet support on the convex part of the blade. The second one considers the application on the concave part of the blade. The modeled directional milling force is applied according to the critical points.

In Fig. 7, a, the directional force of the cutter sample acts on the concave surface at the 1-st critical point of the thin edge of the blade profile. In Fig. 7, b, the directional force of the cutter sample acts on the convex surface at the 4-th critical point of the thick edge of the blade profile.

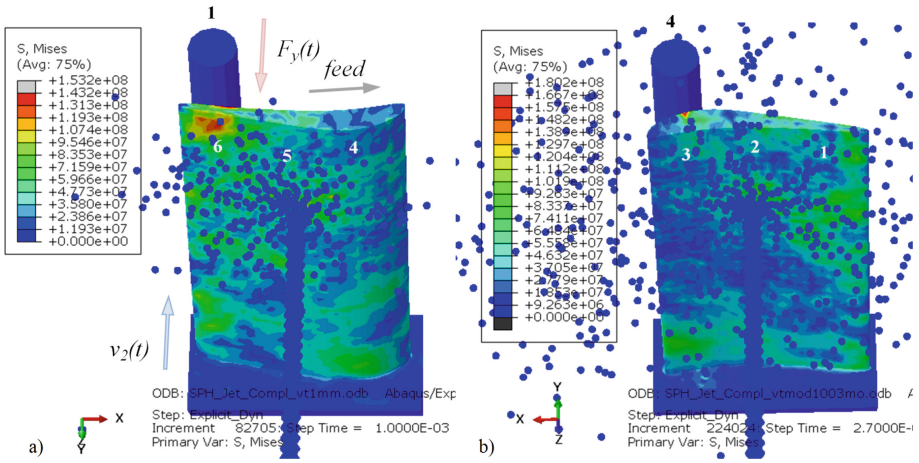

Fig. 7. FEM of the part support based on the SPH method.

According to the obtained results (Fig. 8, Table 3) of fluid jet support modeling, it can be seen that varying the flow velocity allows obtaining displacement values for the different critical points of directional force application within a narrow range of values from 0.01 mm at the first critical point to 0.00911 mm at the fourth one. The studied practical implication of varying fluid jet velocities is the alignment of the deflection at different end mill tool positions. The possible practical implications could be vibration

damping, improved surface finish, optimized material removal rates, and extended tool life.

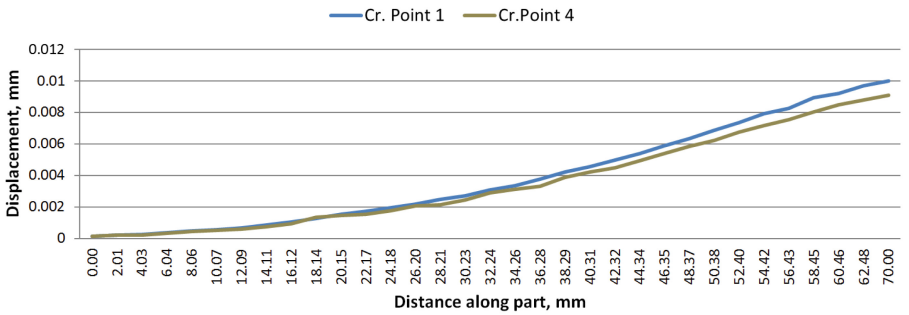

Fig. 8. Modeling of the impact of the fluid jet support on critical points of the part with a flow velocity $v_2 = 50$ m/s (a) and $v_2 = 36$ m/s (b).

Table 3. The deflections along the part from FEM results

Parameter	Value								
The distance along the part, mm	7.77	15.55	23.33	31.11	38.89	46.67	54.45	62.23	70.00
Cr. Point 1 defl., mm	1.35E − 04	4.74 E-04	8.54 E-04	1.74 E-03	2.71 E-03	4.22 E-03	5.90E-03	7.94E-03	1.00E-02
Cr. Point 4 defl., mm	1.31E − 04	4.30 E-04	7.59 E-04	1.54 E-03	2.44 E-03	3.89 E-03	4.96E-03	6.75E-03	9.11E-03

In aligning the overall error for critical points in various end mill tool positions, the indicators correspond to the permissible error equal to ± 0.3 mm in the last controlled section for the lengths up to 100 mm of the free end of the axial turbine blade.

A previous study [3] considered the effect of jet as a function of nozzle diameter. This led to the conclusion about the effective diameter and the SPH method for modeling, which served as the foundation for the current study. Under this condition, the thin-walled part exhibits pronounced curvature and variable stiffness. The variations in the jet velocity are being examined to correct the deflection error caused by the directional cutting force.

Observations reveal that the geometric shape of the wall significantly influences flow dynamics. A convex surface promotes a more significant liquid jet splash, while concave concentrates and sustains the flow, enhancing the jet's effectiveness. The critical points are introduced to consider the corresponding part stiffness variability. However, this solution may contribute to gradations among points regions within permissible error. Therefore, increasing the number of points is rational for actual implementation, which will reduce the discretization error. Additionally, the models consider the single local error maximum, not considering the possible effect of undulated surface errors [29] caused by the tool deflections.

The technique demands multiple models: one for calculating cutting force, requiring a fine mesh, and another for simulating the jet impact, which adds to the overall computation cost. Furthermore, the models focus on static part deformations, excluding dynamic effects like process instabilities in machining thin-walled components. While not a fully standalone solution for finishing process optimization, it is a complementary solution, addressing undesirable interactions in conjunction with other methods.

5 Conclusions

It proposes an approach to reduce machining errors in manufacturing thin-walled parts through adaptive fluid jet support during milling. The cutting force, rooted in a rigid model with thin-walled parts' feature additions, can apply the theoretical algorithm for the adaptive iterative fluid jet support technique. The study focuses on the static problem, dividing the cutter and part into integration segments to model forces in the milling process.

The presented single-point fluid jet support, although beneficial for stabilizing allowance removal and approximating the machining of low-rigid thin-walled parts to more rigid ones. However, the ability to compensate for significant torsion effects is questionable. It is emphasized that the equation for jet force assumes ideal boundary conditions, highlighting the need for adjustments to account for real-world factors such as viscosity, friction, turbulence, and system losses.

It is important to note that the technique provided is based on a static problem, and the algorithm presented is theoretical. The analysis of the F_y component of cutting force reveals disparities in modeling results and predictions at the initial stages, attributed to the analytical model's limitations in considering variability in allowance removal.

The fluid jet support modeling has additional surface roughness and flow boundary layer formation limitations. Despite the limitations, the results demonstrate the effectiveness of varying jet velocity in achieving displacement values for critical points, contributing to overall error alignment in various end milling tool positions. The findings underscore the potential of the proposed technique in reducing processing errors in thin-walled parts machining.

For further research, the approximation of the presented models to actual conditions and experimental validation of the proposed approach are considered to build the framework that aims to create a simulation-based compensation strategy and a combination of high computational efficiency, manageable model complexity, and accurate predictions.

References

1. Pavlenko, I., et al.: An increase in the energy efficiency of axial turbines by ensuring vibration reliability of blade milling. Energies **16**(3), 1511 (2023). https://doi.org/10.3390/en16031511
2. Wimmer, S., Hunyadi, P., Zaeh, M.F.: A numerical approach for the prediction of static surface errors in the peripheral milling of thin-walled structures. Prod. Eng. Res. Devel. **13**, 479–488 (2019). https://doi.org/10.1007/s11740-019-00901-7

3. Kononenko, S., Dobrotvorskiy, S., Basova, Y., Dobrovolska, L., Yepifanov, V.: Simulation of thin-walled parts end milling with fluid jet support. In: Ivanov, V., Trojanowska, J., Pavlenko, I., Zajac, J., Peraković, D. (eds.) DSMIE 2020. LNME, pp. 380–389. Springer, Cham (2020). https://doi.org/10.1007/978-3-030-50794-7_37
4. Petrakov, Y.V., Ohrimenko, O.A., Sikailo, M.O., Myhovych, A.V.: Cutting forces simulation for end milling. J. Eng. Sci. **10**(2), A27–A33 (2023). https://doi.org/10.21272/jes.2023.10(2).a4
5. Ge, G., Du, Z., Yang, J.: Rapid prediction and compensation method of cutting force-induced error for thin-walled workpiece. Int. J. Adv. Manuf. Technol. **106**, 5453–5462 (2020). https://doi.org/10.1007/s00170-020-05050-1
6. Masmali, M., Mathew, P.: An analytical approach for machining thin-walled workpieces. Procedia CIRP **58**, 187–192 (2017). https://doi.org/10.1016/j.procir.2017.03.186
7. Bolar, G., Joshi, S.N.: Numerical modeling and experimental validation of machining of low-rigidity thin-wall parts. In: Pande, S.S., Dixit, U.S. (eds.) Precision Product-Process Design and Optimization. LNMIE, pp. 99–122. Springer, Singapore (2018). https://doi.org/10.1007/978-981-10-8767-7_4
8. Sun, Y., Jiang, S.: Predictive modeling of chatter stability considering force-induced deformation effect in milling thin-walled parts. Int. J. Mach. Tools Manuf **135**, 38–52 (2018). https://doi.org/10.1016/j.ijmachtools.2018.08.003
9. Agarwal, A., Desai, K.A.: Tool and workpiece deflection induced flatness errors in milling of thin-walled components. Procedia CIRP **93**, 1411–1416 (2020). https://doi.org/10.1016/j.procir.2020.04.101
10. Li, Z., Yan, Q., Tang, K.: Multi-pass adaptive tool path generation for flank milling of thin-walled workpieces based on the deflection constraints. J. Manuf. Processes **68**, 690–705 (2021). https://doi.org/10.1016/j.jmapro.2021.05.075
11. Huang, N., Bi, Q., Wang, Y., Sun, C.: 5-Axis adaptive flank milling of flexible thin-walled parts based on the on-machine measurement. Int. J. Mach. Tools Manuf **84**, 1–8 (2014). https://doi.org/10.1016/j.ijmachtools.2014.04.004
12. Zhao, X., Zheng, L., Shi, M., Wang, Y.: Unified model towards service-oriented continuous-discrete hybrid adaptive milling system for thin-walled parts driven by in-process data. IFAC-PapersOnLine **55**(10), 2156–2161 (2022). https://doi.org/10.1016/j.ifacol.2022.10.027
13. Zhao, X., Zheng, L., Wang, Y., Zhang, Y.: Services-oriented intelligent milling for thin-walled parts based on time-varying information model of machining system. Int. J. Mech. Sci. **219**, 107125 (2022). https://doi.org/10.1016/j.ijmecsci.2022.107125
14. Tangestani, R., Chakraborty, A., Sabiston, T., Yuan, L., Ghasri-Khouzani, M., Martin, É.: Multi-scale model to simulate stress directionality in laser powder bed fusion: application to thin-wall part failure. Mater. Des. **232**, 112147 (2023). https://doi.org/10.1016/j.matdes.2023.112147
15. Sulitka, M., Falta, J., Stejskal, M., Kociánová, B.: Integrated force interaction simulation model for milling strategy optimization of thin-walled blisk blade machining. Procedia CIRP **102**, 174–179 (2021). https://doi.org/10.1016/j.procir.2021.09.030
16. Polishetty, A., Goldberg, M., Littlefair, G., Puttaraju, M., Patil, P., Kalra, A.: A preliminary assessment of machinability of titanium alloy Ti 6AL 4V during thin wall machining using trochoidal milling. Procedia Eng. **97**, 357–364 (2014). https://doi.org/10.1016/j.proeng.2014.12.259
17. Wan, X.-J., Hua, L., Wang, X.-F., Peng, Q.-Z., Qin, X.: An error control approach to tool path adjustment conforming to the deformation of thin-walled workpiece. Int. J. Mach. Tools Manuf **51**, 221–229 (2011)
18. Ratchev, S., Govender, E., Nikov, S., Phuah, K., Tsiklos, G.: Force and deflection model-ling in milling of low-rigidity complex parts. J. Mater. Process. Technol. **143–144**, 796–801 (2003)

19. Wang, M.-H., Sun, Y.: Error prediction and compensation based on interference-free tool paths in blade milling. Int. J. Adv. Manuf. Technol. **71**, 1309–1318 (2014)
20. Ramanaiah, B.V., Manikanta, B., Ravi Sankar, M., Malhotra, M., Gajrani, K.: Experimental study of deflection and surface roughness in thin wall machining of aluminum alloy. Mater. Today Proc. **5**, 3745–3754 (2018)
21. Scippa, A., Grossi, N., Campatelli, G.: FEM based cutting velocity selection for thin walled part machining. Procedia CIRP **14**, 287–292 (2014). https://doi.org/10.1016/j.procir.2014.03.023
22. Munoa, J., Sanz-Calle, M., Dombovari, Z., Iglesias, A., Pena-Barrio, J., Stepan, G.: Tuneable clamping table for chatter avoidance in thin-walled part milling. CIRP Ann. **69**(1), 313–316 (2020). https://doi.org/10.1016/j.cirp.2020.04.081
23. Wang, J., Ibaraki, S., Matsubara, A.: A cutting sequence optimization algorithm to reduce the workpiece deformation in thin-wall machining. Precis. Eng. **50**, 506–514 (2017). https://doi.org/10.1016/j.precisioneng.2017.07.006
24. Pavlenko, I., et al.: Using regression analysis for automated material selection in smart manufacturing. Mathematics **10**(11), 1888 (2022). https://doi.org/10.3390/math10111888
25. Ivchenko, O., et al.: Method for an effective selection of tools and cutting conditions during precise turning of non-alloy quality steel C45. Materials **15**(2), 505 (2022). https://doi.org/10.3390/ma15020505
26. Arnaud, L., Gonzalo, O., Seguy, S., Jauregi, H., Peigné, G.: Simulation of low rigidity part machining applied to thin-walled structures. Int. J. Adv. Manuf. Technol. **54**, 479–488 (2011). https://doi.org/10.1007/s00170-010-2976-9
27. Altintas, Y.: Manufacturing Automation: Metal Cutting Mechanics, Machine Tool Vibrations, and CNC Design, 2nd edn. Cambridge University Press, Cambridge (2012)
28. Navarro, P.F., Chiu, P.-H., Higgins, A., Serge, M., Benson, D.J., Nesterenko, V.F.: Shear band patterning and post-critical behavior in AISI 4340 steel with different microstructure. Int. J. Impact Eng **112**, 144–154 (2017). https://doi.org/10.1016/j.ijimpeng.2017.10.011
29. Wimmer, S., Zaeh, M.: The prediction of surface error characteristics in the peripheral milling of thin-walled structures. J. Manuf. Mater. Process **2**(1), 13 (2018). https://doi.org/10.3390/jmmp2010013

The Influence of Cutting Forces on Cracks Formation During the Grinding of Products from Materials Prone to Defect Formation

Maksym Kunitsyn(✉), Anatoly Usov, and Yuriy Zaychyk

Odesa Polytechnic National University, 1, Shevchenko Avenue, Odesa 65044, Ukraine
m.v.kunitsyn@op.edu.ua

Abstract. This study examines how cutting forces impact the formation of cracks and chips on surfaces during the grinding of products. Understanding the structure of the grinding process is crucial for identifying ways to increase the output of suitable parts from materials prone to defect formation during final grinding operations, as primary defects such as cracks and chipping occur precisely during final processing. Friction between the abrasive and the processed metal plays a significant role in forming radial and tangential stresses in the surface layer. As the friction coefficient increases, the zone of maximum stress moves closer to the surface of the part being ground, which affects the formation of grinding cracks. The depth of grinding is one factor determining the appearance of these cracks. Stresses generated in the surface layer during processing with a significant grinding depth with solid circles are tensile, contributing to an intensive cracking process. We considered the stress-deformed state of the surface layer of the processed parts under the action of the component grinding forces of cutting force and friction force to clarify their role in the formation of grinding cracks. Using lubricating and cooling technological media reduces the grinding temperature and friction forces between the wheel and the processed material, thereby reducing the intensity of cracking and chipping.

Keywords: Grinding · Cutting Forces · Friction · Defects · Crack · Abrasive · Surface Layer · Grain · Manufacturing Innovation

1 Introduction

Various technological operations contribute to the appearance of inherited defects in the surface layer, which include non-metallic inclusions, flakes, air pores, microcracks of a shrinkage nature (melting), deformation of crystal grains, cracks of liquid origin (forging, drawing, coarse-graining, accumulation of carbides), chips, ruptures, network of surface cracks, internal cracks, exfoliation (finishing operations), spalling. These defects, being stress concentrators, contribute to the formation of cracks, both in processing the material and during their operation.

© The Author(s), under exclusive license to Springer Nature Switzerland AG 2024
V. Ivanov et al. (Eds.): DSMIE 2024, LNME, pp. 240–250, 2024.
https://doi.org/10.1007/978-3-031-61797-3_20

Losses from defects due to hereditary defects in finishing operations are especially significant. As the final operation for most parts, grinding increases operational properties significantly due to high accuracy and low roughness. It is accompanied by high-temperature exposure, which leads to cauterization and significant failure from the output of suitable products due to the formation of cracks [1].

Reducing defects in the finishing operations of these materials and improving the operational properties of products made are essential national economic tasks, significantly saving material resources, labor intensity, and cost of manufacturing parts [2].

Analysis of the causes of cracking during grinding of alloys with low mechanical properties, such as cast iron-nickel-aluminum-based hard magnetic type (e.g., Alnico AL-CA-36/164 and AL-CA-38/141), determined the choice of cutting forces as a criterion for the conditions for the appearance of grinding cracks on the treated surface. Thus, in [3], experimental studies of the influence of cutting forces during grinding on the quality characteristics of the machined surfaces of parts made of materials prone to cracking without generalization and analysis of the component friction forces in this process are given.

The aim of the study. Investigate the influence of cutting forces on the formation of cracks during grinding products of materials prone to defect formation.

To achieve the goal of the research, it is necessary to consider the following:

1 Patterns of radial and tangential stresses formation in the surface layer of products.
2 The nucleation mechanism of grinding cracks from the friction between the abrasive and the treated metal.
3 To propose technological methods that reduce the grinding temperature and friction forces between the wheel and the processed material, thereby reducing the intensity of defect formation.

2 Literature Review

One of the features of the grinding process is the instability of the cutting forces P_Z and P_Y. The nature of wheel wear mainly determines the nature of their change.

Intense sticking of metal to the cutting grains of the wheel impairs its cutting ability and increases the grinding effort. Blunting of abrasive grains also leads to a change in cutting forces [4]. At the same time, it is possible to increase the cutting forces P_Z and P_Y, compared with a sharp wheel by 1.7 and 3.4 times, respectively [5].

In addition, changing grinding modes, in particular, reducing the wheel's rotation frequency and increasing the speed of the part and the grinding depth, also contributes to increasing the cutting forces [4, 5].

Therefore, it is possible that during mechanical processing, alloys with relatively low strength properties, with a specific combination of modes of cutting forces, especially the tangential component P_Z, determine the conditions of cracking of the treated surfaces.

The grinding operation is the main processing operation of heavily loaded parts made of high-strength steel and alloys, which include gears, shafts, dies, elements of electric machines, and electronics [4]. This operation also applies to products whose working surfaces have increased requirements for accuracy and roughness, which significantly

affect their operational properties [5]. Such products include parts with wear-resistant coatings and highly coercive magnets of the cast iron-nickel-aluminum-based hard magnetic type (e.g., Alnico AL-CA-36/164 and AL-CA-38/141), which are used in modern electrical machines, devices, and apparatus.

The tendency of metals to form cracks during grinding depends on metallurgical and structural heredity, which is determined by smelting methods and the degree of deoxidation, phase transformations in alloys, thermal, chemical-thermal treatment modes, and operations preceding the finish [6]. The parameters that consider the stress state's dependence on the structural components are a set of mechanical characteristics (K_{1C}, K_C, K_{ISC}, and K_{th}) of fracture mechanics [7].

However, currently, available models of thermal processes of diamond-abrasive processing are obtained on the assumption of homogeneity of the materials being polished, and the presence of defects in the technological heredity of the products needs to be considered [8]. In these works, the condition of the surface layer of the part is considered mainly from a qualitative point of view or is evaluated in each case by experimental methods [9]. Thus, the susceptibility of magnetic alloys to crack formation during their grinding processing is associated with the features of their magnetic and crystalline structure, designed to obtain high magnetic properties [10]. The absence of quantitative relationships between the crack resistance of magnets and other properties does not allow us to use the existing information base of defect-free grinding unambiguously [11].

The study of the influence of technological parameters on the formation of cracks and the formation of quality characteristics of grinding surfaces is to be established.

The friction between the abrasive and the processed metal significantly affects the formation of radial and tangential stresses in the surface layer. As the friction coefficient increases, the zone of maximum stress moves to the surface of the workpiece. Such displacement affects the formation of grinding cracks.

3 Research Methodology

Studies of mathematical models of grinding forces [12, 13] show that the forces that participate in grinding consist of two components – actual cutting forces and frictional forces. Simultaneously, the ratio of the actual cutting and frictional forces of the tangent and standard components lie within limits limited to the values of 0.20–0.59.

Experimental studies of grinding forces allow us to consider them by parts in the form of:

$$\begin{aligned} P_y &= P_{yc} + P_{y\mu} \\ P_z &= P_{zc} + P_{z\mu} \end{aligned} \tag{1}$$

where P_y – the normal grinding force; P_z – the tangential force of grinding; P_{yc}, P_{zc} – the normal and tangential components of forces that contribute to chip formation; $P_{y\mu}$, $P_{z\mu}$ – the normal and tangential components of forces caused by friction, respectively.

There is an inverse influence between the grinding force and the zone of the wheel wear plane, provided that the parameters of the kinematic process remain constant, Fig. 1. During the normal grinding process, which guarantees the absence of burning, the normal grinding force P_y increases linearly with the increase of the wear area of the

wheel, indicating that the average contact pressure P between the wear planes and the processing area also increases gradually and proportionally to the hardness of the material being processed. Since the tangential force also increases linearly with an increase in the area of the wear plane, the coefficient of sliding friction μ between the wear planes and the processing area remains constant.

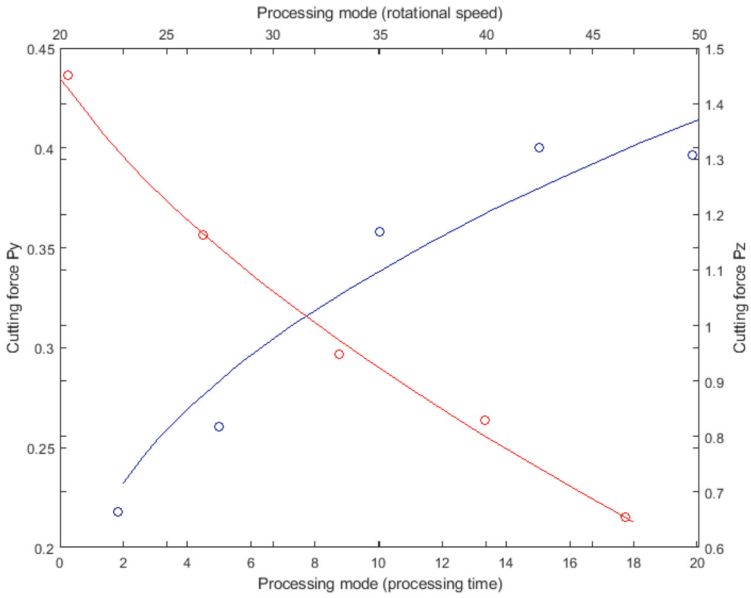

Fig. 1. The influence of processing modes on the value of cutting forces P_y and P_z (e. g. steels 14NiCr14, X12Ni5, 13NiCr14).

The coefficient of sliding friction is equal to the ratio between the slope of the shear force curve and the slope of the normal force curve.

If S_K^* represents the zone of actual contact between the wheel and the workpiece, then:

$$\begin{aligned} P_y &= P_{yc} + S_K^* \overline{P} \\ P_z &= P_{zc} + \mu S_K^* \overline{P} \end{aligned} \tag{2}$$

For the cutting force created by a single grain, the following result can be obtained:

$$\begin{aligned} P_{ey} &= P_{eyc} + P_{ey\mu} = P_{eyc} + \delta_e \overline{P} \\ P_{ez} &= P_{ezc} + P_{ez\mu} = P_{ezc} + \mu \delta_e \overline{P} \end{aligned} \tag{3}$$

where δ_e – the front zone of the active grain (a zone of actual contact of the active grain with the processed surface).

The relationship between the chipping force expressed in formulas (2) and (3) and the cross-section of the chipping was obtained from the results of the experiment (Fig. 2). It is known that the cutting force always has a linear dependence on the chip thickness

d_c. If $d_c = 0$, the cutting force equals the residual compressive force. Therefore, by subtracting the compression force from the total cutting force, we can find the force produced by the chip, which is proportional to the thickness of the raw chip. In the case of a pure chipping process, the following equation $P_E = K_1 Q$ occurs, where K_1 is the specific force of chip formation, included in the normal grinding force.

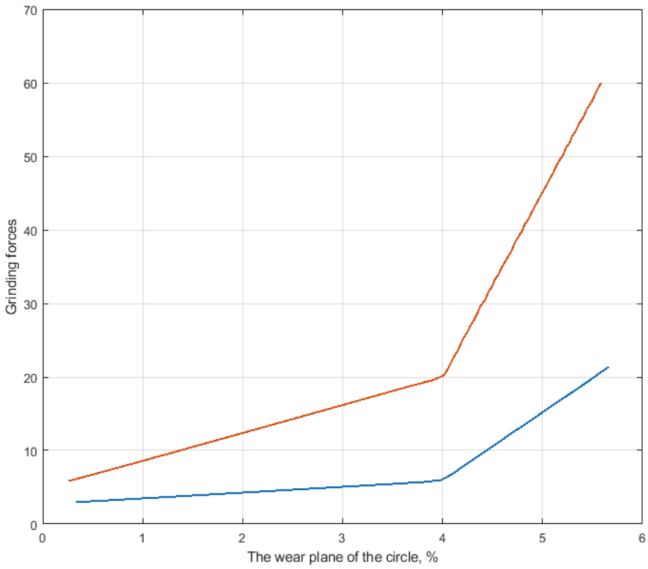

Fig. 2. The influence of the zone of the wheel wear plane on the grinding forces P_y and P_z.

As for the tangential chipping force, it should be noted that if we take the cone-shaped shape of the grains and their orientation in the direction of the radius of the circle, then the following ratio can be obtained:

$$\frac{\mathrm{P}_{ezc}}{\mathrm{P}_{eyc}} = \frac{\pi}{4\mathrm{tg}\,\theta} = \varphi \tag{4}$$

where θ is half the angle of the upper part of the grains. Then:

$$\mathrm{P}_{ezc} = \varphi k_2 Q \tag{5}$$

From Eqs. (3)–(5), it can be found:

$$\mathrm{P}_{ey} = k_1 Q + \delta_e \overline{\mathrm{P}}$$
$$\mathrm{P}_{ez} = \varphi k_1 Q + \mu \delta_e \overline{\mathrm{P}}$$

The normal P'_Y and tangential P'_Z grinding forces per unit of grinding width S^*_T, acting between the wheel and the processing zone are equal to the sum of the normal and

tangential forces of all active grains in the contact zone between the wheel and the processing zone per unit grinding width:

$$\begin{aligned} \mathrm{P}'_y &= \Sigma_{i=1}^{n}\left(\mathrm{P}^i_{eyc} + \mathrm{P}^i_{ey\mu}\right) = \mathrm{P}'_{yc} + \mathrm{P}'_{y\mu} \\ \mathrm{P}'_z &= \Sigma_{i=1}^{n}\left(\mathrm{P}^i_{ezc} + \mathrm{P}^i_{ez\mu}\right) = \mathrm{P}'_{zc} + \mathrm{P}'_{z\mu} \end{aligned} \tag{6}$$

Thus, the chip-forming force is part of the total normal grinding force per unit area of wear, equal to (Fig. 1):

$$\mathrm{P}'_{yc} = \Sigma_{i=1}^{n} k_1 Q_i = k_1 \Sigma_{i=1}^{n} Q_i \tag{7}$$

where ΣQ_i is the total value of all chip cross-sections per unit of grinding width. From here, we can get an expression for ΣQ_i, considering the kinematic parameters of the grinding process in the form:

$$\Sigma_{i=1}^{n} Q_i = \frac{V_g}{V_{k\rho}} t_{\text{ø}\ddot{e}} \tag{8}$$

$$\mathrm{P}'_{yc} = k_1 \frac{V_g}{V_{k\rho}} t_{\text{ø}\ddot{e}} \tag{9}$$

From Eq. (3), the normal component of the total grinding force per unit of grinding width $P'_{Y\mu}$ is given by the formula $P'_{Y\mu} = N\overline{\delta}_e\overline{P}$, where N is the number of all simultaneously working grains per unit of grinding width, and $\overline{\delta}_e$ is the average peak area per active number of grains.

Integrating the function P'_Y over the total contact length from $L = 0$ to $L = L_K$, we obtain:

$$\mathrm{P}'_y = \int_0^{L_k} \mathrm{P}'_y(l)dl \tag{10}$$

Using existing models of forces generated during grinding [12, 13] for working grains, it was found:

$$\mathrm{P}'_{y\mu} = \frac{\overline{\delta\mathrm{P}}A}{1+\alpha}[C_1]^{\beta}\left[\frac{V_g}{V_{k\rho}}\right]^{\alpha}\left[t_{\text{ø}\ddot{e}}\right]^{\frac{1+\alpha}{2}}\left[D_{k\rho}\right]^{\frac{1-\alpha}{2}} \tag{11}$$

where A is the proportionality factor; C_1 is the statistical density of the distribution of the cutting edges of the grains of the circle; α, β are index coefficients associated with the distribution of edges on the periphery of the circle and vary within $0 < \alpha < 2/3$; $S < \beta < 2/3$.

Adding the chip-forming component and the friction component included in the normal grinding force per unit of grinding width, we get:

$$P'_y = k_1 \frac{V_\partial}{V_{k\rho}} t_{\text{ø}\ddot{e}} + \frac{\overline{\delta P}A}{1+\alpha}[C_1]^{\beta}\left[\frac{V_\partial}{V_{k\rho}}\right]^{\alpha} t_{\text{ø}\ddot{e}}^{\frac{1+\alpha}{2}} D_{k\rho}^{\frac{1-\alpha}{2}} \tag{12}$$

Similarly, for the tangential grinding force per unit of grinding width, we have:

$$P'_z = \varphi k_1 \frac{V_\partial}{V_{k\rho}} t_{\text{ø}\ddot{e}} + \frac{\mu\overline{\delta\mathrm{P}}A}{1+\alpha}[C_1]^{\beta}\left[\frac{V_\partial}{V_{k\rho}}\right]^{\alpha} t_{\text{ø}\ddot{e}}^{\frac{1+\alpha}{2}} D_{k\rho}^{\frac{1-\alpha}{2}} \tag{13}$$

Thus, a model of grinding forces consisting of two terms is built. The first term corresponds to the chipping force, and the second to the friction force.

In practice, cracks often appear when grinding in circles with three dull grains. Therefore, it is logical to assume that the nucleation mechanism of grinding cracks is influenced to a greater extent by the components of friction forces $P_{Y\mu}{}'$ and $P_{Z\mu}{}'$.

4 Results and Discussion

To finally clarify their role in the formation of grinding cracks, consider the problem of the stress-deformed state of the surface layer of the processed parts under the action of the component grinding forces - $P'_{Y\mu}$ and $P'_{Z\mu}$.

The mathematical formulation of the problem contains the Lamé Eqs. (14), (15) [14], the right-hand part of which includes the forces - $P'_{Y\mu}$ and $P'_{Z\mu}$. In this case, the boundary conditions will be as follows (16):

$$\begin{array}{c} \frac{\partial\theta}{\partial x}\cdot\frac{1}{1-2\mu}+\Delta\vec{U}=b^T\frac{\partial T}{\partial x};\ \vec{U}=\frac{U}{2G};\ \vec{V}=\frac{V}{2G};\\ \frac{\partial\theta}{\partial y}\cdot\frac{1}{1-2\mu}+\Delta\vec{U}=b^T\frac{\partial T}{\partial y};\ b^T=\frac{4G(1+\mu)}{1-2\mu}\alpha t \end{array} \tag{14}$$

$$\begin{array}{c} \sigma_x(x,y)|_{x=0}=0,\ |y|>a;\\ \tau_x(x,y)|_{x=0}=0,\ |y|>a; \end{array} \tag{15}$$

$$\left(\tau_{xy}+\mu\sigma_x\right)\big|_{x=0}=0,\ u=\frac{x^2}{2R},\ |y|<a \tag{16}$$

The last condition should be understood as follows. Below the circle is a linear relationship between normal pressure and tangential load. In addition, the amount of displacement U in the contact zone $2a$ of the circle with the part is replaced by a parabola for simplification; μ is the coefficient of friction between the abrasive and the treated metal.

We will search for the elastic normal $\sigma_x(x,y)$ and tangential $\tau_{xy}(x,y)$ stresses arising in the surface layer through the Airy stress function $\Phi(x,y)$ [15]:

$$\sigma_x=\frac{\partial^2\Phi}{\partial y^2};\ \sigma_y=\frac{\partial^2\Phi}{\partial x^2};\ \tau_{xy}=-\frac{\partial^2\Phi}{\partial x\partial y} \tag{17}$$

If we use the representation of the stress function $\Phi(x,y)$ through a combination of the complex functions $\Phi(Z)$ and $\Psi(Z)$, $Z=x+i$y and related functions $\overline{\Phi}(Z)$ and $\overline{\Psi}(Z)$ [16, 17]. Then, we get the formulas for the maximum tangential stress $\tau_{xy}^{\max}$ and the main stresses σ_1 and σ_2:

$$\begin{array}{l} \sigma_1=\left[\Phi(Z)+\overline{\Phi}\left(\overline{Z}\right)\right]+\left[\overline{Z}\Phi(Z)+\Phi(Z)\right]\\ \sigma_2=\left[\Phi(Z)+\Phi\left(\overline{Z}\right)\right]-\left[\overline{Z}\Phi(Z)+\Phi(Z)\right]\\ \sigma_1+\sigma_2=\sigma_x+\sigma_y\\ \tau_{xy}^{\max}=\left[\overline{Z}\Phi'(Z)+\Psi'(Z)\right] \end{array} \tag{18}$$

The functions $\Phi(Z)$ and $\Psi(Z)$, in turn, are determined from the relations [15]:

$$\begin{array}{l} \Phi(Z)=-\frac{1}{2\pi i}W_1(Z)+\frac{1}{2\pi i}W_2(Z)\\ \Psi(Z)=-\frac{1}{\pi}W_2(Z)+\frac{1}{2\pi i}W_1'(Z)-\frac{Z}{2\pi}W_2'(Z) \end{array} \tag{19}$$

where $W_1(Z)$ and $W_2(Z)$ are functions of a complex variable, representing Cauchy-type integrals, the densities of which are equal to normal pressure values and tangential forces acting on the part's surface, respectively.

Solving the inhomogeneous Riemann-Hilbert problem Eqs. (14), (15), we determine the function $W_1(Z)$. The specific pressure in the contact zone of the circle with the part is determined by the formula [18, 19]:

$$\sigma_x(0, y) = \frac{\sin \pi \Theta^*}{\pi} \frac{P_y}{\sqrt{a^2 - y^2}} \left(\frac{a + y}{a - y} \right)^{\frac{1}{2} - \Theta^*} \tag{20}$$

where $\theta^* = \frac{1}{\pi} \text{atan} \left[\frac{1-2\nu}{2\rho(1-\nu)} \right]$; ν – the Poisson's ratio; E – the modulus of elasticity of the material being ground.

If $2a = L_k = \sqrt{D_{k\rho} t_{\emptyset \ddot{e}}}$ then the expression for normal stresses can be rewritten as follows:

$$\sigma_x(0, y) = \frac{\sin \pi \Theta^*}{\pi} \frac{P_y}{\sqrt{Dt - y^2}} \left(\frac{\sqrt{Dt} + y}{\sqrt{Dt} - y} \right)^{\frac{1}{2} - \Theta^*} \tag{21}$$

The tangential load τ_{xy}, which contributes to the opening of grinding cracks, is determined by the known pressure:

$$\tau_{xy}(0, y) = \frac{\mu \sin \pi \Theta^*}{\pi} \frac{P_y}{\sqrt{Dt - y^2}} \left(\frac{\sqrt{Dt} + y}{\sqrt{Dt} - y} \right)^{\frac{1}{2} - \Theta^*} \tag{22}$$

It can be noted that the presence of frictional forces between the abrasive and the metal leads to the point where the tangential stress reaches its maximum value, moving to the surface of the part. Figures 3 and 4 show isoclines, that is, lines of equal principal shear stresses in the absence ($\mu = 0$) (Fig. 2 (a)) and in the presence (Fig. 2b) ($\mu \neq 0$) of frictional forces. The significant influence of friction forces on the nature of crack formation is also confirmed by the fact that the trajectory of the cracks is most often located perpendicular to the direction of processing. The characteristic appearance of grinding cracks obtained during the processing of magnets with a dull circle (e.g., Alnico AL-CA-38/141), i.e., when the tangential stresses reach maximum values, is experimentally demonstrated. Existing technological methods that reduce friction between the abrasive and the processed metal are the impregnation of wheels [12, 13], their periodic adjustment, and lubricating and cooling process media.

Various lubricating and cooling technological media, which have diverse compositions and physical and chemical properties, are used during grinding. They have a significant impact on the productivity and quality of the processing of parts due to the reduction of the grinding temperature, [20] the energy spent on overcoming the friction force between the abrasive grains and the bond between the wheel and the processed material, thereby reducing the intensity of the formation of cracks on the surface being ground.

It can be seen from theoretical studies that the value of the coefficient of friction ρ between the abrasive and the processed metal significantly affects the value of tensile

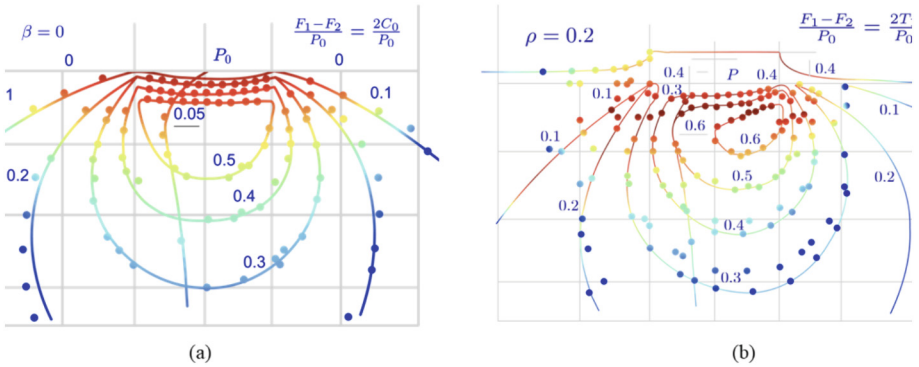

Fig. 3. Distribution of equal main lines of shear stresses (a) in the absence of frictional forces and (b) in the presence of frictional forces.

stresses. As studies [2, 15, 21] show, the grinding coefficient is an authentic reflection of the friction coefficient during grinding. Defect-free grinding of materials with low mechanical characteristics is possible when cutting forces are limited. In particular, the tangential component P_Z, and the coefficient of friction ρ for the abrasive with the processed metal is reduced.

Thus, from studies of the influence of cutting forces on the stress state of the surface layer, one additional condition for defect-free grinding can be constructed [20]:

$$P_z \leq \frac{\pi\sqrt{Dt_{\text{ґё}}}}{KP^2 \sin\pi\theta}\left\{[\tau]_C - \frac{E\rho\sqrt{Rt}}{2(1-\nu^2)\sqrt{R}}\right\}, \tag{23}$$

where $[\tau]$ is the ultimate shear stress value; $\theta = \frac{1}{\pi}\text{atan}\left[\frac{1-2\nu}{2\rho(1-\nu)}\right]$; ρ is the minimum possible value of the coefficient of friction between the abrasive and the treated metal, which is provided using lubricating and cooling technological media and wheel impregnation compositions; K is the ratio coefficient $\frac{P_Y}{P_Z}$.

5 Conclusions

As a result of this study, it was found that after processing, the interaction of the abrasive and the metal significantly influences the formation of radial and tangential stresses on the surface. As the friction coefficient increases, the area of highest stress shifts to the surface, which affects the development of grinding cracks. The depth of grinding is one factor determining the emergence of grinding cracks. The stresses produced in the surface layer during processing with a significant grinding depth with solid circles create tensile forces, intensifying the cracking process. Additionally, the SIF also increases with an increase in grinding depth. Using lubricants and cooling agents reduces the temperature of grinding, the friction between the wheel and the processed material, and the cracking intensity.

References

1. Bhargava, G.K., Sharma, P., Bhardwaj, S., Sharma, I. (eds.) An Introduction To Hard Ferrites: From Fundamentals To Practical Applications. Materials Research Forum LLC (2023)
2. Li, L., et al.: Mechanical behavior and modeling of grinding force: a comparative analysis. J. Manuf. Process. **102**, 921–954 (2023). https://doi.org/10.1016/j.jmapro.2023.07.074
3. Zawada-Tomkiewicz, A., Wierucka, I.: A case study in technological quality assurance of a metric screw thread. Measurement **114**, 208–217 (2018). https://doi.org/10.1016/j.measurement.2017.09.021
4. De Oliveira, D., et al.: Abrasive and non-conventional post-processing techniques to improve surface finish of additively manufactured metals: a review. Prog. Addit. Manuf. **8**(2), 223–240 (2023). https://doi.org/10.1007/s40964-022-00325-3
5. Romanov, P.I.: Influence of process parameters on magnetic abrasive machining efficiency. E3S Web of Conferences, vol. 389, p. 01074. Petersburg, Russia (2023). https://doi.org/10.1051/e3sconf/202338901074
6. Yang, M., et al.: Temperature field model in surface grinding: a comparative assessment. Int. J. Extreme Manuf. **5**(4), 042011 (2023). https://doi.org/10.1088/2631-7990/acf4d4
7. Zhi, G., Li, X., Luo, A., Yang, J., Rong, Y.: An experimental investigation on response of CBN super abrasive's grinding performance and failure characteristics to the grinding speed. Exp. Tech. **41**(2), 117–130 (2017). https://doi.org/10.1007/s40799-016-0159-9
8. Pratap, A., Patra, K., Dyakonov, A.A.: A comprehensive review of micro-grinding: emphasis on toolings, performance analysis, modeling techniques, and future research directions. Int. J. Adv. Manuf. Technol. **104**(1–4), 63–102 (2019). https://doi.org/10.1007/s00170-019-03831-x
9. Schobesberger, M., Helmhagen, S., Mende, S., Berensmeier, S., Fraga-García, P.: From micro to nano: grinding natural magnetite ore for microalgae harvesting. Magnetochemistry **9**(6), 149 (2023). https://doi.org/10.3390/magnetochemistry9060149
10. Zhang, S., Gong, M., Lian, H., Wu, J., Zhu, W., Ou, Z.: Design of a high-speed rotary ultrasonic machining machine tool for machining microstructure of brittle materials. Micromachines **14**(8), 1544 (2023). https://doi.org/10.3390/mi14081544
11. Chen, Z., Xie, J., He, Q., Yang, H., Luo, Y.: Improving metal surface integrity by integrating mechanical stress fields during micron- and nano-abrasive machining. Int. J. Mech. Sci. **240**, 107928 (2023). https://doi.org/10.1016/j.ijmecsci.2022.107928
12. Kühn, F., Hendricks, S., Troß, N., Brimmers, J., Bergs, T.: Experimental analysis on the influence of the tool micro geometry on the wear behavior in gear hobbing. Int. J. Adv. Manuf. Technol. **126**(3–4), 1279–1292 (2023). https://doi.org/10.1007/s00170-023-11158-x
13. Brodyanski, A., Klein, M.W., Merz, R., Smaga, M., Beck, T., Kopnarski, M.: Microstructural changes caused by friction loading in high manganese TWIP steel and case-hardened 16MnCr5. Mater Charact **163**, 110231 (2020). https://doi.org/10.1016/j.matchar.2020.110231
14. Popov, G.Y., Protserov, Y.S.: Axisymmetric problem for an elastic cylinder of finite length with fixed lateral surface with regard for its weight. J. Math. Sci. **212**(1), 67–82 (2015). https://doi.org/10.1007/s10958-015-2649-1
15. Freiman, S.W., Mecholsky, J.J.: The Fracture of Brittle Materials: Testing and Analysis. John Wiley & Sons. New Jersey, United States (2019). https://doi.org/10.1002/9781118147757
16. Fuchs, B.A., Shabat, B.V.: Functions of a Complex Variable and Some of Their Applications. Elsevier, London (2014)
17. Durège, G.E.: Elements of the Theory of Functions of a Complex Variable with Especial Reference to the Methods. Legare Street Press, New Mexico, p. 304 (2023)
18. Gladwell, G.M.L.: Contact problems in the classical theory of elasticity. Springer, Netherlands (2014)

19. Hetnarski, R.B., Ignaczak, J.: The Mathematical Theory of Elasticity. CRC Press, Boca Raton, p. 837 (2016)
20. Usov, A., Morozov, Y., Kunitsyn, M., Tonkonozhenko, A., Chernush, I.: Investigation of the influence of structural inhomogeneities on the strength of welded joints of functionally gradient materials. Proc. Odessa Polytech. Univ. **1**(60), 21–34 (2020). https://doi.org/10.15276/opu.1.60.2020.03
21. Xin, T., Pei, H., Shucai, Y.: Coating and micro-texture techniques for cutting tools. J. Mater. Sci. **57**, 17052–17104 (2022). https://doi.org/10.1007/s10853-022-07704-9

Stiffness of Underpinning Supports for Fixtures

Pavlo Kushnirov[1], Yuliia Denysenko[1,2(✉)], Grigore Pop[3], Bohdan Basov[1], and Oksana Dynnyk[4]

[1] Sumy State University, 116, Kharkivska Street, Sumy 40007, Ukraine
y.denisenko@tmvi.sumdu.edu.ua
[2] Poznan University of Technology, 3, Piotrowo Street, 61-001 Poznan, Poland
[3] Technical University of Cluj-Napoca, B-Dul Muncii, 103-105, 400641 Cluj-Napoca, Romania
[4] Classical Professional College of Sumy State University, 12, M. Nemolota Street, Konotop 41600, Ukraine

Abstract. Machining of large-sized workpieces with low stiffness is an urgent task. Auxiliary supports are used in machine tools to reduce deformations and vibrations of workpieces due to the action of cutting forces. Auxiliary underpinning supports are preferable to self-installing ones since they have a higher intrinsic stiffness. The stiffness of the underpinning support with a vertical support pin and with improved ergonomic properties was determined experimentally using a spring dynamometer and simulation. The stiffness coefficients were calculated, and a graph of the support displacement's dependence on the force's magnitude was constructed. A rotary underpinning support with a spherical base is also considered. This support allows for rotating its moving part in two planes and, accordingly, changes the angles of inclination of the support pin. This expands the technological capabilities of the support since it becomes possible for the support pin to contact inclined or curved surfaces of the workpieces. This support's stress, displacement, and strain at a force of 4 kN were analyzed. Studies have shown the high stiffness of the underpinning support with a spherical base. Modeling of the underpinning support deformations with a spherical base and the workpiece, where the support pin is brought to the inclined inner surface of the workpiece, was also carried out. A comparative analysis of the stiffness coefficients of the considered supports was carried out: the highest stiffness coefficient underpins a vertical support pin.

Keywords: Rigidity · Experimental · Modeling · Pin · Displacement · Spherical Base · Coefficient · Manufacturing Innovation

1 Introduction

Workpieces of extended, large-width, or thin-walled parts (frames of machine tools, housings, elements of aerospace equipment, tables of paper-cutting machines, frames, and plates) have low stiffness. Since such workpieces are subject to cutting forces during machining, the result may be deformation of the workpiece or vibration. These phenomena can arise due to a small number (or non-optimal location) of workpiece support

© The Author(s), under exclusive license to Springer Nature Switzerland AG 2024
V. Ivanov et al. (Eds.): DSMIE 2024, LNME, pp. 251–262, 2024.
https://doi.org/10.1007/978-3-031-61797-3_21

points in the fixture. In places with no support points, the workpiece will elastically deform and bend due to significant force loads (for example, large cutting forces during rough milling). This means that the technological system will have reduced rigidity, so the machining process will not occur with progressive cutting conditions. In turn, this leads to a decrease in productivity and machining quality.

It is essential to secure greater stiffness within the technological system to enhance machining efficiency. Additional auxiliary supports are used in fixtures to increase stiffness in places where deflections of workpieces or vibrations result from cutting forces [1, 2]. Various auxiliary supports are utilized, such as self-installing and underpinning supports. An example of a self-installing support involves a vertically positioned pin (plunger) with a bottom wedge for a self-braking effect. A locking screw presses the pin against this inclined surface. The pin, driven by a spring, ascends until it contacts the workpiece surface on the main supports [3]. However, self-installing supports suffer from inadequate stiffness; the pin-clamping mechanism may sag under substantial cutting forces, leading to subsequent jamming and a failure to fulfill its intended function. Consequently, it is advisable to use auxiliary supports that are not self-installing but underpinning for challenging working conditions. These underpinning supports, owing to their design characteristics, offer greater rigidity, thereby ensuring an overall increase in the stiffness of the technological system [4].

The study aims to determine the stiffness of various types of auxiliary underpinning supports by experimentation and numerical modeling.

2 Literature Review

Utilizing lightweight, large, and structurally efficient thin-walled components has become widespread in the production of aircraft and rockets due to their exceptional strength. Y. Tian [5] introduced an innovative approach to suppress vibrations and deformations during the mirror milling of thin-walled workpieces. This method employs a magnetic follow-up support fixture. Utilizing devices that ensure optimal fixturing element placement enhances machining accuracy for intricate and heavy parts. Adjusting fixturing element positions can be carried out manually [6].

The development of flexible fixtures for processing complex-shaped workpieces, such as "connecting rods," is discussed in [7]. Flexible fixtures are increasingly prominent in manufacturing thin-walled components in the automotive and aerospace industries. By optimizing the installation of workpieces in the fixture, the deformation caused by machining forces and their weight can be minimized [8].

An innovative articulated device for reducing vibrations when milling thin-walled parts has been developed [9, 10]. For this purpose, special torsion springs are used, which do not change the nature of the structure's dynamic characteristics, thus ensuring better control of the achieved dimension of the structure. Due to clamping deformation and vibration issues, holding low-stiffness freeform components during machining is challenging.

Proposed by O. Craig [11], a novel fixture concept seeks to conform to the contours of freeform components by employing arrays of flexible and deformable flexure pins to fill the gaps between locators. Thin-walled aerospace components, characterized by low

stiffness and complex structures, are prone to deformation when exposed to machine tool vibrations, cutting forces, and heat during milling. To address this challenge, a mechanical/magnetorheological composite clamping method has been suggested to dampen vibrations and enhance machining accuracy [12].

Increasing the stiffness of a technological system is an urgent research problem since, due to the poor rigidity, workpiece vibration and deformation become the main factors that limit cutting efficiency. The primary factors constraining cutting efficiency are workpiece vibration and deformation, mainly due to poor rigidity. Typically, auxiliary support is used to increase workpiece stiffness. In this study by S. Chai [13], a novel adaptive auxiliary fixture, which combines the functions of vibration suppression and deformation measurement, is introduced.

Flexible and reconfigurable vacuum holding fixtures are increasingly employed when milling aluminum aircraft skin parts because they are adaptable to several part geometries. However, the low rigidity of the parts seriously limits the widespread deployment of such devices. Therefore, an analysis was carried out of the final thickness achieved for the machined part and the cutting force [14]. It is shown that processing errors depend only on the workpieces' initial geometric shape and the part's fixtures distribution. In addition, a new cutting force model is designed for skins held in flexible fixtures. It allows for optimizing the trajectory, material selection, geometry [15, 16], and support distribution, thus boosting the use of flexible fixtures.

The research [17] showed that an improper fixturing scheme (i.e., magnitudes of clamping forces and fixture layout) leads to undesirable workpiece deformation. A new systematic approach based on elastic mechanics is proposed. The genetic algorithm solves the optimization model to minimize the maximum fixturing-induced deformation of the surface to be machined. Deformations of technological system elements can be quantified using stiffness coefficients. A mechanical model [18] is built to numerically predict the stiffness coefficients of curved fiber-reinforced composites.

The design of a rotary fixture incorporates dynamic machining analysis, as outlined in [19]. The models are presented, including a 2D drawing and a 3D view of the fixture. The paper suggests three alternative methods for mass balancing the rotary fixture using Pro/Mechanism. High manufacturing accuracy is emphasized through fixture and deformation control in the adaptive CNC machining process [20]. The approach involves multi-point positioning and auxiliary support to tackle the challenge of low stiffness. These measures enhance system stiffness and mitigate the deformation of thin-walled parts by altering their force state.

The designed milling fixture [21] contains a clamping setup for a Vertical Milling Machine. The screw clamps are designed in such a way to hold the workpieces rigidly. The fixture is tested using ANSYS Software. The process of designing and manufacturing fixtures for tapered or conical workpieces [22] has its characteristics. Operations that can be performed with this fixture are front-facing, drilling, and boring. The features presented in the article are designed with a minimum number of components. This fixture is created considering the shape and size of a specific workpiece. Also, the design process is done on SolidWorks, and stress, strain, and displacement analyses are carried out.

Thus, since a technological system with reduced rigidity imposes restrictions on cutting modes, it is relevant to design new fixtures that allow rigid installation of workpieces and enable high-performance and high-quality machining.

3 Research Methodology

It is possible to increase the stiffness of the «fixture-workpiece» system using underpinning auxiliary supports. Unlike self-installing supports, in these supports, the vertical pin rests on a wedge with an inclination angle of 8 degrees. This makes it possible to perceive the vertical component of the cutting forces when machining the workpiece.

One of the disadvantages of this type of auxiliary support is that the wedge in the support is moved manually: in this case, there is a danger that excessive manual effort can be applied to the wedge, and the workpiece can rise above the main supports. Also, the lack of ergonomics in the design is a disadvantage of underpinning supports. When the head of the rod presses on the palm of the worker, signaling the need to stop moving the wedge, the worker has some unpleasant sensations in the palm, somewhat painful. This worsens working conditions and causes some health risks.

To improve the ergonomic properties, the auxiliary support can be equipped with a compression spring located in the blind hole of the wedge between the bottom of this hole and the support rod. The presence of a spring between the wedge and the rod reduces the force of the pressure of the rod on the hand significantly, making the contact of the fixing head of the rod with the worker's hand softer and thus reducing health risks (Fig. 1).

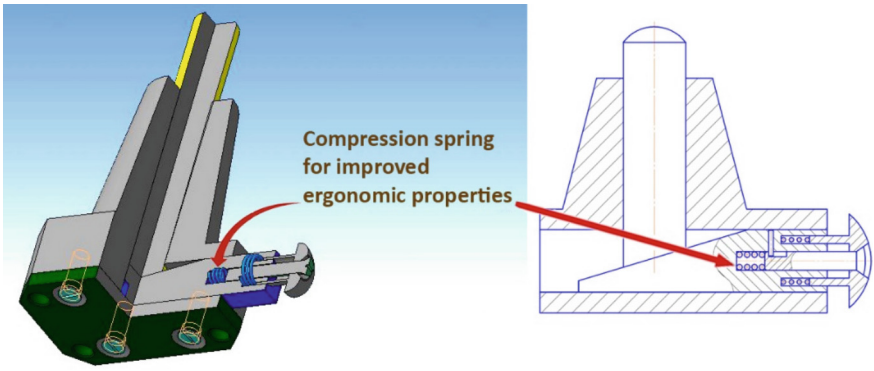

Fig. 1. Underpinning support with vertical support pin.

The stiffness of the main spring, located between the wedge and the button, must be sufficient to move the total mass of the moving parts of the support (button with wedge, rod, springs, support pin). According to ergonomic recommendations [23], the maximum force of a human hand on a button with a main spring should not exceed 145 N. The recommended stiffness of the spring between the wedge and the rod should be 35–60% of the stiffness of the main spring.

Let's consider the experimental research methodology of the stiffness of the auxiliary underpinning support of the fixture. The scheme of the research is shown in (Fig. 2a), and the general view of the setup of the research is shown in (Fig. 2b). We load the underpinning support with a vertical force that simulates the cutting force during workpiece machining using a spring dynamometer. To determine the stiffness, we place the underpinning support on the plane of the table and then apply force through the dynamometer to the supporting pin of the support.

The magnitude of the force changes in the range from 1000 N to 4000 N. The elastic deformation of the underpinning support is determined by the readings of the displacement indicator with a division value of 0.001 mm. For ease of reading, the leg of the indicator is brought to the side lobe, rigidly connected to the support pin. The results obtained during the experiment are entered in the (Table 1).

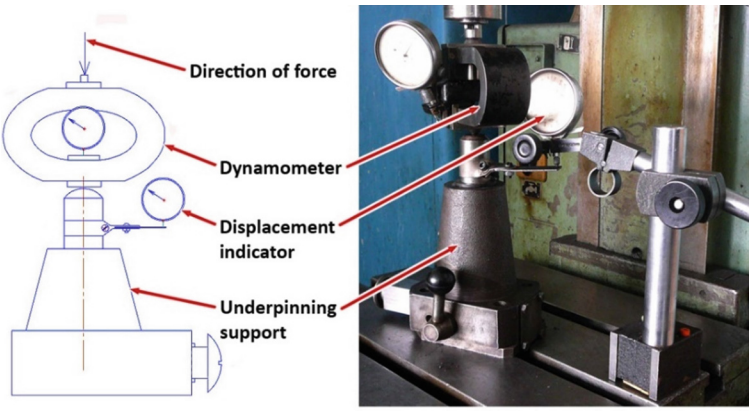

a) b)

Fig. 2. Experimental research of stiffness of auxiliary underpinning support with vertical support pin: a – scheme; b – general view.

The sources of potential errors in the considered experimental approach are the following:

- the presence of two dial indicators inevitably leads to the fact that the inherent errors of these measuring instruments will affect the results of experimental measurements;
- the elastic element bracket, which is part of the dynamometer and is made of metal, can introduce additional errors in the measurement results due to fatigue phenomena in the metal and, as a result, violation of calibrated linear movements.

In addition to the auxiliary underpinning support with a vertical support pin, a rotary underpinning support with a spherical base was also investigated [24]. This spherical base is made movable relative to the fixed part, which makes it possible to rotate the moving part in two planes and, accordingly, change the angles of inclination of the support pin. This is important for making contact with workpiece surfaces that contain non-flat or inclined areas, such as those made along a radius or at an angle (Fig. 3).

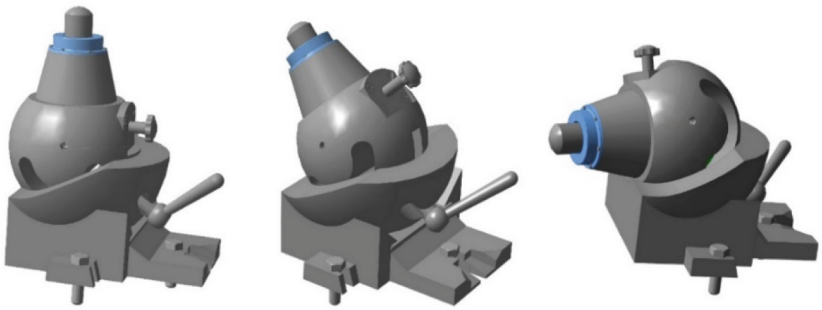

a) b) c)

Fig. 3. Rotary underpinning support with a spherical base and different inclination angles of the support pin: a – 0 degrees; b – 45 degrees; c – 90 degrees.

4 Results and Discussion

Research of the underpinning support displacements was also carried out using SOLIDWORKS Simulation, the results of which are shown in Fig. 4.

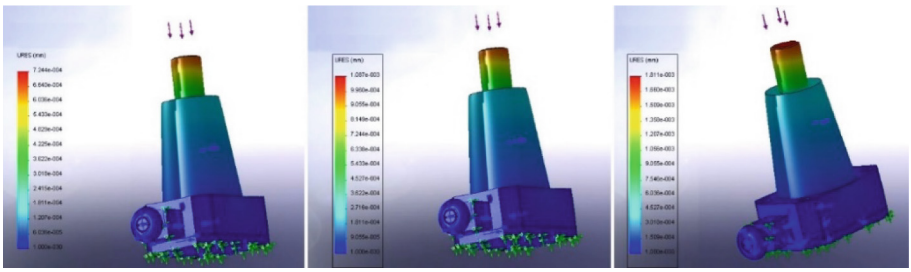

a) b) c)

Fig. 4. Research of displacements of the underpinning support with vertical support pin using SOLIDWORKS Simulation: a – 0.7244 μm (force 1000 N); b – 1.087 μm (force 1500 N); c – 1.811 μm (force 2500 N).

The results obtained during modeling are also entered in Table 1.

We find the underpinning support's average stiffness coefficients as the force-to-displacement ratio. We have for experimental research and modeling in SOLIDWORKS Simulation:

$$k = 753\text{N}/\mu\text{m}(\text{experiment});$$

$$k = 1444\text{N}/\mu\text{m}(\text{modeling}).$$

The reasons for the significant discrepancy between the values of the stiffness coefficients obtained experimentally and by modeling require additional research.

Table 1. Displacement and stiffness coefficient of underpinning support (Fig. 1) – (Fig. 3).

Force [N]	Displacement [μm]		Stiffness coefficient (k) [N/μm]	
	Experiment	Modeling	Experiment	Modeling
0	0	0		
1000	1.4	0.7244	714	1380
1500	1.8	1.087	833	1380
2000	2.9	1.307	690	1530
2500	3.3	1.811	758	1380
3000	3.9	1.961	769	1530
3500	4.5	2.535	778	1380
4000	5.5	2.615	727	1530

According to the obtained data, we plot the dependence of the underpinning support's displacements on the force's magnitude (Fig. 5).

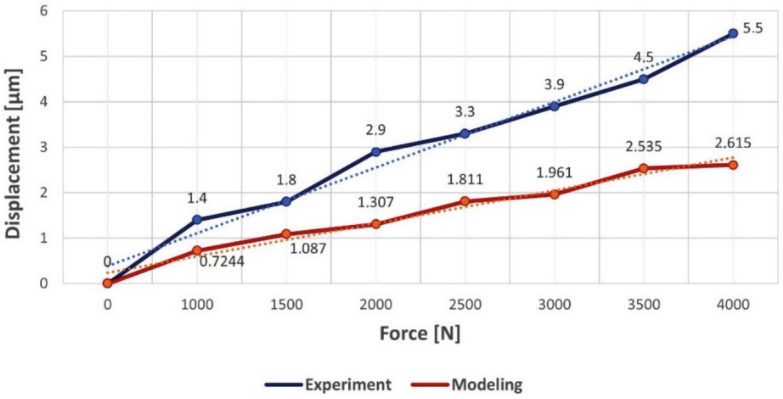

Fig. 5. Displacements of the underpinning support with vertical support pin depending on the magnitude of the force.

The design of the underpinning support with a spherical base was carried out in SOLIDWORKS, and an analysis of stresses, displacements, and deformations at a force of 4000 N was also carried out. The results (for the vertical position of the support pin) are $4.9 \cdot 10^7$ N/m^2 maximum stress Von Mises, 3.5 μm maximum resultant displacement, and $1.55 \cdot 10^{-4}$ is maximum equivalent strain (Fig. 6). The studies carried out showed the high rigidity of the underpinning support with a spherical base: the largest displacements of the support pin due to the action of the force directed along the axis of the support are on the order of 3.5 μm.

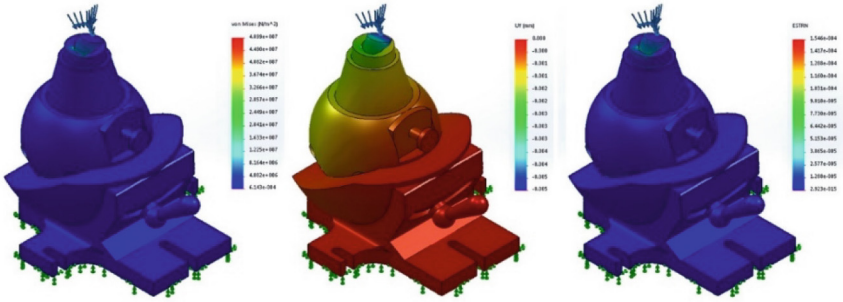

a) b) c)

Fig. 6. Research of rotary underpinning support with a spherical base in SOLIDWORKS: a – stress; b – displacement; c – strain.

The stiffness coefficient of a rotary underpinning support with a spherical base is equal to

$$k = 4000 / 3.53045 = 1133 [N / \mu m]$$

The rotary underpinning support with a spherical base is designed to increase the rigidity of the technological system by bringing the support pin to the area of the workpiece where deformations from cutting forces are possible. An example of such use of a supplied support is shown in the figure, where the support pin is connected to the inclined inner surface of the "Plate" workpiece (Fig. 7).

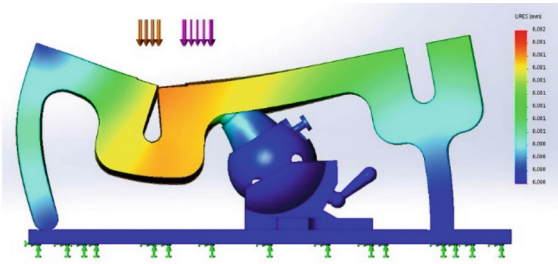

Fig. 7. Research the displacements of the rotary underpinning support with a spherical base and the workpiece in SOLIDWORKS.

The support pin inclines approximately 40°. Modeling in SOLIDWORKS showed that the maximum displacement of the "workpiece – underpinning support with a spherical base" system is 3.6 μm at a force of 4000 N.

The stiffness coefficient of a rotary underpinning support with a spherical base together with the workpiece is equal to

$$k = 4000 / 3.57462 = 1119 [N / \mu m]$$

A comparison of the stiffness of the considered support options (underpinning support with vertical support pin, rotary underpinning support with a spherical base, rotary underpinning support with a spherical base together with the workpiece) is given in Fig. 8. Underpinning support with vertical support pin has the highest stiffness coefficient (k = 1444 N/μm). This can be explained by the more straightforward design of this support, containing fewer parts and contacting surfaces.

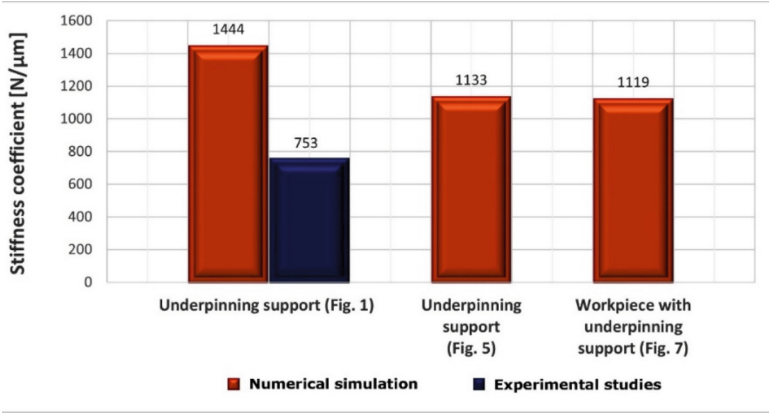

Fig. 8. Comparison of the stiffness of the considered support options.

This research's limitations include considering only two types of underpinnings: those with a vertical support pin and those with a spherical base. Other types of supports, such as auxiliary underpinnings, allow tilting in only one plane. Research on these types of support will be further carried out.

Let us compare our results with those of other authors who have investigated the stiffness of machines and fixtures. In [25], the stiffness of modular fixtures was investigated, namely the influence of the applied force and other parameters on the system's normal stiffness and tangential stiffness. The results (plots in Figs. 9 and 12 [25]) showed that for a force of 4000 N, the displacement values of the fixture elements are in the range of 4 to 8 μm. These values are in the same order (from 2.6 to 5.5 μm for the support with a vertical pin and 3.6 μm for the support with a spherical base). In another work [26], theoretical studies and experimental measurements of the stiffness of the elements of the machining center were carried out. In the modeling process, a force of 100 kg was applied to the end of the spindle. The magnitudes of the obtained displacements [26] at a small extension of the spindle amounted to 6–10 μm, and when the spindle was extended, the stiffness decreased significantly. This confirms that comprehensive studies of stiffness are relevant to improving the efficiency of all elements of the technological system [26, 27].

The limitations of this article include consideration of only two types of underpinning supports (with a vertical support pin and with a spherical base); in future work, the authors are considering the possibility of a more detailed analysis of other types of auxiliary supports.

5 Conclusions

This article examined the designs of underpinning support for fixtures and methods for determining their stiffness. The underpinning supports are used to increase the stiffness of places of the workpiece where deformations may occur due to the action of cutting forces. Studies were carried out on the stiffness of two types of underpinning supports: with a vertical support pin and with a spherical base.

The stiffness coefficients that were determined in this study (k = 753 N/μm; k = 1119 N/μm; k = 1133 N/μm; k = 1444 N/μm) allow quantitative characterization of the designs of auxiliary underpinnings. This provides an opportunity for engineers and technicians planning to use these supports in production to choose various design options, the most acceptable in terms of stiffness.

The scientific novelty of this paper consists of the following:

- by experimental and numerical simulation [numerical simulation], the stiffness coefficients of the under-support with vertical support pin (753 N/μm and 1444 N/μm, respectively) were determined;
- the stiffness coefficient of the support with a spherical base (1133 N/μm) was determined by numerical simulation;
- the spherical base support's stiffness coefficient and the workpiece were determined by numerical simulation (1119 N/μm).

The comparative analysis showed that the most significant stiffness coefficient has the undercarriage with a vertical support pin, although the undercarriage with a spherical base has broader technological possibilities due to a rotating mechanism.

The research results show that engineers and industrial workers now have information about the stiffness parameters of the considered underpinnings and the methods of evaluating their determination.

The research was carried out at the Department of Manufacturing Engineering, Machines and Tools at Sumy State University.

In future work, the authors are considering the possibility of a more detailed analysis of other types of auxiliary supports, for example, supports with an inclination of the support pin in only one plane or supports with rotation of the housing around a vertical axis. After manufacturing support with a spherical base in metal, experimental studies of its rigidity are planned.

Acknowledgment. The research was partially supported by the Polish National Agency for Academic Exchange within the project "Digitalization in mechanical engineering" (agreement no. BNI-UE-2023–2), Ministry of Education and Science of Ukraine (State Reg. No. 0122U200875), the International Association for Technological Development and Innovations (IATDI), Research and Educational Center for Industrial Engineering (Sumy State University), and Ministry of Education and Science of Ukraine (State Reg. No. 0122U200875).

References

1. Kamble, V.D., Mathew, A.T.: Brief review of methodologies for creation of cohesive fixture design. Mater. Today **22**(4), 3353–3363 (2020). https://doi.org/10.1016/j.matpr.2020.04.285
2. Okpala, C.C., Ezeanyim, O.C.: The design and need for jigs and fixtures in manufacturing. Sci. Res. **3**(4), 213–219 (2015). https://doi.org/10.11648/j.sr.20150304.19
3. Borovyk, A.I.: Technological equipment of mechanical assembly production. Kondor, Kyiv (2008). [in Ukrainian]
4. Toporov, O., Bondarev, S.: Auxiliary underpinning support. Inventors for mechanical engineering, 22 (1996)
5. Tian, Y., Xiao, J., Liu, S., Ma, S., Liu, H., Huang, T.: Vibration and deformation suppression in mirror milling of thin-walled workpiece through a magnetic follow-up support fixture. J. Manuf. Process. **99**, 168–183 (2023). https://doi.org/10.1016/j.jmapro.2023.04.074
6. Pandit, H.: Jigs and fixtures in manufacturing. Int. J. Eng. Res. Appl. **12**(10), 50–55 (2022). https://doi.org/10.9790/9622-12105055
7. Ivanov, V., Botko, F., Dehtiarov, I., Pavlenko, I., Trojanowska, J.: Development of flexible fixtures with incomplete locating: connecting rods machining case study. Machines **10**(7), 493 (2022). https://doi.org/10.3390/machines10070493
8. Do, M.D., Son, Y., Choi, H.-J.: Optimal workpiece positioning in flexible fixtures for thin-walled components. Comput. Aided Des. **95**, 14–23 (2018). https://doi.org/10.1016/j.cad.2017.09.002
9. Petrakov, Y.V., Ohrimenko, O.A., Sikailo, M.O., Myhovych, A.V.: Cutting forces simulation for end milling. J. Eng. Sci. (Ukraine) **10**(2), A27–A33 (2023). https://doi.org/10.21272/jes.2023.10(2).a4
10. Kolluru, K., Axinte, D.: Novel ancillary device for minimising machining vibrations in thin wall assemblies. Int. J. Mach. Tools Manuf **85**, 79–86 (2014). https://doi.org/10.1016/j.ijmachtools.2014.05.007
11. Craig, O., Picavea, J., Gameros, A., Axinte, D., Lowth, S.: Conformable fixture systems with flexure pins for improved workpiece damping. J. Manuf. Process. **50**, 638–652 (2020). https://doi.org/10.1016/j.jmapro.2019.12.045
12. Weicheng, G., Yong, Z., Xiaohui, J., Ning, Y., Kun, W., Xiao, L.: Improvement of stiffness during milling thin-walled workpiece based on mechanical/magnetorheological composite clamping. J. Manufact. Process. **68**(A), 1047–1059 (2021). https://doi.org/10.1016/j.jmapro.2021.06.039
13. Chai, S., Ouyang, L., Bi, Q., Yu, J., Zhang, Y.: An adaptive fixture for suppress vibrations and measuring workpiece deformation of thin-walled casings. Procedia CIRP **101**, 322–325 (2021). https://doi.org/10.1016/j.procir.2020.05.269
14. Casuso, M., Rubio-Mateos, A., Veiga, F., Lamikiz, A.: Modeling of cutting force and final thickness for low stiffness 2024–T3 aluminum alloy part milling considering its geometry and fixtures. J. Market. Res. **21**, 2416–2427 (2022). https://doi.org/10.1016/j.jmrt.2022.10.070
15. Ivchenko, O., et al.: Method for an effective selection of tools and cutting conditions during precise turning of non-alloy quality steel C45. Materials **15**(2), 505 (2022). https://doi.org/10.3390/ma15020505
16. Pavlenko, I., et al.: Using regression analysis for automated material selection in smart manufacturing. Mathematics **10**(11), 1888 (2022). https://doi.org/10.3390/math10111888
17. Li, G., Du, S., Huang, D., Zhao, C., Deng, Y.: Elastic mechanics-based fixturing scheme optimization of variable stiffness structure workpieces for surface quality improvement. Precis. Eng. **56**, 343–363 (2019). https://doi.org/10.1016/j.precisioneng.2019.01.004
18. Dai, T., Wei, Y., Tao, C., Huang, J.: Mechanical model of stiffness coefficients prediction of curved fiber reinforced composites considering fiber distribution and aggregation. Compos. Struct. **321**, 117277 (2023). https://doi.org/10.1016/j.compstruct.2023.117277

19. Maniar, N.P., Vakharia, D.P.: Design & development of rotary fixture for CNC with computer aided mass balancing method as pre-mortem tool. In: 2nd International Conference on Innovations in Automation and Mechatronics Engineering, pp. 397–404. Procedia Technology, ICIAME (2014). https://doi.org/10.1016/j.protcy.2014.08.051
20. Wu, D., et al.: Machining fixture for adaptive CNC machining process of near-net-shaped jet engine blade. Chin. J. Aeronaut. **33**(4), 1311–1328 (2020). https://doi.org/10.1016/j.cja.2019.06.008
21. Ramnath, B.V., Elanchezhian, C., Rajesh, S., Prakash, S.J., Kumaar, B.M., Rajeshkannan, K.: Design and development of milling fixture for friction stir welding. Mater. Today **5**(1), 1832–1838 (2018). https://doi.org/10.1016/j.matpr.2017.11.282
22. Rathaur, S., Sanoria, R., Abidi, S.H.A., Gani, A.: Design and Fabrication of CNC Lathe Fixture for Cone. In: Yadav, S., Jain, P.K., Kankar, P.K., Shrivastava, Y. (eds.) Advances in Mechanical and Energy Technology: Select Proceedings of ICMET 2021, pp. 177–186. Springer Nature Singapore, Singapore (2023). https://doi.org/10.1007/978-981-19-1618-2_17
23. EN 1005–3:2002+A1:2008. Safety of machinery - Human physical performance - Part 3. Recommended force limits for machinery operation
24. Ma, H., Wang, K.-Ch., Yang, Ch.-H.: A novel design optimization methodology for machine tools based on computer-assisted engineering and sensor-based measurement techniques. Sens. Mater. **35**(8), 2705–2727 (2023). https://doi.org/10.18494/SAM4442
25. Cioata, V.G., Alexa, V., Ratiu, S.A.: Study of the stiffness of modular fixtures using the finite element method. In: The 10th International Symposium Machine and Industrial Design in Mechanical Engineering, Volume 393, pp. 1–9. Series: Materials Science and Engineering (2018). https://doi.org/10.1088/1757-899X/393/1/012036
26. Kushnirov, P.V., et al.: Rotary auxiliary underpinning support with a spherical base. Patent of Ukraine No. 153759 (2022)
27. Ivanov, V., Pavlenko, I., Liaposhchenko, O., Gusak, O., Pavlenko, V.: Determination of contact points between workpiece and fixture elements as a tool for augmented reality in fixture design. Wireless Netw. **27**(3), 1657–1664 (2021). https://doi.org/10.1007/s11276-019-02026-2

Design of the Technological Route for Sustainable Machining of Functional Surfaces for Automotive Engineering Parts

Yaroslav Kusyi[1(✉)], Nazarii Kusen[1], Andrii Slipchuk[1], Iryna Schuliar[2], and Lolita Pituley[2]

[1] Lviv Polytechnic National University, 12, Bandera Street, Lviv 79013, Ukraine
jarkym@ukr.net

[2] Ivano-Frankivsk National Technical University of Oil and Gas, 15, Karpatska Street, Ivano-Frankivsk 76019, Ukraine

Abstract. Toughening the important demands for the competitiveness of industrial products in general and automotive engineering parts, in particular, requires searching for new effective methods of designing technological routes for machining their functional surfaces. Object-oriented technologies are characterized by using typical technological routes and choosing machining methods based on the criterion of accuracy and quality of surface layers without considering the operation conditions of products and estimation of the level of material degradation of parts. Functionally-oriented technologies consider a large set of technological indicators that affect the formation of operational parameters and reliability characteristics. Sustainable production developing the demands of Industry 5.0 considers economic and social factors and environmental protection when introducing highly efficient technologies. The developed technique of design of the technological route at sustainable machining of functional surfaces for the automotive engineering parts makes it possible to assess the level of parts material exhaustion of a significant area of the specific surface layers by the material homogeneity criterion based on the dispersion of micro-hardness characteristics. Using this technique, the physical processes are analyzed according to the coefficient of variation and the homogeneity coefficient (m) and its derivatives. The machining of a steel shaft is accompanied by a change of the constructively heterogeneous layer of the initial material after blank production to a constructively homogeneous layer of the material of the workpiece with a decrease in the material's susceptibility to its technological damageability from rough treatments to finishing ones.

Keywords: Automotive Engineering · Object-Oriented Technology · Functionally-Oriented Technology · Sustainable Manufacturing · Sustainable Machining · Industrial Growth

© The Author(s), under exclusive license to Springer Nature Switzerland AG 2024
V. Ivanov et al. (Eds.): DSMIE 2024, LNME, pp. 263–275, 2024.
https://doi.org/10.1007/978-3-031-61797-3_22

1 Introduction

The operational conditions of machine parts and automotive engineering differ radically [1, 2]. It was established [3, 4] that wear and fatigue are the most common types of damage to the mating surfaces of responsible parts during their operation. In particular, the executive surfaces of bearings, spools, axles, shafts, gears, etc., which are used in various structures of automotive engineering, work under conditions of friction, intensive wear, fatigue, and aggressive media. However, the sudden failures of critical parts of cars, unlike parts of general mechanical engineering, can have unpredictable consequences and lead to the death of people [5, 6]. Rational selection of promising and inexpensive damping systems with magnetorheological and friction dampers [7, 8] and compelling lubricant compositions of materials with nano-applications [9] is also essential in designing automotive equipment.

Therefore, the principles of sustainable development, the main concepts of Industry 4.0/5.0, must be considered at all phases of the life cycles of automotive products and their parts [10, 11].

The increase in technical requirements for automotive engineering parts led to the improvement of available concepts and the elaboration of new ones for the technological support of requirements for dimensional accuracy, surface engineering indicators, operational parameters, and reliability characteristics of products [12, 13].

Traditional, object-oriented technologies involve step-by-step implementation of the technological and design preparation phases of production using typical manufacturing processes of machining, strengthening, and assembly. The optimization criterion is the minimal technological prime price of parts machining and assembly of units, mechanisms, and machines without a functional and production analysis of the operating conditions of the machines and their parts by a technologist [5, 14].

Functionally-oriented technologies ensure the operational indicators of machine elements according to the regulated reliability indicators in compliance with the necessary design requirements. The technologist develops the production processes of machining certain parts and assembly of products based on the required operating conditions of machine parts [15].

Sustainable manufacturing technologies provide economic, social, and environmental aspects with an optimal combination of cost/operational parameters (reliability characteristics). These technologies are closely associated with the concepts of Industry 5.0, which realizes the desire to return human, social, and ecological aspects to mechanical engineering production [2, 16]. On the other hand, environmental protection is the main task in ensuring sustainable manufacturing demands.

Therefore, developing new approaches in sustainable machining and manufacturing technologies is a current task for the evolution of the modern automotive industry in the framework of Industry 5.0.

The main goal of this paper is to elaborate on a technique for the technological route planning for sustainable machining of responsible automotive engineering parts.

2 Literature Review

The design of technological routes for detailed machining has its parameters for various types of machining [1], in particular, milling [17, 18] and turning [19, 20].

The tabular and estimated methods of the technological route design in product machining are implemented for object-oriented technologies [21, 22].

Technological routes are designed according to regulated accuracy. On the other hand, the designers regulate the quality of functional surfaces. The application of metallic chrome coatings [23], tungsten-free coatings [24, 25], and oxide coatings [26, 27] is promising for increasing the wear resistance of the responsible part for the responsible surfaces of the automotive equipment.

The calculation of estimated refinement characterizes the calculation method of technological route planning for machine parts machining in the framework of object-oriented technologies. Necessary methods of parts machining by cutting are provided using the refinement coefficient ε_i, which takes into account the heredity properties of machined parts between adjacent technological steps [21]:

$$\varepsilon_i = \left[TP_{i-1}\right]/[TP_i], \tag{1}$$

where $[TP_{i-1}]$, $[TP_i]$ are the numerical values of the boundary indicator for the technological step or operation at product manufacturing by cutting, respectively, at the prior and ongoing technological operation or step.

At parts machining, the dimensional accuracy indicators (IT grades) or surface engineering's characteristics (surface roughness (Ra or Rz)) serve the priority criteria for the refinement's calculation [21]:

$$\varepsilon_i = \left[T_{i-1}\right]/[T_i], \tag{2}$$

$$\varepsilon_i = \left[Ra_{i-1}\right]/[Ra_i];\ \varepsilon_i = \left[Rz_{i-1}\right]/[Rz_i], \tag{3}$$

where T_{i-1}, Ra_{i-1}, Rz_{i-1}; T_i, Ra_i, Rz_i are, respectively, the tolerance of the size, surface roughness (Ra, Rz) ensured at the prior and ongoing technological steps.

The estimated refinement $\varepsilon_{est.}$ is determined using the dimensional accuracy indicator or surface roughness [14, 28]:

$$\varepsilon_{est.} = [T_{bl.}]/\left[T_{part}\right], \tag{4}$$

$$\varepsilon_{est.} = [Ra_{bl.}]/\left[Ra_{part}\right];\ \varepsilon_{est.} = [Rz_{bl.}]/\left[Rz_{part}\right] \tag{5}$$

where $T_{bl.}$, $Ra_{bl.}$, $Rz_{bl.}$ Are the tolerance, surface roughness (Ra, Rz) of the blank; T_{part}, $Ra_{part.}$, $Rz_{part.}$ Are the tolerance, the surface roughness (Ra, Rz) of the part by the design demands, respectively.

The number of cutting methods n is counted by [21]:

$$n = \lg(\varepsilon_{est.})/0.46. \tag{6}$$

The verification of the correct choice of cutting methods n is carried out by [28]:

$$\Pi_{i=1}^{n} \varepsilon_i \geq \varepsilon_{est.}. \tag{7}$$

The necessary particularity of functionally-oriented technologies is the primary provision of a set of functional and operating properties of the products parallel engineering according to the specified parameters of accuracy, normative duration of their work, as well as environment protection and economic restrictions. The operational conditions of automotive engineering parts are more complicated than those of other products, which requires considering many technological indicators during their machining or future operations [1, 4].

Therefore, estimated refinements should be calculated for all parameters that affect operational characteristics and reliability indicators, including important microrelief parameters, and the number of cutting methods should be determined by the limiting estimated refinement [14, 28]:

$$\{\varepsilon_{est.1}, \varepsilon_{est.2}, \ldots.., \varepsilon_{est.j}\} \rightarrow \varepsilon_{est.lim.}, \tag{8}$$

where $\varepsilon_{est.1}$, $\varepsilon_{est.2}$, ….., $\varepsilon_{est.n}$ – set of estimated refinements calculated according to the specific operational characteristic or reliability indicator of the parts.

That approach requires more time than object-oriented technologies, but it provides technological process planning based on the priority operational parameters and reliability characteristics of mechanical engineering parts.

Sustainable manufacturing, in general, and sustainable machining are developing rapidly nowadays. Sustainability in product manufacturing can also be ensured by reducing the consumed power at cutting and decreasing waste generation, protecting the environment, and using rational methods of utilization [2, 16].

On the other side, the investigation of physical processes during parts machining, analysis of the material structural states of products during their machining, and search for optimal criteria for the prediction of product behavior at essential stages of their life cycles are the important directions of sustainable manufacturing development [4, 11].

So, the actual task in sustainable machining is to design rational technological processes with minimum required operations of cutting or surface plastic deformation and control of parts to ensure specific operational parameters and reliability characteristics.

3 Research Methodology

3.1 Theoretical Provisions

The development of continuous damage mechanics makes it possible to analyze the reasons for the deterioration of the physical and mechanical properties of the parts materials. Specific physical and mechanical characteristics are employed at product manufacturing to assess the current state of the materials properties of products at phases in their life cycles. For example, the strength and plasticity of the material of the parts are investigated using the processing of results of macro-hardness measurements. However, the measurement results of the absolute (in most cases) or average (in some experiments)

values of the macro-hardness of the product material are ambiguously explained since they depend on specific demands and features of the current measurement methods. So, macro-hardness is presented only as a generic indicator for estimating the elastic and plastic properties of the product material. Conversely, the average hardness value received from experimental research on the material properties of parts needs to include credible data about their stress-strain state [14, 28].

According to the LM-hardness method, Academician A.A. Lebedev substantiated the practicability of analysis of the structural state of product material through derivatives of the absolute values of material parameters, including the dispersion of the measurement results obtained on identical samples under identical conditions. The LM-hardness method is realized by evaluating the dispersion of material macro-hardness of the part as its priority mechanical characteristic [29, 30].

On the other side, homogeneity is a parameter that characterizes the current state of the parts material by processing the results of macro-hardness measurements. Homogeneity is represented by the Weibull law [31]:

$$P(\sigma) = 1 - e^{-\left(\frac{\sigma}{k}\right)^m}, \tag{9}$$

where the material sensitive indicator – the Weibull homogeneity coefficient (WHC) (m) – describes the level of material degradation of products. It is calculated by [28]:

$$m = d(n)/(2.30259 \cdot S(\lg(H)))P, \tag{10}$$

The

$$S(\lg(H)) = \sqrt{\frac{1}{n-1}\Sigma_{i=1}^{n}\left(\lg(H_i) - \overline{\lg(H_i)}\right)^2}, \tag{11}$$

$$\overline{\lg(H_i)} = \frac{1}{n} \cdot \Sigma_{i=1}^{n} \lg(H_i). \tag{12}$$

Other static parameters are used in engineering practice to assess the level of material degradation of products. For example, the coefficient of variation ν evaluates the degree of dispersion of hardness measurement results compared to its average value [28, 29]:

The

$$v = \sqrt{\frac{1}{n-1}\Sigma_{i=1}^{n}\left(H_i - \overline{H}\right)^2/\overline{H}}, \tag{13}$$

where $\overline{H}$ is the average value of the macro-hardness of the product material.

The estimated refinement $\varepsilon_{est.}$ is calculated by the material homogeneity of parts [14, 28]:

$$\varepsilon_{est.} = \left[m_{part}\right]/[m_{bl.}], \tag{14}$$

$$\varepsilon_{est.} = [v_{bl.}]/\left[v_{part}\right], \tag{15}$$

where m_{part}, v_{part}, $m_{bl.}$, $v_{bl.}$ Are the coefficients of homogeneity and the coefficients of variation for the part and blank, respectively.

Refinement for the i-th technological operation or step at known values of the scattering characteristics for the material macro-hardness is determined by studies [14, 28]:

$$\varepsilon_i = \mathrm{m}_i/\mathrm{m}_{i-1}, \tag{16}$$

$$\varepsilon_i = v_{i-1}/v_i, \tag{17}$$

where m_i,v_i, $m_{i\text{-}1}$, $v_{i\text{-}1}$ are WHC and the coefficients of variation at the current and previous technological steps, respectively.

The constant of material A_m is calculated by studies [28]:

$$A_m = ((m+2)/(4m+4))^{1/m}, \tag{18}$$

Besides, the technological damageability D and intensity of its growth are determined by studies [14, 28]:

$$D = (m_{matr.} - m_i)/m_{matr.}, \tag{19}$$

$$j_D = (m_{matr.} - m_i)/m_i, \tag{20}$$

where $m_{matr.}$, m_i – the WHC (m) that is characterized by the dispersion of the macro-hardness of the matrix (base material) and in the i-th section of the product, respectively.

3.2 Laboratory Samples for Experimental Researches

Experimental research was carried out using an overall shaft, which is applied in constructing automotive equipment, transport, and lifting equipment (Fig. 1). The part's material is 37Cr4KD (41CrS4). The blank's type is rolling. The mass of the blank is about 330 kg with overall dimensions Ø of 160 × 2105 mm, and the coefficient of material used is 0.73 [14, 28].

Fig. 1. Shaft.

3.3 Metrological Support of Experimental Research

The macro-hardness of the surface layers of the shaft (Fig. 1) was controlled using a portable tester TD-42, taking into account the weight and dimensions of the workpiece of the shaft. The traditional Brinell hardness measurement method was realized [14, 28]. The macro-hardness of the machined part was controlled in axial sections of shaft necks: Ø 90h7, Ø $125h7_l$ (neck is on the left-hand side), Ø $148h9_l$ (neck is on the left-hand side), Ø $148h9_r$ (neck is on the right-hand side), Ø$125h7_r$ (neck is on the right-hand side) and non-functional surface Ø 156h14 (see Fig. 1). 25–35 measurings of macro-hardness were realized for each surface of the shaft using two series of experiments after each treatment [14, 28].

3.4 Technological Routes Planning at Functional Surfaces Machining

Optimal routes for the responsible surface machining of the shaft were determined by two methods: for object-oriented technologies and sustainable ones using Eqs. (1)–(7) and (14)–(17). The technological routes of surface machining for Ø 90h7, Ø $125h7_l$, Ø and 125h7r consist of rough turning, finish turning, rough grinding, and finish grinding; for Ø $148h9_l$, Ø $148h9_r$ includes rough turning, finish turning, and rough grinding (see Fig. 1) according to the calculations.

4 Results and Discussion

4.1 Processing of the Obtained Results

The results of the optimal technological routes planning for the responsible surfaces of the shaft (see Fig. 1) based on the calculation of estimated refinements (object-oriented machining: criterion – accuracy of machining) and (sustainable machining: criterion – homogeneity of the part surface material) are shown in Fig. 2, where symbols (IT) are described the curves of the dynamics of changes in refinements for the traditional technique; symbols (m) and (ν) are related with the curves of the dynamics of changes in refinements for the LM-hardness method at sustainable machining. It was investigated that there is a decrease in the values of intermediate refinements and tolerance values in the process of transition from rough to finishing machining methods in the production sequence "blank– final part" for both technologies. This is explained by the reduction of dimensional tolerance values for object-oriented machining. At the same time, a similar result is achieved by the developed criterion due to the increase in Weibull coefficients (m) at sustainable machining. The obtained results increase the homogeneity of the shaft's material and structure during the transition to the subsequent treatment and decrease its susceptibility to damage at workpiece machining (see Fig. 2).

Changes in the parameters of the material homogeneity criterion [14, 28] in the production sequence "initial blank –workpiece– part" occur at the machining of the shaft's blank according to the principle of technological heredity of quality indicators of products.

The blank is defined by unsatisfactory homogeneity of the part material of the surface layers, characterized by low WHC values (m = 6.12–11.46) and relatively high values of

the coefficient of variation ν (ν = 9.63–18.77%). The average value of the constant A_m ($A_m = 0.85$) < 0.878 characterizes the state of a structurally heterogeneous material. All functional surfaces of the steel shaft's blank are characterized by a high susceptibility of the material of the surface layers to damageability, which is confirmed by the values of D (D = 0.967–0.983). On the other hand, the intensity of growth of technological damageability j_D is provided by parameters (j_D = 29.541–56.377) (see Fig. 4).

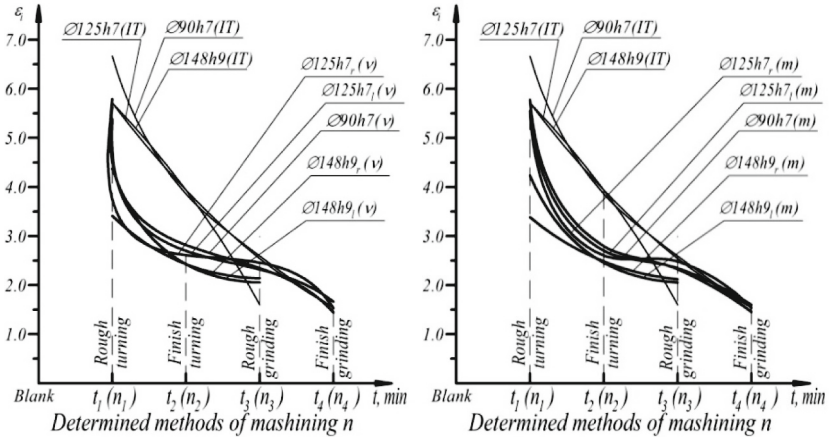

a) b)

Fig. 2. Dynamics of changes in calculated refinements after specific technological steps using criteria of dimensional accuracy and coefficient of variation (a); using criteria of dimensional accuracy and WHC (m) b) according to the specific treatments by machining for the shaft's necks following the technological heredity (t_1 (n_1), t_2 (n_2),…, t_k (n_k) – time durations, for example, 1, 2, *k* technological steps; (*IT*), (*m*), (ν) – the criterions of the dimensional accuracy at machining, WHC and the coefficient of variation, respectively.

An increase in the homogeneity of the surface layers of the workpiece occurs after cutting the defective surface layer after rough turning, which is characterized by a decrease in the values of the coefficient of variation ν (ν = 2.74–3.59%). Removal of the defective near-surface layer of the neck material characterizes the evolution from a structurally heterogeneous state of the material of the blank to a structurally homogeneous state of the workpiece with a simultaneous improvement in the values of A_m (A_m = 0.959–0.967) > 0.878. On the other side, the values of damageability decrease from (D = 0.967–0.983) (for the blank) to (D = 0.883–0.908) (after rough turning) (see Figs. 2, 3 and 4).

Finish turning after rough one determines the further positive dynamics of the growth of WHC (m = 88.03–100.43), material constants (A_m = 0.985–0.986), as well as a decrease in the values of the coefficients of variationν (ν = 1.13–1.28%). At the same time, the absolute values and dispersion of technological damageability decrease.(D = 0.713–0.748) as the intensity of its growth decreases from (j_D = 29.541–56.377) (for the blank) to (j_D = 2.485–2.976) (after finishing turning) (see Fig. 2, 3 and 4).

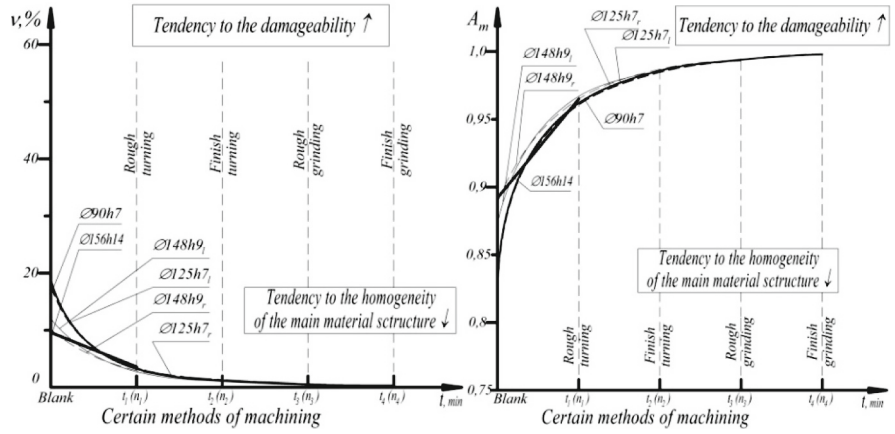

Fig. 3. Change of the coefficient of variation v (a) and the material constant A_m (b) in the surface layers of the shaft necks at its machining.

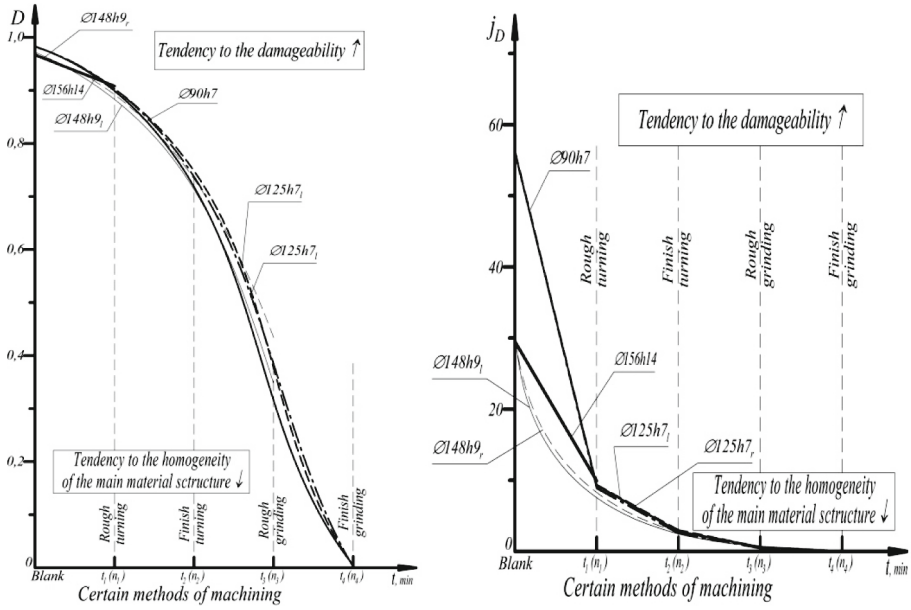

Fig. 4. Change of the damageability D (a) and the intensity of technological damageability growth j_D (b) in the surface layers of the shaft necks at its machining.

Finishing treatment applying grinding of the functional surfaces of the shaft includes rough (preliminary) grinding (for Ø 148h9$_l$, Ø 148h9$_r$) and two-time grinding: rough and finish ones (for Ø 90h7, Ø 125h7$_l$, Ø 125h7$_r$) (see Fig. 1).

The further positive dynamics of increasing the material homogeneity of the functional surfaces is confirmed after a single (rough) grinding of the left and right necks of the steel shaft to the size Ø 148h9, which is ensured by the growth of the WHC (m = 198.23–206.46), the constant A_m ($A_m = 0.993$), reducing the coefficients of variation ν ($\nu = 0.55$–0.57%). At the same time, the absolute values and dispersion of technological damageability D are significantly reduced (D = 0.41–0.434) according to similar dynamics for the intensity of its growth j_D ($j_D = 0.695$–0.766) (see Figs. 2, 3 and 4).

The final grinding of the left and right necks of the steel shaft in sizes Ø 90h7, Ø 125h7 provides the highest homogeneity of the treated surfaces. This is determined by the increasing values of the WHC (m = 333.89–344.59), the stabilization of the constants A_m ($A_m = 0.996$), and decreasing values of coefficients of variation ν ($\nu = 0.33$–0.34) %. The numerical values of technological damageability D (D = 0.015–0.046) and the parameter j_D ($j_D = 0.016$–0.048) are close to zero, which confirms the general tendency towards homogeneity of the material of the finished shaft (Figs. 2, 3 and 4).

The conducted investigations are a continuation of the research of A. Lebedev and his scientific school, but the field of research concerns not only materials science but mechanical engineering. The developed technique for technological route planning at the machining of heavily loaded surfaces of machine parts, particularly in the automotive industry, allows for a comprehensive assessment of the degree of degradation of their material by the criterion of material homogeneity based on the dispersion of microhardness characteristics. The criterion of homogeneity of functional surfaces for machine parts and the indicators that evaluate it have been developed. The proposed technique analyses the physical processes in the surface layers of parts in "real-time" at their machining, in contrast to traditional approaches for technological route planning at product manufacturing. A promising direction for further research is coordinating the results obtained at the development and manufacture stage of machine parts manufacturing with the subsequent approbation of the developed methodology at the operation stage of products in their life cycles.

5 Conclusions

The main conclusions have been made based on the results of our investigations.

Applying the LM-hardness method in engineering practice at parts manufacturing by machining allows for estimating the degradation level of a significant area of functional surfaces, which is especially important for the product's operation under friction, fatigue, etc.

Technological inheritability of the properties of the surface layers of steel machine parts by machining ensures the evolution of structurally heterogeneous material obtained after the blank manufacture into structurally homogeneous material of workpieces and final parts. This is ensured by an increase in WHC from (m = 6.12–11.46) (after the blank manufacture) to (m = 198.23–344.59) (after various methods of grinding) and a decrease in the coefficients of variation ν from ($\nu = 9.63$–18.77%) (after the blank

manufacture) up to ($\nu = 0.33$–0.57%) (after various methods of grinding). The material constant of the product A_m in the production sequence "initial blank –workpiece– detail" at machining of the steel shaft gradually increases from ($A_m = 0.814$) (after the blank manufacture) to ($A_m = 0.966$) (after final grinding). In addition, the dispersion of the A_m values is more significant after the blank manufacture and previous technological machining methods with the stabilization of these parameters for the final technological treatments. This behavior indicates a higher homogeneity of the part material and its structure after final treatments, in contrast to rough and semi-rough methods of machining, and determines necessary demands for optimal technological route planning for the machining of responsible surfaces of products.

At the same time, the technological damageability D decreases from ($D = 0.967$–0.983) (after the blank manufacture) to ($D = 0.015$–0.434) (after various grinding), which ensures the evolution of the structurally heterogeneous material of the steel blanks into the structurally homogeneous material of the final parts.

The proposed technique can be applied to evaluate the dynamics of changes in material homogeneity of mechanical engineering details at their machining, control, field testing, further operation, maintenance, and repair.

Acknowledgment. This research has been conducted as part of the ongoing project "Comprehensive system of functional-oriented planning of machining difficult-to-cut materials for the military-industrial complex (Komplekssys)". It has been funded by the Research Council of Lithuania and the Ministry of Education and Science of Ukraine under the Lithuanian–Ukrainian Cooperation Programme in the Fields of Research and Technologies (Grant No.S-LU-22–6).

References

1. la Monaca, A., et al.: Surface integrity in metal machining - Part II: functional performance. Int. J. Mach. Tools Manuf **164**, 103718 (2021)
2. Davim, J.P. (ed.): Sustainable Machining. MFMT, Springer, Cham (2017). https://doi.org/10.1007/978-3-319-51961-6
3. Kopei, V., Onysko, O., Barz, C., Dašić, P., Panchuk, V.: Designing a multi-agent PLM system for threaded connections using the principle of isomorphism of regularities of complex systems. Machines **11**(2), 263 (2023)
4. Kopei, V.B., Onysko, O.R., Panchuk, V.G.: Component-oriented acausal modeling of the dynamical systems in Python language on the example of the model of the sucker rod string. Peer J. Comput. Sci. **2019**(10), e227 (2019)
5. Stupnytskyy, V., Hrytsay, I.: Computer-aided conception for planning and researching of the functional-oriented manufacturing process. In: Tonkonogyi, V., Ivanov, V., Trojanowska, J., Oborskyi, G., Edl, M., Kuric, I., Pavlenko, I., Dasic, P. (eds.) InterPartner 2019. LNME, pp. 309–320. Springer, Cham (2020). https://doi.org/10.1007/978-3-030-40724-7_32
6. Bucinskas, V., Mitrouchev, P., Sutinys, E., Sesok, N., Iljin, I., Morkvenaite-Vilkonciene, I.: Evaluation of comfort level and harvested energy in the vehicle using controlled damping. Energies **10**(11), 1742 (2017)
7. Dutkiewicz, M., Velychkovych, A., Shatskyi, I., Shopa, V.: Efficient model of the interaction of elastomeric filler with an open shell and a chrome-plated shaft in a dry friction damper. Materials **15**(13), 4671 (2022)

8. Shatskyi, I., Velychkovych, A.: Analytical model of structural damping in friction module of shell shock absorber connected to spring. Shock. Vib. **2023**, 4140583 (2023)
9. Kotsyubynsky, V., Shyyko, L., Shihab, T., Prysyazhnyuk, P., Aulin, V., Boichuk, V.: Multilayered MoS2/C nanospheres as high performance additives to lubricating oils. Mater. Today: Proc. **35**, 538–541 (2019)
10. Cocca, P., Marciano, F., Rossi, D., Alberti, M.: Business software offer for industry 4.0: the SAP case. IFAC-PapersOnLine **51**(11), 1200–1205 (2018)
11. Medvid, I., Onysko, O., Panchuk, V., Pituley, L., Schuliar, I.: Kinematics of the Tapered Thread Machining by Lathe: Analytical Study. In: Tonkonogyi, V., Ivanov, V., Trojanowska, J., Oborskyi, G., Grabchenko, A., Pavlenko, I., Edl, M., Kuric, I., Dasic, P. (eds.) InterPartner 2020. LNME, pp. 555–565. Springer, Cham (2021). https://doi.org/10.1007/978-3-030-68014-5_54
12. Yakovyna, V., Seniv, M., Symets, I., Sambir, N.: Algorithms and software suite for reliability assessment of complex technical systems. Radio Electron. Comput. Sci. Control **4**, 163–177 (2020)
13. Kopei, V., Onysko, O., Odosii, Z., Pituley, L., Goroshko, A.: Investigation of the Influence of Tapered Thread Profile Accuracy on the Mechanical Stress, Fatigue Safety Factor and Contact Pressure. In: Karabegović, I. (ed.) NT 2021. LNNS, vol. 233, pp. 177–185. Springer, Cham (2021). https://doi.org/10.1007/978-3-030-75275-0_21
14. Kusyi, Y., Onysko, O., Kuk, A., Solohub, B., Kopei, V.: Development of the Technique for Designing Rational Routes of the Functional Surfaces Processing of Products. In: Karabegović, I., Kovačević, A., Mandžuka, S. (eds.) New Technologies, Development and Application V. NT 2022. Lecture Notes in Networks and Systems, vol 472, pp. 135–143. Springer, Cham (2022). https://doi.org/10.1007/978-3-031-05230-9_16
15. Stupnytskyy, V.: Features of functionally-oriented engineering technologies in concurrent environment. Int. J. Eng. Res. Technol. (IJERT) **2**(9), 1181–1186 (2013)
16. Davim, P.J.: Manufacturing in digital industries: Prospects for Industry 4.0. Advanced Mechanical Engineering, Book 6. Walter de GruyterGmbh, Berlin/Boston, Germany/USA (2020)
17. Pasternak, S., Danylchenko, Y.M., Storchak, M., Okhrimenko, O.A.: Gear Cutting with Disk-Shaped Milling Cutters. In.: Radzevich, S.P., Storchak, M. (eds). Advances in Gear Theory and Gear Cutting Tool Design, pp. 151–179 (2022)
18. Bembenek, M., Dzienniak, D., Dzindziora, A., Sułowski, M., Ropyak, L.: Investigation of the impact of selected face milling parameters on the roughness of the machined surface for 1.4301 steel. Adv. Sci. Technol. Res. J. **17**(4), 299–312 (2023)
19. Barandych, K.S., Vysloukh, S.P., Antonyuk, V.S.: Ensuring fatigue life of parts during finish turning with cubic boron nitride tools. J. Superhard Mater. **40**(3), 206–215 (2018)
20. Danylchenko, Y., Storchak, M., Danylchenko, M., Petryshyn, A.: Cutting process consideration in dynamic models of machine tool spindle units. Machines **11**(6), 582 (2023)
21. Yurchyshyn, I.I., Lytvynyak, Y.M., Hrytsay, I.Y., et al.: Mechanical Engineering Technology. Handbook for the Performance of Qualification Works. Lviv Polytechnic National University, Lviv (2009)
22. Pavlenko, I., et al.: Using regression analysis for automated material selection in smart manufacturing. Mathematics **10**(11), 1888 (2022). https://doi.org/10.3390/math10111888
23. Bembenek, M., Kopei, V., Ropyak, L.Y., Levchuk, K.: Stressed state of chrome parts during diamond burnishing. Metallofiz. Noveishie Tekhnol. **45**(2), 239–250 (2023)
24. Prysyazhnyuk, P., et al.: Analysis of the effects of alloying with Si and Cr on the properties of manganese austenite based on ab initio modelling. Eastern-Eur. J. Enterprise Technol. **6**(12), 28–36 (2020)

25. Onysko, O., Medvid, I., Panchuk, V., Rodic, V., Barz, C.: Geometric Modeling of Lathe Cutters for Turning High-Precision Stainless Steel Tapered Threads. In: Ivanov, V., Trojanowska, J., Pavlenko, I., Zajac, J., Peraković, D. (eds.) DSMIE 2021. LNME, pp. 472–480. Springer, Cham (2021). https://doi.org/10.1007/978-3-030-77719-7_47
26. Ropyak, L., Shihab, T., Velychkovych, A., Bilinskyi, V., Malinin, V., Romaniv, M.: Optimization of plasma electrolytic oxidation technological parameters of deformed aluminum alloy D16T in flowing electrolyte. Ceramics **6**(1), 146–167 (2023)
27. Ropyak, L., Shihab, T., Velychkovych, A., Dubei, O., Tutko, T., Bilinskyi, V.: Design of a two-layer Al–Al2O3 coating with an oxide layer formed by the plasma electrolytic oxidation of Al for the corrosion and wear protections of steel. Progress Phys. Metals **24**(2), 319–365 (2023)
28. Kusyi, Y., Onysko, O., Kuk, A., Kostiuk, O., Solohub, B.: Improvement of the Technique of Optimal Technological Routes Planning for Machining of the Machine Parts Surfaces. In: Karabegovic, I., Kovačević, A., Mandzuka, S. (eds.) New Technologies, Development and Application VI. NT 2023. Lecture Notes in Networks and Systems, vol 687, pp. 221–232. Springer, Cham (2023). https://doi.org/10.1007/978-3-031-31066-9_23
29. Muzyka, N.R., Shvets, V.P., Boiko, A.V.: Procedure and instruments for the material damage assessment by the LM-hardness method on the in-service scratching of structure element surfaces. Strength Mater. **52**, 432–439 (2020)
30. Ivchenko, O., et al.: Method for an effective selection of tools and cutting conditions during precise turning of non-alloy quality steel C45. Materials **15**(2), 505 (2022). https://doi.org/10.3390/ma15020505
31. Pylypchuk, M.I., Dziuba, L.F., Mayevskyy, V.O., Kopynets, Z.P., Taras, V.I.: The distribution pattern of machining errors on woodworking machine tools. J. Eng. Sci. (Ukraine) **10**(2), A34–A42 (2023). https://doi.org/10.21272/jes.2023.10(2).a5

Surface Morphology and Microstructural Features of LPBF-Printed Superalloy Turbine Blade Subjected to HIP, Heat Treatment, and Shot Peening

Dmytro Lesyk[1,2,3(✉)], Silvia Martinez[1], Bohdan Mordyuk[3], Vitaliy Dzhemelinskyi[1], and Aitzol Lamikiz[1]

[1] University of the Basque Country, 1, Plaza Ingeniero Torres Quevedo, 48013 Bilbao, Spain
dmytro.lesyk@ehu.eus
[2] National Technical University of Ukraine "Igor Sikorsky Kyiv Polytechnic Institute", 37, Prospect Beresteiskyi, Kyiv 03056, Ukraine
[3] G.V. Kurdyumov Institute for Metal Physics of the NAS of Ukraine, 36, Academician Vernadsky Boulevard, Kyiv 03142, Ukraine

Abstract. Laser-based powder bed fusion (LPBF) is one of the attractive methods of powder bed fusion additive manufacturing technology to produce lightweight metal products with complex shapes for the aviation/aerospace industry. In this work, the turbine blades were manufactured applying an industrial LPBF system and commercial Inconel 718 powder. The LPBF-built turbine blade superalloy parts were then thermomechanically post-processed to provide surface integrity and material properties. The hot isostatic pressing and heat treatment were applied to provide the required grain structure and density. The subsurface nanostructuring, compressive residual stress, and a new surface microrelief formation were obtained by a surface shot peening. The results show that the applied combined thermomechanical post-treatment increased the hardening intensity in the subsurface and bulk by ~68% and ~35%, respectively. Shot peening led to a ~50% decrease in surface roughness.

Keywords: Process Innovation · Selective Laser Melting Technology · Additive Manufacturing Post-Processing · Inconel 718 · Turbine Blade · Thermomechanical Treatment · Precipitation Hardening · Surface Nanostructuring

1 Introduction

Today, it is important to carry out new relevant studies in aviation and aerospace, developing new aircraft products using additive manufacturing (AM) technology. By applying traditional methods, such as casting, machining, or forging metals, AM methods allow the production of three-dimensional (3D) part geometries with complex shapes and high

© The Author(s), under exclusive license to Springer Nature Switzerland AG 2024
V. Ivanov et al. (Eds.): DSMIE 2024, LNME, pp. 276–286, 2024.
https://doi.org/10.1007/978-3-031-61797-3_23

precision that are difficult or impossible to implement. In particular, aeronautical metallic/composite products can be manufactured with precision by an innovative powder bed fusion 3D printing technology. The main advantages of powder bed fusion are the automated production of tailored metallic products with high density from 3D models and the suitability of one-of-a-kind parts production [1]. Laser powder bed fusion, electron beam bed fusion, and binder jetting were recently used and compared to manufacture Inconel 625 alloy [2]. The powder layer thickness and particle powder fraction are within 60–100 μm and 10–150 μm, respectively, after the mentioned powder bed fusion techniques [3]. To use powder bed fusion technologies for the production of critical metal parts, there is a need to enhance the properties of the aircraft parts according to industry-approved standards.

2 Literature Review

Additive manufacturing technology is used for the final manufacturing of metal products by adding materials layer by layer and fusion them together in the argon-filled chamber from a computer-aided design model. On the one hand, 3D printing is a relatively new, high-cost technology than casting or machining [4]. On the other hand, it allows producing very strong and high-end complex components, reducing material waste [5].

The capability to use lightweight materials makes laser powder bed fusion (LPBF) technology attractive to the aerospace and aviation industry, which may be applied to manufacturing metallic parts like turbine blades [6]. Titanium and nickel alloys are commonly used in the aviation and aerospace industries, which meet the strict requirements of aircraft engine manufacturers for metallographic and mechanical properties [7]. The LPBF approach is suitable for titanium and nickel alloys, which manufacture strong components that are difficult to machine conventionally [8]. As a result, the LPBF method is promising to manufacture safety-related or spare parts for aviation and aerospace applications. LPBF can shorten the time needed to manufacture turbine blades compared to the casting method [9]. On the other hand, there are almost unlimited opportunities for designing internal passages and structures inside parts for better heat transfer, improved cooling (for example, turbine blades) [8], and fuel/air mixing (for example, burners) [10]. Additionally, the production of the compressor blades using the LPBF approach looks less promising due to significant manufacturing costs. Caiazzo et al. confirmed that the mechanical properties are unaffected by the turbine blades' positioning on the working platform [11]. Moreover, it was found that the LPBF-printed turbine blades can be operated under high pressures and temperatures of about 1250 °C [12]. Thus, the LPBF technology is considered feasible for producing lightweight and complexly shaped metal parts despite the challenges with the LPBF integration for aeronautical applications [13].

It should also be noted that the LPBF-fabricated parts still suffer from different and relatively rough surface roughness/waviness [14], subsurface residual porosity [15], and tensile residual stresses [16] in the near-surface layers. Additionally, columnar grain structures with magnificent dendritic structures and segregation of elements are formed in the LPBF-built alloys due to the high cooling rate [17]. The mechanical properties

differ between the scan and build direction [18]. Thus, the manufacturing mentioned above defects can reduce the fatigue strength of the LPBF-built metal parts.

Recently, various post-processing methods were applied to increase the mechanical properties of the LPBF-built superalloys. The stress relief [19], solution or solution followed by aging [20], hot isostatic pressing (HIP) [21], or heat treatments combined with HIP [22] were used to enhance the surface integrity in the LPBF-manufactured superalloys. Theoretical and experimental studies show that improvement in the functional parameters of the physical and mechanical properties and surface texture/morphology of the turbine blade superalloy parts produced by the LPBF approach is very relevant.

This work is intended to study the effects of the combined thermo-mechanical post-treatment technique on the surface texture, 3D surface roughness parameters, structural and phase composition, hardening intensity, precipitation hardening, and surface nanocrystallization of the turbine blade IN 718 alloy produced using LPBF.

3 Research Methodology

In this work, the turbine blade test components were manufactured by the laser powder bed fusion (LPBF) / selective laser melting (SLM) technique using a Renishaw AM400 system (Fig. 1a) and a nickel-based pre-alloyed Inconel (IN) 718 powder (Fig. 1b). The chemical composition of the used IN 718 powder in weight percent, provided by the Renishaw Company, is the following: ~52.5% Ni, ~19.1% Cr, ~4.89% Nb + Ta, ~3.2% Mo, ~0.85% Ti, ~0.42% Al, ~0.04 Si + Co, < 0.03 C, < 0.02 Mn, < 0.01 N + Cu, < 0.01 P + S, and balance Fe [23]. The powder used was characterized predominantly spherical shaped particles, and the particle size distribution was 10–55 μm (Fig. 1b).

Inconel 718 alloy turbine blades were fabricated in an argon atmosphere using a laser power of 200 W and a scan speed of 700 mm/s. A stripe scanning strategy with a hatch distance of 90 μm and stripe sizes of 5 mm was applied using a laser spot size of about 70 μm. The laser scanning patterns were rotated by an angle of 67° between powder layers of 60 μm (Fig. 1c).

After laser 3D printing, the laser powder bed fused IN 718 alloy samples were subjected to thermomechanical post-processing, which consists of a hot isostatic pressing (HIP), homogenization, and double aging (HA). They shot peening (SP) to enhance the structural phase and stress state.

The hot isostatic pressing tests (a heating temperature of 1160 °C, an argon pressure of 160 MPa, and a holding of 3 h) were performed using an industrial QIH 0.9 × 1.5-2070-1400 MURC press. The homogenization heat treatment was implemented at a heating temperature of 1180 °C and a holding of 1 h, cooling in the furnace. The double aging heat treatment was conducted at 720 °C and a holding of 8 h, followed by furnace cooling to 620 °C and holding for 9 h, cooling in the furnace to 80 °C in argon. The homogenization and aging heat treatments were carried out using industrial equipment [24].

The severe surface plastic deformation of the studied parts was implemented using the shot peening (SP) technique. The turbine blade samples were post-processed by a stream of shots with a diameter of 0.5 mm at a peening pressure of 0.55 MPa in a chamber, providing 100% surface coverage.

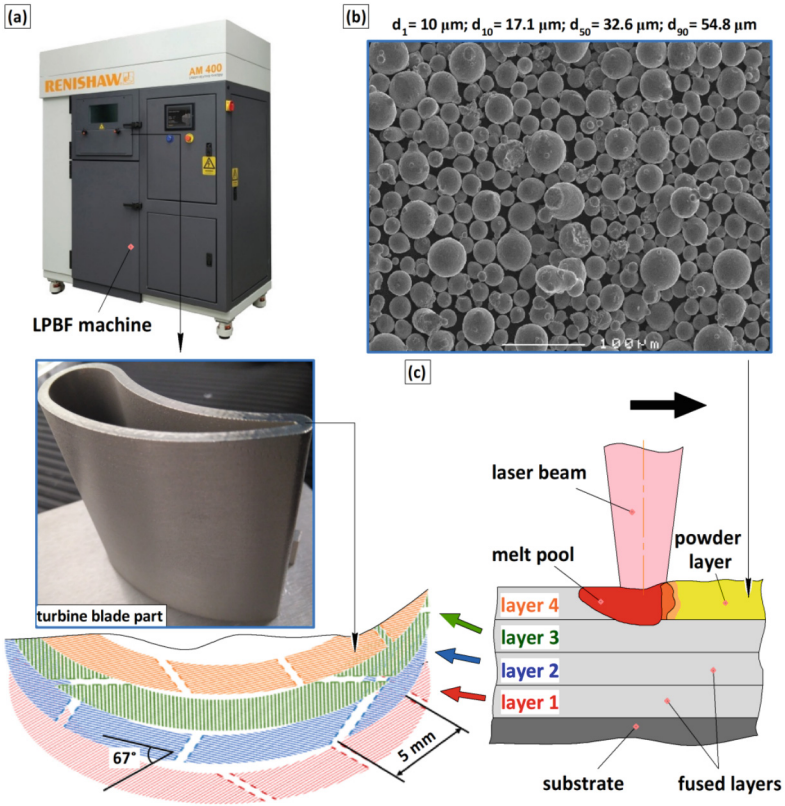

Fig. 1. General view of the Renishaw AM400 system (a), the morphology of the IN 718 powder (b), and LPBF process (c).

The surface morphology and 3D surface roughness parameters were studied by a Mitutoyo Hyper Quick Vision WLI non-contact measuring machine. The X-ray diffraction (XRD) analysis was performed using a Rigaku Ultima IV diffractometer in a CuKα-radiation. The microstructural observation was carried out using a JEOL-CX-II 100 transmission electron microscope (TEM), XL 30 ESEM scanning electron microscope (SEM), and LEICA Reichert Polyvar 2 light optical microscope (LOM). The surface hardness was evaluated using a DIA TESTOR 2Rc hardness tester (10 kgf on the indenter).

4 Results and Discussion

4.1 Surface Morphology

The surface morphology of the LPBF-fabricated and post-treated IN 718 alloy parts analyzed by advanced high-precision and high-resolution optical measuring system is demonstrated in Fig. 2. Non-contact areal surface texture measurements (the research

area was about 0.5 × 0.5 mm) were performed at three different locations for each characterized surface.

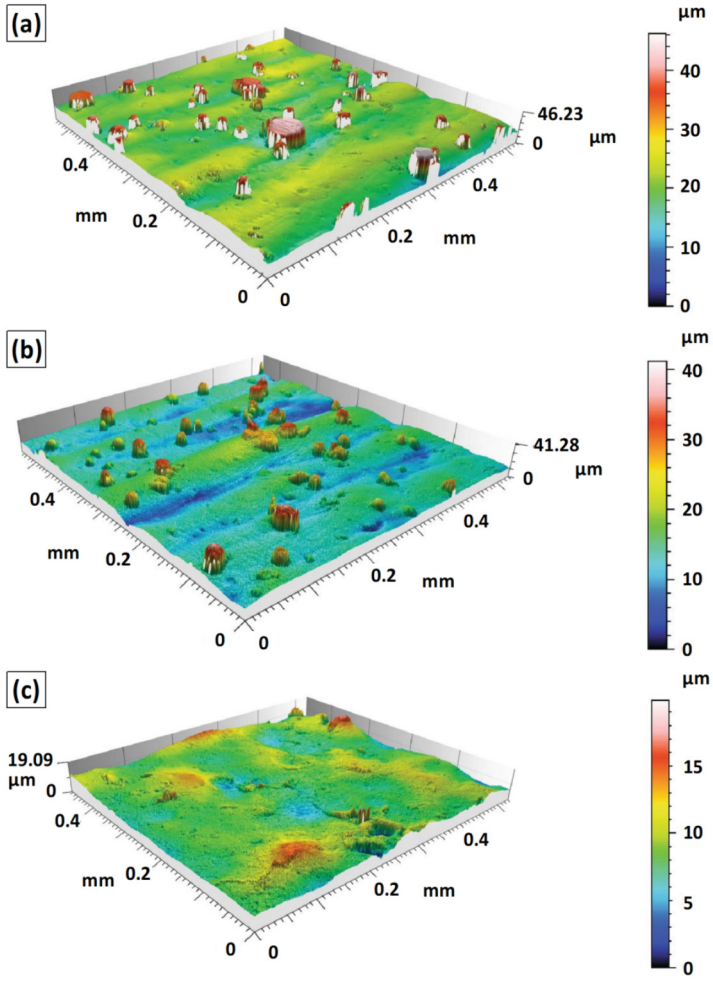

Fig. 2. Surface morphology of the (a) LPBF-produced turbine blade IN 718 alloy parts before and after (b) HIP + HA and (c) HIP + HA + SP post-processing.

The laser scanning passes, spattering powder particles, and partially melted powder particles on the surface may be seen in the LPBF manufactured. Subsequently, HIP + HA-treated superalloy parts (Fig. 2a). The mechanisms of the surface defect formation in the LPBF process are studied in works [25, 26]. In particular, the powder particles are adhered to the LPBF-fused surface without melting due to their existence inside the heat-affected zone [27]. The removal of splatter and weld fumes from the heat-affected zone may be associated with the flow of the shielding gas within the build chamber [26]. The

LPBF-produced turbine blade components exhibit a near-surface porosity accumulation of ~0.67% [21].

Compared to the surface morphology of the Inconel 718 alloy parts produced by LPBF (Rz = 36.5 μm), the HIP + HA processing leads to a slight increase in the maximum height Sz parameter (Sz is the maximum height of the surface texture which is the sum of the absolute values of Sp and Sv). The Sz parameter is about 40 μm after HIP, followed by HA. Increasing the area surface texture parameters after HIP + HA may be related to forming an oxide layer on the surface. Similar results were obtained in the work [26].

The surface finishing by SP provided a new surface texture formation (Fig. 2a), and near-surface material density increased [27]. The surface manufacturing defects were eliminated by severe plastic deformation. The maximum height Sz parameter magnitudes were reduced to 19.23–24.16 μm on the side surfaces of the turbine blade processed by SP.

4.2 Area Surface Roughness

The average area surface roughness magnitudes are presented in Fig. 3. The arithmetical mean height Sa parameter magnitudes of LPBF-built and HIP + HA-treated parts are ranged from 2.14 to 2.44 μm and 2.23 to 2.53 μm, respectively. Compared to the HIP + HA-treated parts, the average Sa parameter values were reduced by %50 after surface finishing used shot peening due to the collisions between the complex shot media and treated surfaces.

The surface roughness improvement was recently achieved after the various surface mechanical treatments, such as sandblasting [26], shot peening [28, 29], and ultrasonic peening [24, 30] of the heat-processed nickel and titanium alloys manufactured by a laser powder bed fusion technology.

4.3 Structural-Phase State and Hardening Intensity

Figure 4 shows the microstructural features observed for the heat-treated and subsequently shot-peened specimens. Application of various microscopic techniques, such as light optical microscopy (LOM), scanning electron microscopy (SEM), and transmission electron microscopy (TEM), allow observing the structural-phase state of the HIP + HA-treated IN 718 alloy parts in different scale levels, i.e., in micro-, meso-, and nano-scales, respectively.

As seen, the HIP + HA thermal post-processing of the LPBF-fabricated IN718 alloy resulted in the formation of homogeneous microstructure with the increased volume fractions of fine γ'/γ'' precipitates (~20 nm) and NbC/TiC carbides (~1–2 μm), providing significant precipitation strengthening due to hindering of the grain coarsening during heat treatment. The resulting grain/crystallite size values were 50–120 μm. The strengthening/hardening intensity of the 718 alloys post-processed by HIP + HA was enlarged by ~35% compared to the LPBF-fabricated part (Fig. 5).

Figure 4d shows the fragments of the XRD patterns with the deconvoluted (220) $\gamma/\gamma'/\gamma''$ X-ray peaks registered for the heat-treated and surface shot-peened parts. These

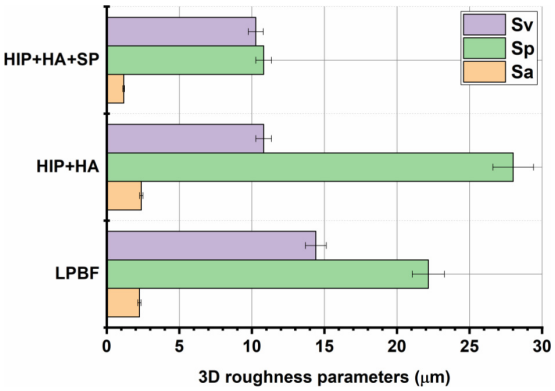

Fig. 3. Area surface roughness parameters of the LPBF-produced turbine blade IN 718 alloy parts before and after HIP + HA and HIP + HA + SP post-processing.

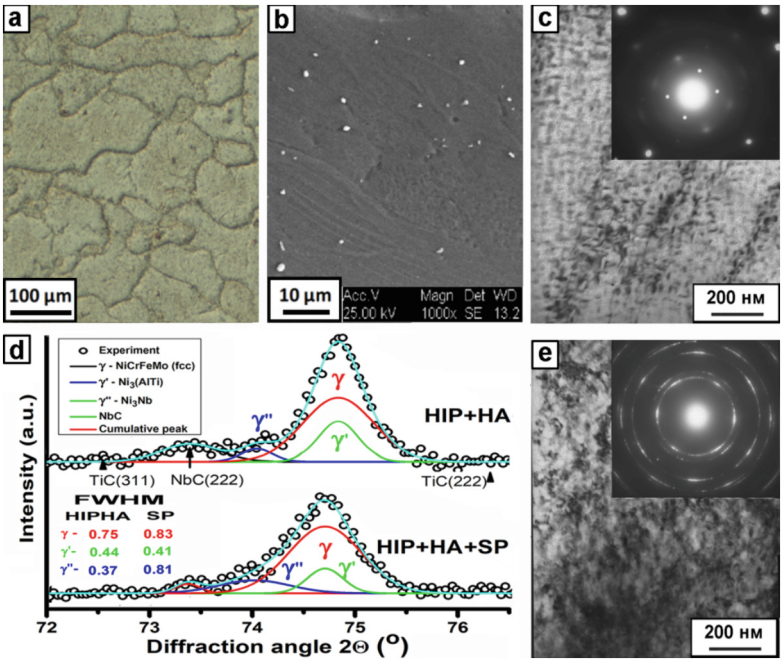

Fig. 4. Microstructural observations of the (a–d) HIP + HA and (d, e) HIP + HA + SP-treated LPBF-built specimens of IN718 alloy by (a) LOM, (b) SEM, (d) XRD, and (c, e) TEM + SAED.

fragments also contain several low-intensity peaks of NbC and TiC carbides. The XRD peak registered after the SP processing is much broadened, which is known to be related to grain/crystallites regiment and lattice microstrains' formation.

Significant grains' refinement owing to SP-induced severe plastic strain of the top surface layer was observed by direct TEM observations and characteristic selective

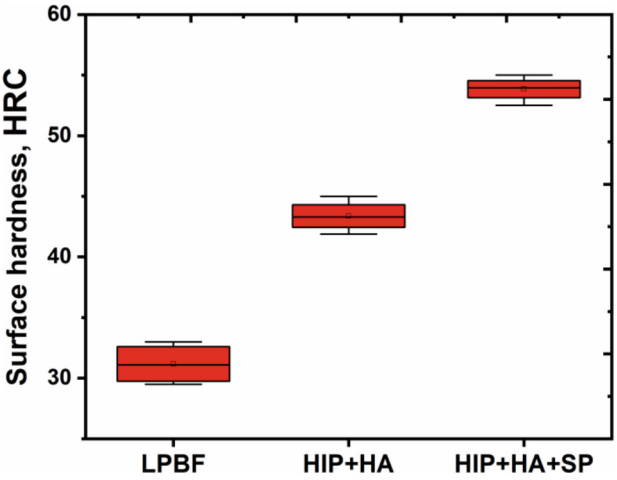

Fig. 5. Surface hardness of the LPBF-produced turbine blade IN 718 alloy parts before and after HIP + HA and HIP + HA + SP post-processing.

area electron diffraction pattern of ring-like type witnesses the formation of the highly misoriented nanoscale grains of 15–20 nm in size (Fig. 4e). Thus, mechanical post-processing by the surface shot peening leads to significant grains' refinement, which is another factor of the observed hardening of the SP-treated IN 718 alloy specimens.

Compared to the surface hardness of the HIP + HA-processed superalloy (~44 HRC), the SP-produced hardness values were increased by ~24%. The near-surface hardening intensity was increased by about 68% after shot peening compared with the LPBF-manufactured IN 718 alloy (Fig. 5). The thickness of the hardened near-surface layer was measured to be 120–140 μm. This layer underwent plastic deformation and became compressed with residual stresses of about –430 MPa on the surface. This is also reported in a similar study [30]. Nevertheless, it should also be noted that the applied thermomechanical post-processing in the sequence HIP + HT + SP is more effective than that of the HT + HIP + SP method [30] through reduction of the yield strength because of the γ'' phase dissolution during the hot isostatic pressing. The HIP + HT + SP technique can be used when higher fatigue performance is required, while the HT + HIP + SP technique may be an exemplary process for improving creep behavior.

5 Conclusions

This work aimed to obtain the IN 718 alloy turbine blade with a required grain structure and phase/residual stress state, enhancing the surface integrity. The combined thermo-mechanical post-processing technique was applied to strengthen and finish the studied heat-resistant alloy. The effects of the hot isostatic pressing followed by heat treatment (homogenization and double aging) and shot peening on the surface properties of the turbine blade IN 718 alloy test parts were studied. The main findings of this study can be summarized as follows.

HIP + HA thermal post-processing leads to the formation of homogeneous microstructure with the increased volume fractions of fine γ'/γ'' precipitates and NbC/TiC carbides, providing significant precipitation strengthening. The hardening intensity of the HIP + HA-treated IN 718 alloy was increased by ~35% (~44 HRC).

SP mechanical post-processing led to significant grains' refinement in the near-surface layer (15–20 nm), providing the compressive residual stresses (–430 MPa on the surface) and increasing the hardening intensity by ~24% (~54 HRC) as compared to the HIP + HA-treated IN 718 alloy.

The severe plastic deformation induced by SP reduced the area surface roughness of the LPBF-built and HIP + HA-treated IN 718 alloy turbine blade to almost 50%.

The study of the crystal orientations by electron backscatter diffraction and electrochemical corrosion behavior of the LPBF-manufactured and thermomechanically post-processed IN 718 alloy parts is planned for further research.

Acknowledgements. The authors, D.A. Lesyk and B.M. Mordyuk, are grateful to the National Research Foundation of Ukraine (NRFU) for the support of the Project within the NRFU Competition "Science for the Recovery of Ukraine in the War and Post-War Periods" (Agreement No. 2022.01/0038). D.A. Lesyk also acknowledges the ADAGIO Fellowship Programme within the European Union's Horizon 2020 research and innovation programme under the Marie Sklodowska-Curie Actions (Agreement No. 101034379).

References

1. Sola, A., Nouri, A.: Microstructural porosity in additive manufacturing: the formation and detection of pores in metal parts fabricated by powder bed fusion. J. Adv. Manuf. Process. **1**, e10021 (2019). https://doi.org/10.1002/amp2.10021
2. Gonzalez, J.A., et al.: Characterization of Inconel 625 fabricated using powder-bed-based additive manufacturing technologies. J. Mater. Process. Technol. **264**, 200–210 (2019). https://doi.org/10.1016/j.jmatprotec.2018.08.031
3. Vock, S., et al.: Powders for powder bed fusion: a review. Prog. Addit. Manuf. **4**, 383–397 (2019). https://doi.org/10.1007/s40964-019-00078-6
4. Wang, X., et al.: Review on powder-bed laser additive manufacturing of Inconel 718 parts. Proc. Inst. Mech. Eng., Part B: J. Eng. Manuf. **231**, 1890–1903 (2017). https://doi.org/10.1177/095440541561
5. John, T.P., et al.: A comparison of traditional manufacturing vs additive manufacturing, the best method for the job. Procedia Manuf. **30**, 11–18 (2019). https://doi.org/10.1016/j.promfg.2019.02.003
6. Babu, S.S., et al.: Additive manufacturing of nickel superalloys: opportunities for innovation and challenges related to qualification. Metall. Mater. Trans. A **49**, 3764–3780 (2018). https://doi.org/10.1007/s11661-018-4702-4
7. Murray, S.P., et al.: A defect-resistant Co–Ni superalloy for 3D printing. Nat. Commun. **11**, 4975 (2020). https://doi.org/10.1038/s41467-020-18775-0
8. Uriondo, A., et al.: The present and future of additive manufacturing in the aerospace sector: a review of important aspects. Proc. Inst. Mech. Eng., Part G: J. Aerosp. Eng. **229**, 2132–2147 (2015). https://doi.org/10.1177/0954410014568797
9. Madara, S.R., et al.: Review of recent development in 3-D printing of turbine blades. Euro. J. Adv. Engg. Tech. **4**, 497–509 (2017)

10. Torres-Carrillo, S., et al.: Environmental analysis of selective laser melting in the manufacturing of aeronautical turbine blades. J. Clean. Prod. **246**, 119068 (2020). https://doi.org/10.1016/j.jclepro.2019.119068
11. Caiazzo, F., et al.: Laser powder-bed fusion of Inconel 718 to manufacture turbine blades. Int. J. Adv. Manuf. Technol. **93**, 4023–4031 (2017). https://doi.org/10.1007/s00170-017-0839-3
12. Wang, X., et al.: A review on the processing of aero-turbine blade using 3D print techniques. J. Manuf. Mater. Process. **6**, 16 (2022). https://doi.org/10.3390/jmmp6010016
13. Early, B., et al.: Characterization of LAM-fabricated porous superalloys for turbine components. J. Eng. Gas Turb. Pow. **139**, 102102 (2017). https://doi.org/10.1115/GT2016-58080
14. Yan, X., et al.: Effect of building directions on the surface roughness, microstructure, and tribological properties of selective laser melted Inconel 625. J. Mater. Process. Technol. **228**, 116878 (2021). https://doi.org/10.1016/j.jmatprotec.2020.116878
15. Wang, F., et al.: Experimental investigation of porosity distribution in selective laser melted Inconel 718. Procedia Manuf. **48**, 807–813 (2020). https://doi.org/10.1016/j.promfg.2020.05.117
16. Raghavan, R., et al.: Residual stress evaluation in selective-laser-melting additively manufactured titanium (Ti-6Al-4V) and Inconel 718 using the contour method and numerical simulation. Addit. Manuf. **22**, 571–582 (2018). https://doi.org/10.1016/j.addma.2018.06.002
17. Raghavan, R., et al.: Effect of different heat treatments on the microstructure and mechanical properties in selective laser melting INCONEL 718 alloy. Mater. Manuf. Process. **32**, 1588–1595 (2017). https://doi.org/10.1080/10426914.2016.1257805
18. Goutianos, S.: Selective laser melting of hot gas turbine components: materials, design and manufacturing aspects. Mater. Sci. Eng. **219**, 012022 (2019). https://doi.org/10.1088/1757-899X/219/1/012022
19. Gruber, K.: Impact of high temperature stress relieving on final properties of Inconel 718 processed by laser powder bed fusion. Mater. Sci. Eng. A **813**, 141111 (2021). https://doi.org/10.1016/j.msea.2021.141111
20. Barros, R.: Laser powder bed fusion of Inconel 718: residual stress analysis before and after heat treatment. Metals **9**, 1290 (2019). https://doi.org/10.3390/met9121290
21. Lesyk, D., Martinez, S., Dzhemelinkyi, V., Lamikiz, A.: Additive manufacturing of the superalloy turbine blades by selective laser melting: Surface quality, microstructure and porosity. In: Karabegović, I. (ed.) NT 2020. LNNS, vol. 128, pp. 267–275. Springer, Cham (2020). https://doi.org/10.1007/978-3-030-46817-0_30
22. Schneider, J.: Microstructure evolution in Inconel 718 produced by powder bed fusion additive manufacturing. J. Manuf. Mater. Process. **6**, 20 (2022). https://doi.org/10.3390/jmmp6010020
23. Sanchez, S., et al.: The creep behaviour of nickel alloy 718 manufactured by laser powder bed fusion. Mater. Des. **204**, 109647 (2021). https://doi.org/10.1016/j.matdes.2021.109647
24. Lesyk, D., Martinez, S., Pedash, O., Dzhemelinskyi, V., Mordyuk, B.: Combined thermomechanical techniques for post-processing of the SLM-printed Ni-Cr-Fe alloy parts. In: Ivanov, V., Trojanowska, J., Pavlenko, I., Zajac, J., Peraković, D. (eds.) DSMIE 2020. LNME, pp. 295–304. Springer, Cham (2020). https://doi.org/10.1007/978-3-030-50794-7_29
25. Ding, R.: Effect of shielding gas volume flow on the consistency of microstructure and tensile properties of 316L manufactured by selective laser melting. Metals **11**, 205 (2021). https://doi.org/10.3390/met11020205
26. Taljaard, D.J.: The effect of sandblasting and bead blasting on the surface finish of dry electrolyte polishing of laser powder bed fusion parts. J. Mater. Eng. Perfor. **32**, 2050–2061 (2023). https://doi.org/10.1007/s11665-022-07259-5
27. Maamoun, A.H.: Influence of shot peening on AlSi10Mg parts fabricated by additive manufacturing. J. Manuf. Mater. Process. **2**, 40 (2018). https://doi.org/10.3390/jmmp2030040

28. Mythreyi, O.V.: Corrosion study of selective laser melted IN718 alloy upon post heat treatment and shot peening. Metals **10**, 1562 (2020). https://doi.org/10.3390/met10121562
29. Ardia, D.T.: Effects of post-processing route on fatigue performance of laser powder bed fusion Inconel 718. Addit. Manuf. **36**, 101442 (2020). https://doi.org/10.1016/j.addma.2020.101442
30. Trudel, E.: Experimental optimization for fatigue life maximization of additively manufactured Ti-6Al-4V alloy employing ultrasonic impact treatment. J. Mater. Eng. Perform. **30**, 2806–2821 (2021). https://doi.org/10.1007/s11665-021-05576-9

Study of Power Parameters of the Screw Spirals Forming

Oleg Lyashuk(✉), Roman Rogatynskyi, Ivan Hevko, Tetiana Navrotska, and Andrii Diachun

Ternopil Ivan Puluj National Technical University, 56, Ruska Street, Ternopil 46001, Ukraine
lyashuk_o@tntu.edu.ua

Abstract. Based on the study of the technological processes of screw spirals manufacturing, the article derives analytical and empirical dependencies for calculating the bending moment, force and design parameters of the screw spirals manufacturing process by the method of tape winding using a forming tool with a rotating sleeve, which allows distributing the load on the forming rollers. The forming tool with a rotating sleeve for screw spirals winding is designed. The analytical dependence for determining the thickness of the spiral after forming by winding method is developed. The bending moment and force parameters for screw spirals winding are determined. The experimental study of the screw spirals winding processes by the forming tool with a rotating sleeve is conducted. After processing the experimental data, the regression equations have been obtained. The response surfaces and two-dimensional cross-sections of the response surfaces of the dependence of the tape winding bending moment on the outer radius of the mandrel, tape thickness, and tape width for 08kp steel and St 3 steel are presented.

Keywords: Forming Tool · Screw Spiral · Bending Moment · Force Parameters · Manufacturing Innovation

1 Introduction

Screw spirals are used as both transport and technological elements in various types of machines and mechanisms, and first of all, in screw conveyors. Much attention has long been paid to their creation. However, the complexity and high energy consumption of their manufacturing processes, as well as increased requirements for quality, reliability, durability, design, and technological parameters of these workpieces, force them to search for progressive ways to obtain them. Therefore, the study of a newly developed method of screw spirals winding with a rotating sleeve is relevant and allows for obtaining new productive technology.

Many methods of screw spirals manufacturing are known. They difference is in the sequence and number of operations, kinematic schemes, the shape of the working elements, and the nature of their contact with the workpiece. The choice of the optimal method of screw spirals manufacturing and the rational design of the forming tool is

© The Author(s), under exclusive license to Springer Nature Switzerland AG 2024
V. Ivanov et al. (Eds.): DSMIE 2024, LNME, pp. 287–298, 2024.
https://doi.org/10.1007/978-3-031-61797-3_24

determined by the following factors: the size and shape of the screw spirals, their physical, mechanical, and technological properties, the requirements for the accuracy of the workpieces and their surface quality.

2 Literature Review

There are six main methods of screw spirals manufacturing: stamping [1], forging [2, 3], casting [4, 5], rolling [6], winding [7, 8], and machining [9, 10].

Many scientists created the theoretical foundations of technological methods of workpieces forming by bending. The solution of theoretical problems for the calculation of bending processes, which are of great practical importance, in particular, for the screw spirals production by the methods of winding on a frame, rolling, and determining their main parameters, is given in the works [11, 12].

Peculiarities of tape bending processes are studied in publications [13–15], which give formulas for determining stresses, bending moments, and forming forces.

Existing methods of screw spiral winding are implemented by winding the tape on different types of frames. Known shaping methods involve bending the tape to these frames with rollers of different types. In general, the existing methods of screw spiral winding are quite similar and differ only in the location of the roller relative to the frame, as well as the location of the tape relative to the roller and the frame [16, 17]. It has been developed and researched a new way of the screw spirals winding with the help of a rotating sleeve, which allows to obtain both broadband spirals and screw spirals with significant internal diameters.

3 Research Methodology

Several variants of screw spirals winding methods and forming tools with a rotating sleeve have been generated, one of which is presented in Fig. 1. The process is implemented using a lathe and a forming tool. Winding of spirals by the rotating sleeve provides performance of the following operation elements: fastening in the chuck of the lathe frame and installation of tape in it; pressing the frame and fixing it with the rear headstock with the supply of a rotating sleeve, which is fixed in the tool holder of the caliper; installing the tape in the guide roller; switching on the main movement of the machine and winding the spiral into a tight package; switching off the main movement of the machine with the removal of the rear headstock and caliper with a rotating sleeve from the frame; removing the coiled screw spiral from the frame.

The description of the forming tool with a rotating sleeve (Fig. 1) and the process of screw spiral winding is presented below. In the chuck of lathe 1, a stepped frame 2 is fixed, which is rigidly located on the left sleeve 3 and with the possibility of axial displacement on the shaped surface 4 of the right sleeve 5. An axial groove is made on the outer edge of the right sleeve 5, into which the L-shaped end of the tape 16 for the screw spiral winding is inserted. The right end of the right sleeve 5 is pressed through the washer by a compression spring 7, the clamping force regulated by a nut 10 through the washer 9 through a trapezoidal threaded connection 8. The right end of frame 2 is pressed by the rear headstock 11 to balance and give the structure rigidity. In the caliper

of machine 13, the holder 14 of the rotating sleeve 12 is rigidly fixed. The rotating sleeve 12 consists of an outer holder in which the bearing 17 and the forming sleeve 18 are located. A guide roller 15 is fixed on the outer edge of the rotating sleeve 12. The support sleeve is also equipped with forming rollers, which help bend the tape into a spiral at its initial formation stage.

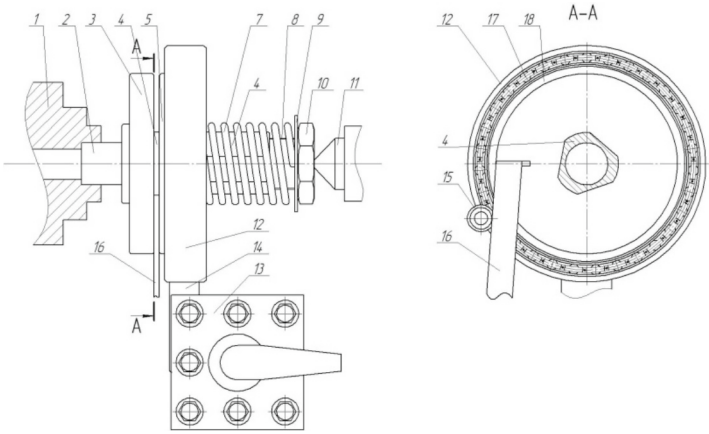

Fig. 1. The forming tool with a rotating sleeve for screw spirals winding.

When winding the tape on the rib with calibration on the outer diameter due to the bending force, which is distributed over the contact zone of the clamping frame, the winding process has its characteristics. To detect them, the winding of tape workpieces with width B_o and thickness H_o by forming a sleeve to the outer radius of the spiral coil R is considered in Fig. 2.

The spiral is formed into a package with an inner radius r. According to [13, 14], when bending (winding) the tape on edge, there is a plane-stress state in which the selected longitudinal elementary layer changes the size of its cross-section in both radial and longitudinal directions.

For practical use, the change of spiral thickness h_ρ depending on the radial parameter ρ can be submitted as:

$$h_\rho = H_0\sqrt{\frac{\rho_0}{\rho}}, \tag{1}$$

where ρ is the radial parameter of the selected longitudinal layer of the wound tape; ρ_0 is the radius of the neutral layer of deformation, the length of which does not change during winding (bending).

The radius of the neutral layer of deformation ρ_0 is

$$\rho_0 = \left(\frac{2\beta r_c}{\sqrt{R}+\sqrt{r}}\right)^2, \tag{2}$$

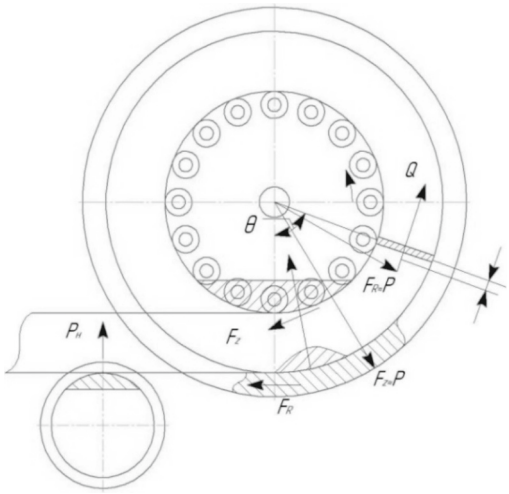

Fig. 2. The calculation scheme of spirals screws winding by the rotating sleeve.

The width of the workpiece should be with zero, the width of the tape – β without, that is, the ratio of the width $B = R\text{-}r$ of the wound spiral to the width of the tape (workpiece) $\beta = B/B_0 = (R–r)/B_0$.

Technologically, the degree of curvature of the bent tape is estimated by the ratio of the length of the outer edge of the screw spiral to the length of the inner edge ψ, which is called the coefficient of non-uniformity of extraction, $\psi = R/r$. Then, the cross-sectional area of the spiral is

$$S_c = \frac{2\beta H_0 r_c\left(\sqrt{R} - \sqrt{r}\right)}{\sqrt{R} + \sqrt{r}} = \frac{4\beta B_0 H_0\left(1 + \psi + \sqrt{\psi}\right)}{3\left(1 + \psi + 2\sqrt{\psi}\right)} \tag{3}$$

and the radius of the center of gravity is

$$r_c = \left(R + r + \sqrt{Rr}\right)/3. \tag{4}$$

Then, the cross-sectional area can be written as

$$S_c = K_s B_0 H_0, \tag{5}$$

where K_s is the coefficient of the cross-sectional area change of the tape when winding,

$$K_s = \frac{4\beta\left(1 + \psi + \sqrt{\psi}\right)}{3\left(1 + \psi + 2\sqrt{\psi}\right)}. \tag{6}$$

Accordingly, the dependence (1) will take the form

$$h_\rho = H_0\sqrt{\frac{\rho_0}{\rho}} = \frac{2\beta H_0 R\left(1 + \psi + \sqrt{\psi}\right)}{3\left(\sqrt{R} + \sqrt{r}\right)\sqrt{\rho}} = \frac{2\beta H_0\left(1 + \psi + \sqrt{\psi}\right)\left(\sqrt{R} + \sqrt{r}\right)}{3\left(1 + \psi + 2\sqrt{\psi}\right)\sqrt{\rho}} \tag{7}$$

In the first approximation, in particular, for spirals with $\psi \geq 2.5$, radius ρ_0 is equal to the neutral stress radius ρ_H ($\rho_0 = \rho_H = \sqrt{Rr}$) and dependence (7) has the form $h_\rho = H_0\sqrt{\sqrt{Rr}/\rho}$.

The scheme of the tape bending to the edge on the outer diameter of the rotating hollow frame (matrix) is considered in Fig. 2. Since the distribution of bending contact stresses is complex and difficult to calculate analytically, we will record the balance of work.

The length of the workpiece element l_0, along which the line of the neutral layer of deformations of radius ρ_0 after winding will not change, is determined by an arc with an angle Θ, $\Theta = l_0/\rho_0$.

The bending moment M_B is determined by a pair of bending forces P, applied to the tape from the action of the guide sleeve (P_r) and forming sleeve (P_R), where $P_R \approx P_r \approx P$. These forces are directed perpendicular to the outer and inner edges in the deformation zone and have components of friction forces μP, where μ is the friction coefficient in the Coulomb-Amonton law. The pressing on the outer edge is done by the hollow sleeve, installed with the possibility of free rotation, and therefore, the friction forces are mainly localized on the guide sleeve in contact with the inner edge of the spiral and are determined by the radial parameter r.

The spiral is formed during shaping by an axial clamping drive sleeve with force F_z, which is technologically acceptable in proportion to the force P by selecting compression springs.

Then, the equation of the balance of work when winding will take the following form:

$$Ql = M_B\theta + k_P\mu rP\theta + k_F\mu rF_z\theta + \varepsilon Ql, \tag{8}$$

where Q is the tangential force, k_P is the coefficient of reduction of the radial parameter of friction forces, k_F is the coefficient of proportionality of the assignment of the axial clamping force, r_F is the radial parameter of force application F_z, $r_F = k_F r$, ε is the relative elongation of the tape, $\varepsilon = r_c/\rho_0 - 1$. Since the pressing of the bent tape takes place in the area with the most significant thickness, i.e., on the inner edge of the spiral, it is taken as the radial parameter r_F, equal to the radius of the inner edge of the coil r, so $k_F \approx 1$.

From there, given that $l \approx r_c\theta$

$$Q = \frac{M_B + \mu rP\left(k_p + k_F k_z\right)}{(1-\varepsilon)r_c}. \tag{9}$$

Consider the components of the dependence (9). The following dependence determines the bending moment

$$M_B = \frac{2\beta H_0(R^2 + 2r\sqrt{rR} - 3rR)}{3}\left(\sigma_{T0} + \prod \ln\sqrt{\frac{R}{r}}\right)\sqrt[4]{\frac{R}{r}} \tag{10}$$

where σ_{TO} is the yield strength of the material, Π is the linear modulus of material hardening.

To confirm the theoretical results, a set of experiments are conducted to study the processes of screw spirals winding by the forming tool with a rotating sleeve and with external radii of the frame $r = 40$–60 mm from the tapes up to 30 mm wide and 1–3 mm thick, which will allow establishing patterns with greater accuracy and peculiarity of the screw spirals forming process, the characteristics of which are presented in Table 1. For these workpieces, the following materials are used: steel 08 kp ($\sigma_{TO} = 276$ MPa, $\mathit{\Pi} = 483$ MPa), St 3 ($\sigma_{TO} = 368$ MPa, $\mathit{\Pi} = 526$ MPa). The forming tool (Fig. 3) was installed on a lathe (Fig. 4). Altivar 71 frequency converter with PowerSuite software v.2.5.0 was used to start the machine's main engine, adjust its speed, and take experimental data. The process of spirals winding (Fig. 5) in the Power Suite window on the computer display shows the engine's torque and winding force over time.

Fig. 3. General view of the elements of the forming tool for the spirals winding by rotating sleeve: 1 - rotating sleeve; 2 - thrust bearing; 3 - straight sleeve; 4 - the left plug; 5 - forming rollers; 6 - guide roller; 7 – spring.

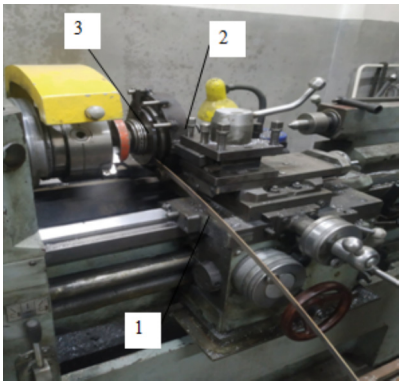

Fig. 4. General view of the spiral winding process by the rotating sleeve: 1 - tape for winding; 2 - the left plug; 3 - rotating sleeve.

To build a mathematical model that characterizes the dependence of the bending moment of the screw spirals winding process by the rotating sleeve with the change of the outer radius of the frame R, tape width B_0 and the thickness of the tape H_0, a full-factor experiment is conducted. Characteristics of factors and values of their levels are given in Table 1.

Fig. 5. Spiral screws wounded in packages.

Table 1. Characteristics of factors and their levels.

Coded factor designation	Factor name	Factor levels value
x_1	Tape thickness H_0, mm	1-2-3
x_2	The external radius of the frame R, mm	40-50-60
x_3	Tape width B_0, mm	10-20-30

The results have been obtained in the format of graphical dependencies in the Power Suite window v.2.5.0, displayed in the oscilloscope window.

4 Results and Discussion

Figure 6 shows the change of the bending moment on the edge of the tape made of steel material St 3 with constant width B_0 and thickness H_0 from the outer radius R of the spiral (the radius of the hollow sleeve).

Figure 7 shows the change of the bending moment M_B from the width B_0 of the tape from material steel St 3 at winding in the hollow forming plug with the external diameter from 100 to 300 mm, with calibration on the external diameter of the spiral.

After converting the expression $R^2 + 2r\sqrt{rR} - 3rR = (R-r)^2 - \left(\sqrt{rR} - r\right)^2$ it follows

$$R^2 + 2r\sqrt{rR} - 3rR = B_0^2\left[1 - \frac{1}{(\sqrt{R/r}+1)^2}\right] = B_0^2\frac{\sqrt{\psi}\left(\sqrt{\psi}+2\right)}{(\sqrt{\psi}+1)^2}. \quad (11)$$

Accordingly, the dependence (10) will take the form

$$M_B = \beta B_0^2 H_0 \frac{\sqrt[4]{\psi}\left(\sqrt{\psi}+2\right)}{3(\sqrt{\psi}+1)^2}\left(\sigma_{T0} + \Pi \ln \sqrt{\psi}\right). \tag{12}$$

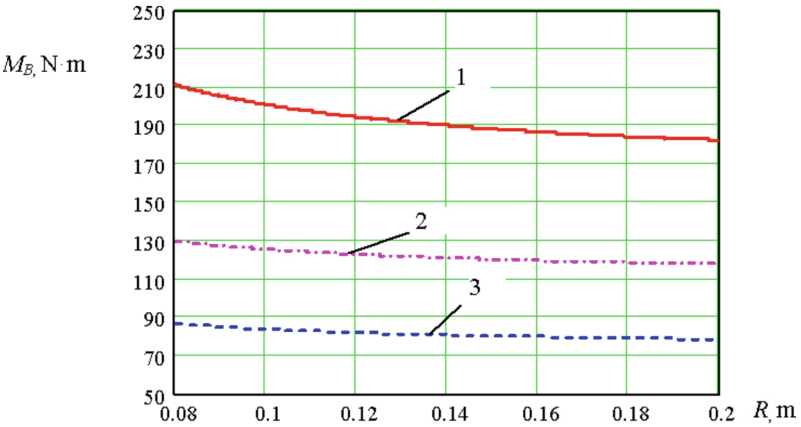

Fig. 6. Changing the bending moment M_B from the outer radius R of the spiral at: 1) $H_0 = 2$ mm, $B_0 = 30$ mm; 2) $H_0 = 3$ mm, $B_0 = 20$ mm; 3) $H_0 = 2$ mm, $B_0 = 20$ mm.

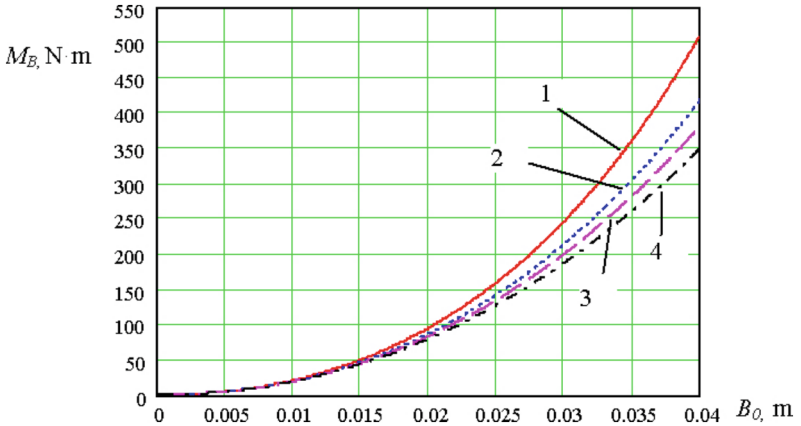

Fig. 7. Changing the bending moment M_B from the width of the workpiece B_0 when winding screw spirals by the rotating sleeve with external radii: 1) $R = 50$ mm; 2) $R = 75$ mm; 3) $R = 100$ mm; 4) $R = 150$ mm.

Taking into account (9) the relationship between the force of retraction of the spiral in the working area of winding and the bending moment will be

$$Q = \frac{M_B\left[1 + \mu\left(k_\mu + k_z k_F\right)\right]}{r_c(1-\varepsilon)} = K_Q \frac{M_B}{r_c}, \tag{13}$$

where the reduction parameter $K_Q = \left[1 + \mu k_\mu (k_P + k_Z k_F)(r/l_P)\right]/(1 - \varepsilon)$.

Accordingly, the winding moment on the drive frame with the end of the spiral fixed and, respectively, on the machine spindle

$$M_W = r_c Q = K_Q M_B = K_\Sigma H_0 B_o^2 (\sigma_{T0} + \Pi \ln \psi), \tag{14}$$

where K_Σ is the complex coefficient depending on the length of the shoulder of the forces application and winding conditions

$$K_\Sigma = 0,25 \beta K_M K_Q = \frac{\beta K_M [1 + \mu k_\mu (k_P + k_e k)]}{4(1 - \varepsilon)} \approx \frac{\beta [1 + \mu k_\mu (k_P + k_e k)]}{4(1 - \varepsilon)\psi^{0,1}} \tag{15}$$

After processing the experimental data, the regression equations have been obtained, which reflect the functional dependence of the change in the bending moment of the tape winding process on the outer radius of the frame, tape thickness, and tape width for the steels 08kp and St 3(Fisher's criteria F = 6.282) and St 3 (Fisher's criteria F = 7.04):

$$\begin{aligned} M_{(H_0,R,B_0)}^{(steel08kp)} &= -938.710 + 31.195R + 15.952B_0 + 2.19H_0B_0 \\ &\quad - 0.28R^2 + 0.141R \quad B_0 - 0.301B_0^2; \end{aligned} \tag{16}$$

$$\begin{aligned} M_{H_{0,R,B_0}}^{(St3)} &= -288.606 + 3.583R + 18.221B_0 + 2.251H_0B_0 \\ &\quad + 0.125RB_0 - 0.314B_0^2. \end{aligned} \tag{17}$$

To construct and analyze the bending moment's dependences on the tape's width, the mandrel's outer radius, and the tape's thickness, we used the Statistisa statistical program package for the PC. Analysis of the randomness of the process was evaluated according to standard methods.

The below figures show the response surfaces and two-dimensional cross-sections of the response surfaces of the dependence of the tape winding bending moment on the outer radius of the mandrel, tape thickness, and tape width for 08kp steel (Fig. 8) and St 3 steel (Fig. 9).

From these graphic dependencies presented in Fig. 8 it can be seen that for steel 08kp with $H_0 = 2$ mm, $R = 50$ mm and the change in B_0 within 10–30 mm, the bending moment of winding acquires the values from 399 N·m till 511 N·m; for St 3 steel (Fig. 9), the winding bending moment increases by 1.07 times and is within the range of 431 N·m till 548 N·m when $H_0 = 2$ mm, $R = 50$ mm and change B_0 within 10–30 mm.

It was established that the energy consumption for forming is reduced by 15% during the winding process using lubricant. For continuous winding devices, it is especially effective to supply lubricant to the coil lifting area along the guide sleeve and in the spiral expansion area, if necessary and if the appropriate mechanism is available.

The calculated bending force R for the strip made of 08kp steel, based on experimental data and regression Eq. (16) for H0 = 2 mm, is in the range of 2410 N to 3210 N. This range exceeds the bending force values obtained in the article [16] (from 1250 N to 1750 N). This can be explained by the occurrence of additional friction moments between the strip and the forming rollers in the tool for winding screw spirals, whereas such rollers are absent in the devices of the article [16]. The developed design of the forming tool with a rotating sleeve for screw spiral winding (Fig. 1) allows expanding the synthesized methods of forming screw spirals presented in the article [17].

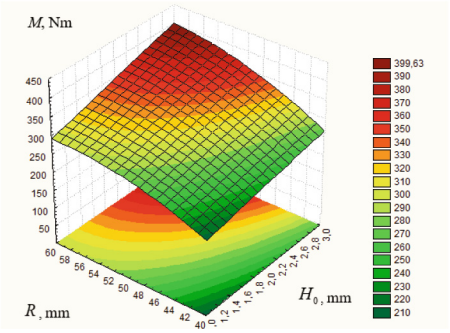

a)

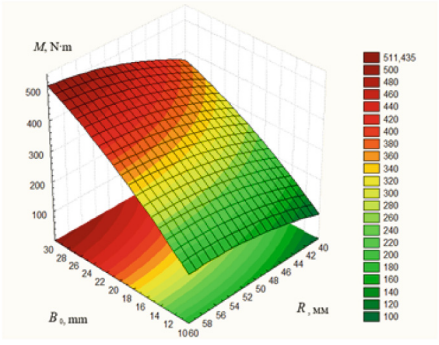

b)

Fig. 8. Response surfaces of the dependences: a) M_B ($_{steel08kp}$) = $f(R, H_0)$; b) M_B ($_{steel08kp}$) = $f(B_0, R)$.

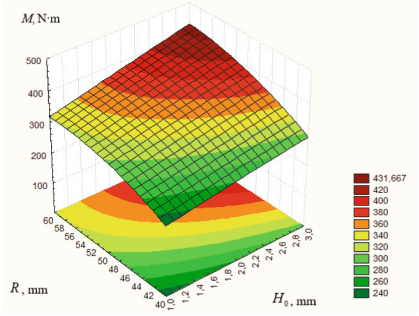

a)

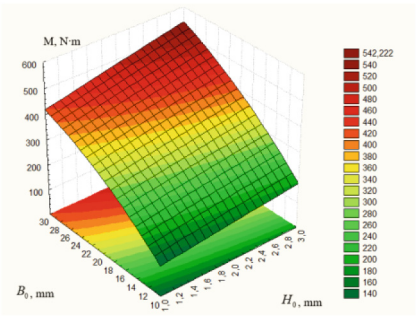

b)

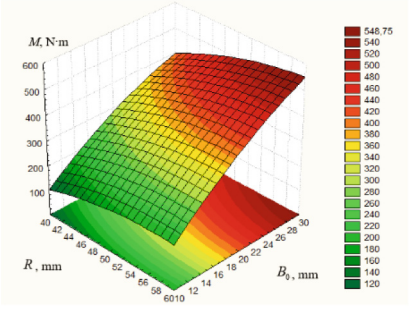

c)

Fig. 9. Response surfaces of the dependences: a) M_B ($_{st3}$) = $f(R, H_0)$; b) M_B ($_{st3}$) = $f(B_0, H_0)$; c) M_B ($_{st3}$) = $f(R, B_0)$.

5 Conclusions

Based on a systematic approach to the study of the technological processes of screw spirals manufacturing, the article derives analytical and empirical dependencies for calculating the power and design parameters of the screw spirals manufacturing process by the method of tapes winding using a forming tool with a rotating sleeve, which allows distributing the load on the forming rollers.

Due to the peculiarity of the tape winding on the frame in many cases, screw workpieces with limited parameters were obtained. The results of the research show that bending is carried out by a force with which shoulder application is extensive enough $l \geq (1...2)r$. In the case of the use of a frame that ensures the stability of the tape on the outer radius during winding, which differs in the scheme of bending force application ($l \leq 0,5r$), it is possible to wind screw spirals with the applied height $b = 12–15$ and higher. In addition, the application of the proposed method is limited by such parameters as the minimum bending radius R_{min}. Depending on the width of the tape and the material used R_{min} $(0.8–1.37)B_0$.

According to the results of the experimental study, it can be seen that for steel 08 kp at $H_0 = 2$ mm, $R = 50$ mm, and change B_0 in the range of 10–30 mm, the bending moment becomes significant: from 399 N·m till 511 N·m. For steel St 3, the bending moment increases by 1.07 times and is within the range of 431 N·m till 548 N·m when $H_0 = 2$ mm, $R = 50$ mm, and change B_0 within 10 - 30 mm.

It has been established that the energy consumption for forming is significantly reduced during the winding process using lubricants. For continuous winding devices, it is especially effective to supply lubricant to the coil lifting area along the guide sleeve and in the spiral expansion area, if necessary and if the appropriate mechanism is available.

References

1. Afzala, M., Maqboola, F., Hajavifardb, R., Buhla, J., Waltherb, F., Bambacha, M.: Modeling the residual stresses induced in the metastable austenitic stainless steel disc springs manufactured by incremental sheet forming by a combined hardening model with phase transformation. Procedia Manufact. **47**, 1410–1415 (2020). https://doi.org/10.1016/j.promfg.2020.04.300
2. Peiai, L., Baoyu, W., Jiapeng, W.: Numerical simulation and experimental study on rotary cold extrusion forming of screw rod. J. Phys. Conf. Ser. **2101**, 012017 (2021). https://doi.org/10.1088/1742-6596/2101/1/012017
3. Shao-Yi, H., Yu-Tuan, C., Guan-Fan, L.: Analysis of sheet metal tapping screw fabrication using a finite element method. Appl. Sci. **6**, 300 (2016). https://doi.org/10.3390/app6100300
4. Yi, L., Pengxiao, Z., Cai, T., Zhi, S.: Effect of lost-foam casting process on properties of spiral blade. Crystals **12**, 1075 (2022). https://doi.org/10.3390/cryst12081075
5. Dai, H.J., D'Souza, N., Dong, H.B.: Grain selection in spiral selectors during investment casting of single-crystal turbine blades: part I. Experimental investigation. metallurgical and materials. Transactions A **42**, 3430–3438 (2011). https://doi.org/10.1007/s11661-011-0760-6
6. Wengfei, P., et al.: Analysis of cross wedge rolling of spiral shaft parts. Procedia Eng. **81**, 322–327 (2014). https://doi.org/10.1016/j.proeng.2014.09.171
7. Lyashuk, O, Diachun, A., Kuchvara, I., Vovk, Y., Dzyura, V.: Study of power parameters of forming profile elliptical screw workpieces. Int. J. Integr. Eng. **4**(13), 142–151 (2021)

8. Hevko, I., Dyachun, A., Lyashuk, O., Martsenko, G.A.: Research the force parameters of forming the screw cleaning elements. INMATEH – Agric. Eng. **49**(1), 77–82 (2016)
9. Vasylkiv, V.: Features of using air-plasma cutting technology for manufacturing of helical flights and auger billets. Sci. J. Ternopil Nat. Tech. Univ. **2**(110), 23–32 (2023). https://doi.org/10.33108/visnyk_tntu2023.02.023
10. Matejic, M., Dragoi, M., Blagojevic, M., Filip, A., Miletic, I.: Progressive screw shaft manufacturing technology. IOP Conf. Series: Mater. Sci. Eng. **1009**, 012038 (2021). https://doi.org/10.1088/1757-899X/1009/1/012038
11. Sanchez Vega, L.R., Hanzon, D.W.: Quantification of large uniaxial Bauschinger effects in sheet metal from pure bending/unbending tests and interferometer techniques. Int. J. Mech. Sci. **118**, 144–154 (2016). https://doi.org/10.1016/j.ijmecsci.2016.09.017
12. Poulin, C., Barrett, T., Knezevic, M.: Inferring post-necking strain hardening behavior of sheets by a combination of continuous bending under tension testing and finite element modeling. Exp. Mech. **60**, 459–473 (2020). https://doi.org/10.1007/s11340-019-00577-1
13. Ahn, K.: Plastic bending of sheet metal with tension/compression asymmetry. Int. J. Solids Struct. **204–205**, 65–80 (2020). https://doi.org/10.1016/j.ijsolstr.2020.05.022
14. Štok, B., Halilovič, M.: Analytical solutions in elasto-plastic bending of beams with rectangular cross section. Appl. Math. Model. **33**, 1749–1760 (2009). https://doi.org/10.1016/j.apm.2008.03.011
15. Sitar, M., Kosel, F., Brojan, M.: Numerical and experimental analysis of elastic–plastic pure bending and springback of beams of asymmetric cross-sections. Int. J. Mech. Sci. **90**, 77–88 (2015). https://doi.org/10.1016/j.ijmecsci.2014.11.006
16. Vasylkiv, V., Pylypets, M., Danylchenko, L., Radyk, D.: Investigation of deflections of winded screw flights and auger billets in the processes of their manufacture. Sci. J. Ternopil Nat. Tech. Univ. **4**(104), 33–43 (2021). https://doi.org/10.33108/visnyk_tntu2021.04.033
17. Vasylkiv, V., Pylypets, M., Danylchenko, L., Radyk, D.: Formalized description and synthesis of schemes for shaping helical flights and auger billets based on the componentic methods. Sci. J. Ternopil Nat. Techn. Univ. **4**(104), 44–57 (2021). https://doi.org/10.33108/visnyk_tntu2021.04.044

The Influence of the Geometry of High-Performance Cutters on the Profile Accuracy of Large-Pitch Tapered Threads: Theoretical Study

Iuliia Medvid, Oleh Onysko(✉), Lolita Pituley, Zinovii Odosii, and Olena Kornuta

Ivano-Frankivsk National Technical University of Oil and Gas, 15, Karpatska Street, Ivano-Frankivsk 76019, Ukraine
oleh.onysko@nung.edu.ua

Abstract. Modern tool manufacturers offer fully profiled cutting cutters with an edge profile identical to the standard. The situation for large-pitch thread screws is significantly bigger because, for the most part, such tools have, at their disposal, special means for setting the cutting carbide insert and adjusting it to create an angle of inclination of the edge λ. This angle is required for an even load on both sides of the edge and to ensure the stability of the cutter before it is worn entirely. The modern scientific theory of the cutting process indicates the need to use another angular parameter - the rake angle, which enables the use of difficult-to-machine materials. Methodologically this theoretical study is about the functional influence of the combination of two angles: the inclination of the cutting edge and the back rake angle, on the accuracy of a large-pitch tapered screw thread made of heavy-duty steel. In this work, it is theoretically proven that for the smallest diameter drill-string tool-joint thread (NC10 thread), the combined influence of the geometric parameters of the back-rake angle $\gamma = 12°$ and the cutting-edge inclination angle $\lambda = 3,74°$ on the accuracy of the half-profile angle of the thread is significant. At the same time, the deviation is 62.7% of the tolerance (±0.75°) according to the standard half-profile angle of 30°, which obviously indicates the minimum possibility of using high-performance cutters for the production of large-pitch tapered threads made of difficult-to-machining materials.

Keywords: Process Innovation · Pin · Box · Drill-String Tool-Joint Tapered Thread · Threading Lathe Tool · Rake Angle · Inclination Angle · Cutting Edge

1 Introduction

The development of alternative renewable energy [1] is usually, to some extent, a trigger for improving traditional oil and gas production technologies and drilling in particular. Large-pitch tapered threads are widely used in connecting drill strings. Such connectors are subject to significant requirements regarding mechanical strength, resistance to the

© The Author(s), under exclusive license to Springer Nature Switzerland AG 2024
V. Ivanov et al. (Eds.): DSMIE 2024, LNME, pp. 299–308, 2024.
https://doi.org/10.1007/978-3-031-61797-3_25

aggressive environment in the well, and the ability to perform multiple effective screwing and unscrewing processes. The accuracy and quality of the threaded surfaces of such connections, to a large extent, allow, not only ensure mechanical strength and simplify the screwing process but also provide a significant improvement in environmental protection [2]. An equally important consequence of improving threading efficiency, accuracy, and mechanical strength is the increase in energy saving during the drilling process, both for fossil carbon energy resources and water resources. The constant increase in the world's demand for drinking water sources puts significant demands on efficiency and savings for industrial drilling, especially in regions with high tourism potential [2]. Therefore, the threaded connection is the most responsible element of drill strings and requires comprehensive consideration regarding their life cycle. In this direction, there are modern scientific approaches to vibrational-centrifugal strengthening for functional surfaces of machine parts [3]. Optimization of cutting modes during sustainable machining of products based on economic criteria is very important [4]. The latest scientific trends are optimization of the technological process based on analysis of technological features [5]. The dependence of intergrade damageability on the technological treatment route was found based on technological heredity [6, 7]. To improve the mechanical and anti-corrosion resistance, an analytical model of the threaded connection of the oil and gas assortment pipes reinforced with chrome coating was developed [8]. To increase the wear resistance of the outer surfaces of couplings and nipples of threaded pipe connections, it is promising to use surfacing coatings from tungsten-free alloys with a high manganese content [9], with double carbo-borides based on it. A significant reduction in wear of the thread profile during screwing and unscrewing of drill pipe thread connectors is suggested by the use of MoS2/C nanospheres as additives to sealing greases for threads [11]. However, innovations in the machining process are the least expensive in terms of materials and the most effective in terms of saving time and improving the quality of parts. For example, methods have been proposed that contribute to the formation of the desired roughness of the treated surfaces during the application of milling [12], end milling [13, 14], and tooth milling [15]. The research proposal of cutting process consideration in dynamic models of machine tool spindle units [16] is promising. Grinding ensures the obtained profile of the thread is close to the theoretical one, while special attention is paid to the rational choice of tool material [17, 18] and cutting modes [19]. However, the most productive from a technological point of view is the actual turning of conical threads with high-performance tools - threading cutters.

2 Literature Review

The experimental work [20] examines the influence of the parameters of the turning process of a tapered large-pitch thread for oil pipe connection. Results show less cutting force is acquired for the cutting tool with a rake angle of 12°. However, this paper does not analyze the accuracy of the cutting that was achieved. Conducting experiments with a made of stainless-steel thread [21] shows the dependence of tool resistance and microhardness of the part surface on the selected feeding method. The papers [22, 23] are about how strong vibrations during turning large-pitch threads influence tool wear [22] and cutting-edge profile resistance [23]. However, these investigations model the cutting

process without examination of the resulting thread accuracy. Work [24] is about different ideas of cutting force measuring in the threading process on a lathe. Sustainability and tool wear for machining of titanium alloy thread in dry and cryogenic conditions are investigated in [25]. Research isn't about tool angles' influence on thread profile accuracy. Threads for drill-string tool joints are regulated by the API Spec. 7 standard. According to this standard, the smallest threads are NC10, NC12, NC13 and NC16. Their diameters range from 25 to 40 mm. Their profile form according to the standard API Spec. 7 is V-0.055 (Fig. 1).

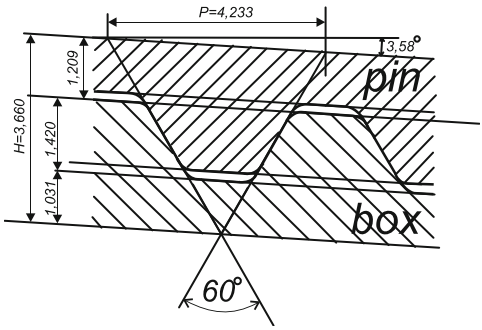

Fig. 1. Tool-joint thread profile of form V-0.055 by API Spec.7.

A tapered thread with a pitch of 4.233 mm and the height of the initial triangle H = 3.66 mm is shown in Fig. 1. The smaller taper diameter is 25.476 mm. Under these parameters, the helical curve lead angle on the first turn is 3.75°. This forces us to use a cutter with an inclination angle $\lambda = 3°–4°$ (Fig. 2). This approach makes it possible to increase the tool's durability. Still, it affects the accuracy of the machined profile [24, 25]. According to calculations, the half (flank) angle increases to 30.24°, which exceeds 30% of the tolerance of 0.75°.

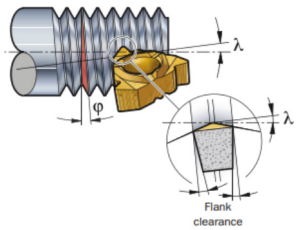

Fig. 2. Application of the inclination angle λ, equal to the thread lead angle.

In the theoretical studies [26], the function of influence on the accuracy of the thread of the rake angle [27], which is used to increase the productivity and stability of the tool when turning large-pitch threads, is described, as suggested by scientists in the work [20]. In a study [26], the theoretical approach of the author Onysko O. is applied, in which the lateral profiles of the DG and EF threads cannot be made by API Spec. 7 if

the cutter has a non-zero value of the inclination angle λ or a non-zero value of the rake angle γ. As a result, in works [26], the difference between the half-profile angles α_{AD} and α_{AB} from the nominal 30° was proved (Fig. 3).

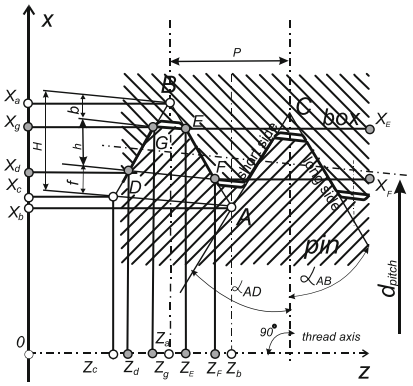

Fig. 3. V-0.055 form of tool-joint thread in ZX coordinates. The *Z* axis runs in the same direction as the axis of the thread, and $H = 3{,}66$ mm, $h = 1{,}242$ mm, $b = 1{,}209$ mm, $P = 4{,}233$ mm.

However, the combined influence of both parameters (inclination angle λ and rake angle γ) on the accuracy of a large-pitch thread is described in a scientific work [26]. The drawback of this work is that the calculation of half-profile angles α is based on trigonometric ratios within the original triangle CAB (sides AC (Fig. 3.) and AB), which led to different results of the deviation of half-profile angles than if only sides DG and EF are presented (Fig. 3). Therefore, the purpose of this work is to combine methods [26, 27] to obtain an optimized functional dependence of the value of the half (flank) angle of a large-pitch thread on the tool geometric parameters: the inclination angle λ and the rake angle γ. There are three different profile curves, as shown in Fig. 4. The red line *DG* corresponds to a standard lateral rectilinear profile, forming a half-profile angle $\alpha = 30 \pm 0{,}75°$. The green curve models the lateral profile formed if a cutter with a rake angle $\gamma = 60°$ is used. The blue curve D_2G_2 models the lateral profile formed if a cutter with a rake angle $\gamma = 12°$ and inclination angle $\lambda = 3°$ is used.

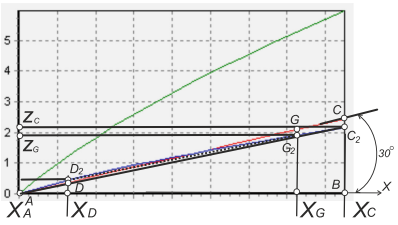

Fig. 4. Models of half angles of the NC10 thread in ZX coordinates: segment AC is made as a result of interpolation along the extreme points of the profile curve thread, DG is a straight segment made based on interpolation of the section of the profile between D and G points.

3 Research Methodology

To study the profile of the NC drill thread of the V-0.055 form according to the API Spec 7 standard, we will use the Cartesian coordinate system XZ in which the Z axis is directed along the axis of the thread (Fig. 3).

To determine the profile of the obtained cut, we will apply the algorithm developed by the authors of this article and presented in [26]. Therefore, in the XZ coordinates presented in Fig. 3, the profile of the cut according to the method [26] corresponds to the profile of the transcendental function:

$$z(x) = tan(\alpha)x\frac{sin\tau}{sin\eta} - \frac{P}{2\pi}\tau, \tag{1}$$

where: $\alpha = 30°$ half angle of the profile of a standard cutting insert;

τ– is determined by the equation:

$$\tau = \eta - arcsin\left(\frac{r_{min}sin\eta}{x}\right)x, \tag{2}$$

where: *rmin* – the radius of the root of the thread, and η is determined by the formula:

$$\eta = \gamma + \mu, \tag{3}$$

where:

$$\mu = \left(\frac{q}{t}\right), \tag{4}$$

where:

$$q = tan\left(\frac{H \cdot cos\varphi}{2sin(60° + \varphi)}\right), \tag{5}$$

where:

$$t = \frac{H \cdot cos\varphi}{sin(60° + \varphi)}\sqrt{\left(\left(1 - sin^2 30° cos^2\lambda\right) - \frac{tan^2(\lambda)}{4}\right)} \tag{6}$$

So, the algorithm represented by formulas (1–6) indicates the functional dependence of the thread profile on its diameter and radius, which is variable for the conical thread, the pitch P, and the angle of inclination λ. Since the algorithm is taken from work [27], the range of profile calculation should be clarified by works [26]; that is, it should be narrowed; for example, the short side of the thread should be determined between points *D* and *G*, not *A* and *C* (Fig. 3). The standard profile (red line in Fig. 4.) is described by the formula:

$$z(x) = tan(\alpha)x \tag{7}$$

Based on the sketch in Fig. 3, the diagram in Fig. 5 is made. In this sketch, point A remains alone, and other points have their counterparts. For example, point *D* of

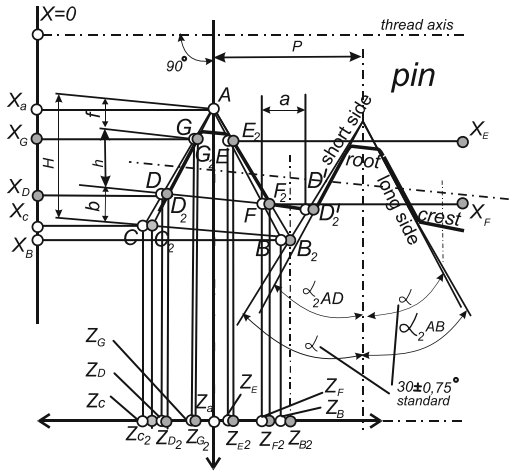

Fig. 5. Sketch for calculating the value of semi-profile angles α2AD and α2AB of the standard and non-standard surface of the tool-joint thread.

the standard profile (Fig. 3) corresponds to point D_2 on the profile constructed by the algorithm (1–6).

The position of the straight segment D_2G_2 of the resulting thread's profile establishes the angle α_{2AD}. A similar explanation can be used for long side E_2F_2 to define the angle α_{2AB}. To evaluate the obtained thread surface, using Fig. 5, the equations can be applied:

$$\alpha_{2AD} = arctg\left(\frac{|Z_{D2} - Z_{G2}|}{|X_D - X_G|}\right) \tag{8}$$

$$\alpha_{2AB} = arctg\left(\frac{|Z_{F2} - Z_{E2}|}{|X_F - X_E|}\right), \tag{9}$$

where: coordinates Z_{D2}, Z_{E2}, Z_{F2}, Z_{G2}, Z_D, Z_E, Z_F, Z_G can be calculated using (1–6) and value of standard coordinates X_D, X_E, X_F, X_G.

The algorithm (8–9) gives a new approach to predicting the thread-profile accuracy depending on the cutting tool's essential geometrical parameters: rake angle γ and inclination angle λ. The standard value of crest flat is a = 1,397 mm. The tolerance Δf of this value isn't defined. But it is clear from Fig. 6 that

$$\Delta a = (z_{F2} - z_F) - (z_{D2} - z_D) \tag{10}$$

4 Results and Discussions

4.1 Initiate Parameters of the Calculations Profile of the Short and Long Side of the NC10 Tapered Thread

The geometric parameters of the tool cutter in the program evaluation are lead angle (inclination angle) $\lambda = 3.74°$. Back rake angle $\gamma = 12°$. The increase in coordinates along the cut axis from right to left from Za = 0 to Zc2 and the step along the X-axis is 0.01 mm (Fig. 5). The point A is located at the start of the list of computed X

coordinates of the profile (Table 1), along with Z1 of the standard profile and Z2 of the transcendental profile. Column Z2− Z1 displays the difference in Z coordinates between the transcendental and standard profiles. Hence, at point A, the coordinate Xa equals 10.29 mm. Consequently, the coordinates Za for Z1 and Z2, corresponding to point A on the curved surface, are set to 0 and highlighted with a frame in Table 1. The other points of the theoretical triangle (standard ABC and transcendent AB2C2) are also shown for the following calculation (Table 1).

Table 1. ZX Coordinate of the standard points (*A, B, C*) and new-received points (*A, B_2, C_2*) of thread theoretical triangle. *- obtained from standard API7.

dots	X, mm	Z1, mm	Z2, mm	Z2 − Z1, mm
A	10.290*	0.000	0.000	0.000
C − C_2	13.950*	2.110	2.110	−0.008
B − B_2	14.090*	2.190	2.240	0.049

4.2 Calculations of the DG- Standard Profile and D2G2 -New Profile of the Short Side of the NC10 Thread

To obtain the coordinates of short side points Z_1 (according to formula (7)) and Z_2 according to formula (1), it is necessary to receive the coordinates X_G and X_{G2} (Fig. 5.):

$$X_G = X_{G2} = X_a + f = 10.290 + 1{,}031 = 11.321(\text{mm}),\ \text{rounded } 11.320 \text{ mm (tab.2)}$$

$$X_D = X_{D2} = X_c - b = 13.950 - 1{,}209 = 12.741(\text{mm}),\ \text{rounded } 12.740 \text{ mm (tab.2)}$$

Table 2. The calculation of the XZ coordinates of the short side profile of thread NC10 of the (newly created points G_2D_2 and standard profile points GD).

dots	X, mm	Z_1, mm	Z_2, mm	$Z_2 - Z_1$, mm
G, G_2	11.320	0.595	0.592	−0.002
D, D_2	12.740	1.410	1.410	−0.006

So, according to data of Table 2 and formula (8): $\alpha_{2AD} = 29.94°$.
That means 0,08% of tolerance of angle $\alpha = 30 \pm 0.75°$.

4.3 Calculations of the EF- Standard Profile E2F2- New Profile of the Long Side of the NC10 Thread

To obtain the coordinates of short side points Z_1 (according to the formula) and Z_2, it is necessary to receive the coordinates X_G and X_{G2} (Fig. 5):

$$X_G = X_{G2} = X_a + f = 10.290 + 1{,}031 = 11{,}321 - 11{,}320\,(\text{mm})$$

$$X_D = X_{D2} = X_c - b = 13.950 - 1{,}209 = 12.741 - 12.740\,(\text{mm})$$

Table 3. The calculation of the XZ coordinates of the long side profile of thread NC10 of the (newly created points E2F2 and standard profile points EF).

dots	X, mm	Z1, mm	Z2, mm	Z2 − Z1, mm
$E\text{-}E_2$	11.320	0.595	0.612	0.018
$F\text{-}F_2$	12.880	1.500	1.530	0.037

So, according to data from Table 3 and formula (8): $\alpha_{2AD} = 30.47°$.

That means 62.7% of tolerance of angle $\alpha = 30 \pm 0.75°$.

Maximum linear displacement along the thread axis – 0.037 mm, which is 2,65% of nominal value a = 1.397 mm.

4.4 Discussions

The NC10 tool-joint thread is an example of a long pitch of 4.233 mm. Accuracy program prediction of machining it using a high-efficiency cutter with a rake angle of $\gamma = 12°$ is offered for machining of stainless steel only [18, 24]. For other types of difficult-to-machine materials, the rake angle may be lower.

The inclination angle of $\lambda = 3.74°$ is not be applied because the shim must be of integer only (3° or 4°) in workshop conditions.

As a result of the application of the specified algorithm (1–9) to evaluate the accuracy of NC10 (27 mm diameter) tool-joint thread, the half angle deviation value from the nominal is obtained −0.47°. This is very much of a deviation −62.7% of the tolerance.

In previous investigations of the profile accuracy of 2 7/8 Reg tool-joint thread, the exceeding of half-angle was only 10% because the diameter of 2 7/8 Reg is 70 mm.

5 Conclusions

Predict evaluation of the profile accuracy of large-pitch thread calculated on the base of the convolute theory of screw (developed by authors) taking to account the geometry parameter threading of difficult-to-machine stainless steel shows the next. In the case of a tiny thread diameter (before 25–30 mm), the deviation of the value of the thread profile angle is more than 60%. In the case of a large thread diameter (more than 70 mm), the deviation of the value of the thread profile angle is only 10%.

In the nearest research, the algorithm prediction of the profile accuracy of the lead screw is planned.

References

1. Liakh, M., et al.: Environmentally-efficient approaches to oil and gas producing sites. E3S Web Conf. **280**, 09002 (2021). https://doi.org/10.1051/e3sconf/202128009002
2. Arkhypova, L.M., Mandryk, O.M., Moskalchuk, N.M., Prykhodko, M.M., Radlovska, K.O.: Renewable energy resources in the system of sustainable development of Carpathian region of Ukraine. J. Phys. Conf. Ser. **1781**, 012010 (2021). https://doi.org/10.1088/1742-6596/1781/1/012010
3. Stupnytskyy, V., Kusyi, Y., Dragašius, E., Baskutis, S., Chatys, R.: Modeling of vibrational-centrifugal strengthening for functional surfaces of machine parts. In: Tonkonogyi, V., Ivanov, V., Trojanowska, J., Oborskyi, G., Pavlenko, I. (eds.) Advanced Manufacturing Processes V. InterPartner 2023. Lecture Notes in Mechanical Engineering, pp. 231–244. Springer, Cham (2024). https://doi.org/10.1007/978-3-031-42778-7_21
4. Kusyi, Y., Kostiuk, O., Kuk, A., Attanasio, A., Cocca, P.: Optimization of Cutting Modes During Sustainable Machining of Products Based on Economic Criteria. In: Tonkonogyi, V., Ivanov, V., Trojanowska, J., Oborskyi, G., Pavlenko, I. (eds.) Advanced Manufacturing Processes V. InterPartner 2023. Lecture Notes in Mechanical Engineering, pp. 167–181. Springer, Cham (2024). https://doi.org/10.1007/978-3-031-42778-7_16
5. Kusyi, Y.M., Stupnytskyy, V.V., Kuk, A.M., Topilnytskyy, V.G.: Development of the fundamental diagram of the formation and transformation of the products properties during their manufacturing. J. Phys. Conf. Ser. **1781**(1), 012027 (2021). https://doi.org/10.1088/1742-6596/1781/1/012027
6. Kusyi, Y.: Technological Inheritability of Product Material Using the Criterion of Technological Damageability. In: Ivanov, V., Trojanowska, J., Pavlenko, I., Zajac, J., Peraković, D. (eds.) DSMIE 2021. LNME, pp. 52–61. Springer, Cham (2021). https://doi.org/10.1007/978-3-030-77719-7_6
7. Kusyi, Y., Kuzin, N.: The dependence of intergrain damageability of casting on the technological treatment route. Eastern-Eur. J. Enterprise Technol. **1**(5), 39–47 (2016). https://doi.org/10.15587/1729-4061.2016.59845
8. Dubei, O.Ya., Tutko, T.F., Ropyak, L.Ya., Shovkoplias, M.V.: Development of analytical model of threaded connection of tubular parts of chrome-plated metal structures. Metallofizika i Noveishie Tekhnologii **44**(2), 251–272 (2022). https://doi.org/10.15407/mfint.44.02.0251
9. Prysyazhnyuk, P., Molenda, M., Romanyshyn, T., Ropyak, L., Romanyshyn, L., Vytvytskyi, V.: Development of a hardbanding material for drill pipes based on high-manganese steel reinforced with complex carbides. Acta Montanistica Slovaca **27**(3), 685–696 (2022). https://doi.org/10.46544/AMS.v27i3.09
10. Bembenek, M., Prysyazhnyuk, P., Shihab, T., Machnik, R., Ivanov, O., Ropyak, L.: Microstructure and wear characterization of the Fe-Mo-B-C—based Hardfacing alloys deposited by flux-cored arc welding. Materials **15**(14), 5074 (2022). https://doi.org/10.3390/ma15145074
11. Kotsyubynsky, V., Shyyko, L., Shihab, T., Prysyazhnyuk, P., Aulin, V., Boichuk, V.: Multilayered MoS_2/C nanospheres as high-performance additives to lubricating oils. Mater. Today: Proc. **35**, 538–541 (2019). https://doi.org/10.1016/j.matpr.2019.10.021
12. Petrakov, Y., Danylchenko, Y., Sapon, S., Sikailo, M.: Surface Relief Formation in Peripheral End Milling. In: Ivanov, V., Trojanowska, J., Pavlenko, I., Rauch, E., Piteľ, J. (eds.) Advances in Design, Simulation and Manufacturing VI. DSMIE 2023. Lecture Notes in Mechanical Engineering, pp. 316–326. Springer, Cham (2023). https://doi.org/10.1007/978-3-031-32767-4_30
13. Petrakov, Y.V., Ohrimenko, O.A., Sikailo, M.O., Myhovych, A.V.: Cutting forces simulation for end milling. J. Eng. Sci. (Ukraine) **10**(2), A27–A33 (2023). https://doi.org/10.21272/jes.2023.10(2).a4

14. Bembenek, M., Dzienniak, D., Dzindziora, A., Sułowski, M., Ropyak, L.: Investigation of the impact of selected face milling parameters on the roughness of the machined surface for 1.4301 steel. Adv. Sci. Technol. Res. J. **17**(4), 299–312 (2023). https://doi.org/10.12913/22998624/170422
15. Pasternak, S., Danylchenko, Y.M., Storchak, M., Okhrimenko, O.A.: Gear Cutting with Disk-Shaped Milling Cutters. In: Radzevich, S.P., Storchak, M. (eds.) Advances in Gear Theory and Gear Cutting Tool Design, pp. 151–179. Springer, Cham (2022). https://doi.org/10.1007/978-3-030-92262-7_5
16. Danylchenko, Y., Storchak, M., Danylchenko, M., Petryshyn, A.: Cutting process consideration in dynamic models of machine tool spindle units. Machines **11**(6), 582 (2023). https://doi.org/10.3390/machines11060582
17. Pavlenko, I., et al.: Using regression analysis for automated material selection in smart manufacturing. Mathematics **10**(11), 1888 (2022). https://doi.org/10.3390/math10111888
18. Ivchenko, O., et al.: Method for an effective selection of tools and cutting conditions during precise turning of non-alloy quality steel C45. Materials **15**(2), 505 (2022). https://doi.org/10.3390/ma15020505
19. Ropyak, L.Y., Vytvytskyi, V.S., Velychkovych, A.S., Pryhorovska, T.O., Shovkoplias, M.V.: Study on grinding mode effect on external conical thread quality. IOP Conf. Series: Mater. Sci. Eng. **1018**(1), 012014 (2021). https://doi.org/10.1088/1757-899X/1018/1/012014
20. An, Q.L., Guo, G.G., Zheng, X.H., Chen, M., Liu, G., Zhang, Y.S.: Experimental study on cutting characteristics for buttress thread turning of 13% Cr stainless steel. KEM **443**, 262–267 (2010). https://doi.org/10.4028/www.scientific.net/KEM.443.262
21. Costa, C.E., Polli, M.L.: Effects of the infeed method on thread turning of AISI 304L stainless steel. J. Braz. Soc. Mech. Sci. Eng. **43**, 253 (2021). https://doi.org/10.1007/s40430-021-02978-7
22. Li, Z., Fu, X., Li, J., et al.: Establishment of vibration wear model for turning large-pitch thread tools and its wear suppression method. Int. J. Adv. Manuf. Technol. **109**, 857–876 (2020). https://doi.org/10.1007/s00170-020-05403-w
23. Fu, X., Li, K., Li, Z., et al.: A SVM-based design method for cutting edge profile stability of large-pitch thread turning tool considering vibration. Int. J. Adv. Manuf. Technol. 2767–2781 (2023). https://doi.org/10.1007/s00170-023-10985-2
24. Krawczyk, B., et al.: Surface topography description of threads made with turning on Inconel 718 shafts. Materials **16**, 80 (2023). https://doi.org/10.3390/ma16010080
25. Zawada-Tomkiewicz, A., Żurawski, L., Tomkiewicz, D., Szafraniec, F.: Sustainability and tool wear of titanium alloy thread cutting in dry and cryogenic conditions. Int. J. Adv. Manuf. Technol. **114**, 2767–2781 (2021). https://doi.org/10.1007/s00170-021-07034-1
26. Onysko, O., Medvid, I., Panchuk, V., Rodic, V., Barz, C.: Geometric Modeling of Lathe Cutters for Turning High-Precision Stainless Steel Tapered Threads. In: Ivanov, V., Trojanowska, J., Pavlenko, I., Zajac, J., Peraković, D. (eds.) DSMIE 2021. LNME, pp. 472–480. Springer, Cham (2021). https://doi.org/10.1007/978-3-030-77719-7_47
27. Medvid, I., Onysko, O., Panchuk, V., Pituley, L., Schuliar, I.: Kinematics of the Tapered Thread Machining by Lathe: Analytical Study. In: Tonkonogyi, V., Ivanov, V., Trojanowska, J., Oborskyi, G., Grabchenko, A., Pavlenko, I., Edl, M., Kuric, I., Dasic, P. (eds.) InterPartner 2020. LNME, pp. 555–565. Springer, Cham (2021). https://doi.org/10.1007/978-3-030-68014-5_54

Theoretical Justification for Increasing Efficiency of Grinding Technological Processes Based on the Reduction of Cutting Temperature

Fedir Novikov[1(✉)], Andrii Hutorov[2], Oleksii Yermolenko[1], Oksana Yermolenko[1], and Andrii Ivashura[1]

[1] Simon Kuznets Kharkiv National University of Economics, 9-A, Nauky Avenue, Kharkiv 61166, Ukraine
NovikovFV@i.ua

[2] National Scientific Center "Institute of Agrarian Economics", 10, Heroiv Oborony Street, Kyiv 03127, Ukraine

Abstract. The aim of the work is a generalized theoretical substantiation of conditions for reducing the cutting temperature durin g grinding to develop effective technological processes for grinding products made of materials with increased hardness. A theoretical solution was obtained, the main parameter of which is the maximum cutting temperature from heating the formed chips. It was theoretically established that when this temperature is reached, it is possible to increase machining productivity many times. By calculation and experiment, it was established that the maximum cutting temperature is many times higher than the melting point of the machined material. Calculations proved an increase in machining productivity by providing a relatively small grinding temperature and applying multipass grinding with a relatively high speed of the workpiece. They also proved an increased grinding temperature by applying depth grinding with a relatively low workpiece speed. Based on an effective process of face grinding by diamond wheels on metal bonds of sealing rings made of hard alloy "Relit" with the application of electroerosion dressing, reducing energy consumption and increasing quality and productivity of processing was developed. An effective process of gear grinding by profile copying (depth grinding) with a highly porous abrasive wheel was developed. This made it possible to reduce the energy consumption of processing, increase productivity up to 5 times, and ensure defect-free processing.

Keywords: Processing Performance · Energy Consumption During Machining · Metal-Bonded Diamond Wheels · Process Innovation

Nomenclature Table

θ	temperature during grinding, deg;
θ_{max}	maximum cutting temperature, deg;
σ	conditional cutting stress, N/mm^2;
a	thermal diffusivity coefficient of the processed material, m^2/s;
λ	coefficient of thermal conductivity of the processed material, W/(m·deg);

© The Author(s), under exclusive license to Springer Nature Switzerland AG 2024
V. Ivanov et al. (Eds.): DSMIE 2024, LNME, pp. 309–318, 2024.
https://doi.org/10.1007/978-3-031-61797-3_26

c specific heat capacity of the processed material, J/(kg·deg);
ρ density of the processed material, kg/m^3;
V_R the removal rate of the workpiece in the direction perpendicular to the grinding wheel direction of motion, m/s;
V_{det} part speed, m/min;
t grinding depth, m;
R_c circle radius, m;
Q_0 specific grinding productivity, mm^2/min;
τ processing time, s;
A cutting work, J;
Q amount of heat, J;
N grinding power, W;
P_z, P_y the tangential and radial component of the cutting force, N;
V_c wheel speed, m/s;
S_Σ total instantaneous cross-sectional area at grinding by all simultaneously working wheel grains, m^2;
B grinding width, m;
m mass of material removed during time τ, kg;
ϑ the volume of material removed during time τ, m^3;
l length of movement of the grinding wheel during time τ, m;
E energy intensity of machining, J/m^3;
α_1 fraction of heat generated during grinding and which goes only into the resulting chips;
α_2 the fraction of heat that goes into the surface layer of the workpiece;
α dimensionless coefficient

1 Introduction

Grinding is the main technological process of finishing mechanical machining of machine parts. However, it is characterized by high energy consumption. This leads to an increase in the thermal stress of the cutting process and the appearance of burns, microcracks, and other temperature defects on the machined surfaces [1, 2], for example, when grinding gears [3], bearings [4], rails [5] and many other products. Therefore, solving the problem of high-quality and high-performance machining during grinding by reducing the cutting temperature is of great scientific and practical importance. In particular, this applies to grinding products made of metal and non-metallic materials of increased hardness, the processing of which is accompanied by low quality and productivity indicators. In this regard, predicting the cutting temperature during grinding is the first step to analyzing and preventing these problems. The study [6] showed that the cutting temperature during grinding of titanium alloys with a diamond wheel can be reduced by decreasing the wheel speed, while for ceramic grinding, it can be decreased by increasing the wheel speed after exceeding a certain value. It has been established [7] that ultrasonic vibration significantly affects the cutting temperature during grinding, reducing it by 10.6%. Thus, using a segmented wheel allowed for reducing the cutting temperature during grinding below the critical limit and excluding the formation

of burns on the machined surface (of the titanium alloy Ti-6Al-4V) [8]. The use of deep-feed grinding [9], metal-bonded diamond wheels [10], and efficient technological media [11, 12] also makes it possible to reduce the cutting temperature significantly. However, these results were obtained experimentally and are valid for particular machining conditions. To select more rational grinding conditions, it is important to have generalized theoretical solutions valid in a wide range of changes in the parameters of the grinding mode, the characteristics of grinding wheels, and other processing conditions. The aim of the work is a generalized theoretical justification of conditions for reducing the cutting temperature during grinding to develop effective technological processes for grinding products made of materials of increased hardness.

2 Literature Review

Much attention is paid to the theoretical analysis of the conditions for reducing the cutting temperature during grinding in the scientific and technical literature. In [13, 14], the finite element method simulation of temperature and energy distribution during cylindrical grinding was carried out. It is shown that the speed of the workpiece affects the distribution of energy into chips more clearly than other grinding parameters. In [15], a three-dimensional model was proposed to determine the temperature change using finite element analysis while grinding a heat-resistant alloy based on Inconel 718 nickel. It was found that the cutting temperature during grinding can be reduced by reducing the depth of the cut or changing other grinding parameters. In [16, 17], mathematical models of the thermal process during grinding were developed, and in [18], the conditions for reducing the cutting temperature during grinding were theoretically substantiated based on the solution of a complex differential equation of heat conduction. However, this traditionally uses experimental data on the distribution of heat released during cutting, escaping into the formed chips and the surface layer of the workpiece [19]. As a result, the obtained solutions are valid only for specific machining conditions and do not reveal the true technological capabilities of the grinding process. This is a significant disadvantage of the known mathematical models for determining the grinding temperature. Therefore, the present work solves the problem of analytical determination of grinding temperature, considering the analytically established pattern of distribution of heat generated during grinding, escaping into the formed chips and the surface layer of the workpiece. This will make it possible to obtain more generalized theoretical (analytical) solutions and to carry out a scientifically based analysis of the conditions for a significant reduction in grinding temperature in wide ranges of changes in the grinding mode parameters for various grinding methods and conditions.

3 Research Methodology

To achieve this goal, the calculation scheme for determining the grinding temperature proposed in [20] was used in this work. In it, the allowance to be removed is represented by a package of adiabatic rods located perpendicular to the direction of motion of the grinding wheel. If we assume that the grinding wheel cuts the adiabatic rods in the grinding process, it is possible to analytically establish the distribution patterns of the

generated heat escaping into the formed chips and the surface layer of the machined part. On this basis, a fundamentally new analytical dependence for determining the grinding temperature is obtained, considering the analytically established distribution of the heat escaping into the formed chips and the surface layer of the workpiece [21]:

$$\theta = \theta_{max} \cdot \left[1 - e^{-\frac{V_R^2}{a} \cdot \tau} \cdot e^{-\frac{\theta}{\theta_{max}}} \right], \tag{1}$$

which after transformation in relative terms takes the form:

$$\left(1 - \frac{\theta}{\theta_{max}} \right) \cdot e^{\frac{\theta}{\theta_{max}}} = e^{-\frac{Q_0}{a} \cdot \sqrt{\frac{t}{2 \cdot R_c}}}, \tag{2}$$

where $\theta_{max} = \frac{\sigma}{c \cdot \rho}$; $a = \frac{\lambda}{c \cdot \rho}$; $\tau = \frac{t}{V_R}$; $V_R = V_{det} \cdot \sqrt{\frac{t}{2 \cdot R_c}}$; $Q_0 = V_{det} \cdot t$.

From dependence (2), it follows that with increasing $Q_0 = V_{det} \cdot t$, the ratio θ / θ_{max} continuously increases, asymptotically approaching unity, i.e. $\theta \to \theta_{max}$ (Fig. 1). Processed material – steel ShX15 (Japanese analog SUJ2, French analog 100C6, English analog 2S135, German analog 1.3505, US analog 52100).

Consequently, under these conditions $\theta \to \theta_{max}$, it becomes possible to virtually unlimitedly increase the specific processing productivity, which can become an essential factor in increasing the efficiency of the grinding process. However, the parameter θ_{max} should be quantitatively assessed and compared with the melting temperature values for the practical use of the obtained solution. If it turns out that the parameter θ_{max} is less than the melting temperature of the material being processed, then it becomes possible to significantly increase the specific processing productivity Q_0 without increasing the grinding temperature θ. If the parameter θ_{max} is greater than the melting temperature of the material being processed, then the grinding temperature θ can only change within the limits limited by the melting temperature of the material being processed. This significantly narrows the technological possibilities of grinding. In this case, the main condition for reducing the cutting temperature θ and increasing Q_0 is to reduce the parameter $\theta_{max} = \sigma / (c \cdot \rho)$ by reducing the conditional cutting stress σ. Thus, the parameter θ_{max} should be considered the main value that allows us to generally assess the level of thermal stress of the grinding process and justify the conditions for reducing the cutting temperature during grinding.

To reveal the physical essence of the parameter θ_{max}, we determine the fraction of heat generated during grinding and which goes only into the resulting chips, based on the condition: $\alpha_1 = \frac{c \cdot m \cdot \theta}{N \cdot \tau} = \frac{\theta}{\theta_{max}}$, where $N = P_z \cdot V_c$; $P_z = \sigma \cdot S_{\sum}$; $S_{\sum} = \frac{Q_0 \cdot B}{V_c}$; $m = \rho \cdot \vartheta$; $\vartheta = B \cdot t \cdot l$; $l = V_{det} \cdot \tau$.

As can be seen, the change in the value corresponds to the change in the ratio θ / θ_{max}, i.e., grinding temperature θ. The more θ, the more α_1. Under the condition $\theta \to \theta_{max}$, the value is $\alpha_1 \to 1$, i.e., all the heat generated during grinding goes into the resulting chips. Consequently, the θ_{max} parameter determines the cutting temperature during grinding, formed from heating only the resulting chips. The fraction of heat that goes into the surface layer of the workpiece is equal to $\alpha_2 = 1 - \alpha_1 = 1 - \theta / \theta_{max}$, i.e., the more θ, the less α_2.

To clarify the obtained solution, we determine the parameter θ_{max} from the condition of equality of the cutting work $A = N \cdot \tau$ and the amount of heat $Q = c \cdot m \cdot \theta_{max}$

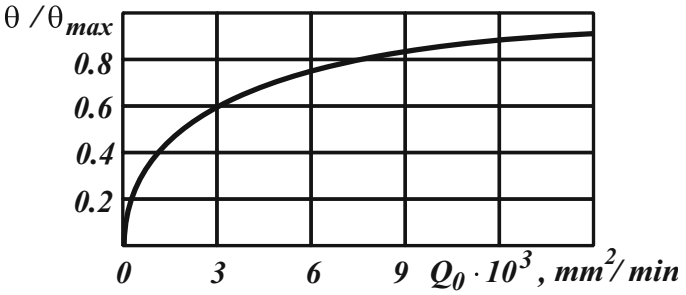

Fig. 1. Dependence θ/θ_{max} on Q_0: processed material – steel ShX15 ($a = 8.4{\cdot}10^{-6}$ m^2/s); t = 10^{-3} m; $R_c = 0.2$ m.

generated during the grinding process and going only into the resulting chips. The result is: $\theta_{max} = \sigma/(c \cdot \rho)$. Consequently, the parameter θ_{max} determines the cutting temperature during grinding, taking into account the heating of only the formed chips, and the parameter θ, included in the dependence (2) determines the cutting temperature during grinding, taking into account the distribution of heat escaping both the formed chips and the surface layer of the workpiece, i.e. $\theta < \theta_{max}$.

In the theory of grinding [19, 20], the maximum grinding temperature is understood as the maximum temperature that occurs in the grinding zone. In fact, from a physical point of view, the maximum grinding temperature should be understood as a conditional (ideal) temperature determined by the parameter θ_{max} since it is the main one in the dependence (2) to determine the conditions for the distribution of heat generated during grinding into the surface layer of the workpiece and the resulting chips.

The conditional cutting stress σ is determined from the dependence $\sigma = P_z/S_{\sum}$ taking into account $P_z = N/V_c$ and $S_{\sum} = Q_0 \cdot B/V_c$. Then $\sigma = N/(Q_0 \cdot B) = E$. The energy intensity of machining (grinding) E equals the conditional cutting stress σ. The dimension J/m^3 = N/m^2. This makes it possible to estimate the energy intensity of machining and compare it with the strength characteristics of the material being processed, which is of great practical importance from the point of view of reducing the force intensity of the machining process. It is possible to determine the parameter $\theta_{max} = \sigma/(c \cdot \rho)$ and evaluate an increase in the specific processing productivity Q_0 by taking experimental values of the parameter σ.

4 Results and Discussion

After solving the dependence (2) with respect to the specific processing productivity $Q_0 = V_{det} \cdot t$, the following dependence can be obtained:

$$Q_0 = a \cdot \left(\frac{2 \cdot R_c}{t}\right)^{0,5} \cdot ln\, \alpha^{-1}, \tag{3}$$

where $\alpha = \left(1 - \frac{\theta}{\theta_{max}}\right) \cdot e^{\frac{\theta}{\theta_{max}}}$.

As can be seen, it is possible to increase $Q_0 = V_{det} \cdot t$ by reducing the grinding depth t, increasing the value α (Table 1), and, accordingly, the ratio θ/θ_{max} by reducing

the conditional cutting stress σ. Moreover, an increase in the ratio θ/θ_{max} has a more significant effect on the machining productivity $Q_0 = V_{det} \cdot t$ than the increase in the grinding depth t. However, as practice shows, the ranges of change of the ratio θ/θ_{max} are considerably limited by the change of the parameter θ_{max}, which at grinding exceeds the melting point of the processed material. So, at flat grinding on the elastic scheme of steel R18 (US analog T1, German analog 1.3355, Polish analog SW18; $c \cdot \rho = 3.72{\cdot}10^6$ J/(m^3·deg)) with abrasive wheel 24A40M36K5 ($V_c = 29.6$ m/s, $V_{det} = 0.1$ m/s, $P_y = 60$ N), conditional cutting stress σ takes on extremely high values: $\sigma = (3.24 \ldots 18.8){\cdot}10^4$ N/mm^2, exceeding the compressive, tensile and shear strength limits of the processed material. Accordingly, $\theta_{max} = \sigma/(c \cdot \rho) = 8710 \ldots 50537.6$ deg is many times higher than the melting point of the material being processed. The critical value θ, at which burns, microcracks, and other temperature defects are not formed on the machined surfaces is 850 deg. Then, the ratio $\theta/\theta_{max} = 0.0168 \ldots 0.0975$ is significantly less than the limit value of unity.

Experimental studies of circular external grinding of T5K10 (in standard ISO – P40, German analog HS345 (HT03), Swedish analog MC131, Polish analog S30 (S30S)) carbide milling cutters with a diamond wheel on a metal bond 1A1 300 × 25 × 5 AC6 200/160 M1–01 4 with the use of electrochemical dressing of the wheel have been carried out. It is established that at processing with grinding mode: $V_{det} = 10$ m/min; $t = 0.2{\cdot}10^{-3}$ m; $V_c = 35$ m/s; $B = 0.025$ m; $Q_0 = 2000$ mm^2/min, there are no burns, microcracks, or other temperature defects on the treated surface. In this case, $\sigma = 8400$ N/mm^2; ($c \cdot \rho = = 2.88{\cdot}10^6$ J/(m^3·deg); $\theta_{max} = \sigma/(c \cdot \rho) = 2910.6$ deg. Taking the critical value $\theta = 850$ deg; $\theta/\theta_{max} = 0.27485$ is obtained. Therefore, the ratio θ/θ_{max} increases with increasing cutting ability of the diamond wheel. This allows for increasing the processing productivity.

In [22], it was experimentally established that during flat grinding with the periphery of an abrasive wheel EB25SM1K alloy ZhC6K ($a = \lambda/(c \cdot \rho) = 3.73 \cdot 10^{-6}$ m^2/s; $\lambda = 16.6$ J/(m·s·deg); $c \cdot \rho = 4.46 \cdot 10^6$ J/(m^3·deg)) with grinding mode: $V_{det} = 0.1$ m/s; $t = 0.02{\cdot}10^{-3}$ m; $R_c = 0{,}1$ m nominal cutting stress $\sigma = 52{\cdot}10^3$ N/mm^2. Chemical composition of ZhC6K alloy: 0.16% C, 11% Cr, 2.75% Ti, 5.5% Al, 4% Mo, 4.5% Co, 2% Fe, 5% W, 0.02% B, 0.4% Mn and 0.4% Si, the rest is Ni (US analog Inconel 718).

Then $\theta_{max} = \sigma/(c \cdot \rho) = 11660$ deg. According to dependency (2):$\theta = 1109$ deg and $\theta/\theta_{max} = 0.095$. The grinding temperature, established experimentally [22], is $\theta = 1000$ deg. Consequently, there is a slight discrepancy between the calculated and experimental values of the grinding temperature – within 11%.

Thus, it was established that the parameter θ_{max}, regardless of the grinding conditions, significantly exceeds the melting temperature of the processed material. Therefore, when grinding, achieving the value and realizing the condition for a significant increase in processing productivity is impossible, which follows from dependence (2). In this case, the grinding temperature θ will be significantly less than θ_{max}. The $\theta \rightarrow \theta_{max}$ value can only be achieved under processing conditions with blade tools, where the energy intensity of processing is significantly less than during grinding [20, 22].

Therefore, the choice of rational parameters of grinding mode, providing the maximum possible productivity of processing, taking into account the limitation on the grinding temperature, can be made using the results of calculations obtained based on

Table 1. Calculated values Q_0 and V_{det} depending on the θ/θ_{max} for different values t (processed material – steel ShX15 ($a = 8.4{\cdot}10^{-6}$ m^2/s); $R_c = 0.2$ m).

$t \cdot 10^{-3}$ m	θ/θ_{max}	0	0.2	0.4	0.6	0.8	0.9	1.0
	α	1	0.9771	0.8951	0.7288	0.4451	0.24596	0
	$\alpha-1$	1	1.023436	1.117193	1.372118	2.246688	4.0657	∞
	$ln\,\alpha-1$	0	0.02	0.11	0.32	0.81	1.4	∞
0.01	Q_0, mm^2/min	0	2016	11088	32256	81648	141120	
	V_{det}, m/min	0	201.6	1109	3225.6	8164.8	14112	
0.1	Q_0, mm^2/min	0	638	3509	10207.6	25839	44660	
	V_{det}, m/min	0	6.38	35.1	102	258.4	446.6	
1.0	Q_0, mm^2/min	0	202	1109	3226	8165	14140	
	V_{det}, m/min	0	0.2	1.11	3.226	8.165	14.14	
10	Q_0, mm^2/min	0	63.8	350.9	989	2584	4466	
	V_{det}, m/min	0	0.0063	0.035	0.1	0.2584	0.44	

dependence (2), shown in Table 1. As can be seen from Table 1, with a small ratio θ/θ_{max}, the speed of the workpiece takes on a relatively high value, which is not always possible on a grinding machine. As the ratio θ/θ_{max} increases, the workpiece speed V_{det} for a given grinding depth t increases even more and is impossible to realize in practice. In this case, it is necessary to increase the grinding depth, i.e., to move into the area of depth grinding and reduce the speed of the workpiece. This is particularly effective for small grinding lengths, using single-pass depth grinding with low workpiece speed $V_{det} = Q_0/t$. In this case, the loss of auxiliary time associated with reversing the machine table is also eliminated [9].

After using the theoretical solution from dependence (3), an effective technological process for flat grinding the end surfaces of sealing rings made of Relit (WC-W2C) hard alloy was developed and introduced into production. Grinding was carried out with the end face of a 12A2 45° 150 × 10 × 3 AC6 125/100 M1–01 4 diamond wheel. Grinding was carried out using an elastic scheme with a specific pressure of 0.7 N/mm^2. The rotation speed of the processed ring was 30 m/min. The electrical discharge dressing of a diamond wheel on a metal bond made it possible to reduce the conditional cutting stress to a value of $\sigma = 3000$ N/mm^2 (as in the previously mentioned example). As a result, an increase in ratio $\theta/\theta_{max} = 0.27$ allowed for achieving process productivity.

Based on dependence (3) and Table 1, with a short grinding length, for example, during gear grinding, in order to reduce the number of wheel passes (auxiliary time) and ensure defect-free processing by reducing the cutting temperature, it is effective to use a single-pass deep grinding scheme with a low part speed V_{det}. Based on this, a high-performance technological process for gear grinding using the profile copying method has been developed on the modern HOFLER RAPID 1250 gear grinding machine to replace the gear grinding process using the lapping method. The removal of a 0.4 mm allowance on each side is performed in 4 passes of a special high-porous profile abrasive T1ESP 400 × 32 × 127 93A46M15WPG11W wheel with a double-conical profile. The longitudinal feed rate is 3 m/min. Processed material – steel 18XGN2MFB (US analog SA-29 Grade (5115), German analog 16 MnCr 5, French analog 16 MC 5 (16 MnCr 5 RR), Italian analog 16 MnCr 5, Chinese analog 15 CrMn (20 CrMn)). This has allowed for an increase in the contact length of the wheel with the machined surface, a reduction in energy consumption and auxiliary time, a 5-fold increase in processing productivity, and defect-free processing.

Thus, in the work analytically in generalized form, the conditions for reducing the thermal stress of the grinding process and, accordingly, the grinding temperature are justified. This allows a scientifically sound approach to developing high-performance and high-quality grinding processes.

5 Conclusions

The work proposes a fundamentally new generalized theoretical approach to justify the conditions for reducing the cutting temperature during grinding. On its basis, a theoretical solution is obtained, the main parameter of which is the maximum cutting temperature resulting from the heating of the formed chips without considering the heating of the surface layer of the workpiece. It is theoretically established that when this temperature is reached, it is possible to increase machining productivity many times. By calculation and experiment, it is established that the maximum cutting temperature is many times higher than the melting point of the machined material due to the extremely high energy consumption of machining. It does not allow for significantly increasing machining productivity. Simultaneously, calculations have established that it is possible to increase the productivity of machining when providing a given relatively small grinding temperature by application of multi-pass grinding with a relatively high speed of the workpiece and when providing a given but increased grinding temperature - by application of high-performance depth grinding with relatively low speed of the workpiece. Based on an effective process of face grinding by diamond wheels on metal bonds of sealing rings made of hard alloy, “Relit” is developed by applying electroerosion dressing, reducing energy consumption and increasing the quality and productivity of processing. An effective process of gear grinding by the method of profile copying (depth grinding) using a highly porous abrasive wheel has been developed, which makes it possible to reduce the energy consumption of processing, increase productivity up to 5 times, and ensure defect-free processing.

References

1. Gupta, S.N., Chak, S.K.: Grinding temperature and its consequences on induced residual stresses during grinding of nickel-based superalloys: a review. Eng. Res. Express **4**, 042002 (2022). https://doi.org/10.1088/2631-8695/acaa1d
2. Reimers, M., Lang, W., Dumstorff, G.: Experimental and numerical investigations in shallow cut grinding by workpiece integrated infrared thermopile array. Sensors **17**(10), 2250 (2017). https://doi.org/10.3390/s17102250
3. Jiang, X., Liu, K., Yan, Y., Li, M., Gong, P., He, H.: Grinding temperature and surface integrity of quenched automotive transmission gear during the form grinding process. Materials **15**(21), 7723 (2022). https://doi.org/10.3390/ma15217723
4. Paiva, R.L., Souza Ruzzi, R., Silva, R.B.: An approach to reduce thermal damages on grinding of bearing steel by controlling cutting fluid temperature. Metals **11**(10), 1660 (2021). https://doi.org/10.3390/met11101660
5. Huang, L.M., et al.: Simulation research on temperature field and stress field during rail grinding. Proc. Inst. Mech. Eng. Part F: J. Rail Rapid Transit **235**(10), 1278–1290 (2021). https://doi.org/10.1177/0954409720984568
6. Wu, C., Li, B., Yang, J., Liang, S.Y.: Comparison of machining temperature in high speed grinding of metallic materials and brittle materials. MATEC Web Conf. **114**, 02006 (2017). https://doi.org/10.1051/matecconf/201711402006
7. Kan, Z., Wenhe, L., Lianjun, S., Heng, M.: Investigation on grinding temperature in ultrasonic vibration-assisted grinding of zirconia ceramics. Mach. Sci. Technol. **23**(4), 612–628 (2019). https://doi.org/10.1080/10910344.2019.1575405
8. Handa, D., Kumar, S., Sarath, B.T.S., Sooraj, V.S.: Simulation of Intermittent Grinding for Ti-6Al-4V with Segmented Wheel. Mater. Today: Proc. **44**(1), 2537–2542 (2021). https://doi.org/10.1016/j.matpr.2020.12.626
9. Ohishi, S., Furukawa, Y.: Analysis of workpiece temperature and grinding burn in creep feed grinding. Bull. JSME **28**(242), 1775–1781 (1985). https://doi.org/10.1299/jsme1958.28.1775
10. Salata, M.: The analysis of the influence of technological parameters on the grinding temperature in the single-pass grinding process of solid carbide end mill flutes. Adv. Sci. Technol. Res. J. **16**(1), 190–202 (2022). https://doi.org/10.12913/22998624/143483
11. De Paiva, R.L., de Souza Ruzzi, R., da Silva, R.B.: An approach to reduce thermal damages on grinding of bearing steel by controlling cutting fluid temperature. Metals **11**, 1660 (2021). https://doi.org/10.3390/met11101660
12. Hadad, M.J., Tawakoli, T., Sadeghi, M.H., Sadeghi, B.: Temperature and energy partition in minimum quantity lubrication-MQL grinding process. Int. J. Mach. Tools Manuf **54–55**, 10–17 (2012). https://doi.org/10.1016/j.ijmachtools.2011.11.010
13. Ding, Z., Jiang, X., Guo, M., Liang, S.Y.: Investigation of the grinding temperature and energy partition during cylindrical grinding. Int. J. Adv. Manufact. Technol. **97**, 1767–1778 (2018). https://doi.org/10.1007/s00170-018-1900-6
14. Lan, S., Jiao, F.: Modeling of heat source in grinding zone and numerical simulation for grinding temperature field. Int. J. Adv. Manufact. Technol. **103**, 3077–3086 (2019). https://doi.org/10.1007/s00170-019-03662-w
15. Sharma, Ch., Ghosh, S., Talukdar, P.: Finite element analysis of workpiece temperature during surface grinding of inconel 718 alloy. In: Proceedings of the 5th International & 26th All India Manufacturing Technology, Design and Research Conference, pp. 420–1–420–6 (2014)
16. Chuprov, I.F., Kaneva, E.A., Mordvinov, A.A.: Equations of Mathematical Physics with Applications to Problems of Oil Production and Gas Pipeline Transportation. Ukhta State Technical University, Ukhta (2004)
17. Oborskii, G.A, Dashchenko, A.F., Usov, A.V.: Systems Modeling. Astroprint, Odessa (2013)

18. Sizyi, Iu.A., Stalinskii, D.V.: Dynamics and Thermal Physics of Grinding. State Enterprise UkrNTC "Energostal", Kharkiv, Ukraine (2016)
19. Malkin, S., Guo, C.: Thermal analysis of grinding. CIRP Ann. **56**(2), 760–782 (2007). https://doi.org/10.1016/j.cirp.2007.10.005
20. Yakimov, O.V., Usov, A.V., Slobodianyk, P.T., Iorgachov, D.V.: Thermophysics of Machining Engineering. Astroprint, Odessa, Ukraine (2000)
21. Novikov, F.V.: Mathematical model for determining the temperature during grinding based on the balance of heat that goes into the formed chips and the workpiece. Bull. Kharkiv Petro Vasylenko Nat. Tech. Univ. Agric. **61**, 23–33 (2007)
22. Yashcheritsyn, P.I., Tsokur, A.K., Yeremenko, M.L.: Thermal phenomena in grinding and properties of processed surfaces. Science and technology, Minsk (1973)

Wear Behaviour and Machining Performance in Milling of INCONEL® 718 of TiAlVN and TiAlN/TiAlVN Coated Tools: A Comparative Study

Naiara Sebbe[1,2(✉)], Filipe Fernandes[1,3], Rúben Costa[2,4], Rita Sales-Contini[1,5], and André Pedroso[1,2]

[1] ISEP, School of Engineering, Polytechnic of Porto, Rua Dr. António Bernardino de Almeida, 4249-015 Porto, Portugal
napvs@isep.ipp.pt

[2] FEUP – Faculty of Engineering, University of Porto, Rua Dr. Roberto Frias, 4200-465 Porto, Portugal

[3] Department of Mechanical Engineering, University of Coimbra, CEMMPRE – Centre for Mechanical Engineering Materials and Processes, Rua Luís Reis Santos, 3030-788 Coimbra, Portugal

[4] Associate Laboratory for Energy, Transports and Aerospace (LAETA-INEGI), Rua Dr. Roberto Frias 400, 4200-465 Porto, Portugal

[5] Technological College of São José dos Campos, Professor Jessen Vidal, Centro Paula Souza Avenida Cesare Mansueto Giulio Lattes, 1350 Distrito Eugênio de Melo, São José dos Campos/SP 12247-014, Brazil

Abstract. INCONEL® 718 is considered a difficult-to-machine material due to its superior mechanical properties. The milling process is the most suitable for machining this alloy due to its flexibility in generating complex shapes. Coated tools doped with some elements, such as Vanadium, have been used to improve process performance. Thus, this work aimed to compare two coatings, TiAlVN and TiAlN/TiAlVN, deposited by the Direct Current Magnetron Sputtering (DC MS) method when milling INCONEL® 718. The analysis was carried out concerning their structure and performance, in terms of surface roughness and wear mechanisms, in the milling process. The parameters changed in the process were the cutting length (L_{cut}) and feed per tooth (f_z). Both coatings were found to have a columnar structure, with the multilayer coating having a smaller grain size. Furthermore, the multilayer coating featured better wear behaviour. The main wear mechanisms identified for both coatings were abrasive and adhesive, with higher intensity in the TiAlVN monolayered coating.

Keywords: Nickel Alloys · Tool Wear Mechanisms · PVD Coatings · Machining · Wear Resistance · Vanadium · Manufacturing Innovation

© The Author(s), under exclusive license to Springer Nature Switzerland AG 2024
V. Ivanov et al. (Eds.): DSMIE 2024, LNME, pp. 319–330, 2024.
https://doi.org/10.1007/978-3-031-61797-3_27

1 Introduction

The machining process is one of the processes most used by companies to transform raw materials into final parts with good quality and surface finish; therefore, it is a process that is always subject to improvement due to its great importance in industrial and scientific terms [1]. The milling operation, a flexible process that produces parts with a perfect surface finish, is the most used in the machining process of INCONEL® 718 [2]. This Ni-superalloy is considered a difficult-to-machine material due to its superior mechanical properties, such as high hardness and low thermal conductivity [3]. However, there is a gap in the literature regarding the milling operation of this alloy. That is, more studies are needed to improve the process. Furthermore, as INCONEL® 718 is a material widely used in the aeronautical and aerospace industry, areas under elevated safety responsibility, the milling process must be optimised, which could lead to reduced process costs and increased tool lifespan.

In addition, recent advances are necessary and are studied by several authors, as is the case with the use of coatings on cutting tools or even on cutting tools' materials and geometries. For example, Akhtar et al. [4] analyzed the influence of machining parameters on the surface integrity of INCONEL® 718 during high-speed milling, comparing cutting tools coated with TiAlN by the PVD process and uncoated SiC whisker-reinforced tools. The authors verified that the surface roughness and the surface integrity obtained by the coated tools were superior. In turn, De Bartolomeis et al. [5] analyzed, based on several studies, the most desired properties for cutting tools in machining this alloy and verified the advantage of these tools having high hardness under elevated temperature, high mechanical and wear resistance, as well as toughness and thermal resistance. Some materials, such as cubic boron nitrides (CBNs), ceramic materials, and carbides, exhibit better behavior when milling this alloy.

Thus, thin coatings have been deposited on cutting tools to improve the milling process. In this aspect, TiAlN-based coatings are widely used and studied nowadays [6], with doping elements, such as Vanadium, being added to improve process performance and tool lifespan. In addition, in the literature, some works focus on the characterization of the coating, depending on its physical and chemical properties [7, 8], with no works being found that evaluate the performance of cutting tools coated with TiAlVN.

Based on that, this work aimed to compare the wear behaviour and process performance of two coatings doped with Vanadium: TiAlVN monolayer and TiAlN/TiAlVN multilayer. These two coatings were selected due to the gap seen in the literature regarding their analysis in the INCONEL® 718 milling process, as well as since this coating can be beneficial in the milling process as it reduces the friction coefficient between surfaces [9], which reduces process wear and consequently increases tool lifespan. Furthermore, multilayer coatings are essential to avoid crack propagation and oxidation resistance [10], which is crucial when machining INCONEL® 718, as it can increase the process temperature [11]. The results obtained here are expected to be used as a basis for future work in terms of optimisation and performance of the milling process.

2 Literature Review

2.1 INCONEL® 718 and Machining Process

INCONEL® 718 is a Ni-superalloy with superior mechanical properties, such as high hardness, low thermal conductivity, good corrosion resistance, oxidation resistance, resistance to creep, and weldability [12]. Therefore, it is considered a difficult-to-machine material [13]. Furthermore, this alloy tends to adhere to cutting tools, which generates more significant abrasive wear and can increase the cutting forces developed [14]. Another critical point of INCONEL® 718, which causes significant abrasive wear in the process, is related to its final metallurgical structure. In this case, a significant amount of hard carbides is found, which increases the wear of the cutting tools and can also cause their respective failure [15]. An example of the presence of hard carbides was found in the work of Polvorosa et al. [16], in which built-up edges were developed as wear mechanisms. The cutting forces developed in the process are also imperative in the machining of INCONEL® 718, as they provide essential information regarding process stability, vibrations, and performance [17]. Furthermore, aiming to analyse the performance of the process and study ways to improve it, some authors focused their work on optimising the machining process with the selection of ideal parameters able to improve the quality of the machined surface and reduce the resulting wear on cutting tools, which is the case of the work by Pinheiro et al. [18], in which, using the Taguchi method, the authors determined the best combination of parameters, such as cutting speed (vc), feed (fz), cutting tool, lubrication mode, so that the performance of the turning process in INCONEL® 718 was improved.

2.2 Coating Deposition

The deposition of coatings on cutting tools has been studied, aiming to improve the performance of the machining process. Deposition can be done through Physical Vapor Deposition (PVD) or Chemical Vapor Deposition (CVD) [19]. Among the PVD methods, one of the most used is the Direct Current Magnetron Sputtering (DC MS) method [20]. This process is auspicious concerning coated tools for machining INCONEL® 718, as it brings many advantages to the coating, such as accurate control of its composition, not causing degradation of the film since deposition is carried out at a lower temperature, and a high deposition rate [21]. Some authors compared the wear behaviour of coated and uncoated tools to verify the advantages of using coatings on cutting tools and improving process performance. This is the case of the work by Jawaid et al. [22], in which the TiN coating deposited through the PVD process was analysed and compared with uncoated tungsten carbide tools in the milling of INCONEL® 718. An improvement in process performance was found when using coated tools, showing a lower amount of wear; however, delamination occurred. TiAlN-based coatings have great potential in machining INCONEL® 718, as they have high hardness, thermal stability, and oxidation resistance [23].

Furthermore, adding doping elements (e.g., Y, Si, Mo, and V) to TiAlN can improve process performance and increase corrosion resistance, crack propagation and adhesion resistance. However, in the case of V, there is a gap in the literature regarding the

performance of this coating in the machining field, with studies being more focused on its characterisation. For example, Xu et al. [7] found that adding V to TiAlN increased its hardness and decreased resistance to oxidation due to the formation of Ti-oxides instead of Al-oxide.

2.3 Wear Mechanisms

Wear mechanisms provide essential information regarding the performance of the process and are related to the interaction between the cutting tool and the workpiece. Furthermore, the chipping formation mechanism is of crucial importance. Based on this, depending on the material to be machined, the tool used, its substrate and geometry, and the parameters used, the mechanisms can appear in different intensities and stages of development, which makes their analysis crucial concerning process optimisation and even further increase the tool life. Regarding the wear mechanisms developed in the machining of INCONEL® 718, abrasive wear and material adhesion with built-up edge formation are commonly observed [24]. Other mechanisms may appear depending on the process parameters and whether coated tools are used.

3 Research Methodology

3.1 Materials

INCONEL® 718 alloy was used as stock material, supplied in a cylindrical shape with a diameter of 158 mm. The material underwent the following heat treatments: (a) Solution annealing at 970 °C, followed by quenching in water; (b) Precipitation hardening at 718 °C for 8 h; (c) Oven cooling at 621 °C for 8 h; (d) Air cooling. Its chemical composition (% wt.) is shown in Table 1.

Table 1. INCONEL® 718 chemical composition (*%wt*) [25].

Ni	Cr	Fe	Nb	Mo	Ti	Al	Co
53.89	18.05	17.78	5.35	2.90	0.96	0.51	0.20
Cu	Si	Mn	B	C	P	N	Mg
0.10	0.080	0.078	0.039	0.023	0.010	0.0070	0.0017

WC-Co end mills tools, grade 6110, with 6% Co as a binder and an average grain size of 0.3 μm were used. The tools were provided by Inovatools, S.A. (Leiria, Portugal) company. The geometry of these tools is shown in Table 2.

Cutting tools coated in two configurations were used: monolayer coating (TiAlVN) and multilayer coating (TiAlN/TiAlVN). The coatings were deposited using Teer Coatings UDP 650 Closed Field Unbalanced DC Magnetron Sputtering equipment. The coating was deposited on the entire cutting part of the tool. The deposition parameters, as well as the methodology used, will be explained in Sect. 3.2.

Table 2. WC-Co end mill tool characteristics and geometry.

Tool geometry dimensions	Value
Tool cutting diameter ($\emptyset_t$)	6 mm
Tool cutting length	13 mm
Chamfer	45°; 0.20 mm
Cutting angle	12°
Clearance angle	10°
Number of flutes	4

3.2 Methods

Coating Deposition. Before starting the deposition process, aiming to eliminate any remaining contamination, the cutting tools were positioned in a chamber at a pressure of 0.003 Pa and subjected to a cleaning process with Ar + ions at −600 V, time of pulse of 1.5 μs and frequency of 250 kHz for 30 min. The first layer deposited was a TiN layer to aid the coating adhesion. The TiAlVN coating was obtained with 3000 W, 2500 W, and 1800 W for the Ti, Al, and V targets. The TiAlN/TiAlVN multilayer coating was deposited with the same parameters. However, the V target oscillated the power between 0 and 1800 W. The deposition process for both cases was carried out under total pressure (Ar + N2) around 0.30–0.34 Pa, and the substrate rotation speed was 12 rpm. The deposition parameters used are shown in Table 3.

Table 3. Parameters selected for deposition of TiAlVN and TiAlN/TiAlVN tool coatings.

Deposition parameters	TiAlVN	TiAlN/TiAlVN
Ti target power (W)	3000	
Al target power (W)	2500	
V target power (W)	1800	0/1800
Bias voltage (V)	−80	
Interlayer thickness (μm)	≈ 0.27	
Thickness (μm)	≈ 1.7	2
Multilayer period (nm)	–	≈ 50

Milling Tests. Machining tests were performed using a HAAS VF-2 (HAAS Automation, Oxnard, CA, USA) three-axis CNC milling centre. A spiral strategy was selected as the INCONEL® 718 part was supplied as a cylinder. Thus, the milling operation was performed from the centre towards the periphery of the part, using a cutting fluid with 5% oil in water. As for the milling parameters, the radial depth of cut (ae) was kept constant to prevent wear-related phenomena. The axial depth of cut (ap) was the same

for all tests and had a value of 0.08 mm. This value was selected through preliminary tests, which showed that higher values, for example, 0.2 mm and 0.1 mm, were too much for tools that failed shortly after the initial plunge. In addition, as the tool diameter (Øt) was 6 mm, the value of ae was decided to be 75% of this value, which is 4.5 mm. The parameters varied in the tests, including fz and Lcut. Parameter fz varied between three distinct values: 0.0525 mm/tooth, 0.07 mm/tooth, and 0.105 mm/tooth, and Lcut varies between 5 m and 15 m. The cutting speed was 100 m/min for all cases. The test conditions are presented in Table 4. Coatings deposited in monolayer and multilayer will be designated as V and MV, respectively, with the number after this letter corresponding to the percentage of feed per tooth and the subsequent cutting length (5 m or 15 m).

Table 4. Milling parameters.

Ref	V_c [m/min]	f_z [mm/tooth]	L_{cut} [m]
V75_5 and MV75_5	100	0.0525	5
V75_15 and MV75_15	100	0.0525	15
V100_5 and MV100_5	100	0.0700	5
V100_15 and MV100_15	100	0.0700	15
V150_5 and MV150_5	100	0.1050	5
V150_15 and MV150_15	100	0.1050	15

Scanning Electron Microscopy (SEM) Analysis. A ZEISS Merlin high-resolution microscope (FEG-SEM) was used to analyse the morphology of the coatings, both on the surface and in the cross-section, with a high voltage of 15 kV, a magnification between × 10,000 and × 50,000, and secondary electrons.

After each test, the roughness of each machined surface was analysed using a Mahr Perthometer M2 profilometer (Mahr, Gottingen, Germany), following the DIN EN ISO 4288:1996 [26]. Measurements considered 0.8 mm as the cut-off distance (λ_c) and 5.6 mm as the measuring length, taken in the tangential and radial direction. The arithmetic average roughness value (R_a) between measurements was considered to evaluate this. Moreover, the wear suffered by the cutting tools in all tested conditions was evaluated through a Hitachi SU3800 scanning electron microscope, using BSE (Backscattered Electrons) mode and at a magnification between × 40 and × 2000, making it possible to analyse the wear mechanisms present and measure VB3 according to ISO 8688–2:1986 [27]. VB3 was selected because it is located close to the chamfer and, therefore, is the wear that most influenced the machined surface quality.

4 Results and Discussion

4.1 Morphology of the Cross-Section and Surface of the Coatings

The morphology of both the cross-section and surface coatings is shown in Fig. 1. The coatings have a columnar morphology, characteristic of the sputtering process using a DC power source [28]. Already on the surface, the coating has rounded grains, which correspond to the top of the columns. It is observed that the size of the grains tends to decrease in the multilayer structure. This occurs due to the alternation of TiAlN layers with TiAlVN layers, the consequent decrease in the thickness of each layer, and the strong competitive growth mode between various crystalline textures [29].

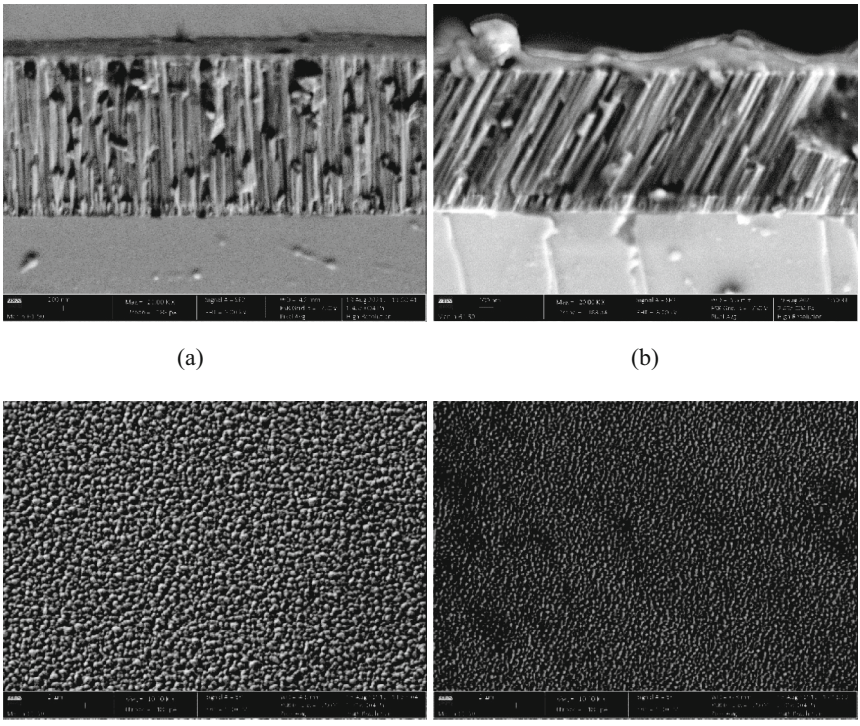

(a) (b)

(c) (d)

Fig. 1. Morphology of the coatings: (a) Cross-section of TiAlVN coating with 2000 kx magnification; (b) Cross-section of TiAlN/TiAlVN coating with 2000 kx magnification; (c) top surface of TiAlVN coating with 1000 kx magnification and (d) top surface of TiAlN/TiAlVN coating with 1000 kx magnification.

4.2 Roughness Analysis

Figure 2 illustrates the results obtained for measuring the surface roughness of the machined part.

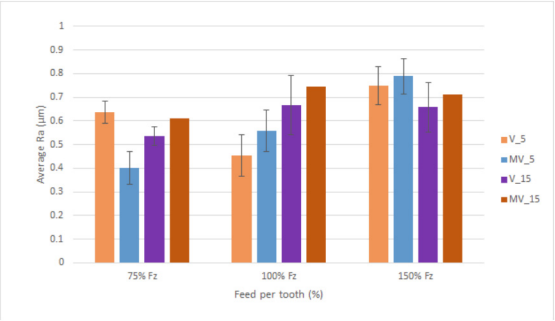

Fig. 2. Surface roughness values for all conditions.

It is noted that there was an increase in surface roughness with the increase in f_z for $L_{cut} = 5$ m. This is justified since lower feed values per tooth generally generate better-machined surface quality [30]. This trend is mainly seen in the MV_5 condition. In the case of condition V_5, with 75% f_z, there was a break in the cutting edge, resulting in a surface roughness greater than 100% f_z. As for the tests carried out at 15 m, the roughness increases from 75% to 100% of the f_z, followed by a slight decrease when increasing to 150% of the f_z. This happens due to the increase in temperature between the part and the cutting tool in the process, which generates a lubricating phase of V_2O_5, reducing friction and improving the machined surface roughness. However, increasing the f_z increases the surface roughness of the machined part [31].

Regarding L_{cut}, it is observed that the higher this parameter is, the higher the roughness is obtained. However, this trend was not observed when comparing conditions V75_5 with V75_15. This is not commonly observed and may be related to the excess vibration in the first condition and the breakage of the cutting tool edge. Commonly, high L_{cut} promotes more significant abrasive wear on the cutting tool, which is especially notable when machining materials such as INCONEL® 718 [32].

Therefore, for higher L_{cut} values, this difference tends to be more significant due to the sustained wear of the cutting tool. Thus, it can be seen that concerning the roughness of the machined surface, tools coated only with a monolayer of TiAlVN presented superior results and performance, as the surface quality was better with lower surface roughness levels when compared to tools with multilayer coating. This is related to the resulting wear and the amount of V, which generated several lubricating phases upon contact between the cutting tool and the machined part.

4.3 Wear Measurement (VB3) and Characterization

Figure 3 shows the results obtained for measuring flank wear.

The L_{cut} was the parameter with the most significant influence on the resulting wear. This behaviour was already expected since the abrasive and accumulated wear increases when the L_{cut} increases [33]. Regarding the influence of variation in f_z, in most conditions, an increase in flank wear is noted with the increase in this parameter. An f_z with higher values generates more localised wear [34]. Furthermore, the f_z is

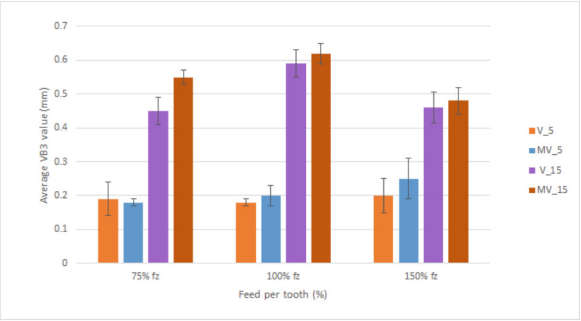

Fig. 3. Flank wear (VB3) for all conditions.

related to the chip formation mechanism, and the formation of fine chips can lead to superior abrasive wear due to the possibility of these chips breaking and, consequently, distinguished flank wear. When comparing the two types of coatings under the same conditions, it is observed that the TiAlVN coating shows less wear, which follows the roughness obtained.

The predominant wear mechanisms were abrasive and adhesive on the tool substrate and the coatings. These wear mechanisms are commonly observed when machining INCONEL® 718, mainly due to the formation of hard chips, which can even cause changes in the geometry of the cutting tool [25]. In the work of Kursuncu et al. [35], even using another coating, in this case, TiAlSiN/TiSiN/TiAlN, abrasion and material adhesion were also identified when milling Inconel 718. Abrasive wear was also identified in the work by Thakur et al. [36]. In addition to this wear, the authors also identified plastic deformation and microchipping. In this case, the coating used was TiN/TiAlN. Figure 4(a) illustrates the presence of abrasive wear in the V150_15 condition.

Regarding adhesive wear, it was mainly observed on the rake face of cutting tools, being in greater quantity on the tool substrate than on the coating. Both coatings showed

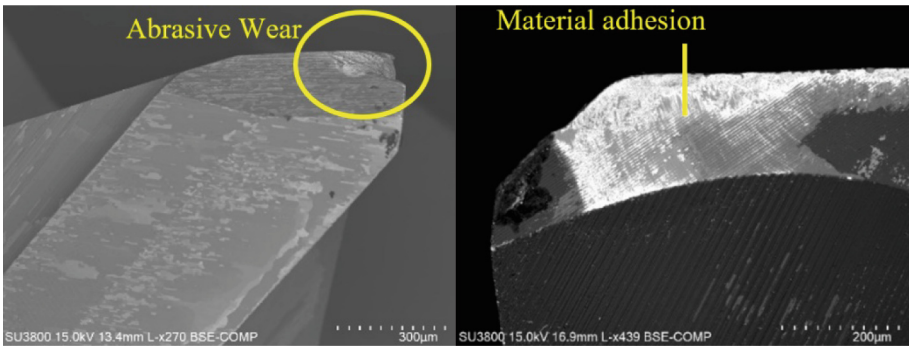

(a) (b)

Fig. 4. Predominant wear mechanisms: (a) abrasive wear in V150_15 condition, and (b) adhered material in MV150_5 condition.

material adhesion. However, the amount of adhered material was more significant in the multilayer coating. Figure 4(b) illustrates the presence of adhered material on the cutting tool, resulting in the MV150_5 condition.

Furthermore, it can be pointed out that there was no coating delamination, showing the importance of using an adhesion layer, which, in this case, was made of TiN. In addition to improving adhesion, this underlayer gives the coatings better resistance to cracking propagation [18].

5 Conclusions

The present work compared the wear behaviour of two coating configurations when milling INCONEL® 718, depending on the variation of machining parameters. The results showed that the TiAlVN and TiAlN/TiAlVN coatings have a columnar structure, with the grains being smaller in the multilayer coating. Concerning the roughness of the machined surface and the resulting wear, the TiAlVN coating presented better results, possibly due to the formation of a lubricating phase. The condition MV100_15 exhibited more significant flank wear, and on the other hand, the lowest flank wear was observed for condition V100_5. As for the machining parameters, the Lcut presented the most significant influence.

However, feed per tooth has also been shown to impact the milling process. Regarding wear mechanisms, abrasive wear, and material adhesion were identified, which was already expected for INCONEL® 718. The results obtained can be used as a basis for future work, given the difficulty of machining INCONEL® 718, mainly in cabling operations.

As future work, it is suggested to analyze the influence of different percentages of Vanadium in the coating and compare the behavior in tools without coatings so that it is possible to verify how the deposition of thin coatings can improve the performance of the process.

References

1. Gouveia, R.M., Silva, F.J.G., Reis, P., Baptista, A.P.M.: Machining duplex stainless steel: comparative study regarding end mill coated tools. Coatings **6**(4), 51 (2016). https://doi.org/10.3390/coatings6040051
2. Paturi, U.M.R., Darshini, B.V., Reddy, N.S.: Progress of machinability on the machining of INCONEL 718: a comprehensive review on the perception of cleaner machining. Clean. Eng. Technol. **5**, 100323 (2021). https://doi.org/10.1016/j.clet.2021.100323
3. Hong, S.J., Chen, W.P., Wang, T.W.: A diffraction study of the γ'' phase in INCONEL 718 superalloy. Metall. and Mater. Trans. A. **32**(8), 1887–1901 (2001). https://doi.org/10.1007/s11661-001-0002-4
4. Akhtar, W., Sun, J., Chen, W.: Effect of machining parameters on surface integrity in high speed milling of super alloy GH4169/Inconel 718. Mater. Manuf. Processes **31**(5), 620–627 (2016). https://doi.org/10.1080/10426914.2014.994769
5. Bartolomeis, A.D., Newman, S.T., Jawahir, I.S., Biermann, D., Shokrani, A.: Future research directions in the machining of Inconel 718. J. Mater. Process. Technol. **297**, 117260 (2021). https://doi.org/10.1016/j.jmatprotec.2021.117260

6. Caliskan, H., Panjan, P., Kurbanoglu, C.: 3.16 Hard coatings on cutting tools and surface finish. In: Hashmi, M.S.J. (eds.) Comprehensive Materials Finishing, pp. 230–242. Elsevier, Oxford (2017). https://doi.org/10.1016/B978-0-12-803581-8.09178-5
7. Xu, Y.X., Chen, L., Pei, F., Yue, J.L., Du, Y.: Thermal stability and oxidation resistance of V-alloyed TiAlN coatings. Ceram. Int. **44**(2), 1705–1710 (2018). https://doi.org/10.1016/j.ceramint.2017.10.100
8. Zhang, J., Chen, L., Kong, Y.: The microstructural, mechanical and thermal properties of TiAlVN, TiAlSiN monolithic and TiAlVN/TiAlSiN multilayered coatings. J. Alloys Compd. **899**, 163332 (2022). https://doi.org/10.1016/j.jallcom.2021.163332
9. Tillmann, W., Momeni, S., Hoffmann, F.: A study of mechanical and tribological properties of self-lubricating TiAlVN coatings at elevated temperatures. Tribol. Int. **66**, 324–329 (2013). https://doi.org/10.1016/j.triboint.2013.06.007
10. Fukumoto, N., Ezura, H., Suzuki, T.: Synthesis and oxidation resistance of TiAlSiN and multilayer TiAlSiN/CrAlN coating. Surf. Coat. Technol. **204**(6), 902–906 (2009). https://doi.org/10.1016/j.surfcoat.2009.04.027
11. Mahesh, K., Philip, J.T., Joshi, S.N., Kuriachen, B.: Machinability of INCONEL 718: a critical review on the impact of cutting temperatures. Mater. Manuf. Processes **36**(7), 753–791 (2021). https://doi.org/10.1080/10426914.2020.1843671
12. Buddaraju, K.M., Ravi Kiran Sastry, G., Kosaraju, S.: A review on turning of INCONEL alloys. Mater. Today Proc. **44**, 2645–2652 (2021). https://doi.org/10.1016/j.matpr.2020.12.673
13. Hosseini, E., Popovich, V.A.: A review of mechanical properties of additively manufactured INCONEL 718. Addit. Manuf. **30**, 100877 (2019). https://doi.org/10.1016/j.addma.2019.100877
14. Toubhans, B., Fromentin, G., Viprey, F., Karaouni, H., Dorlin, T.: Machinability of INCONEL 718 during turning: Cutting force model considering tool wear, influence on surface integrity. J. Mater. Process. Technol. **285**, 116809 (2020). https://doi.org/10.1016/j.jmatprotec.2020.116809
15. Zhou, J., Bushlya, V., Avdovic, P., Ståhl, J.E.: Study of surface quality in high speed turning of INCONEL 718 with uncoated and coated CBN tools. Int. J. Adv. Manuf. Technol. **58**(1–4), 141–151 (2012). https://doi.org/10.1007/s00170-011-3374-7
16. Polvorosa, R., Suárez, A., de Lacalle, L.N.L., Cerrillo, I., Wretland, A., Veiga, F.: Tool wear on nickel alloys with different coolant pressures: comparison of Alloy 718 and Waspaloy. J. Manuf. Process. **26**, 44–56 (2017). https://doi.org/10.1016/j.jmapro.2017.01.012
17. Sousa, V.F.C., Silva, F.J.G., Alexandre, R., Fecheira, J.S., Silva, F.P.N.: Study of the wear behaviour of TiAlSiN and TiAlN PVD coated tools on milling operations of pre-hardened tool steel. Wear **476**, 203695 (2021). https://doi.org/10.1016/j.wear.2021.203695
18. Pinheiro, C., et al.: Effect of machining parameters on turning process of INCONEL 718. Mater. Manuf. Processes **36**(12), 1421–1437 (2021). https://doi.org/10.1080/10426914.2021.1914839
19. Martinho, R.P., Silva, F.J.G., Martins, C., Lopes, H.M.: Comparative study of PVD and CVD coated tools in milling of duplex stainless-steel. Int. J. Adv. Manuf. Technol. **102**, 2423–2439 (2019). https://doi.org/10.1007/s00170-019-03351-8
20. Baptista, A., Silva, F., Porteiro, J., Míguez, J., Pinto, G.: Sputtering Physical Vapour Deposition (PVD) coatings: a critical review on process improvement and market trend demands. Coatings **8**(11), 402 (2018). https://doi.org/10.3390/coatings8110402
21. Yeh, T.-S., Wu, J.-M., Hu, L.-J.: The properties of TiN thin films deposited by pulsed direct current magnetron sputtering. Thin Solid Films **516**(21), 7294–7298 (2008). https://doi.org/10.1016/j.tsf.2008.01.001

22. Jawaid, A., Koksal, S., Sharif, S.: Cutting performance and wear characteristics of PVD coated and uncoated carbide tools in face milling INCONEL 718 aerospace alloy. J. Mater. Process. Technol. **116**(1), 2–9 (2001). https://doi.org/10.1016/S0924-0136(01)00850-0
23. Geng, Z., Shi, G., Shao, T., Liu, Y., Duan, D., Reddyhoff, T.: Tribological behavior of patterned TiAlN coatings at elevated temperatures. Surf. Coat. Technol. **364**, 99–114 (2019). https://doi.org/10.1016/j.surfcoat.2019.02.076
24. Grzesik, W.: Tool wear and damage. In: Advanced Machining Processes of Metallic Materials, pp. 215–239. Elsevier (2017). https://doi.org/10.1016/B978-0-444-63711-6.00012-0
25. Sousa, V.F.C., Fernandes, F., Silva, F.J.G., Costa, R.D.F.S., Sebbe, N., Sales-Contini, R.C.M.: Wear behavior phenomena of TiN/TiAlN HiPIMS PVD-coated tools on milling inconel 718. Metals (Basel) **13**(4), 684 (2023). https://doi.org/10.3390/met13040684
26. ISO 4288:1996 – Geometrical Product Specifications (GPS) – Surface Texture: Profile Method – Rules and Procedures for the Assessment of Surface Texture. International Organization for Standardization, Geneva (1996)
27. ISO 8688-2:1986 – Tool Life Testing in Milling – Part 2: End Milling. International Organization for Standardization, Geneva (1986)
28. Mauer, G., Vaßen, R.: Coatings with columnar microstructures for thermal barrier applications. Adv. Eng. Mater. **22**(6), 1900988 (2020). https://doi.org/10.1002/adem.201900988
29. Aliofkhazraei, M., et al.: Development of electrodeposited multilayer coatings: a review of fabrication, microstructure, properties and applications. Appl. Surf. Sci. Adv. **6**, 100141 (2021). https://doi.org/10.1016/j.apsadv.2021.100141
30. Airao, J., Chaudhary, B., Bajpai, V., Khanna, N.: An experimental study of surface roughness variation in end milling of super duplex 2507 stainless steel. Mater. Today Proc. **5**(2), Part 1, 3682–3689 (2018). https://doi.org/10.1016/j.matpr.2017.11.619
31. Čep, R., et al.: Surface roughness after machining and influence of feed rate on process. Precision machining VII. Key Eng. Mater. **581**, 341–347 (2014). https://doi.org/10.4028/www.scientific.net/KEM.581.341
32. Ostrowicki, N., Kaim, A., Gross, D., Hanenkamp, N.: Effect of various cooling lubricant strategies on turning INCONEL 718 with different cutting materials. Procedia CIRP **101**, 350–353 (2021). https://doi.org/10.1016/j.procir.2021.02.037
33. Dhananchezian, M., Rajkumar, K.: Comparative study of cutting insert wear and roughness parameter (Ra) while turning Nimonic 90 and Hastelloy C-276 by coated carbide inserts. Mater. Today Proc. **22**, 1409–1416 (2020). https://doi.org/10.1016/j.matpr.2020.01.484
34. Zhang, G., Zhang, J., Fan, G., Xu, C., Du, J.: The effect of chip formation on the cutting force and tool wear in high-speed milling INCONEL 718. 2023. Int. J. Adv. Manuf. Technol. (2023). https://doi.org/10.21203/rs.3.rs-2366266/v1
35. Kursuncu, B., Caliskan, H., Guven, S.Y., Panjan, P.: Wear behavior of multilayer nanocomposite TiAlSiN/TiSiN/TiAlN coated carbide cutting tool during face milling of INCONEL 718 superalloy. J. Nano Res. **47**, 11–16 (2017). https://doi.org/10.4028/www.scientific.net/JNanoR.47.11
36. Thakur, D.G., Ramamoorthy, B., Vijayaraghavan, L.: Some investigations on high speed dry machining of aerospace material INCONEL 718 using multicoated carbide inserts. Mater. Manuf. Process. **27**(10), 1066–1072 (2012). https://doi.org/10.1080/10426914.2011.654158

Evaluation of Cutting Fluid Penetration into the Cutting Zone During Grinding of Rolling Rolls

Mykhaylo Stepanov[1], Leonid Polonsky[2], Volodymyr Korniienko[1], Tetyana Tretyak[1], and Maryna Ivanova[1](✉)

[1] National Technical University «Kharkiv Polytechnic Institute», 2, Kyrpychova Street, Kharkiv 61002, Ukraine
maryna.ivanova@khpi.edu.ua

[2] Zhytomyr Polytechnic State University, 103, Chudnivska Street, Zhytomyr 10005, Ukraine

Abstract. The process of cutting fluid penetration into the contact zone of the grinding wheel and workpiece at circular external grinding of rolls of rolling mills and the main factors influencing this process are investigated. It is established that cutting fluid penetration into the contact zone of the grinding wheel and the workpiece is a complex hydromechanical process occurring due to the capillary effect using the finest network of capillaries formed in the contact zone of the grinding wheel and workpiece. It is established that dynamic phenomena in the technological system accompanying the cutting process when grinding rolls exert a significant influence on the penetrating ability of cutting fluid. Based on the research results, recommendations on selecting grinding modes of rolls providing the maximum degree of cutting fluid penetration into the contact zone of the wheel and workpiece are offered. In this case, the maximum increase of "useful" cutting fluid consumption is achieved, which reduces the grinding process's heat intensity at a minimum cutting fluid consumption, thereby increasing the grinding efficiency.

Keywords: Industrial Growth · Grinding · Rolling Rolls · Penetrating Ability · Cutting Fluid · Contact Zone · Arc Length of Contact · Process Innovation

1 Introduction

The reliability and durability of rolling rolls are decisive factors that determine the product quality, productivity, and economic efficiency of rolling mills [1–3]. Due to the complexity of roll production technology and the cyclic nature of their operation at high contact stresses, any unaccounted factor can be decisive in reducing the part's strength [4]. The solution to problems related to the improvement of roll surface quality may result from searching for more perfect grinding technologies [5, 6]. Meanwhile, the question of the technology of the qualitative process of rolls finishing by grinding continues to be difficult and actual even today. The real reserve of growth of processing efficiency by grinding is the rational application of technological lubricating and cooling. The

© The Author(s), under exclusive license to Springer Nature Switzerland AG 2024
V. Ivanov et al. (Eds.): DSMIE 2024, LNME, pp. 331–340, 2024.
https://doi.org/10.1007/978-3-031-61797-3_28

problem's relevance is dictated by the need to study the processing process, considering the specifics of grinding rolling rolls using cutting fluid.

The purpose of this work was to analyze the processes of grinding rolls of rolling mills with the use of cutting fluid and to determine the factors influencing the penetration of cutting fluid into the contact zone of the grinding wheel and workpiece, and on this basis to offer recommendations to increase the degree of penetration of cutting fluid into the contact zone.

2 Literature Review

The mechanism of coolant penetration into the cutting zone has been and remains the subject of numerous studies. Thus, various methods for quantitatively assessing coolant penetration properties are proposed [7, 8]. The coolant's penetrating effect depends on its properties and how it is supplied to the cutting zone. At high cutting speeds, which are characteristic of grinding, penetration of the medium into the cutting zone is very difficult and depends on several factors (Fig. 1). The efficiency of cutting fluid penetration when it is fed into the contact zone under pressure is enhanced. This is favored by additional kinetic energy, which increases the penetrating effect on heavily loaded contact surfaces. A multifunctional tool module has been developed to create favorable penetration conditions into the contact zone of the tool and workpiece, which allows adjusting the cutting fluid flow-by-flow rate and pressuring [9].

The grinding conditions are primarily determined by the arc of contact between the grinding wheel and the workpiece. In the external cylindrical grinding of a roll with longitudinal feed, abrasive grains move along the circumference while the workpiece (grinding wheel) moves along its axis.

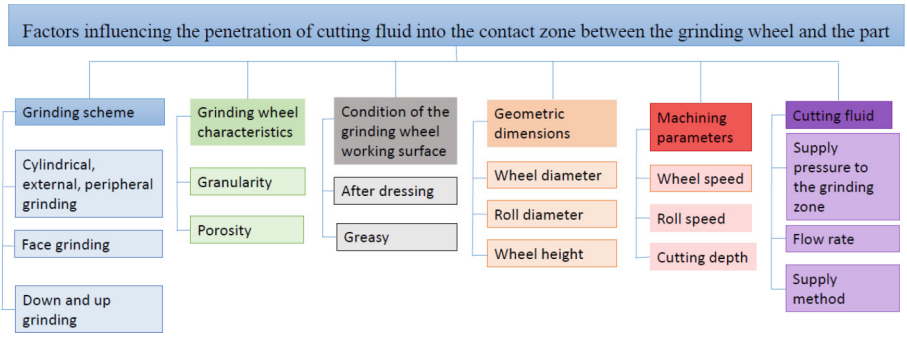

Fig. 1. Factors for analyzing the efficiency of cutting fluid penetration into the cutting zone.

The behavior of the fluid in the contact zone is determined, among other things, by hydraulic parameters (flow rate and pressure), grinding wheel size, and coolant characteristics [10]. The flow rate and pressure critically influence the chip evacuation condition during grinding [11]. Redko S.G. has discovered that the amount of thermal impulses imparted to the ground surface is directly proportional to the length of the arc of contact with the machined surface, the circumferential speed of the wheel, the number of

working grains, and inversely proportional to the workpiece movement speed. The number of thermal impulses is influenced by the depth of the cut, which can be expressed in terms of the contact arc length. Elyanov D.D. and Kulikov A.N. have claimed that increasing the depth of cut and feed (intensity of removal) increases the thickness of the metal layer removed by the grain, the length of the contact arc, the number of abrasive grains involved in the work, cutting force, power consumption and temperature of the ground surface. E.N. Maslov makes the following conclusions from the analysis of the kinematics of the grinding process:

1. The absolute length of the arc of contact between the wheel and the workpiece is small. For example, when the diameter of the grinding wheel $D_{gw} = 600$ mm, the diameter of the workpiece $d_{wp} = 50$ mm, and the cutting depth $t = 0.005$ mm, then the absolute length of the arc of contact is $L = 0.48$ mm.
2. At small values of the cutting depth, the diameter of the wheel has an insignificant effect on the length of the arc of contact.
3. The circumferential speed of the workpiece and longitudinal feed also insignificantly affect the contact arc length.

The analyses (Table 1) of the length of the contact arc during the grinding of rolls on different machines in the shops of different enterprises (mainly metallurgical plants) show that the given value of L is several times greater than the contact length during grinding of workpieces of the most common diameters, which emphasizes the specificity of processing by grinding of rolling rolls.

The rotation of a large-diameter grinding wheel generates circumferential and end-air flows. The air in the pores of the wheel is pushed to the periphery of the wheel by centrifugal force, which creates a vacuum inside the porous structure of the wheel, and new volumes of air are sucked in through the pores. Khudobin L.V. noticed that robust vortex flows are also created by the scallops of the roughness of the surface of the periphery and end of the grinding wheel.

Thus, the intensity of air flows is determined by the characteristics of the lap (granularity, forming roughness of the lap surface, and porosity). The speed of the created air flows is determined by the size (diameter, height), shape, and characteristics of the lap, and it increases with the growth of the lap's speed. In this connection, it seems relevant to conduct research to reveal the factors influencing the penetration of cutting fluid into the contact zone.

3 Research Methodology

It has been established [12] that when the grinding wheel is rotating at a speed of 33 m/s, the air from the periphery of the grinding wheel is thrown off at the same speed, and at a distance of 12.5 mm, the airflow speed is 19.2 m/s. At the same time, directly above the contact zone, an "air wedge" is created, and the pressure which reaches 0.84 MPa.

The following should be considered when evaluating the influence of grinding wheel grain size and porosity on cutting fluid penetration into the contact zone.

At roughing grinding of clad rolled rolls, wheels from zirconium corundum 38A with a high grit size of 125…200 with hardness CT1 on a Bakelite bond are used. Such binder is characterized by high density and practical absence of pores.

Table 1. Contact arc length when grinding rolls.

Company	Machine tool	Rolling roll characteristics	Grinding parameters	Contact arc length, mm
Metallurgical Plant, Rustavi city	«Norton»	Ø 505×3500 cast iron 90HSd (grinding a journal d = 320; l = 400 mm)	Preliminary	4.15
			Final	2.07
Lutuginsky Rolling Rolls Plant	«Landis»	Ø 505×3640 521×3020 900×3955 cast iron HSh 71…85 (grinding a journal d = 300…340 mm; l = 300…385 mm)	Preliminary	6.39
			Final	4.4
Novolipetsk Steel	«Farrel Ginsting»	Ø 1323× 3760…5060 (support) 9×P steel HSh 61…95	Preliminary	4.81
			Final	1.6
Azovstal Iron and Steel Works, Mariupol	ХШ 5-08	Ø 1800×3400 9ХФ steel	Preliminary	3.2
			Final	2.12
	ХШ 5-09	Ø 11030×8400 ЛПХНg cast iron	Preliminary	4.24
			Final	2.10

Use wheels with grit size 16…25 on ceramic or Bakelite bond at final grinding. For very fine grinding, use wheels with grit size 8…10; for polishing, grind with an even smaller grit size, which reduces the generation of the airflow grinding wheel.

Recommended values of cutting fluid supply parameters for grinding with different grinding wheels are given in [13]. Cutting fluid easily penetrates the contact zone between the wheel and the workpiece when its pressure is 10–15% higher than the pressure of the airflow created by the wheel. The growth of air pressure in the contact zone with increased cutting depth and cross-feed is established.

All the above-mentioned gives grounds to assume that at grinding rolls of rolling mills, the influence of air flows generated by grinding wheel and workpiece will be a more significant factor preventing cutting fluid from getting into the contact zone due to much larger diameters of wheel and workpiece than in case of application of serial universal cylindrical grinding machines.

The penetration of cutting fluid into the grinding zone is affected by the air gap that occurs during intermittent contact in machining processes.

Interrupters (scrapers), which must be installed in front of the nozzle, are used to relieve the negative effect of air flows. The air layer in the wedge zone is divided into two

flows: an air boundary layer along the grinding wheel and a reverse flow - reflux along the workpiece, which seriously limits cutting fluid penetration into the contact zone.

There are also known studies aimed at improving the aerodynamic environment around the grinding wheel by destroying turbulent air flows by installing a special nozzle for pumping out air.

Various data on the gap width (thickness of the fluid layer) in the wheel-workpiece contact are known. P.I. Yascheritsyn gives data that the specified thickness of the liquid layer is within 0.005…0.025 mm. Khudobin L.V. claimed that in the data for wheels with 16 and 40-grain sizes, the value of the equivalent slot in the gap is 25…100 μm.

Efimov V.V., by analyzing the profilograms of the working surface of the wheel, established that the equivalent thickness of hydrodynamic contact without taking into account the introduction of grains into the workpiece for ceramic-bonded wheels with a grain size of 16–40 is in the range of 35–150 μm (for wheels with hardness M3-T2).

Although the abrasive grains cut into the metal, the intergrain part of the grinding wheel moves at some distance from the machined surface; due to this, a gap is formed in the narrow part of which hydrodynamic pressure is created.

A formula for determining the value of the aforementioned gap - Yashcheritsyn P.I. and Brankevich E.S. obtained the average distance from the ligament to the machined surface:

$$L_g = (0.1 - 0.5)d_0, \tag{1}$$

where d_0 is the size of abrasive grains.

The gap is represented as an equivalent rectangular slot of a certain width. In other studies, a mathematical model [14] of the change of the channel cross-sectional area in the wheel-workpiece contact (at discrete contact) as a result of increasing cutting fluid contamination, the action of "greasing" and grinding wheel wear was obtained.

B. V. Efimov presented the equivalent height of the free surface of the cutting wheel profile in the form of dependence

$$h_g = \frac{1}{H_o}\int_0^{H_0} f(x)dx, \tag{2}$$

where H_0 is the grinding wheel height; $f(x)$ is the function corresponding to the equation of a broken line along the grain boundary and ligament in the plane of the axial section of the cutting wheel profile.

The hydrodynamic lubrication theory is often used to study cutting fluid flow in the contact zone between the wheel and the workpiece. This theory makes it possible to calculate the minimum necessary cutting fluid flow rate through the contact zone, at which the hydrodynamic lubrication mode is theoretically possible.

V.D. Demidov estimates cutting fluid penetration into the grinding zone by the fluid flow rate through the contact defined by the formula:

$$Q_f = \delta_0 \cdot V_{ww} \cdot H_{gw}, \tag{3}$$

where δ_0 is the minimum reduced thickness of the fluid layer in the wheel-workpiece contact; cap V sub w w is fluid velocity in the wheel-workpiece contact; cap H sub g w is grinding wheel height.

In some studies, the cutting fluid flow through the wheel-workpiece contact is called "useful" [15]. Some studies indicate that the occurrence of hydrodynamic lubrication mode depends on the grinding parameters (cutting conditions, type of grinding - preliminary or final, cutting fluid supply parameters).

The fluid flow rate through the wheel-workpiece contact is represented as the sum of fluid flow rates through the channels formed between the grains:

$$Q = \sum_{i=1}^{n} Q_i', \quad i = 1, 2, 3 \ldots n \tag{4}$$

where n is the number of grains in contact with the workpiece.

The cutting fluid flow rate in each of these channels is determined by the formula:

$$Q_{i\prime} = \frac{\delta}{2}\left[\frac{p(x, y)\delta^2}{GL\mu_f} + V_{gw} + V_{wp}\right], \tag{5}$$

where δ is the width of the equivalent rectangular slot in the channel; L is an arc length of the grinding wheel and workpiece contact; $p(x, y)$ is cutting fluid pressure before contact; μ_f is the dynamic viscosity of cutting fluid; V_{gw}, V_{wp} are velocities of the grinding wheel and workpiece, respectively.

The analysis of formula (5) shows that the flow rate in the channel $Q_{i\prime}$ depends on the parameter L (the length of the contact arcs between the wheel and the workpiece). As the contact length increases, the value of cutting fluid flow rate through the contact zone decreases. Thus, the parameter L affects not only the number of grains involved in the grinding process but also the penetration ability of cutting fluid.

It should be noted that the profile of the grinding wheel surface is complex and variable and contains different high grains (grain tops are located at different heights). Still, despite this, the contact zone can be represented as a set of channels having a trapezoidal shape in cross-section and a length equal to the length of the arc of contact between the grinding wheel and the workpiece.

The cross-sectional area of the channel is determined by the formula

$$A_{ch} = (\Delta - a) \cdot l, \tag{6}$$

where Δ is the average value of grain extension under the bond; a. is the average value of shear thickness; is the average distance between grains at the level of average height.

For the majority of operations, even at rigid dimensions, only the upper part of the wheel relief is involved in grinding work, which for the most common medium grit wheels (16, 25, 40), most used for grinding rolls, is 0.1–0.5 part of the entire height of the profile.

The average distance between the grains at the level of their average height is determined by dividing the length of the abrasive space A by the average number of grains per unit length of the working surface Z, corresponding to the height of their protrusion above the level of the conditional surface of the bond l [16, 17].

$$l = \frac{A}{Z} = \frac{\pi a_0 k_m}{3k_v k_h}, \tag{7}$$

where k_v is the coefficient of volume concentration of grains (coefficient of relative volume occupied by grains), $k_v \leq 1$; k_h is the coefficient of relative height of protrusion of grains above the level of bond ($0 < k_h < 1$) for abrasive materials k_h=0.5–0.9; k_m is coefficient of relative location, for abrasive grains k_m=0.81–0.87; a_0 is characteristic size (maximum size of grains of the main fraction, microns).

4 Results and Discussion

To determine the "useful" cutting fluid flow rate into the cutting zone, design and experimental studies were carried out under the following initial conditions:

- grinding wheel grit size – 16, 25, and 40;
- cutting fluid temperature – 20 °C;
- cutting fluid flow rate variation range – 0.8…1.8 dm^3/(min·mm);
- used machine – Farrell Giustina;
- workpiece - support roll Ø1320x3760, steel 9XΦ (HSh 61…95);
- grinding parameters:
- preliminary $V_{gw} = 31.4$ m/s; $V_{wp} = 1$ m/s; $t = 0.05$ mm; $F = 0.5$ m/min;
- final $V_{gw} = 19.6$ m/s; $V_{wp} = 2$ m/s; $t = 0{,}005$ mm; $F = 2.5$ m/min.

As studies have shown (Figs. 2 and 3), the "useful" flow rate and, consequently, the cutting fluid penetration ability are most influenced by the grinding wheel grit size and grinding mode (parameters of preliminary and final grinding). In this case, enlarging the grinding wheel grit size from 16 to 40 increases the useful flow rate by 4–5 times.

The parameters of preliminary and final grinding have a similar effect. When moving from preliminary to final grinding, there is an increase in the "useful" flow rate by a factor of 4–4.5. The cutting fluid flow rate supplied to the contact zone has much less influence

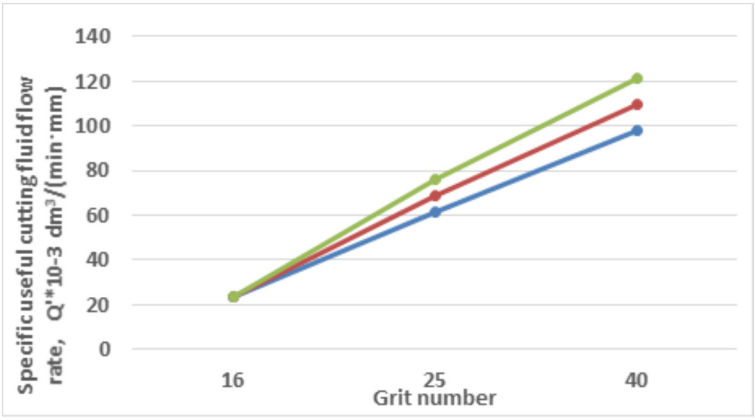

Fig. 2. Influence of grinding wheel grit size and cutting fluid flow rate supplied to the cutting zone on specific "useful" flow rate: preliminary grinding ($V_{gw} = 31.4$ m/s; $V_{wp} = 0.53$ m/s; $t = 0.2$ mm; cutting fluid temperature – 20 °C; 1, 2, 3 - cutting fluid flow rate 0.8; 1.2; 1.8 dm^3/(min·mm) respectively.

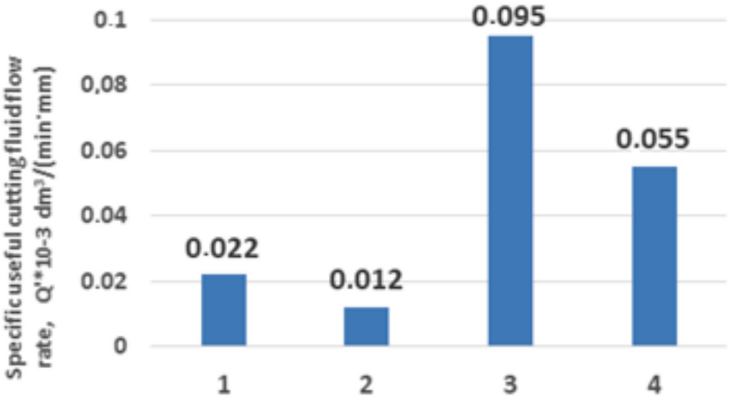

Fig. 3. Influence of grinding mode and wheel grit on specific "useful" cutting fluid consumption: 1, 2 and 3, 4 - grit size 16 and 40, respectively; 1, 3 and 2, 4 - final and preliminary grinding, respectively.

on the "useful" flow rate. Thus, an increase in cutting fluid consumption by a factor of 2.25 contributes to an increase in "useful" consumption by only 1.7%. When using 40-grit grinding wheels, such an increase in cutting fluid flow rate into the contact zone increases "useful" consumption by 19%.

Rolling rolls must have a high uniform hardness after hardening to avoid damage on the working surface. When grinding rolls of chromium steels, the limiting factor is the temperature, above the critical value of which the surface layer is tempered, which leads to a decrease in hardness. So, if a temperature value of 340–360 °C corresponds to a hardness of 70–85 HSD (HRC 52–61), then at a temperature of 460–480 °C the hardness is 50–65 (HRC 39–49).

The task of ensuring the quality of the roll surface by impacting the cooled surface with a cutting fluid can be reduced to the search for inexpensive and, at the same time, accessible ways of delivery to the grinding zone. The design of the coolant supply technique and its location should take into account the peculiarities of the technological operation of grinding the roll to be able to break the air flows created by the rotating at high-speed wheel and workpiece to provide the maximum possibility of getting the coolant into the contact zone with minimum losses of energy and coolant from splashing. In addition, the design must provide the optimum grinding wheel to cutting fluid speed ratio so that the temperature in the contact zone is minimized. The location of the coolant supply technique elements must consider the direction of the reverse airflow along the surface of the roll so that the penetrating ability of the coolant is not limited.

As previously mentioned, the air layer in the wedge-shaped zone is divided into two flows: a boundary layer along the wheel and a reverse air flow reflex along the roll surface, which significantly limits the cutting fluid penetration into the contact zone. When the speed of the wheel increases, the airflow velocity at the periphery of the wheel increases, and the airflow pressure in the wedge also increases. In addition, the reflex tends to become more intense, and the energy of the flow field rises. Thus, the main obstacle to cutting fluid entering the cutting zone when grinding rolls is, on the one

hand, the times longer length of the contact arc due to the large values of the wheel and workpiece diameters, and, on the other hand, the narrowing and lengthening of the zone located near the contact arc.

A survey of hydro- and aerodynamic conditions was carried out by several foreign scientists. Some performed studies in precision machining, others developed mathematical models for constructing temperature fields, and others determined the heat transfer coefficient in the contact zone. However, these studies were conducted on medium-sized machines with small dimensions of wheels and workpieces, and it is hardly applicable to large roll grinding machines. In addition, the relief of the circle's working surface needed to be considered. The maximum helpful flow rate through the contact is 25–50% of the flow rate from the cutting fluid nozzle and is controlled by changing (varying) several factors. This value is overestimated.

The results, which made it possible to determine the value of helpful flow rate for effective surface cooling when grinding rolling rolls, can be used in the:

– designing a rational design of cutting fluid supply technique to the cutting zone;
– specifying the specified initial data for mathematical modeling of thermal processes in the cutting zone.

5 Conclusions

Depending on many factors, cutting fluid penetration into the contact zone between the grinding wheel and the workpiece is a complex hydro-mechanical process. The penetration of the coolant occurs due to (among other things) the capillary effect using the finest network of capillaries formed in the contact zone between the grinding wheel and the workpiece.

Dynamic phenomena accompanying the cutting process and the vibrations of the wheel, workpiece, and other elements of the technological system created during this process significantly influence the ability to penetrate the cutting fluid.

The most significant influence on the penetrating ability to cut fluid into the contact zone of the wheel and the workpiece when grinding rolls of rolling mills is made by the grit size of the grinding wheel and grinding mode. Increasing the grit size from 16 to 40 can increase the "useful" cutting fluid consumption up to 9 times.

There is a 4–4.5 times increase in "useful" cutting fluid consumption at the transition from preliminary grinding to its final stages.

When the cutting fluid flow rate supplied to the cutting zone increases by 2 times, the useful flow rate increases insignificantly - 17–19%.

References

1. Gorbatyuk, S.M., Sedykh, L.V.: Improving the durability of rolling-mill rolls. Metallurgist **54**, 299–301 (2010). https://doi.org/10.1007/s11015-010-9297-y
2. Ilca, I., Miloştean, D., Balazsi, S.: Increasing of rolling mill rolls durability in operation. Part I. J. Eng. Sci. Innov. **6**(2), 147−158 (2021)
3. Kiss, I., Cioata, V.G., Alexa, V.: Increasing the rolling-mill rolls quality - in some multidisciplinary research. Acta Tech. Corvin. Bull. Eng. **3**(2), 31−36 (2010)

4. Dr. Karl Heinrich Schroeder. A basic understanding of the mechanics of rolling mill rolls. https://docslib.org/doc/4136203/a-basic-understanding-of-the-mechanics-of-rolling-mill-rolls, Accessed 21 Nov 2023
5. Practical Roll Techniques: Grinding & Balancing. https://www.valmet.com/globalassets/media/downloads/white-papers/roll-services/wpr_grindandbalance.pdf. Accessed 21 Nov 2023
6. Sun, W., Yuan, T., Wu, Z., et al.: Optimization model of the cold rolling roll grinding volume based on nonlinear fatigue accumulation regulation. J. Fail. Anal. Preven. **23**, 2131–2141 (2023). https://doi.org/10.1007/s11668-023-01767-9
7. Heinzel, C., Kirsch, B., Meyer, D., Webster, J.: Interactions of grinding tool and supplied fluid. CIRP Ann. **69**(2), 624–645 (2020). https://doi.org/10.1016/j.cirp.2020.05.001
8. Nguyen, T., Zhang, L.C.: The coolant penetration in grinding with segmented wheels—Part 1: mechanism and comparison with conventional wheels. Int. J. Mach. Tools Manuf. **45**(12–13), 1412–1420 (2005). https://doi.org/10.1016/j.ijmachtools.2005.01.035
9. Fesenko, A.V., Yevsyukova, F.M., Naboka, E.V., Kolisnyk, M.E., Goncharov, E.V.: Development of a tool module for external intermittent grinding with activation of a lubricating coolant (coolant). Energy Electron. Electromechan. **3–4**(157–158), 4–19 (2021). [in Ukrainian]
10. Dot, T., Snagioka, M., Kawagachi, T., Sakamoto, T.: Behaviour of grinding flied near cutting point. Sci. DND Ind. **58**(2), 55–59 (1984)
11. Jung, J., Ni, J.: Prediction and coolant pressure and volume blow rate in the gundrilling process. Trans. ASME J. Manuf. Sci. End. **125**(4), 696−702 (2003)
12. Fisher, R.S.: Grinding dry with water? Grind. Finish. **3** (1965)
13. Yakimov, A.A., Klimenko, N.N., Shikhareva, Bovnegra, L.V.: Ensuring surface quality during grinding of parts with composite coating. High Technol. Mech. Eng. **1**(28), 206−213 (2018). [in Ukrainian]
14. Stepanov, M.S.: Mathematical description of the area of the channel formed at the contact of a grinding wheel and a workpiece. Bull. Eng. Acad. Ukraine **3**, 199–203 (2001)
15. Stepanov, M.S., Permyakov, A.A.: Effect of cutting fluid nozzle orientation on its useful flow rate through the contact zone. Progress. Technol. Syst. Mech. Eng. Interd. Collect. Scientific Works **27**, 233−238 (2004)
16. Mazur, N.P., Vnukov, Y.N., Grabchenko, A.I., et al.: Fundamentals of the theory of cutting of materials. NTU "KHPI", Kharkov (2013). [in Ukrainian]
17. Chalyj, V., Moroz, S., Tkachuk, A., Zablotskyi, V., Trokhymchuk, I., Stelmakh, A.: Formation of bearings parts waviness in centerless mortise grinding on rigid supports. J. Eng. Sci. (Ukraine) **10**(1), A15–A21 (2023). https://doi.org/10.21272/jes.2023.10(1).a3

Enhancing Service Life and Durability of Machine Parts Through Surface Plastic Deformation

Anastasiia Symonova(✉), Volodymyr Drahobetskyi, and Viktoriia Kulynych

Kremenchuk Mykhailo Ostrohradskyi National University, 20, Pershotravneva Street, Kremenchuk 39600, Ukraine
NSymonova@gmail.com

Abstract. This scientific article explores innovative methods for enhancing the surface strength of machine components to extend service life and durability. The focus shifts to nanostructuring surface layers, introducing impact-friction hardening as a dual-action method without equipment dismantling. Experimental investigations on alloy 110G13L validate the method, showing a 30% increase in the reinforced layer's depth. The research demonstrates the technique's potential for preserving structural integrity, offering prolonged equipment lifespan, heightened operational efficiency, and a positive economic impact. Integrating mathematical models and experimental validations provides a comprehensive understanding of the outcomes of this surface plastic deformation technique. The study introduces impact-friction hardening with torsion, aiming to combine impact and friction elements for enhanced surface strength and operational efficiency in machine components. The literature review highlights the effectiveness of combining impact and friction, while the research methodology details the experimental approach. Results indicate a significant depth increase in the reinforced layer, showcasing the technique's promise for various sectors, including agriculture and mining. The study concludes with insights into future research directions, emphasizing the need for broader material exploration and parameter variation to understand the method's applicability comprehensively.

Keywords: Impact-Friction Hardening · Nanocrystalline Structure · Ultra-Fine-Grained Structure

1 Introduction

Recently, there has been a notable surge in interest within the scientific community regarding methods for enhancing the surface strength of machine and equipment components. The pursuit of surface strengthening methodologies is grounded in the potential to extend the service products' life and durability significantly. While achieving an ultra-fine-grained or nanocrystalline structure is acknowledged as an effective means to enhance strength and wear resistance in machine-building complex products, the challenges associated with this process, particularly in large-sized products, have prompted a shift in focus towards nanostructuring the parts surface layer.

© The Author(s), under exclusive license to Springer Nature Switzerland AG 2024
V. Ivanov et al. (Eds.): DSMIE 2024, LNME, pp. 341–351, 2024.
https://doi.org/10.1007/978-3-031-61797-3_29

Various methods for surface strengthening have been developed and broadly categorized into static and impact methods. Traditional impact strengthening techniques involve impact actions, such as the impact of balls or solid bodies [1], and friction actions, including the rotation of high-speed rollers [2] or other tools on material surfaces, as well as methods employing intense plastic deformation [3]. Notably, these methods typically require stationary equipment and machines to be decommissioned during the hardening process.

This article explores the theoretical foundations and implementation of a surface treatment method known as impact-friction hardening [4]. Unlike traditional methods that often necessitate stationary equipment and machine downtime during hardening, impact-friction hardening offers a promising alternative. This innovative approach to processing the surface layers of machine parts and technological equipment introduces a dual-action method that combines impact and friction elements. This method presents novel opportunities for reinforcing internal and external surfaces without equipment or mechanism dismantling.

When coupled with compact equipment, the proposed impact-friction hardening method not only preserves the structural integrity of machine parts but also averts premature deterioration – all achieved without the downtime associated with conventional hardening processes. This advancement addresses a pressing challenge in various sectors, including agriculture and mining, ensuring a tangible and positive economic impact through prolonged equipment lifespan and enhanced operational efficiency.

In addressing the challenges associated with traditional surface strengthening methodologies and their limitations, this work aims to introduce and explore the innovative impact-friction hardening with torsion as a promising technique, offering enhanced surface strength and operational efficiency in machine components.

2 Literature Review

Many methods, encompassing various modifications and combinations, exist for surface strengthening to achieve an ultra-fine-grained or nanocrystalline layer. These methods were proposed to be categorized based on the external forces or physical influences they employ [5].

The study outlined in reference [6] compares the outcomes of impact hardening and impact hardening combined with torsion. The research conducted on 2C22 steel using impact energy of 3.5 J indicates that the incorporation of torsion yields superior results. This combined approach enables the attainment of a microhardness of 400 MPa at a depth of 300 μm, accompanied by the creation of a fibrous structure with a fiber thickness ranging from 0.13 to 0.23 μm.

In a separate investigation, frictional treatment involving a hemispherical indenter crafted from synthetic diamond demonstrated significant strain hardening of austenitic steel AISI 321, resulting in a microhardness of 710 HV. The total depth of the hardened layer extended to approximately 450 μm, showcasing the formation of nanocrystalline and fragmented ultra-fined-grained structures [7]. Further exploration into the frictional processing of cast iron GG20, utilizing a tool with threaded multidirectional grooves on its working surface, exhibited a remarkable strength increase of over 8 times [8].

The researchers in reference [9] proposed a method known as impact-friction processing, employing a flexible tool. This innovative technique yielded a robust nanostructured surface layer with fragment sizes measuring up to 0.13 μm. Additionally, the authors emphasize the versatility of this method, suggesting its applicability to coating functions.

As elucidated in the findings of reference [10], the efficacy of friction hardening is intricately influenced by several factors, including the hardening conditions, part characteristics, and the attributes of the hardening tool disc. The dynamic interplay between these elements gives rise to a highly concentrated flow of energy in the contact zone generated by the rapid rotation of the tool disc against the processed part. The intensity of this energy flow is contingent upon the properties of the hardening tool disc and the specific hardening conditions. Notably, the material composition, shape, dimensions, and physical-mechanical properties of the tool disc significantly impact the formation of thermal energy flow within the contact zone. An augmented coefficient of friction correlates with increased heat release in the contact zone. The frictional interaction induces simultaneous high-speed shear deformation in the metal's surface layers, resulting in additional heating. Consequently, the contact zone experiences elevated temperatures and stresses during friction hardening.

During friction hardening, the technological environment entering the contact zone undergoes decomposition into ions of its constituent chemical elements. This process triggers mass transfer within the metal's surface layers. The conditions of friction hardening are further influenced by the chemical composition, surface activity of the medium, and its functional properties. Technological media containing polymers, chlorine, and other surface-active components can reduce the surface energy of the metal, thereby facilitating surface deformation processes. Active hydrogen plays a significant role in plasticizing the surface layer, enhancing phase and structural transformations during surface hardening.

An extensive literature review underscores a pronounced interest in surface-strengthening methodologies, particularly those leading to the creation of ultra-fined-grained or nanostructures. Researchers have focused on novel techniques, with friction treatment demonstrating its efficacy in forming a hardened layer. Combining impact with friction has been revealed to deepen the hardened layer, and investigations indicate that torsion intensifies surface hardening processes. In light of these findings, this work will comprehensively explore a combined method for surface layer strengthening, encompassing impact friction and torsion.

3 Research Methodology

Effectively, grain refinement is achieved through intense plastic deformation, particularly during twisting. This involves non-monotonic deformation, creating a pronounced curvature in the deformation trajectory. The substantial contribution to the formation of nanocrystalline structures is facilitated by altering the direction of primary deformations, a phenomenon more efficiently achieved through both torsion and impact-wave loading. These transformative processes are effectively realized under the conditions of impact-friction hardening with torsion, as depicted in Fig. 1.

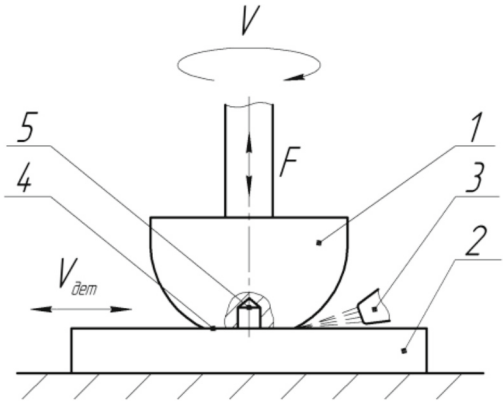

Fig. 1. The method of impact-friction hardening with torsion.

The execution of this method involves the rotation of the tool disc 1, pressed against the processed surface of the part 2. The part 2 moves at a low speed during processing. The contact between the tool and the part results in the surface layer of part 2 being heated to a temperature surpassing phase transformations (Ac3). Ther-mal TS 3 is introduced into the treatment zone, facilitating heat removal from the treated surface. Rapid cooling ensues in the surface layer, leading to the formation of a strengthened layer. To augment the thickness of the hardened layer and enhance the machined surface's quality, a specialized tool 1 with a flat end 4 and a hole 5 is employed.

In the "tool-part" contact zone, the intensity of shear deformation in the surface layer of the metal increases due to additional impact loads F, generated, for example, by a crank crawler mechanism, enabling supplementary slander. At the opening 5, longitudinal impact waves converge, significantly amplifying the depth of the material being strengthened. Previous research in this direction was conducted based on JSC "Motor Sich" (Zaporizhia) for strengthening matrices for stamping parts of a complex spatial shape from blanks with a closed surface. Losses in the strength of the surface of the matrix and its dimensions were compensated by impact-friction additional strengthening in the breaks between shifts or, more often, after 1.5–2 h of the production process. The results are presented in [11].

To substantiate the efficacy of incorporating additional torsion, experimental investigations were conducted on impact-friction strengthening, both with and without torsion, under the following strengthening parameters: velocity (v) = 5 m/min and penetration depth (d) = 0.1 mm. The chosen material for this study was alloy 110G13L.

Microhardness measurements were performed using a CarlZeiss, Jena, Mikrohaterprüfer Hanemann unit equipped with a Vickers pyramid. A consistent load of 0.5 N was applied to ascertain microhardness, and the measurements were conducted 9 to 10 times to ensure accuracy. The relative measurement error did not exceed 10%. The oblique grinding method assesses microhardness variation with the altered layer's depth.

4 Results and Discussion

Examining the impact of a rotating tool on the machined surface was posited the following assumptions:

1. Dynamic sedimentation of the surface layer occurs with the friction of the percussion instrument during its rotation.
2. Instantaneous energy release in the contact zone of the rotating striker was assumed.
3. The yield stress σ_s^{din} is connected with the intensity of deformation rates $\dot{e}_i$ as expressed by $\sigma_s^{din} = G_{S_0}(T)\dot{e}_i^n$, where $G_{S_0}(T)$ and n are constants.

The deformation of the surface layer is illustrated in Fig. 2.

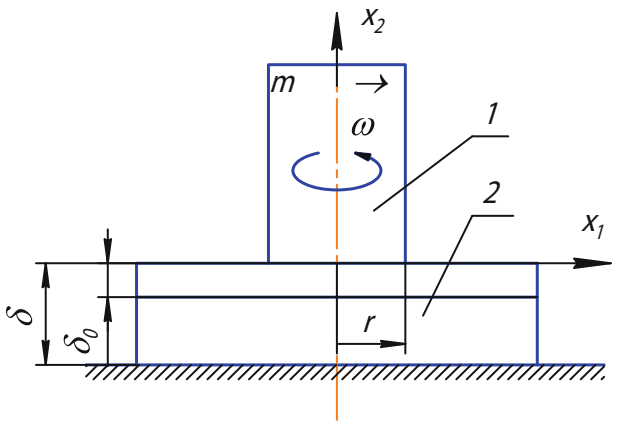

Fig. 2. Dynamic compression of the surface layer with a rotating impact tool: 1 – rotating tool; 2 – the surface layer.

A hard, rotating impact tool of mass m deposits a surface layer with a thickness equal to δ_0 to the current δ. The original speed v_0 of the striker tool is reduced to v.

Equation of tool motion:

$$m\frac{d\dot{x}_{ij}}{dt} = F_0 \cdot G_{S_0} \cdot \dot{\varepsilon}_u^n \cdot \delta_0 \cdot \delta^{-1} \tag{1}$$

or:

$$m\left(\frac{d\dot{x}_{11}}{dt} + \dot{x}_{12}\frac{d\dot{x}_{11}}{dx} + \dot{x}_{12}\frac{d\dot{x}_{12}}{dy}\right) = F_0\left[\frac{2}{3}\left(\delta_{11}^2 - \tau_s^2\right)\cdot\left(\dot{\varepsilon}_{11}^2 - \dot{\varepsilon}_{12}^2\right)^n\right]^{\frac{1}{2}} \cdot \delta_0 \cdot \delta^{-1} \tag{2}$$

where m – the mass of the percussion instrument;$\dot{x}_{11}, \dot{x}_{12}$ – speed components; t – time;F_0 – the area of the percussion instrument;;$\delta_{11}, \dot{\varepsilon}_{11}, \dot{\varepsilon}_{12}$ – stress components and strain intensity; τ_s – yield strength in pure shear.

The solution combines the solutions derived from two scenarios: the impact of an excellent tool with a front flat section onto a plane of plastic material and the interaction problem of a rotating cylinder with a viscous material. We assume that post-impact, the

reinforcing material undergoes a drawing into a wave motion. Subsequently, a flat impact wave initiates propagation from the point of impact, placing the reinforcing material into a state of one-dimensional motion, which is mathematically described by the equation:

$$\left(\rho\frac{d\dot{x}_1}{dt}+\dot{x}_1\frac{d\dot{x}_1}{dx_1}\right)=-\frac{dp}{dx_1}, \tag{3}$$

where x_1 – spatial coordinate with the origin at the point of intersection of the axis of the punch with the processed surface; p, ρ, $\dot{x}_1$ – pressure, density, and speed of particles.

Taking into account the condition of incompressibility, it follows that $\frac{d\dot{x}_1}{dx_1}=0$, then

$$\dot{x}_1(t)=\dot{\delta}, a\cdot\frac{d\dot{x}_1}{dt}=\ddot{\delta}. \tag{4}$$

Equation (3) takes the form:

$$\rho\ddot{\delta}=-\frac{dp}{dt}. \tag{5}$$

On the front section of the tool, was get:

$$p=-\rho\delta\delta\ddot{+}c. \tag{6}$$

Using the ratio, for the impact wave motion parameters:

$$\overline{p}=\frac{\rho_0\rho\dot{\delta}^2}{\rho-\rho_0}. \tag{7}$$

The solution of the equation is reduced to the form:

$$p=\frac{\rho_0\rho}{\rho-\rho_0}(\dot{\delta}^2+\delta\ddot{\delta}). \tag{8}$$

Given that the mass of the striker is equal to the equation of motion, the expression takes the form:

$$m\ddot{\delta}=-\frac{\pi r^2\rho_0\rho}{\rho-\rho_0}(\dot{\delta}^2+\delta\ddot{\delta}). \tag{9}$$

Integrating this equation was getting expressions:

$$the\dot{\delta}=\frac{mv_0}{m+\lambda\delta}, \delta=-\frac{m}{\lambda}+\sqrt{\frac{m^2}{\lambda^2}+\frac{2mv_0t}{\lambda}}, \tag{10}$$

where: $\lambda=\frac{\rho_0\rho\pi r^2}{\rho-\rho_0}$.

Taking into account the fact that the rate of deformation $\dot{\varepsilon}=\frac{\dot{\delta}}{\delta}$, using the ratio, was determined the stresses acting in the surface layer of the reinforcing part:

$$\sigma=\sigma_s\left(\frac{\dot{\delta}}{\delta}\right)^n. \tag{11}$$

To determine the moment of friction forces, the equation for the angular velocity of the surface layer. The material in the contact zone is heated and can be considered viscous. The angular velocity of the material flow was obtained:

$$\frac{dw}{dt} = \eta \frac{d^2w}{dx_1^2}, \tag{12}$$

where ω – angular speed of rotation of the striker; η – viscosity of the material.

The solution of this equation has the form:

$$w = -y_0 exp\left(-\frac{x_1}{\delta}\right). \tag{13}$$

The moment of friction forces is equal to:

$$M = \int_0^r 2\pi r^2 \eta \frac{d\dot{x}_1}{dx_1} dr = y_0 \pi \sqrt{\rho\eta} \cdot R^4, \tag{14}$$

where $\dot{x} = \dot{x}_2 = rw$.

If it is necessary to consider temperature factors, the refined theory of plastic flow or the complicated model of G. Backhaus [12] considers the Bauschinger effect [13]. At the same:

$$dF_1 = \frac{\partial \sigma_i}{\partial T} dT + \frac{\partial \sigma_i}{\partial \varepsilon_i} d\varepsilon + \frac{\partial \sigma_i}{\partial \dot{\varepsilon}_i} d\dot{\varepsilon} + \frac{\partial \sigma_i}{\partial t} dt + \frac{\partial \mu_k}{\partial \varepsilon_i} d\varepsilon + \frac{\partial \mu_k}{\partial t} dt. \tag{15}$$

where σ_i – stress intensity; $\varepsilon_i, \dot{\varepsilon}_i$ – strain intensity and strain rates; T – temperature; t – time; μ_k – parameters characterizing the internal structure of the material, lower index – parameter number.

Establishing deformations that align with the optimal material structure based on operational characteristics and are equivalent to the uniform limit is achievable by employing the Gilman-Johnston formula for the rate of plastic deformations [14].

$$\varepsilon_i = \frac{4}{3} bC_0 \left(n_0 + \frac{3}{4} m\varepsilon_i\right) exp\left[-2\left(D + \frac{3}{4} H \frac{\varepsilon_i}{\sigma_i}\right)\right]. \tag{16}$$

where n_0 – initial density; b – Burgers vector; m – dislocation multiplication factor; H – constant strengthening; C_0 – speed of sound in the transverse direction; D – empirical constant.

At the same time, it was taken into account that the propagation of dislocations is possible when $\tau_{max} > \tau_{kr}$

$$\tau_{kr} = \frac{Gb}{l_d}. \tag{17}$$

In addition, when $e \approx 0.6 \ldots 0.7$, then a high density of dislocations $\approx (2 \ldots 3) \cdot 10^{15}$, m^2 is achieved. It leads to the formation of minimum sizes. When $e \approx 3 \ldots 4$ then the content of such fragments in metals becomes predominant in comparison with larger areas of disorientation [15].

When twisting with draft and impact load, the degree of deformation is determined as follows:

$$thee = \frac{1}{\delta_0}\left\{\int\left(\dot{x}_1^2 + r^2w^2/3\right)dt + \int \dot{x}_1 dt\right\}, \tag{18}$$

where w – angular velocity.

The work of frictional forces is converted into heat. The temperature in the surface layer can be determined using the solution of the thermal conductivity equation for an instantaneous source:

$$T(t) = T_0 + \frac{Q}{2c\rho\sqrt{\pi a^2 t}}, \tag{19}$$

where $T(t)$ – the temperature in the surface layer in the plane of action of the instantaneous source; T_0 – initial temperature of the reinforcing surface layer; Q – the amount of heat released at time $t = 0$; c – specific heat capacity of the material; ρ – material density; a – the thermal conductivity coefficient.

The emergence of curvature of the deformation trajectory is because, under conditions of impact loading, the Cauchy formula has the form [16]:

$$p_{nk} = (\sigma_{ik} \pm \rho v_{ii} c)n_i, \tag{20}$$

where $n, k = 1,2, 3$; $v_{ii} = \frac{dx_{ii}}{dt}$.

The matrix $|\sigma_{ik} + \rho v_{ii} c|$ is a stress tensor for T_σ.

To bring it to a diagonal form, or as a result of solving the problem at a conditional extremum, it is necessary to solve the characteristic equation:

$$\lambda^3 - I_1^d\lambda^2 + I_2^d\lambda^3 - I_3^d\lambda^4 = 0, \tag{21}$$

where λ– Lagrange multiplier, I_1^d, I_2^d, I_3^d – invariants of the stress tensor.

The coefficients of the characteristic equation forming a system of invariants differ from and are equal to the conditions of static loading:

$$I_1^d = \sigma_{11} + \sigma_{22} + \sigma_{33} \pm \rho c(V_{11} + V_{22} + V_{33})$$

$$\begin{aligned} I_2^d = {} & \sigma_{11}\sigma_{22} + \sigma_{22}\sigma_{33} + \sigma_{33}\sigma_{11} + \rho c(\sigma_{11}V_{22} + \sigma_{22}V_{33} + \sigma_{33}V_{11} + \sigma_{22}V_{11} \\ & + \sigma_{33}V_{22} + \sigma_{11}V_{33}) + \rho^2 c^2(V_{11}V_{22} + V_{22}V_{33} + V_{33}V_{11}), \end{aligned} \tag{22}$$

$$\begin{aligned} I_3^d = {} & \sigma_{11}\sigma_{22}\sigma_{33} + \rho c(\sigma_{11}\sigma_{22}V_{33} + \sigma_{22}\sigma_{33}V_{11} + \sigma_{11}\sigma_{33}V_{22}) + \rho^2 c^2(\sigma_{11}V_{22}V_{33} \\ & + \sigma_{22}V_{11}V_{33} + \sigma_{33}V_{11}V_{22}) + \rho^3 c^3 V_{11}V_{22}V_{33} \end{aligned}$$

where $\sigma_{11}, \sigma_{22}, \sigma_{33}$ – main stresses; $V_{11}V_{22}V_{33}$ – speed of movement in the direction of the main axes of the material.

The orientation and magnitude of the guiding cosines are contingent upon the stress tensor invariants, leading to a modification in the curvature of the deformation trajectory.

This study introduces mathematical models to calculate the strengthening force's components. Specifically, the focus is on two key forces: *Ph*, generated through the tool's contact pressure with the machined surface, and *Pz*, the circumferential force arising from the rotation and pressing of the tool against the machined surface. These component forces are mathematically modeled using a design matrix of type 2^3. The resulting mathematical models for determining these forces are expressed in the form of Eqs. (23)–(24):

$$P_{x_2} = 150 \cdot \dot{x}^{0.45} \cdot B^{0.87} \cdot t^{0.8+0.1 \cdot \ln(B)} \tag{23}$$

$$P_{x_1} = 72 \cdot \dot{x}^{0.29} \cdot B^{0.45} \cdot t^{0.7+0.05 \cdot \ln(B)} \tag{24}$$

where $\dot{x}$ – speed of movement of the machine table, m/min; B – width of reinforcement, mm; t – vertical feed, mm.

To determine the thickness of the reinforced layer, a mathematical model was built using a non-composite plan of the 2nd order:

$$\delta_0 = 303 \cdot \dot{x}^{2.15+0.7 \cdot \ln(x)} \cdot B^{6.01-1.9 \cdot \ln(B)} \cdot t^{0.75} \tag{25}$$

The conducted experimental studies for 110G13L alloy yielded the results shown in Fig. 3.

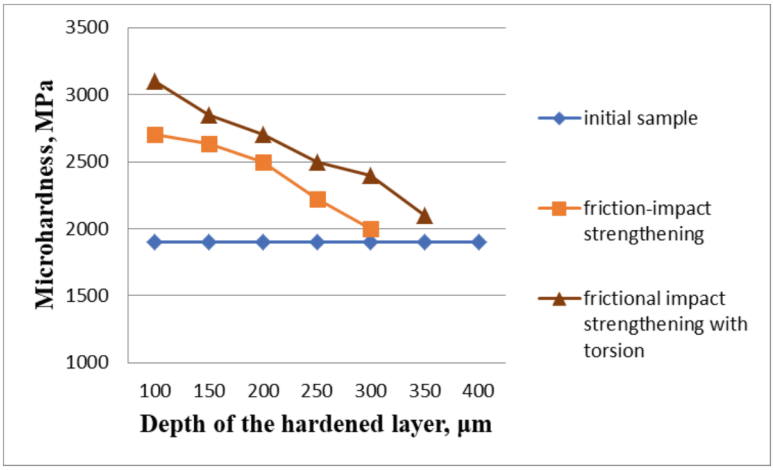

Fig. 3. Comparison of the hardened layer depth obtained by friction hardening without torsion and with additional torsion.

This study explicitly investigates bucket teeth reinforcement on quarry excavators, namely the EKG-10, EKG-8I, and XS 342 RC excavator models.

The study outlined in [6] investigated torsion's impact on impact hardening outcomes. The hypothesis was that the incorporation of torsion could intensify surface hardening processes. The current study aligns with this hypothesis, showcasing a 30%

increase in the depth of the reinforced layer with the introduction of torsion in the impact-friction hardening process.

The method proposed in this study shares similarities with the ultrasonic impact-frictional treatment method introduced by researchers in [17]. The flexibility and versatility of the impact-friction processing method were emphasized, aligning with the current study's objective of providing a dual-action approach without the need for equipment dismantling.

The upcoming research phase entails experimental studies to assess the enhanced operational performance of parts treated through impact-friction hardening with torsion under actual working conditions. The objective is to compare the obtained data with standard conditions, evaluate how the improved surfaces or parts fare in real-world scenarios, and determine their longevity compared to conventional counterparts.

5 Conclusions

The research demonstrates that impact-friction hardening, particularly when coupled with additional torsion, significantly enhances the depth of the reinforced layer by up to 30%. The results obtained in this study are specifically applicable to the 110G13L alloy. The reliability of these findings is supported by experimental validation, where the experimental results demonstrate notable improvements over traditional friction hardening without torsion.

However, it is imperative to acknowledge the limitations inherent in the scope of this study. The focus on a specific alloy, 110G13L, necessitates caution in generalizing the results to other materials. Further research encompassing a broader range of alloys is essential to understand the technique's applicability comprehensively.

Future developments in this line of research should explore the extension of the impact-friction hardening with the torsion technique to diverse materials and geometries. Additionally, investigating the influence of varying hardening parameters and environmental conditions will contribute to refining the method's versatility and reliability.

Acknowledgment. The research was partially supported by the International Association for Technological Development and Innovations (IATDI).

References

1. Lei, Y., Wang, Z., Qi, H.: Strengthening performance optimization of single ball impact treatment by evaluating residual stress. Materials **15**, 3719 (2022). https://doi.org/10.3390/ma15103719
2. Li, G., Xiao, X., Zhang, W., Song, D.: Study on surface fretting friction properties of heat-treated HIP Ti-6Al-4 V alloy after heating-assisted ultrasonic surface strengthening. J. Mater. Process. Technol. **316**, 117942 (2023). https://doi.org/10.1016/j.jmatprotec.2023.117942
3. Symonova, A., Havin, V., Savelov, D.: Choice of the optimal parameters of the ultra-fine grained copper machining. In: Ivanov, V., et al. (eds.) Advances in Design, Simulation and Manufacturing. DSMIE 2019. LNME, pp. 177–185. Springer, Cham (2019). https://doi.org/10.1007/978-3-319-93587-4_19

4. Shahriyari, F., Taghiabadi, R., Razaghian, A., Mahmoudi, M.: Effect of friction hardening on the surface mechanical properties and tribological behavior of biocompatible Ti-6Al-4V alloy. J. Manuf. Processes **31**, 776−786 (2018). https://doi.org/10.1016/j.jmapro.2017.12.016
5. Morshed-Behbahani, K., Zakerin, N.: A review on the role of surface nanocrystallization in corrosion of stainless steel. J. Market. Res. **19**, 1120–1147 (2022). https://doi.org/10.1016/j.jmrt.2022.05.094
6. Katiyar, S., Dixit, P.M.: Simulation of softening in high pressure torsion process using continuum damage mechanics model. Proc. Inst. Mech. Eng. Part C: J. Mech. Eng. Sci. **236**(1), 424−439 (2022). https://doi.org/10.1177/09544062211033883
7. Makarov, A.V., et al.: Effect of hardening friction treatment with hard-alloy indenter on microstructure, mechanical properties, and deformation and fracture features of constructional steel under static and cyclic tension. Surf. Coat. Technol. **205**(3), 841–852 (2010). https://doi.org/10.1016/j.surfcoat.2010.08.025
8. Gurey, V., Maruschak, P., Hurey, I., Dzyura, V., Hurey, T., Wojtowicz, W.: Dynamic analysis of the thermo-deformation treatment process of flat surfaces of machine parts. J. Manuf. Mater. Process **7**, 101 (2023). https://doi.org/10.3390/jmmp7030101
9. Li, R.-L., Li, M.-Z., Qiu, N.-J., Cai, Z.-Y.: Surface flexible rolling for three-dimensional sheet metal parts. J. Mater. Process. Technol. **214**, 2 (2014). https://doi.org/10.1016/j.jmatprotec.2013.09.008
10. Hurey, I., Gurey, V., Hurey, T., Bartoszuk, M., Wojtowicz, W.: The wear resistance during oscillating friction of steel specimens with strengthened nanocrystalline layers. In: Tonkonogyi, V., Ivanov, V., Trojanowska, J., Oborskyi, G., Pavlenko, I. (eds.) Advanced Manufacturing Processes V. InterPartner 2023. LNME, pp. 265–275. Springer, Cham (2023). https://doi.org/10.1007/978-3-031-42778-7_24
11. Drahobetsky, V.V., et al.: New solution for plastic deformation process intensification. Metallurgist 65, 1108–1116 (2022). https://doi.org/10.1007/s11015-022-01253-x
12. Backhaus, G.: Theory versus experiment. Rigid Body Mech. **6**, 12–129 (1967)
13. Soboyejo, W.O.: Mechanical Properties of Engineered Materials. Marcel Dekker, New York (2003)
14. Bergström, Y.: A dislocation model for the stress-strain behaviour of polycrystalline α-Fe with special emphasis on the variation of the densities of mobile and immobile dislocations. Mater. Sci. Eng. **5**(4), 193–200 (1970). https://doi.org/10.1016/0025-5416(70)90081-9
15. Utyashev, F.Z., Raab, G.I.: Effect of the deformation zone on the structure refinement in metals. **104**, 582−594 (2007). https://doi.org/10.1134/S0031918X0712006X
16. Cremer, J.T.: Neutron scatter physics and differential cross sections. In: Advances in Imaging and Electron Physics, Chapter 3, vol. 173, pp. 167−274. Elsevier (2012). https://doi.org/10.1016/B978-0-12-396969-9.00003-3
17. Makarov, A.V., Lezhnin, N.V., Chalina, M.A., Volkova, E.G.: Surface hardening of austenitic stainless steel via ultrasonic impact-frictional treatment. AIP Conf. Proc. **2509**, 020127 (2022). https://doi.org/10.1063/5.0085657

Statistical Comparison of Manual and Automatic Sampling at Enterprises

Jozef Trojan[1(✉)] and Milan Fil'o[2]

[1] Technical University of Kosice, 9, Park Komenskeho, 042 00 Kosice, Slovak Republic
jozef.trojan@tuke.sk
[2] Ecoinvestment, 1037/3, Republic Square, 110 00 Praha 1, Czech Republic

Abstract. The presented article deals with a detailed analysis of the state of the issue. It is about the characteristics of the organization and the description of its current state, as well as the description, procedure, and comparison of the sampling process in organizations. Next, the specific problems of the process are defined, and in connection with them, a new sampling system is designed, which is fully automated. The article is more specifically focused on statistically significant differences between manual and automatic sampling of business commodities such as coal ore, concentrate, and pellets, which are then submitted for comparison. Sample tests are necessary to make a comparison. The test results are subsequently recorded in the sample test reports. Both manual and automated samples are analyzed using statistical tests to determine if there are statistically significant differences between the data. Such tests were also done in organizations.

Keywords: Industrial Growth · Automatic Sampling · Manual Sampling · Statistical Characteristics

1 Introduction

The organization is dedicated to sampling coal ore, concentrate, and metallurgical coke transported by belt transport P1 and P2 and sampling pellets transported by belt transport P17. Conveyor belts along which the material is transported.

The raw materials that arrive on these belts are brought to the organization by rail, and after the entrance checks, they are transported by trucks to a place called the ore field, where they are piled into large piles. The picker and stacker machines take care of this establishment, depending on whether an existing pile or a completely new one is being removed from the pile. Each pile has its marking, numerically and with the name of where it comes from. Raw materials are later removed from the piles according to precise calculations calculated by process engineers based on the requirements of the management or the operation itself. All the raw materials that make up not only but significantly the charge for blast furnaces can be found at the ore site. The mine must be regularly inspected, and the piles must be recalculated to match the quantities of raw materials delivered [1–5]. The ore field can be seen in Fig. 1.

© The Author(s), under exclusive license to Springer Nature Switzerland AG 2024
V. Ivanov et al. (Eds.): DSMIE 2024, LNME, pp. 352–361, 2024.
https://doi.org/10.1007/978-3-031-61797-3_30

Fig. 1. Ore field.

2 Literature Review

2.1 Manual Sampling

Every tool used must correspond to the nature of the work and must be in good condition, i.e., it must not be damaged. Manual sampling is performed using a sampling shovel. The sample is then placed in a bucket and later transported. The sample is taken for further processing or directly to the laboratory, where the sample analysis is performed.

The size of the blade is determined according to the belt from which the sample is taken. The longer one is used for the P1 belt, and the shorter one for the P2 belt. Subsequently, the sample is taken by inserting the paddle into the material flow, as shown in Fig. 2.

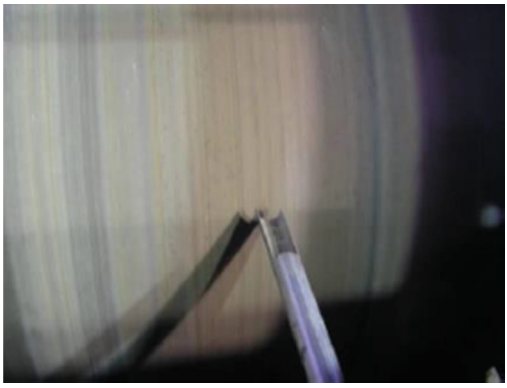

Fig. 2. Inserted sampling scoop into the material flow.

The material is poured into the prepared bucket, and the procedure is repeated until the sampling is completed. The bucket with the sample is taken to the Quality Control laboratory, where it undergoes further processing. Other processing that is carried out in

such a laboratory includes, for example, grinding, crushing, sieving, sorting, strength or hardness tests, abrasion resistance tests, drying or, on the contrary, wetting, and last but not least, various weighing's, such as weighing before processing and after processing or in the state dry and wet. The sample processed in this way becomes the basis of the analysis. An analysis is carried out, especially a chemical one, in which the presence of individual elements and their amount in a given sample is determined. Based on these data, samples are later tested or, for example, analyzed by statistical tests [6–10].

2.2 Automatic Sampling

Automatic sampling is carried out with the help of hammer sampling, also called rotary hammer sampling, and can be seen in Fig. 3.

Fig. 3. Rotary hammer removal.

With its arrangement and design, the automatic sampling line guarantees the regular collection of primary sub-samples of the sampled material to create a rough sample that represents the shipments per the relevant standards (ISO 3082). The sampler meets the conditions for representative sampling and storage of sub-samples in such a way as to limit the possibility of accidental errors caused by the operator. Procuring sub-samples, including further processing, is automatically done without operator intervention. The installed sampler with the completed certificate becomes a benchmark for quality control of the supplied material in customer-supplier relations. It meets the requirements set out in ISO 3082 (iron ore).

Primary sub-samples from belt transport are collected by hammer sampling directly from the moving belt. The sampling vessel cuts through the entire fuel flow in a circular path and throws partial samples into its dump. An electric gearbox ensures that the collection container is driven. It is started according to the set time interval of collection, provided that the belt with the sampled material is running and the minimum height of the layer of this material is determined on the belt. The rest position of the collection container is before the top dead center (outside the material flow). It is set in motion by a signal from the automatic control system (in an imposed time cycle) or manually

with a button. After running the track, i.e., j. when the partial sample is poured into the hopper, it stops at the signal from the limit switch (induction sensor). If it is not turned on, the control system must ensure the shutdown after a specific set time (3 s). In this case, a malfunction must be signaled with the stoppage of the entire previous belt transport cascade. Otherwise, there would be a risk of a dangerous collapse of the sampled material on the belt at the point of hammer removal. Monitoring the position of the collection container is doubled. The second inductive sensor is connected to a voltage independent of the sampler voltage. The partial sample falls from the sampling hopper into the container of the skip conveyor, which transports it to the plate divider, where it is divided. The divided partial sample then falls through the sample pipe into the collection container of the homogenization quarter, where it is stored. The unseparated residue from the divider (the so-called waste) is lifted through the waste pipe directly onto the existing conveyor belt. After completing the sampling of the expected shipment, the sampler operator starts the mixing device of the homogenizing quarter in manual mode and immediately opens the rotary knife cap manually. After opening the cap, the collected sample in the container falls directly into the prepared sample containers. He then adjusts the required sample weight for the laboratory (to a minimum of 10 kg) and manually dumps the remaining sample (the so-called waste) onto the existing conveyor belt. During this activity, the sampling of the new shipment is blocked [11–15].

3 Research Methodology

3.1 Comparison of Manual and Automatic Sampling in Terms of Statistically Significant Differences

To correctly perform statistical tests, it is necessary to know the essential statistical characteristics - average and standard deviation, as shown in Table 1. They are determined based on data from test reports.

Table 1. Basic statistical characteristics.

T-test						
Elements and compounds	Manual sampling			Automatic sampling		
	N	Mean	StDev	N	Mean	StDev
Fe	10	54.75	1.85	10	55.28	1.56
SiO_2	10	15.27	2.12	10	14.36	2.43
S	10	0.02	0.005	10	0.02	0.03
Humidity	10	4.72	0.13	10	5.07	0.38

The data from the subscriptions were entered into the protocols. Ten withdrawals were made. The commodities that were taken were coal ore, concentrate, and pellets. Collections were both manual and automatic, and the compared elements and compounds

are total iron Fe, silicon dioxide SiO2, sulfur S, and moisture. For individual data, it is necessary to calculate the variance and mean values. In this case, the mean value means the mean (because it is usually distributed data), and the variance means the standard deviation. Based on the calculated data, whether the data from the sample test reports are statistically significantly different is determined. If statistically significant differences are found, manual and automatic sampling work differently, and the samples taken will have different results after laboratory analysis.

3.2 T-Test

One of the statistical tests that are performed is the T-test, for the execution of which it is necessary to establish hypotheses.

Hypotheses established in the organization were:

H0- Null hypothesis: There is no difference between the mean values.

H1- Alternative hypothesis: There is a difference between the mean values.

Evaluation of Hypotheses

For elements and compounds, we accept the H0 hypothesis and reject the H1 hypothesis.

In the case of humidity, on the other hand, we reject hypothesis H0 and accept hypothesis H1.

Considering the results of the comparison of all parameters, we can conclude that the average values are almost the same regardless of the sampling method, whether it is manual or automatic sampling.

A graphic example of such a comparison is the so-called boxplots. Boxplots that show the distribution of data and its current location. They indicate the percentage content of the observed element/compound in the samples. Based on the graph's appearance, we can determine the dispersion, standard deviation, and their sizes and locations. We can understand where 50% of our data resides using this view.

Boxplot comparisons of two elements/compounds are shown in Figs. 4 and 5.

3.3 Bonett and Levenes Test/Method

As with the T-test, these tests must state the hypotheses:

H0- Null hypothesis: There is no difference between the standard deviations.

H1- Alternative hypothesis: There is a difference between the standard deviations.

As is already evident based on the hypotheses, a comparison of standard deviations is used to assess whether they are statistically different.

The p values after performing both tests are shown in Table 2.

Evaluation of Hypotheses

The evaluation of the hypotheses is the same as that of the previous test.

For elements and compounds, we accept the H0 hypothesis and reject the H1 hypothesis.

In the case of humidity, on the other hand, we reject hypothesis H0 and accept hypothesis H1.

A graphical comparison of the results of the two elements/compounds of Bonett's and Levene's tests can be seen in the following Figs. 6 and 7.

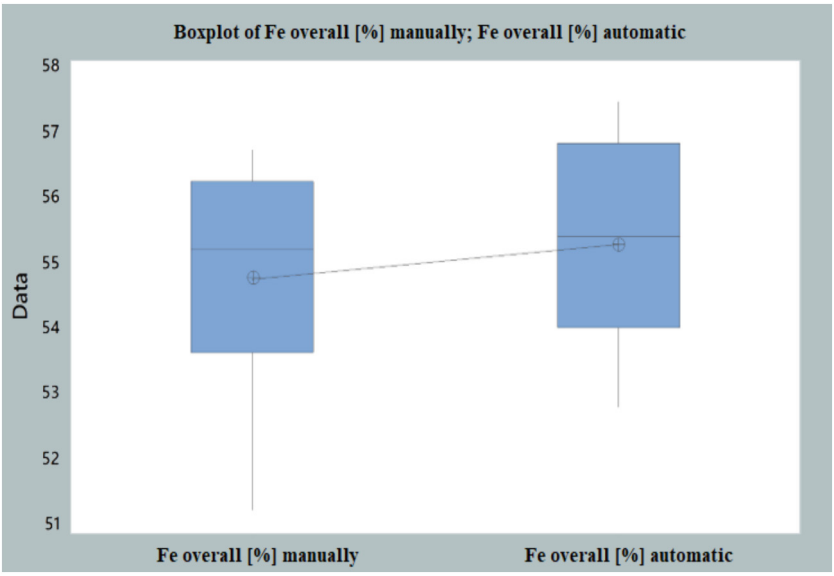

Fig. 4. Boxplot for percent Fe content.

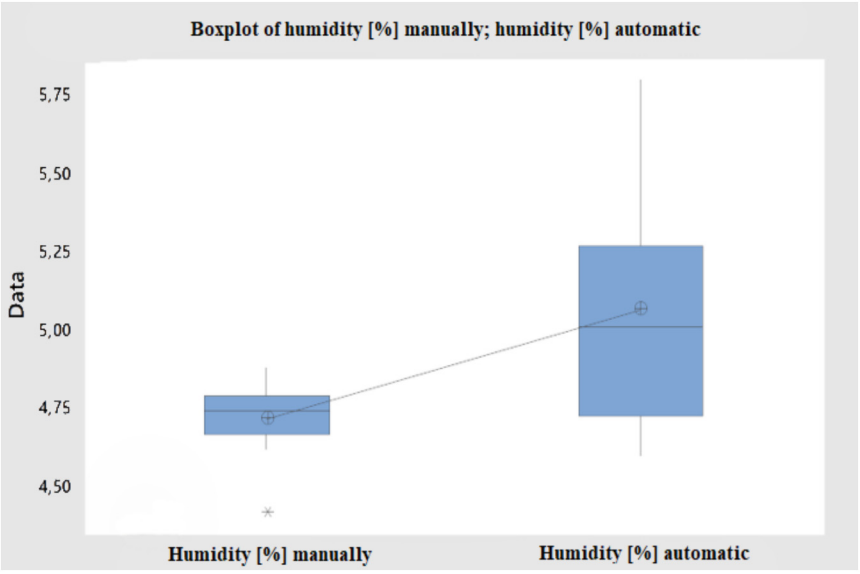

Fig. 5. Boxplot for percent moisture content.

Table 2. P-values after performing the tests.

P-value	Fe	SiO_2	S	Humidity
Bonett's test	0.618	0.648	0.538	0.035
Levene's test	0.606	0.852	0.731	0.032

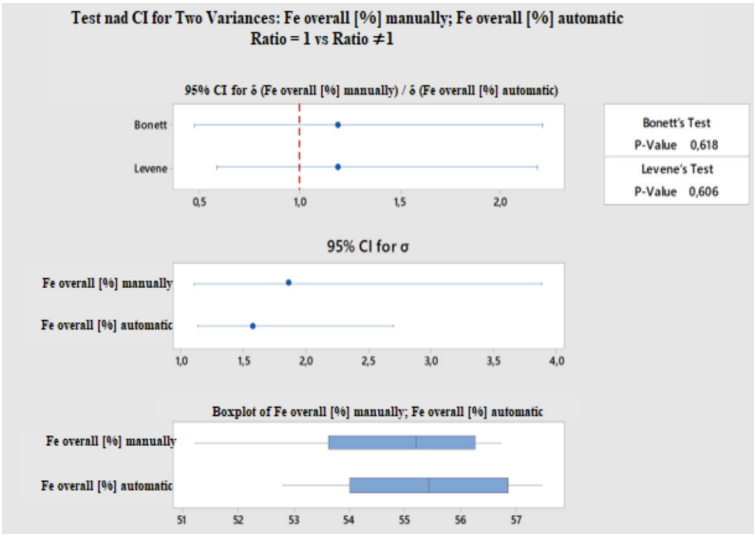

Fig. 6. Test for element Fe.

4 Results and Discussion

4.1 T-Test Result

The result of such a test, in which the essence is to monitor the average percentage content of elements in the samples, is to determine whether there is a statistically significant difference between the samples. If not, it is possible to claim that the samples are identical. If so, the samples can be said to be different.

We can work towards such a finding with the help of the p-value. The value describes the probability that we will get the value of the test statistic. Still, this value must be greater or equal to the value obtained, assuming that the null hypothesis is true. [3] (The p-value is a priori before the data is obtained from the experiment).

By p-value, we mean the lowest level of significance at which it is possible to reject the null hypothesis. Hypothesis H0 is rejected at the significance level α if the p-value is less than or equal to α ($\alpha = 0.05$). It follows that if the p-value is less than 0.05, we can say there is a statistically significant difference between the percentage values of the quality elements in the samples taken manually and automatically.

The p values ($\alpha = 0.05$) after performing the T-test for the observed qualitative characteristics can be seen in Table 3.

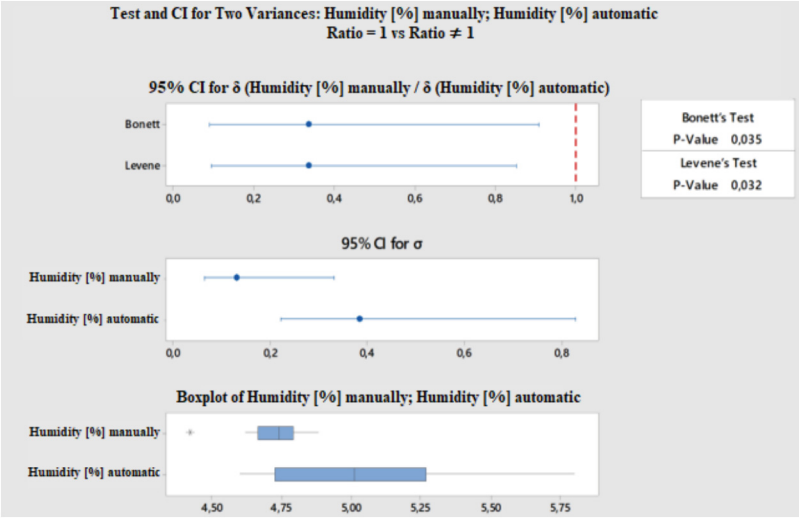

Fig. 7. Humidity test.

Table 3. P-values after T-test.

Elements and compounds	Fe	SiO_2	S	Humidity
P-value	0.496	0.382	0.841	0.021

Based on the resulting values from the T-test, we can say that the statistical difference between the data is visible only in the case of humidity. For the other qualitative elements and compounds Fe, SiO2, and S, the difference in percentage content is not statistically significant. Therefore, it is possible to point out that the sampling method has no influence and did not affect the results in this case.

4.2 The Result of the Bonett's and Levene's Test

These tests result in the finding that similar to the T-test, the differences in standard deviations are not statistically significant. The difference in values occurred only in humidity.

5 Conclusions

Based on the performed tests, it was concluded that manual or automatic sampling provides a sample whose resulting values are equal to or are very similar; they are not statistically significantly different. Statistically significant differences in values occurred only in the case of humidity.

In both tests, the evaluation of the hypotheses was the same.

A significant difference between manual and automatic sampling is that it is impossible to manually sample the entire set, as only one sample is taken. Automatic sampling uses a sampler that samples the entire set - samples are taken regularly at intervals. With automatic sampling, a representative sample is obtained, while a manually taken sample creates a random sample for us.

Acknowledgment. This article was created by the implementation of the grant project APVV-17-0258 Digital engineering elements application in innovation and optimization of production flows, APVV-19-0418 Intelligent solutions to enhance business innovation capability in the process of transforming them into innovative businesses, VEGA 1/0438/20 Interaction of digital technologies to support software and hardware communication of the advanced production system platform, KEGA 020TUKE-4/2023 Systematic development of the competence profile of students of industrial and digital engineering in the process of higher education and VEGA 1/0508/22 Innovative and digital technologies in manufacturing and logistics processes and system.

References

1. Krajčovič, M., Plinta, D.: Adaptive inventory control system for material items with continuous non-stationary demand. Manag. Prod. Eng. Rev. **5**(1), 11–20 (2014). https://doi.org/10.2478/mper-2014-0002
2. Dulina, L., Rakyta, M., Sulirova, I., Šeligova, M.: Improvement of the production system 2017. In: Smart City 360°, 2nd EAI International Summit. EAI, Ghent (2017). https://doi.org/10.4108/eai.14-2-2017.152173
3. Markulik, M., Cehlár, R., Kozel, R.: Process approach in the mining conditions. Acta Montanist. Slovaca **23**(1), 46–52 (2018)
4. Trebuňa, P., Poór, P., Halčinová, J.: Example for determining of metrics (degree of dissimilarity) of objects cluster analysis. In: 2013 International Conference on Frontiers of Energy. Environmental Materials and Civil Engineering (FEEMCE 2013), pp. 317–320. DEStech Publications, Shanghai (2013)
5. Straka, M., Bindzár, P., Kaduková, A.: Utilization of the multicriteria decision-making methods for the needs of mining industry. Acta Montanist. Slovaca **19**(4), 199–206 (2014)
6. Heydorn, K., Esbensen, K.: Sampling and metrology. Accredit. Quality Assur. **9**(7), 391–396 (2004). https://doi.org/10.1007/s00769-004-0808-z
7. Choi, W., Kurfess, T.R., Cagan, J.: Sampling uncertainty in coordinate measurement data analysis. Precis. Eng. **22**(3), 153–163 (1998). https://doi.org/10.1016/S0141-6359(98)00011-7
8. Juran, J.M., Godfrey, A.B.: Juran's Quality Handbook. McGraw-Hill, New York (1998)
9. McMillen, N.: Statistical Process Control and Company-Wide Quality Improvement. IFS, Bedford (1991)
10. Adams, M.J.: Chemometrics in Analytical Spectroscopy. The Royal Society of Chemistry, Cambridge (1995)
11. Havlík, T.: Sampling of Solid Materials. s.l. Emilena Plus (2006)
12. Kábele, P., Edl, M.: Increasing the efficiency of the production process due to using methods of industrial engineering. In: Ivanov, V., et al. (eds.) Advances in Design, Simulation and Manufacturing II. DSMIE 2019. LNME, pp. 126−137. Springer, Cham (2020). https://doi.org/10.1007/978-3-030-22365-6_13

13. Mucha, J., Szuwarzynski, M.: Sampling errors and their influence on accuracy of zinc and lead content evaluation in ore from the Trzebionka mine (Silesian-Cracow Zn-Pb ore district, Poland). Chemom. Intell. Lab. Syst. **74**(1), 165–170 (2004). https://doi.org/10.1016/j.chemolab.2004.03.014
14. Donskoi, E., Suthers, S.P., Fradd, S.B., et al.: Utilization of optical image analysis and automatic texture classification for iron ore particle characterization. Miner. Eng. **20**(5), 461–471 (2007). https://doi.org/10.1016/j.mineng.2006.12.005
15. Fu, X., Wei, S.M., Liu, Y., Hu, M., Cao, S.M.: Design of the automatic sample preparation system. In: 2015 International Conference on Advanced Mechatronic Systems (ICAMECHS), Beijing, pp. 567−570 (2015)

Quality Assurance

Improvement of the Assembly Technology Quality by Determining the Closing Link Size Under Thermal Stress

Hanna Hrinchenko[1(✉)], Roman Trishch[2,3], Viktoriia Kniazieva[1], and Nataliia Antonenko[1]

[1] Ukrainian Engineering Pedagogics Academy, 16, Universytetska Street, Kharkiv 61003, Ukraine
hrinchenko@uipa.edu.ua

[2] National Aerospace University "Kharkiv Aviation Institute", 17, Chkalova Street, Kharkiv 61070, Ukraine

[3] Mykolas Romeris University, 20, Ateities Street, 08303 Vilnius, Lithuania

Abstract. The study aims to improve the quality of the thermal assembly technology of engineering elements by introducing a methodology for determining the size of the closing link in the calculation of assembly dimensional chains, taking into account the influence of temperature gaps. The presented analysis of the technological preparation of production revealed the need to include the calculation of dimensional chains as one of the elements of dimensional analysis, which is determined by a set of calculation and analytical procedures carried out during the development and analysis of structures and technological processes. The effectiveness of dimensional chain calculation using the probabilistic method largely depends on the extent to which the influence of random factors on the values of the component links and the closing link is considered. Studies have confirmed that the calculation of the nominal value of the closing link does not meet the requirements set forth when compared with the results obtained during the calculation without considering the influence of temperature gaps. However, the practical assembly of the feed pump rotor, taking into account the influence of temperature gaps, can lead to an improvement in the axial assembly accuracy by 5% to 13% and a decrease in the gap between the ends of the rotor wheel and the discharge disk by 6% to 10% without the need to use additional technological equipment.

Keywords: Technology Quality · Thermal Assembly · Dimensional Chain · Assembly Accuracy · Manufacturing Innovation

1 Introduction

One of the components of Ukraine's successful entry into the global trade market is the production of competitive products, especially in those industries that traditionally provide the country's exports. Machine building is a key knowledge-intensive industry

© The Author(s), under exclusive license to Springer Nature Switzerland AG 2024
V. Ivanov et al. (Eds.): DSMIE 2024, LNME, pp. 365–375, 2024.
https://doi.org/10.1007/978-3-031-61797-3_31

in the country, as its development is crucial for ensuring the quality of products in other sectors of the national economy. The main task of modern machine building is to produce high-quality and competitive products. The quality of products depends on the quality of manufacturing of individual parts and their assembly process.

Assembly is the final stage of manufacturing machines and mechanisms, which largely determines the operational reliability and durability of the product. Notably, most of the assembly work is manual, sometimes requiring a lot of physical labor and high skill. Therefore, the economic performance of an enterprise, in many cases, depends on the labor intensity of assembly production, and the problem of improving the quality and productivity of assembly is one of the most critical issues in the scientific and technological progress of modern engineering.

2 Literature Review

Assessing the quality of processes that ensure the reliability and safety of complex engineering and other production systems requires a comprehensive approach. Ensuring the quality of technological equipment requires careful analysis at various stages: design, assembly, and operation [1]. The quality of assembly can be affected by many factors, including those not directly related to the assembly process [2], such as errors in thermal, mechanical, and other types of part processing. These errors can directly or indirectly manifest themselves either in the assembly process or the assembled product and thus worsen its quality.

Such concepts were detailed in the research works [3, 4]. Thus, the authors of [3] proposed a universal method for determining assembly line errors and proved its impact on the overall productivity of processes. The impact of assembly errors by the nature of their manifestation (random and systematic), by the type of fit, interposition of elements, deformations, the state of mating surfaces, and others are considered in [4].

The methodology for rapid identification of geometric errors of three-axis machine tools using machine tool measurements, which allows identifying the linear positioning error and two straightness errors of any linear axis of machines with Cartesian kinematics, as well as the perpendicularity error between the axes, is presented in [5]. A continuation of this work was the method proposed by the authors of [6] for identifying thermoelastic errors of three-axis machine tools using measurements on the machine adapted to the conditions of the shop. The presented method is suitable for the one-time identification of geometric errors caused by manufacturing inaccuracies, assembly-related deviations, and wear and for the identification of thermally induced geometric errors over a long period. Since the artifact is scalable, it can be adapted to different machine sizes. Thus, the presented method is versatile and inexpensive to measure geometric and especially thermoelastic errors. At the same time, the authors do not consider improving the quality of assembly from the point of view of considering the factors that indirectly affect the technology.

The technology for assembling a connection of a particular type (cylindrical, conical, flat, and threaded) is chosen based on the nature of the fit, taking into account its accuracy, the dimensions of the parts and their accuracy, shape, and surface roughness errors, structural elements (chamfers, boring, grooves), and the required accuracy of the relative

position of the parts in the connection. Papers [7, 8] discuss the main parameters that parts entering the assembly process must have. The most critical stage in the design of the technology is the design of the assembly operation itself based on the calculation of the assembly of parts. The validity of the calculation depends on the degree to which the influence of the previously listed factors is considered, as well as on the kinematic, stiffness, power, and dynamic characteristics of the technological equipment. The authors of [7] proposed a model that describes the variation of the dimensional chain of mechanical components associated with the stroke. The geometric characteristics of assembly parts are discretized as a set of coordinate points, and several linear dimensional chains equivalently replace the traditional geometric dimensional chain. For each linear dimensional chain, the reference point of the assembly of the two parts is deformed under gravity and thermal effects, resulting in the dimensional chain being out of alignment. In this paper, the closure of the dimensional chain is guaranteed by replacing the zero point of the assembly with a plane defined by the three highest points. Paper [8] proposes a mathematical gearing model, including profile deviation, pitch deviation, and geometric deviation, developed by combining traditional profile modeling with the small displacement torsor (SDT) method. Based on this mathematical model, a tooth contact analysis method that considers various deviations and a program for calculating the transmission error were developed.

Studies [9–11] considered issues related to solving the problem of assembling parts into an assembly unit on cylindrical landing surfaces. During tension assembly, parts should be made with chamfers since their absence leads to the unassemblability of the product due to the high probability of resting on the end surfaces or assembly with damage to the edges along the contour of the landing surface [9]. The presence of chamfers is of great importance, especially during automatic assembly. Moreover, this is the main requirement for the part's manufacturability in assembly. The issue of assembling joints with small gaps and tension is discussed in more detail in [10]. A slight misalignment of the axes of the parts leads to their jamming, and a slight increase in the assembly force leads to the formation of burrs. During the assembly of such joints, using various correction devices, it is necessary to ensure small eccentricity and skew angle of the axes in automatic mode [11].

As mentioned earlier, accuracy is one of the most important quality indicators [12–15]. To predict assembly accuracy in the virtual assembly process, the authors of [12] proposed a technology for automatically generating and solving the assembly dimensional chain concerning fit deviation. By preprocessing the selected assembly model, basic information about the relevant parts is obtained and stored in the corresponding chain table, the data obtained is processed, and according to a certain search direction, the increasing and decreasing links are determined, and the dimensional chain is generated. When assembling, the main technical requirements are maintaining the accuracy of the position, rotation, and linear movement of components and parts relative to any base surfaces [13]. The accuracy of the relative position of the parts, if there is no thrust shoulder on the workpiece, depends on the accuracy of the assembly mechanism [14]. The most significant effect in solving the complex problem of accuracy, productivity, and cost-effectiveness of manufacturing products (machines and devices) is generally achieved

when this problem is solved from three main perspectives that characterize all stages of production and operation: design and operational, technological, and metrological [15].

The work aims to improve the quality of assembly technology by determining the size of the closing link of assembly dimensional chains, considering the temperature gaps that occur during assembly under thermal effects.

3 Research Methodology

Studies to determine the size of the closing link were carried out on samples and natural products: the shaft and rotor wheels of the feed pump of the SVPT-340–1000 LMZ type.

The research methodology included:

1. selection of materials, design of components;
2. calculation of the assembly dimensional chain of the multi-element connection by the probabilistic method without taking into account the influence of the material's thermal expansion;
3. preparation of samples and equipment for experiments;
4. determining the size of the closing link after assembling the feed pump rotor without considering the influence of thermal expansion of the material.

When choosing the materials of the samples, the requirements were based on the fact that they should be the most common in the industry, meet the minimum manufacturing costs, and meet the research objectives. Therefore, the material used was steel 45. The chemical composition and mechanical properties are shown in Table 1.

Table 1. Chemical composition and mechanical properties of metal samples.

Steel grade	Chemical composition, %					Mechanical properties		
	C	Si	Mn	S	P	Temporary resistance σ_v, kg/mm^2	Relative elongation, %	Hardness, H_B
45	0.47	0.28	0.6	0.088	0.028	68	19	167–179

The general view of the studied parts is shown in Fig. 1.

The controlled dimension is the distance between the ends of the bushings during assembly by heating. In order to conduct a study of the dimensional dispersion process, at least 80 tests are required.

Pumps of this type are among thermal power plants' most critical auxiliary machines. The special operating conditions of the pump require that all rotor parts (in addition to being securely fastened against the effects of the operating environment) should also be able to expand freely. For this purpose, the axial dimensions must be precisely maintained. The rotor is a multi-element assembly with a shaft and six stainless steel impellers mounted in series. The wheels are mounted on the shaft with tension. A general view of the rotor assembly is shown in Fig. 2.

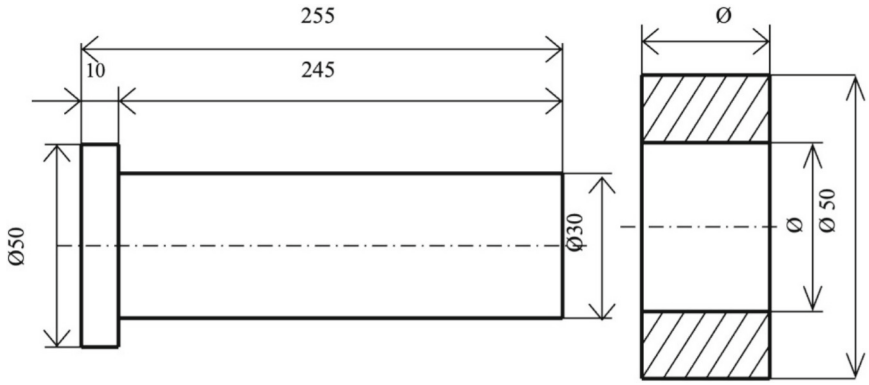

Fig. 1. General view of the experimental sample.

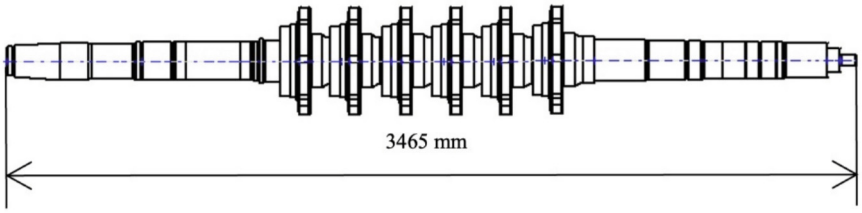

a)

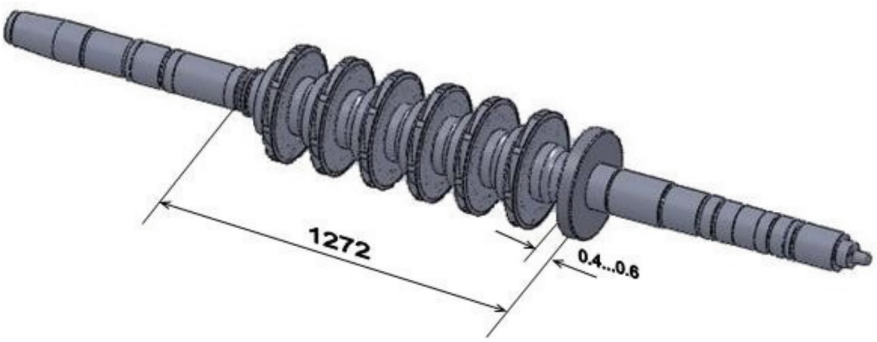

b)

Fig. 2. Feed pump rotor assembly: (a) general view; (b) three-dimensional view.

All parts are large-sized - the inner diameter of the rotor wheel is 164.8 mm; the width of the rotor wheel's landing surface is 195 mm; the total length of the shaft is 3465 mm. The diameter of the landing surface along the shaft length is 1272 mm.

The rotor is assembled using induction heating, which has the following advantages: the ability to program the heating parameters of the product, preventing the blades from

overheating to dangerous temperatures that lead to material weakening, obtaining a mating surface without scratches or deformations, and increasing labor productivity. The disadvantage of such an assembly is the difficulty in maintaining dimensional accuracy due to the linear expansion of materials due to temperature.

Calculating the assembly dimensional chain involves obtaining a gap between the ends of the wheel and the hub of the discharge disc of a certain size. For this purpose, a dimensional unit diagram was built based on the drawing "Rotor. Assembly drawing PN 1500-350" (Fig. 3).

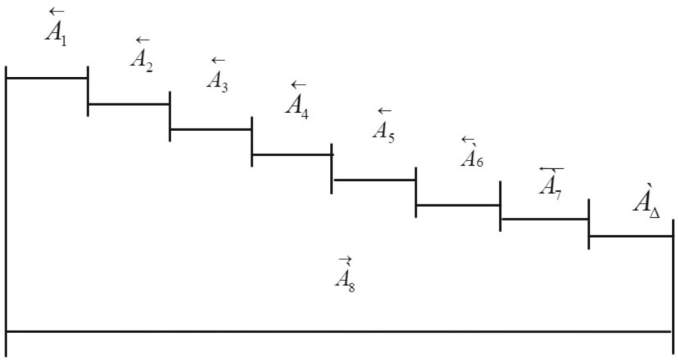

Fig. 3. Diagram of the dimensional chain of the assembly unit.

Dimension A_1 is a component of the reducing link, equal to the distance between the end of the first wheel and the end of the shaft stage; dimensions A_2, A_3, A_4, A_5, A_6, A_7 are the component reducing links of the assembly dimensional chain, which have the value of the length of the wheel landing surface; A_8 is a component of the increasing link, which has the value of the total length between the ends of the first wheel and the discharge disk; A_Δ is a closing link, which has the value of the distance between the ends of the last rotor wheel and the discharge disk.

4 Results and Discussion

Since the rotor production is small-scale and the number of links in the dimensional chain exceeds four, the solution to the problem was realized by probabilistic summation.

From the service purpose of the mechanism, it follows that the minimum gap between the end of the last rotor wheel and the end of the discharge disk should be 0.4 mm $\left(\Delta_{O_\Delta}\right)$, and the maximum – 0.6 mm $\left(\Delta_{I_\Delta}\right)$. Therefore, the clearance tolerance field is equal to:

$$\delta_\Delta = \Delta_{I_\Delta} - \Delta_{O_\Delta} = 0.6 - 0.4 = 0.2\,\text{mm}.$$

The coordinate of the center of the tolerance field of the closing link:

$$\Delta_{C_\Delta} = \frac{\left(\Delta_{I_\Delta} + \Delta_{O_\Delta}\right)}{2} = (0.6 + 0.4)/2 = 0.5\,\text{mm}.$$

The solution to the direct problem is summarized in Table 2.

For the component links, column 1 shows the number of the component's links, column 2 shows its nature, and column 3 shows the nominal size. In column 4, we entered the values of the squares of the tolerance units of all component links based on the specified nominal size of each link.

In column 5, the number of tolerance units was determined by the formula

$$a = \frac{\delta_\Delta}{\sqrt{\sum_{i=1}^{m-1} i_i^2}}, \tag{1}$$

where i_i – the tolerance unit of the i component link.

The qualification of all links in the dimensional chain, except for one of the optional links (in this case, link A8 was left), was determined by the value of a and recorded in column 6.

Next, the dimensional tolerances of the component links, except for one, were determined according to regulatory requirements based on the nominal size (column 3) and qualification (column 6) and entered in columns 7 and 8. Half of the tolerance field of the closing link and component links was determined by the formulas:

$$\frac{\delta_\Delta}{2} = \frac{\Delta_{I_\Delta} - \Delta_{O_\Delta}}{2}; \quad \frac{\delta_i}{2} = \frac{\Delta_{I_i} - \Delta_{O_i}}{2}.$$

The data obtained were entered in column 9, squared, and recorded in column 10. The expression determined the remaining half of the tolerance field of the component link:

$$\frac{\delta_x}{2} = \sqrt{\left(\frac{\delta_\Delta}{2}\right)^2 - \sum_{i=1}^{(m-1)-1} \left(\frac{\delta_i}{2}\right)^2 \xi^2}$$

where ξ is the transmission ratio, which may have different meanings and values depending on the type of dimensional chain.

Thus, in this case, the transmission ratio is equal to one for a linear chain for increasing component links. For decreasing component links, the transmission ratio is "–1".

Then, the coordinates of the centers of the tolerance fields Δ_{C_i} can be determined for all the component links except one.

The obtained values were recorded in column 11, where the individual coordinates of the midpoints of the tolerance fields of the increasing $\Delta_{C_{ii}}$ and decreasing $\Delta_{C_{di}}$ links were summed up. The coordinate of the center of the tolerance field of the remaining component link was determined by the following expression:

$$\Delta_{C_x} = \left(\Delta_{C_\Delta} + \sum\nolimits_{i=1}^{m-1} \Delta_{C_{ii}}\right) - \sum\nolimits_{i=1}^{(m-1)-1} \Delta_{C_{di}}$$

The limit deviations of the remaining component link were defined as $\Delta_{O_x} = \Delta_{C_x} + 0.5\delta_x$; $\Delta_{O_x} = \Delta_{C_x} - 0.5\delta_x$, and recorded in the remaining graphs.

To solve the inverse task, it is necessary to determine the closing link's nominal value without considering the material's linear expansion and its maximum deviations.

$$A_\Delta = \sum_{i=1}^{n} \xi_{A_i} A_i = -102 + (-195) \cdot 6 + 1272 = -1272 + 1272 = 0.$$

$$\Delta_{O_\Delta} = \left(\sum_1^m \Delta_{Oi} - \sum_1^n \Delta_{Ii} \right) \pm K_i \sqrt{\sum_1^{m+n} \left(\frac{T_i}{2} \right)^2}$$

$$\Delta_{O_i} = (743 - 243) + 100 = 600\,\mu m$$

$$\Delta_{I_i} = (743 - 243) - 100 = 400\,\mu m$$

where T_i – temperature value for a particular link.

Next, to determine the accuracy of the compilation, the risk coefficient and the value of the risk percentage were found

$$t = \frac{0.5T_\Delta}{\sqrt{\sum_1^{m+n} \lambda_i^2 \left(\frac{T_i}{2} \right)^2}} = \frac{100}{\sqrt{81 + 864 + 166}} = \frac{100}{33.3} \approx 3.$$

In this case, for $t = 3$, the risk percentage is 0.27 percent. Thus, the tolerances of the component links are within the limits of economic accuracy, and the assembly will be performed with complete interchangeability. This means that the individual parts or components have been manufactured precisely within specified tolerances, allowing them to be easily replaced without compromising overall assembly performance or functionality.

Achieving cost-effective tolerance accuracy is critical in manufacturing processes because it helps maintain efficiency and cost-effectiveness. This means that components are manufactured to a high quality and meet the required standards, ensuring a smooth assembly process with minimal errors or necessary adjustments. This can lead to optimization of the production process, waste reduction, and overall product quality improvement, which is confirmed in [5, 6].

Let's determine the nominal value of the closing link of the dimensional chain, taking into account the linear expansion of the material:

$$A_\Delta = \sum_{i=1}^{n} \left(\xi_{A_i} A_i - \left(\beta_{OTi} l_i T_{OTi} + \Delta_{C_i} \right) \right) = -102 + (-192.9) \cdot 6 + 1272 = -1259.4 + 1272 = 12.6 \text{ mm}$$

The next step is to assemble the feed pump rotor and determine the gap size between the ends of the last wheel and the discharge disk under production conditions with or without additional technological operations.

The proposed method can be used for any distribution and has a number of advantages over known methods. The estimates obtained by this method are consistent and unbiased. These estimates are almost optimal because they are optimal for the sample size $n = 2$, and for the sample size $n \geq 7$, they almost coincide with the known optimal estimates of the parameters of the distributions for which they were found.

Table 2. Calculation of the dimensional chain of an assembly unit.

Link No	Link characteristics	Nominal size, mm	Tolerance unit squared	Number of tolerance units squared	Qualitet	Limit deviation μm		Half of the tolerance field, μm	Half of the tolerance fields in quadrats, μm	Coordinate of the center of the tolerance field, μm
						upper	lower			
-	Closing					600	400	100	10000	500
1	Decreasing	102	4.709	26.9	8	54	0	27	729	27
2	Decreasing	195	8.410		8	72	0	36	1296	36
3	Decreasing	195	8.410		8	72	0	36	1296	36
4	Decreasing	195	8.410		8	72	0	36	1296	36
5	Decreasing	195	8.410		8	72	0	36	1296	36
6	Decreasing	195	8.410		8	72	0	36	1296	36
7	Decreasing	195	8.410		8	72	0	36	1296	36
8	Increasing	1272				782	704	38.67	1495	743
	Total:		55.169							

Further research is based on the development of regulatory support with normative parameters of the gap value for different temperature values to improve the quality of assembly in mechanical engineering under thermal effects based on the theory of calculation of assembly dimensional chains. The development of regulatory support with normative parameters of the gap value at different temperatures aims to provide recommendations that improve the overall quality of the assembly process in mechanical engineering. This approach considers the effect of temperature on components and aims to ensure the accuracy and reliability of assembly in various environmental conditions. It will complement the known normative parameters of the characteristics of assembly units and the reference points of the assembly of two parts deformed by gravity, the thermal effect, as a result of which the dimensional chain is shifted and determined by the three highest points described in [7].

5 Conclusions

The efficiency of dimensional chain calculation using the probabilistic method depends mainly on the extent to which the influence of random factors on the values of the constituent links and the closing link is considered.

Until now, the existing methods of dimension chain calculation were based on outdated normative documents, which, in some cases, are unacceptable to use. The calculation of the assembly dimensional chain in conditions of thermal influence by the heating method based on the carried out researches in work normative material which allows for increasing the accuracy of calculation of dimensional chain at the expense of account of the influence of temperature gaps is offered.

Studies on determining the size of the closing link during the calculation of assembly dimensional chains, taking into account the influence of temperature gaps, have shown

that the result of calculating the nominal value of the closing link does not meet the task in hand, compared to the results obtained during the calculation without taking into account the influence of temperature gaps. However, the practical implementation of the assembly of the rotor of the SVPT-340-1000 LMZ feed pump type, taking into account the influence of temperature gaps, makes it possible to increase the assembly accuracy in the axial direction by 5–13% and reduce the size of the gap between the ends of the rotor wheel and the discharge disk by 6–10% without the use of additional technological equipment.

References

1. Hrinchenko, H., Kupriyanov, O., Khomenko, V., Khomenko, S., Kniazieva, V.: An approach to ensure operational safety for renewable energy equipment. In: Koval, V., Olczak, P. (eds.) Circular Economy for Renewable Energy. Green Energy and Technology, pp. 1−17. Springer, Cham (2023). https://doi.org/10.1007/978-3-031-30800-0_1
2. Kupriyanov, O., Trishch, R., Dichev, D., Hrinchenko, H.: Experimental Studies on the form error effect of the part mounting surface on the strength quality parameter of the interference fit joints. In: Tonkonogyi, V., Ivanov, V., Trojanowska, J., Oborskyi, G., Pavlenko, I. (eds.) Advanced Manufacturing Processes V. InterPartner 2023. LNME, pp. 369–378. Springer, Cham (2024). https://doi.org/10.1007/978-3-031-42778-7_34
3. Ribeiro, J., Pinheiro, R., Soares, S., Valente, A., Amorim, V., Filipe, V.: Automated detection of refilling stations in industry using unsupervised learning. In: Silva, F.J.G., Ferreira, L.P., Sá, J.C., Pereira, M.T., Pinto, C.M.A. (eds.) Flexible Automation and Intelligent Manufacturing: Establishing Bridges for More Sustainable Manufacturing Systems. FAIM 2023. LNME, pp. 1157–1163. Springer, Cham (2024). https://doi.org/10.1007/978-3-031-38165-2_132
4. Ramesh, R., Mannan, M., Poo, A.: Error compensation in machine tools — a review. Int. J. Mach. Tools Manuf **40**(9), 1235–1256 (2000). https://doi.org/10.1016/S0890-6955(00)00009-2
5. Breitzke, A., Hintze, W.: Workshop-suited geometric errors identification of three-axis machine tools using on-machine measurement for long term precision assurance. Precis. Eng. **75**, 235–247 (2022). https://doi.org/10.1016/j.precisioneng.2022.02.006
6. Breitzke, A., Hintze, W.: Workshop-suited identification of thermo-elastic errors of three-axis machine tools using on-machine measurement. Precis. Eng. **85**, 72–88 (2024). https://doi.org/10.1016/j.precisioneng.2023.09.009
7. Hu, M., Ma, J., Zhao, W.: Variable dimensional chain of stroke-related mechanical assemblies. Proc. Inst. Mech. Eng. Part B: J. Eng. Manuf. **230**(5), 909–922 (2016). https://doi.org/10.1177/0954405416636984
8. Xu, R., Huang, K., Guo, J., Yang, L., Qiu, M., Ru, Y.: Gear-tolerance optimization based on a response surface method. Trans. Can. Soc. Mech. Eng. **42**(3), 309–322 (2018). https://doi.org/10.1139/tcsme-2018-0006
9. Liu, Z., Zhou, S., Qiu, C., Tan, J.: Assembly variation analysis of complicated products based on rigid–flexible hybrid vector loop. Proc. Inst. Mech. Eng. Part B: J. Eng. Manuf. **233**(10), 2099–2114 (2019). https://doi.org/10.1177/0954405418816851
10. Xue, D., Yu, J., Li, Y., Zhang, H., Tong, X.: An advanced rigid-flexible hybrid assembly deviation analysis method for aerostructures. Adv. Eng. Inform. **58**, 102173 (2023). https://doi.org/10.1016/j.aei.2023.102173
11. Yi, Y., Liu, T., Yan, Y., et al.: A novel assembly tolerance analysis method considering form errors and partial parallel connections. Int. J. Adv. Manuf. Technol. (2022). https://doi.org/10.1007/s00170-022-09628-9

12. Xueguang, L., Huizhong, H., Fei L., Penghui L.: Research on assembly accuracy prediction based on UG secondary development. In: Proceedings of the SPIE 12309, International Conference on Advanced Manufacturing Technology and Manufacturing Systems (ICAMTMS 2022), 123090B (2022). https://doi.org/10.1117/12.2645675
13. Lu, C., Wang, S.-L.: An approach to evaluating product assembly precision considering the effect of joint surface deformation. Proc. Inst. Mech. Eng. C J. Mech. Eng. Sci. **228**(14), 2604–2617 (2014). https://doi.org/10.1177/0954406213519758
14. Dhupia, J.S., Powalka, B., Ulsoy, A.G., Katz, R.: Effect of a nonlinear joint on the dynamic performance of a machine tool. ASME. J. Manuf. Sci. Eng. **129**(5), 943–950 (2007). https://doi.org/10.1115/1.2752830
15. Kumar, U.V., Schmitz, T.L.: Spindle dynamics identification for receptance coupling substructure analysis. Precis. Eng. **36**(3), 435–443 (2012). https://doi.org/10.1016/j.precisioneng.2012.01.007

Integration of Statistical Analysis and Machine Learning Techniques for Enhanced Quality Control in Candle Oil Cartridge Manufacturing

Monika Kulisz[1](✉), Katarzyna Antosz[2], and Edward Kozłowski[1]

[1] Lublin University of Technology, 38, Nadbystrzycka Street, 20-618, Lublin, Poland
m.kulisz@pollub.pl

[2] Rzeszow University of Technology, 8, Powstańców Warszawy, 35-959, Rzeszów, Poland

Abstract. Quality control is crucial in production and plays a key role in ensuring the delivery of superior products. The research presented in this paper aimed to establish a robust decision-support tool to enhance the production oversight process in candle oil cartridge manufacturing. The study included two stages. The first stage was concentrated on isolating and identifying the critical factors that have a significant statistical influence on product quality. Following this, advanced machine learning techniques such as the Support Vector Machine, Regression Trees, K-Nearest Neighbors, and the Artificial Neural Network were harnessed. These models showcased validation accuracies that ranged from 84.5% to 86.9%. Notably, the ANN model emerged as the best due to its unmatched AUC value, which indicates its effectiveness for accurate classification. These insights shed light on the enormous potential of state-of-the-art methods in overcoming manufacturing challenges and pave the way for industries to adopt and integrate rigorous quality control mechanisms.

Keywords: Quality Control · Support Vector Machine · Regression Trees · K-Nearest Neighbors · Artificial Neural Network · Industrial Innovation

1 Introduction

Quality control in the production area has always been a key aspect, characterized by a constant pursuit of stability. A stabilized process ensures the production of high-quality products, significantly reduces the number of products that do not meet the desired standards and specifications [1, 2], and eliminates the hidden quality nonconformities [3]. Historically, the emphasis was on identifying defective products at the end of the production process to prevent their delivery to consumers [4]. Various methods and tools, such as the one discussed by Duong et al., have been used to calculate the product quality index by analyzing product paths and production batches [5]. Schötz et al. further presented a methodology for optimizing the arrangement of quality control steps to reduce quality-related costs in mass production [6].

However, as the intricacies of production processes evolved, so did the challenges. Identifying elements that disrupt the smooth flow of production has become increasingly

© The Author(s), under exclusive license to Springer Nature Switzerland AG 2024
V. Ivanov et al. (Eds.): DSMIE 2024, LNME, pp. 376–387, 2024.
https://doi.org/10.1007/978-3-031-61797-3_32

complex, especially considering the considerable amount of data generated and the complexity of its analysis [7]. This led to a shift in focus towards recognizing the input parameters responsible for the emergence of defective products [8]. The digital era, characterized by advances in data analytics and machine learning, has played a key role in refining these methods [9]. Jamwal et al., for instance, emphasized the potential benefits of machine learning techniques when applied to address sustainability challenges in manufacturing [10].

The study's main objective was to create a decision-support instrument to help supervise the manufacturing process in a company producing oil cartridges for candle production. A significant challenge in producing these cartridges is the significant deviation of the product weight from its intended value. Approximately 5% of the total production is outside the acceptable range, adversely impacting profitability. Deviations from the weight tolerance increase the risk of not fulfilling client specifications as previously agreed.

The research aims to identify the factors that affect the quality of the inserts. In this way, the company can make informed decisions to reduce the production of substandard products. The conclusions garnered from this study will be used to develop a system plan focused on continuous supervision of production indicators, thus improving quality control.

The research methodology takes place in two separate stages. Initially, the focus was on identifying crucial elements that statistically influence the quality of the inserts. Subsequently, an in-depth analysis of the production process was carried out based on data obtained from the company. These data were subjected to rigorous statistical analysis. Machine learning techniques were used in the final stage to improve the decision-making process. This part of the research focuses on developing a model that predicts the quality of the resulting products.

2 Literature Review

Continuous manufacturing has further accentuated the evolution of quality control methodologies. Karst et al. presented the potential benefits of improving product quality control [11]. Moreover, it is essential to integrate quality control concepts into classic production models, as shown by Pan et al., who have paved the way for more efficient and cost-effective production processes [12]. Furthermore, introducing Cyber-Physical Production Systems (CPPS) has revolutionized industries like metal casting. Lee et al. demonstrated the effectiveness of CPPS in predicting metal casting quality using a combination of the Internet of Things (IoT), artificial intelligence, and simulations [13].

With the proliferation of advanced technologies, there are constant efforts to automate and optimize quality prediction in multistage manufacturing systems. Fields such as machine learning, neural networks, and decision models are increasingly used to help predict quality, making manufacturing processes more sustainable and efficient [14–16].

Integrating data analytics, machine learning, and continuous production methodology can contribute to ensuring appropriate quality standards for the received products and thus achieve an appropriate level of customer satisfaction [17–19].

The article consists of several chapters, including an introduction. Section 2 discusses the research problem and methodology, while Sect. 3 presents the results and discussion.

Finally, Sect. 4 presents the conclusions. This work is a continuation of the research presented in [20].

3 Research Methodology

3.1 Description of the Process

The whole process is shown in Fig. 1. There are eight separate phases in the analyzed production procedure. First, the raw materials for candle production, mainly paraffin, are taken from the warehouse. Automated machines then sort these materials into designated plastic containers. Once sorted, these containers are positioned. They are then directed to an automated mechanism that attaches a wick to them, a process called "crimping". Simultaneously, another station prepares the paraffin wax to fill these containers.

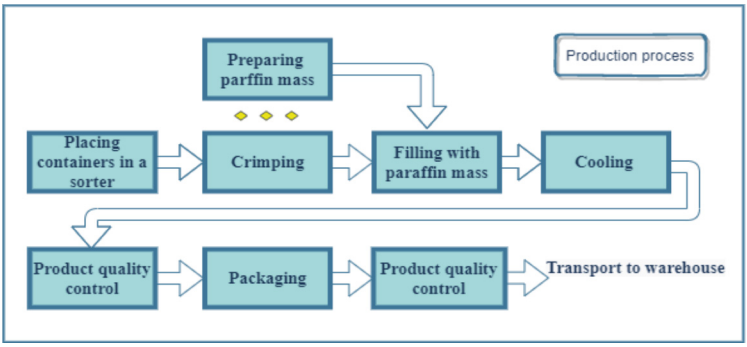

Fig. 1. Flow chart of the analyzed manufacturing process.

After crimping, the containers are sent to the assembly line. Here, they are methodically arranged at regular intervals using special equipment. The next step is the first phase of paraffin filling, which reaches about half the desired weight. A secondary filling mechanism adds more paraffin as it moves along the conveyor. This process allows the initial layer of paraffin to solidify partially.

After filling, the containers are sent to a cooling lane where the paraffin solidifies completely. Quality checks follow. A combination of manual control by production and quality control personnel and automatic control using sensors in dedicated chambers is used. Any product that does not meet quality standards is removed immediately.

The next stage involves packaging and labeling of the products. Specialized robotic arms with suction capabilities stack these products. Each stack is then wrapped in protective film and marked. This marking includes essential details such as the production line, date specifications, and a unique code ensuring product traceability for future references or complaints.

Finally, these labeled products are packed into various types of packaging, such as flap cartons or skid-friendly displays. Another round of visual inspection is performed on the boxed stacks during this packing process. After approval, these products are stretch-wrapped and sent to the finished goods warehouse.

3.2 Data Collection and Preliminary Analysis

In the initial stage of the research, categories and the scope of data collection were determined. Process data is presented in Table 1.

Table 1. Description of variables.

Variable	Unit of Measure	Description
x1	°C	Oil mass temperature in the tank
x2	°C	Worm temperature
x3	°C	Baths temperature
x4	°C	Filling machines temperature
x5	°C	Nozzle temperature
x6	s	Priming time
x7	°C	Temperature in the tunnel
x8	s	Cooling time
x9	–	Day of the week
x10	–	Shift
x11	–	Operator

Two types of product quality were distinguished: OK, representing a compliant product, and NOK, indicating a non-compliant product. Data was collected from November 1, 2022, to June 30, 2023. The collected information was analyzed. Preliminary tools such as a boxplot were used to identify anomalies. The detected irregularities were eliminated from the data set. Table 2 presents the main statistics related to the input variables.

We utilized the chi-square statistical method to determine the factors influencing the product quality based on the collected data. The chi-square value was determined by the Formula (1):

$$\chi^2 = \sum \frac{(O-E)^2}{E} = \sum_{i=1}^{k} \sum_{j=1}^{p} \frac{\left(n_{ij} - E_{ij}\right)^2}{E_{ij}} \tag{1}$$

This value follows an asymptotic χ^2 distribution with *(k-1)(p-1)* degrees of freedom. In this context, Observed values are denoted as n_{ij}, and Expected values are based on the product of the marginal totals. The chi-square method is often used to verify the independence between two categorical variables. For this study, a contingency table was developed, and the expected frequency for each cell was calculated using the product of its column and row totals divided by the overall number of observations.

With the product quality-labeled as OK/NOK, we applied the tests H_0: $x_1 = x_2 = \cdots = x_{11}$, $andH_1$: $x_1 \neq x_2 \neq \cdots \neq x_{11}$, using chi-square with a null hypothesis and a confidence level set at $\alpha = 0.05$. The outcomes of this analysis are displayed in Table 3, x8 was omitted due to its constant value (Table 2).

Table 2. Basic statistics for input variables.

Variable	Average	Minimum	Maximum	Std. Dev
x1	41.35	40.00	44.00	0.83
x2	21.61	20.10	22.50	0.79
x3	56.14	55.00	57.00	0.54
x4	42.87	40.00	45.30	1.19
x5	42.87	40.00	45.30	1.19
x6	1.01	1.00	1.20	0.05
x7	15.92	15.30	16.50	0.33
x8	20.00	20.00	20.00	0.00
x9	2.96	1.00	5.00	1.45
x10	2.02	1.00	3.00	0.82
x11	2.02	1.00	3.00	0.82

Table 3. Chi-square test results.

Var	x1	x2	x3	x4	x5	x6	x7	x9	x10	x11
R	−0.473	−0.127	0.163	0.072	0.072	0.004	−0.210	0.027	0.037	0.037
t(N-2)	−14.58	−3.467	4.495	1.961	1.961	0.109	−5.825	0.735	1.013	1.013
p-value	0.000	0.005	0.008	0.049	0.060	0.913	0.000	0.462	0.311	0.311

From the data in Table 3, it is clear that several factors significantly influence product quality, such as x1 (p-value = 0.000), x2 (p = 0.005), x3 (p = 0.008), x4 (p = 0.049), and x7 (p = 0.000). These results highlight key factors of product quality from a statistical perspective.

This leads to the following questions: "Which factors should a company prioritize for continuous quality control?", "Which of them are the most crucial?". To answer this question, in subsequent research, machine learning methods such as Support Vector Machine (SVM), Regression Trees (RT), K-Nearest Neighbours (KNN), and Artificial Neural Network (ANN) were used to create models that detail the shifts in product quality based on process metrics.

3.3 Machine Learning Methods Methodology

To predict whether the received product meets the quality requirements or not, classification models were developed using several machine learning methods: Support Vector Machine (SVM), Regression Trees (RT), K-Nearest Neighbours (KNN), and Artificial Neural Network (ANN). The modeling process was conducted in Matlab R2023a. The first three models were constructed using the Classification Learner App toolbox, while the ANN was developed using the Neural Network Pattern Recognition App toolbox.

The selection of the mentioned machine learning methods – SVM, RT, KNN, and ANN – was based on their strengths and advantages for classification tasks. These methods represent different paradigms in machine learning, allowing for a comprehensive exploration of potential model structures, thereby increasing the chances of identifying an approach that is particularly well-suited to the problem. SVM is a powerful linear classifier that can handle non-linear data through the kernel trick, making it adept at managing high-dimensional data and finding optimal hyperplanes that maximize the margin between classes. Regression Trees, on the other hand, divide the data space into regions and are valuable when interactions between variables are suspected, with the added benefit of providing a graphical representation that is easier to interpret than some other models. KNN is a non-parametric method that bases decisions on the proximity of data points in the feature space, proving useful when decision boundaries are irregular. Artificial Neural Networks, inspired by biological neural networks, can approximate any continuous function and are particularly effective for problems where the relationship between input and output is intricate and non-linear. Furthermore, each method has a track record of successful applications across various classification problems in various domains, underscoring their general applicability and robustness. Additionally, Matlab R2023a offers comprehensive toolboxes and functions that streamline the implementation, training, and validation of these methods, enhancing the modeling process's efficiency.

The approach emphasizes meaningful distinctions between classes for the K-Nearest Neighbor (KNN) method. Several distance metrics include Euclidean, City Block, Chebyshev, Minkowski (cubic), Mann-Halanobis, Cosine, Correlation, Spearman, Hamming, and Jaccard. The algorithm is set to consider 10 neighbors for classification. Three options have been analyzed regarding weighting the distance: Equal, Inverse, and Squared Inverse. In addition, data standardization was enabled (Yes) or not (No).

For SVM, the training process incorporates different kernel functions. These functions include the Gaussian, linear, quadratic, and cube kernels. Both the kernel scale and the box constraint parameters are set to automatic, allowing the software to determine the optimal values during the training process.

The RT methodology is tailored to capture moderate distinctions between classes. The maximum number of splits is limited to 20, ensuring a medium number of leaves for finer class discrimination. The split criterion is defined, but the surrogate decision splits are turned off, meaning that surrogate splits are not used in the tree-building process.

Finally, for the Artificial Neural Network (ANN), the training process uses the scaled conjugate gradient algorithm. The softmax activation function was employed to obtain the probability of belonging to each class. The number of neurons in the hidden layer, ranging from 10 to 100, is determined experimentally. The dataset partitioning allocates 70% to training, with the remaining 30% divided equally between test and validation, each receiving 15%. The network architecture is a single hidden layer.

The input layer of the model consists of five neurons (variables x1, x2, x3, x4, and x7), while the output layer contains a single neuron (a classifier with two values 0 or 1). A classifier value 1 indicates that the received product meets the quality requirements, whereas 0 indicates that it does not. The quality of the models was determined based on the accuracy of the validation set.

4 Results and Discussion

As a result of the research, various machine learning models were trained to predict product quality. The best-obtained models for each type, including SVM, RT, KNN, and ANN, exhibited validation accuracies ranging from 84.5% to 86.9%. In addition to accuracy, the models were also evaluated for prediction speed, ranging from 4,100 observations per second (obs/sec) for ANN to 16,000 obs/sec for SVM, and training times, ranging from 1.6938 s for KNN to 8.9805 s for ANN. These results and details on prediction speed, training time, and model hyperparameters are presented in Table 4.

Table 4. Training parameters for the best models: SVM, RT, KNN, and ANN.

Training results	SVM	RT	KNN	ANN
Accuracy (Validation)	84.5%	86.8%	86.9%	86.9%
Prediction speed [obs/s]	16000	5300	11000	4100
Training time [s]	2.235	5.6647	1.6938	8.9805
Model Hyperparameters	Preset: Linear SVM Kernel function: Linear Multiclass method: One-vs-One	Preset: Medium Tree Maximum number of splits: 20 Split criterion: Gini's diversity index	Preset: Cubic KNN Distance metric: cubic Distance weight: equal Standardize data: Yes	Preset: Neural Network Layer size: 25 Activation: Softmax Iteration limit: 1000

The images (Fig. 2 and Fig. 3) presented display the results of four classification models: SVM, RT, KNN, and ANN. The first set of images (Fig. 2) shows the confusion matrix for each model, illustrating the number of true positives, true negatives, false positives, and false negatives classifications. The second set of images (Fig. 3) represents ROC curves, highlighting the ability of each model to differentiate between classes. The AUC (Area Under the Curve) value is also calculated for each curve, serving as a performance metric for the classifier.

From the results, distinctions in model performance can be observed. The SVM model has a relatively high number of false positives, 101, while correctly predicting 611 true positives. The RT model shows a more balanced profile with 79 false positives and 606 true positives but has the lowest AUC value of 0.6115 among the models, suggesting limitations in its classification efficiency. The KNN and ANN models show similar confusion matrix patterns, with KNN showing 79 false positives and 607 true positives and ANN mirroring these numbers exactly. However, the KNN model's AUC of 0.6257 is overshadowed by ANN's superior AUC of 0.735, indicating its overall ability for correct classification.

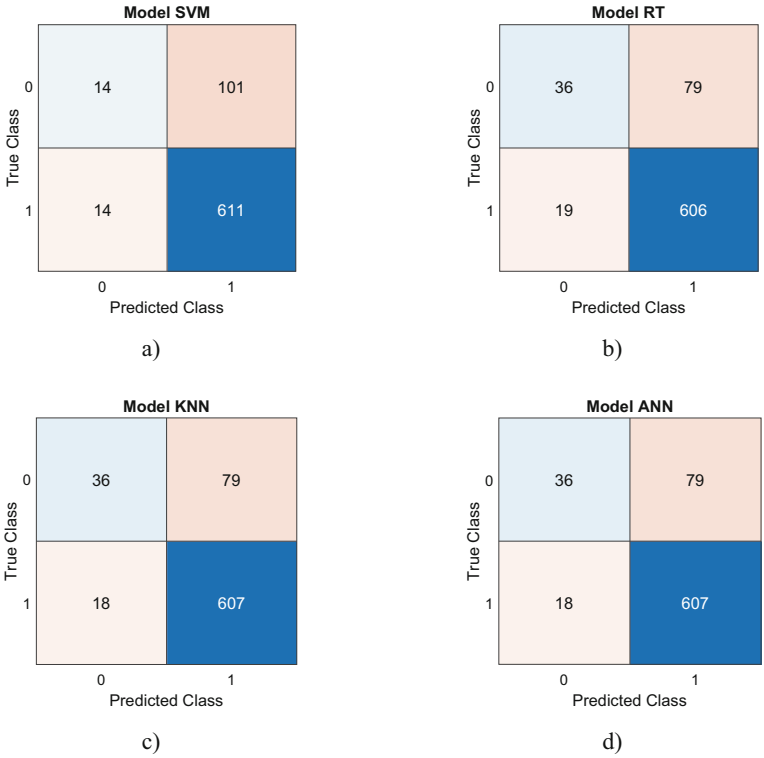

Fig. 2. Confusion Matrix for SVM (a), RT (b), KNN (c), and ANN (d).

In the ROC curves shown in Fig. 3, true positive rates are plotted against false positive rates, providing a visual representation of model performance at various thresholds. For example, the ROC curve for the ANN model shows an AUC of 0.735, indicating a strong ability to discriminate between classes. The other SVM, RT, and KNN models have lower AUC values of 0.6803, 0.6115, and 0.6257, respectively, indicating less robust performance than ANN.

In light of the above, the results for the ANN model were analyzed in more detail. Therefore, the confusion matrix and ROC curve for each data set: training, testing, and validation are presented below.

Figures 4 and 5 present performance metrics of a machine or statistical learning model in the form of ROC curves and confusion matrix. Figure 4 displays four confusion matrices representing different data sets: Training, Validation, Test, and All. Each matrix illustrates the performance of a classification model. The training data confusion matrix reveals an accuracy of 86.5%, with the model correctly identifying 611 out of 706 instances. The validation set decreases slightly to 85.6% accuracy, with 90 false negatives marring its record. The Test set shows the highest accuracy at 90.1%, indicating that the model performs exceptionally well on unseen data. Considering all the data combined, the overall accuracy is 86.9%.

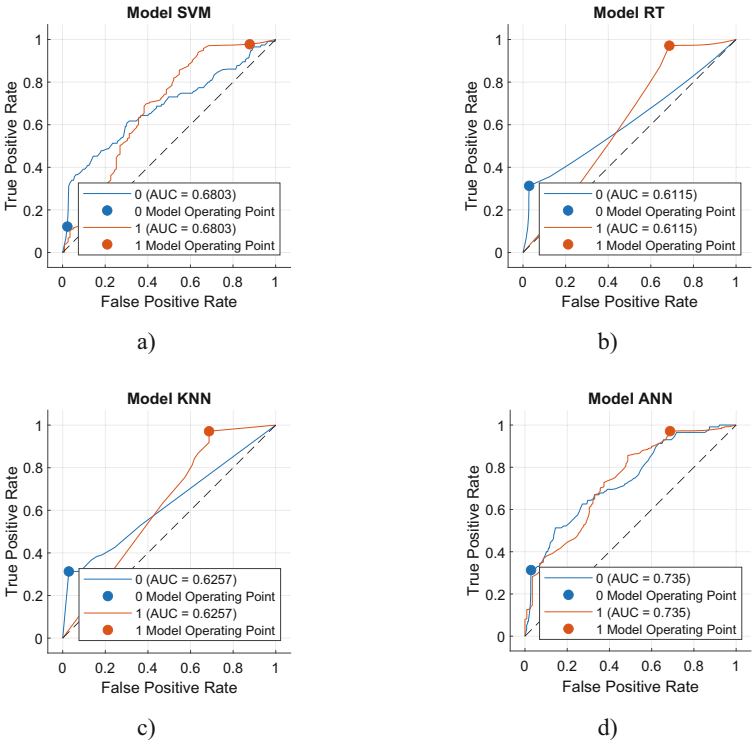

Fig. 3. Receiver Operating Characteristic (ROC) Curves: for SVM (a), RT (b), KNN (c), and ANN (d).

The ROC curves for the training, validation, test, and overall sets, as illustrated in Fig. 5, indicate the model's good predictive capabilities since they all lie above the diagonal. The ANN model's exemplary AUC values and accuracy metrics across different datasets, clearly represented in the figures, confirm its superior predictive capability. These results provide compelling evidence for the ANN model's deployment in practical settings where reliable and accurate predictions are paramount.

This study focused on identifying key factors affecting the quality of wax inputs in candle production, employing advanced statistical techniques and machine learning. The results, indicating a significant influence of factors such as oil tank temperature (x1), worm temperature (x2), filling temperature (x4), and cooling time (x7) on product quality, align with findings from other authors in this field. For instance, research by Wang et al. [3] also emphasized the importance of process parameter control in ensuring product quality. Similarly, Jamwal et al. [10] highlighted the potential of machine learning techniques in addressing quality challenges in manufacturing. However, this study extends the field by integrating statistical analysis with diverse machine learning methods, allowing for a deeper understanding and prediction of product quality.

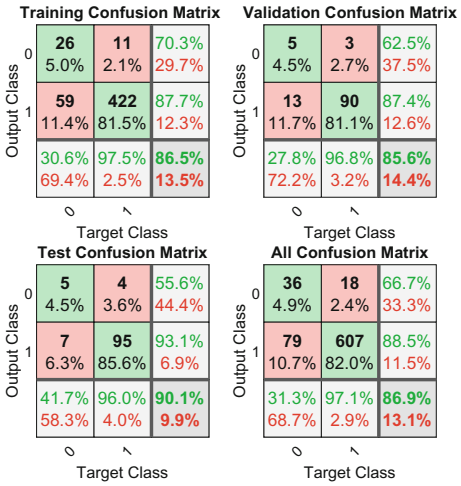

Fig. 4. Confusion matrix for the ANN model for training, test, and validation data.

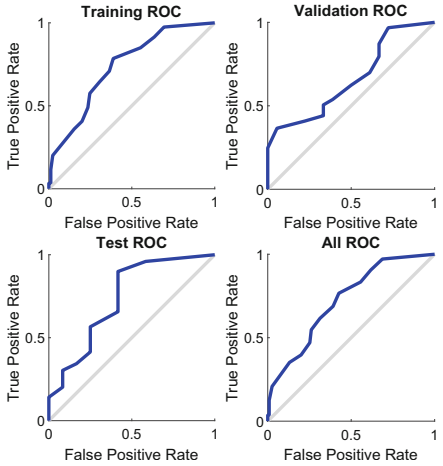

Fig. 5. ROC Curves for the ANN model for training, test, and validation data.

5 Conclusions

This research focused on creating a decision-support model to improve the quality of oil cartridges in candle production. A significant challenge facing the industry is the difference in product weight, which directly impacts profitability and customer satisfaction. Factors influencing product quality were identified through a comprehensive analysis of the manufacturing process and the use of both statistical and machine learning methods. Preliminary statistical analysis revealed key factors such as x1, x2, x3, x4, and x7 that significantly impact product quality. Further research used machine learning techniques, namely SVM, RT, KNN, and ANN, to predict product quality based on these factors.

The models were trained and achieved validation accuracies ranging from 84.5% to 86.9%. ANN was the best choice among all the models due to its highest AUC value, indicating its overall ability to classify correctly. These results highlight the potential of using advanced methods to address manufacturing challenges and provide a foundation for companies to implement robust quality control measures.

The findings of this research have significant implications for the manufacturing industry, particularly in quality control contexts. The statistical methods and machine learning employed the ANN model that exhibited the highest AUC value, suggesting new approaches to monitoring and improving product quality. However, the study also has its limitations. Primarily, the analysis is limited to data from a single manufacturing facility, which may affect the generalizability of the results. Moreover, focusing solely on selected process parameters may overlook other important factors influencing product quality. Therefore, these results should be interpreted considering these limitations.

Future research should consider incorporating additional process variables and extending the analysis to other manufacturing facilities to enhance the generalizability of the findings. Long-term studies to assess how changes in the manufacturing process affect product quality under various conditions would also be valuable. Furthermore, exploring other machine learning and artificial intelligence techniques that might provide better insights into complex relationships between process parameters and product quality would be a worthwhile direction for future research in this area.

References

1. Mikulić, D., Dolaček, Z.: Quality of concrete structures through standards application. Appl. Codes Design Regulat. **1**(1), 81–87 (2005)
2. Antosz, K., Kluz, R.: Analyze of process quality capability with one side specification limit. Technol. Autom. Montażu **2**, 49–52 (2018)
3. Wang, J., Liu, X., Wang, X., Jin, K.: Process machining allowance for reliability analysis of mechanical parts based on hidden quality loss. Eksploatacja i Niezawodnosc – Maintenance and Reliability **25**(4) (2023)
4. Riccetti, S.: End product quality control. In: Ricetti, S. (ed.) Designing Food Safety and Equipment Reliability Through Maintenance Engineering, pp. 297–324. CRC Press, Boca Raton (2014)
5. Duong, L.T., Travé-Massuyès, L., Subias, A., Barbosa Roa, N.: Assessing product quality from the production process logs. Int. J. Adv. Manuf. Technol. **2**(5), 1–13 (2021)
6. Schötz, S., Koller, J., Döpper, F.: Decision support methodology to reduce quality-related costs within mass production. In: Proceedings of the International Technology Management Conference, pp. 1–10. Springer, Heidelberg (2018)
7. Estrada-Vargas, A.P., Lopez-Mellado, E., Lesage, J.-J.: Input-output identification of controlled discrete manufacturing systems. Int. J. Syst. Sci. **45**, 456–471 (2014)
8. Galaktionova, Y.A., Ibragimova, E.K., Bekisheva, E.V.: On product quality control. Fibre Chem. **38**(1), 79–82 (2006)
9. Yan, H., Sergin, N.D., Brenneman, W.A., Lange, S.J., Ba, S.: Deep multi-task learning from quality prediction of multistage manufacturing systems. J. Qual. Technol. **53**, 526–544 (2021)
10. Jamwal, A., Agrawal, R., Sharma, M., Kumar, A., Kumar, V., Garza-Reyes, J.: Machine learning applications for sustainable manufacturing: a bibliometric-based review for future research. J. Enterp. Inf. Manag. **2**(5), 1–20 (2021)

11. Karst, D.J., Steinebach, F., Šoóš, M., Morbidelli, M.: Process performance and product quality in an integrated continuous antibody production process. Biotechnol. Bioeng. **114**, 298–307 (2017)
12. Pan, E., Jin, Y., Wang, S., Cang, T.: An integrated EPQ model based on a control chart for an imperfect production process. Int. J. Prod. Res. **50**(23), 6891–6903 (2012)
13. Lee, J., Noh, S., Kim, H.-J., Kang, Y.-S.: Implementation of cyber-physical production systems for quality prediction and operation control in metal casting. Sensors **18**(5), 1428 (2018)
14. Workman, M., Chen, D.Z., Musa, S.: Machine learning for predicting perovskite solar cell opto-electronic properties. Drones **7**(1), 1–15 (2020)
15. Kaščak, J., Husár, J., Knapčíková, L., Trojanowska, J., Ivanov, V.: Conceptual use of augmented reality in the maintenance of manufacturing facilities. In: Trojanowska, J., Kujawińska, A., Machado, J., Pavlenko, I. (eds.) Advances in Manufacturing III. MANUFACTURING 2022. Lecture Notes in Mechanical Engineering, pp. 241–252. Springer, Cham (2022). https://doi.org/10.1007/978-3-030-99310-8_19
16. Pavlenko, I., et al.: Using regression analysis for automated material selection in smart manufacturing. Mathematics **10**(11), 1888 (2022). https://doi.org/10.3390/math10111888
17. Kozłowski, E., Borucka, A., Oleszczuk, P., Jałowiec, T.: Evaluation of the maintenance system readiness using the semi-Markov model taking into account hidden factors. Eksploatacja i Niezawodność – Maintenance and Reliability **25**(4) (2023). https://doi.org/10.17531/ein/172857
18. Rogalewicz, M., Kujawińska, A., Feledziak, A.: Ensuring the reliability and reduction of quality control costs by minimizing process variability. Maintenance Reliability/Eksploatacja i Niezawodnosc **25**(2) (2023)
19. Trojanowska, J., Husár, J., Hrehova, S., Knapčíková, L.: Poka Yoke in smart production systems with pick-to-light implementation to increase efficiency. Appl. Sci. **13**(21), 11715 (2023). https://doi.org/10.3390/app132111715
20. Antosz, K., Gola, A., Paśko, Ł., Malheiro, T., Gonçalves, A.M., Varela, L.: Six sigma and random forests application for product quality system control development. In: International Scientific-Technical Conference MANUFACTURING, pp. 99−112. Springer, Cham (2022)

An Analysis of Machined Surface Quality Using TiAlTaN-Coated Tools in AMPCO® Milling Operations

Francisca Nogueira[1], André Pedroso[1(✉)], Francisco Silva[1,2], Raul Campilho[1,2], and Rita Sales-Contini[1,3]

[1] ISEP, Polytechnic of Porto, R. Dr. António Bernardino de Almeida, 4249-015 Porto, Portugal
afvpe@isep.ipp.pt

[2] Associate Laboratory for Energy, Transports and Aerospace (LAETA-INEGI), Rua Dr. Roberto Frias, 400, 4200-465 Porto, Portugal

[3] Technological College of São José dos Campos, Professor Jessen Vidal, Centro Paula Souza, Avenida Cesare Mansueto Giulio Lattes, 1350 Distrito Eugênio de Melo, São José dos Campos/SP 12247-014, Brazil

Abstract. Over the years, a consistent evolution has been observed in developing materials for industrial applications and chip-start cutting processes. Improving cutting tools by applying advanced coatings has demonstrated great significance by extending tool life (TL) and ensuring improved surface quality. With the development of a wide range of coatings, it is crucial to analyse, understand, and investigate the phenomena that occur during metal cutting. The primary objective of this study is to assess, identify, and quantify the evaluation of the machined surface quality of milled AMPCO® (a Cu-Be alloy) with WC-Co uncoated and TiAlTaN-coated tools using Physical Vapour Deposition (PVD). Regarding this, milling tests were performed, and surface roughness (SR) evaluations were assessed while varying cutting length (Lcut) and feed rate (f) at three distinct levels. The results obtained with WC-Co uncoated differed from those obtained with TiAlTaN-coated tools. Parameters f and Lcut significantly influenced the quality of the machined surface. TiAlTaN-coated tools performed notably worse than uncoated tools, indicating that the coating did not provide any advantages, mainly due to the lack of adhesion.

Keywords: Cu-Be Alloys · Machining Processes · PVD-Coated Tools · Uncoated Tools · Surface Analysis · Surface Integrity · Surface Roughness · Manufacturing Innovation

1 Introduction

Cu-Be alloys have excellent wear resistance and noteworthy properties such as thermal conductivity (k) and electrical resistivity (ρ_R) [1]. These alloys, known for their hardness and resistance to seizing and galling [2], are suitable for various applications, including

© The Author(s), under exclusive license to Springer Nature Switzerland AG 2024
V. Ivanov et al. (Eds.): DSMIE 2024, LNME, pp. 388–398, 2024.
https://doi.org/10.1007/978-3-031-61797-3_33

bearings, bushings [2, 3], electrical components, fasteners, and pumps. One specific variant, the C17200 Cu-Be alloys, detailed in ASTM B 194 – 15 [4], finds widespread use in industries like aerospace for producing tools and moulds for challenging environments [5, 6]. Regrettably, limited research has explored the interaction between Cu-Be workpieces and diamond tools [7, 8]. Machining Cu-Be alloys still poses great challenges due to material adhesion caused by significant ductility, leading to rapid Tool Wear (TW). Zuo et al. [9] studied adhesive rate variation and crystal adhesion's effect on WC-Co carbide tool damage. The authors found that microstructures, like cracks, adhesives, and adhesive layers, significantly impact tool damage, making the coating more susceptible and less predictable. This adhesive effect directly influences cutting performance, surface friction, and TL. As a result, extensive research efforts have focused on addressing these challenges, with techniques like EDM being explored and known for their effectiveness in moulding cavities production [6]. Dong et al. [10] introduced an effective method for machining high aspect ratio micro-holes in the C17200 Cu-Be alloy [4]. This approach combines micro-Electrical Discharge Machining (EDM) with deionised water and in situ Powder Mixed Electrical Discharge Machining (PMEDM) using boron carbide additives. Surface quality of high aspect ratio micro-holes was improved, reducing the arithmetic average roughness (R_a) from 2.65 μm to 0.92 μm. Engineered materials like Cu-Be alloys have broad applications across engineering domains [11]. Conventional machining processes face issues such as TW, Build-Up Edge (BUE), and grain lattice micro-tearing due to their high hardness and fatigue strength at elevated temperatures (T).

2 Literature Review

AMPCO®, a commercial term for Cu-Be alloys, is widely used in plastic injection moulding due to its high thermal conductivity and hardness, significantly reducing moulding cycle times. However, hard Be particles pose challenges in achieving smooth surfaces through conventional machining methods [12, 13]. Cu and its alloys are vital in various industries, and the surface quality is crucial for their performance. With their unique properties, these materials introduce complexities in processing and manufacturing due to their hardness and potential toxicity. Ongoing research is essential to address these challenges and enhance the effective use and long-term sustainability of these materials. Sousa et al. [6] studied the machining of AMPCO® but with Diamond-Like Carbon (DLC) coated tools and concluded that the coating did not positively affect the machined surface's quality.

The choice of milling AMPCO® with TiAlTaN-coated [14, 15] tools for the investigation stems from its paramount importance in the injection mould industry, making research in this domain precious for industry optimisation. This paper intends to encompass the effect of varying cutting length (L_{cut}) and feed rate (f) on surface roughness (SR) of AMPCOLOY®83 workpieces and TW while using TiAlTaN-coated and WC-Co uncoated tools. AMPCO® offers excellent surface finish and thermal conductivity, which are fundamental for mould cavities, allowing better surface finishing of the injected parts and reduced injection cycle times. However, its machining aspect holds intrigue due to

the dearth of information and scientific research about this alloy. Addressing this deficiency presents an essential and captivating challenge, offering potential contributions to the engineering scientific community.

3 Research Methodology

3.1 Material to be Machined

The machined base material in this work was a Cu-Be alloy called AMPCOLOY®83, supplied by AMPCO® Metal Portugal, Ltd. (Porto, Portugal), in its forged state. It was supplied as a parallelepiped block of 150 × 150 × 101.6 mm^3. It contains a significant weight content (*wt %*) of Cu, making it an excellent alloy for good ρ_R, k, wear resistance, and high hardness (Table 1).

Table 1. Physical and mechanical properties of the provided AMPCOLOY®83.

Mechanical Property	Value	Units
E	128	GPa
σ_u	1140	MPa
σ_y	1000	
HV	376	HV
ε_u	5	%
ρ	8260	kg/m^3

Caption: ε_u – strain at fracture

3.2 Cutting Tools

The milling tools supplied by InovaTools, S.A. (Marinha Grande, Portugal) are made of tungsten carbide (WC, grade 6110, Fig. 1) with an average grain size of 0.3 μm and a *wt %* = 6% Co binder. Six uncoated WC-Co tools and six TiAlTaN-coated tools were employed for the experiments, each featuring a thicker and longer shank to reduce vibrations during machining (Table 2). Clearance Face (CF), the Rake Face (RF), and the Top Face (TOP) are defined under the ISO 3002–1:1982 [16] standard.

Understanding the cutting tool's geometry and various facets is essential. The TiAlTaN coating, employed for safeguarding the milling cutters during machining, was produced using the Physical Vapor Deposition (PVD) method. This process utilised a High-Power Impulse Magnetron Sputtering (HiPIMS) power source in TEandM (Coimbra, Portugal). An average value of 3.369 μm of coating thickness (t) can be assumed, with a relatively insignificant standard deviation (SD) of ± 0.045 μm. This t is suitable for milling tools and is not critical in compromising adhesion.

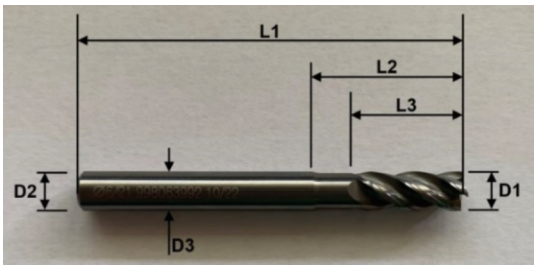

Fig. 1. Schematic diagram of the cutting tool dimensions.

Table 2. Dimensions of the milling cutters in mm (except for z).

Ref	D1	D2	D3	L1	L2	L3	z
288.060.00	6.00	6.00	5.50	57	13	21	4

Caption: z – number of teeth/cutting wedges

3.3 Milling Process

A CNC machine DMG/Mori Seiki DMU 60 eVo (Deckel Maho) was used to conduct machining tests to assess the quality of the machined surface. The details of the setups can be found in Table 3. The milling strategy involved rough linear machining, with the radial depth of cut (a_e or RDOC) set at 60% of the tool's diameter ($Ø$) and the axial depth of cut (a_p, or ADOC) at 0.5 mm to simulate finishing milling. The tools reference can be followed by "T0", representing the WC-Co uncoated tools, or "T1" for the TiAlTaN-coated ones. It is then accompanied by "L", "F", and "S", representing the L_{cut}, f, and s, respectively.

Besides the experimental plan on Table 3, the machining strategy encompasses down-milling with lubrication. The lubricant ratio used is 10% oil to 90% water. Forces and T measurements, as well as vibration analysis, were not conducted. Nonetheless, vibration analysis could have been conducted with the same modus operandi as in [17] and [18].

3.4 SR Testing

SR measurements were conducted with a Mahr Perthometer M2 profilometer with a minimum reading of 0.01 μm. The SR analysis includes parameters like R_z (average of maximum heights between consecutive peaks) and R_t (height between the deepest valley and highest peak along the evaluation length), following ISO 21920–2:2021 [19] standard measurements. Each test used a cut-off (λ_c) of 0.8 mm as the reference, covering seven segments for a total length of 5.6 mm [20]. The first and last segments were excluded from the measurements to mitigate potential errors stemming from probe inertia and acceleration. Machining process stability was necessary, and SR measurements were taken immediately after each machining trial in both transverse and longitudinal directions.

Table 3. An experimental plan with milling parameters was used in the setups.

Tool Reference	Coated	f (mm/min)	L_{cut} (m)
T0L27F750S126	No	750	26.8
T0L54F750S126		750	53.6
T0L74F750S126		750	73.7
T0L27F1500S126		1500	26.8
T0L54F1500S126		1500	53.6
T0L74F1500S126		1500	73.7
T0L27F750S126	Yes	750	26.8
T0L54F750S126		750	53.6
T0L74F750S126		750	73.7
T0L27F1500S126		1500	26.8
T0L54F1500S126		1500	53.6
T0L74F1500S126		1500	73.7

4 Results and Discussion

4.1 Machined Surface Assessment

SR Obtained Results

An analysis of the machined SR evaluation under various cutting conditions and with different tool types is presented in this section. After each test, a profilometer was used to measure SR values in transverse and longitudinal directions. Tool references for TiAlTaN-coated and uncoated WC-Co tools are listed in Tables 4 and 5, with three tools in each setup. The presented R_a, R_z, and R_t values represent the mean ($\bar{X}$) and standard deviation (SD) of three SR measurements in both longitudinal and transverse directions for each tool.

Analysis of L_{cut} Influence on R_a

R_a values from milling operations are displayed in Fig. 2, which summarises data concerning the transverse direction SR, while Fig. 3 focuses on the longitudinal direction SR, offering a comprehensive view of the results.

In the transverse direction, WC-Co uncoated tools yield lower values than the TiAlTaN-coated ones, where the impact of L_{cut} seems more pronounced. R_a increase is evident with the increment in L_{cut}, attributed to the heightened TW resulting from the longer machining, negatively affecting the machined surface's quality. The maximum R_a value is achieved with the TiAlTaN-coated tool, which reached $L_{cut} = 73.7$ m at $f = 1500$ mm/min. Notably, TiAlTaN-coated tools perform better with $L_{cut} = 27.8$ m (Fig. 3), indicating potential benefits for lower values; however, the graph suggests a higher TW rate for TiAlTaN-coated tools than WC-Co uncoated ones, as observed for $f = 750$ mm/min. WC-Co uncoated cutters consistently exhibit lower SR values than

Table 4. Measurements of transverse SR.

Tools Reference	Coated	R_a (μm)	R_z (μm)	R_t (μm)
T0L27F750S126	No	0.370 ± 0.047	1.992 ± 0.199	3.542 ± 0.600
T0L54F750S126		0.428 ± 0.016	1.992 ± 0.178	3.576 ± 0.537
T0L74F750S126		0.470 ± 0.022	2.228 ± 0.109	3.654 ± 0.552
T0L27F1500S126		0.747 ± 0.031	3.410 ± 0.487	6.194 ± 0.893
T0L54F1500S126		0.780 ± 0.092	3.468 ± 0.249	6.194 ± 0.372
T0L74F1500S126		0.812 ± 0.040	4.152 ± 0.479	7.146 ± 0.656
T1L27F750S126	Yes	0.453 ± 0.035	2.264 ± 0.308	3.108 ± 0.692
T1L54F750S126		0.484 ± 0.019	2.334 ± 0.324	3.992 ± 1.059
T1L74F750S126		0.584 ± 0.055	3.120 ± 0.164	4.192 ± 0.557
T1L27F1500S126		0.816 ± 0.063	4.136 ± 0.267	5.054 ± 0.772
T1L54F1500S126		0.940 ± 0.036	4.834 ± 0.438	6.872 ± 1.057
T1L74F1500S126		1.092 ± 0.084	5.256 ± 0.362	7.078 ± 0.585

Table 5. Measurements of longitudinal SR.

Tools Reference	Coated	R_a (μm)	R_z (μm)	R_t (μm)
T0L27F750S126	No	0.248 ± 0.035	1.502 ± 0.205	1.660 ± 0.196
T0L54F750S126		0.266 ± 0.055	1.614 ± 0.262	2.088 ± 0.256
T0L74F750S126		0.360 ± 0.017	1.926 ± 0.662	2.090 ± 0.931
T0L27F1500S126		0.363 ± 0.016	2.066 ± 1.099	2.440 ± 1.268
T0L54F1500S126		0.384 ± 0.050	2.192 ± 0.278	2.490 ± 0.240
T0L74F1500S126		0.432 ± 0.060	2.654 ± 0.452	2.962 ± 0.553
T1L27F750S126	Yes	0.175 ± 0.050	1.404 ± 0.582	1.574 ± 1.127
T1L54F750S126		0.334 ± 0.012	1.790 ± 0.305	1.938 ± 0.295
T1L74F750S126		0.496 ± 0.039	2.540 ± 0.709	3.230 ± 0.728
T1L27F1500S126		0.799 ± 0.079	4.488 ± 0.477	4.710 ± 0.674
T1L54F1500S126		1.054 ± 0.027	4.532 ± 0.802	4.742 ± 1.753
T1L74F1500S126		1.347 ± 0.097	4.784 ± 1.522	6.060 ± 1.555

their coated competitors, indicating that the coating has not yielded an advantage for this tool substrate.

TiAlTaN-coated tools under the $f = 1500$ m/min condition display a notable increase in R_a, comparable to the condition at $f = 750$ mm/min (Fig. 2 and Fig. 3). Furthermore, the consistent trend observed is that shorter L_{cut} values result in lower R_a values for both WC-Co and TiAlTaN-coated tools. The coating degradation is more pronounced at $L_{cut} =$

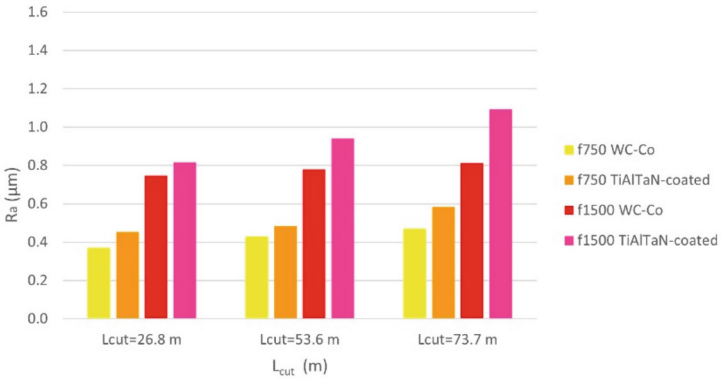

Fig. 2. R_a values in the transverse direction function of L_{cut}.

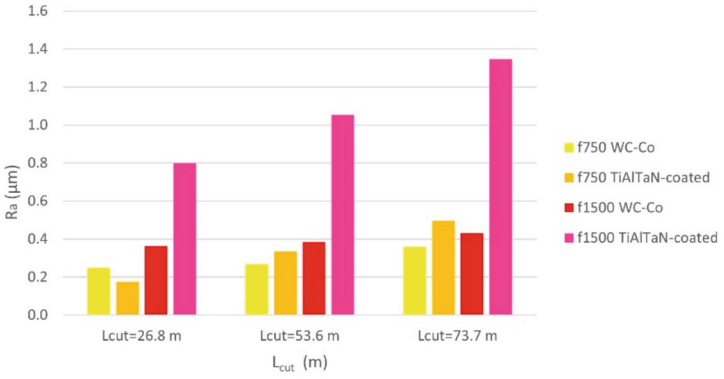

Fig. 3. R_a values in the transverse direction function of L_{cut}.

73.7 m, leading to a decline in the machined surface quality. Weak adhesive strength, $L_{C2} < 22$ N, leads to coating delamination. This separation makes tool coatings susceptible to three-body abrasion, decreasing tool performance and surface quality in machining; hence, the R_a values are so high for $f = 1500$ mm/min, in Fig. 3. It is evident from Fig. 2 and Fig. 3 that as L_{cut} increases, both in the transverse and longitudinal directions, R_a also increases [21]. For the same L_{cut}, in the case of the longitudinal direction and $f = 1500$ mm/min, there is a much more significant discrepancy between TiAlTaN-coated and WC-Co uncoated. According to [22], the SR of a machined alloy was analysed. It was also concluded that R_a increased with an increase in f, observing that, in general, the values in the transverse direction are much higher than in the longitudinal direction, which in turn can be easily explained by the fact that, during transverse measurement, the roughness gauge may have been placed between concavities or protrusions, being perpendicular to these irregularities and naturally measuring higher roughness in this direction (striae).

Analysis of F Influence on R_a

Figure 4 presents the R_a values about f and tool typology for the transverse direction. There is an apparent increase in R_a with the increase in L_{cut}. Consequently, at higher f, the uncoated WC-Co tools demonstrate superior performance as indicated by their lower Ra values than the TiAlTaN-coated tools.

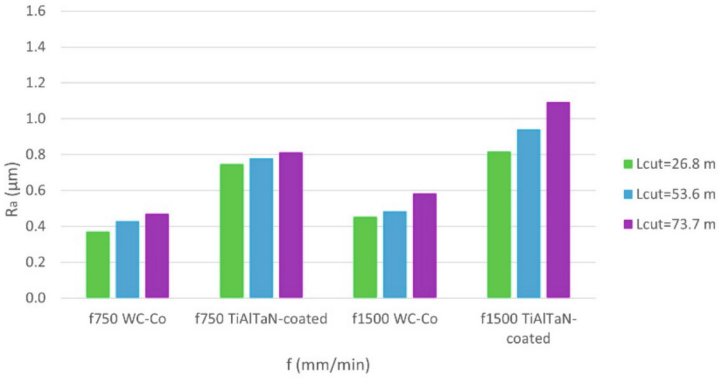

Fig. 4. R_a values in the transverse direction based on f.

An evident trend is a decrease in machined surface quality with an increase in L_{cut} in both transverse and longitudinal directions. Moreover, the transverse values consistently exceeded the longitudinal values for the WC-Co tools. Figure 5 illustrates the R_a values concerning the f and tool type for the longitudinal direction. A significant difference between feed rates of $f = 750$ mm/min and $f = 1500$ mm/min is evident for the TiAlTaN-coated tools, highlighting the detrimental impact of altering f on the coating.

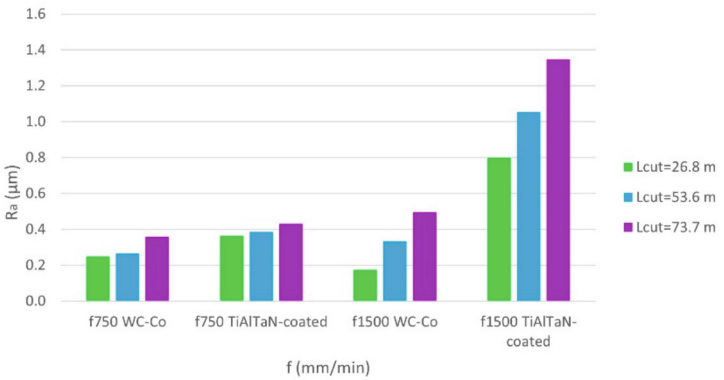

Fig. 5. R_a values in the longitudinal direction based on f.

Surface quality deteriorates with increased L_{cut}., and SR values are lower at f = 750 mm/min compared to f = 1500 mm/min. At higher f, the tool coating degrades,

causing surface irregularities due to coating delamination and more severe abrasion mechanisms, resulting in elevated R_a values. Increasing f led to higher SR for both TiAlTaN-coated and WC-Co uncoated tools in all conditions and directions; however, TiAlTaN-coated tools showed a slight advantage with shorter L_{cut} values (Fig. 5) due to the protective role of the coating when cutting AMPCO®. The same trend was observed in Fig. 5, with slightly higher SR values for TiAlTaN-coated tools at higher f and both tool types in longitudinal and transverse SR, $f = 1500$ mm/min resulted in significantly rougher surfaces compared to $f = 750$ mm/min, highlighting the impact of the f parameter on machined surface quality. In summary, the overall quality of the machined surface was satisfactory, with reasonable R_a values.

Nevertheless, doubling the f led to almost a twofold increase in R_a values, concluding that the f parameter affects the machined surface's quality [23, 24] in this experimental procedure. Notably, TiAlTaN-coated tools consistently showed higher SR values than WC-Co uncoated tools, indicating that the coating choice may not be ideal, mainly due to adhesion issues to the substrate. Thus, further investigations should consider this and increase the adhesions using an adequate interlayer. This paper is intended to be a resume of a more extensive article that encompasses the machined surface quality assessment, TW mechanisms [25], and evaluation [26].

5 Conclusions

This study assessed the impact of f and L_{cut} on the SR of both WC-Co uncoated and TiAlTaN-coated tools. The findings align with existing literature on these parameters. The results showed that f and L_{cut} influenced R_a, R_t, and R_z. The lowest values were achieved for the lower f and L_{cut} setups, indicating that higher f and L_{cut} led to poorer SR. TiAlTaN-coated tools consistently exhibited higher R_a values than WC-Co uncoated tools, likely due to coating defects and rapid degradation during use. The trends in R_a were comparable to uncoated tools but with significantly higher values, and SR was lower for lower f and L_{cut} values.

Moreover, the coating did not improve machined surface quality, resulting in high R_a values and coating cracks in several tools. These issues were attributed to poor coating adhesion and suboptimal deposition conditions. This study will significantly contribute to the endeavours of the injection mould industry in the milling of AMPCO® using TiAlTaN-coated tools, underscoring the significance of research for industrial optimisation. As for future work, performing further machining experiments, including turning and drilling for roughing and finishing tasks, would be welcoming to gain insights into the material's performance and contribute to the scientific understanding of machining alloys such as AMPCOLOY®.

Acknowledgement. The authors thank ISEP and INEGI for their support. The work is developed under the "DRIVOLUTION – Transition to the factory of the future", with the reference DRIVOLUTION C644913740-00000022 research project, supported by European Structural and Investments Funds with the "Portugal 2020" program scope.

References

1. Rouxel, B., Mischler, S., Logé, R., Igual Munoz, A.: Wear behaviour of novel copper alloy as an alternative to copper-beryllium. Wear **524–525**, 204817 (2023). https://doi.org/10.1016/j.wear.2023.204817
2. Baragetti, S., Terranova, A., Vimercati, M.: Friction behaviour evaluation in beryllium–copper threaded connections. Int. J. Mech. Sci. **51**(11), 790–796 (2009). https://doi.org/10.1016/j.ijmecsci.2009.09.004
3. Sharma, A., Joshi, S.S., Datta, D., Balasubramaniam, R.: Modeling and analysis of tool wear mechanisms in diamond turning of copper beryllium alloy. J. Manuf. Process. **56**, 439–450 (2020). https://doi.org/10.1016/j.jmapro.2020.04.053
4. International A ASTM B 194 - 15. Standard Specification for Copper-Beryllium Alloy Plate, Sheet, Strip, and Rolled Bar. American Society for Testing and Materials International, Pennsylvania (2015). https://doi.org/10.1520/B0194-15
5. Ramesh, B., Venkatesh, R., Abraham, D., Clement, S., Ronadson, B., Elayaperumal, A.: Optimization of process parameter levels during conventional milling of beryllium copper alloy using end mill. Int. J. Adv. Res. Sci. Eng. **1**, 57–63 (2013)
6. Sousa, V.F.C., Castanheira, J., Silva, F.J.G., Fecheira, J.S., Pinto, G., Baptista, A.: Wear behavior of uncoated and coated tools in milling operations of AMPCO (Cu-Be) alloy. Appl. Sci. **11**(16), 7762 (2021). https://doi.org/10.3390/app11167762
7. Campbell, F.C.: Chapter 3 - Magnesium and Beryllium. In: Campbell, F.C. (eds.) Manufacturing Technology for Aerospace Structural Materials, p. 93−118. Elsevier Science, Oxford (2006). https://doi.org/10.1016/B978-185617495-4/50003-2
8. Sharma, A., Datta, D., Balasubramaniam, R.: An investigation of tool and hard particle interaction in nanoscale cutting of copper beryllium. Comput. Mater. Sci. **145**, 208–223 (2018). https://doi.org/10.1016/j.commatsci.2018.01.011
9. Zuo, J., Lin, Y., Zhong, P., Liu, Y.: Investigation on adhesive wear process of tool coating surface under high-adhesive rate environment in cutting Beryllium-copper C17200 alloy. Mater. Lett. **279**, 128488 (2020). https://doi.org/10.1016/j.matlet.2020.128488
10. Dong, S., Wang, Z., Wang, Y., Zhang, J.: Micro-EDM drilling of high aspect ratio micro-holes and in situ surface improvement in C17200 beryllium copper alloy. J. Alloy. Compd. **727**, 1157–1164 (2017). https://doi.org/10.1016/j.jallcom.2017.08.162
11. Dong, S., Wang, Z., Wang, Y.: Research on micro-EDM with an auxiliary electrode to suppress stray-current corrosion on C17200 beryllium copper alloy in deionized water. Int. J. Adv. Manuf. Technol. **93**(1), 857–867 (2017). https://doi.org/10.1007/s00170-017-0478-8
12. Lipa, M., Durocher, A., Tivey, R., Huber, T., Schedler, B., Weigert, J.: The use of copper alloy CuCrZr as a structural material for actively cooled plasma facing and in vessel components. Fusion Eng. Des. **75–79**, 469–473 (2005). https://doi.org/10.1016/j.fusengdes.2005.06.056
13. Gallo, P., Berto, F., Lazzarin, P., Luisetto, P.: High temperature fatigue tests of Cu-be and 40CrMoV13.9 alloys. Procedia Mater. Sci. **3**, 27−32 (2014). https://doi.org/10.1016/j.mspro.2014.06.007
14. Sousa, V.F.C., Silva, F.J.G.: Recent advances on coated milling tool technology—a comprehensive review. Coatings **10**(3), 235 (2020). https://doi.org/10.3390/coatings10030235
15. Sousa, V.F.C., Da Silva, F.J.G., Pinto, G.F., Baptista, A., Alexandre, R.: Characteristics and wear mechanisms of TiAlN-based coatings for machining applications: a comprehensive review. Metals **11**(2), 260 (2021). https://doi.org/10.3390/met11020260
16. ISO ISO 3002-1:1982(E). Basic Quantities in Cutting and Grinding — Part 1: Geometry of the Active Part of Cutting Tools—General Terms, Reference Systems, Tool and Working Angles, Chip Breakers. International Organization for Standardization, Geneva (1982)

17. Silva, F.J.G., Martinho, R.P., Martins, C., Lopes, H., Gouveia, R.M.: Machining GX2CrNiMoN26-7-4 DSS alloy: wear analysis of TiAlN and TiCN/Al2O3/TiN coated carbide tools behavior in rough end milling operations. Coatings **9**(6), 392 (2019). https://doi.org/10.3390/coatings9060392
18. Martinho, R.P., Silva, F.J.G., Martins, C., Lopes, H.: Comparative study of PVD and CVD cutting tools performance in milling of duplex stainless steel. Int. J. Adv. Manuf. Technol. **102**(5), 2423–2439 (2019). https://doi.org/10.1007/s00170-019-03351-8
19. ISO ISO 21920-2:2021(E). Geometrical Product Specifications (GPS) — Surface Texture: Profile — Part 2: Terms, Definitions and Surface Texture Parameters. International Organization for Standardization, Geneva (2021)
20. Chang, W.-R., Hirvonen, M., Grönqvist, R.: The effects of cut-off length on surface roughness parameters and their correlation with transition friction. Saf. Sci. **42**(8), 755–769 (2004). https://doi.org/10.1016/j.ssci.2004.01.002
21. Buj-Corral, I., Vivancos-Calvet, J., Domínguez-Fernández, A.: Surface topography in ball-end milling processes as a function of feed per tooth and radial depth of cut. Int. J. Mach. Tools Manuf. **53**(1), 151–159 (2012). https://doi.org/10.1016/j.ijmachtools.2011.10.006
22. Wang, W., Kweon, S.H., Yang, S.H.: A study on roughness of the micro-end-milled surface produced by a miniatured machine tool. J. Mater. Process. Technol. **162–163**, 702–708 (2005). https://doi.org/10.1016/j.jmatprotec.2005.02.141
23. Hung, N.P., Zhong, Z.W., Lee, K.K., Chai, C.F.: Precision grinding and facing of copper-beryllium alloys. Precis. Eng. **23**(4), 293–304 (1999). https://doi.org/10.1016/S0141-6359(99)00024-0
24. Martinho, R.P., Silva, F.J.G., Baptista, A.P.M.: Cutting forces and wear analysis of Si3N4 diamond coated tools in high speed machining. Vacuum **82**(12), 1415–1420 (2008). https://doi.org/10.1016/j.vacuum.2008.03.065
25. Pedroso, A.F.V., et al.: A comprehensive review on the conventional and non-conventional machining and tool-wear mechanisms of INCONEL®. Metals **13**(3), 585 (2023). https://doi.org/10.3390/met13030585
26. Nogueira, F.R., et al.: A comparative study on the wear mechanisms of uncoated and TiAlTaN-coated tools used in machining AMPCO® alloy. Coatings **14**(1), 4 (2024). https://doi.org/10.3390/coatings14010004

Metrological Support of the Thermal Vision Method of Defectoscopy

Volodymyr Tonkonogyi, Maryna Holofieieva(✉), Alexandr Orgiyan, Yurii Holofieiev, and Oleksii Buriachenko

Odessa National Polytechnic University, 1, Shevchenko Avenue, Odesa 65044, Ukraine
mgolofeyeva@gmail.com

Abstract. Various non-metallic heterogeneous materials and structures are widely used in many industries. Undoubtedly, the use of such mediums and the quality of construction materials require the development of countermeasures and measurement of their parameters. The most promising are non-destructive methods, among which thermal control methods can be singled out. The article is devoted to studying the influence of mechanical stimulation parameters on the distribution of temperature fields with the acoustic infrared thermometric method of counter products made of non-metallic heterogeneous materials. This method is based on the emergence of temperature fields in materials with structural defects under the influence of vibration. Experimental studies of carbon plate defects in the form of "dull drilling" were carried out on a specially designed stand for the excitation of mechanical vibrations. The dependence of the parameters of thermal processes on the frequency of mechanical vibrations, the time of their impact, and the distance from the point of application of the vibrations to the defective zone was determined. At the same time, the temperature contrast was used as an optimization criterion, as a natural characteristic of comparing thermal control procedures. Considering the anisotropy of the physic and mechanical properties of the material under study, the control was carried out in two positions of the plate relative to the direction of propagation of mechanical oscillations: at an angle of 45° to the fibers and perpendicular to it.

Keywords: Non-Metallic Heterogeneous Materials · Non-Contact Measurement · Acoustic Infrared Thermometric Method · Defectoscopy · Metrological Support · Mechanical Stimulation · Anisotropy · R&D Investment

1 Introduction

Nowadays, we can note the increasing use of non-metallic heterogeneous media as structural materials, characterized by improved properties compared to traditional materials, such as increased vibration resistance, non-magnetism, low electrical conductivity, low weight, high rigidity and strength, and biological neutrality. It is known that replacing traditional materials with heterogeneous ones reduces the material capacity of products several times while increasing their working life and reliability. In addition, labor intensity is reduced due to improved manufacturability [1]. This makes it possible to expand

© The Author(s), under exclusive license to Springer Nature Switzerland AG 2024
V. Ivanov et al. (Eds.): DSMIE 2024, LNME, pp. 399–408, 2024.
https://doi.org/10.1007/978-3-031-61797-3_34

their use in mechanical engineering, the aerospace industry, medicine, and construction. However, the question of the quality of products from the specified class of materials arises on the way [2]. First, this refers to the presence of various defects, such as cracks, delamination, pores, and uneven distribution of the medium's components in the product's volume. The complex structure of non-metallic heterogeneous materials determines the stochastic nature of their characteristics and the anisotropy of their properties [3].

It should be noted that products made of non-metallic heterogeneous materials are complex objects of control. From the point of view of metrological support, any heterogeneous object can be interpreted as complex by increasing the number of parameters that are considered when building a model representation due to the selection of structural levels during the analysis of the physical and mechanical characteristics of the material from which the object is made. Any heterogeneous object can be represented at the microstructure, submacrostructure, and mesostructure levels, depending on the purpose and tasks of measurements for automated management [4].

Measuring the characteristics of the specified class of materials requires developing new or improving existing methods due to their specific characteristics. Undoubtedly, the most promising nowadays are non-destructive countermeasures and measurement methods, among which thermal methods can be singled out [5]. Their advantage is visibility and the absence of the need to use complex and expensive equipment. Here, the informative parameter is the distribution of thermal fields on the surface of the object of control, anomalies that can signal the presence of an artifact in the volume of the product [6].

There are passive and active methods of thermal control. Passive methods do not require stimulation of the object. Thermal energy is released in it as a result of functioning. As for active methods, they require additional energy to produce excess heat. There are different ways of stimulating thermal energy, for example, convective, optical, and ultrahigh frequency. The vibration method of excitation can be considered promising [7]. The research aims to study the influence of mechanical stimulation parameters on the distribution of temperature fields during the acoustic infrared thermometric method of counter products made of non-metallic heterogeneous materials.

2 Literature Review

It is known that temperature fields arise due to mechanical vibrations in materials (including non-metallic heterogeneous ones) with structural defects. This is due to the dissipation of vibration energy in the defective zones of the structure, especially on the cracks, and the release of excess heat in them [8]. The emergence of temperature gradients due to the transformation of mechanical energy into thermal energy is also characteristic of solid bodies' stretching, compression, and destruction [9]. Sometimes, it is possible to observe the release of thermal energy without disturbing the material's structure. Such an effect can be caused, for example, by mechanical hysteresis that occurs during cyclic loading of materials. However, within the fluidity of the material [10], significant temperature effects do not appear [11]. Another reason for releasing heat due to plastic deformation is the initiation and propagation of cracks and other types of damage. Such a process is local [12, 13].

We should also note the independence of the change in temperature in proportion to the sum of the deformations from their direction, and, accordingly, we can say that the thermoelasticity analysis does not allow us to conclude the nature and direction of the deformation [14, 15].

Considering the above, we see the perspective of using thermal methods to study and measure the characteristics of the parameters of internal processes occurring in non-metallic heterogeneous medium [16]. Thermal control methods are based on the interaction of the thermal field of the object with the heat-sensitive element, the transformation of the parameters of the studied thermal field into an electrical signal, and its transmission to the recording device [17, 18].

To date, the work of the source of thermal stimulation of defects is based on a mechanical method [19]. Its advantage over classical methods of thermal excitation is the absence of temperature changes in defect-free zones [20]. This makes it possible to reduce the signal/noise ratio and increase the accuracy of determining the location of the defect in the structure of a non-metallic heterogeneous material [21].

The implementation of the acoustic infrared thermometric method is based on the thermoelastic effect. Therefore, it is necessary to use the appropriate mechanical stimulation, the frequency of which lies within the limits of the sound and ultrasonic ranges [22].

Figure 1 shows the schematic diagram of flaw detection of products made of non-metallic heterogeneous objects using the acoustic infrared thermometric method.

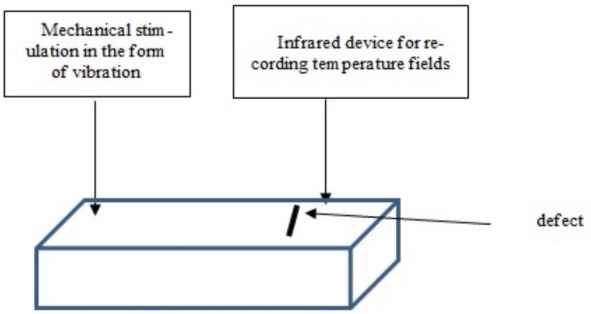

Fig. 1. Schematic diagram of flaw detection of products made of non-metallic heterogeneous objects using the acoustic infrared thermometric method.

3 Research Methodology

A series of experiments was conducted to determine the optimal conditions for the mechanical stimulation of thermal energy release on defects in the structure of non-metallic heterogeneous materials. The optimality of the mechanical influence was determined from the point of view of its duration, frequency, and direction of propagation of oscillations. At the same time, the temperature contrast $\Delta\theta$ was used as an optimization criterion, as a natural characteristic of comparing thermal control procedures.

Figure 2 shows the appearance of the developed experimental stand for the excitation of mechanical vibrations during the registration of defects in non-metallic heterogeneous materials (formation of cracks, delaminations, etc.).

Fig. 2. Appearance of the stand for excitation of mechanical vibrations during registration of defects in non-metallic heterogeneous materials.

The stand contains a cast-iron plate on which an unbalanced rotor (electric motor) is mounted. The plate is installed on four elastic-flexible support rods, which are rigidly connected to the base of the device and the plate. A sample of the tested material is pressed against the end of the plate, which can change its position relative to the striker. The striker is installed in a clamping device with the possibility of movement along the tested sample in the vertical direction to change the point of application of the shock pulse.

The impact force pulse's direction coincides with the plate's oscillations in the horizontal plane and perpendicular to the plane of the sample. In the initial position, the striker's top is tangent to the sample's surface under investigation. Figure 3 shows the basic diagram of the stand.

The PRL-6 variable speed control device ensured the change in the frequency of oscillations with a voltage change range of 127–220 V. This ensured a change in the frequency of mechanical oscillations of the plate from 15 Hz to 80 Hz. When the frequency of excitation changes, the amplitudes of plate oscillations change.

In the study of thermal processes occurring during the acoustic infrared thermometric method of flaw detection at different frequencies of mechanical oscillations, in order to ensure the same experimental conditions, preservation of the amplitude of oscillations was ensured by changing the gaps between the striker and the investigated plate. This made it possible to maintain changes in the amplitude of oscillations at a level of no more than 10–15%.

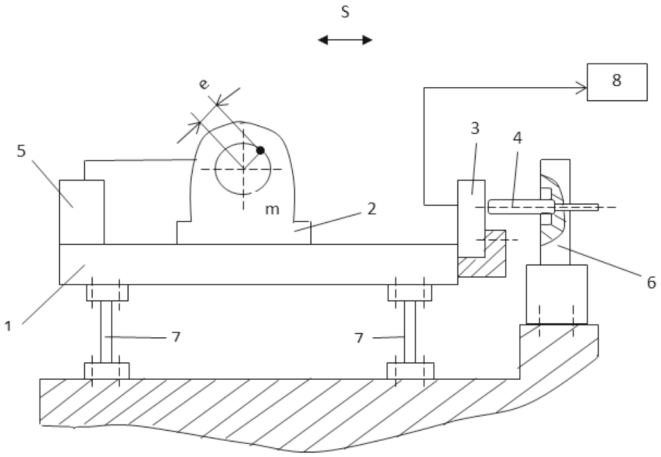

Fig. 3. Schematic diagram of the stand for excitation of mechanical vibrations during registration of defects in non-metallic heterogeneous materials: 1 – cast iron plate with dimensions of 500 × 300 × 25 mm; 2 – engine with power N = 5.5 W; 3 – sample under investigation; 4 – fight; 5 – the device for stepwise adjustment of rotation speed PRL-6; 6 – fighting body; 7 – flexible rods (4 pcs. 40 × 8 mm) located in the corners of the plate; 8 –vibration spectrum analyzer 795M.

The horizontal oscillations of the plate arise under the action of the horizontal component of the centrifugal force. In the vertical direction, plate vibrations do not occur due to the design features of the stand.

The value of the unbalanced mass and the value of the eccentricity *e* were chosen so that the amplitude of the plate vibrations in the horizontal plane varied within (0.02–0.8) mm. The amplitude of bending vibrations of the sample varied within (0.05–0.1) μm. The frequency of periodic shock excitations varied within (25–78) Hz.

Thus, the horizontal oscillations of the plate in the experiments that ensured the formation of shock pulses arose due to inertial excitation. The plate oscillations with the sample under study were recorded using a vibration spectrum analyzer 795M, in which the piezoelectric sensor AC102-1A was used as the primary transducer. Visual reproduction of oscillation oscillograms was displayed on a personal computer.

Control of experimental samples in the form of a carbon plate measuring 4 × 80 × 130 mm with defects in the form of "dull drilling" was carried out. The sample was installed on the base of the technological equipment and fixed to the experimental stand.

The distance from the point of introduction of mechanical vibrations to the defective zone of the tested platinum in each series of experiments was kept constant. Moreover, it should be noted that the temperature contrast increased as the specified distance decreased. Stimulation was carried out with packs of punches, which created periods of "heating" and "cooling down".

Considering the anisotropy of the physical and mechanical properties of the material under study (including stiffness and, accordingly, the natural frequency of oscillations), the control was carried out in two positions of the plate relative to the direction of propagation of mechanical oscillations: at an angle of 45° to the fibers and perpendicular to it.

4 Results and Discussion

The results of the research on selecting optimal parameters of mechanical stimulation of thermal energy in the acoustic infrared thermometric method of flaw detection of non-metallic heterogeneous materials are shown in Tables 1 and 2.

Table 1. Results of research at the position of plate I (propagation direction of mechanical vibrations at an angle of 45° to the fibers).

Frequency of oscillations, Hz	The measured parameter	Time of excitement, s				
		2	3	4	5	6
25	θ_d/θ_{df}	26.4/24.0	26.5/25.0	26.8/24.2	26.9/24,	26.9/24.4
	$\Delta\theta$	2.4	2.5	2.6	2.6	2.5
57	θ_d/θ_{df}	26.8/24.4	26.9/24.4	26.9/24.2	26.9/24.2	26.9/24.4
	$\Delta\theta$	2.4	2.5	2.7	2.7	2.5
78	θ_d/θ_{df}	27.1/23.7	28.2/24.2	28.2/24.3	28.2/24.5	28.2/25.0
	$\Delta\theta$	3.3	4.0	3.9	3.7	3.2

$\Delta\theta$ – the temperature difference in defective and defect-free zones.
θ_d – the temperature in the defective zone.
θ_{df} – the temperature in a defect-free zone.

For example, Fig. 4 shows thermograms obtained during control of the tested plate at a frequency of 78 Hz.

Figures 5 and 6 show the graphs obtained from the results of the studies given in Tables 1 and 2.

Table 2. Results of research at the position of plate II (the direction of propagation of mechanical vibrations perpendicular to the fibers).

Frequency of oscillations, Hz	The measured parameter	Time of excitement, s				
		2	3	4	5	6
25	θ_d/θ_{df}	28.3/25.2	29.1/25.1	29.1/25.6	29.1/25.6	29.2/25.8
	$\Delta\theta$	3.1	4.0	3.5	3.5	3.4
57	θ_d/θ_{df}	28.7/25.5	28.9/25.1	29.0/25.2	29.0/25.4	29.0/25.4
	$\Delta\theta$	3.2	3.8	3.8	3.6	3.6
78	θ_d/θ_{df}	29.0/25.6	29.1/25.6	29.3/25.7	29.3/25.7	29.4/26.1
	$\Delta\theta$	3.4	3.5	3.6	3.6	3.3

The perspective of using thermal methods of studying and measuring the characteristics of the parameters of internal processes occurring in non-metallic heterogeneous

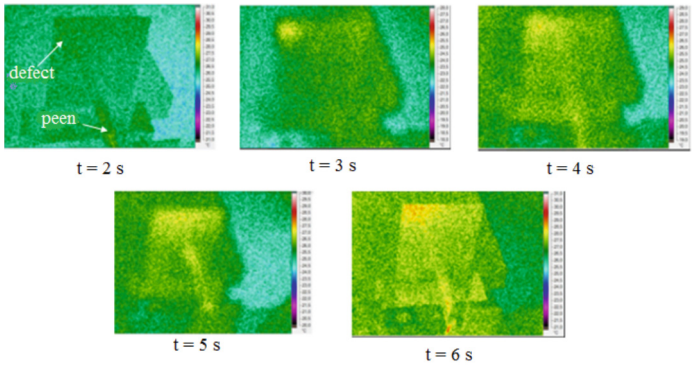

Fig. 4. Thermograms obtained during mechanical stimulation with a frequency of 78 Hz of thermal processes using the acoustic infrared thermometric method of flaw detection of a carbon plate.

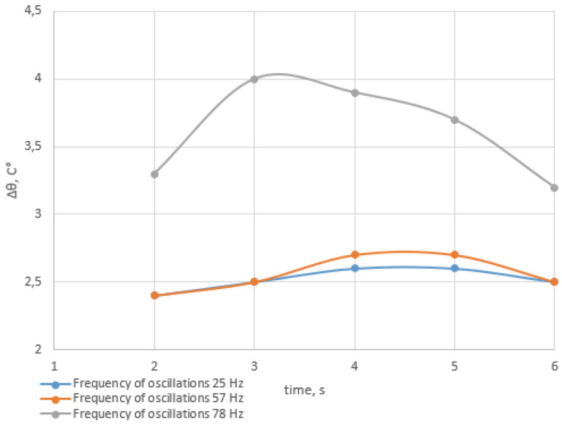

Fig. 5. Changes over time in the temperature contrast between defective and defect-free zones on the thermogram at the position of the plate I (propagation direction of mechanical vibrations at an angle of 45° to the fibers).

media is shown. The acoustic infrared thermometric method of flaw detection of products from the specified class of materials, based on the thermoelastic effect, is considered.

An experimental stand for the excitation of mechanical vibrations during the registration of defects in non-metallic heterogeneous materials (formation of cracks, delaminations, etc.) has been developed.

A series of experiments was conducted to determine the optimal conditions for the mechanical stimulation of thermal energy release on defects in the structure of non-metallic heterogeneous materials. The optimality of the mechanical influence was determined from the point of view of its duration, frequency, and direction of propagation of oscillations. At the same time, the temperature contrast $\Delta\theta$ was used as an optimization criterion, as a natural characteristic of comparing thermal control procedures.

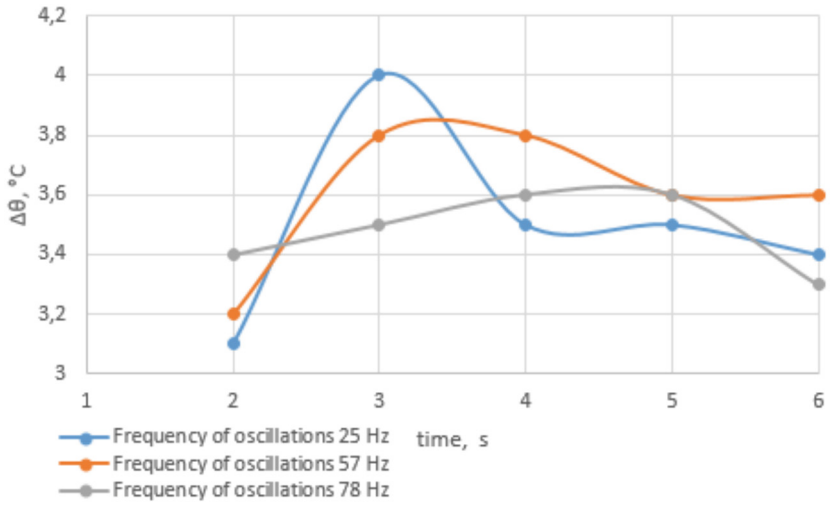

Fig. 6. Changes over time in the temperature contrast between defective and defect-free zones on the thermogram at the position of plate II (the direction of propagation of mechanical vibrations is perpendicular to the fibers).

5 Conclusions

The analysis of the results of the study of experimental samples leads to the following conclusions. The temperature difference in the defective and defect-free zones changes slightly over time, although the dependence graphs have some maxima. Accordingly, at these moments, higher visual contrasts are observed on the thermogram of the investigated surface. The decrease in $\Delta\theta$ with an increase in the time of mechanical stimulation is most likely due to a greater diffusion of thermal energy in the material (similar to how it occurs during optical stimulation).

The dependence of temperature contrast on the frequency of oscillations of mechanical stimulation of thermal processes is noted. Moreover, according to the data in Tables 1 and 2, the absolute values of the temperatures in the defective and defect-free zones slightly increase with the frequency of mechanical oscillations. This, most likely, is related to the change in the total energy of vibrations introduced into the material, which is, of course, one of the main factors that affect the amount of thermal energy released during the control of products by the acoustic infrared thermometric method. As expected, the distance from the point of their application to the defective zone is a significant factor influencing the temperature contrast between defective and defect-free zones.

It is shown that the anisotropy of the physical and mechanical properties of a non-metallic heterogeneous material in different directions of propagation of mechanical vibrations leaves an imprint on the pattern of thermal fields excited by the acoustic infrared thermometric method of flaw detection of products from the specified class of materials.

References

1. Dorofeyev, V., Pushkar, N., Zinchenko, H.: The influence of concrete structure on the destruction of reinforced concrete bended elements. In: Blikharskyy, Z. (eds.) Proceedings of Eco-Comfort 2020. LNCE, vol. 100, p. 103−111 (2021). https://doi.org/10.1007/978-3-030-57340-9_13
2. Dorofeyev, V., Myronenko, I., Pushkar, N.: The effect of technological damage on the properties and reliability of construction materials and structures. Appl. Mech. Mater. **908**, 149–156 (2022)
3. Biswas, A., Shapiro, V., Tsukanov, I.: Heterogeneous material modeling with distance fields. Computer Aided Geometric Design **21**(3), 215–242 (2004). https://doi.org/10.1016/j.cagd.2003.08.002
4. Blanter, M.S., Golovin, I.S., Neuhauser, H., Sinning, H.-R.: Internal Friction in Metallic Materials. Springer-Verlag, Berlin (2007)
5. Aliha, M.R.M., Imani, D.M., Salehi, S.M., Shojaee, M., Abedi, M.: Mixture optimization of epoxy base concrete for achieving highest fracture toughness and fracture energy values using Taguchi method. Composites Commun. **32**, 101150 (2022). https://doi.org/10.1016/j.coco.2022.101150
6. Fomin, O., Lovska, A., Khara, M., Nikolaienko, I., Lytvynenko, A., Sova, S.: Adapting the load-bearing structure of a gondola car for transporting high-temperature cargoes. Eastern-Euro. J. Enterprise Technol. **2**(7(116)), 6–13 (2022). https://doi.org/10.15587/1729-4061.2022.253770
7. Tonkonogyi, V., Holofieieva, M., Levynskyi, O., Klimov, S., Turmanidze, R.: Fractal dimension using the acoustic infrared thermal method of inspection of non-metallic heterogeneous materials. In: Tonkonogyi, V., Ivanov, V., Trojanowska, J., Oborskyi, G., Pavlenko, I. (eds.) Advanced Manufacturing Processes V. InterPartner 2023. LNME, pp. 389–398. Springer, Cham (2024). https://doi.org/10.1007/978-3-031-42778-7_36
8. Tonkonogyi, V., Holofieieva, M., Holofieiev, Y., Klimov, S., Naumenko, Y., Dašić, P.: Prediction of defects in the structure of non-metallic heterogeneous materials. J. Eng. Sci. (Ukraine) **10**(2), C19–C25 (2023). https://doi.org/10.21272/jes.2023.10(2).c3
9. Jiangang, S.: Analysis of data processing methods for pulsed thermal imaging characterisation of delaminations. Quantitative InfraRed Thermography J. **10**, 9–25 (2013). https://doi.org/10.1080/17686733.2012.757860
10. Ivchenko, O., et al.: Method for an effective selection of tools and cutting conditions during precise turning of non-alloy quality steel C45. Materials **15**(2), 505 (2022). https://doi.org/10.3390/ma15020505
11. Marani, R., Palumbo, D., Reno, V.: Modeling and classification of defects in CFRP laminates by thermal non-destructive testing. Compos. B Eng. **135**, 129–141 (2018). https://doi.org/10.1016/j.compositesb.2017.10.010
12. Vavilov, V.I., Nesteruk, D., Khorev, V.L.: Ultrasonic and inductive IR thermographic procedures as newly - emerged technigues in thermal NDT. Annual Journal of Electronics **6**(2), 102–109 (2012)
13. Buchacz, A., Baier, A., Płaczek, M., Herbuś, K., Ociepka, P., Majzner, M.: Development and analysis of a new technology of freight cars modernization. J. Vibroengineering **20**(8), 2978–2997 (2018). https://doi.org/10.21595/jve.2018.192061
14. Kainer, K.U.: Metrix Composites. Custom-made Materials for Automative and Aerospace Engineering. WILEY – VCH (2006)
15. Pavlenko, I., et al.: Using regression analysis for automated material selection in smart manufacturing. Mathematics **10**(11), 1888 (2022). https://doi.org/10.3390/math10111888

16. Maladague, X.: Theory and practice of infrared technology for nondestructive testing, Wiley Series in Microwave and Optical Engineering. John Wiley & Sons, New York (2001)
17. Ahmed, J., Gao, B., Woo, W.L.: Wavelet-Integrated alternating sparse dictionary matrix decomposition in thermal imaging cfrp defect detection. IEEE Trans. Industr. Inf. **15**(7), 4033–4043 (2019). https://doi.org/10.1109/TII.2018.2881341
18. Saeed, N., Omar, M.A., Abdulrahman, Y.: A neural network approach for quantifying defects depth, for nondestructive testing thermograms. Infrared Phys. Technol. **94**, 55–64 (2018). https://doi.org/10.1016/j.infrared.2018.08.022
19. Rao, D.S.P.: Infrared thermography and its applications in civil engineering. Indian Concrete J., 41–50 (2008)
20. Valancius, K, Skrinska, A.: Transient heat conduction process in the multilayer wall under the influence of solar radiation. In: Proceedings Improving human potential program, pp. 179–185. PSA, Almeria, Spain (2002)
21. Morgun, B., Turmanidze, R., Morgun, J., Shvahirev, P., Levynskyi, O.: Method for Measuring the temperature in the elements of a wind turbine multiplier. In: Tonkonogyi V., Ivanov V., Trojanowska J., Oborskyi G., Pavlenko I. (eds.) Advanced Manufacturing Processes II. InterPartner 2020. LNME, p. 695−703. Springer, Cham (2021). https://doi.org/10.1007/978-3-030-68014-5_67
22. Karpiuk, V., Syomina, Y., Antonova, D.: Bearing capacity of common and damaged CFRP-strengthened R. C. beams subject to high-level low-cycle loading. Mater. Sci. Forum **968**, 185−199 (2019). 10,4028/www.scientific.net/MSF.968.185

Virtual Device for Assessing the Geometric Parameters' Reliability Control for Mechanical Products Depending on the Tool Accuracy

Oleksandr Voichyshen, Serhii Patsera, Vitalii Derbaba(✉), and Oleksandr Bohdanov

Dnipro University of Technology, 19, Dmytra Yavornytskoho Avenue, 49005 Dnipro, Ukraine
tmm-univer@ukr.net

Abstract. There is an urgent need for remote tools and research methods in the current conditions of training qualified specialists for work in the engineering industry. Therefore, this work aims to create a virtual device for assessing the reliability of control of the product's geometric parameters. The Monte Carlo approach was applied jointly with the simulation of control procedures. The software environment NI LabVIEW 7.1 is used to automate the computer modeling. The virtual device opens up the possibility of predicting the range of values of the selected control reliability criterion depending on the technological forming system's accuracy. It limits the measuring device's error under certain assumptions about the type of random argument distribution. The ratio of the sum of correctly rejected and correctly accepted products to the total statistical sample is proposed as a control reliability criterion. An algorithmic model of a computer experiment was proposed. It was also implemented in the Flat Sequence Structure of the LabVIEW program, which consists of a certain number of subdiagrams or frames executed sequentially. The study aims to determine the dependence of the selected reliability criterion on the maximum permissible limit of random measurement error. Scientific novelty: graphs showing the dependence of the selected reliability criterion on the maximum permissible limit of random measurement error under specific initial data and limitations in process modeling. Practical implementation: The created virtual device allows a series of computer experiments.

Keywords: Monte Carlo Method · Reliability Criterion · Limiting Error · Computer Experiments · NI LabVIEW · Industrial Innovation

1 Introduction

The quality requirements of produced products and the accuracy requirements of measuring the size of parts are constantly increasing in modern production conditions in industries such as transport engineering, aviation, aerospace, and medicine. According to these trends, there has been a rapid development of the technical capabilities of control and measuring devices in recent years. However, this trend leads to a steady increase in measuring device costs. The task of justifying the rational choice of measuring device

© The Author(s), under exclusive license to Springer Nature Switzerland AG 2024
V. Ivanov et al. (Eds.): DSMIE 2024, LNME, pp. 409–421, 2024.
https://doi.org/10.1007/978-3-031-61797-3_35

accuracy continues to be relevant. However, there is an essential gap in the research published in recent years, which consists of the absence of methodological support for calculating the validity of control procedures concerning the geometric parameters of mechanical engineering products, which would be based on modern computer information technologies.

To solve this problem, a method for modeling and calculating a numerical criterion for the validity of control procedures on the platform NI LabVIEW has been proposed.

Structurally, the article contains an analysis of information sources, a description of the methodological approach to determining the initial data in the study, a selection of a criterion for calculating the validity of geometric parameters control, a description of software implementation both in Microsoft Excel and based on NI LabVIEW, data on the results of statistical simulation modeling of the validity of shaft diameter control.

2 Literature Review

Analysis of literature sources on the topic of this article revealed the following trends. The rapid and massive development of technology is a challenge for higher education to continue adapting and innovating to maintain academic quality [1]. The successful implementation of information technologies in higher education institutions has led to the solution of many problems, which resulted from the use of adequate conceptual models of innovation [2]. The multiple statistical simulation method (Monte Carlo) and method for assessing the deviation of a cylindrical surface of a product on a large number of measurement points are examples of such conceptual models.

For example, in the work [3], it was noted that Supplement 1 to GUM (GUM S1) has recently been proposed based on probability density functions (PDFs) using the Monte Carlo method (MCM). In order to solve the problem of the number of Monte Carlo trials needing to be selected prior, the adaptive Monte Carlo method (AMCM) described in GUM S1 is recommended to control the quality of the numerical results provided by MCM.

The advancement of measurement has led to rigorous demands for the accuracy and efficiency of roundness evaluation of minimum zone circles (MZC) for profiles with massive points [4]. The research results published in the article [5] showed that the fast hybrid roundness evaluation algorithm (HCGPSO) was accurate and improved efficiency by an average of 64%.

Monte Carlo (MC) analysis remains one of the most valuable scientific computing techniques due to its simplicity and broad applicability. MC-modeling is a probabilistic approximation method to identify uncertainty in risk assessment due to its simplicity and broad applicability [6].

In the publication [7], it was proven that when developing information technologies at extensive complex technical facilities, it is necessary, on the one hand, to minimize risks and, on the other, to set an acceptable threshold value for a specific parameter.

In the publication [8], a composite surface roughness model is considered for the first time, considering a random component's influence on the cutting tool's geometric parameters.

The mathematic models and statistical simulation methods of acceptance inspection of the components' geometries and calculation of their presorting parameters are developed. Based on the developed mathematical models, the computer modeling guidelines using the Monte Carlo presorting processes method during the acceptance inspection are compiled. The realization is carried out based on Microsoft Excel. Methodical instructions are used in academic activities. They can be used in drafting business plans for making decisions during pre-production, which is characterized by a stochastic character, including for the purposes of machinery enterprises [9].

In recent years, the constant development of computer technology has contributed to the widespread use of the program NI LabVIEW™, which should be considered as a hierarchy of "virtual instruments" [10].

For example, in the work [11], the development of hardware and software for the testing system for asynchronous motors was completed using LabVIEW. The graphical nature of LabVIEW facilitates the development of working code and allows for quick drag-and-drop built-in functions to simplify the collection, analysis, control, and exchange of data [12]. Publication [13] presents the results of developing and operating a multilayer distributed mixed virtual network laboratory (Virtual NetLab) based on LabVIEW. The work [14] focuses on demonstrating the use of a modern LabVIEWTM tool, which can help better transform the teaching and learning experience, enriching the learning process.

The book [15] shows how Fuzzy Logic Type 1 and Type 2 based on LabVIEW FPGA™ helps students studying integrated control systems design and program these controllers more efficiently and understand the benefits of using fuzzy logic in doing so. The work [16] gives step-by-step recommendations for automating measurements and creating automation systems based on LabVIEW.

The report [17] includes the LabVIEW library with tools designed for theoretical and experimental research in the field of robotics. The library contains more than 350 virtual instruments to support kinematics. The graphical programming environment LabVIEW [18] has already become a general-purpose programming environment. An efficient code execution environment is also a benefit of LabVIEW. The article [19] presents the LabVIEW Academy using the example of its implementation at the Poznań University of Technology.

To ensure that the mobile robot saved energy, using machine learning, it was ensured that it waited close to the point where more orders were coming. The developed methods were designed using the NI LabVIEW environment. By selecting the appropriate LabVIEW front panel settings, the PID controller parameters of a second-order linear system can be quickly determined [20].

Thus, as a result of analyzing the sources of information, the following methods of computer modeling of procedures for monitoring the geometric parameters of products were selected:

- Simulation method for modeling the control procedure of a geometric parameter for compliance with the tolerance field.
- Monte Carlo method for modeling random errors of a measuring instrument.
- NI LabVIEW environment for software implementation of a virtual instrument for automating computer experiments.

3 Research Methodology

3.1 Typical Accuracy Requirements for Mechanical Engineering Products

The initial data for the conducted computer experiments were:

- Typical requirements for accuracy of the cylindrical shaft surface, which is the basic element for rolling bearings (Fig. 1);
- Typical requirements of statutory documents for the measuring device's maximum error (Fig. 2).

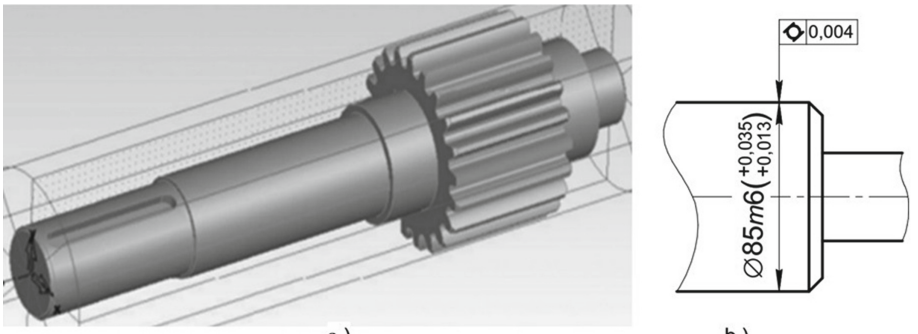

Fig. 1. Typical requirements for accuracy of the cylindrical shaft surface designed for bearings fit: a) 3D model of the shaft, b) tolerance class.

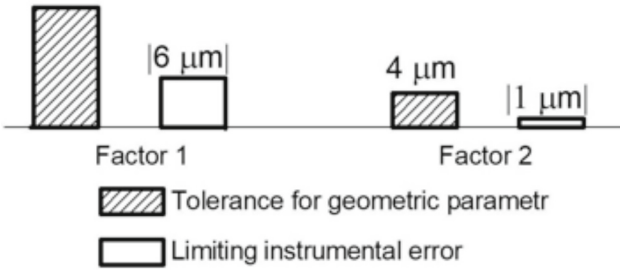

Fig. 2. Typical requirements for the maximum error value of the measuring device.

3.2 Criterion Selection for Calculating the Reliability of Geometric Parameters Control

The simulated control result was evaluated according to the conditional criterion β_*tri* as the validity indicator. If, as a result of modeling, the linear dimension of the part turns out to be such that it meets the requirements for the surface (Fig. 1), then the product's suitability is evaluated by a score $\beta_tri = 1$. Conversely, when the size falls outside

the range of the tolerance zone, then the score $\beta_tri = 0$. A logic formula was used to program the control procedure

$$IF(AND(e_tri >= ei; e_tri <= es); 1; 0), \quad (1)$$

where es and ei – the upper and lower normalized deviate of tolerance zone, according to ISO 286–1:2010,

e_tri– size deviation, obtained by Monte Carlo simulation with zero measurement error.

Using a logical formula

$$IF(AND(e_\Delta i >= ei; e_\Delta i <= es); 1; 0) \quad (2)$$

resimulation of the control procedure was carried out. In this case, $e_\Delta i$ – size deviation, obtained by Monte Carlo simulation with account for random error of the measuring device.

4 Results and Discussion

4.1 Program Implementation in Microsoft Excel

The results of statistical and simulation modeling of the control process with a slightly reduced level of technology accuracy (for descriptive reasons) and regulated maximum device error are given in Table 1. Not all lines are displayed in the given table.

Table 1. An example of the results of statistical-and-simulation modeling of the linear dimensions control procedures Ø85m6.

No	e_tri [μm]	β_tri	Δ i [μm]	$e_\Delta i$ [μm]	β_Δi	Sorting products by category			
						Accepted		Not accepted	
						Correctly accepted, (CA)	Incorrectly accepted, (IA)	Correctly rejected, (CU)	Incorrectly rejected, (IU)
1	18.0	1	1.5	19.5	1	1	0	0	0
33	12.8	0	2.7	15.5	1	0	1	0	0
73	12.6	0	−3.8	8.8	0	0	0	1	0
96	32.0	1	3.9	35.9	0	0	0	0	1
Σβ_tri [%]		97	Σ$\beta_\Delta i$ [%]		93	92	1	2	5

The measurement results are sorted into four categories: correctly accepted products (CA), incorrectly accepted products (IA), correctly rejected products (CU), and incorrectly rejected products (IU).

In this article, as a numerical criterion of control reliability, it is proposed to apply the ratio of the sum of correctly rejected and correctly accepted products to the total volume of the statistical sample according to the formula

$$RADC = (\Sigma CA + \Sigma CU)/(\Sigma CA + \Sigma IA + \Sigma CU + \Sigma IU), \tag{3}$$

where $RADC$ – designation of the numerical criterion of control reliability.

4.2 Program Implementation Based on NI LabVIEW

The software environment NI LabVIEW has proven itself perfectly in many scientific and technical projects and is a recognized international standard for data collection systems and simulation of technological procedures. This software package integrates easily into complex technical hardware-software complexes. At the same time, LabVIEW provides wide opportunities for use in the educational process along with its professional direction.

That particular property of the software environment demonstrates that the measuring device's random error when controlling the part's geometric parameter is the reason for false recognition of the part's suitability. However, actual dimensional drift is outside tolerance. Similarly, mistaken recognition of a certain number of parts, the actual dimensions of which are within the tolerance zone, as invalid takes place. Figures 3 , 4, 5, 6, 7, 8, 9, 10 and 11 shows a few program codes (with comments) for blocks of the algorithmic model.

In market research, similar categories are used, namely the risks of the manufacturer and the customer.

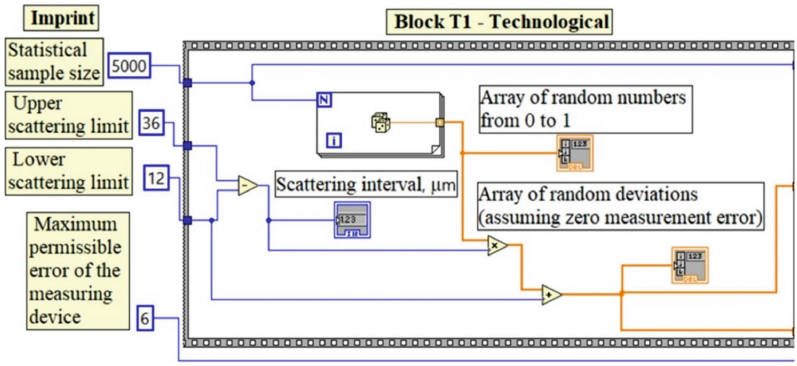

Fig. 3. Program code of the production module T1.

Figures 3 , 4, 5, 6, 7, 8, 9, 10 and 11 show the digitized algorithmic model of the virtual device developed by the authors of this work. This device aims to determine the reliability of control procedures related to the accuracy of the geometric parameters of mechanical engineering products.

In Fig. 3 on the left, the initial data entered by the virtual device user are digitized in Numeric Constant format. On the right is the program code of the processing unit, designed to simulate random deviations of the shaft journal diameter under zero measurement error.

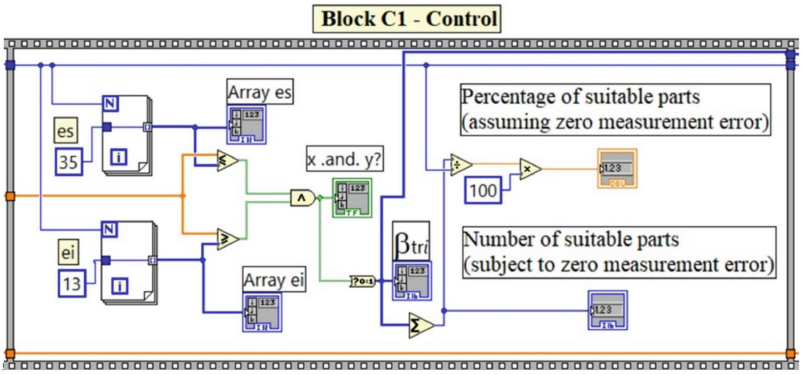

Fig. 4. Program code for modeling the control procedure and determining the proportion of suitable products evaluated by the criterion β*tri* (subject to zero measurement error).

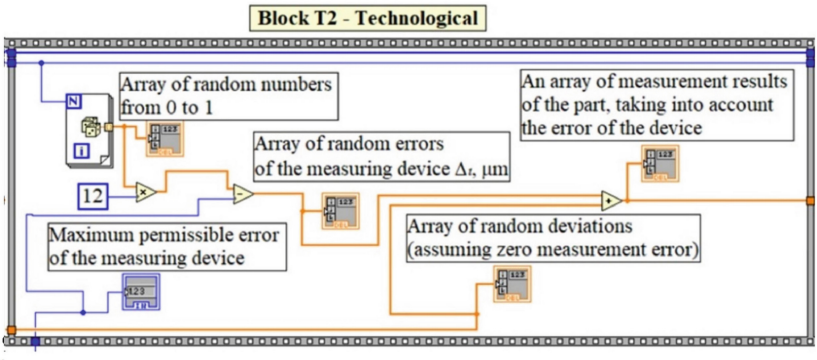

Fig. 5. The sequence of modeling the results of measurements of parts, considering the random error of measurements.

In Fig. 5, the program code is placed inside the Flat Sequence Structure and provides for the creation of an array of random numbers within the interval from 0 to 1 by the Monte Carlo method, transforming this array into an array of random measurement errors.

Figure 6 shows the code of the procedure for control and determination of the specific gravity of suitable products according to the criterion β_Δ*i* (by the presence of a measurement error).

Figure 7 shows the program code for determining the percentage of correctly accepted (CA) products using a logical formula

$$IF(AND(\beta_tri = 1; \beta_\Delta i = 1); 1; 0). \quad (4)$$

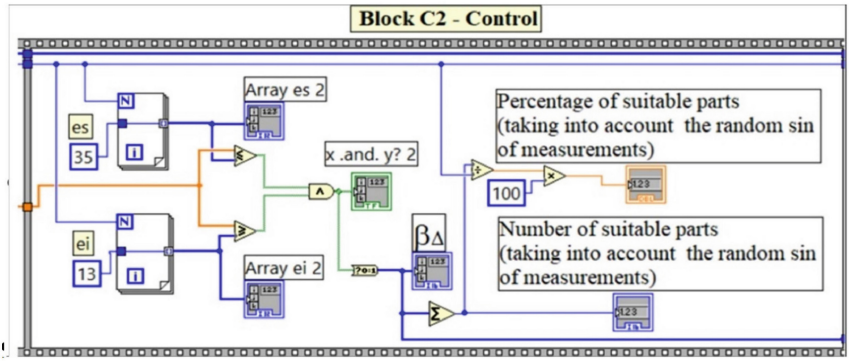

Fig. 6. Program code of the control module C2.

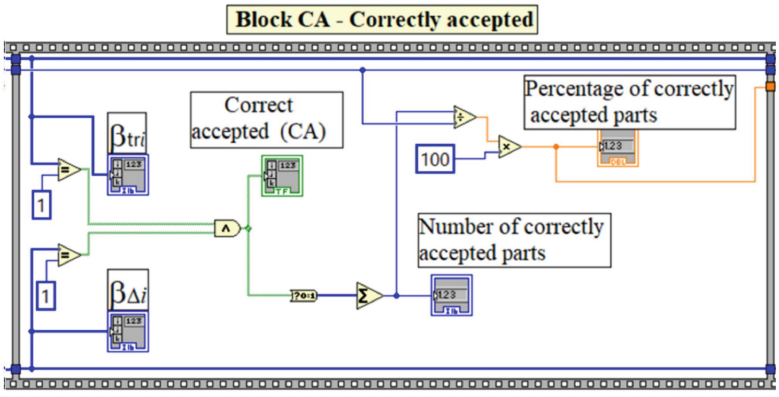

Fig. 7. Program code of the CA module – simulation of parts sorting procedure into a group of correctly accepted ones.

Figure 8 shows the program code for determining the percentage of correctly unaccepted (CU) products using a logical formula

$$IF(AND(\beta_tri = 0; \beta_\Delta i = 0); 1; 0). \tag{5}$$

Figure 9 shows the program code for determining the percentage of incorrectly accepted (IA) products using a logical formula

$$\text{Table 2.}IF(AND(\beta_tri = 0; \beta_\Delta i = 1); 1; 0). \tag{6}$$

Figure 10 shows the program code for determining the percentage of incorrectly rejected (IU) products using a logical formula

$$IF(AND(\beta_tri = 1; \beta_\Delta i = 0); 1; 0). \tag{7}$$

Figure 12 shows a general view of the front panel of the created virtual tool.

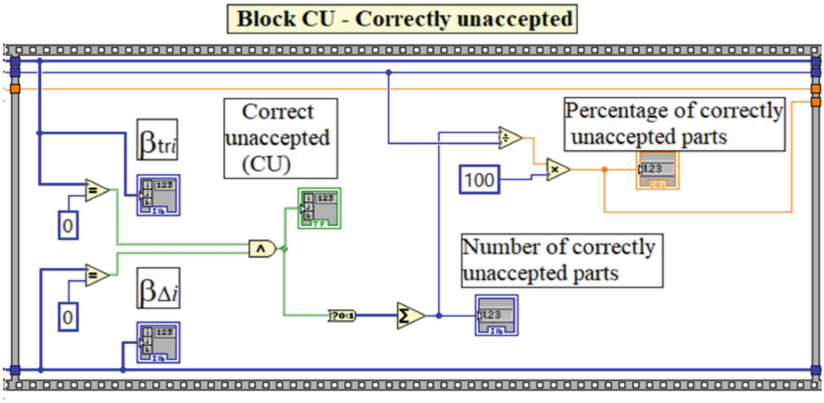

Fig. 8. Program code of the CU module – simulation of the procedure for sorting parts into a group of correctly rejected.

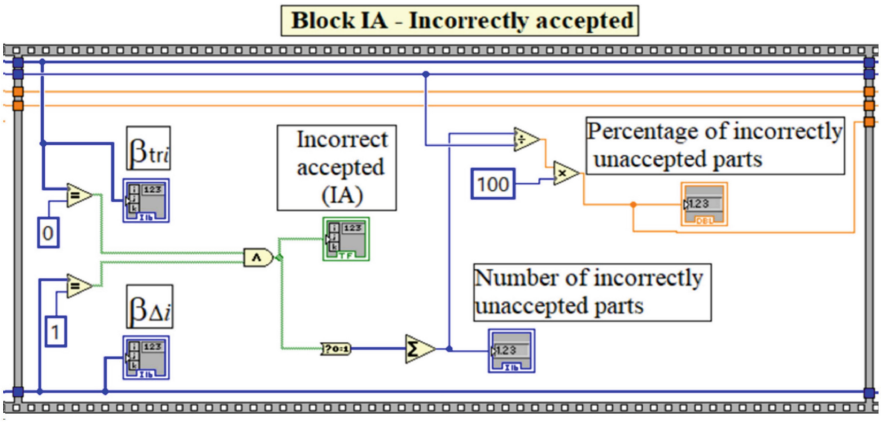

Fig. 9. Program code of the IA module – simulation of parts sorting procedure into a group of incorrectly accepted ones.

On the left side of the front panel, there are fields for introducing the initial numerical values of the modeling process parameters, and on the right are fields for displaying the results of a computer experiment: the value of the RADC criterion for the validity of control procedures and a virtual display for reproducing graph of the dependence of the specified criterion on the magnitude of measurement errors.

4.3 Results of Statistical-and-Simulation Modeling

Study results are shown in Fig. 13. The obtained control reliability dependencies for three classes of technological systems: I, N, and L – increased, normal, and reduced accuracy, respectively.

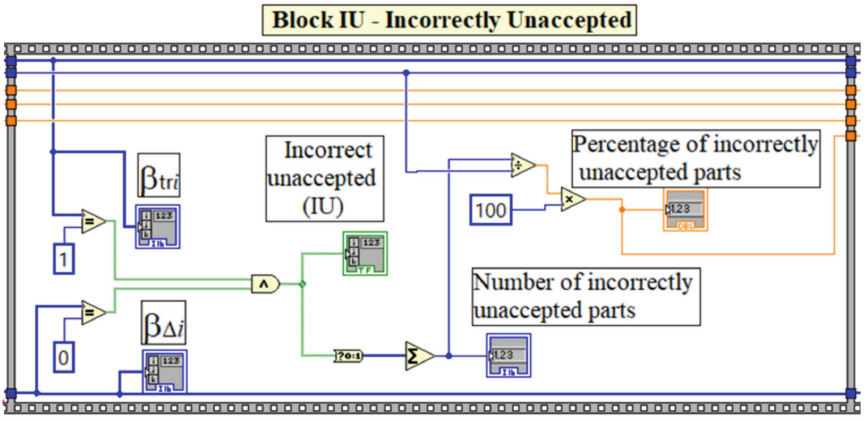

Fig. 10. Program code of the IU module – simulation of parts sorting procedure into a group of incorrectly rejected ones.

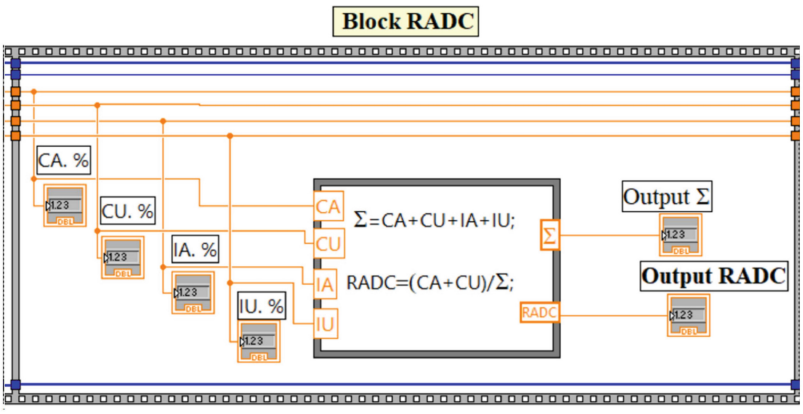

Fig. 11. Program code of the RADC module – for calculating the reliability indicator of product size control.

The validation criterion of control (RADC) is based on the indicators CA, CU, IA, IU, evidence of applicability (adequacy) of which is presented in the authors' previous article [9]. Therefore, there is reason to consider the RADC criterion to meet the applicability requirements (adequacy).

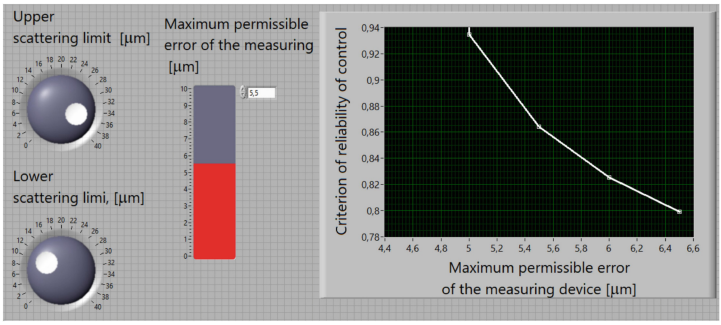

Fig. 12. A general view of the front panel of the created virtual instrument.

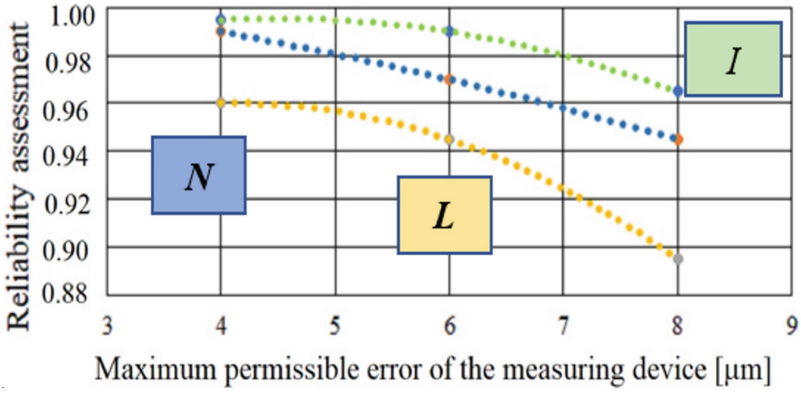

Fig. 13. The results of statistical-and-simulation modeling of the reliability of shaft diameter control.

4.4 Discussion

By comparing working hypotheses and the results of previous studies, the following positions can be identified:

Previously, graph-analytical and tabulated methods for calculating probabilistic control characteristics were used [9].

1. The mentioned methods were based on complex analytical expressions and numerous tables and graphs, which did not ensure the adequacy of calculations for scientific research.
2. To overcome these difficulties, the authors of the work [9] proposed and justified the method of statistical simulation modeling. However, this method was limited only to monitoring the geometric parameters of involute gears.
3. In addition, the work [9] does not consider the issues of automation of scientific research in this direction or the possibility of applying it to related areas of mechanical engineering.

The main directions for further research are:

1. Application of fuzzy logic methods to justify decisions regarding selecting the best virtual instrument options.
2. Clarification of the type of distribution of random measurement errors or measurement uncertainty level.

5 Conclusions

The main results and conclusions are as follows. Innovative methodological support has been created for calculating the validity of control procedures based on the geometric parameters of mechanical engineering products based on modern computer information technologies.

The ratio of the sum of correctly accepted and correctly rejected products to the total volume of the statistical sample is proposed as a numerical criterion of control reliability of geometric parameters of engineering products.

The method of modeling control procedures, originally combined with the Monte Carlo method, is applied to count the number of correctly accepted, incorrectly accepted, correctly rejected, and incorrectly rejected parts.

Determining factors affecting the reliability criterion value of control procedures were the value of the normalized limiting measurement error and the numerical value of the tolerance on the product size.

The scientific novelty lies in the graphical dependence of the selected validation criterion on the maximum permissible limit of random measurement error considering accepted limitations and initial data for modeling.

The created virtual device for assessing the control reliability of geometric parameters of engineering products depending on the tool accuracy was successfully implemented in the educational process in the preparation of MSc. in specialty 131 Applied Mechanics.

References

1. Ramdhani, M.A., Priatna, T., Maylawati, D.S., Sugilar, H., Mahmud, M., Gerhana, Y.A.: Diffusion of innovations for optimizing the information technology implementation in higher education. In: 2021 9th International Conference on Cyber and IT Service Management (CITSM), Bengkulu, Indonesia, pp. 1−8 (2021). https://doi.org/10.1109/CITSM52892.2021.9588892
2. Huda, M.Q., Sa'adah, N.U.: Measurement model of information technology implementation effectiveness. In: 2014 International Conference on Cyber and IT Service Management (CITSM), South Tangerang, Indonesia, pp. 21−24. (2014). https://doi.org/10.1109/CITSM.2014.7042168
3. Wen, X., Zhao, Y., Wang, D., Pan, J.: Adaptive Monte Carlo and GUM methods for the evaluation of measurement uncertainty of cylindricity error. Precision Eng. **37**(4), 856−864 (2013). https://doi.org/10.1016/j.precisioneng.2013.05.002
4. Liu, F., et al.: An Iterative minimum zone algorithm for assessing cylindricity deviation. Measurement 213, 112738 (2023). https://doi.org/10.1016/j.measurement.2023.112738
5. Bai, X., et al.: A fast hybrid roundness evaluation algorithm based on computational geometry and particle swarm optimization for profiles with massive points. Measurement **223**, 113798 (2023). https://doi.org/10.1016/j.measurement.2023.113798

6. Khalid, M.: Monte Carlo analysis for probabilistic risk assessment. Encyclopedia of Toxicology 4th edn. Academic Press (2023). https://doi.org/10.1016/B978-0-12-824315-2.00109-3
7. Poliarus, O., Lebedynskyi, A., Chepusenko, Y.: Method, model, and information technology for determining the value of measurement information in the interests of safety of technical objects. Bull. Kharkiv National Automobile Highway Univ. **99**, 138−145 (2022). https://doi.org/10.30977/BUL.2219-5548.2022.99.0.138
8. Bohdanov, O., Protsiv, V., Derbaba, V., Patsera, S.: Model of surface roughness in turning of shafts of traction motors of electric cars. Naukovyi Visnyk Natsionalnoho Hirnychoho Universytetu **1**, 41–45 (2020). https://doi.org/10.33271/nvngu/2020-1/041
9. Derbaba, V., Zil, V., Patsera, S.: Evaluation of the adequacy of the statistical simulation modeling method while investigating the components presorting processes. Sci. Bull. Nat. Mining Univ. **5**(143), 45–50 (2014)
10. Kodosky, J.: LabVIEW. National Instruments, USA. In: Proceedings of the ACM on Programming Languages, vol. 4, pp. 1–54 (2020). https://doi.org/10.1145/3386328
11. Song, R.Y.: Research on testing system of asynchronous motor based on LabVIEW. In: Tong, X., Liano, W. (eds.) Proceedings of the 2016 2nd International Conference on Materials Engineering and Information Technology Applications, vol. 107, p. 401−404. Atlantis Press, Paris (2017)
12. Ursutiu, D., Samoila, C., Jinga, V.: Creative developments in LabVIEW student training (Creativity Laboratory - LabVIEW Academy). In: Proceedings of 2017 4th experiment@international conference (exp. At 207), Faro, Portugal, pp. 309−312 (2017). DOI: https://doi.org/10.1109/EXPAT.2017.7984399
13. Zhao, C.X.: Study of remote experiment management based on LabVIEW. In: Sun, Q., Xu, X. (eds.) Proceedings of the 2016 International Conference on Education, Management and Computing Technology (ICEMCT 2016), Yangzhou, China, vol. 59, p. 19−23 (2016). https://doi.org/10.2991/icemct-16.2016.5
14. Patil, R.: Learning made easy By LabVIEWTM software tool. In: Natarajan, R. (eds.) In: Proceedings of the International Conference on Transformations in Engineering Education, pp. 111−121. Springer, New Delhi, India (2014). https://doi.org/10.1007/978-81-322-1931-6_16
15. Ponce-Cruz, P., Molina, A., Brian MacCleery, B.: Fuzzy Logic Type 1 and Type 2 Based on LabVIEW™ FPGA. Springer, Cham (2016). https://doi.org/10.1007/978-3-319-26656-5
16. Dubey, K., Narang, N., Negi, P., Ojha, V.: LabVIEW based Automation Guide for Microwave Measurements. Springer, Singapore (2018). https://doi.org/10.1007/978-981-10-6280-3
17. Olaru, A., S. Olaru, S., Mihai, N.: Proper Virtual LabVIEW™ Instrumentation Library for the Assisted Research in Robotics. In: 2018 6th RSI International Conference on Robotics and Mechatronics (IcRoM), Tehran, Iran, pp. 215−222 (2018). https://doi.org/10.1109/ICRoM.2018.8657550
18. Velychko, O., Kulish, Y.: Automation of measurements on the state standard of the unit of phase shift angle between two voltages. Measuring Equipment Metrol. **84**(1), 18–24 (2023). https://doi.org/10.23939/istcmtm2023.01.018
19. Pawlowski, P., Dabrowski, A., Samulnik, G.: LabVIEW Academy. Przeglad Elektrotechniczny **94**(8), 71–74 (2018). https://doi.org/10.15199/48.2018.08.19
20. Kulaç, N., Engin, M.: Developing a Machine Learning Algorithm for Service Robots in Industrial Applications **11**(421), 1–19 (2023). https://doi.org/10.3390/machines11040421

Supply Chain and Transportation

Real-Time Driver Drowsiness Detection Using Transfer Learning

P. M. Fernando[1], Ranil Sugathadasa[1], M. Mavin De Silva[1,2(✉)], Amila Thibbotuwawa[3], and T. Sivakumar[1]

[1] University of Moratuwa, Moratuwa 10400, Katubedda, Sri Lanka
mavinds@uom.lk

[2] Extreme Energy-Density Research Institute, Nagaoka University of Technology, Nagaoka, Niigata 940-2188, Japan

[3] Center for Supply Chain, Operations and Logistics Optimization, University of Moratuwa, 10400 Moratuwa, Katubedda, Sri Lanka

Abstract. Among the primary causes of traffic accidents, drowsy driving is identified, which poses a significant threat to road safety on a global scale, emphasizing the need to address this issue effectively to ensure road safety. The consequences of drowsy driving are far-reaching, impacting numerous lives and underscoring the urgent need for a real-time system capable of early and accurate detection of driver sleepiness. Addressing this critical issue, this research introduces a machine learning model to monitor driver drowsiness and classify the drowsiness status. Leveraging the advancements in Transfer Learning techniques and utilizing the ResNet50 model specifically trained for drowsiness detection. Through extensive evaluations conducted using the NTHU-DDD dataset, the proposed machine learning model has consistently demonstrated superior performance compared to recent advanced approaches in drowsiness detection. The achieved validation accuracy of 87.8% with the optimized ResNet50 model highlights the system's reliability and potential to impact road safety significantly.

Keywords: Deep Learning · Drowsiness Detection · ResNet50 · Road Safety · Process Innovation

1 Introduction

In recent years, the global demand for modern transportation has surged, leading to a significant increase in the number of vehicles on the roadway. Globally, road accidents stand out as a prominent cause of fatalities, as stated by the World Health Organization, with approximately 1.35 million lives lost each year and an additional 20 to 50 million non-fatalities occurring [1]. Driver-related factors have been identified as the primary cause of these accidents. Among the primary causes of road accidents is sleepy driving, which poses a significant threat to road safety on a global scale. Therefore, numerous drivers and pedestrians lose their lives or suffer severe injuries due to drowsy driving incidents [2].

© The Author(s), under exclusive license to Springer Nature Switzerland AG 2024
V. Ivanov et al. (Eds.): DSMIE 2024, LNME, pp. 425–436, 2024.
https://doi.org/10.1007/978-3-031-61797-3_36

Detecting driver drowsiness has become an essential methodology for preventing accidents and enhancing the performance of Driver Monitoring Systems [3], ultimately improving road safety. Drowsiness detection methods in the literature can be classified into three main categories: measurements based on vehicle parameters, physiological assessments, and computer vision approaches [4]. Vehicle-based and physiological methods are less practical for real-world applications due to the need for multiple sensors and complex data processing [5]. Computer vision techniques, particularly those based on machine learning, have shown promising results in driver drowsiness detection that often requires invasive sensors, making them less accessible and cost-effective. Using a camera, behavioral data involves capturing eye, face, and head movements. To attend the crucial challenge of driver drowsiness detection and enhance road safety, this research aims to develop a machine learning model for drowsiness detection using transfer learning techniques. In recent years, transfer learning techniques have achieved substantial attention in drowsiness detection [6]. The model can effectively extract relevant features for drowsiness detection, even with limited labeled data, leveraging the knowledge learned from the pre-training phase.

The intended research endeavors to advance the domain of detecting driver drowsiness by creating an inventive system that improves road safety through continuous real-time monitoring. By combining computer vision, machine learning, and transfer learning techniques, the proposed system has the potential to substantially decrease the number of accidents caused by drowsy drivers, ultimately saving lives while minimizing societal costs associated with road traffic crashes.

2 Literature Review

Driver safety is a paramount concern in the automotive industry, necessitating the development of robust driver detection systems. With drowsy driving being a leading cause of accidents [1], real-time monitoring of driver behavior has become essential for preventing potential collisions and ensuring road safety. The National Highway Traffic Safety Administration states that drowsy driving is accountable for many accidents yearly [7]. To address this problem, advanced driver detection classifications that can accurately identify and provide timely warnings have gained significant attention [2]. Deep learning algorithms have shown remarkable capabilities in driver detection tasks [8]. Machine learning models can effectively detect signs of drowsiness or distraction by analyzing various data sources such as facial expressions, eye movements, head pose, and physiological signals [9]. These models learn patterns and features from large-scale datasets, allowing them to generalize well and make accurate predictions in real-time scenarios [10].

The use of transfer learning in driver detection provides various advantages. Initially, it enables more efficient training of models by leveraging pre-existing knowledge [4]. Instead of training a model from scratch, transfer learning allows the use of pre-trained models as a starting point, reducing training time and computational resources. Secondly, transfer learning helps address the issue of limited labeled data, which is often a challenge in driver detection. Moreover, transfer learning facilitates the development of more robust and accurate driver detection models [9]. This enhances the reliability and performance

of the detection system, leading to more effective alerting mechanisms. However, gaps still need to be addressed to enhance the accuracy and robustness of these systems [11, 12].

As summarized in the above table, there are many researches were conducted for detecting driver drowsiness. Convolutional Neural Networks (CNNs) have garnered considerable interest in driver detection thanks to their capability to extract pertinent features from visual inputs, including facial images and eye movement data [9]. Researchers have explored various CNN architectures for driver detection, achieving impressive results. One widely used CNN architecture is the VGGNet [12]. Recurrent Neural Networks (RNNs) have shown promise in capturing temporal dependencies and sequential patterns in driver behavior data. Long Short-Term Memory (LSTM) network is one of the popular types of RNNs [14]. It utilized LSTM networks to detect driver drowsiness by analyzing eye movement data, such as eyelid closure duration, blink rate, and gaze direction [3]. Transfer learning enables the adaptation of the learned representations to a target domain with limited labeled data. This approach is precious in driver detection, where data collection and annotation can be costly and time-consuming. For instance, AlexaNet's pioneering CNN architecture has been fine-tuned to specialized driver drowsiness datasets [4]. A recent study proposed a real-time distracted driver recognition system based on visual attention analysis [9]. Domain adaptation serves as an approach in transfer learning, aiming to reduce the distribution disparity between the source and target domains [13]. By aligning the distributions of the source and target domains, the model can generalize well to the target domain with limited labeled data [6].

Furthermore, transfer learning can also be applied in a multi-task learning framework [11]. For instance, developed a predictive modeling approach for driver's lane change intention recognition using a deep learning approach [16]. They formulated where the model was trained to simultaneously predict the lane change intention and the steering angle [6, 11]. Another CNN architecture used for transfer learning is ResNet [9]. It employs residual connections, enabling the network to learn residual mappings between layers and alleviate the vanishing gradient problem. By using residual connections, ResNet can build deeper networks without sacrificing performance. While numerous studies have explored driver drowsiness detection, there remains a notable gap in research specifically employing the ResNet50 model [9]. This study aims to address this void by delving into the fine-tuning of the ResNet50 model, striving to enhance its performance and accuracy in the realm of driver drowsiness detection. In doing so, we endeavor to contribute valuable insights and advancements to this underexplored facet of research.

3 Research Methodology

The proposed architecture follows a two-step process. First, the model is trained for extracting features from input images using the ResNet50 architecture. The network is fine-tuned specifically for drowsiness classification, distinguishing between drowsy and non-drowsy states. Trained model architecture is illustrated in Fig. 1.

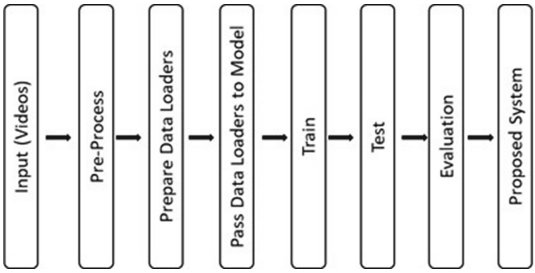

Fig. 1. Overall Architecture.

3.1 Dataset

This dataset was gathered by National Tsing Hua University's (NTHU) Computer Vision Lab (Figs. 2, 3) [16]. The dataset encompasses various subjects from diverse ethnic backgrounds, capturing their facial expressions and behaviors while simulating different driving scenarios covering regular driving, yawning, exhibiting a slow blink frequency, dozing off, and erupting in laughter.

Fig. 2. Different Behaviors of the same scenario [16].

Moreover, the dataset covers day and night illumination conditions to account for realistic driving environments. The resolution of these videos is 640x480 pixels in AVI format. The frame rates varied based on the driving scenarios: the Night Bare Face and Night Glasses scenarios were recorded at 15 fps, while the Bare Face, Glasses, and Sunglasses scenarios were recorded at 30 fps (Table 2).

The training dataset provides 18 subject folders. Each subject will contain five scenarios (with & without glasses in daylight, with & without glasses at night, with sunglasses), and each scenario will contain 4 videos with different situations and corresponding annotation files (Table 3).

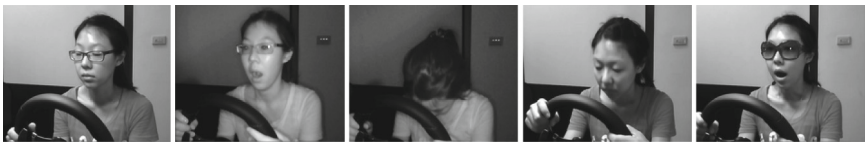

Fig. 3. Different scenarios of same behavior [16].

Table 1. Recent methods were used based on the NTHU dataset.

Methods	Accuracy
Histogram Oriented Gradient & Naïve Bayes [13]	85.62%
seven DMF [3]	83.44%
CNN LSTM [14]	75.80%
Scale-Pruned 3D CNN [8]	78.48%
RF [15]	78.70%
MSTN [13]	82.61%
Transfer Learning (AlexNet, VGG-FaceNet, FlowImageNet) [4]	85.00%
Human [13]	80.83%

Table 2. Driver Behaviors.

Behaviors	Description
Yawning	Head drops forward when feeling drowsy
Nodding	Widely open mouth due to tiredness
Looking aside	Looks in both directions, turning their head
Talking & laughing	Talking and laughing while driving
Sleepy-eyes	Closes eyes due to drowsiness
Drowsy	The driver appears sleepy and tired, with nods, slow blinks, and yawns
Stillness	Driving in a standard manner

The assessment dataset consists of four subject folders with five videos depicting different scenarios and annotation files. The videos showcase diverse situations, including transitions between drowsy and non-drowsy states. The recent access date for this database is June 2023.

3.2 Resnet50

The ResNet50 architecture, addresses the challenges of training deep neural networks by introducing residual blocks. ResNet50 consists explicitly of 50 layers, allowing for extracting intricate features and patterns from images. It delivered exceptional results in

Table 3. Four Situations of Videos.

Situation	Description
"yawning.avi"	The video contains yawning activities
"slowBlinkWithNodding.avi"	The video contains sleepy and nodding activities
"sleepyCombination.avi"	A mix of drowsy activities, such as a combination of sleepy eyes, yawning, and nodding
"nonsleepyCombination.avi"	non-drowsy behaviors such as laughing, talking, and looking aside

the ImageNet Large Scale Visual Recognition competition (Fig. 4) [17]. Fine-tuning and customization of ResNet50 will be performed to optimize its performance specifically for drowsiness classification [9].

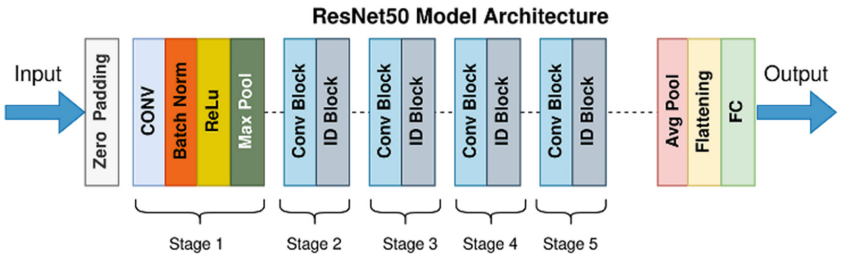

Fig. 4. ResNet50 Model Architecture [17].

3.3 Server Specifications

A lambda server with carefully chosen hardware specifications is employed to facilitate the training process of a driver drowsiness detection model. It includes a high-end Nvidia RTX A6000 GPU with substantial memory, Ubuntu 20.04.1 as the stable operating system, X86_65 CPU architecture with 14 CPUs for parallel processing, and CUDA version 12.0 for accelerated computations. This well-configured server enables efficient training, resulting in a robust and accurate driver drowsiness detection system.

4 Results and Discussion

With a particular focus on evaluating the performance of our trained model. To assess the effectiveness of our model, we utilized the widely adopted accuracy metric, which quantifies the percentage of instances correctly classified by the model. Following an extensive training process spanning 50 epochs, we achieved a commendable accuracy of 87.8%, as illustrated in Fig. 5 below.

The attainment of an accuracy of 87.8% serves as a significant milestone in our research endeavor. This metric accurately demonstrates the model's ability to classify instances within the designated classes. By correctly predicting the labels of the majority of instances, our model showcases a strong ability to comprehend and interpret the relevant features present in the dataset. The 50-epoch training process was instrumental in refining the model's predictive capacity [13]. As the training progressed, we observed a consistent enhancement in accuracy, indicating the model's capacity to adapt and improve its classification performance over time.

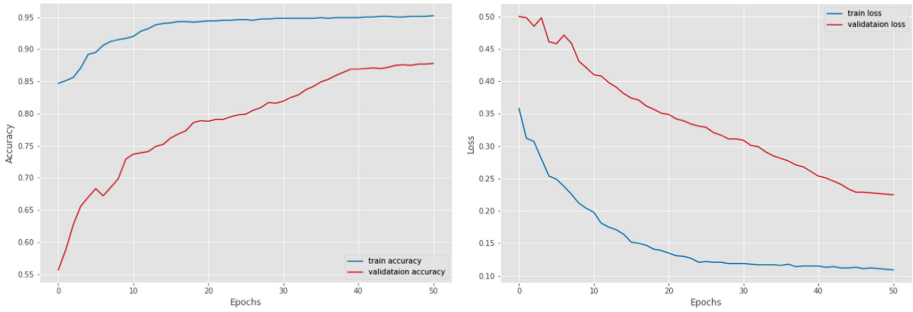

a) b)

Fig. 5. Train Accuracy (a) and Train loss and validation loss (b).

The gradual increase in accuracy suggests that the model effectively acquired knowledge from the training data, progressively refining its decision-making capabilities and successfully capturing the underlying patterns and relationships within the dataset. We also investigated the influence of different constraints and hyperparameters on the model's performance. Our experiments revealed that specific settings had a noticeable influence on the accuracy. For instance, increasing the batch size led to improved accuracy, while adjusting the learning rate affected the convergence speed. These findings highlight the importance of parameter optimization in achieving optimal performance. Considering the accuracy achieved by 87.8%, we conclude that our model has demonstrated promising results in addressing the research problem. However, there is still room for improvement, as some challenging cases resulted in misclassifications. Future research should explore advanced techniques, such as incorporating temporal information or leveraging additional data sources, to enhance the model's accuracy and robustness. In this research phase, we employed video data to estimate the model performance for driver drowsiness detection. The testing phase involved analyzing diverse videos captured in real-world driving scenarios. The images presented below depict the results obtained from our extensive testing process, providing valuable insights into the effectiveness of our model.

In Fig. 6, images 1,2,3,4 illustrate the accuracy achieved by our model in correctly classifying instances of drowsy drivers. The accuracy metric measures the percentage of correctly identified drowsy instances among all instances analyzed. Images 5,6,7,8 showcase the precision and recall values attained by our model. Precision signifies the

percentage of accurately classified non-drowsy instances to all instances classified as non-drowsy. On the other hand, recall indicates the proportion of correctly classified drowsy and non-drowsy instances out of all actual instances. Our model accomplished a 0.85 precision value and 0.92 recall value, demonstrating its ability to identify and capture instances of driver drowsiness accurately. However, as depicted in images 6 and 9, the model faced difficulties in accurately classifying frames as drowsy or nondrowsy, mainly due to drivers wearing sunglasses. Relying solely on facial features, the model needed help to detect drowsiness effectively. This limitation can be overcome by incorporating additional sensors like ECG, EOG, EMG, and HRV and utilizing their data for improved accuracy.

Fig. 6. Sample Images.

4.1 Proposed Real-Time Drowsiness Monitoring System

The system we're suggesting relies on Firebase as the database for smooth data management (see Fig. 7). Input data, which includes timestamp, latitude, longitude, and drowsy/non-drowsy values, is transmitted using arrays to ensure organized storage. Afterward, the data undergoes training in the ResNet50 model to classify inputs into either drowsy or non-drowsy states. If output 1 indicates drowsiness, OpenCV tracks and generates output 2 with time frequency. If output 2 also indicates a drowsy stage, it triggers a warning buzzer. Both output 1 and output 2 continuously update the database with time and GPS data. This database is connected to a mobile application, allowing real-time monitoring of driver drowsiness throughout their route.

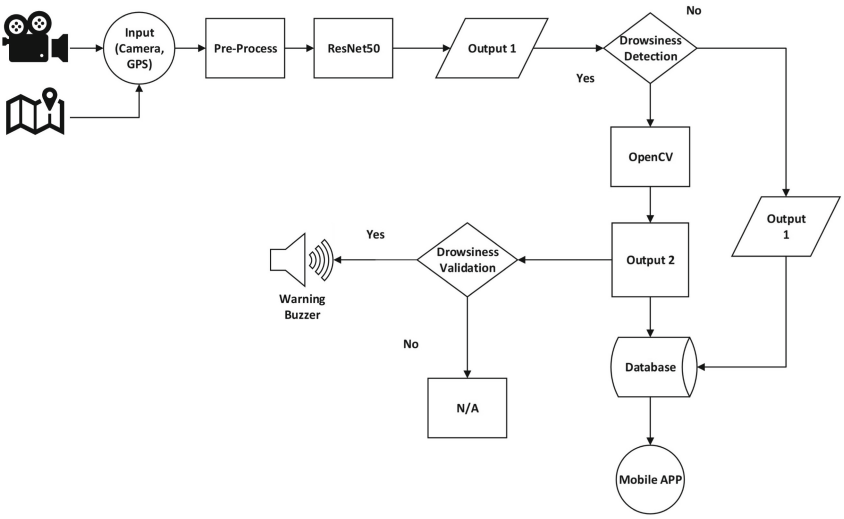

Fig. 7. Proposed Architecture.

4.2 Limitations

The proposed system acknowledges certain limitations that may affect its real-world effectiveness. One of the main concerns is the generalizability of the drowsiness detector. The ResNet50 model used for drowsiness detection is trained solely on the NTHU dataset, which may not encompass the full range of real-world driving conditions [8, 13, 18]. Incorporating diverse datasets that cover various driving conditions is recommended to improve the model's performance and generalizability. Furthermore, repetitive ambient changes that occur during driving, such as variations in lighting conditions. These changes can impact the accuracy of drowsiness detection rates. And drivers' external factors and individual characteristics should be considered for a comprehensive drowsiness detection system.

4.3 Future Direction

Incorporate External Factors and Vehicle Parameters. Integrating additional sensors is essential, considering the influence of external factors and vehicle parameters. External factors, such as varying road conditions, weather conditions, time of day, and individual driving patterns, can significantly impact driver alertness. Additionally, vehicle parameters, including speed, comfort, and driving dynamics, can be crucial in determining driver drowsiness.

Collaboration with the Automotive Industry and Regulatory Bodies. To ensure the practical implementation and widespread adoption of the drowsiness detection system, collaboration between researchers, the automotive industry, and regulators is crucial for effective and industry-compliant drowsiness detection systems. This collaborative approach enhances scientific rigor, ensures commercial viability, and facilitates real-world application.

Continuous Improvement and Updates. To enhance the accuracy and effectiveness of the system, leveraging recently developed models such as YOLOv7, ResNet101, and ResNet152 that excel in transfer learning can be advantageous.

Development of a Mobile Application. As a future direction, developing a dedicated mobile application that seamlessly integrates with the drowsiness detection system is essential. And a practical impact on road safety should be discussed.

5 Conclusions

Driver drowsiness significantly contributes to road accidents, and addressing this issue is crucial for ensuring road safety. The study has introduced an innovative system designed to mitigate accidents resulting from driver drowsiness. The proposed system leverages the power of deep learning and utilizes the ResNet50 model, which has been specifically trained for drowsiness detection. Through extensive evaluations conducted using the NTHU-DDD dataset, the proposed machine learning model has consistently demonstrated superior performance compared to recent advanced approaches in drowsiness detection. The system operates in two fundamental steps. The first step captures a continuous stream of frames, typically obtained from a camera mounted inside the vehicle. These frames are then subjected to preprocessing to extract relevant features that help accurately detect driver drowsiness. The trained ResNet50 model performs a two-class classification, determining whether the driver is drowsy or non-drowsy. Additionally, the model estimates the Real-time drowsiness percentage based on the labeled training data. To enhance the system's effectiveness, the outputs of the model and the corresponding GPS location data are stored in a Firebase database. A mobile application has been developed using React Native to facilitate real-time monitoring of driver drowsiness. This application utilizes the data stored in the Firebase database to allow users to monitor the drowsiness levels of multiple drivers throughout their routes. The application presents a comprehensive display where users can view the names of drivers and their real-time drowsiness percentages. A color-coded scheme is implemented to aid the quick identification of at-risk drivers, with green indicating non-drowsy states and red indicating drowsy states. Moreover, the mobile application offers a detailed view of drivers' drowsiness levels along their route. This feature provides real-time information on the severity and duration of drowsiness periods. Importantly, if users identify a potential risk, they can immediately contact the driver through the application. This proactive approach enables timely intervention, thus preventing potential accidents caused by driver drowsiness.

In conclusion, this research has presented a comprehensive system for driver drowsiness detection and real-time monitoring, combining deep learning techniques, Transfer Learning, mobile application development, and a Firebase database. The proposed system performs better than current methods, as substantiated by thorough evaluations of the NTHU-DDD dataset. The successful validation accuracy of 87.8% with the optimized ResNet50 model highlights the system's reliability and potential to significantly impact road safety by combining cutting-edge technologies and user-friendly mobile

applications. It empowers users to monitor and take proactive measures to prevent accidents caused by drowsy driving. The envisioned drowsiness detection system can seamlessly integrate in future iterations with external variables and vehicular parameters. By collaborating with the automotive industry, the practical usefulness of this system can be systematically evaluated. Recognizing the necessity to enhance precision and efficacy, exploring new machine learning models becomes essential. As articulated in this study, the practical viability of the mobile application monitoring system should be methodically developed. With further advancements and refinements, this system has the potential to enhance road safety and save lives significantly.

References

1. Global status report on road safety 2018. World Health Organization, Geneva (2018)
2. Said, S., AlKork, S., Beyrouthy, T., Hassan, M., Abdellatif, O.E., Fayek Abdraboo, M.: Real time eye tracking and detection- A driving assistance system. Adv. Sci. Technol. and Eng. Syst. **3**, 446–454 (2018). https://doi.org/10.25046/AJ030653
3. Bekhouche, S.E., Ruichek, Y., Dornaika, F.: Driver drowsiness detection in video sequences using hybrid selection of deep features. Knowl Based Syst. **252**, 109436 (2022). https://doi.org/10.1016/j.knosys.2022.109436
4. Muhammad, K., et al.: Deep learning for safe autonomous driving: current challenges and future directions. IEEE Trans. Intell. Trans. Syst. **22**(7), 4316–4336 (2021). https://doi.org/10.1109/TITS.2020.3032227
5. Kaplan, S., Guvensan, M.A., Yavuz, A.G., Karalurt, Y.: Driver Behavior Analysis for Safe Driving: A Survey. IEEE Trans. Intell. Transp. Syst. **16**, 3017–3032 (2015). https://doi.org/10.1109/TITS.2015.2462084
6. Ritheesh, V.R.Y., Reddy, S., Rajan, R.G.: Driver drowsiness detection and alert system using YOLO. In: 2022 International Conference on Innovative Computing, Intelligent Communication and Smart Electrical Systems (ICSES), pp. 1–6 (2022). https://doi.org/10.1109/ICSES55317.2022.9914261
7. Report a Vehicle Safety Problem. https://www.nhtsa.gov/report-a-safety-problem?gad=1&gclid=CjwKCAjw4ZWkBhA4EiwAVJXwqYoTOT2NfA3UtDkiL8-Y0ez0e7BOrR3Hi_GyGHAmgKdTgfnaY-j3pRoCiooQAvD_BwE&gclsrc=aw.ds#index, (Accessed 11 June 2023)
8. Yu, J., Park, S., Lee, S., Jeon, M.: Driver Drowsiness Detection Using Condition-Adaptive Representation Learning Framework. IEEE Trans. Intell. Transp. Syst. **20**, 4206–4218 (2019). https://doi.org/10.1109/TITS.2018.2883823
9. Dua, M., Shakshi, Singla, R., Raj, S., Jangra, A.: Deep CNN models-based ensemble approach to driver drowsiness detection. Neural Comput. Appl. **33**, 3155–3168 (2021). https://doi.org/10.1007/s00521-020-05209-7
10. Weerapura, V., Sugathadasa, R., De Silva, M.M., Nielsen, I., Thibbotuwawa, A.: Feasibility of digital twins to manage the operational risks in the production of a ready-mix concrete plant. Buildings **13**, 447 (2023). https://doi.org/10.3390/buildings13020447
11. Balam, V.P., Sameer, V.U., Chinara, S.: Automated classification system for drowsiness detection using convolutional neural network and electroencephalogram. IET Intel. Transport Syst. **15**, 514–524 (2021). https://doi.org/10.1049/ITR2.12041
12. Hashemi, M., Mirrashid, A., Shirazi, A.B.: Driver safety development real time driver drowsiness detection system based on convolutional neural network. SN Comput Sci. **1**, 289 (2020). https://doi.org/10.1007/s42979-020-00306-9

13. Bakheet, S., Al-Hamadi, A.: A Framework for instantaneous driver drowsiness detection based on improved HOG features and naïve bayesian classification. Brain Sci. **11**, 240 (2021). https://doi.org/10.3390/BRAINSCI11020240
14. Guo, J.M., Markoni, H.: Driver drowsiness detection using hybrid convolutional neural network and long short-term memory. Multimed Tools Appl. **20**, 29059–29087 (2018). https://doi.org/10.1007/S11042-018-6378-6
15. Gwak, J., Hirao, A., Shino, M.: An Investigation of early detection of driver drowsiness using ensemble machine learning based on hybrid sensing. Appl. Sci. **10**, 2890 (2020). https://doi.org/10.3390/APP10082890
16. Weng, C.-H., Lai, Y.-H., Lai, S.-H.: Driver drowsiness detection via a hierarchical temporal deep belief network. In: Chen, C.S., Lu, J., Ma, K.K. (eds.) Computer Vision – ACCV 2016 Workshops. ACCV 2016. LNCS, vol. 10118, pp. 117–133. Springer, Cham (2016). https://doi.org/10.1007/978-3-319-54526-4_9
17. Chaudhari, P., Choromanska, A., Soatto, S., Rossbroich, J., Gygax, J., Zenke, F.: Image classification based on RESNET. J. Phys. Conf .Ser. **1634**, 012110 (2020). https://doi.org/10.1088/1742-6596/1634/1/012110
18. Rami, V., Chirra, R., Reddy Uyyala, S., Krishna, V., Kolli, K.: Deep CNN: a machine learning approach for driver drowsiness detection based on eye state. Revue d'Intelligence Artificielle **33**(6), 461–466 (2019). https://doi.org/10.18280/ria.330609

Risk Assessment at Unsignalized Intersections Based on Human-Road-Environment-Vehicle System Applying Fuzzy Logic

Ievgen Medvediev[1,2], Dmitriy Muzylyov[3], Vitalii Ivanov[4,5(✉)], Jakub Montewka[1], and Justyna Trojanowska[6]

[1] Gdansk University of Technology, 11/12, Gabriela Narutowicza Street, 80-233 Gdansk, Poland
[2] Volodymyr Dahl East Ukrainian National University, 17, John Paul II Street , Kyiv 01042, Ukraine
[3] State Biotechnological University, 44, Alchevskyh Street, Kharkiv 61002, Ukraine
[4] Sumy State University, 116, Kharkivska Street, Sumy 40007, Ukraine
ivanov@tmvi.sumdu.edu.ua
[5] Technical University of Kosice, 1, Bayerova Street, 08001 Presov, Slovak Republic
[6] Poznan University of Technology, 5, M. Sklodowskej-Curie Sq., 60-965 Poznan, Poland

Abstract. The constant increase in motorization level and traffic density increases risks due to dangerous situations for road participants. Therefore, assessing the accident level of road network elements has been an urgent task over the past decades. However, existing approaches mainly rely on traffic flow parameters and account for dynamic vehicle characteristics. The research aims to design a model accounting for uncertain factors (weather conditions and pedestrian wear color) that directly impact the accident rate. For this, the mathematical toolkit of fuzzy logic is used. The study presented in this paper has yielded a model for assessing accident risk at unsignalized intersections. This model, known as the Fuzzy Model, considers various factors such as human behavior, road conditions, environmental factors, and vehicle characteristics. The model proposes accounting for the factors included in the four subsystems (Human-Road-Environment-Vehicle) that determine the transport mega system. Fuzzy Logic MATLAB Toolbox was used for modeling, and the model was assembled using Simulink Environment tools. The simulation used a full-factor experiment 3^4 for four factors at three variation levels for each parameter. A set of accident risk factors was obtained for 81 conducted tests. Based on the modeling, a 3-level table of accident risk measurement was formed at unsignalized intersections depending on the pedestrian's clothing color, intersection equipment level (illumination), weather conditions, and vehicle speed. The study results are due to a novel accident risk system that can be used for operational measures to increase safety levels at an unsignalized intersection.

Keywords: Sustainable Traffic · Pedestrian · Wear Colors · Car · Safety · Highway · Road · Risk Factor · Fuzzy Model · Sustainable Supply Chain

© The Author(s), under exclusive license to Springer Nature Switzerland AG 2024
V. Ivanov et al. (Eds.): DSMIE 2024, LNME, pp. 437–448, 2024.
https://doi.org/10.1007/978-3-031-61797-3_37

1 Introduction

Establishing the accident level in advance could be the initial step to assessing road safety. Thus, it becomes possible to implement appropriate technical measures to improve traffic safety. It is significant for unsignalized intersections or complex traffic junctions.

However, current accident assessment methods primarily consider traffic management factors, traffic flow parameters, vehicle conditions, and driver ergonomics. A more advanced system of estimated parameters is used less often. Only factors that can be quantified using technical means of traffic monitoring or the behavior and psychophysiological state of the driver are considered [1–3]. Existing approaches are based on data that does not imply possible fuzziness in the original database [4–6]. Expressing non-quantitative factors affecting safety in a clearer coordinate system is possible [7]. Therefore, the current assessment systems only consider some relevant factors.

The study proposes a fuzzy inference model that considers classical and fuzzy p variables based on the Human-Road-Environment-Vehicle System (HREVS). The research objectives are to design a fuzzy model that assesses the risk level of accidents at unsignalized intersections based on HREVS elements.

2 Literature Review

As part of modeling accident risks, fuzzy logic was used to assess the safety of traffic participants, with pedestrian clothing color being considered a significant factor. For this, a system of new indicators was used: behavioral psychology of pedestrians and drivers with intuitive methods. This was an innovative idea in modeling the risk of an accident using a fuzzy intuitionistic theory that allows you to assess indecision in pedestrians flexibly' and drivers' behavior [8].

Turkish scientists have demonstrated how a fuzzy inference system can provide drivers with real-time hazard risk information. The designed model considers the frequency of accidents, technical characteristics of tires, and weather conditions [9]. Unfortunately, this model does not show accident risk based on the characteristics of pedestrian flows.

When assessing accident risk, various methods are used, including fuzzy logic, neural network modeling, and linear methods. Similar models predict the relationship between capacity and state of roads under various weather-climatic conditions with the risk of road disasters [10]. Hazard risk consideration based on machine learning when considering driver behavior as a black box system is shown in the study [11]. The new approach is to assess the risks of traffic jams or accidents on the road when organizing network interaction between unmanned vehicles. When managing risks, processing a large amount of data is crucial, especially when received intensively [13].

Several developments have the application aspect of applying a fuzzy inference model. The study [14] presents an example of using fuzzy logic for micro-simulation modeling and risk assessment based on weather and traffic volume data. The dependence of the driving risk is assessed in the study [15] according to intelligent accident prevention, which a fuzzy model of traffic parameters assesses. An expert assessment system of fuzzy inference is used when assessing road accident risk due to the pedestrians'

ontology, considering their location, speed, and movement trajectories [16]. Study [17] presents a model of fuzzy output with the possibility of predicting risk depending on traffic parameters and highway characteristics, but weather conditions and time of day should be considered.

Several studies allow for the prediction of emergency risk depending on the road infrastructure [18 – 20], the occurrence of traffic jams in highway sections [21], and the use of a multi-criteria model [22]. Models designed due to fuzzy logic are used for the same approaches [23, 24].

Through a literature review, it has been identified that there are current knowledge gaps in the development of a fuzzy model capable of assessing the risk of accidents. These gaps mainly apply to road sections without a focus on prevention, assessing the risk based on one or two subsystem parameters of the Human-Road-Environment-Vehicle System, and considering the subject's or pedestrian's behavior separately. The main issue of current knowledge in risk assessment for road traffic tasks is that the existing solutions need to allow consideration of datasets of various nature, none for a proper account of data uncertainty.

Thus, the need for development is justified, and the novelty of the proposed fuzzy model, which will comprehensively consider each HREVS element when assessing the accident risk in unsignalized intersections, is emphasized.

3 Research Methodology

Using fuzzy logic to assess the risks of accidents at unsignalized road intersections offers several advantages. Firstly, it reduces the impact of data uncertainty on the response function when considering the causes of risk occurrence. Secondly, it enables using different variables to establish a pattern of influence on the response function. Finally, fuzzy logic provides better evaluation results by allowing linguistic variables to describe factors that are not easily quantified.

In the study, we understand the risk definition as follows: risk is uncertainty about and severity of the consequence of dangerous situations or accidents at road networks due to HERVS concerning safety at unsignalized road intersections. Therefore, the accident risk on unsignalized intersections, R_a, due to HREVS factors is written in mathematical form as follows:

$$R_a = f(HREVS), \tag{1}$$

where *HREVS* - Human-Road-Environment-Vehicle system factors determine the accident rate at unsignalized road crossings.

The following three main tasks should be resolved to achieve the study objectives:

- selection of one factor from each subsystem characterizing the Human-Road-Environment-Vehicle System, which has the highest impact level on the accident risk occurrence at unsignalized intersections;
- a fuzzy model designed for accident risk assessment at unsignalized intersections based on the mathematical formalization of fuzzy inference according to the Mamdani algorithm;

– Approach development to accident risk assessment at unsignalized intersections based on fuzzy model modeling results, considering the HREVS elements.

To justify the selection of impact factors on the accident risk at unsignalized intersections, a diagram of traffic dependence on the HREVS subsystems (Fig. 1) was designed.

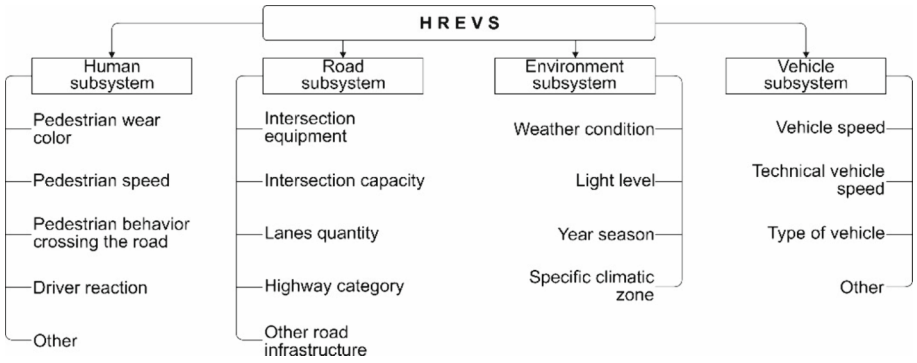

Fig. 1. Human-Road-Environment-Vehicle System Influencing Factors on Accident Risk at Unsignalized Intersections.

The most sensitive (most important) factors are selected from each HREVS subsystem due to previous studies that justify the significance of their impacts on the response function (risk assessment of accidents at unsignalized road intersections). The following part of the paper provides explanations for choosing each factor. The future-designed fuzzy model could help to establish the individual and collective significance of input variables to the accident risk, using it as a response function.

In the human subsystem, one factor determining a crash's severity is the color and brightness of road users' clothes [25]. Significantly, pedestrian clothing increases the accident risk at intersections due to road sections' insufficient illumination. Because it seems problematic to set the level linearly depending on the clothes' color using standard approaches, the study proposes considering pedestrian wear color as the first input parameter in the fuzzy model. The impact rate of pedestrians' clothes color and brightness on the accident risk, accounting fuzzy logic theory, can be traced to.

In the "Road" subsystem, one of the main factors affecting pedestrian safety is the intersection equipment and other related parameters of the road infrastructure [26, 27]. Therefore, the intersection equipment level is used as the second input parameter for a fuzzy model. Hence, fuzzy logic shows the impact of this indicator on accident risk in Fig. 3.

That's why intersection equipment should use modern controllers to monitor road conditions and display warning signs, increasing safety. However, advanced equipment is only used on main highways, which allows not only to inform drivers but also to regulate traffic parameters (flow speed, density, and direction). The intersection illumination also plays a significant role, especially in the lack of visibility.

Fig. 2. Impact pedestrian wear color on the risk of accident.

Fig. 3. Impact intersection equipment on the risk of accident.

Weather conditions, as a critical factor in the environmental subsystem, significantly affect the risk of accidents. This indicator is not explicitly expressed in quantitative equivalent. However, its failure to consider reduces the objectivity of existing estimates. A statistical experiment has proven that car crashes increase from 71% to 84% in the case of rain and reduced visibility [28]. Therefore, weather conditions (Fig. 4) are considered as a third input parameter when developing a fuzzy model.

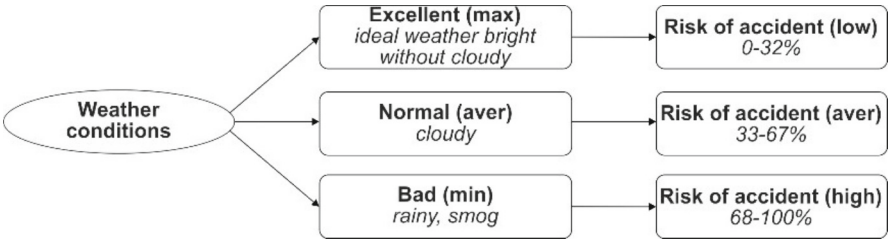

Fig. 4. Impact of weather conditions on the risk of accident.

The vehicle speed predetermines the emergency risk on the road in the first place. Therefore, this indicator is necessary for any model that assesses the possibility of an emergency on the road. The selection of the speed factor is reasonable because it is the primary indicator of a vehicle's dynamics. This factor linearly influences the probability of an accident, meaning that increased speed decreases safety.

The dependence of accident level on vehicle speed due to fuzzy logic theory is depicted in Fig. 5.

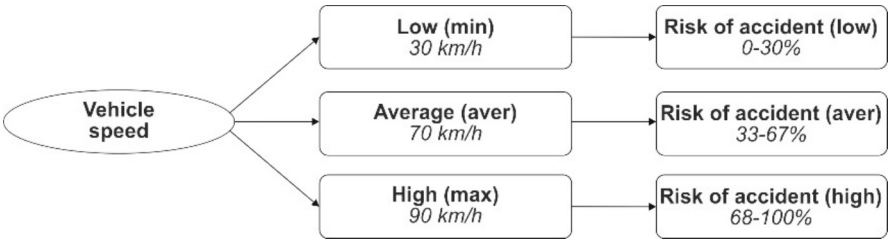

Fig. 5. Impact vehicle speed on the risk of accident.

The risk definition given in formula (1) may be specified as follows, due to Figs. 2, 3, 4 and 5:

$$R_a = f(PWC, VS, WC, IE) \tag{2}$$

where *PWC* - The "Human" subsystem factor that considers the pedestrian attire color; *VS* - the "Vehicle" subsystem factor considering vehicle speed, [km/hour]; *WC* - Environmental subsystem factor, which takes into account weather conditions; *IE* - factor of the Road subsystem, taking into account the level of the intersection equipment, [unit].

The following modeling framework can describe the investigation technology, Fig. 5.

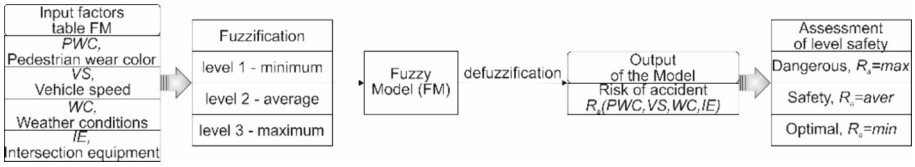

Fig. 6. Modelling framework.

To assess the relationships between linguistic variables that determine the level of variation for each incoming factor, the following conceptual scheme (Fig. 7) is designed on the accident risk value as a response function:

The Mamdani algorithm is used as a fuzzy inference model for generating the rules displaying dependence of the output parameter (target function), R_a, on the input model indicators (*PWC*, *VS*, *WC*, *IE*). In this case, the mathematical formulation of fuzzy inference for a fuzzy model in general is presented as:

$$IF\ PWC\ is\ ...AND\ IE\ is...AND\ VS\ is...AND\ WC\ is...THEN\ Ra\ is... \tag{3}$$

The Fuzzy Model architecture was assembled in MATLAB Simulink according to the research framework (Fig. 6) and the conceptual diagram of the relationship of input parameters with the response function (Fig. 7). Structurally, the model is presented in the MATLAB modeling environment in Fig. 8.

Modeling involves considering all possible variation levels for each input factor. Since there are four input parameters with three levels of variation each, a complete 3^4-factorial experiment is required to assess all possible accident risk situations. The

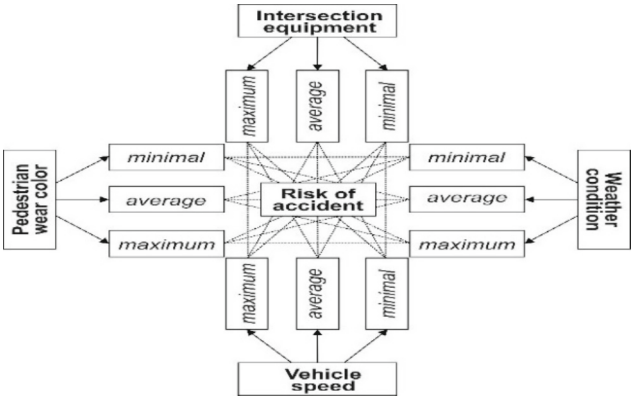

Fig. 7. Conceptual scheme of relationships between input factors and risk accidents.

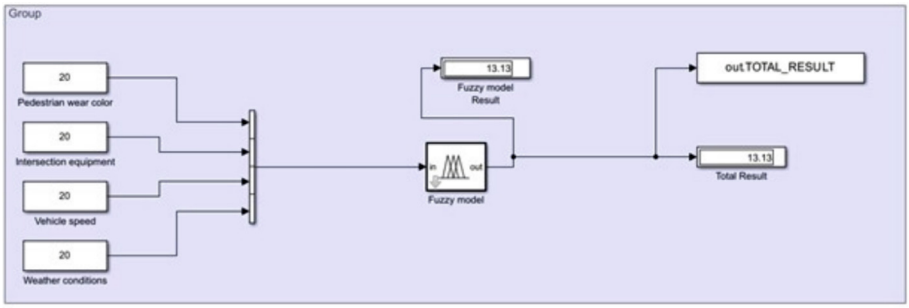

Fig. 8. Fuzzy Model Architecture assembled by Simulink MATLAB.

fuzzy inference rule set for 81 tests according to Experiment Plan 3^4 is generated using the Fuzzy MATLAB Toolbox (Fig. 9).

The rules of fuzzy output presented make it possible to determine the value of the accident risk on unsignalized intersections. This indicator defines the safety level depending on the input parameters.

It is important to note that the model's practical implementation relies on simulated rules. The set of fuzzy inference rules presented in Fig. 8 considers all possible situations where input factors affect the likelihood of risk occurring at an unsignalized road intersection. By incorporating a fuzzy model based on these rules into an automatic road monitoring system, it becomes possible to respond quickly to any changes in the situation and adjust the operating conditions of the traffic flow around the intersection.

Let's take the example of a pedestrian crossing an intersection to understand modeling principles better. If the pedestrian's clothes are dark, the intersection is poorly lit, and the car is moving at 30 km/h or less with good weather conditions, the risk of accidents is low. This is because the positive values of the other two balance out the negative impact of the first two factors. Similar scenarios exist for each situation, and each group's risk values are presented in the Results and Discussion section.

	Rule	Weight	Name
1	If pwc is min and ie is min and vs is min and wc is min then ra is min	1	rule1
2	If pwc is aver and ie is min and vs is min and wc is min then ra is min	1	rule2
3	If pwc is max and ie is min and vs is min and wc is min then ra is min	1	rule3
4	If pwc is min and ie is aver and vs is min and wc is min then ra is min	1	rule4
5	If pwc is aver and ie is aver and vs is min and wc is min then ra is aver	1	rule5
6	If pwc is max and ie is aver and vs is min and wc is min then ra is aver	1	rule6
7	If pwc is min and ie is max and vs is min and wc is min then ra is min	1	rule7
8	If pwc is aver and ie is max and vs is min and wc is min then ra is min	1	rule8
9	If pwc is max and ie is max and vs is min and wc is min then ra is aver	1	rule9
10	If pwc is min and ie is min and vs is aver and wc is min then ra is min	1	rule10
11	If pwc is aver and ie is min and vs is aver and wc is min then ra is aver	1	rule11
12	If pwc is max and ie is min and vs is aver and wc is min then ra is aver	1	rule12
13	If pwc is min and ie is aver and vs is aver and wc is min then ra is min	1	rule13
14	If pwc is aver and ie is aver and vs is aver and wc is min then ra is aver	1	rule14
15	If pwc is max and ie is aver and vs is aver and wc is min then ra is aver	1	rule15
16	If pwc is min and ie is max and vs is aver and wc is min then ra is aver	1	rule16
17	If pwc is aver and ie is max and vs is aver and wc is min then ra is aver	1	rule17
18	If pwc is max and ie is max and vs is aver and wc is min then ra is aver	1	rule18
19	If pwc is min and ie is min and vs is max and wc is min then ra is min	1	rule19
20	If pwc is aver and ie is min and vs is max and wc is min then ra is aver	1	rule20
21	If pwc is max and ie is min and vs is max and wc is min then ra is aver	1	rule21
22	If pwc is min and ie is aver and vs is max and wc is min then ra is aver	1	rule22
23	If pwc is aver and ie is aver and vs is max and wc is min then ra is aver	1	rule23
24	If pwc is max and ie is aver and vs is max and wc is min then ra is max	1	rule24
25	If pwc is min and ie is max and vs is max and wc is min then ra is aver	1	rule25
26	If pwc is aver and ie is max and vs is max and wc is min then ra is max	1	rule26
27	If pwc is max and ie is max and vs is max and wc is min then ra is max	1	rule27
28	If pwc is min and ie is min and vs is min and wc is aver then ra is min	1	rule28
29	If pwc is aver and ie is min and vs is min and wc is aver then ra is aver	1	rule29
30	If pwc is max and ie is min and vs is min and wc is aver then ra is aver	1	rule30
31	If pwc is min and ie is aver and vs is min and wc is aver then ra is min	1	rule31
32	If pwc is aver and ie is aver and vs is min and wc is aver then ra is aver	1	rule32
33	If pwc is max and ie is aver and vs is min and wc is aver then ra is aver	1	rule33
34	If pwc is min and ie is max and vs is min and wc is aver then ra is aver	1	rule34
35	If pwc is aver and ie is max and vs is min and wc is aver then ra is aver	1	rule35
36	If pwc is max and ie is max and vs is min and wc is aver then ra is aver	1	rule36
37	If pwc is min and ie is min and vs is aver and wc is aver then ra is min	1	rule37
38	If pwc is aver and ie is min and vs is aver and wc is aver then ra is aver	1	rule38
39	If pwc is max and ie is min and vs is aver and wc is aver then ra is aver	1	rule39
40	If pwc is min and ie is aver and vs is aver and wc is aver then ra is aver	1	rule40
41	If pwc is aver and ie is aver and vs is aver and wc is aver then ra is aver	1	rule41
42	If pwc is max and ie is aver and vs is aver and wc is aver then ra is aver	1	rule42
43	If pwc is min and ie is max and vs is aver and wc is aver then ra is max	1	rule43
44	If pwc is aver and ie is max and vs is aver and wc is aver then ra is max	1	rule44
45	If pwc is max and ie is max and vs is aver and wc is aver then ra is max	1	rule45
46	If pwc is min and ie is min and vs is max and wc is aver then ra is aver	1	rule46
47	If pwc is aver and ie is min and vs is max and wc is aver then ra is aver	1	rule47
48	If pwc is max and ie is min and vs is max and wc is aver then ra is aver	1	rule48
49	If pwc is min and ie is aver and vs is max and wc is aver then ra is max	1	rule49
50	If pwc is aver and ie is aver and vs is max and wc is aver then ra is max	1	rule50
51	If pwc is max and ie is aver and vs is max and wc is aver then ra is max	1	rule51
52	If pwc is min and ie is max and vs is max and wc is aver then ra is max	1	rule52
53	If pwc is aver and ie is max and vs is max and wc is aver then ra is max	1	rule53
54	If pwc is max and ie is max and vs is max and wc is aver then ra is max	1	rule54
55	If pwc is min and ie is min and vs is min and wc is max then ra is min	1	rule55
56	If pwc is aver and ie is min and vs is min and wc is max then ra is aver	1	rule56
57	If pwc is max and ie is min and vs is min and wc is max then ra is aver	1	rule57
58	If pwc is min and ie is aver and vs is min and wc is max then ra is aver	1	rule58
59	If pwc is aver and ie is aver and vs is min and wc is max then ra is aver	1	rule59
60	If pwc is max and ie is aver and vs is min and wc is max then ra is min	1	rule60
61	If pwc is min and ie is max and vs is min and wc is max then ra is aver	1	rule61
62	If pwc is aver and ie is max and vs is min and wc is max then ra is max	1	rule62
63	If pwc is max and ie is max and vs is min and wc is max then ra is max	1	rule63
64	If pwc is min and ie is min and vs is aver and wc is max then ra is aver	1	rule64
65	If pwc is aver and ie is min and vs is aver and wc is max then ra is aver	1	rule65
66	If pwc is max and ie is min and vs is aver and wc is max then ra is aver	1	rule66
67	If pwc is min and ie is aver and vs is aver and wc is max then ra is aver	1	rule67
68	If pwc is aver and ie is aver and vs is aver and wc is max then ra is aver	1	rule68
69	If pwc is max and ie is aver and vs is aver and wc is max then ra is max	1	rule69
70	If pwc is min and ie is max and vs is aver and wc is max then ra is max	1	rule70
71	If pwc is aver and ie is max and vs is aver and wc is max then ra is max	1	rule71
72	If pwc is max and ie is max and vs is aver and wc is max then ra is max	1	rule72
73	If pwc is min and ie is min and vs is max and wc is max then ra is aver	1	rule73
74	If pwc is aver and ie is min and vs is max and wc is max then ra is max	1	rule74
75	If pwc is max and ie is min and vs is max and wc is max then ra is max	1	rule75
76	If pwc is min and ie is aver and vs is max and wc is max then ra is max	1	rule76
77	If pwc is aver and ie is aver and vs is max and wc is max then ra is max	1	rule77
78	If pwc is max and ie is aver and vs is max and wc is max then ra is max	1	rule78
79	If pwc is min and ie is max and vs is max and wc is max then ra is max	1	rule79
80	If pwc is aver and ie is max and vs is max and wc is max then ra is max	1	rule80
81	If pwc is max and ie is max and vs is max and wc is max then ra is max	1	rule81

Fig. 9. Rules of Fuzzy Inference according to modeling by MATLAB.

4 Results and Discussion

Based on modeling results in the MATLAB environment, surfaces of impact on the accident risk value were designed for each pair of incoming HREVS factors. The factor "Pedestrian wear color" is characterized by significant uncertainty, but it is difficult to predict using probabilistic methods. After all, it is pretty challenging to predict the clothes the pedestrian will wear. It is especially problematic for specific road sections. Therefore, the dispatcher responsible for monitoring the road situation can only react promptly to the impact of this factor. Figure 10 depicts the dependence of the pedestrian wear color effect in combination with other factors (weather conditions, vehicle speed, and intersection equipment) on the risk of an emergency at an unsignalized intersection.

The accident risk value increases slightly when the "Pedestrian wear color", *PWC*, the input value is low. This tendency is displayed in Fig. 10(a)-Fig. 10 (c). This fact corresponds with logic and previous statistical studies that justify that the brighter the color of wear (the minimum *PWC* level in the fuzzy model), the better pedestrian identification on the road. Therefore, we achieve a higher safety level. This fact confirms the validity of the results obtained from a fuzzy model when assessing accident risk.

Due to 81 study cases modeling, according to fuzzy inference rules (Fig. 9), a set of 81 situations was obtained (Fig. 11). Each situation at an unsignalized road intersection is characterized by its response function value, representing the accident risk.

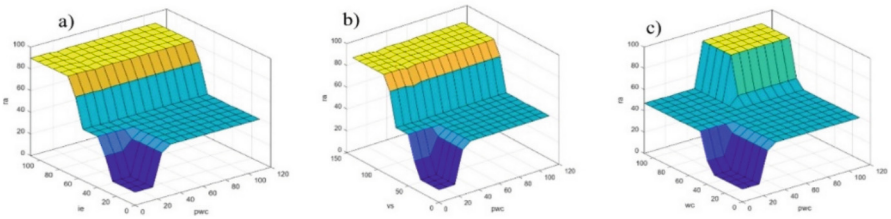

Fig. 10. Simulations Results of Fuzzy Inference by MATLAB Environment visualization of Fuzzy Inference for risk accident at unsignalized intersection associated with a) pedestrian wear color and intersection equipment; b) pedestrian wear color and vehicle speed; c) pedestrian wear color and weather conditions.

Figure 11 shows that three levels of emergency risk have been obtained. Analysis of the results indicates that the number of hazardous situations (green) is 26 out of 81 possible. In this case, the response function is maximum, $R_a = \max$, and the estimated value of the accident risk from the fuzzy model is greater than 47.5. Therefore, it can be argued in this case that the safety level for traffic participants, in particular pedestrians, is the lowest, i.e., "Dangerous" according to Fig. 7. The appearance of such a situation indicates that it is necessary to urgently improve the driving conditions, for example, increase the level of illumination, recommend reducing the speed limit. The use of suitable technical tools can enable the prompt implementation of such actions.

If the obtained accident risk value does not exceed 10.54, it is related to Ra = min. It means that the safety level at the unsignalized intersection of the road is "Optimal." Only 15 such situations (red) exist in the general sample (81 tests). High safety indicates a sufficient level of traffic management in the area under consideration.

Ra1	Ra2	Ra3	Ra4	Ra5	Ra6	Ra7	Ra8	Ra9
Ra10	Ra11	Ra12	Ra13	Ra14	Ra15	Ra16	Ra17	Ra18
Ra19	Ra20	Ra21	Ra22	Ra23	Ra24	Ra25	Ra26	Ra27
Ra28	Ra29	Ra30	Ra31	Ra32	Ra33	Ra34	Ra35	Ra36
Ra37	Ra38	Ra39	Ra40	Ra41	Ra42	Ra43	Ra44	Ra45
Ra46	Ra47	Ra48	Ra49	Ra50	Ra51	Ra52	Ra53	Ra54
Ra55	Ra56	Ra57	Ra58	Ra59	Ra60	Ra61	Ra62	Ra63
Ra64	Ra65	Ra66	Ra67	Ra68	Ra69	Ra70	Ra71	Ra72
Ra73	Ra74	Ra75	Ra76	Ra77	Ra78	Ra79	Ra80	Ra81

MAX of Risk accident 26
AVER of Risk accident 40
MIN of Risk accident 15

Fig. 11. Modeling results for risk accident at the unsignalized intersection by Fuzzy Model.

According to the modeling results, the largest number of situations is characterized by an average risk of accidents at unsignalized intersections, Ra = aver, which determines a sufficient level of "Safety". Such situations (yellow) are the most, almost 50% of the total, i.e., 40 units. The calculated value from the fuzzy model for the average accident risk ranges from 10.54 to 47.5. However, "Safety" does not mean that the driving of road sections cannot lead to an accident. Therefore, these situations should be considered as primary signals of the possibility of the traffic situation deterioration. It gives a certain

margin of time for response, for example, informing drivers about the need to reduce the speed limit.

However, the following aspects are the limitations of the fuzzy model:

- accident risk is determined based on accounting for only one factor from each subsystem included in the Human-Road-Environment-Vehicle System;
- model does not consider the traffic flow density and intensity;
- model does not consider the year season;
- modeling results consider the conditions when all factors appear from each subsystem with a certain level of variation at each study test.

Despite certain limitations, the authors claim the model can still accurately assess accident levels at road sections and unsignalized intersections. The model considers all the factors from subsystems that comprise the Human-Road-Environment-Vehicle System. These limitations do not affect the results obtained from the model.

The modeling results obtained can be compared to previous approaches. Still, the proposed model is a new solution that enables the simultaneous consideration of factors expressed as quantitative and fuzzy in the presented set of HREVS elements. Therefore, a more comprehensive evaluation was observed when comparing the results of accident risk assessment based on other studies (such as [14, 16]) when using the proposed model. It implies that forecasting the risk situation at an unregulated intersection will be more accurate as a diverse set of factors is considered.

5 Conclusions

This study aimed to develop a fuzzy model for determining the emergency risk on unsignalized road sections, considering Human-Road-Environment-Vehicle System factors. The proposed fuzzy model was one of the first steps to simultaneously use diverse initial parameters that can be accurately specified quantitatively (vehicle speed, intersection equipment level) and unclarity expressed (pedestrian wear color, weather conditions).

The fuzzy model was implemented in the MATLAB modeling environment, and its structure was assembled using the Simulink Toolbox. The 81 one fuzzy inference rule due to the Mamdani algorithm was modeled to cover the entire set of possible cases, corresponding to the full-factor experiment 3^4.

The results of the accident risk calculation, R_a, made it possible to define three levels of safety for pedestrians. At $R_a = \min$, an "Optimal" level of safety is achieved, and at $R_a = \max$ - "Dangerous". Almost 50% of the results correspond to the average level of accident risk, which characterizes a sufficient level of safety on the road section.

The designed fuzzy model allows further research and considers additional variables of the traffic situation, which allows operating with big data when making correct management decisions, significantly expanding the model to include additional parameters or addressing the noted limitations. Thus, these aspects will become the direction of further scientific developments.

Acknowledgment. The research was partially supported by the Polish National Agency for Academic Exchange within the project "Digitalization in mechanical engineering" (agreement no. BNI-UE-2023–2), European Union's Marie Skłodowska-Curie Actions under MSCA4Ukraine funding scheme (project number 1233438), EU NextGenerationEU through the Recovery and Resilience Plan for Slovakia under the project No. 09I03–03-V01–00094, and International Association for Technological Development and Innovations.

The authors would like to express their gratitude to Yehor Baklanov, Senior Software Engineer, for his informational support, recommendations, and assistance in setting up the Fuzzy Model.

References

1. Hu, Z., Zhou, J., Zhang, E.: Improving traffic safety through traffic accident risk assessment. Sustainability **15**, 3748 (2023)
2. Trojanowski, P., Trusz, A., Stupin, B.: Correlation between accidents on selected roads as fundamental for determining the safety level of road infrastructure. In: Ivanov, V., Trojanowska, J., Pavlenko, I., Rauch, E., Peraković, D. (eds.) Advances in Design, Simulation and Manufacturing V. DSMIE 2022. LNME, p. 104−113. Springer, Cham (2022). https://doi.org/10.1007/978-3-031-06025-0_11
3. Volkov, V., Taran, I., Volkova, T., Pavlenko, O., Berezhnaja, N.: Determining the efficient management system for a specialized transport enterprise. Naukovyi Visnyk Natsional-noho Hirnychoho Universytetu **4**, 185–191 (2020)
4. Druzhinin, E., Haidabrus, B., Psarov, O., Cheranovskiy, V.: Analysis of project implementation methods and models throughout risk management. In: Nechyporuk, M., Pavlikov, V., Kritskiy, D. (eds.) Integrated Computer Technologies in Mechanical Engineering - 2022. ICTM 2022. LNME, vol. 657, pp. 583–597. Springer, Cham (2023). https://doi.org/10.1007/978-3-031-36201-9_49
5. Vojtov, V., et al.: Modeling of traffic flows sustainability on highway network stretches. Appl. Sci. **13**, 9307 (2023)
6. Pohudina, O., Morikova, A., Haidabrus, B., Kiyko, S., Druzhinin, E.: Comparison of Metoheuristic Search Methods for the Task of Choosing a Rational Set of Measures to Risks' Respond. In: Nechyporuk, M., Pavlikov, V., Kritskiy, D. (eds.) Integrated Computer Technologies in Mechanical Engineering - 2020. ICTM 2020. LNNS, vol. 188, pp. 657–666. Springer, Cham (2021). https://doi.org/10.1007/978-3-030-66717-7_56
7. Medvediev, I., Muzylyov, D., Shramenko, N., Nosko, P., Eliseyev, P., Ivanov, V.: Design logical linguistic models to calculate necessity in trucks during agricultural cargoes logistics using fuzzy logic. Acta Logistica -Inter. Sci. J. about Logist. **7**(3), 155−166 (2020)
8. Mandar, M., Karim, L., Boulmakoul, A., Lbath, A.: Triangular intuitionistic fuzzy number theory for driver-pedestrians interactions and risk exposure modeling. Proc. Comput. Sci. **109**, 148–155 (2016)
9. Koçar, O., Dizdar, E.: A risk assessment model for traffic crashes problem using fuzzy logic: a case study of Zonguldak Turkey. Int. J. Transp. Res. **14**(5), 492–502 (2022)
10. Yeole, M., Jain, R., Menon, R.: Road traffic accident prediction for mixed traffic flow using artificial neural network. Mater. Today: Proc. **77**, 832–837 (2022)
11. Yuksel, A.S., Atmaca, S.: Driver's black box: a system for driver risk assessment using machine learning and fuzzy logic. J. Intell. Trans. Syst. **25**(5), 482–500 (2021)
12. Shaikh, R.A., Thayananthan, V.: Risk-based decision methods for vehicular networks. Electronics **8**, 627 (2019)

13. Haidabrus, B., Protsenko, S., Rosenberger, P., Grabis, J.: Data Analysis of readiness programs of machine-building enterprises. in: ivanov, V., Trojanowska, J., Pavlenko, I., Zajac, J., Peraković, D. (eds.) Advances in Design, Simulation and Manufacturing III. DSMIE 2020. LNME, pp. 128–136. Springer, Cham (2020). https://doi.org/10.1007/978-3-030-50794-7_13
14. Alam, M.J., Habib, M.A., Quigley, K.: Critical infrastructure renewal: a framework for fuzzy logic based risk assessment and microscopic traffic simulation modelling. Trans. Res. Proc. **25**, 1397–1415 (2016)
15. Xie, L., Zhang, J., Cheng, R.: Comprehensive evaluation of freeway driving risks based on fuzzy logic. Sustainability **15**(1), 810 (2022)
16. Castro, J., Delgado, M., Medina, J., Ruiz-Lozano, M.: An expert fuzzy system for predicting object collisions. Its application for avoiding pedestrian accidents. Expert Syst. Appli. **38**(1), 486−494 (2010)
17. Gaber, M., Wahaballa, A.M., Othman, A.M., Diab, A.: Traffic accidents prediction model using fuzzy logic: Aswan desert road case study. J. Eng. Sci. **45**(1), 28–44 (2017)
18. Wang, H., Zheng, L., Meng, X.: Traffic accidents prediction model based on fuzzy logic. In: Tan, H., Zhou, M. (eds.) Advances in Information Technology and Education. CCIS, vol. 201, pp. 101–108. Springer, Berlin, Heidelberg (2011). https://doi.org/10.1007/978-3-642-22418-8_14
19. Barreno, F., Romana, M.G., Santos, M.: Fuzzy expert system for road type identification and risk assessment of conventional two-lane roads. Expert. Syst. **39**(9), e12837 (2022)
20. Maraj, E., Kuka, S.: Prediction of Road Accidents using Fuzzy Logic. J. Multidisciplinary Eng. Sci. Technol. **6**(12), 11245–11248 (2019)
21. Liu, H.-W., et al.: Cloud model-based fuzzy inference system for short-term traffic flow prediction. Mathematics **11**, 2509 (2023)
22. Stanković, M., Stević, Ž, Das, D.K., Subotić, M., Pamučar, D.: A new fuzzy MARCOS method for road traffic risk analysis. Mathematics **8**, 457 (2020)
23. Demčák, J., Lishchenko, N., Pavlenko, I., Pitel', J., Židek, K.: The experimental SMART manufacturing system in SmartTechLab. In: Trojanowska, J., Kujawińska, A., Machado, J., Pavlenko, I. (eds.) Advances in Manufacturing III. MANUFACTURING 2022. LLNME, vol. 2, pp. 228–238. Springer, Cham (2022). https://doi.org/10.1007/978-3-030-99310-8_18
24. Zidek, K., Pitel, J., Pavlenko, I., Lazorik, P., Hosovsky, O.: Digital twin of experimental workplace for quality control with cloud platform support. In: Knapcikova L., Balog M., Perakovic D., Perisa M. (eds) 4th EAI International Conference on Management of Manufacturing Systems. EAI/Springer Innovations in Communication and Computing, pp. 135–145. Springer, Cham (2020). https://doi.org/10.1007/978-3-030-34272-2_13
25. Hosseinian, S.M., Gilani, V.N.M., Mirbaha, B., Kordani, A.A.: Statistical analysis for study of the effect of dark clothing color of female pedestrians on the severity of accident using machine learning methods. Math. Probl. Eng. **2021**, 5567638 (2021)
26. Pljakić, M., Jovanović, D., Matović, B.: The influence of traffic-infrastructure factors on pedestrian accidents at the macro-level: The geographically weighted regression approach. J. Safety Res. **83**, 248–259 (2022)
27. Zaleta, O.M., Povstyanoy, O.Y., Ribeiro, L.F., Redko, R.G., Bozhko, T.Y., Chetverzhuk, T.I.: Automation of optimization synthesis for modular technological equipment. J. Eng. Sci. (Ukraine) **10**(1), A6–A14 (2023). https://doi.org/10.21272/jes.2023.10(1).a2
28. Becker, N., Rust, H.W., Ulbrich, U.: Weather impacts on various types of road crashes: a quantitative analysis using generalized additive models. Eur. Transp. Res. Rev. **14**, 37 (2022)

Green Logistics System: Cargo Bikes as an Alternative to Light Trucks

Natalya Shramenko[1](✉), Christoph Hupfer[1], Vladyslav Shramenko[1,2], and Piotr Trojanowski[3]

[1] Baden-Württemberg Institute of Sustainable Mobility, Karlsruhe University of Applied Sciences, 30, Moltkestrasse, 76133 Karlsruhe, Germany
natalya.shramenko@bw-im.de
[2] Vytautas Magnus University, 58, K. Donelaičio Street, 44248 Kaunas, Lithuania
[3] West Pomeranian University of Technology in Szczecin, 17, al. Piastów, 70-310 Szczecin, Poland

Abstract. To reduce the negative impact of transport on the climate, important steps are the transition to more sustainable energy sources, the development of public transport, and the promotion of electric and other environmentally friendly modes of transport. Various mobility concepts (such as delivery with electric vans, cargo bicycles, the use of mobile micro-hubs, and automated deliveries using robots, drones, or autonomous vehicles) demonstrate approaches to creating a foundation for alternative and environmentally friendly urban logistics. In densely populated cities, electric cargo bicycles are becoming increasingly popular as a replacement for vans and cars to deliver groceries and parcels. The research aims to assess the effectiveness of using cargo bicycles as an alternative to cars for transporting small consignments within city limits. A simulation model has been developed to form cargo transportation routes within the city. The model is based on applying a genetic algorithm and considers specified constraints on time, distance, and available resources (vehicles and personnel). The study compared different technologies for serving customers of a supermarket chain (pendulum routes and distribution-assembly routes). At the same time, modeling was carried out for the conditions of use of various vehicles (an electric cargo bike and a car). The experiment results showed that the use of cargo bicycles significantly reduces emissions of harmful substances, decreases energy consumption, leads to lower delivery costs, provides companies with greater flexibility in organizing logistics processes, and, at the same time, has a significant positive social impact.

Keywords: Greenhouse Gases · Delivery Routes · Last Mile · Optimization · Genetic Algorithm · Small Consignment of Goods · Simulation Model

1 Introduction

By 2030, demand for urban delivery, driven by the growth of e-commerce, is expected to increase last mile by 78%, leading to a 36% increase in the number of delivery vehicles in the world's 100 largest cities. This growth in delivery is accompanied by an increase

© The Author(s), under exclusive license to Springer Nature Switzerland AG 2024
V. Ivanov et al. (Eds.): DSMIE 2024, LNME, pp. 449–461, 2024.
https://doi.org/10.1007/978-3-031-61797-3_38

in greenhouse gas emissions of almost 30%. With increased carbon emissions, traffic congestion is projected to increase by more than 21%, which equates to adding 11 min to each passenger's daily commute time [1].

Sustainable mobility and logistics are important aspects of sustainable urban development [2] and significantly impact business performance, safety, the environment, and overall quality of life [3]. Achieving an optimal supply chain and route can lead to significant cost savings for businesses and enhance their competitiveness in the market. Reducing harmful emissions while transporting goods is another challenge companies face [4].

Companies aim to develop measures to reduce the negative impact of transportation activities on the environment. A priority direction is the creation of more eco-friendly and sustainable supply chains based on implementing environmentally friendly delivery technologies, including using environmentally friendly modes of transportation [5]. This task is highly relevant because goods are usually transported using trucks that use much fuel, which leads to more pollution with CO_2 emissions and makes the already busy city traffic more congested [6]. The use of electric vehicles in urban logistics processes reduces fuel use and reduces emissions while increasing the availability and flexibility of the logistics system [7]. Survey results from 2017 and 2021 also show a significantly growing interest in cargo bikes among the German population. Thus, awareness of cargo bikes increased from 38 to 63%; purchase potential increased from 7 to 12%; willingness to use cargo bike rental systems increased from 16 to 28% [8].

In this paper, we aim to check the efficiency of transporting small consignments in the city using cargo bicycles as an alternative to trucks. By comparing different service technologies, we seek to determine the effectiveness and potential benefits of using cargo bicycles regarding fuel consumption, environmental impact, and traffic load.

The object of the study is the functioning process of the urban freight distribution system. The subject of the study includes customer service technologies for small cargo shipments within the city limits. The research goal is to assess the efficiency of using cargo bicycles as an alternative to freight vehicles for transporting small cargo shipments within the city.

2 Literature Review

Logistics costs are an extremely significant category due to their relatively high revenue share. Based on surveys of enterprises, it was found that logistics occupies an average of 17.08% of profits, with transportation costs being the most significant component of logistics costs, with the participation of 36.1% of the total amount, that is, an average of 6.16% of revenue [9]. In addition, the share of the logistics component for agriculture products reaches up to 50% of the total cost of production [10].

For high-quality customer service during cargo transportation, it is necessary not only to deliver a given cargo volume but also to complete it within a specific time frame, which complicates the formation of distribution routes and the choice of a rational carrying capacity of vehicles that provide delivery. Such an optimization task is called a Vehicle Routing Problem (VRP) [11, 12].

As a result of the organization process analysis of cargo transportation, several limitations were defined: formation of irrational routes, ignoring the client's requirements for

on-time cargo delivery, and using automobiles of irrational cargo capacity on routes [13]. Logistics companies and distribution centers are responsible for planning and organizing small cargo delivery from cargo railway stations, port terminals, airports, large shopping centers, and logistical complexes to the end consumers, including malls, restaurants, hotels, mini-markets, and individual citizens [14]. The concept of small cargo delivery relates to reducing the total length of routes and minimizing the number of trucks used for transportation [15].

Major international logistics companies are actively testing and employing cargo bicycles as a fast, cost-effective, and environmentally friendly transportation option in urban areas [16]. In densely populated cities, electric cargo bicycles are increasingly replacing vans and cars to deliver goods (such as food and parcels) to their destinations [17]. An effective urban logistics system contributes to the more cost-effective delivery of goods, and its effectiveness is reflected in the ability of stakeholders to ensure delivery, taking into account quantity, location, time, and customer satisfaction [18, 19]. Managing such a system is complicated by the involvement of various stakeholders, the restrictions imposed by the urban structure, and the high level of retail trade [20].

The rational organization of any technological process at cargo delivery, including optimization of vehicle routes, reduces delivery costs and reaches the synergetic effect [21]. Therefore, in small cargo transportation, they attempt to organize the transportation of goods on advanced planned and collected cargo routes for more effective rolling stock use.

It is possible to make a conclusion based on the conducted analysis of scientific papers by researchers [22] and on the practical experience of transportation services for cargo owners. This observation indicates that in planning and organizing distribution routes for delivery services to cargo owners, particularly for many clients, the focus is often placed solely on the carrier's perspective. As a result, the interests of consignors and consignees, who are concerned about the timely transportation of their cargo, should be addressed or addressed. This situation highlights a decline in the quality of transportation services. Meanwhile, optimizing routes in cities has some features that should contribute to developing new models. Heuristic methods can be used to create distribution routes for many customers, and much attention is paid to genetic algorithms [23].

Thus, the improvement of existing and development of new scientific and practical decisions, methods, and models on planning and the organization of delivery routes is necessary to improve the quality of the transportation service directed to meet the requirements of cargo owners fully.

3 Research Methodology

Forming transportation routes for small cargo shipments within the city is carried out in several stages. In the first stage, the transportation problem is solved, involving determining an optimal transportation plan for distributing goods from a set of supply sources to a set of demand destination points while minimizing the overall transportation costs. The simplex method is employed to enhance the solution and find the optimal transportation plan.

To form distribution routes when servicing a large number of clients (more than 17), a Genetic Algorithm (GA) was used.

The application of GA to the traveling salesman problem demonstrates its effectiveness in solving complex routing and optimization challenges. Benefits of applying genetic algorithms to the traveling salesman problem:

- GA can find approximate solutions in conditions where achieving an exact solution is challenging, providing global optimization of routes;
- GA is effective in handling large datasets;
- the algorithms can quickly adapt to changing conditions and requirements, making them suitable for dynamic environments and variables in the traveling salesman problem.

Thus, a Genetic Algorithm can be used to find an optimal or near-optimal solution that minimizes the total cost or distance traveled by a fleet of vehicles to serve a group of customers, considering various constraints such as a limited number of goods in warehouses, vehicle capacity, time windows, travel time for vehicles, depot limits, customer priority, service times, etc.

3.1 Problem Formalization

The research was conducted using the example of Lidl supermarkets located in Karlsruhe, Germany.

The Lidl supermarket group offers non-food items through the Lidl online store. Currently, the offering is limited to non-food items; however, potential buyers may also purchase long-lasting food products through the Lidl online store. Potential online customers for Lidl supermarkets include cafes, bakeries, restaurants, and private individuals. Modeling the functioning of the distribution system in the city of Karlsruhe is illustrated using the example of 6 Lidl supermarkets (Fig. 1) and 50 potential customers.

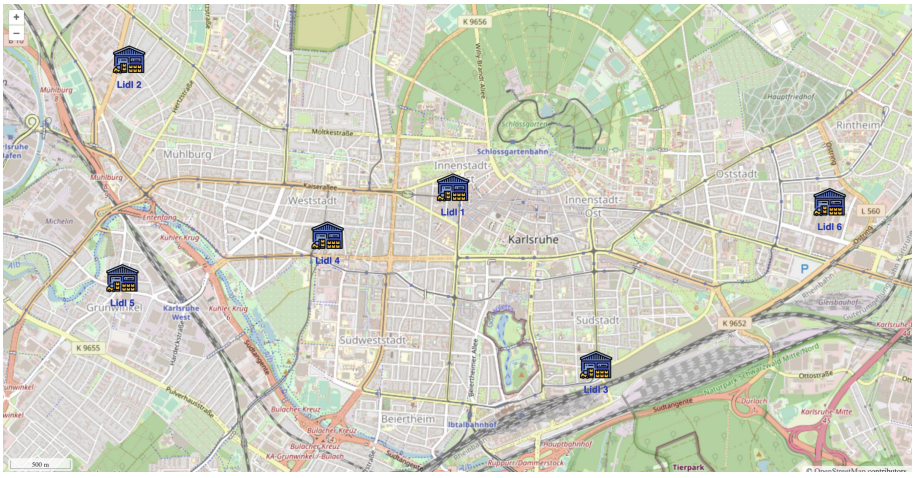

Fig. 1. The locations of the 6 LIDL supermarkets in Karlsruhe city.

The names and locations of potential online customers for Lidl supermarkets, the availability of products in Lidl supermarkets, and the demand for products from customers are random variables, the values assumed for experimental purposes.

3.2 Supply Chain Formation Technologies

The distribution system can be based on various route organization technologies. The following route organization technologies are examined in the study:

- formation of pendulum routes, where one customer is served along the route, and then the vehicle returns empty to the loading point (Fig. 2);
- formation of distributive-assembled routes, where from a specified loading point, the vehicle delivers products to one customer, then returns empty to the next loading point, from where it delivers goods to the next customer (Fig. 3).

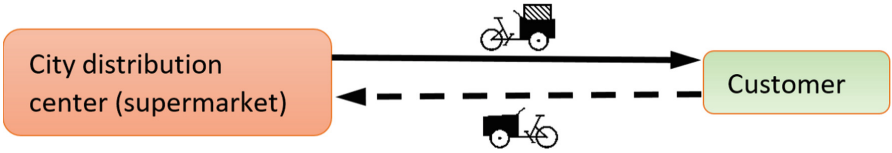

Fig. 2. Scheme of the pendulum route.

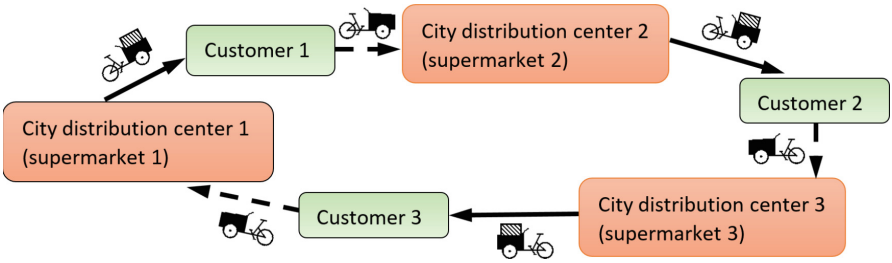

Fig. 3. Distributive-assembled route schemes for small cargo transportation.

The delivery of products from the supermarkets to the customers is carried out using vehicles of the same type and model.

Advantages of cargo bikes for transporting commercial goods in the city:

- environmentally friendly transportation;
- take up relatively little space on the road;
- require significantly less parking space;
- independence from parking spaces;
- bicycles do not pay emissions tax or parking fees in congested city centers;
- low cost of operation, maintenance, and capital investments;
- faster (no traffic jams) and targeted delivery of cargo to the consumer (which is especially important for urgent delivery and for the delivery of perishable goods);

– the cyclist does not require high qualifications compared to a car driver (a driver's license is not required to operate a cargo bike);
– lower energy consumption compared to a car;
– high maneuverability on the road; accessibility to pedestrian areas;
– provide mobility in urban environments; low noise level;
– positive effect on the health of the cyclist and his stress state.

Thus, it is necessary to conduct a comparative analysis of the performance indicators of different vehicles on the generated routes for different service technologies (pendulum and distributive-assembled routes).

3.3 Formalization of the Distribution Process

The organization of the transportation process on delivery routes is based on reducing the total distance traveled by vehicles:

$$\sum_{k=1}^{m} d_k \rightarrow \min \tag{1}$$

where m – the number of vehicles;

d_k - the length of the route of the k-th vehicle.

The mathematical model of the given problem will have the following form:

$$C = \sum_{k=1}^{m} C_k \cdot d_k \rightarrow \min \tag{2}$$

where C - total daily CO_2 emissions, g;

C_k - the well-to-tank emissions related to electricity production for the k-th type of vehicle, g/km.

The model incorporates the following constraints:

– total carrying capacity of vehicles (based on the characteristics of the fleet);
– operating time of vehicles on routes;
– drivers' working hours on routes;
– number of vehicles.

As a result of route planning for all alternative types and models of vehicles (cars and bicycles), it is necessary to evaluate the performance indicators for the period under consideration (day):

– total driving distance;
– total empty driving distance;
– total loaded driving distance;
– required number of vehicles;
– time spent on routes;
– required number of drivers;
– total greenhouse gas emissions.

4 Results and Discussion

4.1 Modeling the Process of Forming Cargo Transport Routes Within the City

A simulation model with a user interface was developed to model the process of forming routes for transporting small consignments of goods within the city.

The potential demand for products from Lidl supermarkets in Karlsruhe was used as the initial data for modeling the delivery process, coming from 50 potential online customers (bakeries, cafes, restaurants). The demand for products is distributed according to a normal distribution with a mean parameter $\mu = 75$ kg and a standard deviation $\delta = 25$ kg (Fig. 4).

It was assumed that all supermarkets in the network operate for 10 h and have identical product assortments available for online ordering, requiring no special transport conditions. The quantity of supermarket products is randomly generated with a maximum deviation of 15% from the required amount according to demand. Vehicles (cars, cargo bicycles) are strictly assigned to supermarkets, meaning the starting point at the beginning of the working day and the vehicle return point after transportation at the end of the working day coincide. The technical speed for a cargo bicycle is set at 11 km/h; for a cargo car, the technical speed is 23 km/h. The duration of drivers' working time is limited to 8 h per day, but in justified cases, it should be at most 9 h.

It should be taken into account that when applying genetic algorithms to solve the traveling salesman problem, there are certain limitations to consider:

- for large datasets or complex instances of the traveling salesman problem, the computational complexity of genetic algorithms can be significant, requiring substantial computational resources;
- genetic algorithms provide approximate solutions but do not guarantee to find the optimal path;
- the effectiveness of genetic algorithms often depends on choosing an appropriate fitness function and the correct configuration of parameters, such as population size, crossover probability, and mutation rate.

When using genetic algorithms, it is crucial to consider these limitations and carefully tune their parameters for the specific traveling salesman problem at hand.

4.2 Cost Minimizing Transportation Problem

To achieve the optimal distribution of goods from supply to demand, assigning each customer to the most suitable supermarket, we solved an open problem of minimizing transportation costs. In Table 1, a part of the optimal transport plan for delivery by bicycles is presented. This plan considers the arising demand and supply, helping determine the best way to distribute products from supermarkets among individual customers.

Customer	Product Type	Amount, kg
Antalya Restaurar	Flour	92
Arabischer Schaw	Flour	61
Asmara Restaurar	Flour	104
Back Eck	Flour	106
Badische Backstu	Flour	106
Bakery Schmidt -	Flour	96
Bruno Steinbeck (	Flour	111
Bäckerei Bruno St	Flour	40
Bäckerei Konditor	Flour	64
Bäckerei Konditor	Flour	54

Fig. 4. Fragment of demand from small customers.

4.3 Discussion of the Results of Simulation Modeling

Pendulum Routes

Pendulum routes are transportation routes where vehicles return to the location from which the last delivery was made before proceeding to the next destination. When establishing these routes, it is assumed that each vehicle is assigned to a specific supermarket and carries out deliveries exclusively from that supermarket. A simulation of delivering goods from each supermarket to different customers, one after another, using VUF XXL bicycles, was conducted (Fig. 5). The total distance of this route is 147.77 km. To make these deliveries, 5 bicycles are needed.

Similarly, we modeled the delivery of goods through pendulum routes from each supermarket to different customers using Volkswagen Golf VIII cars. The total length of these routes is 177.27 km, requiring 5 trucks for the deliveries.

Generalized indicators of vehicle performance on pendulum routes (Table 2) demonstrate the advantages of cargo bicycles for delivering products in the city. However, the

operating time on the routes needs to be balanced for such a scenario for delivering goods to customers.

```
Route number 4: Lidl 5 →(111 kg) Bruno Steinbeck GmbH
→(0 kg) Lidl 5 →(29 kg) Bäckerei Konditorei Lörz →(0
kg) Lidl 5 →(54 kg) Bäckerei Konditorei Steinbeck →(0
kg) Lidl 5 →(60 kg) Bäckerei Meier →(0 kg) Lidl 5
Number of loaded routes: 4
Loaded driving distance: 10.11 km
Empty driving distance: 10.63 km
Deadhead driving distance: 0 km
Driving time: 0.9 hours
Loading and unloading time: 1 hours
Total driving distance: 20.74 km
Total time: 1.9 hours

Total energy consumption: 2.22 kWh
Total CO2 emissions: 1182.16 grams
Total time: 26.68 hours
Total loaded driving distance: 73.6 km
Total empty driving distance: 74.17 km
Total deadhead driving distance: 0 km
Total driving distance: 147.77 km
```

Fig. 5. Fragment of the performance indicators' calculation results for deliveries processed by the VUF XXL cargo bicycle using pendulum routes.

Table 1. A part of the optimal transportation plan allocates the goods from supply sources to demand destinations when using bicycle delivery.

	Lidl 1	Lidl 2	Lidl 3	Lidl 4	Lidl 5	Lidl 6
Antalya Restaurant	0	0	92	0	0	0
Arabischer Schawarma	0	0	61	0	0	0
Asmara Restaurant	0	0	0	104	0	0
Back Eck	106	0	0	0	0	0
Badische Backstub' (Karlsruhe)	106	0	0	0	0	0
Bakery Schmidt - Innovation in baking tradition	96	0	0	0	0	0
Bruno Steinbeck GmbH	0	0	0	0	111	0
Bäckerei Bruno Steinbeck GmbH	10	0	0	30	0	0
Bäckerei Konditorei Lörz	0	0	0	64	0	0
Bäckerei Konditorei Steinbeck	0	0	0	0	54	0
Bäckerei Meier	0	0	0	0	60	0

Table 2. The performance indicators for formatted pendulum routes for various types of vehicles.

Indicator	VUF XXL	Volkswagen Golf VIII
Required number of vehicles per day, units	5	5
Total distance traveled, km	147.77	177.27
Total distance traveled with cargo, km	73.6	84.15
Total distance traveled without cargo, km	74.17	93.12
Total delivery time, h	26.68	20.96
Total energy consumption	2.22 kWh	10.64 L
Total daily CO2 emissions, g	1182.16	20386
Required number of drivers per day, units	5	5

Table 3. The performance indicators for formatted distributive-assembled routes for various types of vehicles.

Indicator	VUF XXL	Volkswagen Golf VIII
Required number of vehicles per day, units	5	4
Total distance traveled, km	153.25	183.6
Total distance traveled with cargo, km	73.59	84.15
Total distance traveled without cargo, km	79.66	99.45
Total delivery time, h	27.19	29.95
Total energy consumption	2.3 kWh	11.02 L
Total daily CO2 emissions, g	1226	21114
Required number of drivers per day, units	5	4

Distributive-Assembled Routes.
A simulation of delivering goods using distributive-assembled routes was conducted. These distributive-assembled routes differ from pendulum routes in that vehicles may not necessarily return to the location of their last delivery but instead proceed to another warehouse for the next delivery.

In this case, we need to determine the sequence of N transfers of goods from supermarkets to customers, where N represents the number of non-zero values in the optimal transport plan. So, following our model's constraints, the task is to reduce the required number of vehicles and evenly distribute the delivery of goods among multiple vehicles. We want to achieve this without significantly increasing the delivery distance and other critical performance indicators of the delivery routes.

Figure 6 presents a fragment of the performance metrics for the route generated by applying a genetic algorithm for bicycle-based deliveries. In this particular case, we need 5 bicycles, and the total distance of the routes is 153,25 km.

Generalized performance indicators of vehicles on distributive-assembled routes.

```
Route for the bicycle (VUF XXL 6): Lidl 6 →(29 kg) Ok-
tave →(0 kg) Lidl 6 →(62 kg) Bäckerei-Konditorei Richard
Nussbaumer Karlsruhe-Waldstadt →(0 kg) Lidl 1 →(121 kg)
SAMIS Restaurant →(0 kg) Lidl 1 →(69 kg) Mediterrane
Karlsruhe- Restaurant →(0 kg) Lidl 4 →(40 kg) Bäckerei
Meier_5 →(0 kg) Lidl 5 →(60 kg) Bäckerei Meier →(0 kg)
Lidl 5 →(111 kg) Bruno Steinbeck GmbH →(0 kg) Lidl 5
→(29 kg) Firo Kebap →(0 kg) Lidl 1 →(122 kg) Spezi-
alitäten-Bäckerei ANA & ANDA →(0 kg) Lidl 1 →(18 kg) Ox-
ford Pub - Bier & Burger →(0 kg) Lidl 6
Number of loaded routes: 10
Loaded driving distance: 17.93 km
Empty driving distance: 19.21 km
Deadhead driving distance: 2.35 km
Driving time: 3.59 hours
Loading and unloading time: 2.5 hours
Total driving distance: 39.49 km
Total time: 6.09 hours

Total energy consumption: 2.3 kWh
Total CO2 emissions: 1226 grams
Total time: 27.19 hours
Total loaded driving distance: 73.59 km
Total empty driving distance: 68.6 km
Total deadhead driving distance: 11.06 km
Total driving distance: 153.25 km
```

Fig. 6. Fragment of the performance indicators' calculation results for deliveries processed by the VUF XXL cargo bicycle using distributive-assembled routes with the application of a genetic algorithm.

(Table 3) also demonstrate the advantages of cargo bicycles for delivering products in the city.

The results of simulation modeling of the product delivery process in the dynamic urban environment for various route formation technologies (pendulum routes, distributive-assembled routes) indicate the advantage of using cargo bicycles within the city. This is due to lower energy costs and a significant reduction in emissions of harmful substances into the atmosphere. At the same time, the vehicle operating times on routes and the required number of vehicles are balanced with each other.

5 Conclusions

In the face of climate change, using environmentally friendly modes of transportation becomes increasingly crucial. In urban freight transport, electric cargo bicycles emerge as an alternative to freight trucks, offering significant advantages in energy efficiency, road space utilization, and environmental impact in densely populated city areas.

To experiment with the organization of small-batch transport for multiple customers within the city, we developed a simulation model based on a genetic algorithm. This model considers predefined constraints on time, distance, and available resources (vehicles and personnel).

During the research, simulation experiments were conducted on the route formation process for transporting goods from 6 supermarkets to 50 customers within the city. The

modeling is grounded in using a genetic algorithm and is performed for different types of vehicles (cargo bikes and cars) and different transportation organization technologies for serving customers: pendulum and distributive-assembled routes.

The study compares various route formation technologies for serving small product customers, demonstrating the feasibility of using cargo bicycles for urban freight delivery. The experiment results show that distributive-assembled routes are the most effective technology for organizing routes to serve small consumers. Thus, for such a scenario of delivering goods to customers using cargo bikes, the total distance traveled could be reduced by 16.5%, and the total delivery time on routes could be reduced by 9.2%. At the same time, the use of cargo bicycles significantly reduces emissions of harmful substances (for the considered problem total daily CO2 emissions when using the cargo bike VUF XXL were 1226 g per day of operation; total daily CO2 emissions when using the car Volkswagen Golf VIII on routes is 21114 g per day of operation), lowers energy consumption leading to reduced delivery costs, provides companies with greater flexibility in organizing logistics processes, and has important social effects (increased street space, reduced noise, decreased need for parking spaces).

Thus, the research results aim to encourage businesses and local authorities to collaborate on developing and testing freight delivery schemes for small customers in densely populated city areas based on the use of cargo bicycles. This approach reduces environmental impact, cuts delivery costs, and contributes to improving the quality of life in cities.

References

1. World economic forum. The Future of the Last-Mile Ecosystem (2020). https://www3.weforum.org/docs/WEF_Future_of_the_last_mile_ecosystem.pdf, (Accessed 17 Sep 2023)
2. Kauf, S.: City logistics – a strategic element of sustainable urban development. Trans. Res. Proc. **16**, 158–164 (2016). https://doi.org/10.1016/j.trpro.2016.11.016
3. European Commission Transport in the European Union – current trends and issues. (2019). https://ec.europa.eu/transport/sites/transport/files/2019-transport-in-the-eu-current-trends-and-issues.pdf, (Accessed 21 Nov 2023)
4. Škultéty, F., Beňová, D., Gnap, J.: City Logistics as an imperative smart city mechanism: scrutiny of clustered EU27 Capitals. Sustainability **13**, 3641 (2021). https://doi.org/10.3390/su13073641
5. Elbert, R., Rentschler, J.: Freight on urban public transportation: a systematic literature review. Res. Trans. Bus. Manag. 45, Part A, 100679 (2022). https://doi.org/10.1016/j.rtbm.2021.100679
6. Diana, M., Pirra, M., Woodcock, A.: Freight distribution in urban areas: a method to select the most important loading and unloading areas and a survey tool to investigate related demand patterns. Eur. Transp. Res. Rev. **12**, 40 (2020). https://doi.org/10.1186/s12544-020-00430-w
7. Akkad, M.Z., Bányai, T.: Multi-objective approach for optimization of city logistics considering energy efficiency. Sustainability **12**, 7366 (2020). https://doi.org/10.3390/su12187366
8. Potenziale & Marktgröße von Cargobikes. https://www.cargobike.jetzt/potenziale-marktgroesse/, (Accessed 30 Dec 2023)
9. Ślusarczyk, S.K.: Beata: Logistics costs identification in SME in Poland. Adv. Logist. Syst. 91–96 (2013)

10. Wajszczuk, K.: The Role and importance of logistics in agri-food supply chains: an overview of empirical findings. Logist. Trans. **2**(30), 47–55 (2016)
11. Braekers, K., Ramaekers, K., Nieuwenhuyse, I.V.: The vehicle routing problem: state of the art classification and review. Comput. Ind. Eng. **99**, 300–313 (2015). https://doi.org/10.1016/j.cie.2015.12.007
12. Li, H., Liu, Yi., Chen, K., Lin, Q.: The two-echelon city logistics system with on-street satellites. Comput. Indus. Eng. **139**, 105577 (2020). https://doi.org/10.1016/j.cie.2018.12.024
13. Ezquerro, S., Romero, J.P., Moura, J.L., Benavente, J., Ibeas, Á.: Minimizing the impact of large freight vehicles in the city: a multicriteria vision for route planning and type of vehicles. J. Adv. Transp. **2018**, 1732091 (2018). https://doi.org/10.1155/2018/1732091
14. Shramenko, N., Muzylyov, D., Shramenko, V.: Methodology of costs assessment for customer transportation service of small perishable cargoes. Int. J. Bus. Perform. Manag. **21**(1/2), 132–148 (2020)
15. Bjørgen, A., Ryghaug, M.: Integration of urban freight transport in city planning: lesson learned. Transp. Res. Part D: Transp. Environ. **107**, 103310 (2022). https://doi.org/10.1016/j.trd.2022.103310
16. Sheth, M., Butrina, P., Goodchild, A., et al.: Measuring delivery route cost trade-offs between electric-assist cargo bicycles and delivery trucks in dense urban areas. Eur. Transp. Res. Rev. **11**, 11 (2019). https://doi.org/10.1186/s12544-019-0349-5
17. Fontaine, P., Minner, S., Schiffer, M.: Smart and sustainable city logistics: Design, consolidation, and regulation. Eur. J. Oper. Res. **307**(3), 1071–1084 (2023). https://doi.org/10.1016/j.ejor.2022.09.022
18. Russo, F., Comi, A.: Investigating the Effects of city logistics measures on the economy of the city. Sustainability **12**(4), 1439 (2020). https://doi.org/10.3390/su12041439
19. Bachofner, M., Lemardelé, C., Estrada, M., Pagès, L.: City logistics: challenges and opportunities for technology providers. J. Urban Mobility **2**, 100020 (2022)
20. Rześny-Cieplińska, J., Szmelter-Jarosz, A.: Environmental sustainability in city logistics measures. Energies **13**(6), 1303 (2020). https://doi.org/10.3390/en13061303
21. Shramenko, N.: Methodology for evaluation of synergy effect in terminal cargo delivery system. Actual Problems Econ. **182**, 439–444 (2016)
22. Cattaruzza, D., Absi, N., Feillet, D., González-Feliu, J.: Vehicle routing problems for city logistics. EURO J. Trans. Logist. **6**(1), 51–79 (2017). https://doi.org/10.1007/s13676-014-0074-0
23. Wirsansky, E.: Hands-On Genetic Algorithms with Python: Applying genetic algorithms to solve real-world deep learning and artificial intelligence problems. Packt Publishing (2020)

Assessing External Supply Risk: Perspectives from a Low Middle-Income Country

Praveena Somaweera, Dilina Kosgoda, and H. Niles Perera(✉)

University of Moratuwa, Moratuwa 10400, Katubedda, Sri Lanka
hniles@uom.lk

Abstract. Global disruptions due to causes such as the COVID-19 pandemic and the Russia-Ukraine conflict have highlighted the vulnerability of the agri-food supply chain and its impact on food security. Sri Lanka, facing its economic crisis and food scarcity due to these disruptions, ranks 79th out of 113 countries regarding food security. Wheat is the second most consumed cereal in the country. Thus, Sri Lanka must assess the external risks associated with wheat imports to ensure a smooth supply. However, there needs to be more comprehensive research on the risks of relying on imported food in the extant literature, particularly regarding factors including import dependence, supplier country reliability, and transit risks. To address this research gap, the study employed the Herfindahl-Hirschman Index and Shannon-Wiener Index to assess the external wheat supply risk in Sri Lanka. The analysis showed that despite the relatively low overall risk, high dependence on Russia and other high-risk countries increased the wheat supply risk. This study recommends reducing import percentages from high-risk countries and diversifying supply to low-risk countries to mitigate risks. The study also found that the level of political risk in supplier countries had a more significant impact on supply risk than the distance and import shares of the supplier countries. Further, the study provides valuable insights into Sri Lanka's external wheat supply risk and recommends measures to mitigate risks and enhance food security. The findings are generalizable to low and middle-income countries with similar characteristics.

Keywords: Food Security · Supply Chain Risk Assessment · Supply Chain Resilience · Import Dependency · Herfindahl-Hirschman Index

1 Introduction

Supply chain management has evolved into a complex and interconnected network of businesses across different countries, driven by globalization. This interconnectedness offers numerous opportunities for businesses to optimize costs and gain a competitive advantage. The availability of resources plays a crucial role in supply chains, and international trade helps balance deficits and surpluses, preventing issues like food and energy insecurity. For example, oil-rich countries lacking arable land rely heavily on imports to meet their food needs [1].

© The Author(s), under exclusive license to Springer Nature Switzerland AG 2024
V. Ivanov et al. (Eds.): DSMIE 2024, LNME, pp. 462–474, 2024.
https://doi.org/10.1007/978-3-031-61797-3_39

However, it also introduces risks that need to be anticipated, managed, and mitigated, which otherwise could cause various types of losses for organizations. The COVID-19 pandemic and the Russia-Ukraine conflict have attracted the attention of industry practitioners and academics towards the vulnerability of global supply chains. These events have created disruptions in supply chains, and most countries that rely on food imports need help to maintain an uninterrupted supply from their external suppliers. As a result of countries failing to supply their essential food items, food insecurity has been exacerbated worldwide. On the other hand, Sri Lanka has faced economic crises and food shortages, leading to social unrest. The country ranks 79th out of 113 countries regarding food security, with 10% of the population experiencing moderate to severe food insecurity [2]. Therefore, establishing a resilient supply chain is crucial to guaranteeing food security in Sri Lanka.

Sri Lanka heavily depends on imports to meet its food requirements, especially for wheat, the second most consumed cereal in the country. There are many other cereal types that are imported into the country, but wheat is less widely consumed by people than wheat. With wheat being an important cereal to Sri Lanka, contributing to 12% of per day per capita calorie consumption [3], and Sri Lanka entirely depending on imports to meet this daily demand, it is vital to ensure that the country's wheat supply chain is resilient. Despite the importance of supply chain resilience, there is limited research on the risks associated with imported food in Sri Lanka and globally [4]. Existing studies have not adequately measured or assessed the levels of risk linked to external food supply. Thus, this study aims twofold: to measure and analyze the external supply risk of wheat in Sri Lanka and to assess the sensitivity of this risk to external factors.

This study considers several factors influencing the external wheat supply risk. Namely, Sri Lanka's import dependency on wheat, the political and business-related risks in supplier countries, and the transit risks during shipment. This study further examines the diversity and security of Sri Lanka's wheat import supply chains. By understanding the level of risk and its sensitivity to external factors, policymakers and businesses can make informed decisions to mitigate risks and enhance food security. Thus, the findings of this study can provide valuable insights for policymakers and businesses to mitigate risks, enhance supply chain resilience, and ensure food security.

The paper begins with a comprehensive literature review, and it is followed by the methodology of the research study. The study's main findings are presented in the analysis and results section. A thorough discussion of the findings is included in the discussion section. Further, managerial implications and potential future directions for new research are included in this section.

2 Literature Review

2.1 Food Security

Food security is a global issue that affects both developing and high-income countries. Primary causes of hunger and food insecurity stem from climate-related disturbances, crop diseases, economic upheavals, and instances of war and conflicts [5]. Inadequate access to food has wide-ranging consequences for health, productivity, and social well-being. The Global Food Security Index evaluates countries based on various factors and

has reported a decline in the strength of the global food system. The Global Report on Food Crises 2022 highlights the urgent need for assistance in addressing hunger worldwide.

International trade is crucial in balancing food imbalances and ensuring food security, particularly for import-dependent developing nations [6]. Cereal trade stabilizes food supply globally. The increased utilization of outsourced production, distribution, and logistics creates complex connections within the global supply chain, elevating the level of risk exposure [7]. Therefore, it is important to understand the configuration and interconnections between countries in the international trade network to identify the supply risks that are associated with them. For example, the COVID-19 pandemic highlighted the vulnerability of external supply chains and the risks of import concentration [8]. Hence, assessing the impacts of supply chain disruptions is necessary to build a more resilient and secure global food trade network.

2.2 Food Supply Chain Risk Management

Efficient management of risks related to external food supplies is crucial for maintaining food security. Recent events like the Ukraine-Russia crisis and export bans during the COVID-19 pandemic highlight the need for proactive measures. Over the last decade, there has been a significant surge in the need for Supply Chain Risk Management (SCRM), particularly in the past five years, driven by the increase in worldwide risks. SCRM enables government and industry to protect against identified threats to supply chains while fortifying their ability to withstand potential risks [9]. It is essential to comprehend the risk context by assessing both the probability and severity of these risks. This understanding plays a vital role in devising an effective strategy to mitigate supply chain risks. Previous research focuses on assessing risks using self-sufficiency and import dependency theories. Higher self-sufficiency ratios indicate better food availability, but dependence on imports for intermediate input should be considered. Assessing external supply risks requires analyzing the dependence of domestic production on imports. Various studies have explored supply chain risk management in the food industry, including collaborative efforts, resilience models, quality assurance systems, and performance indicators for food quality measurement [10].

Supply chain resilience (SCR) refers to the capacity to bounce back from an unexpected drop in performance to the intended level by implementing measures to either recover or adapt to the situation [11]. It involves both reactive and proactive measures to ensure continuous functioning and competitive advantage [12]. Food supply chain resilience is critical in ensuring a consistent and sufficient supply of suitable food despite unexpected disturbances. Recent events like the COVID-19 pandemic and the Russia-Ukraine conflict have highlighted the vulnerability of global food supply chains, impacting food prices and security. Building resilience in agricultural food supply chains is essential to address climate change, soil degradation, harvest failures, and population growth. SCR is crucial for business continuity and sustainability, with retailers actively developing supply resilience. A wide range of risks, spanning from natural calamities and geopolitical unrest to cyber threats and supplier insolvencies, pose significant challenges. To adeptly handle these risks, businesses must thoroughly grasp the critical issues and evolving patterns within SCRM [7]. Resilient supply chains help withstand future risks

and maintain smooth operations. Researchers and practitioners focus on different stages of supply chain risk management, proposing frameworks and approaches for assessing and mitigating risks. Decision-making now considers ecological and social factors alongside costs and benefits. Regular risk assessments and proactive management are vital for business continuity in volatile environments.

Assessing risks in food supply chains is complex due to various challenges faced by firms, especially SMEs, such as lack of expertise and limited resources. Despite these challenges, risk assessment is essential for reducing waste, ensuring food security, and developing robust strategies [9]. Categorization and classification of risks aid in understanding and managing potential risks. Researchers have explored the relationship between risk factors and organizational performance, focusing on operational risks, supply failures, uncertain demand, and market price variations. All stakeholders should know risks and adopt a systematic approach to manage them and effectively achieve high supply chain performance.

2.3 Situation in Sri Lanka

As a country with a food deficit, Sri Lanka is heavily impacted by the global food situation. Rising prices negatively affect national and household food security, hindering the country's ability to import food. Factors like trade balance deficit, declining foreign reserves, increased foreign debt, and macroeconomic conditions contribute to food availability at the national level, impacting household food security [13].

According to the Global Food Security Index (GFSI) 2022, Sri Lanka ranks 77th out of 113 countries in terms of food security. Cereals, particularly rice and wheat, are the primary sources of calorie supply in Sri Lanka. Cereals accounted for 55% of the total calorie supply between 2013 and 2017, with rice contributing nearly 40% of the calories [3]. The availability of cereals per capita varied during this period. Wheat, which is entirely imported, serves as the second primary source of cereal supply. The availability of wheat is crucial for Sri Lanka's food security, as it heavily relies on imports to meet its cereal needs. At the same time, rice is produced domestically, with only the deficit being imported.

This high reliance on wheat for consumption in Sri Lanka consequently highlights the importance of securing an uninterrupted inflow of wheat into the country to ensure the country's food security. The advancements in global events like war and terrorism, economic crises, and other natural and artificial turmoil can cause the above disruptions. Therefore, assessing the potential risks of wheat imports and aligning import strategies accordingly is highly critical.

3 Research Methodology

The research utilized the Herfindahl-Hirschman Index (HHI) and the Shannon-Wiener Index (SWI) to assess the external wheat supply risk and diversity of wheat suppliers in Sri Lanka. These indices are commonly used in industrial organizations to measure market concentration. However, they have also been adapted to evaluate risks associated with relying on foreign food supplies, like discussions on energy security [14]. Factors

such as import dependency, political instability of exporting countries, and the risk associated with shipping are considered when using these indices for food security assessments. In our study, the external wheat supply risk of Sri Lanka depends on the level of risk that each of the above factors possesses since they can disrupt the smooth flow of the country's wheat supply chain.

The HHI measures supplier concentration, while the SWI emphasizes source consolidation, giving more weight to minor trading partners [4]. While previous studies have considered factors like substitutability between energy sources, we should have included this factor in our assessment of wheat supply risk as wheat is not easily substitutable.

In our research, we employ the Herfindahl-Hirschman Index (HHI) to evaluate the external supply risk of wheat in Sri Lanka. We consider three key factors to assess this risk:

1. The extent of Sri Lanka's reliance on wheat imports, known as import dependency.
2. The level of political and business-related risks in the countries where Sri Lanka imports wheat.
3. The level of risk associated with transportation and transit during the shipment of wheat.

Drawing inspiration from the study conducted by [14], we developed an equation to calculate Sri Lanka's external wheat supply risk as shown in Eq. (1):

$$EWSR = \left[\sum_i \left(\frac{M_i}{\sum M_i}\right)^2 r_i d_i\right] ID \tag{1}$$

In our assessment of the external wheat supply risk in Sri Lanka, we considered various factors. One crucial factor is the import dependency of the country (*ID*), which is calculated by dividing the total quantity of wheat imported (M_i) from each country by the total domestic supply quantity of wheat in Sri Lanka. Since Sri Lanka relies entirely on wheat imports and does not produce or export wheat domestically, the import dependency is crucial in evaluating the country's wheat supply risk.

We also incorporated a risk assessment variable (r_i) to account for the exporting countries' political and business risks. This variable helps to identify potential threats to the external wheat supply chain. Additionally, we included the distance between the exporting countries and Sri Lanka (d_i) to capture supply chain disruptions that may occur during the transit of the shipment. While the ideal approach would involve analyzing the specific path taken by each wheat import, we used the distance between countries as a proxy for transit risk. The rationale is that longer distances increase the number of countries the shipment passes through, thereby potentially increasing its vulnerability to threats.

Considering these factors, we calculated the External Wheat Supply Risk (ESWR) value, which indicates the level of risk associated with Sri Lanka's wheat imports. A higher ESWR value suggests a higher risk when relying on a single country with a high-risk assessment score. A lower ESWR value indicates a lower risk when importing from multiple countries with lower-risk assessment scores and reducing dependence on imports.

We initially adjusted the equation that Hubbard and Hubbard (2013) proposed to incorporate the factors influencing external supply risk. The modified equation can be expressed as in Eq. (2):

$$DES = -\left[\sum_i \left(\frac{M_i}{\sum_i M_i}\right) ln\left(\frac{M_i}{\sum Mi}\right)(1 - r_i)\right]\frac{1}{ID} \tag{2}$$

To ensure the SWI index covers a wide range and produces positive values, we have multiplied it by -1, as shown above. A value of DES close to zero shows a high level of wheat risk in the supply, indicating the insecurity of external supplies. Conversely, higher DES values suggest a more secure wheat supply, implying a lower level of import risk. Therefore, the equation demonstrates how diversifying external suppliers can reduce the risks associated with external supplies.

It is essential to recognize that even if suppliers are not inherently risky and distances are not significant, relying heavily on a concentrated group of sources itself poses a risk. In other words, the level of source consolidation, rather than diversification, can be a risk factor.

In addition to utilizing the HHI and SWI, we conduct a sensitivity analysis to examine how these indices respond to the factors influencing external supply risk that we have considered. This analysis aims to assess how the HHI and SWI values change when various factors are modified, such as Sri Lanka's level of import dependency. Such analysis provides valuable insights for policymakers when making critical decisions regarding supplier selection or switching under different circumstances.

A similar study [1] was conducted for the UAE, which showed similar results to that of Sri Lanka. Even though the two countries are vastly different regarding macroeconomic factors, they share a similarity in that they heavily depend on imports to fulfill domestic food necessities. But, unlike previous studies conducted by [4, 14, 15], our research differs as it focuses on a national level and specifically on a country that relies entirely on imports to meet its domestic wheat needs. Additionally, we incorporate a sensitivity analysis to investigate the behavior of the HHI against the considered factors, which enhances our understanding of the level of risk the country faces when making decisions related to wheat imports.

4 Results and Discussion

4.1 Analysis and Results

Sri Lanka depends on multiple nations to meet its internal need for wheat. Canada, Russia, USA, Australia, and India have consistently served as suppliers of wheat to Sri Lanka throughout the years. Additionally, Romania and Ukraine have emerged as preferred options for the country regarding wheat supply. The concentration of import quantities from these wheat-exporting countries to Sri Lanka between 2015 and 2021 is depicted in Fig. 1.

Figure 2 shows that less significant suppliers in previous years gained larger import shares in 2021, possibly due to market changes caused by the COVID-19 pandemic, such as export bans and restrictions imposed in exporting countries like Ukraine. These

factors led to reduced export volumes and increased prices globally, affecting importing volumes for countries. Higher import shares pose a higher risk to importing countries, according to the HHI equation, as disruptions could jeopardize the import volume. Sri Lanka relies entirely on imports to meet its domestic demand for wheat since it doesn't produce locally. Unlike countries like the UAE, Sri Lanka doesn't re-export wheat but exports wheat flour through companies like Prima and Serendib, making it a major exporter of wheat flour. This demonstrates that Sri Lanka imports wheat for domestic consumption and to meet international demand for wheat flour and related products.

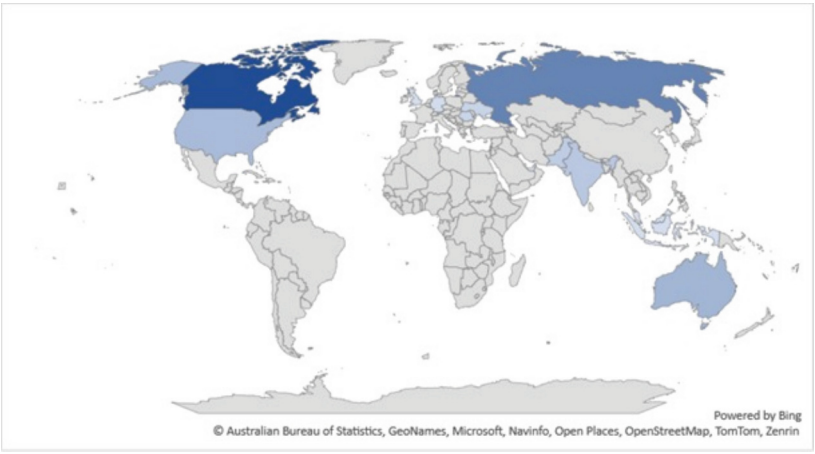

Fig. 1. Sri Lanka's wheat-supplying countries.

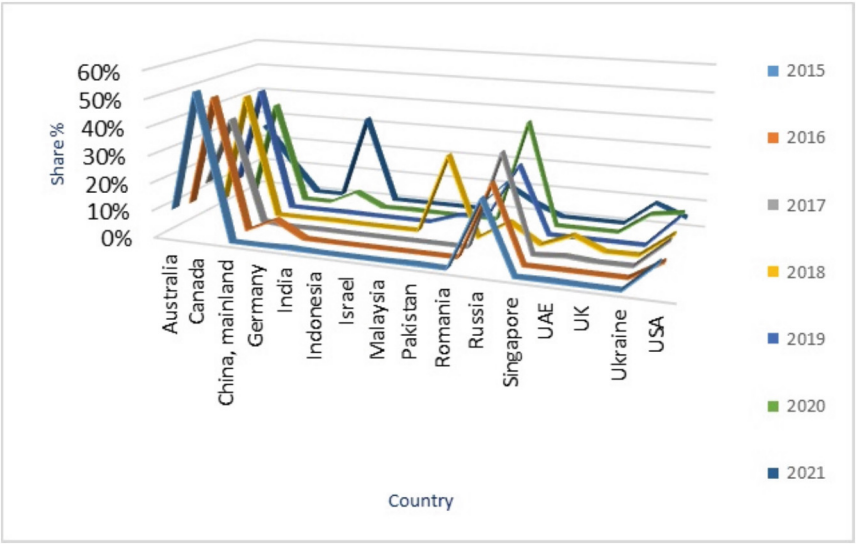

Fig. 2. Wheat import shares of Sri Lanka's wheat suppliers.

According to Fig. 3, it is evident that the total quantity of wheat imported by Sri Lanka has consistently exceeded its domestic supply, except in the year 2016. This suggests that Sri Lanka experienced a wheat deficit in 2016. The highest amount of wheat imports occurred in 2020, despite Covid-19 restrictions, while the lowest was recorded in 2016. While the domestic supply quantity remained relatively stable, the total imported quantity trended upward over time.

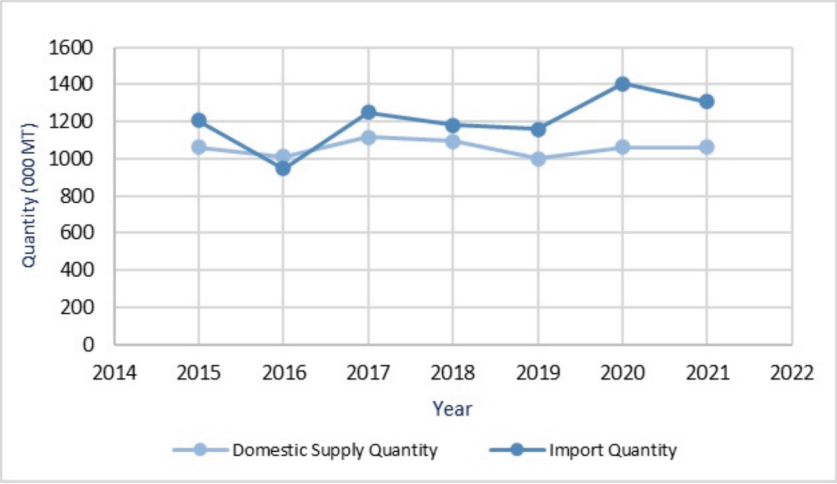

Fig. 3. Total import quantity vs. domestic supply quantity.

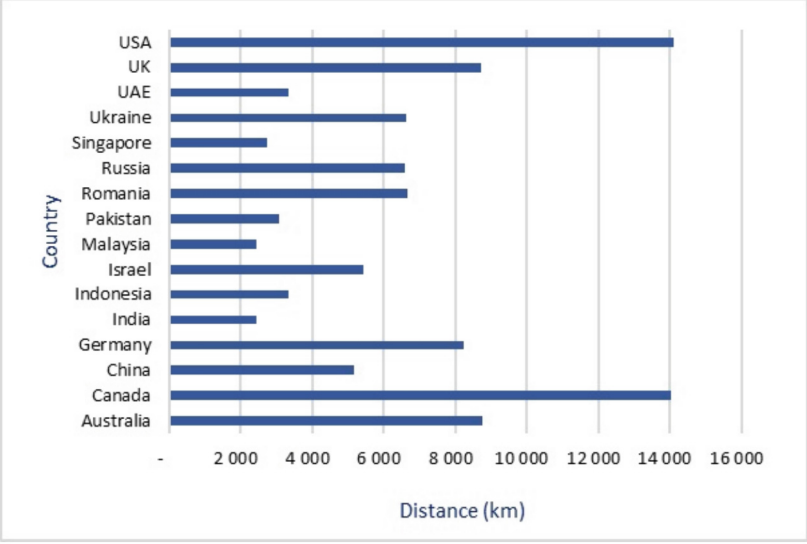

Fig. 4. Distance between the capitals of wheat supplier countries and Sri Lanka.

Our study incorporates supply chain disruptions by considering the distance of shipment, as longer distances increase the risk of disruptions. Figure 4 displays the distances between the capitals of exporting countries and Sri Lanka's capital, Sri Jayewardenepura Kotte. The furthest countries (>6000 km) include the USA, Canada, Australia, the United Kingdom, Germany, Ukraine, Russia, and Romania (categorized as 3). Moderately distant countries (3000 km–6000 km) are denoted as 2, while countries closest to Sri Lanka (<3000 km) are denoted as 1. In 2021, Sri Lanka reduced its import share from Canada (from 37.21% to 12.67%) and likely allocated it to nearby India and Australia, giving them 32.32% and 26.07%, respectively, their highest shares ever.

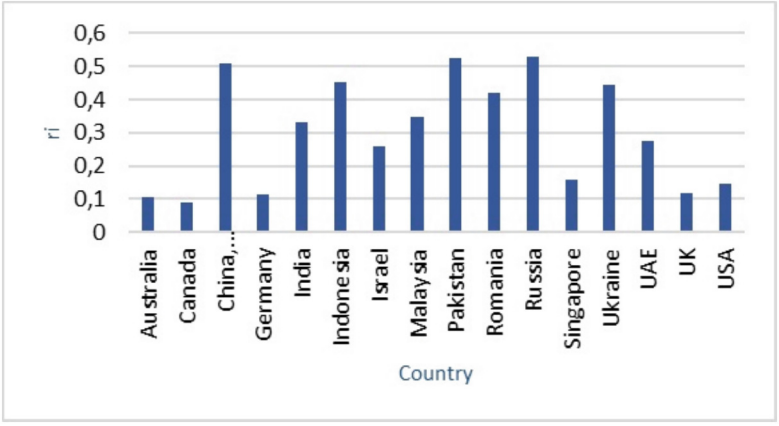

Fig. 5. Level of political and business-related risks in exporting country.

Figure 5 displays the political and business-related risks in Sri Lanka's wheat-exporting countries. As per the data extracted by the Political Risk Services, 2022, Russia and Pakistan have the highest risk assessment variables, followed by Ukraine and Romania, indicating political instability compared to other exporting countries. In 2021, Sri Lanka significantly reduced its wheat import share from Russia to 4.7% after reaching 38.3% in 2020. The exact reason for this change is unclear, but it may be related to the Covid-19 pandemic's impact on wheat prices and export volumes. The impact of the Russia-Ukraine conflict on Sri Lanka's wheat imports could not be assessed due to a lack of data sources.

Figure 6 illustrates Sri Lanka's external wheat supply risk using the indices HHI and SWI. The average HHI value over the period from 2015 to 2021 was 0.21, indicating a relatively low external supply risk during this time. The highest HHI value was observed in 2020 (0.36), attributed to Sri Lanka reducing imports from the secure yet distant country Australia and increasing imports from insecure and distant countries such as Russia and Ukraine. In contrast, the lowest HHI value was seen in 2021 (0.11) when Sri Lanka shifted imports from Russia to India and Australia.

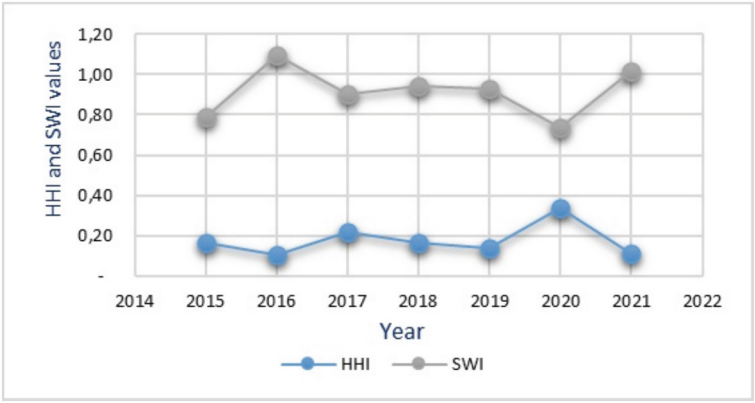

Fig. 6. HHI and SWI values of Sri Lanka from 2015–2021.

When it comes to the SWI, the average value for the period from 2015 to 2021 was 0.92. The highest SWI value was observed in 2016 as1.10, indicating a high diversity of external wheat suppliers and a lower level of external supply risk. The main factors contributing to this high value were the low import dependency in 2016 and the use of more suppliers. On the other hand, the lowest SWI value was recorded in 2020 (0.74), indicating a relatively high external supply risk and a less diverse supplier base. This was primarily caused by high import dependency and increased reliance on less secure countries like Russia and Ukraine.

Figure 7 shows the variation of the aggregate external supply risk and the contribution of a high-risk country like Russia and a low-risk country like Canada to the overall risk. Russia represents countries with relatively higher levels of political risk, whereas Canada represents countries with relatively lower levels of political risk. Canada is much farther from Sri Lanka than Russia is and is, therefore, more likely to be prone to supply chain

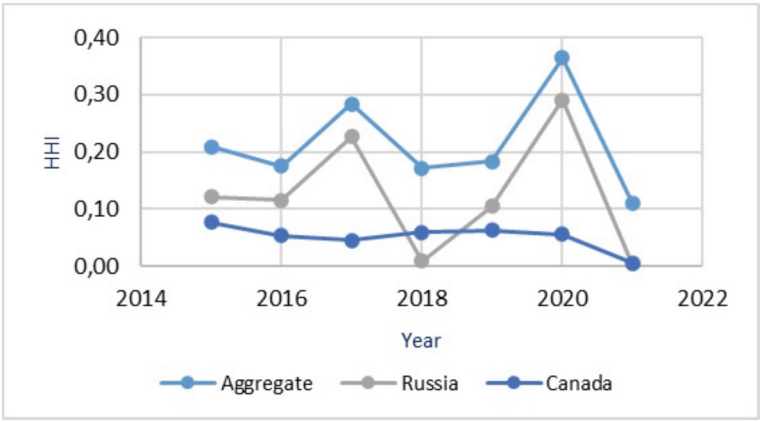

Fig. 7. Aggregate external wheat supply risk Vs risk contributions of Russia and Canada.

disruptions due to distance. Import quantities in Canada have also been higher than those in Russia in most of the years during the considered period. Russia has been the major contributor to the aggregate external supply risk. This suggests that the external supply risk is more responsive to the level of political risk in supplier countries than the distance to the supplier countries and their respective import shares. Therefore, it can be deduced that the higher the level of political risk in supplier countries, the higher the level of contribution to the aggregate external wheat supply risk of Sri Lanka.

4.2 Discussion

During the considered period, Sri Lanka's external supply risk of wheat remained low at an average of 0.21. The highest HHI value, which indicates a greater risk, was recorded in 2020 (0.34), while the lowest, which indicates a small risk, was observed in 2021 (0.11). The significant fluctuation in 2020 was primarily due to a reduction in Australia's import share (from 9.45% to 0.93%) and an increase in the import shares of Russia (from 24.86% to 38.30%) and Ukraine (from 0.01% to 8.14%). Despite being geographically farther from Sri Lanka, Australia had a lower level of political instability (0.1) compared to Russia (0.53) and Ukraine (0.45), which were considered higher-risk suppliers. In 2021, Sri Lanka reduced its import share of Russia to 4.7% while increasing the import shares of Australia (from 0.93% to 26.07%) and India (from 5.1% to 32.21%). This decision led to a significant drop in the external wheat supply risk, reaching its lowest point since 2015. Australia and India were politically stable and considered less risky than Russia. Additionally, India's closer proximity to Sri Lanka further contributed to its favorable position as a wheat supplier.

Another noteworthy finding was that years with higher import shares of Russia ($>20\%$) corresponded to higher external supply risk, whereas years with lower import shares ($<10\%$) saw lower risk. This highlights the importance of diversifying wheat suppliers to reduce risk, as heavy reliance on a single country, particularly one with high-risk levels, increases vulnerability. Supplier diversification was measured using the Supplier Weighted Index (SWI), with the highest SWI recorded in 2016 (1.10) and the lowest in 2020 (0.75). The variation was mainly driven by the level of wheat import dependency, with 2016 exhibiting a low import dependency and 2020 experiencing a high import dependency.

The study also examined the sensitivity of external supply risk to import shares and import dependency by analyzing the cases of Russia and Canada. Despite Russia's closer proximity to Sri Lanka, the supply risk increased significantly with its import share compared to Canada. This indicates that the risk assessment of a supplying country has a more significant impact on the total external supply risk than the distance factor. Additionally, the rate of increase in supply risk for both countries was higher with increasing import shares than with Sri Lanka's level of wheat import dependency. Furthermore, analyzing the sensitivity of external supply risk to import shares and risk assessment using Russia and Canada as base situations revealed that supply risk increases at a higher rate with the risk assessment variable than with distance and import shares.

4.3 Practical Implications

Our study provides valuable insights into the external supply risk of wheat in Sri Lanka, including the diversity of wheat suppliers. We highlight the impact of risk levels in supplying countries on Sri Lanka's wheat supply risk and recommend reducing dependence on high-risk countries like Russia, Ukraine, Romania, and Pakistan. Despite their distance from Sri Lanka, we suggest increasing import shares from lower-risk countries such as Canada, Australia, and the USA. Our findings can assist the government and wheat importers assess external supply risk based on supplier countries and import shares.

Due to data availability constraints, we did not consider the fungibility factor assumed in [4, 14]. The cost factor or trade-offs in measuring external supply risk were not considered. Further, our assessment only focuses on short-term measures. Future research can explore incorporating additional risk factors to enhance the accuracy and applicability of the measurement.

5 Conclusions

Supply chain management in the era of globalization presents both opportunities and risks. Ensuring a resilient food supply chain is crucial for countries like Sri Lanka that heavily rely on food imports. However, more research must be conducted to measure and assess the risks associated with imported food. This study aims to fill this gap by evaluating the external supply risk of wheat in Sri Lanka and examining its sensitivity to various external factors. Our study focused on measuring the external supply risk of wheat in Sri Lanka, considering factors such as import dependency, political/business risks, distance to suppliers, and supplier diversification. Utilizing the Herfindahl-Hirschman and Shannon-Wiener indexes, we analyzed data from 2015–2021, revealing that Sri Lanka has been importing wheat from multiple regular suppliers. While the overall supply risk of wheat in Sri Lanka was low, heavy dependence on high-risk countries like Russia increased supply risks. The study also identified the sensitivity of supply risk to import shares, risk levels of supplier countries, distance, and import dependency. Assigning higher import shares to low-risk countries and diversifying suppliers can effectively reduce Sri Lanka's external wheat supply risk. These findings provide valuable insights for the government and wheat-importing bodies to assess and manage the risk associated with wheat imports in Sri Lanka and similar countries susceptible to import risks.

Acknowledgment. The authors wish to acknowledge the financial support given by the Norwegian Program for Capacity Development in Higher Education and Research for Development (NORHED II – Project number 68085), the "Politics and Economic Governance" sub-theme, the project "Enhancing Lean Practices in Supply Chains: Digitalization", which is a collaboration between the University of Stavanger (Norway), ITB (Indonesia), and the University of Moratuwa.

References

1. Manikas, I., Sundarakani, B., Anastasiadis, F., Ali, B.: A framework for food security via resilient agri-food supply chains: the case of UAE. Sustainability **14**, 6375 (2022). https://doi.org/10.3390/su14106375

2. The Economist Group, "Global Food Security Index (GFSI)," Econ. Intell. Unit. https://impact.economist.com/sustainability/project/food-security-index/#global-overview, (Accessed 10 Dec 2023)
3. Department of Census and Statistics, Food balance sheet 2013–2017. http://www.statistics.gov.lk/Agriculture/StaticalInformation/Foodbalancesheet/FoodBalanceSheet2013-2017-Report, (Accessed 10 Dec 2023)
4. Hubbard, L.J., Hubbard, C.: Food security in the United Kingdom: external supply risks. Food Policy **43**, 142–147 (2013). https://doi.org/10.1016/J.FOODPOL.2013.08.006
5. Mottaleb, K.A., Kruseman, G., Snapp, S.: Potential impacts of Ukraine-Russia armed conflict on global wheat food security: a quantitative exploration. Glob. Food Sec. **35**, 100659 (2022). https://doi.org/10.1016/j.gfs.2022.100659
6. Araujo-Enciso, S.R., Fellmann, T.: Yield variability and harvest failures in Russia, Ukraine and Kazakhstan and their possible impact on food security in the Middle East and North Africa. J. Agric. Econ. **71**(2), 493–516 (2020). https://doi.org/10.1111/1477-9552.12367
7. Emrouznejad, A., Abbasi, S., Sıcakyüz, Ç.: Supply chain risk management: a content analysis-based review of existing and emerging topics. Supply Chain Anal. **3**, 100031 (2023). https://doi.org/10.1016/j.sca.2023.100031
8. Zheng, X., Zhang, L.: Risk assessment of supply-chain systems : a probabilistic inference method. Enterp. Inf. Syst., 1–20 (2020). https://doi.org/10.1080/17517575.2020.1762004
9. Choudhary, N.A., Singh, S.: Risk assessment in supply chains : a state-of-the-art review of methodologies and their applications. Ann. Oper. Res. **322**(2), 565–607 (2023). https://doi.org/10.1007/s10479-022-04700-9
10. Manning, L., Soon, J.M.: Building strategic resilience in the food supply chains. Electronic Libr. **34**(1), 1–5 (2016)
11. Ozdemir, D., Sharma, M., Dhir, A., Daim, T.: Supply chain resilience during the COVID-19 pandemic. Technol. Soc. **68**, 101847 (2022). https://doi.org/10.1016/j.techsoc.2021.101847
12. Sugathadasa, P.T.R.S., Perera, H.N., Liyanage, A.K.: Effective management of manufacturing supply chain risks: a Sri Lankan perspective. Eng. J. Inst. Eng. Sri Lanka **53**(3), 63 (2020). https://doi.org/10.4038/engineer.v53i3.7421
13. Sanderatne, N., De Alwis, S.: National and Household Food Security in Sri Lanka (2014)
14. Le Coq, C., Paltseva, E.: Measuring the security of external energy supply in the European Union. Energy Policy **37**(11), 4474–4481 (2009). https://doi.org/10.1016/j.enpol.2009.05.069
15. Ali, B.M., Manikas, I., Sundarakani, B.: Food security in the United Arab Emirates: external cereal supply risks. Cogent Econ. Financ. **10**(1) (2022). https://doi.org/10.1080/23322039.2022.2149491

Optimizing the Process of Obtaining and Maintaining Rainforest Alliance Certification in the Sri Lankan Supply Chain

Kavitha Wickramaarachchi[1], W. Madushan Fernando[1(✉)], Amila Thibbotuwawa[1], H. Niles Perera[1], and Peter Nielsen[2]

[1] Center for Supply Chain, Operations and Logistics Optimization, University of Moratuwa, Bandaranayake Mawatha, Moratuwa 10400, Sri Lanka
madushanfernando69@gmail.com

[2] Department of Materials and Production, Aalborg University, Fredrik Bajers Vej 7K, 9220 Aalborg East, Denmark

Abstract. This research aims to optimize acquiring and maintaining the Rainforest Alliance certification in the Sri Lankan tea supply chain by introducing a blockchain framework. To address the challenges in the certification process, a specialized blockchain framework is developed by conducting unstructured interviews with industry experts. The main challenges identified during the unstructured interviews were limited resources and knowledge for smallholders, coordination and record-keeping complexities for tea estates and stakeholders, and the time-consuming and expensive adaptation of practices for manufacturers, particularly those with complex supply chains. To assess the influence of various blockchain success factors on the proposed network within the tea industry, Interpretive Structural Modeling (ISM) and Matrice d'Impacts Croisés Multiplication Appliquée à un Classement (MICMAC) analyses are employed. The ISM analysis highlights "immutability" as the foremost driving factor for blockchain success, closely followed by "transparency" and "data accuracy." In terms of dependence on power, "efficiency" emerges as the most influential factor, complemented by the significance of "trust" and "integrity." The structured level partition reveals three categories of success factors: bottom-level factors are highly influential, intermediate-level factors act as facilitators, and top-level factors, while less influential individually, are vital for overall success, relying on lower-level alignment. While relying on expert opinions and subjective judgments, a foundational step is taken toward advancing sustainable supply chain management practices in the tea industry.

Keywords: Blockchain Framework · Rainforest Alliance · Sustainability Certifications

1 Introduction

The tea industry in Sri Lanka significantly contributes to the country's foreign exchange earnings and job creation. It is pivotal in supporting the nation's trade balance and economic stability. In 2022, the tea industry contributed approximately 0.5% to Sri

© The Author(s), under exclusive license to Springer Nature Switzerland AG 2024
V. Ivanov et al. (Eds.): DSMIE 2024, LNME, pp. 475–486, 2024.
https://doi.org/10.1007/978-3-031-61797-3_40

Lanka's GDP, with tea exports constituting about 10.6% of the total exports for that year and 70% manufactured by tea small holders [1]. This economic impact underscores the importance of the industry [2]. Moreover, the tea sector offers employment to over one million individuals, including a substantial proportion of women, contributing to social empowerment and gender equality [1].

However, the sustainability of the Sri Lankan tea industry is challenged by various factors, including cost-cutting measures affecting tea quality, deforestation leading to soil erosion and habitat loss, biodiversity concerns, economic challenges, and environmental issues such as energy usage and greenhouse gas emissions [3].

This research intends to optimize the process of obtaining and maintaining Rainforest Alliance certification in Sri Lanka (Sustainable certification) because sustainability certifications will effectively address the sustainability issues in the tea industry.

2 Literature Review

2.1 Sustainability Certifications

Sustainability certifications effectively address specific concerns, such as child labor practices, health and safety standards, and disciplinary measures, leading to improved working conditions and responsible business conduct [4]. They have also contributed to transforming corporate social responsibility (CSR), integrating social and environmental considerations into business policies and practices [5]. By aligning with sustainability certifications, companies adopt sustainable practices as part of their core operations, resulting in a more comprehensive approach to CSR. Additionally, sustainability certifications reinforce existing state regulations by acting as complementary mechanisms, promoting compliance with higher social and environmental standards [6]. They create a synergistic effect with regulations, enhancing responsible business practices and fostering a sustainable supply chain management culture. Longitudinal studies demonstrate that compliance with certifications leads to notable improvements in workers' rights and conditions, indicating their role as catalysts for positive change [7]. Contrary to the perception of greenwashing, sustainability certifications have demonstrated meaningful contributions towards the United nation's sustainable development goals [8].

A comprehensive literature review reveals numerous challenges impeding the effective implementation of sustainability certifications in supply chains. One significant challenge is the difficulty multinational corporations (MNCs) face in identifying entities beyond the first tier of their supply chains, limiting visibility and monitoring capabilities [9]. Local companies also need more resources and updated practices, hindering their ability to meet certification requirements [10]. Conflicting demands from buyers, emphasizing sustainability while pressuring for commercial goals, create supplier dilemmas [9]. Uneven distribution of costs and responsibilities within the supply chain contributes to behavioral issues and a need for more transparency [11]. Understanding these challenges is essential for developing effective strategies to overcome them and realizing the full potential of sustainability certifications in promoting responsible practices.

2.2 Significance of Rainforest Alliance Certification

The significance of Rainforest Alliance certification in the context of tea farms in Kenya and its impact on various environmental and social aspects has been researched and analyzed [12]. The certification has positively affected certified tea farms in Kenya, particularly in terms of environmental and social factors. Sustainability certifications like Rainforest Alliance aim to establish a stronger connection between consumers and producers, encouraging ethical consumer choices and supporting sustainable production practices [13]. The organization engages in collaborative projects with sustainability buyers to train farmers in sustainability practices, building capacity, and knowledge among farmers [14].

Multinational corporations such as Unilever, Van Rees, and Tata Global Beverages have demonstrated their commitment to Rainforest Alliance certification [15–17]. Unilever has set ambitious goals for sustainable sourcing, including tea, and has been actively training and educating tea smallholders in Vietnam [15]. An internationally recognized consumer goods corporation has established a goal to obtain Rainforest Alliance certification for all its tea products, aligning with consumer market trends and increasing demand for sustainable production practices [18]. By pursuing Rainforest Alliance certification, the company aims to maintain a competitive edge and satisfy consumer expectations regarding sustainability.

2.3 Blockchain Technology in Supply Chains

Blockchain technology, integrating smart contracts and IoT, enhances supply chain visibility, automates processes, and ensures product authenticity [19]. This improves economic sustainability through traceability, transparency, and decentralization, contributing to environmental and social sustainability [20]. The introduction of blockchain in agriculture facilitates visible information on carriers, stakeholder registration, logistics, and product details while maintaining rigorous documentation [21]. Three blockchain types are public (e.g., Bitcoin), private (e.g., Corda), and consortium—offer diverse permission levels and governance structures in the networks [22].

3 Research Methodology

Literature mentioned the significance of the Rainforest Alliance certification to the sustainability of the tea supply chain. This research aims to come up with a solution that eases up the process of obtaining and maintaining Rainforest Alliance certification in the Sri Lankan tea supply chain by using the attributes of blockchain technology and below Fig. 1 showcases steps in methodology.

An unstructured interview session was held with tea industry experts representing various stakeholders. Table 1 shows the demographic of the industry experts who participated in the unstructured interview sessions.

In this study, Interpretive Structural Modeling (ISM) [23] and Matriced' Impacts Croises Multiplication Appliquées a un Classement (MICMAC) analyses were employed to assess how the blockchain success factors introduced by Yadav & Singh, 2020 impact the proposed blockchain solution. Expert interviews provided the input data for this analysis.

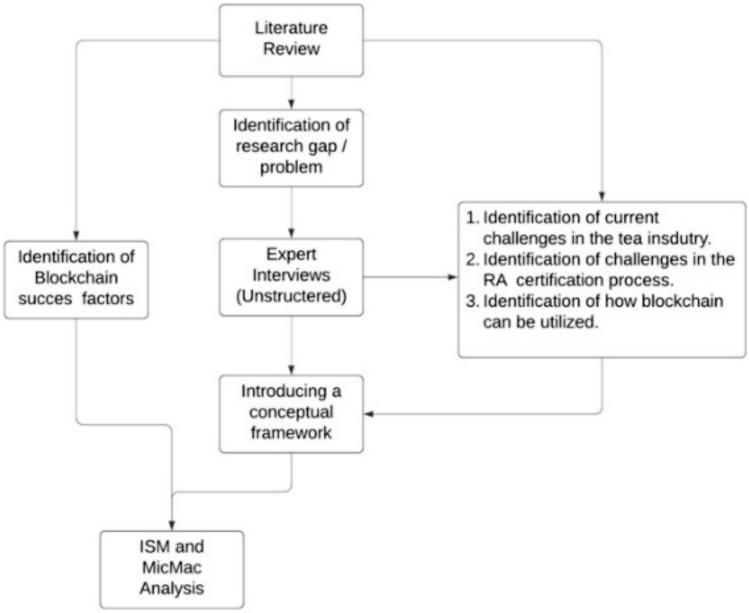

Fig. 1. Steps in methodology.

Table 1. Expert demographic.

Organization	Number of experts	Administration Level / Designation
Auditor (Accredited certification body)	2	Management
Tea Estate	1	Senior Management
Rainforest Alliance	1	Management/Consultant
Tea Small Holdings Development Authority	2	Management/Field officer
Tea brokerage firm	1	Management
Tea exporter	1	Management
Total Experts	8	

4 Results and Discussion

4.1 Challenges Identified in the Process of Obtaining and Maintaining the Rainforest Alliance

Tea Small Holders. Tea smallholders face obstacles in implementing sustainable practices and meeting certification requirements due to limited resources and technical knowledge. Financial constraints make it challenging to access necessary investments,

and a lack of information on certification standards and best practices hinders their efforts. Support and resources are needed to help tea smallholders overcome these barriers and participate effectively in the certification process.

Tea Estates. Tea estates face significant challenges in obtaining and maintaining Rainforest Alliance certification. This involves coordinating various departments, maintaining extensive records, and undergoing labor-intensive audits.

Accredited Auditors. The auditing process for Rainforest Alliance certification demands substantial resources in terms of time, personnel, and expertise. Complex data collection and verification have been challenging, especially with manual documentation.

Manufacturers, Warehousing, and Transportation Stakeholders. Meeting certification standards often necessitates significant changes to current practices, which is time-consuming and expensive. Managing the documentation and record-keeping of compliance-related data is particularly challenging for large-scale manufacturers with complex supply chains.

4.2 Blockchain Network Selection

Due to its specific requirements, a consortium blockchain network is the preferred solution for optimizing the Rainforest Alliance certification process.

- Enhanced Privacy and Control - The certification process involves multiple stakeholders sharing sensitive information. A consortium blockchain provides controlled access, ensuring data privacy while maintaining transparency among members.
- Trusted Network of Participants - Consortium blockchains comprise trusted organizations committed to common goals. This ensures that only authorized, trustworthy participants are part of the network, reducing the risk of fraud or malicious activities.
- Efficient Consensus Mechanism - Consortium blockchains can implement efficient consensus mechanisms tailored to the stakeholders' needs, unlike public blockchains with potentially untrusted nodes. This streamlines transaction validation and verification.
- Improved Scalability and Performance – Consortium blockchains offer better scalability and performance for handling the high transaction volume in the certification process, ensuring efficient processing.
- Governance and Decision-making – Consortium blockchains enable collective agreement on governance and decision-making rules among members, ensuring fair and transparent certification process management, collaboration, dispute resolution, and decision-making.

4.3 Introduction of Blockchain Framework

Figure 2 showcases the proposed blockchain network, and arrows support the information and smart contracts flow in the process.

Also, the proposed solution involves establishing a consortium blockchain network as a single platform for the identified key stakeholders in the tea supply chain and the

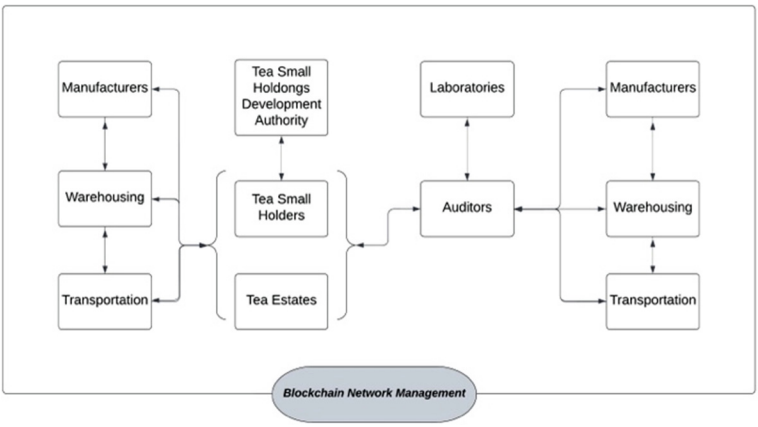

Fig. 2. Proposed blockchain framework.

Rainforest Alliance certification process. This network allows for secure and transparent information sharing, collaboration, and real-time stakeholder communication.

Through the consortium blockchain network, stakeholders can securely exchange certification-related data, such as audit reports, supply chain information, and compliance records. This streamlined sharing process enhances trust, accountability, and traceability throughout the certification process. By utilizing the proposed blockchain network, tea small holders can provide auditors and manufacturers with secure access to their cultivation practices and compliance records, ensuring transparency and accountability across the supply chain. Tea estates can quickly provide the necessary documentation to demonstrate their adherence to sustainability standards, and testing labs can securely share test results with relevant parties.

The proposed framework facilitates the automation of specific processes through the use of smart contracts. These contracts can automatically trigger actions or notifications based on predefined rules and criteria, reducing manual intervention and streamlining the certification process. The framework also establishes a transparent and immutable audit trail, allowing stakeholders, including the Rainforest Alliance, to verify the authenticity and integrity of certification-related data easily. This enhances the credibility of the certification process and builds trust among stakeholders and consumers.

4.4 Interpretive Structural Modeling

Table 2 displays chosen blockchain success factors, while Fig. 3 presents the final reachability matrix. Additionally, Table 3 illustrates the ISM level partition, and Fig. 4 showcases the ISM model.

Based on the analysis (Fig. 4), "immutability" was identified as the blockchain success factor with the highest driving power, followed by "transparency" and "data accuracy." In terms of dependence power (Fig. 4), "efficiency" was the most influential factor, followed by "trust" and "integrity." A structured level partition (Fig. 5) consisting of nine levels facilitated the categorization of factors and represented their relationships.

Table 2. Blockchain success factors were used for the analysis.

Blockchain success factors	
Efficiency (B1)	Immutability (B9)
Effectiveness (B2)	Reliability (B10)
Operation speed (B3)	Decentralization (B11)
Quality (verification and validation) (B4)	Data accuracy (B12)
Transparency (B5)	Traceability (B13)
Security (B6)	Integrity (B14)
Disintermediation (B7)	Cost reduction (B15)
Trust (B8)	Save energy (B16)

	B1	B2	B3	B4	B5	B6	B7	B8	B9	B10	B11	B12	B13	B14	B15	B16	DRIVING POWER
B1	1	1	1	0	0	0	0	0	0	0	0	0	0	0	1	1	5
B2	0	1	0	1	0	0	0	0	0	0	0	0	0	0	0	0	2
B3	1	1	1	0	0	0	0	0	0	0	0	0	0	0	0	0	3
B4	0	1	0	1	1	0	0	1	0	0	0	0	1	1	0	0	6
B5	0	1	0	1	1	0	0	1	0	1	0	0	0	1	1	0	7
B6	0	1	0	0	0	1	0	1	0	1	0	1	0	1	0	0	6
B7	0	1	1	0	0	0	1	0	0	0	0	0	0	0	1	1	5
B8	0	1	0	0	0	0	0	1	0	0	0	0	0	1	0	0	3
B9	0	1	0	1	1	1	0	1	1	1	0	1	0	1	0	0	9
B10	0	1	0	1	0	0	0	1	0	1	0	0	0	1	0	0	5
B11	0	0	1	0	1	0	0	0	0	0	1	0	0	0	0	0	3
B12	0	1	1	1	0	0	0	1	0	1	0	1	0	1	0	0	7
B13	0	1	0	0	1	0	0	1	0	1	0	0	1	0	0	0	5
B14	0	1	0	0	0	0	0	1	0	1	0	0	1	1	0	0	5
B15	0	1	0	0	0	0	0	0	0	0	0	0	0	0	1	0	2
B16	0	1	0	0	0	0	0	0	0	0	0	0	0	0	0	1	2
DEPENDENCE POWER	2	15	5	6	5	2	1	9	1	7	1	3	3	8	4	3	

Fig. 3. Final Reachability Matrix.

This partitioning was used to develop a model visually depicting the interdependencies between success factors through one-way and two-way connected arrows in an ISM digraph, as shown in Fig. 5. Further examination of the ISM diagram in Fig. 5 revealed three categories of success factors.

- Bottom-level success factors (B9, B6, B12, B4) were deemed highly influential and played a crucial role in shaping the overall success of the blockchain network. Addressing these factors is essential to establish a strong foundation for the system's success.

Table 3. Level Partition.

Success factors	Reachability set (Row)	Antecedent set (Column)	Intersection Level	Level
B1 - Efficiency	B1, B2, B3, B15, B16	B1, B3	B1, B3	3
B2 - Effectiveness	B2, B4	B1, B2, B3, B4, B5, B6, B 7, B8, B9, B10,12, B13, B14, B15	B2, B4	1
B3 - Operation speed	B1, B2, B3	B1, B3, B7, B11, B12	B1, B3	2
B4 - Quality	B2, B4, B5, B8, B13, B14	B2, B4, B5, B9, B10, B12	B2, B4, B5	7
B5 - Transparency	B2, B4, B5, B8,10, B14, B15	B4, B5, B9, B11, B13	B4, B5	4
B6 - Security	B2, B6, B8, B10, B12,14	B6, B9	B6	8
B7 - Disintermediation	B2, B3, B7, B15, B16	B7	B7	3
B8 - Trust	B2, B8, B14	B4, B5, B, B8, B9, B10, B12, B13, B14	B8, B14	2
B9 - Immutability	B2, B4, B5, B6, B8, B9, B10, B12, B14	B9	B9	9
B10 Reliability	B2, B4, B8, B10, B14	B5, B6, B9, B10, B12, B13, B14	B10, B14	3
B11 Decentralization	B3, B5, B11	B11	B11	5
B12 Data Accuracy	B2, B3,4, B8, B10, B12, B14	B6, B9, B12	B12	7
B13 Traceability	B2, B5, B8, B10, B13	B4, B13, B14	B13	5
B14 Integrity	B2, B8, B10, B13, B14	B4,5, B6, B8, B9, B10,12, B14	B8, B10, B14	6
B15 Cost reduction	B2, B15	B1, B5, B7, B15	B15	2
B16 Save energy	B2, B16	B1, B7, B16	B16	2

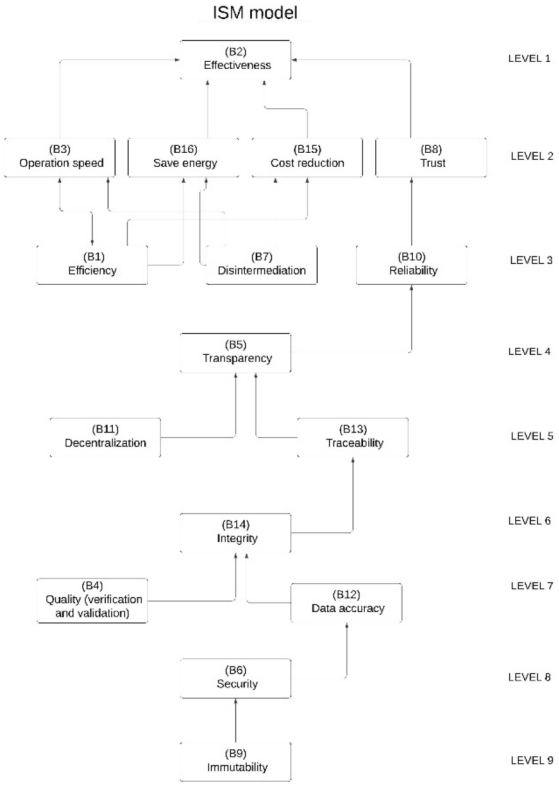

Fig. 4. ISM model.

- Intermediate-level success factors (B14, B13, B11, B5) acted as intermediaries, connecting bottom-level factors with top-level factors. While not the most influential, they contributed to the overall success by facilitating the flow of factors within the network.
- Top-level success factors (B1, B7, B10, B3, B15, B16, B8, B2) had a relatively lower influence on other success factors but were vital for the overall success of the blockchain network. They depended on the alignment and support of lower-level and intermediate-level factors to achieve their full potential.

4.5 MICMAC Analysis

Figure 5 below illustrates the MICMAC analysis, which classifies the success factors of blockchain.

Most factors are in the autonomous cluster, indicating they are relatively easier to achieve. B2 and B8 are in the dependent cluster, aligning with the ISM model's top-level

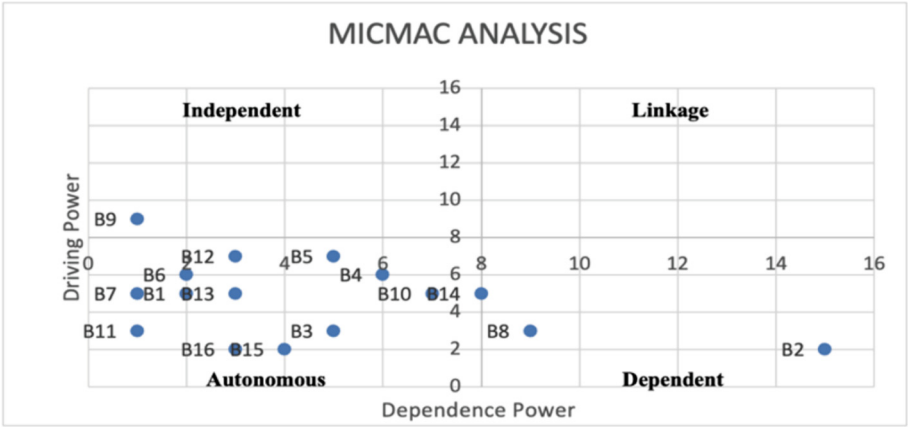

Fig. 5. MICAMAC analysis.

factors. No factors were in the linkage cluster. B9 is in the independent cluster, emphasizing its importance. The analysis provides insights for researchers and stakeholders to focus efforts effectively. However, the research has limitations, including generalizability, sample size impact, depth of investigation, conceptual nature, external factors' influence, and the need for future practical implementation studies and pilot studies.

5 Conclusions

In conclusion, this research addresses a critical research gap in the sustainable certification processes within the Sri Lankan tea supply chain by proposing a blockchain framework for optimizing the Rainforest Alliance certification. The existing challenges faced by tea smallholders, tea estates, and other stakeholders necessitated a novel approach to enhance efficiency and transparency in the certification process.

The methodology employed involved unstructured interviews with industry experts, leading to developing a specialized blockchain framework. Interpretive Structural Modeling (ISM) and Matrice d'Impacts Croisés Multiplication Appliquée à un Classement (MICMAC) analyses were crucial components of the research methodology, providing valuable insights into the blockchain success factors and their interdependencies.

The significant findings of this study highlight the key challenges faced by tea smallholders, tea estates, and accredited auditors in the Rainforest Alliance certification process. These challenges, ranging from limited resources and knowledge to coordination complexities, underscore the need for a tailored solution. The proposed blockchain framework, particularly a consortium blockchain network, emerges as a preferred solution, offering enhanced privacy, control, and efficiency in the certification process.

For future research, exploring the practical implementation and impact of the proposed blockchain framework in the Sri Lankan tea supply chain is imperative. Further studies can delve into the scalability and adaptability of blockchain technology in

other agricultural supply chains. Additionally, longitudinal research can assess the long-term effects of blockchain integration on sustainability certifications and the overall tea industry.

References

1. Wijayasiri, J., Arunatilake, N., Kelegama, S.: Sri Lanka tea industry in transition: 150 years and beyond. Institute of Policy Studies of Sri Lanka (2018)
2. Central Bank of Sri Lanka: Annual Report 1 (2022)
3. International Labour Organization: Future of Work for Tea Smallholders in Sri Lanka (2018)
4. Yu, X.: Impacts of corporate code of conduct on labor standards: a case study of reebok's athletic footwear supplier factory in China. J. Bus. Ethics **81**, 513–529 (2008). https://doi.org/10.1007/S10551-007-9521-2/METRICS
5. Mzembe, A.N., Lindgreen, A., Maon, F., Vanhamme, J.: Investigating the drivers of corporate social responsibility in the global tea supply chain: a case study of eastern produce limited in Malawi. Corp. Soc. Responsib. Environ. Manag. **23**, 165–178 (2016). https://doi.org/10.1002/CSR.1370
6. Amengual, M.: Complementary labor regulation: the uncoordinated combination of state and private regulators in the dominican republic. World Dev. **38**, 405–414 (2010). https://doi.org/10.1016/J.WORLDDEV.2009.09.007
7. Egels-Zandén, N.: Revisiting supplier compliance with MNC codes of conduct: recoupling policy and practice at chinese toy suppliers. J. Bus. Ethics **119**, 59–75 (2014). https://doi.org/10.1007/S10551-013-1622-5/TABLES/2
8. DeFries, R.S., Fanzo, J., Mondal, P., et al.: Is voluntary certification of tropical agricultural commodities achieving sustainability goals for small-scale producers? a review of the evidence. Environ. Res. Lett. **12** (2017). https://doi.org/10.1088/1748-9326/AA625E
9. Soundararajan, V., Brown, J.A.: Voluntary governance mechanisms in global supply chains: beyond CSR to a stakeholder utility perspective. J. Bus. Ethics **134**(1), 83–102 (2014). https://doi.org/10.1007/S10551-014-2418-Y
10. Silva-Castañeda, L.: A forest of evidence: third-party certification and multiple forms of proof—a case study of oil palm plantations in Indonesia. Agric. Hum. Values. **29**, 361–370 (2012). https://doi.org/10.1007/S10460-012-9358-X
11. Acquier, A., Valiorgue, B., Daudigeos, T.: Sharing the shared value: a transaction cost perspective on strategic CSR policies in global value chains. J. Bus. Ethics **144**, 139–152 (2017). https://doi.org/10.1007/S10551-015-2820-0/TABLES/1
12. Ochieng, B.O., Hughey, K.F.D., Bigsby, H.: Rainforest alliance certification of Kenyan tea farms: a contribution to sustainability or tokenism? J. Clean. Prod. **39**, 285–293 (2013). https://doi.org/10.1016/J.JCLEPRO.2012.07.048
13. Eden, S., Bear, C., Walker, G.: Mucky carrots and other proxies: problematising the knowledge-fix for sustainable and ethical consumption. Geoforum **39**, 1044–1057 (2008). https://doi.org/10.1016/J.GEOFORUM.2007.11.001
14. Our Approach | Rainforest Alliance. https://www.rainforest-alliance.org/approach/. accessed 31 May 2023
15. Unilever. https://www.unilever.com/planet-and-society/. Accessed 01 June 2023
16. Van Rees. https://vanrees.com/. Accessed 01 June 2023
17. Tata Consumer Products. https://www.tataconsumer.com/. Accessed 01 June 2023
18. Munasinghe, A., Cuckston, T., Rowbottom, N.: Sustainability certification as marketisation: rainforest Alliance in the Sri Lankan tea production industry. Account. Forum **45**, 247–272 (2021). https://doi.org/10.1080/01559982.2021.1893053

19. Cao, Y., Yi, C., Wan, G., et al.: An analysis on the role of blockchain-based platforms in agricultural supply chains. Transp. Res. E Logist. Transp. Rev. **163** (2022). https://doi.org/10.1016/J.TRE.2022.102731
20. Munir, M.A., Habib, M.S., Hussain, A., et al.: Blockchain adoption for sustainable supply chain management: economic, environmental, and social perspectives. Front Energy Res. **10** (2022). https://doi.org/10.3389/FENRG.2022.899632/BIBTEX
21. Vangipuram, S.L.T., Mohanty, S.P., Kougianos, E., Ray, C.: AgroString: visibility and provenance through a private blockchain platform for agricultural dispense towards consumers. Sensors **22**, 8227 (2022). https://doi.org/10.3390/S22218227
22. Types of Blockchains Explained- Public Vs. Private Vs. Consortium. https://www.blockchain-council.org/blockchain/types-of-blockchains-explained-public-vs-private-vs-consortium/. Accessed 07 June 2023
23. Aruchunarasa, B., Fernando, W.M., Perera, H.N., et al.: Barriers to additive manufacturing implementation in plastic waste management - a case study from a developing economy. In: IEEE International Conference on Industrial Engineering and Engineering Management, pp. 1438–1442 (2022). https://doi.org/10.1109/IEEM55944.2022.9989644
24. Yadav, S, Singh, S.P.: Blockchain critical success factors for sustainable supply chain. Resour. Conserv. Recycl. **152** (2020). https://doi.org/10.1016/J.RESCONREC.2019.104505

Engineering Education

Designing the Educational Content for the Industry 4.0 Competency Model

Peter Arras[1](✉) and Galyna Tabunshchyk[2,3]

[1] KU Leuven, 5, Jan De Nayerlaan, 2860 Sint Katelijne Waver, Belgium
peter.arras@kuleuven.be
[2] National University "Zaporizhzhia Polytechnic", 64 Zhukovskogo, Zaporizhzhia 69063, Ukraine
[3] FH Dortmund, IDiAL, 23, Otto-Hahn Street, Dortmund, Germany

Abstract. In this paper, authors reflect on the methodology used in the Work4Ce-project (Cross-domain competencies for healthy and safe work in the 21st century) to build a competency model for Industry 4.0 in an Education 4.0 environment. The competency model is a tool that clarifies the skills, knowledge, and attitudes a person needs to perform a job in a particular environment and describes what is necessary for a student for a learning module. The methodology of building this model can generally be used to define competency models and build courses in a setup with distributed stakeholders. In a co-creation setup with OpenCops and a Joint Educational system, the different international partners create open educational resources on the different topics for Industry 4.0. The educational resources should serve different target groups: (engineering) students and professionals needing to update and extend their knowledge on the topic.

Keywords: Work4ce · OpenCop · Open Educational Resources · Sustainable Education

1 Introduction

The Work4Ce-project ("Cross-domain competencies for healthy and safe work in the 21st century") addresses the need for educational resources to prepare for the future workplace (Work 4.0) [1]. The project starts from the observation that in a world where the digital transformation of the workplace and processes is constantly speeding up, employees (and employers) need new and different sets of knowledge and skills to do their jobs successfully. The competence to work efficiently in a digitally transformed world ranges from basic digital skills (obviously) to working in a new setting where colleagues work in distributed teams at other geographical locations and even in other time zones. This was highlighted in the recent Covid pandemic when colleagues could no longer meet physically. All of these impact the way people work (and live).

The Work4Ce project aims to define competency models (sets of required skills, knowledge, and attitudes) and learning materials to prepare students and professionals with the tools to cope with this changing environment.

© The Author(s), under exclusive license to Springer Nature Switzerland AG 2024
V. Ivanov et al. (Eds.): DSMIE 2024, LNME, pp. 489–497, 2024.
https://doi.org/10.1007/978-3-031-61797-3_41

In the project, interdisciplinary curricula and modules are developed, and (virtual) university-enterprise collaboration is organized to assess the practical value of the curricula to improve the potential employability of the graduates. Implementing a co-production approach of teachers and industry experts, new, job-related competency models for the workplace of the future (Work 4.0) are defined.

A competency model is a set of guidelines that define the skills, knowledge, and general competencies/attitudes required for employees to perform a job professionally. Competency modeling is a tool used explicitly by the human resources department of an organization to assess candidates during the employment process, as well as for employee talent management and performance management.

Competency modeling is an important asset in the recruitment process as it allows companies to ensure that new, onboarded employees have the core skills and knowledge required for the job. The competency model is a basis for recruiters in defining adequate job descriptions, and for potential employees, it creates a well-defined framework of expectations.

A competency model is also a basis for the talent management of employees. From the moment of recruiting through training and development, HR and coaches have a better overview of the skills that need to be present or developed in their co-workers. As such, a track for (lifelong)learning can be defined.

Competency modeling allows companies to set targets and properly assess employees during evaluation sessions. It gives direction to employees by defining areas for improvement.

In the paper, the authors will discuss the process of coming to the competency model for the course module on Industry 4.0 and give a short outline of the curriculum and the competency model.

2 Literature Review

Educational institutions should be able to react to the quickly changing requirements of the labor markets, and an approach to working with broadly defined competency models was piloted in the Work4Ce project. To derive a competency model, the necessary learning outcomes must first be defined.

Learning outcomes are defined as statements of what a learner knows, understands, and can do after completing the learning process. In the EQF (European Qualification Framework) [2, 3], learning outcomes are thus defined in terms of knowledge, skills, and competence which are defined as follows [4]:

- Knowledge is the outcome of the assimilation of information through learning. It is the body of facts, principles, theories, and practices related to a field of work or study. In the context of the EQF, knowledge is described as theoretical.
- Skills are the ability to apply knowledge and use know-how to complete tasks and solve problems. In the EQF, skills are described as cognitive or practical skills.
- Competence is the proven ability to use knowledge, skills, and personal, social, and methodological abilities in work or study situations and in professional and/or personal development. In the EQF, competence is described in terms of responsibility and autonomy.

Learning Outcomes, Competencies, and Qualifications are to be formulated according to the EQF [2] and the ESG (European Standards and Guidelines) [3]. A guideline for formulating learning outcomes is given in [5].

The shift of competencies required for people to work in a digitally transformed world is evident in the context of Industry 4.0 implementation, which involves accents on agile and digital transformation processes [6].

The authors provided research on the impact of university-business cooperation for Industry 4.0 in the manufacturing industry. It highlights the gaps, especially in understanding the importance of digital competencies [7].

The authors consider the importance of developing the competency model in the cross-border projects [8]. A conceptual model of the competence-based selection of the team is suggested in the different projects.

The authors [9] investigate the roles of the competence centers in supporting the small and medium enterprises towards the Industry 4.0 paradigm.

The maturity model for competency development for Industry 4.0 has also transformed during the last few years [10].

In the Work4Ce project, the competency model was defined in an expert group, OpenCop (Open Community of Practice), and hereunder, the authors look at the model for the module on Industry 4.0. The creation of learning environments and experiences in Cops (Communities of Practice) that bring our learners together to form learning communities was stated by [11].

3 Research Methodology

Creating and assuring a general competency model for a thematic course so that it is relevant to be used by academia and industry was tackled using a combination of Open Communities of Practice, a Joint Educational Ecosystem, and Open Educational resources.

As the target audiences for the educational resources are threefold (master students, academic staff, and industry employees), each with a different outcome, the competency model should describe all necessary skills, knowledge, and attitudes. To make the model consistent in use for all target groups, it is necessary to have all stakeholders participate in defining the model.

Therefore, an Open Community of Practice (OpenCop) comprises academic staff, industry representatives, and other stakeholders. Since Work4ce is an international project, OpenCop is also an international group with participants from different countries and backgrounds. The task of the OpenCop is to define the competency model (describing what knowledge, skills, and overarching competencies employees need on a topic– and so students need to acquire during studying), to design and create the course/learning materials, to do the reviewing and release process of the learning materials. The different process steps to come to course materials are described in Fig. 1. OpenCop leads to co-creating content and ideas between all stakeholders [1].

As the OpenCop is a task force distributed in space and time, a Joint Educational Ecosystem and collaboration space was created so that all can work on the same ideas and content.

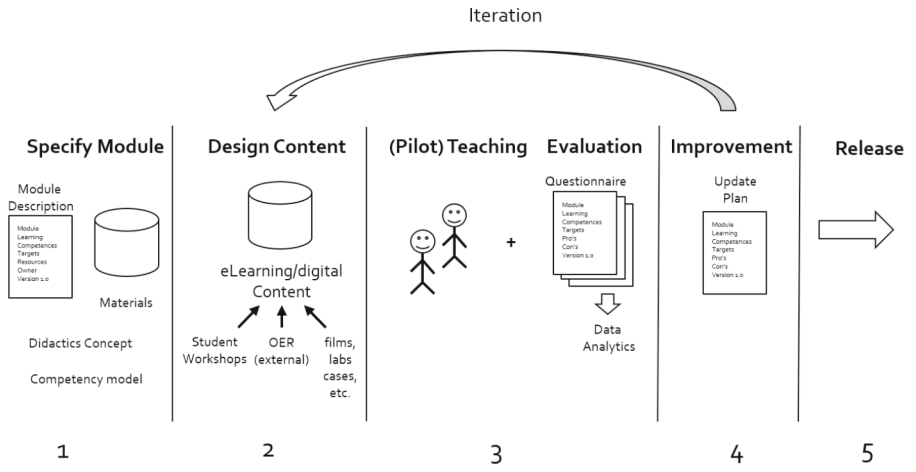

Fig. 1. Process flow of course materials design.

The Work4Ce portfolio of modules for workers to perform in a digitally transformed world includes Working in distributed teams (as workforces are dispersed in time and place, Managing digital change (as a conversion of a traditional workplace into a digital one requires adaptation), Life cycle thinking and sustainable management, Developing digital business ecosystems (the future world more entrepreneurship is desired) and technical modules Industry 4.0, Digital technologies.

As a case study, we look at the development of the Industry 4.0 Module, which aims to introduce some key Industry 4.0 technologies to students and workers. The module on Industry 4.0 consists of a core course, which is obligatory, and several electives to reach a minimum of 9ECTS. Using this structure allows the use of the module for the different target groups, as for each group, a different content collection can be taken. This is visualized in (Fig. 2), where the blue color represents the total of the module contents, the dark blue the core course(s), and the turquoise the elective(s).

- Core course: Introduction to Industry 4.0 and consequences for project and financial management (3ECTS).
- Elective courses on Technologies used in Industry 4.0: IoT (2ECTS), Digital Twins (2ECTS), Additive Manufacturing (2ECTS), Quality of industrial systems/predictive maintenance/condition monitoring (2ECTS), Data analysis for Industry 4.0 (2ECTS), BIM (Building Information Modeling) (2ECTS).
- Each module comes with a set of described competencies (which is the competency model), and each course within the module has its' elaborated set of competences described in 3 categories: knowledge, skills, general (or overarching) competences. The latter is sometimes commonly described as soft skills or transversal skills. This competency model is agreed upon in the OpenCop; as such, it is used for students to describe what they need to study, for industry as a method of measuring the capabilities of their staff, and for academic staff as a requirement for being able to use and teach the module component courses. The competencies are described according to the European "Guidelines for the Description of Learning Outcomes" [9].

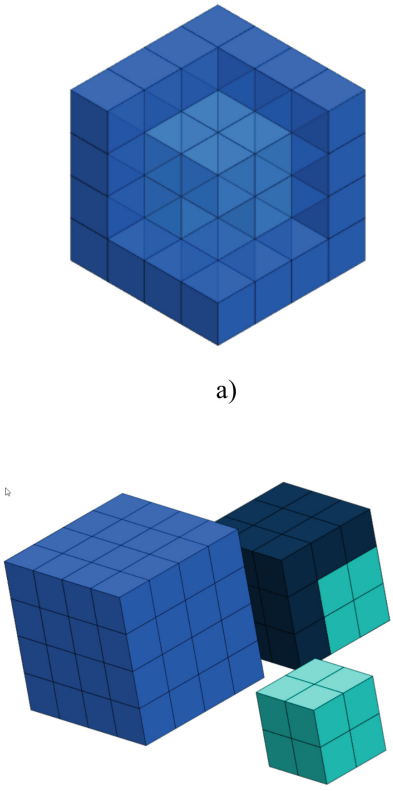

Fig. 2. Knowledge Cube of Module content: a: module knowledge cube which consists of core courses and electives; a) a total of module knowledge educational e-learning programs and resources; b) selection depending on the target audience.

It is essential to develop quality digital media to develop course materials to be used as Open Educational Resources afterward in a setting with different universities in different countries. Incorporating existing open resources/materials is planned in the OpenCop and described in the learning activities. The learning activity plan guides teaching staff on using digital materials in their classrooms (physical and/or virtual). It describes each course and the educational format in which specific outcomes will be reached. Formats, e.g., seminars, self-study eLearning, case studies, assignments, and lab sessions. It helps teaching staff structure their courses and allows differentiation between the target groups with different formats.

The construction of decent digital materials is done according to the KU Leuven learning lab approach, "Quick guide to blended course design" (https://www.kuleuven.be/english/education/leuvenlearninglab/support/quick-guide-blended-course-design/quick-guide-blended-course-design), which give a ready-made guide to convert existing course materials in useable digital learning materials.

For the quality assurance of the materials, a review process is defined with checklists for digital media and course materials so that members of OpenCop can quickly review the developed materials and check against desired learning outcomes.

4 Results and Discussion

In the Work4Ce project, the development of educational resources starts from an agreed competency model that covers (mostly) the complete set of knowledge, skills, and abilities. The competency sets and outline for the educational resources are discussed and decided in OpenCops (Open Communities of Practice), with members from academia, companies, and societal stakeholders. The OpenCop also reviews and finally publishes the educational resources.

A target group analysis was made to develop e-learning materials for the different target groups (Table 1). From this analysis, a description of the competency model was derived after discussion with the expert OpenCop to satisfy the needs of each target group.

The developed competency model for the Industry4.0 module as a whole:

- Students learn the roots of digital transformation towards Industry 4.0 and understand how to overcome the challenges of digital transformation projects.
- Students learn about the key emerging technologies at the core of Industry 4.0 to understand the technological challenges for a digital transformation towards Industry 4.0.
- Students learn about the consequences of introducing Industry 4.0 into an organization: change management and effects on project management.
- Students can propose argued steps to implement digital transformation (technologies, project management techniques) in an industry 4.0 setting.

Elaborated for the core course "Introduction to Industry 4.0 and consequences for project and financial management." This translates into the following competency description (Table 2).

For each elective course, similar lists of competencies have been defined.

The developed course material is piloted in short summer schools, university courses, and short modules for business. In the summer school in Dortmund (September 2023), 27 students from 6 different universities participated. During this summer school, for the module Industry4.0, students had to work on a case to create a concept of a collaborative workspace for an e-business, using knowledge and insights from the courses "Io", "Digital twins", and "Safe workplaces".

Table 1. Different target group audiences.

Target group	Prerequisite	Current job position	Needs	Prospective Job Field
Master level student	Bachelor in technology domains (IT, Engineering) Technological knowledge on software/computational thinking, on technology (general), on electronics, on basic knowledge on office applications,	Student	gain knowledge on technologies of the 21st century and see the interrelations between technologies and the connections to existing industrial installations/machines/plants to understand how projects will span and connect various applications	Master-level position in engineering or design sectors Position as project manager
Lifelong learning student	Bachelor/Master in technology domains (IT, Engineering) or equivalent experience	Professional	Trained in specific courses of the module on new technologies External motivation to keep learning (motivation to dedicate to the module may be hindered by other factors such as work deadlines and family tasks…)	Improvement of position in the current or new organization Update of knowledge to be able to function in a digitally transformed organization
Academic Staff	Technological knowledge on software/computational thinking, on technology (general), on electronics, on basic knowledge on office applications,	Teacher	being able to make connections between technologies of the 21st century and existing industrial installations/machines/plants being able to guide the digital transformation towards an interconnected environment	

Table 2. Competency model acquired knowledge, skills, competencies.

Knowledge	Skills	General competences
• Students will learn the roots of digital transformation towards Industry 4.0 • Student understands how to overcome the challenges of digital transformation projects • Students know of actual cases from different industries • Students know business and organization demands related to Industry 4.0 • Student will outline the challenges of the organization to deal with Industry 4.0 • Students will know the management processes that Industry 4.0 projects require	• Students will be able to integrate the knowledge about industry evolution towards Industry 4.0 • Students can utilize tools and techniques of project management in Industry 4.0 projects • Students can analyze the projects in Industry 4.0 • Students can utilize financial systems needed for Industry 4.0	• Student can describe the challenges that Industry 4.0 can address • Student can enumerate the main technologies related to Industry 4.0 • Students will be able to monitor work processes related to project and finance management in Industry 4.0

5 Conclusions

In the Work4Ce project, groups of stakeholders – gathered in OpenCops (Open Communities of Practice) – defined competency models for different modules important to the digitally transformed world.

By setting the competency model according to the needs of different target groups (students, industrial workers, academic staff), course definition and course material development became much more structured and effective. The description of competencies in a model requires a standardized format of formulation so that different stakeholders interpret the competencies in a similar way. Finding common ground for defining competencies is a key to successful implementation so that universities and the labor field know they are discussing the same thing.

Taking the competency model for a teaching module from the start of development and incorporating existing (Open educational) resources became easier and led to better materials.

Acknowledgment. This work is partly carried out with the support of Erasmus + KA2 projects WORK4CE "Cross-domain competencies for healthy and safe work in the 21st century" (619034-EPP-1–2020-1-UA-EPPKA2-CBHE-JP) and ProDiT: Projects for the Digital Transformation Project Reference: 621745-EPP-1–2020-1-DE-EPPKA2-KA.

References

1. Tabunshchyk, G., Arras, P., Wolff, C.: Development of cross-domain competences for work 4.0. In: Auer, M.E., Rüütmann, T. (eds.) Educating Engineers for Future Industrial Revolutions. ICL 2020. Advances in Intelligent Systems and Computing, vol. 1328, pp. 205–211. Springer, Cham (2021). https://doi.org/10.1007/978-3-030-68198-2_18
2. EU: The European Qualifications Framework: supporting learning, work and cross-border mobility. Publications Office of the European Union, Luxembourg (2018)
3. EU: Standards and Guidelines for Quality Assurance in the European Higher Education Area (ESG). https://enqa.eu/index.php/home/esg/. Accessed 05 Dec 2023
4. Rajala, S.A.: Beyond 2020: preparing engineers for the future. Proc. IEEE **100**, 1376–1383 (2012). https://doi.org/10.1109/JPROC.2012.2190169
5. Gruen, G., Tritscher-Archan, S., Weiß, S.: Guidelines for the Description of Learning Outcomes. ZOOM partnership (2009)
6. Szabó, P., M´lkva, M., Marková, P.; Samáková, J., Janík, S.: Change of competences in the context of industry 4.0 implementation. Appl. Sci. **13**, 8547 (2023). https://doi.org/10.3390/app13148547
7. Eriksson, K., Bränneby, E., Hagelin, M.: An educational model for competence development within simulation and technologies for industry 4.0. In: 2021 Winter Simulation Conference (WSC), pp. 1−12. IEEE (2021). https://doi.org/10.1109/WSC52266.2021.9715395
8. Mikhridinova, N., Ngereja, B.J., Hussein, B., Van Petegem, W., Otegi-Olaso, J.R., Wolff, C.: Competence-based support for project-based learning in virtual settings. In: Auer, M.E., Pachatz, W., Rüütmann, T. (eds.) Learning in the Age of Digital and Green Transition. ICL 2022. Lecture Notes in Networks and Systems, vol. 634, pp. 246–257. Springer, Cham (2023). https://doi.org/10.1007/978-3-031-26190-9_25
9. Ietto, B., Ancillai, C., Sabatini, A., Carayannis, E.G., Gregori, G.L.: The role of external actors in SMEs' human-centered industry 4.0 adoption: an empirical perspective on Italian competence centers. IEEE Trans. Eng. Manage. **71**, 1057−1072 (2022). https://doi.org/10.1109/TEM.2022.3144881
10. Treviño-Elizondo, B.L., García-Reyes, H.: An employee competency development maturity model for industry 4.0 adoption. Sustainability **15**, 11371 (2023). https://doi.org/10.3390/su151411371
11. Rogers, J.: Communities of practice: a framework for fostering coherence in virtual learning communities. Educ. Technol. Soc. **3**, 384–392 (2000)

Implementation of the Methodical System for the Development and Application of Eco-Oriented Pedagogical Technologies

Andrii Kalenskyi(✉), Tetiana Gerliand, Oksana Lapa, Tetyana Pyatnichuk, and Olha Haiduk

Institute of Vocational Education of the National Academy of Educational Sciences of Ukraine, 98a, Vito-Lithuanian Lane, Kyiv 03045, Ukraine
kaa_1959@ukr.net

Abstract. The article discloses a methodical system that could enable the designing and introduction of eco-oriented pedagogical technologies (EPT) into professional engineering education, which is a subsystem of the methodical eco-oriented education system and the following characteristics: integrity, components, structurality, compactness, functionality, multi-level, controllability and connection with the environment. It includes a set of interrelated components: methodology (methodological approaches: activity, competence, technological, systemic and personality-oriented approaches and principles: humanization of prognostication, design of conditions for preserving the gene pool of the biosphere; compensability; interdisciplinary and systematic; concept: use methods of development and application of EPT in the professional training of engineering students, which include complex of techniques with their specific forms, methods and means environmental knowledge and formation of appropriate behavior in solving pedagogical, environmental, environmental and health-preserving tasks, which will contribute to the achievement of harmony in relations between people, society, technologies, machines and environment); content (definition and terms for the development and application of EPT in professional education; information-theoretical knowledge about the state of development and application of EPT; knowledge about the processes of development and application of EPT); methods (forms of training; methods of eco-oriented training, eco-oriented training technology; training tools); evaluation and results (components of the formation of the teacher's readiness to implement EPT in his own professional activity are: value-motivational, informational-knowledge, reflective-active, control-evaluative). The result of implementing a methodical system for developing and applying EPT was predicted to improve the teachers' readiness level to implement them in their professional activities.

Keywords: Vocational Education · Training · Engineering Students · Methodical System · Eco-Oriented Technology · Methodological Approaches · Ecological Competence · Sustainable Education

© The Author(s), under exclusive license to Springer Nature Switzerland AG 2024
V. Ivanov et al. (Eds.): DSMIE 2024, LNME, pp. 498–508, 2024.
https://doi.org/10.1007/978-3-031-61797-3_42

1 Introduction

Ukraine shares the goals of the EU's climate policy. Our country was one of the first in Europe to ratify the Paris Climate Agreement. In August 2020, the Government of Ukraine informed the EU governing bodies of Ukraine's participation in the European Green Deal [1]. Green Competencies (GreenComp) consist of twelve competencies grouped into four areas [2]:

- Competencies embodying the values of sustainable development (sustainability, justice, promotion of nature).
- A system of competencies for understanding sustainable development (critical thinking, ability to formulate and solve problems).
- Competencies for predicting a sustainable future (literacy, adaptability, research thinking).
- Competences of political leadership (individual or collective activity to implement the ideals of sustainable development).

The research aims to describe the system for developing and introducing EPT in the professional training of engineering students.

2 Literature Review

Curricula and professional internship programs must be transformed in the medium and long term to help engineering students develop new skills for the green transition: technical theory and practice are complemented by soft skills and new ways of thinking [3]. The educational programs themselves, during various types of educational activities, should primarily address issues of environmental awareness and climate-friendly behavior [4]. Vocational education and training schools (VET schools) should review and update curricula to meet labor market demand and prepare graduates with green skills: ecodesign, leadership, management, urban planning, greening, communication, waste management, procurement, and finance [5]. VET-school programs should combine vocational skills relevant to all economic cycles, jobs, and work practices with key competencies that include strong basic skills, digital, transversal, environmental, and other life skills [6]. The findings on the problem that refers to the value-oriented teaching models while forming the vital competencies [7] were considered in the current research. The methodical system for professional training of technically skilled workers with elements of the dual form of education was studied. It included a set of interrelated components and aimed to improve the quality of professional activity of engineering graduates, particularly environmental [8].

The results of the existing environmental education models [9, 10] were the basis for the current study: cognitive-value, epistemological, epistemological-activity, informational-personal, abstract-declarative, educational, and ideological.

The research literature addresses the production of green products and materials, for example, eco-innovation strategy in manufacturing [11], an overview of potential ecological applications in the construction industry [12], and the digital transformation of eco-innovation in peatlands (Paludiculture) [13], which facilitates the production of green products and services in real-time.

The ideas of purposeful influence on the environmental competence of engineering students while developing and accessing their creative potential were also considered in our research [14, 15] as engineers act inside the human – machines – technologies – environment system in their professional activity. Engineers are expected nowadays and in the future, to be able to find non-conventional ecologically friendly solutions following the customer-oriented approach and realizing effectively their project and designing activity [16].

Considering the achievements of national scientists and foreign experience in environmental education, we have concluded that to ensure the quality formation of environmental competence of graduates, it is necessary to scientifically substantiate and implement a methodical system for developing and applying EPT in the professional training of engineering students.

3 Research Methodology

To identify the leading methodical approaches to development and application of EPT in vocational education we considered innovative pedagogical ideas, theories and modern educational paradigms, following were identified (see Fig. 1): activity (evelopment and application of EPT leads to active, versatile, productive, maximally independent educational activity of education seekers), competence (development and application of EPT is aimed at the formation and development of key and subject competences of the individual and, first of all, ecological), technological (EPTs carry out accurate instrumental management of the educational process and guarantee the achievement of its goals and objectives), systemic (the study of development and application of EPT is carried out as a whole set of elements in a set of relationships and connections between them) and personality-oriented (EPT contribute to the creation of an atmosphere for the formation of individuality, personal development, self-realization, the ability to reflect, adapt, self-defense and self-determination of students) approaches.

Research methods: theoretical – analysis and generalization of pedagogical and methodical literature on the chosen problem to outline the principal and categorical apparatus used for the research; empirical methods were used for observation of the educational process, conversations with students, teachers; a pedagogical experiment was provided to check the effectiveness of the methodical system after its implementation.

4 Results and Discussion

The necessity, generality, and compulsory nature of environmental education as a condition for the formation of the environmental culture of society are enshrined in numerous laws on environmental protection and documents on education in Ukraine. The sustainable development concept puts the issue of improving Ukrainian environmental education and upbringing quality on the agenda [16].

The current situation in environmental education significantly depends on the level of development and relevant competence of the teacher, who is directly responsible for shaping the student's personality. The EPT design and application could solve the problem mentioned in the professional training of engineering students.

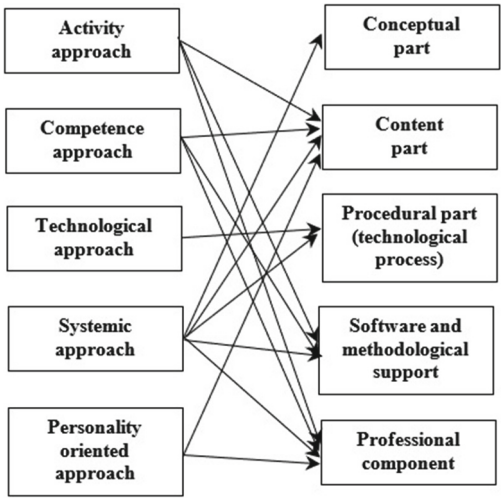

Fig. 1. The influence of methodological approaches on the structural components of pedagogical technology.

Analysis of the category "pedagogical technology" shows that the structure of environmentally oriented pedagogical technologies includes [17]:

1. Conceptual part of environmentally oriented technology (short description of concepts, hypotheses, and relationships which could help understand it).
2. Content part (goals of environmental education, scope and nature of the content of environmentally oriented education).
3. The procedural part is the technological process (organization of the educational process, methods of cognitive and environmental activity of students, methods and forms of teacher's work, and learning diagnostics).
4. Software and methodical support of the environmentally oriented educational process (curricula and programs, teaching aids, teaching, and diagnostic tools).
5. Professional component (reflection dependence of successful functioning and reproduction of the designed environmentally oriented pedagogical technology on the level of teacher's pedagogical skills).

Environmentally orientated pedagogical technologies have the following features:

– they are more complex, being fragments of the environmental education of society with their structural and functional diversity. These are complex and highly complex systems, which are a combination of specific subsystems that combine a significant number of elements and connections;
– they are characterized by less determinism and "rigidity". As a rule, these are adaptive systems characterized by flexible parameters and the ability to change toward the needs of the environment;
– time-moving systems. Their activities can determine the content of pedagogical technology, or they can act as a mechanism for its implementation, have certain conditions

and results, which gives dynamics to ecologically oriented pedagogical technology, making it a process that is constantly changing;
– ecologically oriented pedagogical technologies are characterized by variability, that is, diversity caused by the presence of individuals with their uniqueness, while a person acts as the driving force of these technologies, determining their diversity;
– ecologically oriented pedagogical technologies should be translators of such widespread principles of society as efficiency and optimality, systematicity, goal setting, self-development, synergy, and humanism;
– system becomes an eco-oriented technology when defined as a specific construct for realizing the urgent needs of a person, society, and environment.

Having analyzed the domestic and foreign experience of developing and applying environmentally oriented pedagogical technologies in VET schools, we can state that they are aimed at carrying out measures to reproduce nature-based, environmentally optimal living and working conditions for all participants in the educational process, arrangement of the adjacent territory of the institution; creation of «green and living corners»; participation in environmental activities; ensuring life safety (creating a safe learning and working conditions; organizing vocational training according to the rules about the actions in hazardous situations), etc.

Based on this, we can distinguish other groups of pedagogical technologies, for example, the dual form of learning, within which there are certain types of learning technologies [7], which can become environmentally oriented if their content is filled with this aspect, after all, such technologies should ensure that students are aware of the specifics of the impact of environmental factors on living organism; the importance of different types of adaptations of living things to the environment; the role cycle of matter and energy in the processes of interaction natural environment; the essence process of the cycle of matter in ecosystem as means of its restoration; the interconnection of global, regional and local problems; the relationship between the the environment state and human health; the impact of human activity on the environment; the importance of forecasting and modelling the relationship between society and natural systems; the possibilities of science and technology in the implementation of environmentally safe professional activities [8].

Representatives of most regions of Ukraine and the city of Kyiv took part in the anonymous survey conducted to study the current state (the ascertaining stage) of the development and application of EPT in the professional training of engineering students.

According to respondents, the following factors reduce the quality of VET schools: distance learning (53.6%) and poor methodical and material and technical equipment (17.4%). In comparison, the quality of vocational training is improved by highly qualified teaching staff (32.1%) and the institution's provision of the necessary teaching equipment and methodical materials (42.2%).

Teachers use eco-oriented pedagogical technologies in their professional activities: from time to time (66.7%), constantly (24.7%), and not at all (8.6%).

The most important ways to develop and apply EPT in teachers' professional activities are using Internet resources (32.4%) and in-depth study of new developments in teaching methods (32.6%).

Our respondents get the necessary information on environmental issues mainly from the Internet (72.3%). They use verbal or visual (35.4%) and interactive (25.2%) to cover environmental issues in their professional activities.

To organize environmental activities, respondents need environmental knowledge (26.5%), methodical developments (20.4%), and practical skills (18.7%).

We understand the readiness of teachers of VET schools to develop and apply environmentally oriented pedagogical technologies as an integral formation of personality, that is, complex, multifaceted, contradictory, gradual actions in the continuous process of theoretical and practical teaching activity, their sustainable motivation and volitional efforts aimed at solving environmental and valeological problems against the background of positive emotional perception of reality, the formation of beliefs and appropriate behavior in solving pedagogical, ecological, environmental and health-protective tasks in synthesis with the established attitudes to the innovative organization of the educational process, namely the development and application of EPT aimed at mastering environmental knowledge and developing the relevant skills of engineering students [18].

Structurally, the readiness of teachers of VET schools to develop and apply environmentally oriented pedagogical technologies consists of the following components: value-motivational, informational-knowledge, reflective-active, and control-evaluative.

Based on theoretical analysis of modern scientific works on the research problem and results of the ascertaining experiment, three levels of readiness of teachers of VET schools to develop and apply environmentally oriented pedagogical technologies are identified: high level – characterized by the highly professional ability to develop these technologies for professional training of students; middle level –associated with the transfer of learned algorithms for their development and application to conditions of the actual educational process; low level – inherent in teachers who use some aspects of environmentally oriented activities in professional training of engineering students, based on the experience of colleagues.

The respondents self-assessed their readiness to develop and apply environmentally oriented pedagogical technologies in the professional training of engineering students (see Table 1).

Table 1. Levels of teachers' readiness to develop and apply eco-oriented pedagogical technologies (ascertaining stage).

Component	Low level (%)	Medium level (%)	High level (%)
value-motivational	8.1	72.7	19.2
informational-knowledge	9.4	76.2	14.4
reflective-active	9.5	75.8	14.7
control-evaluative	4.3	69.5	26.2

To achieve the goal of environmental education, a specific pedagogical system should be formed that focuses on the formation of healthy environmental thinking

and consciousness of students, which leads to positive changes in attitudes towards the environment and the formation of environmentally responsible future professionals.

The methodical of environmentally oriented education is a model of the educational process that integrates its environmental content and environmentally oriented teaching technology. It is aimed at achieving the learning goal (protection of the environment as well as rational application of natural resources), is based on the content of environmentally oriented education, reflects psychological and pedagogical teaching methods that contribute to the achievement of the goal, determines the environmentally oriented activities of participants in the learning process, their interaction model, their approach to the use of resources (elements) of the environmentally oriented learning environment (teaching aids) used to provide environmental education.

Thus, by methodical of ecologically oriented education, we mean a model of the educational process that reflects orderly interrelationships between goals of environmental education, ecologically oriented teaching technology, learning content (aimed at sustainable development), participants in the educational process, and the means of the educational environment.

Integrated sets of such methodical can form environmentally oriented methodical systems. The presence of system-forming factor (factors) integrates a set of environmentally oriented teaching methods that allows us to speak of this integrated set as an environmentally oriented methodical system. The system-forming factors of such systems can be the kinship and content proximity of individual components of specific methods of environmental education or their combinations: learning objectives (harmonization of relations in the nature-human-society system), environmentally oriented learning content, environmentally oriented educational technologies and elements of learning tools systems.

The methodical system of ecologically oriented education, derived from the pedagogical system, should retain the main features of this system. Otherwise, it is impossible to link (define) these concepts.

Thus, the methodical system of development and application of EPT in vocational education is a subsystem of the methodical system of environmentally oriented education.

All systems are characterized by the following common features: integrity, componentry, structure, compactness, functionality, multilevelness, controllability, and connection with the environment.

Features of the methodical system for development and application of EPT: the presence of components (methodical, content, methodical, evaluation and result); the presence of an internal structure of links between the components of environmentally oriented pedagogical technologies; the presence of certain level of integrity, when the system obtains an integral result after the interaction of its components (high readiness of the teacher to develop and apply environmentally oriented pedagogical technologies in professional the presence of system-forming links that unite components, blocks, parts into single system of environmentally oriented pedagogical technologies; interconnection with other systems (it is a subsystem of the methodical system of environmental education).

The methodical system consists of a set of interrelated components (Fig. 2):

- methodology (methodological approaches: activity, competence, technological, systemic and personality-oriented approaches; principles: humanization of forecasting, designing conditions for preserving the biosphere gene pool; compensatory; interdisciplinary and systemic; concept: use of methods of development and application of EPT in the professional training of education seekers, which include a set of methods, techniques, means and forms of acquiring environmental knowledge and forming appropriate behavior in solving pedagogical, ecological, environmental and health protection tasks that will contribute to harmony between a human, society and the environment; objective: to provide methodical support for the development and application of EPT in the professional training of education seekers as a specific process aimed at targeted acquisition of knowledge about the environment, healthy lifestyle, and instilling in students the ability to find means in environment to realize human rights to health and favorable environment);
- content (definition and terms for the development and application of EPT in professional education; information-theoretical knowledge about state eco-oriented pedagogical technologies designing and application of; knowledge about processes of development and application of EPT; knowledge organization of psychological and pedagogical evaluation);
- methods (forms of training; methods of eco-oriented training, eco-oriented training technology; training tools);
- evaluation and results (components of formation of the teacher's readiness to implement EPT in his professional activity are value-motivational, informational-knowledge, reflective-active, control-evaluative).

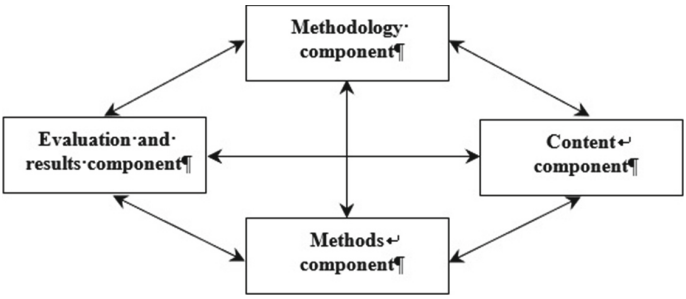

Fig. 2. Components of the methodical system for development and application of EPT.

The learning conditions directly act as component of the methodical system [12]. The learning conditions as component of the methodical system were defined and assessed according to the methodology given in [19]. The first learning condition was the formation of positive motivation among teachers to develop and apply EPT in the professional training of education seekers. This consolidates the positive attitude of those who teach this pedagogical activity.

In turn, there is a need to improve the content of EPT in the professional training of engineering students, which led to the choice of the second learning condition – the environmental orientation of the content of professional training subjects.

The third learning condition is the pedagogical integration of the professional training process. Based on the identified trends, the concept of "integration" is considered a general scientific phenomenon that reflects the most general and essential properties of the phenomena of different sciences by the canons, personifying their most general properties and connections.

Pedagogical integration of the educational process, in turn, requires the use of innovative pedagogical technologies in the training of engineering students. Thus, the fourth learning condition has been identified – educational and methodical support for using environmentally oriented pedagogical technologies to master professional training subjects by education seekers.

The result of implementing the methodical system for the development and application of EPT (formative stage) is the formation of the teacher's readiness to implement them in their professional activities.

The high level of readiness of teachers of VET schools to develop and apply environmentally oriented pedagogical technologies ensures the successful socialization of education seekers and their cultural and ethical integration into modern society. The leading factor in the ecological education of the individual is the universal human values learned by them while preserving the environment (see Table 2).

Table 2. Levels of formation of teachers' readiness to develop and apply eco-oriented pedagogical technologies (formation stage).

Component	Low level (%)	Medium level (%)	High level (%)
value-motivational	3.7	27.8	68.5
informational-knowledge	9.3	35.2	55.6
reflective-active	9.3	37.0	53.7
control-evaluative	3.8	32.0	64.2

Based on analysis of the results obtained after implementing the methodical system for the development and application of EPT (formative stage), the formation of the components of the teacher's readiness for their implementation in his professional activity is better. Indicators of readiness are higher than at the ascertaining stage, namely: value-motivational (48,3% more respondents have a high level after the formative stage); informational-knowledge (41,2% more respondents have a high level); reflective-active (high level in 53,7% of respondents, which is 39,0% more); control-evaluative (64,2% of respondents have a high level, which is 38,0% more).

The Swede M. [9] analyzed the main trends in the development of environmental education in foreign countries. Lukyanova L. [10] substantiates the structure of the technology of studying the ecological course, which includes the following organizational and methodological components: 1) systematization and generalization of ecological knowledge; 2) development of an appropriate educational complex. Gerliand T. [10]

substantiated the complex pedagogical conditions for developing the readiness of teachers of professional (vocational and technical) education institutions to develop and apply eco-oriented technologies in the professional training of future skilled workers.

However, our research has proven that only the implementation of a methodological system for the development and application of eco-oriented pedagogical technologies can give a guaranteed result: the formation of the teacher's readiness to implement these technologies in his professional activity.

5 Conclusions

Implementation of the methodical system for the development and application of EPT was carried out by implementing the following stages: diagnostic and prognostic (monitoring and diagnosis of problems of the development and application of EPT that must be implemented). The improvement qualifications of pedagogical workers on these problems have been resolved); project-organizational (processes of development and application of EPT; knowledge of the organization of psychological and pedagogical assessment; application in technologies of a set of techniques, methods, forms and means of ecological knowledge and the development of appropriate behavior in solving educational, environmental, nature protection and health-improving tasks that will contribute to the achievement of harmony in relationship between man, society and the environment); innovative and active (pedagogical integration of the process of professional training, phenomenon that reflects the most general and essential properties of phenomena in various sciences in accordance with canons, personifying their most general properties and connections and unites complex of eco-oriented educational methods and, thus, allows to speak about this integrated population as an eco-oriented methodical system); reflexive-evaluative (presentation of the results of developed eco-pedagogical technologies; evaluation of the results of this activity; holding of conferences, webinars on the development and application of EPT; determination of changes in the level of teachers' readiness to implement them in their educational activity).

The expected result of introducing the methodical system into the process of eco-oriented pedagogical technology development and application was the high readiness of the teacher to implement those technologies in the educational process while training engineering students.

The next stage of our research in 2024 is the development of practical manuals and their distribution in vocational education institutions of the agricultural sector. The results of implementing these manuals will be presented to the scientific community.

References

1. Smenkovsky, A.Yu.: The European Green Course and the climate policy of Ukraine: analyst. add. NISD, Kyiv (2022). https://doi.org/10.53679/NISS-analytrep.2022.12
2. Bianchi, G., Pisiotis, U., Cabrera Giraldez, M.: GreenComp The European sustainability competence framework. JRC Science for Policy Report. Publications Office of the European Union, Luxembourg (2022)
3. Cedefop, OECD. Apprenticeships for greener economies and societies. Cedefop reference series. https://www.cedefop.europa.eu/en/publications/3091. Accessed 11 Nov 2023

4. Arasinah, K., Ridzwan, C.R., Mohd, B.R., Faizal, A.N.Y., Normah, Z., Haryanti, M.A.: Exploring green skills: a study on the implementation of green skills among secondary school students. Int. J. Acad. Res. Bus. Soc. Sci. **7**(12), 327–346 (2017). https://doi.org/10.6007/IJARBSS/V7-I12/3615
5. Sern, L., Zaime, A., Fong, L.: Green skills for green industry: a review of literature. J. Phys.: Conf. Ser. **1019**, 012030 (2018). https://doi.org/10.1088/1742-6596/1019/1/012030
6. Council of the European Union Council Recommendation of 24 November 2020 on vocational education and training (VET) for sustainable competitiveness, social fairness and resilience. Official Journal of the European Union. https://eur-lex.europa.eu/legal-content/EN/TXT/?uri=CELEX%3A32020H1202%2801%29. Accessed 11 Nov 2023
7. Mozolev, O., Khmara, M., Yashchuk, I., Kravchuk, L., Matviichuk, V., Kalenskyi, A., et. al.: The Influence of Value-oriented Teaching upon Vital Competences Formation of 7–9 Years Old Pupils during Physical Education Lessons. Universal J. Educ. Res. **8**(6), 2352–2358 (2020). https://doi.org/10.13189/ujer.2020.080619
8. Kalenskyi, A., Gerliand, T., Kravets, S., Homeniuk, D., Nagayev, V.: Dual educational system of professional training of future skilled workers. In: Ivanov, V., Trojanowska, J., Pavlenko, I., Rauch, E., Piteľ, J. (eds.) Advances in Design, Simulation and Manufacturing VI. DSMIE 2023. Lecture Notes in Mechanical Engineering, pp. 369–378. Springer, Cham (2023). https://doi.org/10.1007/978-3-031-32767-4_35
9. Shved, M.: Trends in the development of foreign environmental education. Bulletin of Lviv University. Pedagogical series **17**, 167–174 (2003). https://doi.org/10.30970/vpe.2003.17.6410
10. Lukyanova, L.B.: Implementation of modern technology of ecological knowledge in vocational training. Modern information technologies and innovative teaching methods in training specialists: methodology, theory, experience, problems **3**, 230–235 (2003)
11. Rowan, N.J., Murray, N., Qiao, Y., O'Neill, E., Clifford, E., Barceló, D., Power, D.M.: Digital transformation of peatland eco-innovations ('Paludiculture'): Enabling a paradigm shift towards the real-time sustainable production of 'green-friendly' products and services. Science of The Total Environment 838, Part 3, 156328 (2022). https://doi.org/10.1016/j.scitotenv.2022.156328
12. Janahi, N.A., Durugbo, C.M., Al-Jayyousi, O.R.: Eco-innovation strategy in manufacturing: a systematic review. Clear Eng. Technol. **5**, 100343 (2021). https://doi.org/10.1016/j.clet.2021.100343
13. Silva, G., Kim, S., Aguilar, R., Nakamatsu, J.: Natural fibers as reinforcement additives for geopolymers – a review of potential eco-friendly applications to the construction industry. Sustain. Mater. Technol. **23**, e00132 (2020). https://doi.org/10.1016/j.susmat.2019.e00132
14. Sosnytska, N., Titova, O., Symonenko, S., Kravets, O.: Examining the creative potential of engineering students. In: Nadykto, V. (eds.) Modern Development Paths of Agricultural Production, pp. 299–306. Springer, Cham (2019). https://doi.org/10.1007/978-3-030-14918-5_31
15. Titova, O., Ishchenko, T., Yershova, L., Bazyl, L., Kruchek, V.: Entrepreneurial mindset development in engineering students through a business canvas approach. In: Ivanov, V., Trojanowska, J., Pavlenko, I., Rauch, E., Piteľ, J. (eds.) Advances in Design, Simulation and Manufacturing VI. DSMIE 2023. Lecture Notes in Mechanical Engineering, pp. 400–409. Springer, Cham (2023). https://doi.org/10.1007/978-3-031-32767-4_38
16. On the main principles (strategy) of the state environmental policy of Ukraine for the period up to 2030. Legislation of Ukraine. https://zakon.rada.gov.ua/laws/show/2697-19#Text.ua/laws/show/2697-19#Text. Accessed 11 Nov 2023

The Model for Professional Competence Development of Engineering Teachers at Colleges

Petro Luzan[1], Olena Titova[1,2(✉)], Iryna Mosia[1], Tetiana Pashchenko[1], and Gulshan Navruzova[3]

[1] Institute of Vocational Education of the National Academy of Educational Sciences of Ukraine, 98a, Vito-Lytovskyi Lane, Kyiv 03045, Ukraine
olena.titova@tsatu.edu.ua

[2] Dmytro Motornyi, Tavria State Agrotechnological University, 18, B. Khmelnitsky Avenue, Melitopol 72312, Ukraine

[3] Tajik State University of Finance and Economics, 64/14, Nakhimov Street, 734067 Dushanbe, Republic of Tajikistan

Abstract. The main task for engineering teachers at college is to organize a specific environment that could provide students with creative and professional development. So, the teachers must be well prepared to perform their professional activities effectively and supply their students with essential knowledge and skills, preparing them for innovative engineering activities, diverse paths in their field, and engineers' leading roles. Therefore, the research aimed to model the college engineering teachers' professional development process. To achieve the research goal at the first stage, the teachers' competence composition was clarified based on an analysis of the psychological structure of teachers' activity and its subject-specific side. For that purpose, 389 respondents (teachers, instructors, managers from public Ukrainian colleges, and employers) were interviewed in 2023. Then, the structural and content model for developing the teacher's professional competence was designed. The developed pedagogical model reflected and imitated the studied phenomenon's process and specific properties and characteristics. The model could be used in further research devoted to the features of the competence development of an engineering teacher at college to define the process stages, scientifically substantiate the effective technologies and means, and develop diagnostic methods for assessing the levels of teacher's competence.

Keywords: Engineering Education · Teaching Skills · Engineering Students · Pedagogical Model · Continuing Professional Development

1 Introduction

In dealing with problems of vocational education for engineering students, scientists should consider that the goal of university studying is not just training the students for specific purposes in their future jobs but equipping them with some universal skills they

© The Author(s), under exclusive license to Springer Nature Switzerland AG 2024
V. Ivanov et al. (Eds.): DSMIE 2024, LNME, pp. 509–520, 2024.
https://doi.org/10.1007/978-3-031-61797-3_43

will need in their lives [1]. To be successfully employed, engineering graduates should be able to analyze the situation, define a problem, communicate, propose an optimal technical solution, and be part of a team, leader, or idea generator. Therefore, teachers must organize an environment for their engineering students that widens and deepens their creative and professional potential. Since university courses serve as the common starting point for engineers, the teachers are responsible for such things as student learning enhancement, engagement in a professional atmosphere as well as interdisciplinary collaboration, treatment engineering beyond a technical solution, development of a creative learning environment which will allow them to think in a non-standard way for the decisions and consequences. Thus, the teachers have to be well prepared for the function of organizing students' effective professional development, individual work, and work in a team, help them to identify and understand the knowledge and skills essential to succeed, show engineering students diverse paths in the field and engineers' more prominent role [2, 3]. Considering the plenty of new emerging approaches, means, and technologies which, on the one hand, could be used by the teachers to develop their professional competence, but, on the other hand, could confuse as there are a lot of different products, we would predict that the success of the teachers' professional development will depend on the precise organization of the process and careful selection of the content. The novelty of the current research was in the attempt to implement the scientific approaches to the purposeful development of teaching skills for engineering teachers and the creation of such circumstances that enable their successful continuous professional development to provide high-quality and productive training for engineering students at colleges. Thus, the current research aimed to develop a model that could present the structure and content of the engineering teachers' professional development process in the conditions of a college educational environment. For that purpose, the following tasks were set:

- To define the teachers' competence types that were demanded in the current educational practice;
- To weigh the importance of each competence type;
- To design a structural and content model to develop the teacher's professional competence.

2 Literature Review

The analysis of publications was focused on finding an answer to the question: what should be the process of the teacher's pedagogical skills development? The general answer could be retrieved from UNESCO's teachers' training mission: to create and use knowledge for "inclusive, resilient and democratic societies" [4]. That requires teachers to treat their professional competence as an integrated thing that will provide sustainable development of society [5, 6]; therefore, they should be critically analyzed and supported with advanced theoretical concepts and practical tools [7, 8]. A great deal of research was devoted to the problem of the teacher's competence in engineering teachers training as well as general education teachers [9–11]. The findings included the approaches to the development of active learning context and competencies necessary for active learning, effective digital technologies application for engineering students [12], factors

that influence online teaching competence [13], competence methods application in engineering education [14], innovation competencies as well as the ability to motivate students' innovativeness and organize engineering students' outcomes assessment [14, 15]. Another vital aspect under study was the teachers' training to succeed in an inclusive classroom [16, 17].

To implement in practice, the conclusions and provisions of the theory are usually formulated in the form of conditions (requirements) and rules. To solve practical problems, scientists increasingly focus on developing learning conditions to influence individuals' acquirement of relevant skills [18, 19]. The current research's novelty was analyzing existing approaches to determine the strategy and tactics for developing the college engineering teachers' professional competence as a continuous technological process. Here, the studied positions were considered to stipulate specific directions for developing the college educational process and were predicted to improve the professional competence of engineering teachers at colleges.

It is worth agreeing with the researchers [20] that to solve a scientific problem in education, one should consider many previous scientific ideas and positions but justify and experimentally verify only those with a specific scientific novelty.

3 Research Methodology

To solve the problem of purposeful development of the professional competence of an engineering teacher at college, a conceptual system of the research was developed, as well as basic definitions ("professional development", "professional competence", "professional competence of an engineering teacher at college, etc.) were considered. Then, the methodological approaches, factors, and conceptual ideas of the development of the studied phenomenon were substantiated, as well as the principles, factors, and learning conditions of the systematic development of teachers' professional competence [11]. The process of purposeful development of teachers' professional competence was modeled. That could enable the further study of the peculiarities, clarify the stages, define and scientifically substantiate the effective methods, forms, means, and technologies, as well as specify diagnostic methods for assessing the levels of competence development of an engineering teacher at a college.

Based on the logical rules for defining concepts, the professional competence of an engineering teacher at a college was formulated as an integrative property that included some components or competence types. To design specific methods and technologies for developing teachers' professional competence, the components and types of teachers' professional competence were defined using two approaches at the first stage of the experiment. On the one hand, the psychological structure of the professional competence of an engineering teacher at college was analyzed, and based on the published findings on the point [10, 15], 5 components were distinguished. They were motivation, value, cognitive-informational, behavior and activity, personal reflection, emotion, and volition. On the other hand, according to the specific teaching activity, a list of teachers' competence types demanded in the current educational practice was defined using a Google Forms survey provided in 2023. The survey engaged 389 respondents (employers, teachers, instructors, and managers from public Ukrainian colleges). Among the given list of

the components of a teacher's professional competence, the respondents singled out the 9 main ones most often pointed out. They included training competence, educational competence, methodical competence, subject competence, informational and digital competence, environmental competence, inclusive competence, research competence, and communicative competence.

At the second stage of the experimental work, 26 experts (including engineering teachers at colleges and universities as well as scientists who deal with educational problems) weighed the importance of each competence type (which will be named as 'competence' further) based on pairwise comparisons between the competences using an analytic hierarchy process (AHP) tool. The goal was to rank the competencies in order of their importance. For that purpose, instead of looking at all of the competencies at once, the comparisons between two items at a time were made. Then, all of those comparisons were put into a chart (Table 1), which enabled the creation of a detailed picture of each competence's importance. Each cell in the chart was a pairwise comparison of the column competence (A) versus the row competence (B). A versus B, a particular scale, which was from 0 to 1, was used to judge between a pair of competencies. On the scale, a 1 meant that the expert preferred A over B. In the case where B was preferred over A, the expert put 0. A 0.5 was used when the competencies were equally important. The comparison of A versus B was the reciprocal of that value for B versus A. Since the same competencies were compared, the diagonal cells had a 0 value. In the last element of each row and each column, all the values in that row or column were summed up. The total of all the values in the table was the Ranks Sum, which showed that the chart was completed correctly.

Expert data were processed to determine the importance of the professional competence types. In the Table 1, the data of each line was added, and the competence Rank R in the general ranking system was determined. The competence with the highest rank was assigned a Competence Weight equal to 1. For example, in Table 1, the competence No. 1 had the highest rank. The Competence Weight of each competence type was determined by the formula (1):

$$P_i = \frac{\sum P_{max} \cdot R_i}{R_{max}}, \tag{1}$$

where $P_{max} = 1$ is the degree of importance of the competence with the highest rank; R_i is the rank of the competence; R_{max} is the highest rank (in Table 1, $R_{max} = 7$).

For example, competence No. 3 (see Table 1) had a rank R3 = 2.5; with Rmax = 7, the Competence Weight of competence No. 3, according to the first expert, was equal to 0.36. The rest of the calculations were performed similarly using the data received from all the experts. Based on the results of the calculations, a matrix, which presented the Competence Weights according to the assessment by each expert (P_1, P_2 ... P_{26}), was compiled (Table 2). Based on the obtained P_i data, the average value of the Competence Weight was determined according to the formula (2):

$$P_{av} = \frac{\sum P_{ij}}{n}, \tag{2}$$

where n is the number of experts, n = 26.

To determine the dispersion of experts' assessments for each type of teacher's professional competence, the formula for the case of a small sample was used:

$$S_i = \sqrt{\frac{\sum (P_i - P_{av})^2}{n-1}}, \tag{3}$$

where n is the number of experts; P_{ij} is the Competence Weight of the i-th competence in the opinion of the j-th expert; the value $n - 1$ determines the number of degrees of freedom.

In the third stage, using the principle of conceptual minimalism in combination with the maximum informativeness of the modeled subject [21], we designed a structural and content pedagogical model for the teachers' competence development. Its visualization is presented in Fig. 1.

4 Results and Discussion

The main feature of the pedagogical activity of an engineering teacher at college is determined by the subjects of their work. On the one hand, the subjects include people (human-to-human relationships) and, on the other hand, technical objects (machines, mechanisms, parts, materials, types of energy, etc.). An engineering teacher must convey complex technical knowledge to the students, teach them to think creatively, analyze production and technological situations, find optimal problem-solving options, develop their interest in technology, and purposefully form hard and soft skills. That requires the teacher to have perfect possession of engineering knowledge, know advanced ways of production, and know prospects for developing technologies and equipment. In addition, the teacher should simultaneously be an efficient educator, a methodologist, and an organizer of the educational process. Thus, engineering teachers should be dynamic, mobile individuals capable of continuous professional development and systematically mastering the latest educational and production technologies.

Therefore, the professional development of an engineering teacher at college is a continuous process of progressive and humanistic formation of a teacher's personality that strives for constant improvement, self-affirmation, career growth, and development of a new quality of professional and pedagogical action. The pinnacle of a teacher's professional and personal development, formation, and improvement, particularly in complex, changing conditions, is achieving the highest – creative level of professional competence.

The following definition was formulated to deal with the problem of purposeful development of the teacher's professional competence. Thus, the professional competence of an engineering teacher at college was defined as an integrative property of a person, which is manifested in the pedagogical activity, behavior, and actions of an expert and determines their readiness and ability to perform the work functions in a qualified manner due to a balanced combination of the engineering, technical, psychological, pedagogical, methodical, organizational, subject-branch (special), environmental, legal, etc. knowledge as well as skills necessary to develop students' personality. The professional competence also includes teachers' moral and ethical values as well as such specific

professional qualities as a creative attitude to educational activities, developed technical thinking, perseverance, purposefulness, responsibility; endurance, self-control, tolerance, kindness; pedagogical observation and attentiveness; perfect command of scientific and technical language; inspiration and intuition; optimism; pedagogical tact; health and appearance, etc. That could determine sufficient levels of engineering students' education and training at colleges.

At the first stage, according to the results of the analysis of the psychological structure of pedagogical activity, the following structural components of teachers' competence as an integrative property were distinguished: motivation and value (involved the formation of motives, aspirations for innovative engineering and teaching activity, value orientations of the teacher to master high levels of professionalism); cognitive-informational (included the complex of theoretical and procedural knowledge in engineering, pedagogy, psychology, teaching methods, digital technologies, scientific approaches of the field being taught, etc.); behaviour and activity (presented a set of abilities and skills that ensure the quality implementation of the teaching functions); personal reflexion (included regulation of one's own life activities, ability to reflect in professional activity); emotion and volition component meant the ability to understand one's own emotional state when dealing with teaching situations; perseverance in self-development, purposefulness of actions in the informational and educational environment of the college. That structure could be further used as the base for diagnostic instrument development.

On the other hand, the subject-specific teacher's activity must be analyzed. Therefore, the competencies (or competence types) that a college teacher should demonstrate were determined. In particular, respondents indicated that currently, the main types of professional competence were training, didactic, subject, methodological, environmental, inclusive, health-preserving, economic, research, communicative, projective, evaluative-analytical, organizational, psychological, autopsychological, cultural, conflictological, information and digital, educational, prognostic, legal, social, political and creative. Among the given list of components of a teacher's professional competence, the 9 main ones, which the respondents most often pointed out, were singled out. They included the training competence (the teacher's ability to train others, to transfer their own knowledge, to form skills and abilities in students, as well as the ability to learn and improve their own professional level); the educational competence (an integrative personal and activity quality of a teacher, which ensures their theoretical and practical readiness and ability to effectively implement the educational function in a holistic educational process); the methodological competence (a teacher's ability to develop educational and methodological documentation, methods of preparing and conducting educational classes, other didactic materials and teaching aids); the subject competence (theoretical and practical readiness of a teacher for teaching a separate engineering discipline, course, etc.); the information and digital competence (the ability of a teacher to navigate in the information environment, find and process information, apply digital technologies in the educational process of a college); the environmental competence (an ability to apply ecologically friendly approaches in professional and life situations, guided by the priority of environmental values and non-pragmatic motivation for interacting with the environment); the inclusive competence (an ability to provide professional support to the students with

special educational needs, taking into account their individual requirements, opportunities, abilities and interests, to create conditions that ensure the functioning of an inclusive educational environment at a college); the research competence (an individual's ability to carry out scientific research in a particular field of science using general and special scientific methods); and the communicative competence as the ability of a person to choose and technologically effectively apply proper methods of communication.

In the second stage of the experimental work, the experts compared the selected competencies in pairs. For that, a paired comparison chart was filled out (Table 1).

Table 1. Expert assessment results for the importance of professional competence types of engineering teachers at colleges (expert No. 1).

No (A)	Number (No) of the teacher's professional competence (B)									Rank R_i	Competence Weight, P_i
	1	2	3	4	5	6	7	8	9		
1	0.0	0.5	1.0	0.5	1.0	1.0	1.0	1.0	1.0	7	1.00
2	0.5	0.0	1.0	0.5	1.0	0.5	0.5	1.0	1.0	6	0.86
3	0.0	0.0	0.0	0.0	0.5	1.0	0.0	0.5	0.5	2.5	0.36
4	0.5	0.5	1.0	0.0	0.5	1.0	0.5	1.0	0.5	5.5	0.79
5	0.0	0.0	0.5	0.05	0.0	1.0	0.5	1.0	0.0	3.5	0.50
6	0.0	0.5	0.0	0.0	0.0	0.0	0.5	0.0	0.0	1	0.14
7	0.0	0.5	1.0	0.05	0.5	0.5	0.0	1.0	0.0	4	0.57
8	0.0	0.0	0.5	0.0	0.0	1.0	0.0	0.0	0.0	1.5	0.21
9	0.0	0.0	0.5	0.5	1.0	1.0	1.0	1.0	0.0	5	0.71
Ranks Sum										36	

Note: The numbers of the teacher's professional competencies: 1 was the training competence; 2 was the educational competence; 3 was the methodical competence; 4 was the subject competence; 5 was the informational and digital competence; 6 was the environmental competence; 7 was the inclusive competence; 8 was the research; 9 was the communicative competence

In that order, the calculations for the data received from the 26 experts were performed. Based on the results of determining the Competence Weights for the competencies, a matrix was compiled (Table 2 and Table 3). The table presented the results of the assessment by each expert (P_1, P_2 ... P_{26}).

So, according to the results of the 26 experts' assessment, it was established that in the actual educational process, the most demanded (important, significant) were the training and the communicative competencies: their Competence Weights appeared to be 0.76 and 0.75, respectively. The Competence Weight of the information and digital, the subject, the methodical, and the educational competencies were approximately the same, in the range from 0.68 to 0.65. The last positions (7, 8, and 9) were given to the inclusive (0.49), the research (0.38), and the environmental (0.31) competencies.

To discuss the obtained results, we should highlight that the positions of the training, the communicative, the information and digital, the subject, the methodical, and the

Table 2. The matrix of the results of determining the Competence Weights types for the professional competence of engineering teachers at colleges (part 1).

No	P_1	P_2	P_3	P_4	P_5	P_6	P_7	P_8	P_9	P_{10}	P_{11}	P_{12}	P_{13}	P_{14}
1	1.00	1.00	1.00	0.71	0.88	0.93	0.88	0.08	0.82	1.00	0.79	0.71	1.00	0.92
2	0.86	1.00	0.82	0.64	0.63	0.53	0.25	0.54	0.73	0.71	0.43	0.79	0.67	0.67
3	0.36	0.43	1.00	0.71	0.50	0.67	1.00	0.77	0.64	0.43	0.57	0.43	0.73	1.00
4	0.79	0.64	0.36	0.86	1.00	1.00	0.38	0.62	0.64	0.36	0.71	1.00	0.93	1.00
5	0.50	0.21	0.27	1.00	0.13	0.40	0.50	0.77	0.64	0.43	1.00	0.71	0.40	1.00
6	0.14	0.07	0.09	0.43	0.00	0.40	0.00	0.38	0.64	0.29	0.14	0.43	0.13	0.33
7	0.57	0.79	1.00	0.00	0.63	0.27	0.75	1.00	1.00	0.14	0.00	0.57	0.40	0.08
8	0.21	0.43	1.00	0,14	0.25	0.07	0.13	0.46	0.73	0.86	0.50	0.00	0.00	0.08
9	0.71	0.57	1.00	0,64	0.50	0.53	0.63	0.92	0.73	0.93	1.00	0.50	0.53	0.92

Table 3. The matrix of the results of determining the Competence Weights types for the professional competence of engineering teachers at colleges (part 2).

No	P_{15}	P_{16}	P_{17}	P_{18}	P_{19}	P_{20}	P_{21}	P_{22}	P_{23}	P_{24}	P_{25}	P_{26}	P_{av}	S_i
1	0.58	0.62	0.71	0.56	0.25	0.92	0.63	0.85	0.73	0.69	0.75	0.69	0.76	0.05
2	0.67	1.00	0.43	0.88	0.44	0.54	0.56	0.54	0.55	0.62	0.67	0.85	0.65	0.03
3	0.25	0.08	0.86	0.56	0.63	0.85	0.63	1.00	1.00	0.54	1.00	0.77	0.67	0.06
4	0.50	0.92	0.57	0.31	0.44	0.62	0.63	0.54	0.73	0.54	0.83	0.85	0.68	0.04
5	1.00	0.77	0.93	0.63	0.44	0.92	1.00	0.85	0.64	0.54	0.42	1.00	0.66	0.07
6	0.33	0.46	0.07	0.06	0.75	0.31	0.38	0.00	0.64	0.38	0.75	0.46	0.31	0.05
7	0.83	0.62	0.29	0.19	0.44	0.31	0.00	0.46	0.36	1.00	0.67	0.38	0.49	0.10
8	1.00	0.15	0.29	0.31	0.13	0.08	0.13	1.00	1.00	0.62	0.17	0.15	0.38	0.11
9	0.83	0.92	1.00	1.00	1.00	1.00	0.56	0.31	0.91	0.62	0.75	0.38	0.75	0.04

educational competencies were expected and followed the other findings [12, 13]. On the other hand, the fact that the inclusive, the research, and the environmental competencies got last positions in the list contradicted the published results [6, 7, 17] and the goals of sustainable development. That result requires a more profound study to reveal the reasons for such an opinion among college teachers and the measures focused on explaining and justifying the importance of inclusive, research, and environmental competencies for the engineering teacher at a college.

At the final stage of the research, a structural and content pedagogical model for the development of engineering teacher's professional competence was designed and visualized (see Fig. 1). Structurally, the model consisted of four interdependent blocks

that functionally combine some aspects of the development system of the phenomenon under study.

GOAL		**to ensure continuous development of engineering teachers' professional competence at a college**
Methodological and target block	Target landmarks	To develop the structural components of professional competence as an integrative property of the individual (motivation and value, cognitive-informational, behaviour and activity, personal reflection, emotion and volition)
		To develop the main varieties of professional competence (training, educational, methodical, subject, informational and digital, environmental, inclusive, research, communicative)
	Methodological approaches	*General*: systemic, activity, person-oriented, axiological, communicative
		Specific: competence, environmental, informational, humanistic, synergistic, technological
	Principles	*General*: scientific, connection between theory and practice, activity and consciousness, systematicity, accessibility, visibility
		Specific: continuity, prioritization of self-education, design, modularity, fundamentality, integration
Organizational and subject block	Stages	Motivation → Formation → Diagnostics and Correction
	Directions	*Formal education* — certificated training, internship
		Non-formal education — corporate training, research activity, implementation of the educational process
		Informal education — self-development, self-education
	Subjects of interaction	Teachers of technical disciplines, students, methodologists, scientists, teaching staff at educational institutions, etc.
Content and technology block	Content	Innovative knowledge and ability to implement training, educational, methodical, research, etc. types of pedagogical activity at a college
	Means	Natural objects and object-spatial images: machines, mechanisms, parts, layouts, models, dummies, demonstration stands, virtual laboratories
		Educational, scientific, methodical, reference literature
		Electronic educational resources
	Implementation tools	*Methods*: explanatory-illustrative, reproductive, problem-informational, heuristic, research, gamification
		Forms: problem lectures, seminars-discussions, trainings, webinars, self-education based on the Internet resources
		Innovative pedagogical technologies
Diagnostic and resultative block	Diagnostics	*Criteria*: motivational, cognitive, activity, reflexive, volitional *Corresponding indicators*
		Levels of development: basic, elementary, intermediate, advanced
	Expected result	**Positive changes in the levels of engineering teachers' professional competence, the growth of the teachers' abilities to effectively implement various types of innovative pedagogical activity**

Fig. 1. Visualization of the structural and content model of professional competence development of engineering teachers at college.

The newly characterized structure of the investigated competence follows the other published findings on the problem. It requires testing and can be further used in developing and diagnosing the phenomenon of college engineering teachers' professional competence.

The presented pedagogical model can be treated as a specific system that reflects and imitates certain properties, signs, and characteristics of the research object and the principles of its internal organization and function, presented in a straightforward form. For a more detailed study of the development processes of engineering teachers' professional competence at college, it is necessary to organize an experimental research project when the presented model could be applied and tested.

To discuss the results of the current research and the presented model, it should be noted that the content confirmed the elements of a pedagogical model, including Organizational, Content, Methodological, and Technological aspects presented in [22]. On the other hand, the pedagogical model focused on the engineering teachers' high professional level and their subject conceptual understanding by improving critical thinking skills, as justified in [23]. As for the educational practice, the ideas of the 4 "Cs" [24] were reflected in the content and structure of the studied phenomenon. It also must be emphasized that the concept of the developed pedagogical model considered its function in carefully planning a teaching and learning process at college. The process of teachers' professional development should be based on the existing theories (psychological, social, educational, learning, philosophical, etc.), take into account the learning goals and content, be focused on the students features and needs as well as the educational environment and assessment procedure as it was substantiated in [25, 26].

5 Conclusions

The problem of purposeful development of the professional competence of an engineering teacher at college was under study. The definition of the term "professional competence of an engineering teacher at college" was given based on the logical rules for defining concepts. The term was formulated as an integrative property, which included some components or competence types. The psychological structure was analyzed, and 5 components were distinguished: motivation and value, cognitive-informational, behavior and activity, personal reflection, emotion, and volition. The analysis of the subject-specific teacher's activity enabled to determine and range 9 main competence types according to their importance (as the experts assessed them): the training (with Competence Weight 0.76), the communicative (0.75), the subject (0.68), the methodical (0.67), the informational and digital (0.66), the educational (0.65), the inclusive (0.49), the research (0.38) and the environmental (0.31) competences. The process of purposeful development of teachers' professional competence was modeled. The model was based on the methodological approaches, factors, conceptual ideas, and learning conditions of systematically developing teachers' professional competence. The model included four interdependent blocks: Methodological and target, Organizational and subject, Content and technology, and Diagnostic resultative that functionally combine certain elements of the development system of the phenomenon under study.

The ideas contained in the pedagogical model determined the strategy and tactics of developing the teachers' professional competence as a continuous technological process with a specific structure, theoretical and methodological dependencies, and prognostic trends.

The prospects for further scientific research are seen in the experimental verification, appropriate adjustment, and introduction of the structural and content model for

the purposeful development of the professional competence of engineering teachers at colleges into the educational practice.

References

1. Walters, H.D., K.M. Bockorny.: Relevance of general education: an assessment of undergraduate business students. e-J. Bus. Educ. Scholarship Teach. **12**(3), 34–43 (2018)
2. Skenes, K., Rabb, R.J., Washuta, N.J., Righter, J.: Teaching engineering in the general education curriculum. In: Proceedings of 2020 First-Year Engineering Experience, 32109. East Lansing, Michigan (2020)
3. Fagette, P., Chen, S.-J., Baran, G., Samuel, S., Kiani, M.: Engineering a general education program: designing mechanical engineering general education courses. Innov. High. Educ. **38**, 117–128 (2012). https://doi.org/10.1007/s10755-012-9231-2
4. UNESCO: Social & Human Sciences. https://www.unesco.org/en/social-human-sciences. Accessed 20 Jan 2023
5. Vare, P., et al.: Devising a competence-based training program for educators of sustainable development: lessons learned. Sustainability **11**(7), 1890 (2019). https://doi.org/10.3390/su11071890
6. Lozano, R., Barreiro-Gen, M., Lozano, F.J., Sammalisto, K.: Teaching sustainability in European higher education institutions: assessing the connections between competences and pedagogical approaches. Sustainability **11**(6), 1602 (2019). https://doi.org/10.3390/su11061602
7. Imara, K., Altinay, F.: Integrating education for sustainable development competencies in teacher education. Sustainability **13**(22), 12555 (2021). https://doi.org/10.3390/su132212555
8. Weng, S.-S., Liu, Y., Dai, J., Chuang, Y.-C.: A novel improvement strategy of competency for Education for Sustainable Development (ESD) of University teachers based on data mining. Sustainability **12**(7), 2679 (2020). https://doi.org/10.3390/su12072679
9. Katalin, H., Zsófia-Irén H., Szentes, E.: Existing and to be developed teacher competences in engineer teacher training. Contemporary Educ. Res. J. **10**(4) (2020). https://doi.org/10.18844/cerj.v10i4.5212
10. Ca-Nguyen, D., Phuong-Ngo, T., Thang–Ngoc, H., Hai-Luong, D., Lien-Nguyen, H., Thang-Nguyen, T.: A policy review of criteria and competencies for teaching staff of general education in Vietnam. Cogent Educ. **9**(1) (2022). https://doi.org/10.1080/2331186X.2022.2133889
11. Titova, O., Luzan, P., Ishchenko, T., Kabysh, M., Homeniuk, D.: Improvement of professional competence of general education teachers for engineering curriculum. In: Tonkonogyi, V., Ivanov, V., Trojanowska, J., Oborskyi, G., Pavlenko, I. (eds.) Advanced Manufacturing Processes V. InterPartner 2023. Lecture Notes in Mechanical Engineering, pp. 379–388. Springer, Cham (2024). https://doi.org/10.1007/978-3-031-42778-7_35
12. Neves, R., Lima, R., Mesquita, D.: Teacher competences for active learning in engineering education. Sustainability **13**(16), 9231 (2021). https://doi.org/10.3390/su13169231
13. Aidoo, B., Macdonald, A., Gyampoh, A.O., Baah, K.A., Tsyawo, J.: Factors influencing teachers' online teaching competence in higher education. Soc. Educ. Res. **3**(1), 148–160 (2022). https://doi.org/10.37256/ser.3120221315
14. Cruz, M.L., Saunders-Smits, G.N., Groen, P.: Evaluation of competency methods in engineering education: a systematic review. Europ. J. Eng. Educ. **45**(5), 729–757 (2020). https://doi.org/10.1080/03043797.2019.1671810

15. Sosnytska, N., Titova, O., Symonenko, S., Kravets, O.: Examining the creative potential of engineering students. In: Nadykto, V. (eds.) Modern Development Paths of Agricultural Production 2019, pp. 299–306. Springer, Cham (2019). https://doi.org/10.1007/978-3-030-14918-5_31
16. Carvalho, G.D.G. de, Corrêa, R.O., Carvalho, H.G. de, Vieira, A.M.D.P., Stankowitz, R. de F., Kolotelo, J.L.G.: Competencies and Performance of Engineering Professors: Evidence from a Brazilian Public University. Ingeniería E Investigación **38**(3), 33–41 (2018). https://doi.org/10.15446/ing.investig.v38n3.70998
17. LaShorage, S., Karen, T.-B.: Enhancing teacher competency through co-teaching and embedded professional development. J. Educ. Training Stud. **3**(3), 117–125 (2015)
18. Murphy, M., Destin, M.: Promoting inclusion and identity safety to support college success. The Century Foundation (2016). https://tcf.org/content/report/promoting-inclusion-identity-safety-support-college-success/. Accessed 12 Jan 2023
19. Gagné, R.M.: The Conditions of Learning, 4th edn. Holt, Rinehart & Winston, New York (1985)
20. Gagné, R.M., Medsker, K.L.: The conditions of learning: training applications. Harcourt Brace, Fort Worth (1996)
21. Koper, R.: Conditions for effective smart learning environments. Smart Learn. Environ. **1**(5) (2014). https://doi.org/10.1186/s40561-014-0005-4
22. Department of Education and Training, issuing body & Victoria. The pedagogical model (2018). http://nla.gov.au/nla.obj-2339258399. Accessed 12 Jan 2023
23. Behar, P.: Constructing pedagogical models for E-learning. I. J. Adv. Corporate Learn. **4**, 16–22 (2011). https://doi.org/10.3991/ijac.v4i3.1713
24. Ali-Corlu, M., Sencer-Corlu, M.: Scientific Inquiry based professional development models in teacher education. Educ. Sci. Theory Practice **12**(1), 514–521 (2012)
25. Pedagogical model. ESCADE Ramon Llull University. https://www.esade.edu/en/about-us/mission-values/holistic-education/pedagogical-model. Accessed 12 Jan 2023
26. Arufe-Giráldez, V., Sanmiguel-Rodríguez, A., Ramos-Álvarez, O., Navarro-Patón, R.: News of the pedagogical models in physical education-a quick review. Int. J. Environ. Res. Public Health **20**(3), 2586 (2023). https://doi.org/10.3390/ijerph20032586

Motivation Principles of Self-management in the Professional Training of Engineers Under the Conditions of Forming the Creative Competence

Viktor Nagayev(✉), Yuliia Sahachko, Galyna Nagayeva, Sergii Chervonyi, and Yevhenii Beznos

State Biotechnological University, 44, Alchevskih Street, Kharkiv 61002, Ukraine
nagaevviktor1966@gmail.com

Abstract. The article aims to model the motivational mechanisms of the formation of the creative experience of future engineers based on the identification of contradictions in the management of educational activities and the development trends of the pedagogical process of training specialists in the engineering field. Modern methodological approaches and theoretical and empirical methods were used in the research: questionnaires, testing, time series analysis, modeling creative situations, pedagogical experiment, statistical analysis, and reference comparison (to identify the system of student motivation for engineering professional activity. The proposed model of forming engineering personnel's creative experience depends on the motivation level. The motivational structure of the engineer's professional competence in the system of his professional training is analyzed. Didactic methods of activating the motivational support of the educational process and components of educational management in the self-management conditions of students' educational and creative activities were studied. A justified structure of the technological stages of students' self-motivation in the conditions of the digital educational space. The effectiveness of the proposed self-motivation model in future engineers' educational activity by means of self-correction and self-development of personality is proven.

Keywords: Motivation · Management · Self-Organization · Educational Activities · Managerial Competence · Professional Training · Engineering Creativity

1 Introduction

In today's innovative educational space, one of the inhibiting aspects of increasing the efficiency of engineering training is the low level of student motivation for productive, independent work. Therefore, in the educational process of professional training of engineering personnel, the pedagogical problem of activating students' independent work based on the introduction of motivational mechanisms to encourage students to participate in creative educational activities arises [1, 2].

© The Author(s), under exclusive license to Springer Nature Switzerland AG 2024
V. Ivanov et al. (Eds.): DSMIE 2024, LNME, pp. 521–530, 2024.
https://doi.org/10.1007/978-3-031-61797-3_44

According to the results of the aspect analysis of the professional activity of engineering personnel, it was determined that in the conditions of the digital economy and the decentralization of production, the demand for engineers who are able not only to solve complex technological tasks of innovative search, to make creative scientifically based decisions, but also to show high leadership abilities, to show competences, is sharply increasing in related fields, to ensure constant self-development [3, 4].

Based on the modeling of production situations and the survey of engineering personnel of enterprises and organizations of the Kharkiv region (Ukraine), we determined that only 16–18% of engineering specialists work at the level of creative experience. Other scientists testify to similar trends, which reflect the insufficient preparation of engineers for creative activity [5].To confirm these conclusions, we will conduct a sociological survey of production workers and students of engineering specialties regarding the motivation of professional training and the determination of the role of creativity in the production activity of engineers. The results of the survey proved that a significant percentage of respondents proved the high importance of motivational support (84%) and the need to form creative experience of future engineering personnel in the process of their professional training (78%) [6]. On this basis, it was concluded that the creative orientation of engineers of the modern generation is the main prerequisite for their effective production activity under the conditions of self-motivation skills.

2 Literature Review

The problem of motivational support in the educational process is highly urgent because the efficiency of the future production activity of the future specialist engineer depends significantly on motivational factors. Therefore, in the pedagogical environment, it is essential to find motivational factors - motivators of educational and creative activity that fundamentally affect the future specialist as an educational system subject [7].

Let's consider the theoretical foundations of the motivation of the educational process [8]. Figure 1 shows the diagram of the relationship between the concepts of "needs", "interests", and "motives", which largely determine the process of self-management of motivational educational and creative activities of the student [9]. These elements comprise the combination of algorithms' structure for motivational educational activities, which is determined by multifactorial conditions [9].

While studying at an educational institution, a student is influenced by many factors that encourage him to study and increase or decrease motivation (hinder successful studies). A motive is an internal drive to activity related to satisfying defined needs, a set of internal and external conditions that cause personality activity. Motives are the basis of an individual's activity and an essential component of the structure of human activity [10]. As a rule, the motive is realized in the goal of the activity, although in practice, they may not coincide. For example, getting a higher rating may be motivated by the student's desire to realize respect and the prospect of an excellent job in an engineering position.

An essential component of the motivation of a particular activity is the combination of motives and goals of the activity [11, 12]. Motives and goals of activity condition each other. A feature of the interdependence of motives and goals of activity is that the

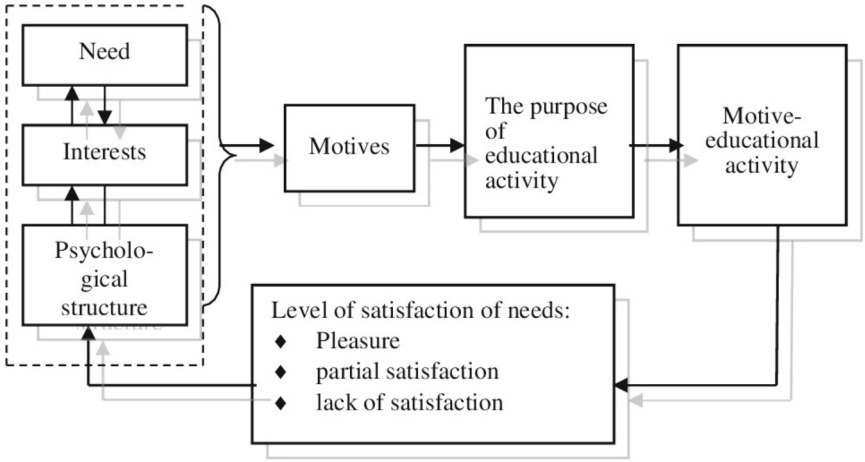

Fig. 1. The self-management process model motivates the students' educational activity.

motive acts as a reason for setting specific goals. For example, for the desire to obtain an engineering education to become the goal of an individual's activity, the presence of appropriate motives is required (the desire to master an engineering specialty, the desire for practical implementation in society, an effort to prove one's high level of production potential, etc.). Goals and motives are not identical, although sometimes they coincide (if the motive prompts a separate partial action). For example, when a student works on solving educational tasks, seeking to master specific professional knowledge and skills. These aspects were analyzed from the perspective of internal and external motivation factors for educational activities [13]. A student's motivational behavior is based on a person's needs and motivation. A drive is a desire to satisfy needs based on the feeling of lacking something. Psychologists have determined that needs and urges are the main motives for action [14]. For example, a future engineer feels the need for complex, interesting creative work, and this prompts him to try to achieve the goal by receiving a task that will ensure the satisfaction of this need. Therefore, the teacher must also be a good motivator who helps students discover internal creative motives for professional activity [15]. Such activity within the limits of achieving the goal will be motivational behavior.

An equally significant component of motivational behavior is the concept of "interest" (a form of manifestation of the cognitive need of an individual, which is directed at the relevant subject as something valuable for it). The interests of an individual can be highly diverse (equipment, technology, nature, etc.). The main thing about this concept is that, having shown interest in the relevant subject, future engineers can make this interest a means of achieving professional goals [16].

The results of many pedagogical studies prove that one of the essential points that reveals the pedagogical essence of high-quality motivated educational activity of students is a set of motives [17, 18]. For example, the motives of students' high-quality educational and creative activity can be fairness and objectivity of the evaluation by the thrower, the opportunity to improve in professional and professional training to realize their creative

and intellectual abilities, the prospect of suitable employment, and others. These factors are purely individual and depend on many circumstances, but a higher school teacher needs to study and consider them. In this context, the teacher's task is not to force the future engineer specialist to learn but to encourage learning so that the learning process becomes naturally necessary and desirable.

It should be noted that the motives of students' activity can be external and internal [19]. External - those offered by the teacher (for example, rating evaluation, incentive coefficients), and internal - those generated by the psychological structure of the individual, his level of education, morality, culture (for example, such motives can be the self-expression of a future engineer, the desire for creativity, self-improvement). As a result of the student's awareness of primary (natural) and secondary (material and spiritual) needs, there are specific incentives for productive actions, thanks to which these needs are satisfied. For example, Titova O., Luzan P., and other researchers consider engineering creativity as a resource potential that allows identifying various areas of learning that can be supported by information technologies (activation of multimedia tools, automation of technological techniques for improving the graphic design, organization of a creative educational environment, optimization research activities and control of learning outcomes [20]. At the same time, researchers focus on the algorithmization of students' motivational activities [21].

As a result of the awareness of primary (natural) and secondary (material and spiritual) needs, acquirers have specific incentives to act, which satisfies these needs. In this context, it is essential to develop mostly internal motives because they correspond to the needs of a higher order, according to A. Maslow [19]. For example, a significant internal motive for quality educational activity is the creative learning process. According to our research, 78% of future engineers want to work in a creative educational environment with a high level of individualization of the learning content. For this, it is necessary to humanize the educational process and to develop didactic systems with decentralized influence based on the process of self-motivation of students. Many studies have proven that the internal needs of students in the competition are, in most cases, much stronger than the external motivation from the teacher [23]. In this context, the educational process built in the form of game production models creates an effective internal motivation system for future engineers to engage in professional activity.

At the same time, to obtain a potentially sustainable motivational system for training engineering personnel, the implementation of the principles of motivation must take into account Adams' procedural motivational theory of justice, according to which the student constantly compares his achievements and received rewards with the corresponding components of other subjects of the educational process [8]. At the same time, the value (valence) of the reward is subject to subjective interpretation, which determines the need for the teacher to study the student's needs and provide motivational factors that would individually satisfy these needs.

Also, in training engineering personnel, it is essential to determine the priority motives since this psychological category is subjective and historical. For example, the Kharkiv Scientific Center of Management-Education Didactics conducted surveys of students of engineering majors over the past 20 years on the importance of motivations for activity [5]. Thus, in the early 2000s, the most significant motive was the

desire to receive an automatic assessment; in the 2010s, the desire to study in a creative environment; in the 2020s, students mostly care about their rating, which can become a reason for suitable employment ensuring an influential career as an engineer.

Analyzing the existing scientific-methodical and didactic support for the training of engineers, we concluded that the current state of engineering education needs to ensure the proper training of specialists with the qualities mentioned above [24]. On this basis, the principal contradiction between the need for the formation of creative abilities of engineers and the insufficient development of the theoretical and methodological foundations of the motivational management of the educational process was formulated. Several contradictions confirm this contradiction, the solution of which is based on the problem of self-management of students' educational activities. To solve these problems, it is necessary to improve the pedagogical process of training engineering personnel based on technology and using a management approach with the student's active role as a management subject [25].

3 Research Methodology

At the ascertainment stage of the experiment, the motivation of engineering primary students for initial activities was clarified by studying their value attitude interest in independent and individual work; the level of knowledge, skills, and abilities to implement the self-management process is determined; the level of formation of qualities characteristic of a future specialist in the field of engineering was investigated. Students of the State Biotechnological University (Kharkov) majors 192 "Construction and Civil Engineering", 193 Geodesy and Land Management, and 208 "Agroengineering" took part in the survey. The role of experts was played by teachers, production workers, postgraduate students, part-time students, and postgraduate students, who observed students during a specific period (semester), conducted questionnaires and surveys, and analyzed the results of self-assessment of students' motivational activities.

The exploratory stage of the experiment aimed to develop a research concept based on the definition of a hypothesis, scientific laws, and principles of motivational activity for future engineers. Based on the clarification of the theoretical and methodological foundations of the educational process, a complex of didactic tools for the motivational activity of students was substantiated, establishing the quantitative and qualitative composition of the experiment participants. The following research methods were used at this stage: forecasting, designing, and organizational modeling.

At the control stage of the pedagogical experiment, a comparative assessment of the effectiveness of the proposed model of motivational activity was made according to the developed methodology of student self-management; the reliability of the scientific hypothesis was evaluated. The following research methods were used at this stage: correlation-regression, survey, and graphic.

4 Results and Discussion

To organize an effective motivational influence and achieve the research goals, we have developed a two-level pedagogical technology for managing students' motivational activities [22]. The first stage of the experiment concerned the development of individual

elements of this technology on the example of relevant educational programs of various specialties, with the separation of the motivational component - the rating assessment of students' educational activities. For this purpose, based on the State Biotechnological University, research was conducted on the influence of the didactic model of student self-management on their motivational activity. The research hypothesized that a high level of students' motivation will create prerequisites for their creative activity, which should be the basis for the formation of a high level of formation of creative experience for future engineers. This assumption was based on the preliminary analysis of the student survey regarding motivational factors.

The purpose of the study was to determine students' self-motivation level while attending classroom classes and the influence of this factor on the development of creative abilities and professional training of future engineers. As a result, quantitative and qualitative indicators were determined, which made it possible to monitor the motivational nature of the creative activity of students studying in the self-management of motivational activity (SMA) and the traditional system of education (TES).

We will conduct a dispersion analysis of the above data. According to the traditional education system, we have the following results: the range of variation between the maximum and minimum value of attending classes for all specialties was 44%; coefficients of variation (mechanical engineers – 14.62%; construction engineers – 17.95%; land management engineers – 22.78%; average – 18.45%).

The average level of class attendance was 66.8%. According to the SMA model, the range of variation between this indicator's maximum and minimum value was 26%. At the same time, the coefficients of variation were as follows: mechanical engineers – 9.15%; civil engineers – 10.2%; land surveying engineers - 11.79%; the average is 10.38%. Average class attendance by students was 68.2%.

The analysis of these results indicates qualitative changes in students' motivation regarding forming their value-oriented qualities (self-awareness, self-motivation, self-expression, etc.) manifested in increased creative activity. Under these conditions, students work more regularly and intensively. At the same time, the very nature of attending classes changes. They show more creative activity in the middle of the academic semester, and, on the contrary, with the traditional system, the teacher feels the activity of students at the beginning and end of studying the discipline. According to the proposed model of student self-management, we have a motivational influence on the psychological aspects of the individual's activity, creating a clear positive idea of the possibility of achieving the desired result.

Taking into account the above provisions, it is possible to propose the following mathematical model of motivation of the process of self-management of learning in the training of engineers:

$$R = PSI\,x\ A\ x\ M\ x\,F\ x\,V \tag{1}$$

where: R – expected results of educational activity in the form of formed creative experience; PSI – components of the psychological structure of the individual (interests, needs, character, temperament); A – the activity of educational activity; M – motivation of creative activity; F – the fairness of the assessment of self-management of learning; V – the value (valence) of motivational conditions.

According to the results of the pedagogical experiment, it can be noted that the nature of the level of students' motivation in the model of self-management of learning differs significantly from the same indicator in the traditional system of education. This explains and simultaneously proves the change in the motivation of future engineers, which affects their psychological aspects of self-development. They are interested in working more regularly, rhythmically, and qualitatively during the semester because they have a clear idea of the direct dependence of their final grade on the results of their engineering creativity. The result is higher creative activity, which ultimately leads to professional growth of engineering professionals.

However, in contrast to the qualitative assessment of class attendance (level of motivation), its quantitative assessment (students' presence in class), as shown by the research results, does not directly affect students' academic performance and the formation of creative experience. To prove this point, we will calculate the variance-regression analysis of the dependence of students' academic performance on class attendance according to the self-management model of motivational activity (SMA) and the traditional education system (TES) on the example of engineering disciplines.

According to the experiment results, regression equations were obtained, proving that engineering creativity does not depend on class attendance. Moreover, the regression coefficients (a = –0.012766, a = –0.008959) show that there is an inverse relationship between these indicators:

$$\text{Ysma} = 5.396796 - 0.012766\ \text{X1} \tag{2}$$

$$\text{Ytes} = 4.644335 - 0.008959\ \text{X2} \tag{3}$$

Regression coefficients show that with an increase in the frequency of attending classes by 1%, there is no increase in the level of engineering creativity. Still, on the contrary, it decreases by 0.012766% and 0.008959%, respectively. The coefficients of determination (Rd = 0.28690078, Rd = 0.25486737) prove that about 25–28% of the total variation of the resulting characteristic is determined by the action of these factors. So, according to the calculations of the statistical indicators of the coincidence of the results of the evaluation of the actual data of engineering creativity and the attendance of students' classes, it can be determined by the following indicators of pair correlation: $R_К = -0.54$ (according to SMA) and $R_К = -0.50$ (according to TSN), respectively, which indicates lack of direct connection between the studied factors. The study's results proved that only the qualitative aspect of students' attending classes (their motivational creative activity) is the main factor characteristic of the formation of creative experience. Further research as part of a formative experiment based on the correlation analysis of dynamic series also proved a close connection between the level of creative experience formation and future engineers' creative activity. At the same time, the pairwise correlation coefficient between these factors during the pedagogical experiments was 0.87.

The above results can be compared with studies in the field of activation of motivational support for educational activities of engineering personnel [2, 7]. It should be noted that the comparison of these research results confirms our hypothesis about the possibility of increasing the motivational component of the educational process through the

implementation of self-didactic functions of students (self-management of educational and creative activities). At the same time, the study [3] emphasizes the importance of parity subject-subject relations between the teacher and the student within the framework of the implementation of facilitation functions by the teacher in the virtual environment. To implement these pedagogical conditions, we also confirm the need for differentiation of pedagogical influence with the possibility of managing the motivational basis of students' educational and creative activity in the conditions of SMART educational technologies.

However, our research was conducted on the example of engineers of agro-industrial production, which requires further testing of the educational and methodological support of self-study motivation at the level of specialists of various specializations. Considering the modern experience of training engineering personnel [13, 20], it is necessary to ensure the development of a factor model of student self-study motivation at the level of adaptive pedagogical influence. Such a situational motivational model of self-management of learning will optimize the resource provision of pedagogical influence and increase the productivity of training future engineers.

5 Conclusions

Engineering creativity is essential to engineers' professional competence when facing innovative challenges related to modern technical and technological problems. Creatively gifted engineers in production conditions take risks more often than their less creative colleagues; they know how to adapt to the changes in their environment. Also, creative engineering personnel are a source of constant innovations and inventions; they quickly adapt to new conditions and adequately perceive the connections between the elements of the technical system, which in modern society determines the competitive advantages of the engineering industry.

The above processes and psychological-pedagogical conditions for increasing the motivation of students' engineering creativity prove the need to develop a system of didactic forms and means of managing educational and creative activities to ensure high self-motivation of students' creative activity in the pedagogical process. Based on the results of a questionnaire survey of students of engineering majors regarding the introduction of the model of self-management of motivational activities (SMD) into the educational process, we concluded that the proposed didactic direction is highly effective, as evidenced by the feedback of managers of enterprises in which future engineers underwent industrial practice.

We have proven that the presence of motives also depends on the educational and cultural level of the applicants. Thus, students with high basic training prefer creative forms of organization of the educational process, while students with a lower level of training pay more attention to the teacher's control system. It should be added that in training engineers, improving the motivational function of control is essential. Knowledge control (on an exam or a test) is not only a form of knowledge assessment but also a decisive motivating factor for a student's quality education.

The studies proved the validity of the proposals regarding including the main provisions of motivational theories in the educational process of vocational training of

engineering personnel. Taking into account the results of previous studies on the problem of increasing the motivation of engineering creativity, we have proposed adequate didactic models at the macro- and micro-levels of a higher education institution (didactic games in the system of activation and step-by-step control of knowledge; case models of the analysis of industrial situations; variable forms of research activity according to the priority areas of science development and techniques; educational studios: "School of a young engineer", "Agrarian engineer - a creative profession"; optional course "Creativity in the conditions of self-development of an engineer"), which take into account the content of the training of engineering personnel, as well as the individual psychological needs of a specialist in production conditions.

References

1. Bourgeois-Bougrine, S., Buisine, S., Vandendriessche, C., Glaveanu, V., Lubart, T.: Engineering students' use of creativity and development tools in conceptual product design: what, when and how? Thinking Skills Creativity **24**, 104–117 (2017). https://doi.org/10.1016/j.tsc.2017.02.016
2. Kožuh, A.: Didactic skills in the field of developing creativity and innovativeness of a student. Int. J. Cognit. Res. Sci. Eng. Educ. **8**(1), 69–79 (2020)
3. Bun, P., Trojanowska, J., Ivanov, V., Pavlenko, I.: The use of virtual reality training application to increase the effectiveness of workshops in the field of lean manufacturing. In: 4th International Conference of the Virtual and Augmented Reality in Education, VARE 2018, pp. 65–71 (2018)
4. Hadgraft, R.G., Kolmos, A.: Emerging learning environments in engineering education. Australas. J. Eng. Educ. **25**(1), 3–16 (2020). https://doi.org/10.1080/22054952.2020.1713522
5. Nagayev, V., Vertegel, V., Nagayeva, G., Kovalenko, O., Smihunova, O.: A model of formation of professional and creative competences for engineers based on information and digital technologies. In: Ivanov, V., Trojanowska, J., Pavlenko, I., Rauch, E., Piteľ, J. (eds.) Advances in Design, Simulation and Manufacturing VI. DSMIE 2023. Lecture Notes in Mechanical Engineering, pp. 390−399. Springer, Cham (2023). https://doi.org/10.1007/978-3-031-32767-4_37
6. Mamchych, T., Myroniuk, L., Royko, L.: Information and communication technologies usage experience at teaching of mathematical disciplines in the terms of the distance learning. Comput.-Integrated Technol. Educ. Sci. Prod. **39**, 70–77 (2020). https://doi.org/10.36910/6775-2524-0560-2020-39-12
7. Zheng, J., Wu, G., Li, H.: Motivating civil engineering students' creativity: actor-partner interdependence approach. J. Civil Eng. Educ. **146**(1) (2020)
8. Madsen, K.B.: Modern theories of motivation. Copenhagen (1974)
9. Norström, P., Hallström, J.: Models and modelling in secondary technology and engineering education. Int. J. Technol. Des. Educ. **33**(50), 1797–1817 (2023)
10. Cropley, D.H.: Promoting Creativity and Innovation in Engineering Education. Psychology of Aesthetics Creativity and the Arts 9(2) (2015)
11. Aldakheel, E., Rajaei, H.: Cloud computing in computer science and engineering education. In: Proceedings ASEE Annual Conference and Exposition, pp. 25.318.1−25.318.15. San Antonio, Texas (2012)
12. Vries, P., Klaassen, R., Kamp, A.: Emerging technologies in engineering education: can we make it work? In: 13th International CDIO Conference Proceedings. University of Calgary (2017)

13. Lean Filho, W., Nesbit, S., et al.: New Developments in Engineering Education for Sustainable Development. Springer, Switzerland (2016). https://doi.org/10.1007/978-3-319-32933-8
14. Hernandez-de-Menendez, M., Morales-Menendez, R.: Technological innovations and practices in engineering education: a review. Int. J. Interact. Des. Manuf. **13**, 713–728 (2019). https://doi.org/10.1007/s12008-019-00550-1
15. Cropley, D.H., Cropley, A.J.: Engineering creativity: A systems concept of functional creativity. Creativity across domains: Faces of the muse **1**(15), 169–185 (2005)
16. Strilets, O.: Pedagogical conditions of professional training of skilled machine-building industry workers by the dual form of education. Professional Pedagogies **2**(23), 19–26 (2021). https://doi.org/10.32835/2707-3092.2021.23.19-26
17. Symonenko, S., Zaitseva, N., Titova, O., Vynogradova, M.: Development of communicative competence as a precondition of competitive software engineer formation. In: Nadykto, V. (eds.) Modern Development Paths of Agricultural Production, pp. 307–315. Springer, Cham (2019). https://doi.org/10.1007/978-3-030-14918-5_32
18. Sosnytska, N., Titova, O., Symonenko, S., Kravets, O. Examining the creative potential of engineering students. In: Nadykto, V. (eds.) Modern Development Paths of Agricultural Production, pp. 299−306. Springer, Cham (2019). https://doi.org/10.1007/978-3-030-14918-5_31
19. Maslow, A.: Motivation and personality. New York (1954)
20. Titova, O., Luzan, P., Sosnytska, N., Kulieshov, S., Suprun, O.: Information and Communication Technology Tools for Enhancing Engineering Students' Creativity. In: Ivanov, V., Trojanowska, J., Pavlenko, I., Zajac, J., Peraković, D. (eds.) Advances in Design, Simulation and Manufacturing IV. DSMIE 2021. Lecture Notes in Mechanical Engineering, pp. 332−340 Springer, Cham (2021). https://doi.org/10.1007/978-3-030-77719-7_33
21. Luzan, P., Koshuk, O., Titova, O., Mosia, I.: The technology of the learning outcomes test development. In: Tonkonogyi, V., Ivanov, V., Trojanowska, J., Oborskyi, G., Pavlenko, I. (eds.) Advanced Manufacturing Processes III. InterPartner 2021. Lecture Notes in Mechanical Engineering, pp. 687−696. Springer, Cham (2022). https://doi.org/10.1007/978-3-030-91327-4_66
22. Gorbunova, K., Nagayev, V., Litvinchuk, S., Ulitina, K., Gannichenko, T.: Integration of end-to-end and dual learning as a guarantee of quality professional training for future power engineers. In: Ivanov, V., Trojanowska, J., Pavlenko, I., Rauch, E., Peraković, D. (eds.) Advances in Design, Simulation and Manufacturing V. DSMIE 2022. Lecture Notes in Mechanical Engineering, pp. 542–551. Springer, Cham (2022). DOI: https://doi.org/10.1007/978-3-031-06025-0_53
23. Svyrydiuk, V., Luzan, P., Svyrydiuk, O., Titova, O., Popova, O.: Electronic textbooks as means for developing professional competencies of engineering students. In: Tonkonogyi, V., Ivanov, V., Trojanowska, J., Oborskyi, G., Pavlenko, I. (eds.) Advanced Manufacturing Processes III. InterPartner 2021. Lecture Notes in Mechanical Engineering, pp. 707−716. Springer, Cham (2021). https://doi.org/10.1007/978-3-030-91327-4_68
24. Koshuk, O.B: Perspective directions of modernization to vocational training of future mechanical engineers agricultural industry. Sci. J. Innov. Sol. Modern Sci. **8**(17), 24–36 (2017)
25. Bilousova, L., Gryzun, L., Sherstiuk, D., Shmeltser, E.: Cloud-based complex of computer transdisciplinary models in the context of holistic educational approach. In: CEUR Workshop Proceedings 2433, pp. 336–351 (2019)

Author Index

A
Antonenko, Nataliia 365
Antosz, Katarzyna 376
Arras, Peter 489
Aruväli, Tanel 3
Azamfirei, Victor 51

B
Babenko, Eugene 152
Badovskyi, Olexandr 139
Balaniuk, Anna 139
Basov, Bohdan 251
Basova, Yevheniia 111, 223
Beketov, Oleksandr 152
Beznos, Yevhenii 521
Bohdanov, Oleksandr 409
Buriachenko, Oleksii 399
Butdee, Suthep 212

C
Çakir, Orhan 188
Campilho, Raul 388
Chervonyi, Sergii 521
Ciszak, Olaf 164
Costa, Rúben 319

D
De Angeli, Antonella 63
De Marchi, Matteo 3
De Silva, M. Mavin 425
Dehtiarov, Ivan 164
Denysenko, Yuliia 251
Derbaba, Vitalii 409
Diachun, Andrii 287
Dobrotvorskiy, Sergey 223
Drahobetskyi, Volodymyr 341
Druzhinin, Evgeniy 124
Dudarev, Igor 39
Dynnyk, Oksana 251
Dzhemalyadinov, Ruslan 188
Dzhemelinskyi, Vitaliy 178, 276
Dzhemilov, Eshreb 188

E
Edl, Milan 139
Evtuhov, Artem 164

F
Fernandes, Filipe 319
Fernando, P. M. 425
Fernando, W. Madushan 475
Fil'o, Milan 352
Filina-Dawidowicz, Ludmiła 89
Frego, Marco 63
Frolov, Mykhaylo 200

G
Gerliand, Tetiana 498
Gorovyi, Dmytro 111
Grabis, Janis 124
Grochala, Daniel 178

H
Haidabrus, Bohdan 100, 124
Haiduk, Olha 498
Hevko, Ivan 287
Holofieiev, Yurii 399
Holofieieva, Maryna 399
Hrinchenko, Hanna 365
Hruska, Matej 178
Hupfer, Christoph 449
Hutorov, Andrii 309

I
Ivanov, Vitalii 164, 437
Ivanova, Maryna 331
Ivashura, Andrii 309

© The Editor(s) (if applicable) and The Author(s), under exclusive license to Springer Nature Switzerland AG 2024
V. Ivanov et al. (Eds.): DSMIE 2024, LNME, pp. 531–533, 2024.
https://doi.org/10.1007/978-3-031-61797-3

J
Janmanee, Pichai 212

K
Kalenskyi, Andrii 498
Kharchenko, Oleksandr 223
Kliment, Marek 15, 28
Kniazieva, Viktoriia 365
Kolesnikova, Kateryna 124
Kononenko, Serhii 223
Konstantinidis, Fotios K. 51
Kopec, Ján 15, 28
Korniienko, Volodymyr 331
Kornuta, Olena 299
Kosgoda, Dilina 462
Kozechko, Valentyn 152
Kozłowski, Edward 376
Kulisz, Monika 376
Kulynych, Viktoriia 341
Kunitsyn, Maksym 240
Kusen, Nazarii 263
Kushnirov, Pavlo 251
Kusyi, Yaroslav 263

L
Lamikiz, Aitzol 276
Lapa, Oksana 498
Larshin, Vasily 39
Laukhin, Dmytro 152
Lesyk, Dmytro 178, 276
Lishchenko, Natalia 39
Luzan, Petro 509
Lyashuk, Oleg 287
Lynnyk, Olena 111

M
Martinez, Silvia 276
Matiscák, Matúš 15
Matt, Dominik T. 3
May, Gökan 51
Medvediev, Ievgen 437
Medvid, Iuliia 299
Mizerák, Marek 28, 75
Montewka, Jakub 437
Mordyuk, Bohdan 178, 276
Mosia, Iryna 509
Mrowiński, Piotr 89
Muzylyov, Dmitriy 437

N
Nagayev, Viktor 521
Nagayeva, Galyna 521
Navrotska, Tetiana 287
Navruzova, Gulshan 509
Nielsen, Peter 475
Nogueira, Francisca 388
Novikov, Fedir 309

O
O'Donnell, Garret 39
Oborskyi, Gennadii 139
Odosii, Zinovii 299
Onysko, Oleh 299
Orgiyan, Alexandr 139, 399
Ostroha, Ruslan 164

P
Pashchenko, Tetiana 509
Patsera, Serhii 409
Pavlenko, Ivan 111
Pedroso, André 319, 388
Peer, Angelika 63
Pekarčíková, Miriam 28, 75
Perera, H. Niles 462, 475
Pituley, Lolita 263, 299
Polonsky, Leonid 331
Pop, Grigore 251
Psarommatis, Foivos 51
Pyatnichuk, Tetyana 498

R
Rauch, Erwin 3
Rogatynskyi, Roman 287
Rott, Nataliia 152

S
Sahachko, Yuliia 521
Sait, Unais 63
Sales-Contini, Rita 319, 388
Schuliar, Iryna 263
Sebbe, Naiara 319
Shramenko, Natalya 449
Shramenko, Vladyslav 449
Silva, Francisco 388
Sivakumar, T. 425
Slipchuk, Andrii 263
Solokha, Vasyl 200
Somaweera, Praveena 462

Stepanov, Mykhaylo 331
Sugathadasa, Ranil 425
Symonova, Anastasiia 341

T
Tabunshchyk, Galyna 489
Thibbotuwawa, Amila 425, 475
Titova, Olena 509
Tonkonogyi, Volodymyr 399
Trebuňa, Peter 15, 75
Tretyak, Tetyana 331
Trishch, Roman 365
Trojan, Jozef 75, 352
Trojanowska, Justyna 111, 437
Trojanowski, Piotr 89, 449
Troynina, Anastasiya 89
Trubin, Dmytro 223
Tsyganov, Volodymyr 200

U
Usov, Anatoly 240
Uysal, Alper 188

V
Vaniev, Eldar 188
Voichyshen, Oleksandr 409

W
Wickramaarachchi, Kavitha 475

Y
Yermolenko, Oksana 309
Yermolenko, Oleksii 309

Z
Zaychyk, Yuriy 240